B cell and antibody responses to SARS-CoV-2 in people living with HIV

Emma Touizer

A thesis submitted for the degree of

Doctor of Philosophy

Division of Infection and Immunity
University College London

March 2024

Declaration

I, Emma Touizer, confirm that the work presented in this thesis is my own. Where information has been derived from other sources, I confirm that this has been indicated in the thesis.

Emma Touizer

Abstract

People living with HIV (PLWH) have ongoing immune dysfunction despite successful antiretroviral treatment. In PLWH, B cells and antibodies phenotype, function, and development are disrupted. However, there is still no clear investigation into how this overall B cell disruption in PLWH leads to the worse serological outcomes observed in vaccination. This thesis aims to characterise the humoral and cellular response made by PLWH against a novel pathogen, SARS-CoV-2, following infection or vaccination.

Participants were either recruited following SARS-CoV-2 infection (47 PLWH and 35 HIV-negative controls) or following 1, 2 or 3 doses of SARS-CoV-2 vaccines (111 PLWH and 64 HIV-negative controls). SARS-CoV-2 infection provided a sufficient stimulus so that PLWH's binding and neutralising antibody titres were comparable to HIV-negative controls. However, following SARS-CoV-2 vaccination, PLWH's serological output was lower compared to HIV-negative controls after each vaccine dose, regardless of previous SARS-CoV-2 infection. After the 1st vaccine dose, the neutralisation response of PLWH was delayed compared to HIV-negative controls. This delay was associated with lower frequencies of spike-specific memory B cells (MBC) and perturbed MBCs phenotype characterised by higher levels of atypical MBCs. After the 3rd vaccine dose, PLWH still had lower titres and breadth of neutralising antibodies, alongside perturbed MBCs phenotype compared to HIV-negative controls despite having similar frequencies of spike-specific MBCs. To answer if this MBC defect leads to improper recall responses in PLWH and thus inadequate affinity maturation, 10 PLWH and 10 HIV-negative individuals were chosen to sequence their bulk and antigen-specific BCR repertoire after each dose of SARS-CoV-2 vaccination. This showed that at the clonal level, PLWH's antibody repertoire was less diverse and skewed towards aberrant somatic hypermutation.

Altogether, this thesis showed that despite adequate antigenic stimulation, PLWH struggle to overcome their initial MBCs defect and thus are less able to make a successful serological response.

Impact statement

Since the beginning of the HIV pandemic, it has been clear that people living with HIV (PLWH) were at greater risk of opportunistic infections and poorer vaccination outcomes. This thesis aims to characterise the B cell and antibody response of PLWH in infection and vaccination against a novel pathogen, SARS-CoV-2. At the start of this project there was a scarcity of data investigating how the lower serological responses seen in PLWH against other pathogens tie in with the well-characterised defect in the memory B cell phenotype of PLWH or how these differences play out at the clonal level.

The UK's PLWH population is slowly ageing thanks to successful antiretroviral treatment which controls their HIV viraemia. However, this also means that the normal effect of immunosenescence with age may be compounded by any residual immune dysfunction preventing PLWH from making adequate vaccination responses. This problem was highly relevant in the climate of a novel global COVID-19 pandemic, as when this work started there was no data on SARS-CoV-2 immunogenicity in PLWH. The results included in this thesis represented the first evidence that PLWH made an equivalent antibody response to SARS-CoV-2 infection compared to HIV-negative controls. It was then important to understand how well PLWH would respond to SARS-CoV-2 vaccination. This thesis showed that a minimum level of T cell mediated reconstitution is required for the generation of a post-vaccination antibody response. However, past this there was still some level of residual B cell dysfunction which led to poorer serological outcomes after SARS-CoV-2 vaccination in PLWH, perturbed memory B cell (MBC) phenotype and lower diversity in PLWH's antigen specific antibody repertoire as assessed by next-generation sequencing. However, there was a heterogeneity in the quality of these response amongst PLWH likely due to different HIV treatment histories/varying levels of ongoing immune perturbation. Overall, this thesis provides new insights as to why PLWH make poorer responses to vaccines than the general population. This knowledge can be leveraged with further investigation into the mechanism of MBC disruption to improve vaccination strategies in PLWH.

Acknowledgements

The first and biggest thank goes to my supervisor, Laura McCoy. Laura kindly welcomed me in her lab in the middle of the pandemic, and since then has provided me with invaluable support (scientific, career-wise and even at times emotional) and excellent mentorship. Laura has been endlessly patient and kind when everything went right (a rare occurrence) but most importantly when everything went wrong. I could not have wished for a better supervisor.

I'd like to thank my thesis committee Mala Maini and Matt Reeves for their kindness, enthusiasm, and guidance in pushing me to think outside the B cell box.

None of this would have been possible without my funders, the UCL-Birkbeck MRC DTP.

Within the McCoy lab, Luke Muir has been a bastion of knowledge in the face of an endless stream of silly questions. Luke taught me a lot of the techniques vital for this project and most importantly was always game to team-up against Sarah/Peter or Chloe to rile them up. Sarah Griffith, Peter Thomas and Chloe Rees-Spear have been incredible companions in PhD (mis)fortune. Their friendship over these past 4 years has meant the world. Rosemarie Ford came right when everything was falling apart and never once complained whilst doing yet another bit of blood processing/ neutralisation/PCR, she has been a massive help and an overall star. The rest of the McCoy lab past and present: Chris Pinder, Dylan Jankovic, Olivia Payne and Amanda Duhlin have all played a part in providing an incredible environment to work in. I also had the pleasure of mentoring two great students Ethan Shum and Asha Marshall, which was incredibly rewarding. Ethan's hard work directly contributed to this project by purifying a lot of IgG out of plasma at record speed.

Another big thank goes to my other office mates from the Cruciform and the Pears along the years for letting me distract them/distracting me or even for the rare scientific discussion: AK Reuschl, Dejan Mesner, Aljawharah Alrubayyi, Kelly Da Costa, Noshin Hussain, Jonida Kokici, Eddy Arbe-Barnes, Doug Fink, George Finney and the many other members of the Maini-Pallett-Swadling supergroup. A special thank goes to Anna Jeffery-Smith who kindly showed me the B-cell phenotyping ropes that were key to this thesis. Janani Sivakumaran Nguyen provided excellent technical help for everything sorting and flow. Emma Morris and Tom Fox helped shape the bigger

picture during the COVID grant meeting discussion. I'm also thankful for everyone that shaped my scientific journey in my previous lab stints during my BSc/MSc/PhD rotations.

This work has relied heavily on the incredible clinical teams at the Mortimer Market Centre and Ian Charleson Day Centre. A special thank goes to Paulina Prymas, Aran Dhillon and Connor McAlpine at MMC and Tom Fernandez, Tom Allan and Johnny Edwards at ICDC. These names are only the tip of the clinical team iceberg at both sites who contributed to this project. Most importantly I am incredibly grateful for all the study participants who kindly took the time in the middle of a pandemic to give us some blood for research.

On a personal note, I'd like to thank my friends from both homes: Camille L, Camille P, Christie, Claire, Imogen, Lola, Mathilde, Megan, Rachel and Raphaëlle who have made sure that I was hardly working at time instead of working too hard.

My parents, Caroline & Yves have unconditionally supported me and given me all the opportunities I needed to get where I am today, none of this would be possible without their hard work and love. My sister Laura for keeping me on my toes and being my friend since day one.

I'd like to thank my cat Benjie for reminding me of what really mattered: her. She has been incredibly helpful by repeatedly trying to sit between me and my keyboard to make sure writing this thesis took as much time as possible, I have not questioned her logic.

Finally, I am afraid that no words will ever be good enough to thank Maria who has been behind me every step of the way during this PhD, kept me grounded and sane and given so much meaning to this work. This PhD is dedicated to you. You are the best at everything. I love you.

UCL Research Paper Declaration Form

referencing the doctoral candidate's own published work(s)

Please use this form to declare if parts of your thesis are already available in another format, e.g. if data, text, or figures:

- *have been uploaded to a preprint server*
- *are in submission to a peer-reviewed publication*
- *have been published in a peer-reviewed publication, e.g. journal, textbook.*

This form should be completed as many times as necessary. For instance, if you have seven thesis chapters, two of which containing material that has already been published, you would complete this form twice.

1. **For a research manuscript that has already been published** (if not yet published, please skip to section 2)

a) **What is the title of the manuscript?**

Characterization of humoral and SARS-CoV-2 specific T cell responses in people living with HIV

b) **Please include a link to or doi for the work**

https://doi.org/10.1038/s41467-021-26137-7

c) **Where was the work published?**

Nature Communications

d) **Who published the work?** (e.g. OUP)

Nature Publishing Group

e) **When was the work published?**

05 October 2021

f) **List the manuscript's authors in the order they appear on the publication**

Aljawharah Alrubayyi, Ester Gea-Mallorquí, **Emma Touizer**, Dan Hameiri-Bowen, Jakub Kopycinski, Bethany Charlton, Natasha Fisher-Pearson, Luke Muir, Annachiara Rosa, Chloe Roustan, Christopher Earl, Peter Cherepanov, Pierre Pellegrino, Laura Waters, Fiona Burns, Sabine Kinloch, Tao Dong, Lucy Dorrell, Sarah Rowland-Jones, Laura E. McCoy & Dimitra Peppa

g) **Was the work peer reviewed?**

Yes

h) **Have you retained the copyright?**

Yes

i) **Was an earlier form of the manuscript uploaded to a preprint server?** (e.g. medRxiv). If 'Yes', please give a link or doi)

Yes (https://www.biorxiv.org/content/10.1101/2021.02.15.431215v1)

If ‘No’, please seek permission from the relevant publisher and check the box next to the below statement:

☒

*I acknowledge permission of the publisher named under **1d** to include in this thesis portions of the publication named as included in **1c**.*

2. **For a research manuscript prepared for publication but that has not yet been published** (if already published, please skip to section 3)

3. **For multi-authored work, please give a statement of contribution covering all authors** (if single-author, please skip to section 4)

   I led the experimental work and analysis which relates to Figure 1 of this publication (all neutralisation and binding antibody data) and corresponding supplementary figures. Samples were processed and all the T-cell related data was experimentally led by my co-first authors Aljawharah Alrubayyi and Ester Gea-Mallorquí. The original draft of the manuscript was written by Aljawharah Alrubayyi, Ester Gea-Mallorquí, Laura McCoy, Dimitra Peppa and myself. Only the neutralisation and binding antibody data is directly used in this thesis, the rest of the data in this publication is discussed where relevant in the discussion sections of this thesis and referenced accordingly.

4. **In which chapter(s) of your thesis can this material be found?**

   Chapter 1-7.

5. **e-Signatures confirming that the information above is accurate** (this form should be co-signed by the supervisor/ senior author unless this is not appropriate, e.g. if the paper was a single-author work)

   Candidate

   Emma Touizer

   Date:

   12/03/2024

   Supervisor/ Senior Author (where appropriate)

   Laura McCoy

   Date

   13/03/2024

1. **For a research manuscript that has already been published** (if not yet published, please skip to section 2)

a) **What is the title of the manuscript?**

Failure to seroconvert after two doses of BNT162b2 SARS-CoV-2 vaccine in a patient with uncontrolled HIV

b) **Please include a link to or doi for the work**

https://doi.org/10.1016/S2352-3018(21)00099-0

c) **Where was the work published?**

Lancet HIV

d) **Who published the work?** (e.g. OUP)

Elsevier

e) **When was the work published?**

June 2021

f) **List the manuscript's authors in the order they appear on the publication**

Emma Touizer, Aljawharah Alrubayyi, Chloe Rees-Spear, Natasha Fisher-Pearson, Sarah A Griffith, Luke Muir, Pierre Pellegrino, Laura Waters, Fiona Burns, Sabine Kinloch, Sarah Rowland-Jones, Ravindra K Gupta, Richard Gilson, Dimitra Peppa, Laura E McCoy

g) **Was the work peer reviewed?**

Yes

h) **Have you retained the copyright?**

Yes

i) **Was an earlier form of the manuscript uploaded to a preprint server?** (e.g. medRxiv). If 'Yes', please give a link or doi)

If 'No', please seek permission from the relevant publisher and check the box next to the below statement:

☒

*I acknowledge permission of the publisher named under **1d** to include in this thesis portions of the publication named as included in **1c**.*

2. **For a research manuscript prepared for publication but that has not yet been published** (if already published, please skip to section 3)

3. **For multi-authored work, please give a statement of contribution covering all authors** (if single-author, please skip to section 4)

I led the experimental work and analysis which relates to all neutralisation and binding antibody data of this publication. Samples were processed by Sarah Griffith and Chloe-Rees Spear and all the T-cell related data was experimentally led by my co-first author Aljawharah Alrubayyi. The original draft of the manuscript was written by Aljawharah Alrubayyi, Laura McCoy, Dimitra Peppa and myself. Only the neutralisation and binding antibody data is directly used in this thesis, the rest of the data in this publication is discussed where relevant in the discussion sections of this thesis and referenced accordingly.

4. **In which chapter(s) of your thesis can this material be found?**

   Chapter 1-7.

5. **e-Signatures confirming that the information above is accurate** (this form should be co-signed by the supervisor/ senior author unless this is not appropriate, e.g. if the paper was a single-author work)

   Candidate

   Emma Touizer

   Date:

   12/03/2024

   Supervisor/ Senior Author (where appropriate)

   Laura McCoy

   Date

   13/03/2024

1. **For a research manuscript that has already been published** (if not yet published, please skip to section 2)

a) **What is the title of the manuscript?**

Characterization of humoral and SARS-CoV-2 specific T cell responses in people living with HIV

b) **Please include a link to or doi for the work**

https://doi.org/10.1016/j.isci.2022.105862

c) **Where was the work published?**

iScience

d) **Who published the work?** (e.g. OUP)

Cell Press

e) **When was the work published?**

20 January 2023

f) **List the manuscript's authors in the order they appear on the publication**

Emma Touizer, Aljawharah Alrubayyi, Rosemarie Ford, Noshin Hussain, Pehuén Pereyra Gerber, Hiu-Long Shum, Chloe Rees-Spear, Luke Muir, Ester Gea-Mallorquí, Jakub Kopycinski, Dylan Jankovic, Anna Jeffery-Smith, Christopher L. Pinder, Thomas A. Fox, Ian Williams, Claire Mullender, Irfaan Maan, Laura Waters, Margaret Johnson, Sara Madge Michael Youle, Tristan J. Barber, Fiona Burns, Sabine Kinloch, Sarah Rowland-Jones, Richard Gilson, Nicholas J. Matheson, Emma Morris, Dimitra Peppa, Laura E. McCoy

g) **Was the work peer reviewed?**

Yes

h) **Have you retained the copyright?**

Yes

i) **Was an earlier form of the manuscript uploaded to a preprint server?** (e.g. medRxiv). If 'Yes', please give a link or doi)

Yes (https://www.biorxiv.org/content/10.1101/2022.11.11.516111v1)

If 'No', please seek permission from the relevant publisher and check the box next to the below statement:

☒

*I acknowledge permission of the publisher named under **1d** to include in this thesis portions of the publication named as included in **1c**.*

2. **For a research manuscript prepared for publication but that has not yet been published** (if already published, please skip to section 3)

3. **For multi-authored work, please give a statement of contribution covering all authors** (if single-author, please skip to section 4)

   I led the experimental work and analysis which relates to Figure 1,2 and 3 of this publication (all pseudovirus neutralisation antibody data, binding antibody data and MBC phenotyping) and corresponding supplementary figures. Samples were processed by myself with help of Aljawharah Alrubayyi, Rosemarie Ford, Noshin Hussain, Chloe Rees-Spear, Luke Muir and Dylan Jankovic. Rosemarie Ford, Hiu-Long Shum and Dylan Jankovic assisted with pseudovirus related experiments. Pehuén Pereyra Gerber carried out all the live neutralisation work which is described in this thesis. All the T-cell related data was experimental led by my co-first author Aljawharah Alrubayyi. The original draft of the manuscript was written by Aljawharah Alrubayyi, Laura McCoy, Dimitra Peppa and myself. Only the neutralisation, binding antibody and MBC phenotyping data are directly used in this thesis, the rest of the data in this publication is discussed where relevant in the discussion sections of this thesis and referenced accordingly.

4. **In which chapter(s) of your thesis can this material be found?**

   Chapter 1-7.

5. **e-Signatures confirming that the information above is accurate** (this form should be co-signed by the supervisor/ senior author unless this is not appropriate, e.g. if the paper was a single-author work)

   Candidate

   Emma Touizer

   Date:

   12/03/2024

   Supervisor/ Senior Author (where appropriate)

   Laura McCoy

   Date

   13/03/2024

Statement of contributions

Luke Muir optimised the semi-quantitative assay used in Chapter 3 and 4.

Hiu-Long ‘Ethan’ Shum assisted experimentally with the IgG purification and neutralisation data presented in Chapter 4.

Rosemarie Ford, Dylan Jankovic and Chloe Rees-Spear assisted experimentally with the neutralisation data presented in Chapter 4.

Pehuén Pereyra Gerber (Matheson Lab, University of Cambridge) carried out all the experimental work for the live neutralisation data used in Chapter 4 (Figure 4.5).

Anna Jeffery-Smith optimised the memory B cell phenotyping flow cytometry assay used in Chapter 5.

Chloe Rees-Spear carried out all the transfection for protein purification whilst Sarah Griffith carried out all the size exclusion chromatography for the production of biotinylated spike and RBD protein used in Chapter 5 and 6.

Janani Sivakumaran Nguyen and Laura McCoy helped setting-up the sorter for spike-specific sorting in Chapter 6.

Rosemarie Ford and Peter Thomas helped generating the bulk BCR libraries used in Chapter 6.

UCL Genomics sequenced the prepared NGS libraries used in Chapter 6.

Table of contents

Declaration **2**

Abstract **3**

Impact statement **4**

Acknowledgements **5**

UCL Research Paper Declaration Form **7**

List of figures **20**

List of tables **23**

Abbreviations **24**

Introduction **27**

1.1. B cells and antibodies **27**

1.1.1. B cell origins and early development *27*

1.1.2. B cell activation and germinal centre reaction *30*

1.1.3. Antibody development, structure and function. *34*

1.1.4. Memory B cell response phenotype, function and potential extrafollicular origin. *39*

1.1.5. The 'normal' BCR repertoire. *43*

1.2. SARS-CoV-2 ..... **44**

1.2.1. A brief history of SARS-CoV-2 and other coronaviruses. *44*

1.2.2. SARS-CoV-2 virus lifecycle. *47*

1.2.3. SARS-CoV-2 variants of concern *50*

1.2.4. Vaccines. *54*

1.2.5. Antibody responses to SARS-CoV-2 infection and vaccination *58*

1.2.6. Heterogeneity and the impact of variants on the antibody responses to SARS-CoV-2. ..... *60*

1.2.7. Convergent/public antibody responses in SARS-CoV-2. ..... *61*

1.2.8. B cell responses to SARS-CoV-2. ..... *62*

1.2.9. Other cell-specific responses to SARS-CoV-2. ..... *64*

1.3. Human Immunodeficiency Virus-1 ..... **66**

1.3.1. HIV-1 emergence and lifecycle. *66*

1.3.2. T cells, immune reconstitution and ART treatment. 69
1.3.3. HIV-specific antibody responses in PLWH. 73
1.3.4. The BCR repertoire in PLWH. 74
1.3.5. B cell defects in PLWH. 75
1.3.6. Responses to vaccines in PLWH. 79
1.3.7. Impact of SARS-CoV-2 infection and vaccination in PLWH. 80

1.4. Aim & Hypothesis 83

2. Methods 84

2.1. Study cohort sampling & ethics. 84
2.1.1. Convalescent cohort. 84
2.1.2. Vaccination cohort. 85

2.2. Blood processing 86

2.3. Enzyme-linked immunosorbent assays (ELISA). 87
2.3.1. S1 and N semiquantitative ELISAs 87
2.3.2. Total IgG ELISAs 87

2.4. IgG purification 88

2.5. Cell Culture 89

2.6. Pseudovirus neutralisation 89
2.6.1. Pseudovirus plasmid transformation and preparation. 89
2.6.2. Pseudovirus production and titration. 90
2.6.3. Pseudovirus neutralisation assays. 91

2.7. Live neutralisation 92

2.8. Protein production for spike and RBD 92
2.8.1. Transfection 92
2.8.2. His GraviiTap purification of spike and RBD proteins. 93
2.8.3. Size exclusion chromatography. 93

2.9. Memory B cell flow cytometry phenotyping 93

2.10. Spike-specific B cell sorting. 94
2.10.1. Staining PBMCs for spike-specific sorting. 94
2.10.2. Lysis plate preparation for sorted cells. 96

2.11. Single-cell PCR pipeline..... 96
2.11.1. cDNA generation and nested PCR steps for sorted single spike-specific B cells. 96
2.11.2. Agarose gel quality control (QC) check. 100
2.11.3. Sanger sequencing. 100
2.12. Bulk-cell PCR pipeline..... 100
2.12.1. Dry pellet preparation. 100
2.12.2. RNA extraction for dry pellets and previously thawed cells. 100
2.12.3. cDNA generation and nested PCR steps for 100 sorted spike-specific B cells and previously thawed cells. 101
2.12.4. cDNA generation and nested PCR steps for dry pellets. 103
2.12.5. Barcode indexing. 105
2.12.6. NGS MiSeq Sequencing. 108
2.13. Bioinformatic analysis. 108
2.13.1. Low throughput BCR library preparation and quality control. 108
2.13.2. High throughput BCR library preparation and quality control. 108
2.13.3. Clonal assignment, gene usage and somatic hypermutation. 109
2.13.4. Diversity measurements. 110
2.14. Statistics..... 111
3. Humoral responses to SARS-CoV-2 infection in PLWH 112
3.1. Summary 112
3.2. Cohort design. 114
3.3. Combined S1 and N antibody detection indicates previous SARS-CoV-2 infections. 116
3.4. Similar levels of SARS-CoV-2 specific binding antibodies in PLWH and HIV-negative controls at a convalescent timepoint..... 120
3.5. Optimisation of pseudovirus assay for the detection of SARS-CoV-2 neutralising antibodies. 122
3.6. Equivalent titres of WT neutralising antibodies in PLWH and HIV-negative controls after SARS-CoV-2 infection. 127

3.7. Convalescent donors, regardless of HIV status, have lower neutralising activity to the SARS-CoV-2 B.1.1.7 variant and to SARS-CoV-1. 130

3.8. No association between SARS-CoV-2 specific antibody titres and CD4 count or CD4:CD8 ratio. 133

3.9. Discussion..... 135

4. Humoral responses to SARS-CoV-2 vaccination in PLWH..... 143

4.1. Summary 143

4.2. Failure to seroconvert following 2 vaccine doses of COVID-19 vaccination in a participant with advanced HIV..... 144

4.3. Vaccination cohort design..... 148

4.4. Lower levels of binding S1 antibodies in SARS-CoV-2 naïve PLWH compared to HIV-negative control. 152

4.5. Lower levels of WT neutralisation in PLWH across all timepoints, regardless of previous COVID-19 infection..... 156

4.6. Limited breadth of the neutralising response to the Omicron BA.1 variant in PLWH. 161

4.7. Production of a neutralising response is delayed in PLWH..... 165

4.8. Binding and neutralising responses are predictive of one another. .. 169

4.9. PLWH require more binding antibodies to produce neutralisation titres than HIV-negative controls. 172

4.10. Differences in vaccine platforms do not explain the serological defect seen in PLWH. 174

4.11. No clear association between CD4 count, CD4:CD8 ratio and serological output following vaccination. 176

4.12. Discussion..... 180

5. Memory B cell responses to SARS-CoV-2 vaccination in PLWH 192

5.1. Summary 192

5.2. Cohort design and flow gating strategy 193

5.3. Ongoing disruption in *de novo* memory B cell response after the 1st vaccine dose. 196

5.3.1. Prior infection gives an advantage in the generation of a robust spike-specific MBC response. 196

5.3.2. Perturbed global memory B cell phenotypes are associated with a delay in the development of neutralisation. 201

5.3.3. No difference in isotype usage after the 1st vaccine dose. 205

5.4. B cell disruption after the 3rd vaccine dose underpins a limited recall response in PLWH. 208

5.4.1. Similar levels of spike-specific MBCs between PLWH and HIV-negative controls regardless of prior infection. 208

5.4.2. The inherent global memory B cell dysfunction is still present after the 3rd vaccine dose in PLWH but is lessened in the spike-specific memory B cells. 213

5.4.3. Higher expression of IgM in spike-specific MBCs of PLWH reflects a maturity defect. 216

5.5. No association between MBC dysfunction and CD4 count or CD4:CD8 ratio. 218

5.6. Discussion 221

6. Modulation of the B cell receptor repertoire post SARS-CoV-2 vaccination in PLWH 230

6.1. Summary 230

6.2. Sub-study design and sorting strategy for BCR sequencing 231

6.3. NGS pipeline output. 237

6.4. Limited clonal overlap between early bulk BCR repertoires and spike-specific BCR was observed at the final timepoint. 240

6.5. Higher frequency of public clonal lineages in HIV-negative controls than in PLWH. 242

6.6. PLWH participants included for BCR sequencing have normalised MBC phenotype. 246

6.7. V gene usage differs between spike-specific clones and non-specific clones. 248

6.8. Aberrant somatic hypermutation in PLWH. 251

6.9. Lower levels of repertoire diversity in the spike-specific repertoire of SARS-CoV-2 naïve PLWH. 253

6.10. Higher diversity is associated with better serological output. 257

6.11. Discussion. 259

7. Discussion 266

7.1. Results summary. 266

7.2. Overall limitations of this thesis. 268

7.3. Perspectives. 269

7.3.1. What is needed for a working B cell response? 269

7.3.2. What does an effective clonal response look like? 270

7.3.3. What does this study tell us about the kind of vaccines PLWH and other immunocompromised populations need? 272

References 275

List of figures

Chapter 1: Introduction

Figure 1.1.1: *B cell development……29*

Figure 1.1.2: *B cell maturation in secondary lymphoid organs.……33*

Figure 1.1.3: *Generation of diversity in the antibody repertoire.……37*

Figure 1.1.4: *Putative directionality between MBCs phenotypes…….....42*

Figure 1.2.1: *Similarity between SARS-CoV-2 and other human coronaviruses……46*

Figure 1.2.2: *SARS-CoV-2 genome, virus and spike protein structure……49*

Figure 1.2.3: *SARS-CoV-2 variants of concern……52*

Figure 1.2.4: *Impact of vaccination in the COVID-19 pandemic in the UK……..57*

Figure 1.3.1: *HIV replication cycle……..68*

Figure 1.3.2: *Model of immune reconstitution on ART……72*

Figure 1.3.4: *Summary of B cell dysfunction in chronic HIV……..78*

Chapter 3: Humoral responses to SARS-CoV-2 infection in PLWH

Figure 3.3*: A semi-quantitative ELISA against N and S1 IgG-specific antibodies can delineate between SARS-CoV-2 infection and previous cross-reactive hCoV responses……..119*

Figure 3.4*: PLWH and HIV-negative controls have similar titres of S1 and N IgG-specific antibody titres following SARS-CoV-2 infection……121*

Figure 3.5*: Optimisation of a pseudovirus assay for the detection of SARS-CoV-2 antibodies in PLWH…….....125*

Figure 3.6*: PLWH and HIV-negative controls have similar titres of neutralizing antibodies against SARS-CoV-2 WT following SARS-CoV-2 infection……...129*

Figure 3.7*: PLWH and HIV-negative controls have similar titres of neutralising antibodies against SARS-CoV-2 WT following SARS-CoV-2 infection……...132*

Figure 3.8*: No association between SARS-CoV-2 specific antibody titres and CD4 count or CD4:CD8 ratio…..……134*

Chapter 4: Humoral responses to SARS-CoV-2 vaccination in PLWH

Figure 4.2*: Failure to seroconvert following 2 vaccine doses of COVID-19 vaccination in a participant with advanced HIV……147*

Figure 4.4*: Lower levels of binding S1 antibodies in SARS-CoV-2 naïve PLWH compared to HIV-negative control……155*

***Figure 4.5**: Lower levels of neutralising antibodies in PLWH against SARS-CoV-2 WT across all timepoints, regardless of previous COVID-19 infection……159*
***Figure 4.6**: Lower levels of neutralising antibodies in PLWH against SARS-CoV-2 Omicron BA.1 across all timepoints, regardless of previous COVID-19 infection…163*
***Figure 4.7**: Production of a neutralising response is delayed in PLWH……167*
***Figure 4.8**: Binding and neutralising responses are predictive of one another……170*
***Figure 4.9:** PLWH require more binding antibodies to produce neutralisation titres than HIV-negative controls……173*
***Figure 4.10**: Differences in vaccine platform do not explain the serological defect seen in PLWH……175*
***Figure 4.11**: No clear association between CD4 count, CD4:CD8 ratio and serological output following vaccination……...178*

Chapter 5: Memory B cell responses to SARS-CoV-2 vaccination in PLWH

***Figure 5.2:** B cell phenotyping flow cytometry gating strategy……194*
***Figure 5.3.1:** Prior infection gives an advantage in the generation of a robust spike-specific MBC response……....199*
***Figure 5.3.2**: Perturbed global memory B cell phenotypes are associated with a delay in the development of neutralisation……203*
***Figure 5.3.3:** No difference in isotype usage after the 1st vaccine dose……207*
***Figure 5.4.1:** Similar levels of spike-specific MBCs between PLWH and HIV-negative controls regardless of prior infection……..211*
***Figure 5.4.2:** The inherent global memory B cell dysfunction is still present after the 3rd vaccine dose in PLWH but is lessened in the spike-specific memory B cells….215*
***Figure 5.4.3:** Higher expression of IgM in spike-specific MBCs of PLWH reflects a maturity defect……..217*
***Figure 5.5:** No association between MBC dysfunction and CD4 count or CD4:CD8 ratio……....219*

Chapter 6: Modulation of the B cell receptor repertoire post SARS-CoV-2 vaccination in PLWH

***Figure 6.2.1**: Participants included for BCR sequencing demonstrate representative binding and neutralisation abilities……233*
***Figure 6.2.2:** Schematic of BCR sequencing strategy……...235*

Figure 6.2.3: *Gating strategy for spike-specific B cell sorting……...236*
Figure 6.3: *Retrieval of BCR sequences and distinct clonal lineages across all timepoints and groups……239*
Figure 6.4: *Limited clonal overlap between bulk and spike-specific timepoints……241*
Figure 6.5: *Trend towards higher frequency of public clonotypes in HIV-negative controls than in PLWH……244*
Figure 6.6: *PLWH participants included for BCR sequencing have normalised MBC phenotype……247*
Figure 6.7.1: *V gene usage differs between spike-specific BCRs and non-specific BCRs……..249*
Figure 6.7.2: *PLWH and HIV-negative controls have the same V gene usage in their spike-specific BCR repertoire……250*
Figure 6.8: *Aberrant somatic hypermutation in PLWH……..252*
Figure 6.9: *Lower levels of diversity in SARS-CoV-2 naïve PLWH……255*
Figure 6.10: *Higher diversity is associated with better serological output……258*
Figure 6.11: *Model of the impact of chronic HIV infection on the MBC and BCR repertoire……...263*

List of tables

Chapter 2: Methods

Table 2.9: *Staining panel for MBC phenotyping……94*

Table 2.10.1: *Staining panel for spike-specific MBC sorting……..95*

Table 2.11.1: *PCR conditions for amplification of the BCR's heavy chain VDJ region from single sorted cells……..98*

Table 2.11.2: *Primers for the single-cell sequencing pipeline.……99*

Table 2.12.3: *PCR conditions for amplification of the BCR's heavy chain VDJ region from 100 sorted spike-specific B cells and previously thawed cells……103*

Table 2.12.4: *PCR conditions for amplification of the BCR's heavy chain VDJ region from dry pellets……104*

Table 2.12.5.1: *PCR conditions for the final indexing PCR……..105*

Table 2.12.5.2: *Primers for the bulk sequencing pipeline……107*

Chapter 3: Humoral responses to SARS-CoV-2 infection in PLWH

Table 3.2*: Characteristics and demographic information for the convalescent cohort……115*

Chapter 4: Humoral responses to SARS-CoV-2 vaccination in PLWH

Table 4.3.1*: Demographic information for the vaccine cohort……150*

Table 4.3.2*: Breakdown of participants' vaccination history at each timepoint for the vaccine cohort……...151*

Abbreviations

ACE-2	Angiotensin-converting enzyme 2 receptor
ADCC	Antibody-dependent cellular cytotoxicity
ADCP	Antibody-dependent cellular phagocytosis
AID	Activation-induced cytidine deaminase
AIDS	Acquired immunodeficiency syndrome
AM	Activated memory B cell
AP	Alkaline phosphatase
ART	Antiretroviral treatment
ASC	Antibody-secreting cells
AtyM	Atypical memory B cell
BAFF	B-cell activating factor
BCR	B cell receptor
bnAb	Broadly neutralising antibody
bp	Base pair
CDR	Complementarity-determining region
CLP	Common lymphoid progenitors
COVID-19	Coronavirus infectious disease 2019
CSR	Class switching recombination
DMEM	Dulbecco's modified eagle's medium
DMSO	Dimethylsulfoxide
DN	Double negative memory B cell
dNTP	Deoxyribonucleotide triphosphate
DPSO	Days since symptom onset
DSB	Double stranded breaks
DTT	Dithiothreitol
DZ	Dark zone
EDTA	Ethylene diamine tetra acetic acid
ELISA	Enzyme-linked immunosorbent assays
Fab	Fragment antigen binding
FBS	Foetal bovine serum
Fc	Fragment crystallisable
FcR	Fc receptor
FCS	Furin cleavage site
FDC	Follicular dendritic cells
FFluc	SARS-CoV-2 Papain-like protease activatable circularly permuted firefly luciferase
FWR	Framework region
GC	Germinal centre
HAART	Highly active anti-retroviral therapy

hCoV	Human coronavirus
HIV	Human Immunodeficiency Virus
HSC	Haematopoietic stem cells
ID_{50}	Dilution at which 50% of the virus is inhibited
Ig	Immunoglobulin
IGH	Immunoglobulin heavy chain
IGHD	Immunoglobulin heavy chain diversity region
IGHJ	Immunoglobulin heavy chain joining region
IGHV	Immunoglobulin heavy chain variable region
IGK	Immunoglobulin light chain (kappa)
IGL	Immunoglobulin light chain (lambda)
IM	Intermediate memory B cell
INSTI	Integrase nuclear strand transfer inhibitors
LB	Luria-Bertani
LPS	Lipopolysaccharide
LZ	Light zone
MBC	Memory B cell
MERS-CoV	Middle-East respiratory syndrome coronavirus
MHC	Major histocompatibility complex
MOI	Multiplicity of infection
mRNA	Messenger RNA
MWU	Mann Whitney's U test
N	SARS-CoV-2 Nucleocapsid/nucleoprotein protein
NGS	Next-generation sequencing
NHEJ	Non-homologous end-joining
NK	Natural killer cells
NNRTI	Non-nucleoside reverse transcriptase inhibitor
NRTI	Nucleoside reverse transcriptase inhibitor
NTD	N-terminal domain
OD	Optical density
PBMC	Peripheral blood mononuclear cells
PBS	Phosphate buffered saline
PCR	Polymerase chain reaction
PI	Protease inhibitors
PLWH	People living with HIV
QC	Quality control
RAG1/2	Recombination-activating genes 1/2
RBD	Receptor binding domain
RLU	Relative light unit
RM	Resting memory B cell
RPM	Rotation per minute

RPMI	Roswell Park Memorial Institute media
RSS	Recombination signal sequence
RT	Room temperature
RT-PCR	Real-time polymerase chain reaction
RTC	Replication transcription complex
S1	SARS-CoV-2 Spike subdomain 1
S2	SARS-CoV-2 Spike subdomain 2
SARS-CoV-1	Severe acute respiratory syndrome coronavirus 1
SARS-CoV-2	Severe acute respiratory syndrome coronavirus 2
SHM	Somatic hypermutation
TCR	T cell receptor
TdT	Terminal deoxynucleotidyl transferase
Tfh	T follicular helper cells
TLM	Tissue-like memory B cell
TLR	Toll-like receptor
TMPRSS2	Transmembrane serine protease 2
TNF	Tumour necrosis factor
VDJ	Variable Diversity and Joining gene s rearrangement
VOC	Variant of concern
WHO	World Health Organisation
WT	Wildtype

1. Introduction

1.1. B cells and antibodies

1.1.1. B cell origins and early development

In the mid-20th century, concurrent observations of a lack of immunoglobulin (Ig) in humans despite the presence of a thymus, and of loss of antibody production in chickens which had been bursectomized (Cooper M et al., 1965; Glick et al., 1956). This led to the adoption of the name "B" cells, a reference to the 'bursa of Fabricius' found in birds, as the in-human bone-marrow-derived source of antibodies (Roitt et al., 1969). Early development of B cells occurs in the bone marrow (or foetal liver) and is structured around the sequential formation of a complete B cell receptor (BCR) and the maintenance of tolerance (***Figure 1.1.1***). In the bone marrow, haematopoietic stem cells (HSC) are multipotent cells which give rise to either myeloid or lymphoid cells like B cells. Common lymphoid progenitors (CLP), which arise from HSCs, represent the first cells which are committed to the lymphoid lineage (Kondo et al., 1997). The earliest fate commitment to become a B cell, rather than a T or natural killer (NK) cell, occurs at the pro-B cell stage (Allman et al., 1999). Pro-B cells already express un-rearranged germline Ig genes, and only from the pro-B cell stage onwards can they express recombination-activating genes 1/2 (RAG1/2) and terminal deoxynucleotidyl transferase (TdT), both of which are essential for variable-diversity-joining gene (VDJ) recombination (Hardy et al., 1991; Oettinger et al., 1990). The exact process of VDJ recombination will be further explained in **section 1.2.3**. The pro-B cell stage is divided between early, when D to J rearrangement happens on the heavy chain at both alleles; and late, when V to DJ rearrangement happens (Hardy et al., 1991). This initial rearranged heavy chain (pre-BCR) is paired alongside a constant μ chain (IgM), Igα, Igβ and a surrogate λ_5 light chain (Karasuyama et al., 1993) to test for improper rearrangement. Only pro-B cells with a functional pre-BCR will be selected via pre-BCR signalling to proliferate (Hess et al., 2001), and the others will be largely eliminated via apoptosis (Lu and Osmond, 1997).

At the pre-B cell stage, the V and J genes of the light chain are rearranged first at the κ locus, then at the λ locus (Hardy et al., 1991; Reth et al., 1987), with only one of these rearranged light chains expressed alongside the pre-BCR. The pre-BCR/μ

chain/Igα/Igβ complex will be tested with the newly rearranged light chain for self-reactivity. Any B cells that recognise self-antigens will be deleted by either apoptosis (Lu and Osmond, 1997; Nemazee and Buerki, 1989), or by anergy (Goodnow et al., 1988) to maintain central tolerance. Additionally, BCRs can be re-edited to select for non-self-reactivity (Gay et al., 1993; Tiegs et al., 1993).

Effectively, this process yields an immature IgM B cell with a functional BCR composed of a rearranged heavy and light chain which can recognize a non-self-antigen. These cells have also lost the ability to edit their BCR (Melamed et al., 1998). During this entire process, 90% of the cells which have committed to the B cell lineage will be lost selection process (Rolink et al., 1998).

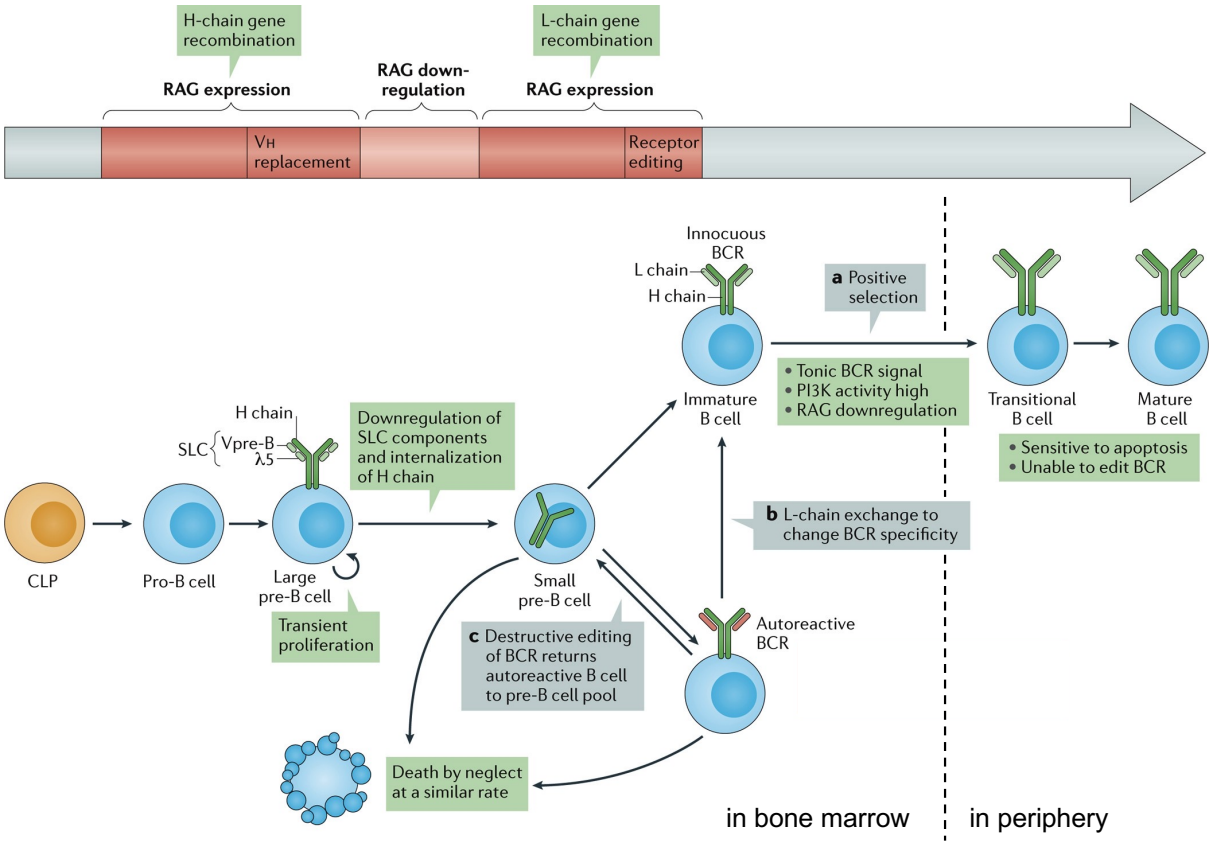

Figure 1.1.1: *B cell development. In the bone marrow, a CLP will commit to the B cell lineage and become a pro-B cell, sequential rearrangement of the heavy and light chain happens at the pre-B cell stage. Testing of the rearranged BCR for binding to self-antigen will lead to either re-editing of the BCR to re-test for self-reactivity or B cell death by apoptosis or anergy. B cells with non-self-reactive BCRs will be positively selected to progress their maturation in the periphery. Adapted from* (Nemazee, 2017).

1.1.2. B cell activation and germinal centre reaction

Immature B cells with innocuous BCRs can now move from the bone marrow into the periphery in secondary lymphoid organs such as the spleen, lymph nodes or the gut. New emigrants in the secondary lymphoid organs are immature B cells which are also known as transitional and both express IgD and IgM on their surface alongside CD10, CD24 and CD38 (Carsetti et al., 1995; Palanichamy et al., 2009). Transitional B cells can further be divided into three populations (T1, T2, T3), with T1 and T2 B cells prone to additional selection to remove any self-reactive BCRs i.e., to maintain peripheral tolerance (Palanichamy et al., 2009; Wardemann et al., 2003), whilst the exact role of T3 is poorly understood. Some transitional B cells may play a regulatory role (Evans et al., 2007). Additionally, autoreactive B cells will be anergic and less able to signal through their BCR through the B-cell activating factor (BAFF) (Lesley et al., 2004). Progressive loss of CD10, CD24 and CD38 characterises the transition from transitional to naïve B cells.

Antigen recognition by the BCR is the first necessary step for B cell activation and formation of a germinal centre (GC). Naïve B cells can encounter antigens in a T-cell-dependent or independent fashion. T cell-independent antigens are less well understood but can directly activate B cells due to their complex structures which can cross-link BCRs and thus trigger BCR signalling (type II antigens such as polysaccharides) or by activating toll-like receptors (TLRs) (type I antigens such as LPS or CpG) (Allman et al., 2019; Liu et al., 2022b). Alternatively, antigens are presented in a T cell-dependent manner on subcapsular sinus macrophages or follicular dendritic cells (FDCs) (Carrasco and Batista, 2007; Suzuki et al., 2009) which will lead to internalisation of the BCR-antigen antigen complex, processing, and presentation of the antigen on B cells' major histocompatibility complex II (MHC). This antigen-dependent activation of B cells will make them migrate towards the T cell zone - B cell zone border, which is mediated by the expression of CCR7, CXCR5 and EB12 (Cyster et al., 2000; Förster et al., 1999; Gatto et al., 2011). In the meantime, naïve CD4 T cells also need to be activated to differentiate into T follicular helper cells (Tfh). T cell activation and differentiation into Tfh is mediated by FDCs which can present processed antigens to T cells on their MHC, this will upregulate the transcription factor Bcl6 which is essential for the maintenance of a GC reaction (Choi et al., 2011). Finally, at the T-B cell zone border, activated B cells and Tfh cells can interact. Here, via its

MHC the B cell presents processed cognate antigen to the Tfh, and in return, the B cell receives Tfh help in the form of a costimulatory signal by CD40L binding to CD40 on the surface of the B cell (Basso et al., 2004). This interaction leads to the production of cytokines like IL-21 which will lead to either the formation of a GC or an extrafollicular response (Lee et al., 2011), the latter of which will be discussed at greater length in **section 1.1.4**. Overall, Tfh cells help lead to the rapid proliferation of GC B cells. The entry of B cells into GC is not fully understood but may depend on their affinity (Schwickert et al., 2011). Recent evidence has highlighted that the majority of CSR (further discussed in **section 1.1.3**) happens following Tfh-B cell interactions but before entry in the GC and SHM (Roco et al., 2019).

The GC can be divided into two zones the dark zone (DZ) and light zone (LZ) along a chemokine gradient of CXCR5 and CXCR4, upregulation and downregulation of these cytokines dictate the movement of B cells between the LZ and DZ (Allen et al., 2004). B cells first migrate towards the DZ where they are called centroblasts. Within the DZ, there is further proliferation of centroblasts named clonal expansion and somatic hypermutation (SHM). SHM is mediated by activation-induced cytidine deaminase (AID), which introduces mutations in the VDJ (Muramatsu et al., 1999). AID converts cytosine to uracil and has a preference for introducing these mutations in the complementarity-determining regions (CDR) of the VDJ (reviewed in (Schramm and Douek, 2018)) which as discussed in **section 1.1.3**, are essential for binding. Overall SHM provides additional diversity to the antibody repertoire and adaption to pathogens encountered. This leads to the creation of a large pool of clonal variants which can then enter the LZ where the B cells, now known as centrocytes, will test their newly mutated BCRs. Within the LZ, there is a large network of FDCs which can present antigens and B cells with higher-affinity BCRs will more readily capture the antigen presented by FDCs. These B cells will then be able to present antigen to Tfh cells in the LZ and as such receive more help and co-stimulatory-survival signals. On the other hand, B cells with low-affinity BCRs which did not receive sufficient Tfh help will die via apoptosis (Gitlin et al., 2015; Le et al., 2008; Liu et al., 2015; Shih et al., 2002). This process of selection of high-affinity B cells is termed affinity maturation. High-affinity B cells which receive Tfh cell help can re-enter the DZ for further rounds of clonal expansion and SHM to improve their affinity (Victora et al., 2010), alternatively they can exit the GC to become memory B cells (MBC) or antibody-secreting B cells

(ASCs). ASCs can be divided into long-lived plasma cells which reside in the bone marrow whilst short-lived plasma cells also called plasmablasts will circulate throughout the periphery like MBCs. Unswitched MBCs are first to exit the GC, then switched MBCs and finally long-lived plasma cells (Weisel et al., 2016).

Altogether the process of B cell development, activation and maturation in the germinal centre leads to the formation of highly diverse long-lived memory and plasma cells which can readily respond to be recalled upon re-exposure to their antigen. Of note, plasma cells cannot re-enter the GC, but MBCs have been shown to be able to re-enter GCs to improve their affinity maturation (Mcheyzer-Williams et al., 2015). However, recent data has shown that most B cells which enter the GC are naïve (Mesin et al., 2020).

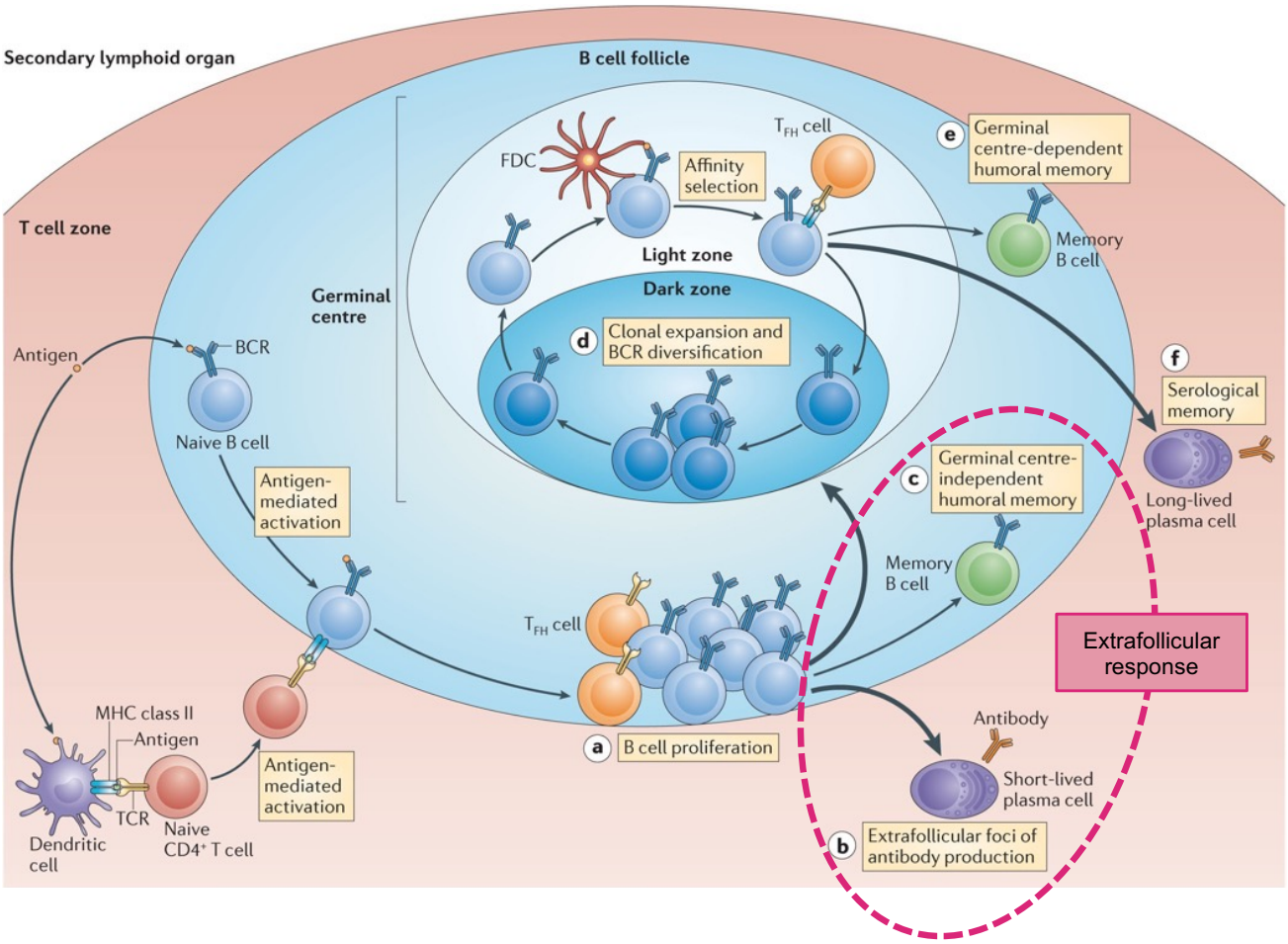

Figure 1.1.2: *B cell maturation in secondary lymphoid organs. Immature/naïve B cells can be activated by antigens in a T cell-dependent or independent manner. Interaction with a cognate Tfh cell allows B cells to proliferate and move away from the B-T cell border to form GCs. In the GC, activated B cells will further proliferate in the dark zone via a process of clonal expansion which generates diversity by SHM, they can then move into the light zone where FDCs will present them with antigens to affinity-select the best BCRs. B cells with high affinity can receive T cell help from Tfh cells and can either exit the GC to become memory B cells or long-lived plasma cells or re-enter the DZ to go through sequential rounds of SHM and affinity maturation. Alternatively, activated B cells can be educated outside of the GC via the extrafollicular pathway and generate MBCs and short-lived plasma cells. Adapted from* (Kurosaki et al., 2015).

1.1.3. Antibody development, structure and function.

Each antibody molecule is made up of a pair of identical heavy chains (IGH) and a pair of identical light chains (IGL for lambda or IGK for kappa). Each heavy chain is encoded by one variable gene (V), one diversity (D), one joining (J) gene and one constant (C) gene. Similarly, each light chain is encoded by one V gene, one J gene and a small portion of the C gene. The antibody can be divided into two parts. First, the variable region or Fab (fragment antigen binding), which contains the heavy chain VDJ plus the first CH domain of the C heavy chain and the light chain's VJ plus the first CH domain of the C light chain. Secondly, the constant region or Fc (fragment crystallisable) which is made of the rest of the C chain' CH domains. Between the Fc and Fab is found the hinge region which can affect antibody flexibility, as seen with the longer hinge of IgG3 which affects Fab and Fc function (Foss et al., 2022). The main locus for IGH genes is found on chromosome 14q32.33. So far, up to 46 functional IGHVH, 23 IGHD and 6 IGHJ genes are documented to exist within this locus in humans. Similarly, up to 38 functional IGKV, 5 IGKV and 33 IGLV, IGL5 have been documented to exist in the lambda light chain locus on chromosome 22q11.22 and kappa light chain locus on chromosome 2p11.2 respectively in humans. Alongside these known functional genes, many more exist that are not functional. When accounting for all the possible rearrangement combinations on the heavy and light chain and SHM, as many as ~$2x10^{12}$ antibody sequences could be generated (Lefranc and Lefranc, 2023).

VDJ recombination (***Figure 1.1.3A***) is a sequential process which occurs during B cell development in the bone marrow/foetal liver. Each V, D or J gene region within the heavy or V and J gene region within the light chain loci are flanked by recombination signal sequences (RSS) which are used by RAG1/2 (Oettinger et al., 1990; Schatz et al., 1989; Tonegawa, 1983) to mediate VDJ recombination. Two genes flanked by RSS sequences will be brought in proximity by the activity of an array of transcription factors like Pax5, IRF4 or IKAROS (reviewed by (Schatz and Ji, 2011)). These RSS sequences can then be recognized and bound by RAG1/2, which will induce double-stranded breaks (DSB). These DSBs are exclusively repaired by non-homologous end-joining (NHEJ) which will introduce additional base pairs at each joining event and therefore additional diversity (Cui and Meek, 2007). An added layer of diversity comes from TdT which can add additional base pairs (Landau et al., 1987). The order of

recombination (D-J then V-DJ or V-J for light chain) is maintained by the alternating length of a spacer region within the RSS sequences to avoid improper recombination (Van Gent et al., 1996). As discussed in **section 1.1.1**, the heavy chain is rearranged before the light chain. Additionally, the kappa chain will be rearranged before the lambda light chain (Mehr et al., 1999). To avoid the expression of two different BCRs with potentially two different specificities on each allele, one allele is excluded via the process of allelic exclusion (Ten Boekel et al., 1998; Löffert et al., 1996; Sonoda et al., 1997). Further rearrangement on the light and heavy chain can occur to avoid a self-reactive rearrangement (Gay et al., 1993; Tiegs et al., 1993). Antigen binding is mediated by the Fab domains, more specifically by the variable regions comprising the VDJ portion of the heavy chain and VJ portion where incredible diversity has been generated through VDJ recombination, SHM and CSR. The heavy and light chain can be divided into framework regions (FWR) 1 to 4 and complementary determining regions (CDR) 1 to 3. The CDRs form loops at the N-terminus of the antibody (***Figure 1.1.3C***)), and together they form the bulk of the paratope, the portion of the antibody which can directly bind to the antigen. CDR1 and CDR2 are directly encoded by either the IGHV or IGL/KV. The CDRH3s (and CDRL/K3s) have been the most implicated in determining the binding (Chothia et al., 1989; Kabat and Wu, 1991) as they are the source of greater diversity since they comprise the end of the V gene, the entire D gene and the start of the J gene, i.e., most of their sequence has been changed from germline by VDJ recombination and SHM. Following the same logic, two recombination events must happen to produce a complete CDRH3 (D-J than V-DJ) whilst only one recombination produces a CDRL3 (V-J), as joining is imprecise it is therefore understood that there is a greater potential for diversity in CDRH3s than in CDRL3s.

The constant region dictates effector function, with 5 isotypes available (IgM, IgD, IgG, IgA and IgE). The isotype usage of a B cell depends on the first available C chain gene found on the heavy chain locus e.g., if the first available gene is Cμ, IgM is used and so on. To change isotype, B cells go through CSR (***Figure 1.1.3B***) where AID can bind to any switch regions which are found upstream of each C gene (except Cδ) and deaminate them (Muramatsu et al., 2000). This will induce the formation of DSBs and the excision of C genes in between (Catalan et al., 2003). This process is irreversible,

i.e., if a B cell has class switched to IgG4, this B cell and its progeny cannot class switched to any excised C chain but only IgE and IgA2.

The first available isotype is IgM (Cμ), which is expressed on all immature B cells alongside IgD and as such IgMs are the first secreted antibodies after immune stimulation. IgM antibodies have a lower affinity for their antigen than the other isotypes, hence the benefit of class-switching (Mäkelä et al., 1970). When secreted they can form pentameric structures which increase their avidity, compensating for lower affinity and allowing them to form immune complexes and activate the complement system (Collins et al., 2002). IgD is a splice variant of IgM and is only found on naïve B cells which are yet to class-switch, its function is poorly understood. The most abundant Ig in the blood is IgG, encoded by the Cγ genes. IgGs are further divided into 4 isotypes numbered based on abundance: IgG1, IgG2, IgG3 and IgG4. IgG1 and IgG3 usage is preferred against viral antigens, whilst IgG1, IgG2 and IgG4 are preferentially used against bacterial antigens (Ferrante et al., 1990). Due to its position in the locus, IgG3 is the first available IgG isotype for class-switching. It has been proposed that IgG4 may play an important role in inflammatory responses (reviewed in (Trampert et al., 2018)). IgAs are an integral part of mucosa and site-specific response and are the second most abundant Ig in the blood. Two sub-isotypes of IgA exist, IgA1 and IgA2. Of note, IgA can form dimers in those mucosal sites (reviewed in (Woof and Mestecky, 2005)). Therefore, IgAs in those mucosal/barrier tissue sites may play an important role for immediate protection (Azzi et al., 2022; Blutt and Conner, 2013; Havervall et al., 2022; Sheikh-Mohamed et al., 2022). Finally, IgEs are mostly involved in allergy responses (reviewed in (Galli and Tsai, 2012)). On top of binding and neutralising, antibodies can mediate other functions through their Fc region such as opsonisation or binding to different factors of the complement pathway for complement activation. Additionally, each isotype has a range of corresponding receptors (FcR) which can be inhibitory or activatory and are involved in diverse processes like antibody-dependent cellular cytotoxicity (ADCC) and antibody-dependent cellular phagocytosis (ADCP) which feed back into the rest of the adaptive immune system.

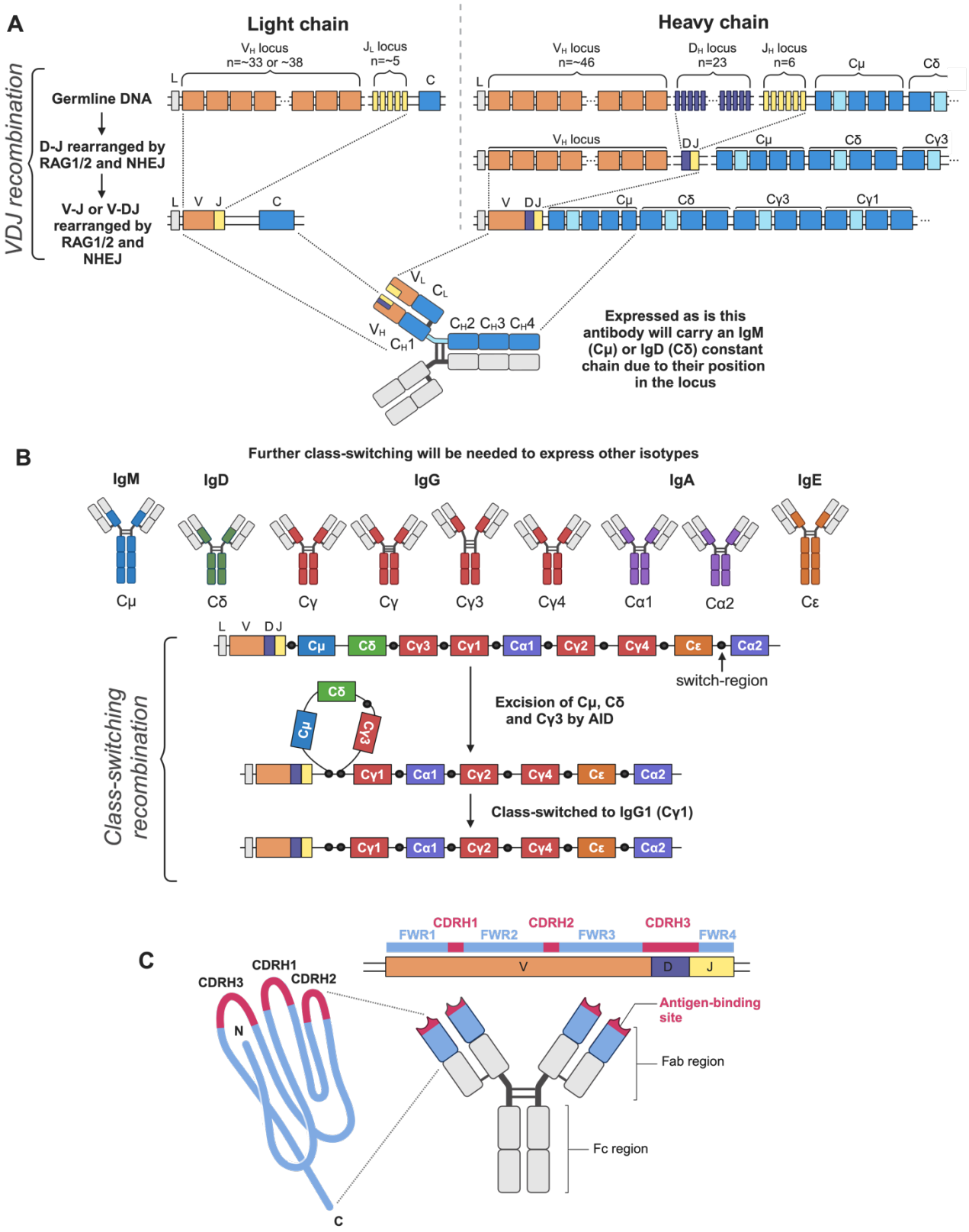
A
Light chain
Heavy chain
VDJ recombination
Germline DNA
D-J rearranged by RAG1/2 and NHEJ
V-J or V-DJ rearranged by RAG1/2 and NHEJ
Expressed as is this antibody will carry an IgM (Cμ) or IgD (Cδ) constant chain due to their position in the locus
B
Further class-switching will be needed to express other isotypes
IgM
IgD
IgG
IgA
IgE
switch-region
Excision of Cμ, Cδ and Cγ3 by AID
Class-switched to IgG1 (Cγ1)
Class-switching recombination
C
CDRH1
CDRH2
CDRH3
FWR1
FWR2
FWR3
FWR4
Antigen-binding site
Fab region
Fc region

Figure 1.1.3: *Generation of diversity in the antibody repertoire.* ***A.*** *Recombination of the light and heavy chain variable region (VJ or VDJ) by RAG1/2 activity. NHEJ of D-J and V-DJ or V-J segment introduces diversity by the random addition of nucleotides.* ***B.*** *Class-switching (mediated by AID) is essential to change isotype usage from IgM/D.* ***C.*** *Example VDJ sequence and corresponding CDR and FWR regions. Overall, the structure of the variable region comprising the heavy chain's VDJ and light VJ dictates antigen binding. Diagram created with biorender.com.*

1.1.4. Memory B cell response phenotype, function and potential extrafollicular origin.

B cells can be considered MBCs when they have encountered antigen. Additionally, MBCs should be present in a steady state and therefore possess some form of longevity and be able to respond upon re-exposure (Weisel and Shlomchik, 2017). Additionally, memory B cells have been described by their expression of CD27, which is a tumour necrosis factor (TNF) receptor, (Klein et al., 1998; Tangye et al., 1998), and by the absence of IgD surface expression, although some MBCs do not express CD27 as discussed later. Both IgG+ and IgM+ B cells can be MBCs (Dogan et al., 2009; Pape et al., 2011).

The 'length' of the memory B cell responses can vary from one pathogen to the next. An example of the long-lasting character of memory B cells can be found in a study looking at individuals who were alive during the 1918 H1N1 influenza pandemic. 90 years on, these individuals' sera still showed neutralizing activity against the 1918 H1N1 virus, and critically strain-matched HA-specific antibodies could be isolated from B cells showing that circulating memory B cells can provide long-lived immunity (Yu et al., 2008). Similarly, MBCs and antibodies were shown to stay stable over the course of 26 years for a range of pathogens included in routine vaccination (Amanna et al., 2007).

Several classifications can be used to identify B cells overall (reviewed by (Sanz et al., 2019)). Throughout this thesis, CD27 and CD21 are used to discriminate between important sub-phenotypes of MBCs after excluding IgD+ B cells. CD21 is also known as complement receptor 2/C3d receptor and acts as a co-receptor for the BCR to increase BCR signalling (Cherukuri et al., 2001). Resting MBCs (CD27+ CD21+) are considered to be the classical memory B cell subtype associated with quiescent B cells which are poised to respond upon re-exposure. In a steady state, they comprise the bulk of the memory B cell compartment. Activated MBCs (CD27+ CD21-) represent a more transcriptionally active subtype which are reactivated upon re-exposure (Ellebedy et al., 2016) and may be primed to further differentiate into ASCs (Lau et al., 2017). Intermediate (or switched naïve) MBCs (CD27- CD21+) are generally less mutated than CD27+ MBCs (Wu et al., 2011), even if they comprise a large proportion of the recall MBC population (Zurbuchen et al., 2023). As such they may be a precursor population to resting/activated MBCs.

The exact role of the last MBC phenotype, CD21- CD27- atypical MBCs is less well understood. They are part of normal vaccination responses (Sutton et al., 2021; Zurbuchen et al., 2023) but are notoriously known to be increased in many chronic conditions. From a nomenclature point of view, atypical MBCs discussed in this thesis can be thought of as the equivalent to other well-characterised MBC subtypes seen in a plethora of acute and chronic infections, in auto-immunity, or in ageing. In the field of HIV, the name of 'tissue-like' memory B cells (TLMs) has been preferentially used to describe CD21- CD27- B cells (Moir et al., 2008a). This is based on the original description of a CD27- memory B cells expressing FcLR4 subtype preferentially found in the tonsils (the tissue in 'tissue-like') which had a high level of SHM akin to classical MBC expressing CD27 (Ehrhardt et al., 2005). Their role in HIV is discussed at greater length in **section 1.3.5**. Similarly, they have been identified to be increased in other chronic infections such as hepatitis B (Burton et al., 2018), hepatitis C (Doi et al., 2014; Oliviero et al., 2015) and in malaria where they are referred to as atypical MBCs (Portugal et al., 2015). The term DN2 B cell (for double negative 2) is often used in the wider auto-immunity literature based on their lack of expression of IgD and CD27 (referred to as DN B cells), coupled with lack of expression of CD21 (or CXCR5) and expression of CD11c (Jenks et al., 2018; Wei et al., 2007). With this classification, DN1 (CD21+ CD11c-) are the equivalent to this thesis' activated MBCs whilst DN3 (CD21- CD11c-) may represent another subtype of atypical MBCs. Finally, increased numbers of IgD- CD27- have also been observed in the elderly population (Colonna-Romano et al., 2009), where these MBCs are now known as 'age-associated B cells' or ABCs. Throughout this thesis, the name atypical MBCs is used to refer to B cells lacking CD21 and CD27 expression (where IgD+ or CD10+ cells have been excluded first).

Additional studies have identified the expression of CD11c (Jenks et al., 2018; Song et al., 2022; Winslow et al., 2017), Tbet (Knox et al., 2017; Song et al., 2022; Winslow et al., 2017; Yang et al., 2022), and FcLR5 (Ehrhardt et al., 2008; Kim et al., 2019; Li et al., 2016) as useful markers to identify atypical MBCs. Additionally, CD11c+ B cells have been identified as a potential precursor of ASCs (Golinski et al., 2020). CD11c+ B cells might be induced by Tfh outside of GC (Song et al., 2022), which has been associated with extrafollicular response. The extrafollicular pathway is thought to bypass the GC education of MBCs to more rapidly produce short-lived ASCs like

plasmablast and memory B cells (reviewed in (Elsner and Shlomchik, 2020)). This pathway has been suggested to be the main source of atypical MBCs in an autoimmune context (Jenks et al., 2018). Altogether it has been noted that atypical MBCs are less able to respond to antigen or signal through their BCR upon interaction with their cognate antigen. Coupled with their increased expression of inhibitor receptors like FcLR5, this has led to the belief that they represent an exhausted subtype of B cells which may be a dead-end in the differentiation pathway of MBCs (Ambegaonkar et al., 2020; Kardava et al., 2014; Portugal et al., 2015). However, this has yet to be conclusively shown. Further to this, several studies (Reyes et al., 2023; Sutton et al., 2021) have suggested that there might be different sub-phenotypes with different roles within atypical MBCs.

Overall, CD27- CD21- atypical B cells appear in various contexts although all involve improper inflammation processes. Lack of clearance of the inflammatory-causing stimuli probably leads to the persistence of high levels of atypical MBCs and despite the heterogeneity of disease state, they appear to share transcriptional profiles (Holla et al., 2021). Recently, the formation and maintenance of atypical B cells has been associated with the transcription factor Zeb2 (Dai et al., 2024; Gao et al., 2024). A recent study highlighted that there is significant transcriptional overlap and plasticity between resting and activated MBCs, whilst atypical MBCs may represent an alternative differentiation pathway (Lopes de Assis et al., 2023) (***Figure 1.1.4***). Of note, while it has been hypothesised that their persistence is clearly associated with disease, antigen-specific atypical MBCs have been associated with a protective influenza response (Burton et al., 2022) and broad neutralisation profiles against SARS-CoV-2 (Carr et al., 2023).

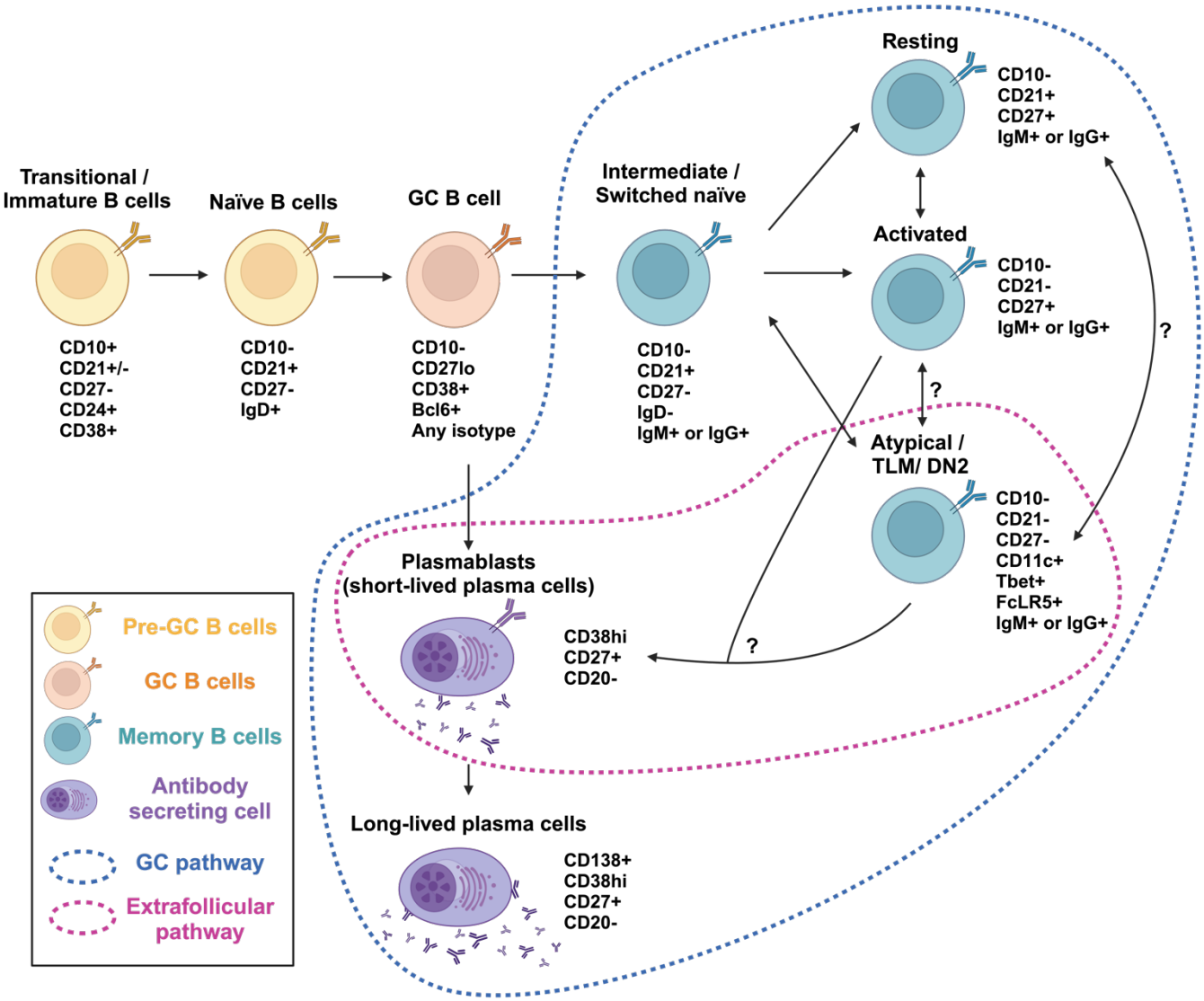

Figure 1.1.4: *Putative directionality between MBCs phenotypes. Schematic of the interaction between the different subtypes of memory B cells and ASCs, arrow direction describes directionality. Typical markers to identify these B cell populations are indicated alongside* (Sanz et al., 2019). *Naïve B cells can enter the GC, and following the GC reaction, B cells can differentiate into ASCs or into memory B cells. There is plasticity between the different phenotypes. Alternatively, the extrafollicular pathway may directly give rise to atypical MBCs and short-lived plasma cells/plasmablasts. In peripheral blood, GC B cells and long-lived plasma cells cannot be confidently identified. Diagram created with biorender.com.*

1.1.5. The 'normal' BCR repertoire.

As mentioned earlier the number of possible BCRs that can be generated is estimated to be ~$2x10^{12}$ (Lefranc and Lefranc, 2023), which is greater than the total amount of BCRs expected to exist in one individual at approximately $5x10^{9}$ (Briney et al., 2019). Practically, this means that there is little overlap between the BCR repertoire of any given two individuals (Wang et al., 2015). However, rare overlapping BCRs do occur and are termed public or convergent antibodies and as they are relatively common in SARS-CoV-2 they are discussed in greater detail in **section 1.2.7**. In humans, the most common usage of a VH family is IGHV3 followed in order by IGHV4, IGHV1, and IGHV5 with IGHV2, IGHV6, and IGHV7 are much being much rarer (Brezinschek et al., 1995; Volpe and Kepler, 2008). Within this, the most commonly used IGHV gene is IGHV3-23 (Volpe and Kepler, 2008). Other IGHV genes of interest include IGHV4-34, which has been associated with the recognition of self-reactive epitopes and commensal bacteria (Schickel et al., 2017; Tipton et al., 2015). This may be caused by the presence of N-glycosylation motifs within the CDR regions of IGHV4-34 (Sabouri et al., 2014). In general, public and private BCRs which use similar VH genes and have a similar function will generally use a similar VL gene (Jaffe et al., 2022).

Between tissues, there is significant overlap between the BCRs found in the peripheral blood, bone marrow, spleen and in the lung, whilst there is less overlap in the BCRs found in the aforementioned tissues and the gut (Meng et al., 2017). In children, the BCR repertoire rapidly evolves due to encounters with routine childhood vaccination and infection. Over this time, SHM will increase for all isotype bar IgE. Generally, there are higher levels of SHM and clonal diversity in adults than in children due to more exposure to various pathogens (Nielsen et al., 2019). In adults, the memory B cell repertoire stays stable over time, with recurrent sequencing of BCRs from B cells which were stimulated years prior (Phad et al., 2022). This shows that BCR sequencing from RNA derived from peripheral blood mononuclear cells (PBMC) is a logical way to sample a representative pool of BCRs which reflects the variety of BCRs found in tissues and across time.

1.2. SARS-CoV-2

1.2.1. A brief history of SARS-CoV-2 and other coronaviruses.

The first cases of a novel respiratory disease in Wuhan (China) were reported in mid-December 2019. The aetiological agent for this respiratory disease went on to be recognized as a virus from the *Coronaviridae* family (Wu et al., 2020) and named first 2019-nCoV, then given the official name 'Severe Acute Respiratory Syndrome Coronavirus 2' or SARS-CoV-2, based on its similarity to the previous coronavirus SARS-CoV, with the disease named 'COVID-19' for coronavirus infectious disease 2019 by the World Health Organisation (WHO, 2020a). SARS-CoV-2 went on to spread beyond China to the rest of the world and was officially declared a pandemic in early March 2020 by WHO (WHO, 2020b). This led to worldwide lockdown orders in many countries from March 2020 onwards, with the UK officially entering lockdown in late March 2020. In the UK, COVID-19-related restrictions continued throughout 2020, 2021 and until March 2022 (UK Government, 2022). As of the 4th of February 2024, the WHO reports that since the start of the SARS-CoV-2 pandemic in 2020, more than 774 million COVID-19 cases and more than 7 million COVID-19 deaths have been reported worldwide (WHO, 2024), with more than 230,000 deaths in the UK alone (UKHSA, 2023a).

In early 2020, it was expected that the general population would be immunonaïve for SARS-CoV-2 as globally few individuals were ever infected by SARS-CoV-1. However, SARS-CoV-2 is part of the wider family of *Coronaviridae* (***Figure 1.2.1A***). So far, six other human coronaviruses (hCoVs) have been identified. Four of the hCoVs (229E, NL63, OC43, and HKU1) are now known to be endemic within the general population and are frequently the causal agent of common-cold, particularly in children (Aldridge et al., 2020; Galanti et al., 2019; Walsh et al., 2013). It is now understood that even in early 2020 there was a general level of pre-existing immunity provided by seasonal coronaviruses hCoVs infections for SARS-CoV-2 (Guo et al., 2020; Ng et al., 2020; Pickering et al., 2020; Wang et al., 2020). It is not thought that these cross-reactive provided much protection against SARS-CoV-2 infection (Anderson et al., 2021). On the other hand, the other two pre-2020 coronaviruses had not circulated widely throughout the general population. Firstly, the closest relative of SARS-CoV-2 (***Figure 1.2.1B***), SARS-CoV, is now often khown as SARS-CoV-1 to

avoid confusion (and referred throughout this thesis as SARS-CoV-1). SARS-CoV-1 was the causal agent (Drosten et al., 2003; Rota et al., 2003) of a major outbreak of severe and often fatal pneumonia in Eastern Asia (mostly China and Hong Kong) from 2002 to 2004. Secondly, the Middle-East respiratory syndrome coronavirus (MERS-CoV), which was responsible for several outbreaks first in the Middle East and then in Korea between 2012 and 2018 (Zaki et al., 2012). Both SARS-CoV-1 and MERS-CoV have had higher case-fatality rates than SARS-CoV-2 (Pormohammad et al., 2020). This higher propensity to kill or severely sicken the host seen with SARS-CoV-1 and MERS-CoV severely limits transmissibility and may explain why both viruses never spread beyond their initial outbreak unlike with other hCoVs and or SARS-CoV-2.

Infection with SARS-CoV-2 can lead to disease with vastly different degrees of severity from asymptomatic infection to death. Commonly reported symptoms include a mix of local and systemic symptoms such as coughing, myalgia, fatigue, fever, sore throat, loss or change of sense of smell/taste or gastrointestinal problems. More severe cases can lead to low oxygen saturation, which untreated can lead to respiratory failure requiring ICU treatment and generalised organ dysfunction. Older individuals (McMichael et al., 2020), individuals with immunosuppression/immunodeficiency (particularly transplant and cancer patients) (Leston et al., 2024) and those with comorbidities such as cardiovascular disease, respiratory disease or diabetes (Yang et al., 2020) are at higher risk of severe COVID-19 disease. Severe COVID-19 disease has also been associated with a higher risk of developing Long COVID, a poorly understood long-term illness which can impact multiple organs (reviewed in (Davis et al., 2023)).

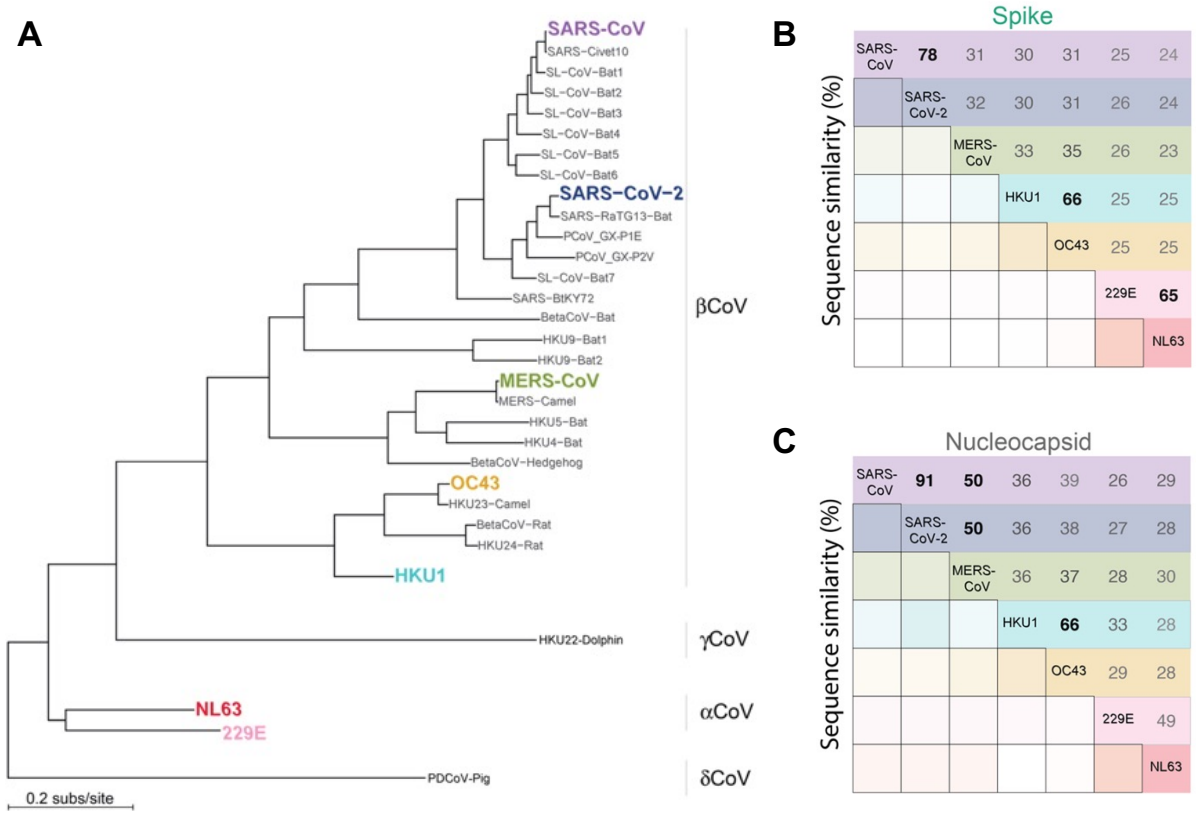

Figure 1.2.1: *Similarity between SARS-CoV-2 and other human coronaviruses. This figure is adapted from* (Lewitus et al., 2023). ***A.*** *Phylogenetic tree showing relations between the different hCoVs (bolded and in colour) and selected animal CoVs.* ***B.*** *Percent identity matrix between the sequence of different hCoVs for the whole spike protein and* ***C.*** *for the nucleocapsid/nucleoprotein protein.*

1.2.2. SARS-CoV-2 virus lifecycle.

As a betacoronavirus, SARS-CoV-2 is a single-stranded positive-sense RNA virus. SARS-CoV-2 genome is roughly 30kb in length and is made up of four structural proteins: spike protein or S, envelope protein or E, membrane protein or M and nucleocapsid/nucleoprotein or N (***Figure 1.2.2A-B***). Additionally, the genome is comprised of several non-structural proteins and accessory proteins. The non-structural proteins are encoded by ORF1a and ORF1b, together these non-structural proteins (Nsp1-16) form the replicase or replication transcription complex (RTC). The exact role of the accessory proteins (ORF3a, 3b, 3c, 3d, 6, 7a, 7b, 8, 9b, 9c and 10) is less well understood although many play a role in evading host innate immune responses (reviewed in (Sievers et al., 2023)), such as ORF8 which interacts with spike to modulate its availability on virions (Kim et al., 2023). Spike, M and E are found on the surface of the virus whilst N sits inside the viral particle. The M and E proteins are necessary for viral particle assembly and potentially budding (Cao et al., 2021; Zhang et al., 2022a). N protein is a multifunctional protein. Its main role is facilitating the packaging of the RNA genome, N can also modulate inflammation or the host cell cycle (Pan et al., 2021; Wu et al., 2023).

Spike protein has a size of roughly 180-200 kDa and is made up of two subunits S1 and S2 and forms homotrimers. The S1 subunit contains the receptor binding domain (RBD) and N-terminal domain (NTD), both can directly bind to the entry receptor. S1 is separated from S2 by the furin cleavage site (FCS). S2 provides the membrane fusion peptide (FP) to mediate entry and is anchored in the viral membrane via its transmembrane domain (TM) (***Figure 1.2.2B-C***). Compared to S1, S2 is relatively well conserved between the different hCoVs (Walls et al., 2020) (***Figure 1.2.2D***). Spike mediates cell entry via the interaction of its RBD on the S1 subunit with the angiotensin-converting enzyme 2 receptor (ACE-2) on the host cell (Shang et al., 2020; Walls et al., 2020). Spike is found on the viral particle in a prefusion conformation, the interaction between RBD and ACE-2 will trigger the sequential cleavage of the spike protein into S1 and S2 at the FCS (Hoffmann et al., 2020), then of S2 at the S2' site by available proteases (mostly transmembrane serine protease 2 (TMPRSS2) and cathepsin L) (Bayati et al., 2021; Hoffmann et al., 2020). As spike is the main target of neutralising antibodies following SARS-CoV-2 infection and vaccination (see **section 1.2.4**), neutralising antibodies often directly or indirectly

disrupt the interaction between spike and ACE-2. Depending on the availability of TMPRSS2 on the cell surface, internalisation of the virus will happen either via clathrin-mediated endocytosis or by direct fusion between the viral and host cell membrane (Bayati et al., 2021). The viral particle will then uncoat in the cytoplasm, where the viral genome will be first translated to produce the proteases needed to transcribe the RNA genome (reviewed in (Malone et al., 2022)). The newly produced structural proteins are then inserted (spike, M, E) into vesicle membranes at the Golgi or ER, whilst N will form a viral ribonucleoprotein with the viral RNA. The ribonucleoprotein and embedded structural proteins can then be assembled into a viral particle and released from the cells (Scherer et al., 2022).

The main tissue of tropism of SARS-CoV-2 is the respiratory mucosae which is concordant with the high expression of ACE-2 and TMPRSS2 on epithelial cells alongside the respiratory track (Hou et al., 2020a; Sungnak et al., 2020). These two receptors are also highly expressed in the digestive tract (Zhang et al., 2020), which is known to be a major site of SARS-CoV-2 infection. Due to its multiple potential sites of infection, side effects from COVID-19 disease can be multi-systemic.

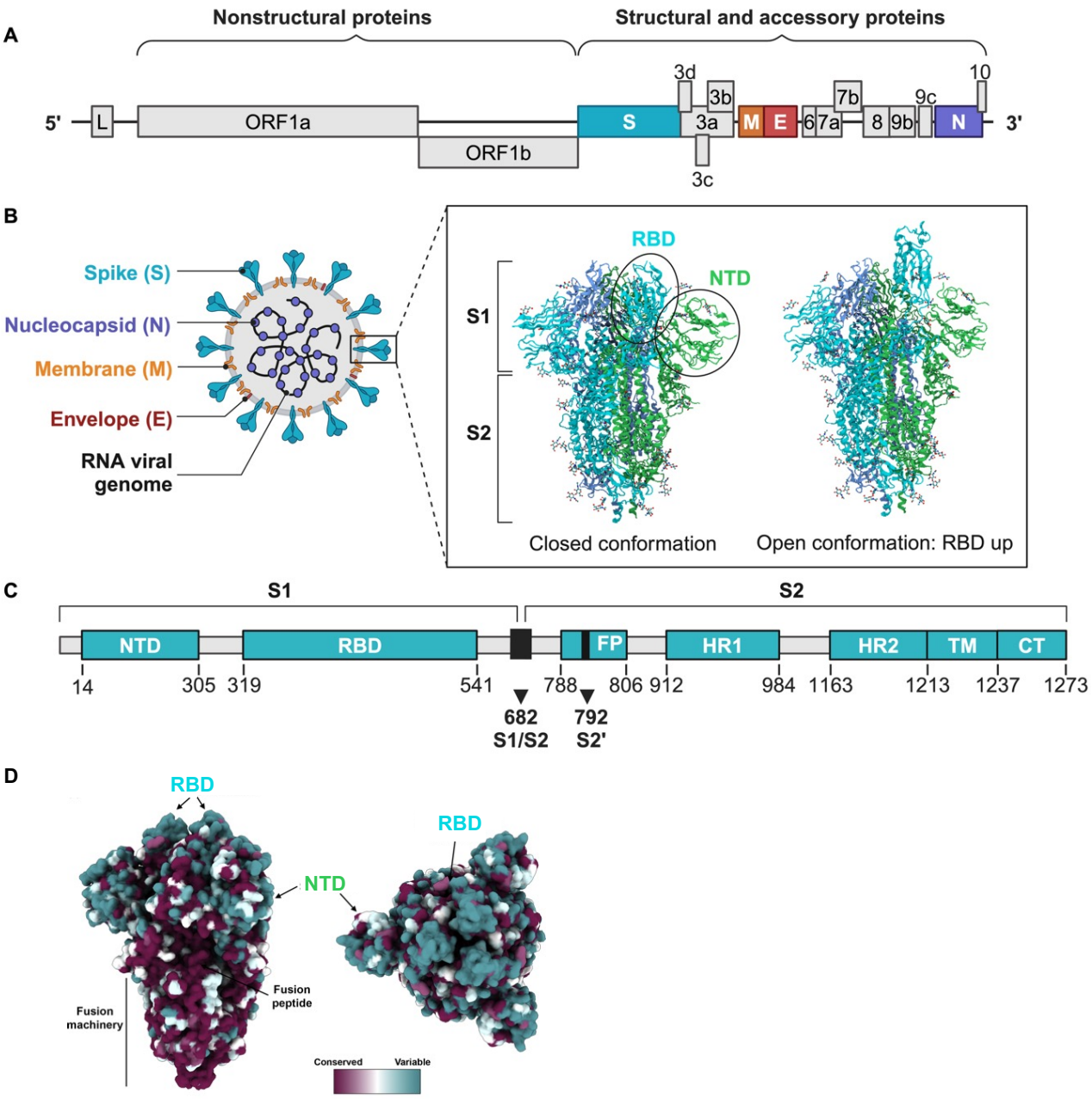

Figure 1.2.2: *SARS-CoV-2 genome, virus and spike protein structure.* ***A.*** *SARS-CoV-2 genome.* ***B.*** *Schematic of SARS-CoV-2 virus structure with insert showing the crystal structure of the spike glycoprotein in the closed and open conformation (PBD: 6VXX and 6VYB).* ***C.*** *SARS-CoV-2 spike protein domains and sub-domains (NTD= N-terminal Domain, RBD= receptor binding domain, FP= fusion peptide, HR1 & HR2= heptad repeat domain 1&2; TM= transmembrane domain; CT= cytoplasmic tail). D. Conservation between the SARS-CoV-2 spike protein and other SARS-CoV-like virus spike protein. Diagram created with biorender.com, C is adapted from* (Walls et al., 2020).

1.2.3. SARS-CoV-2 variants of concern

The first isolated SARS-CoV-2 sequence, Wuhan-hu-1 was isolated in early January 2020 in Wuhan (Wu et al., 2020) and is widely referred to as wild-type (WT) SARS-CoV-2. The first evidence of viral evolution from SARS-CoV-2 came from the rapid change from the use of an aspartic acid to a glycine in position 614 of the spike protein from March-April 2020 onward (Korber et al., 2020). This D614G change became ubiquitous due to its increased infectivity (Hou et al., 2020b; Weissman et al., 2021) and transmissibility (Volz et al., 2021), virtually all SARS-CoV-2 sequences since have included this point mutation.

The first variant of concern (VOC) identified was the alpha variant or B.1.1.7 in the UK in the winter of 2020 (Rambaut et al., 2020), with nine point mutations in the spike protein (***Figure 1.2.3***). B.1.1.7 quickly became the dominant circulating strain worldwide and caused an important new wave of cases and death (Davies et al., 2021a) in what at the time was a mostly immune-naïve population as vaccination had only just begun. Overall, the B.1.1.7 variant was more transmissible than Wuhan-hu-1 (Davies et al., 2021b, 2021a; Volz et al., 2021). Increased infectivity was partly mediated by the del69-70 and N501Y changes within the RBD (Collier et al., 2021a; Greaney et al., 2021; Meng et al., 2021). However, overall, antibody titres gained via vaccination were only modestly decreased against the B.1.1.7 variant (Collier et al., 2021a; Greaney et al., 2021; Rees-Spear et al., 2021; Starr et al., 2021).

The next variant was the beta or B.1.351 variant which emerged in South Africa in late 2020 (Tegally et al., 2021). As with B.1.1.7, B.1.351 retained the N501Y mutation and on top had the E484K mutation on the RBD which has been widely associated with escape from antibody neutralisation (Cele et al., 2021a; Wang et al., 2021a). Against B.1.351, there was no longer any vaccine-mediated neutralisation with two doses of AZD1222 (Madhi et al., 2021a) whilst neutralisation was slightly reduced with BNT216b2 (Abu-Raddad et al., 2021).

The delta variant or B.1.617.2 first arose in India in the spring of 2021 before becoming the globally dominant variant over the summer of 2021 (***Figure 1.2.3B***). This variant presented 10 point mutations within the spike protein, of note one mutation P681R helped increase cleavage of the spike protein and therefore facilitated entry and replication efficiency (Liu et al., 2022c; Mlcochova et al., 2021). This led to a relative

decrease in neutralising titres and vaccine efficacy from Alpha (Lopez Bernal et al., 2021; Mlcochova et al., 2021).

Omicron BA.1 or B.1.1.529.1 emerged in South Africa/Botswana in late 2022 (Viana et al., 2022). Since that point, Omicron and its subsequent variants have been the dominant circulating strain (UKHSA, 2023b) (***Figure 1.2.3A-B***). Omicron BA.1 has 36 point mutations within spike, however, some of the changes present in BA.1 have been lost in newer Omicron variants. Overall, Omicron BA.1 presented a large antigenic change from previous variants (***Figure 1.2.3A-C***) which meant that most individuals had largely reduced if not abrogated neutralising titres after two doses of COVID-19 vaccination which highlighted the need for a third vaccine dose to neutralise BA.1 (Cameroni et al., 2021; Cele et al., 2021b; Garcia-Beltran et al., 2022; Liu et al., 2022a; Planas et al., 2021). The dominance of Omicron over B.1.617.2 in late 2021 was probably driven by the large antibody escape it generated (Cao et al., 2022) coupled with a differential entry strategy (Willett et al., 2022).

The cause of variant emergence is not conclusively understood, although several hypotheses have been proposed. Persistent infections with high levels of viral evolution have been documented in immunocompromised hosts (Cele et al., 2022; Clark et al., 2021; Kemp et al., 2021; Maponga et al., 2023; Riddell et al., 2022) but also in asymptomatic individuals with long term infections (Ghafari et al., 2024). In general, asymptomatic infections and lack of routine surveillance in some parts of the world could mean that variants are not being detected in a timely manner. Finally, SARS-CoV-2 has a wide tropism and therefore can be found in animal reservoirs as seen in minks (Munnink et al., 2021) or white-tailed deers (Chandler et al., 2021), where host constraints on viral escape may be different than the ones seen in human which could lead to the generation of diverse variants that could cross-over again to humans.

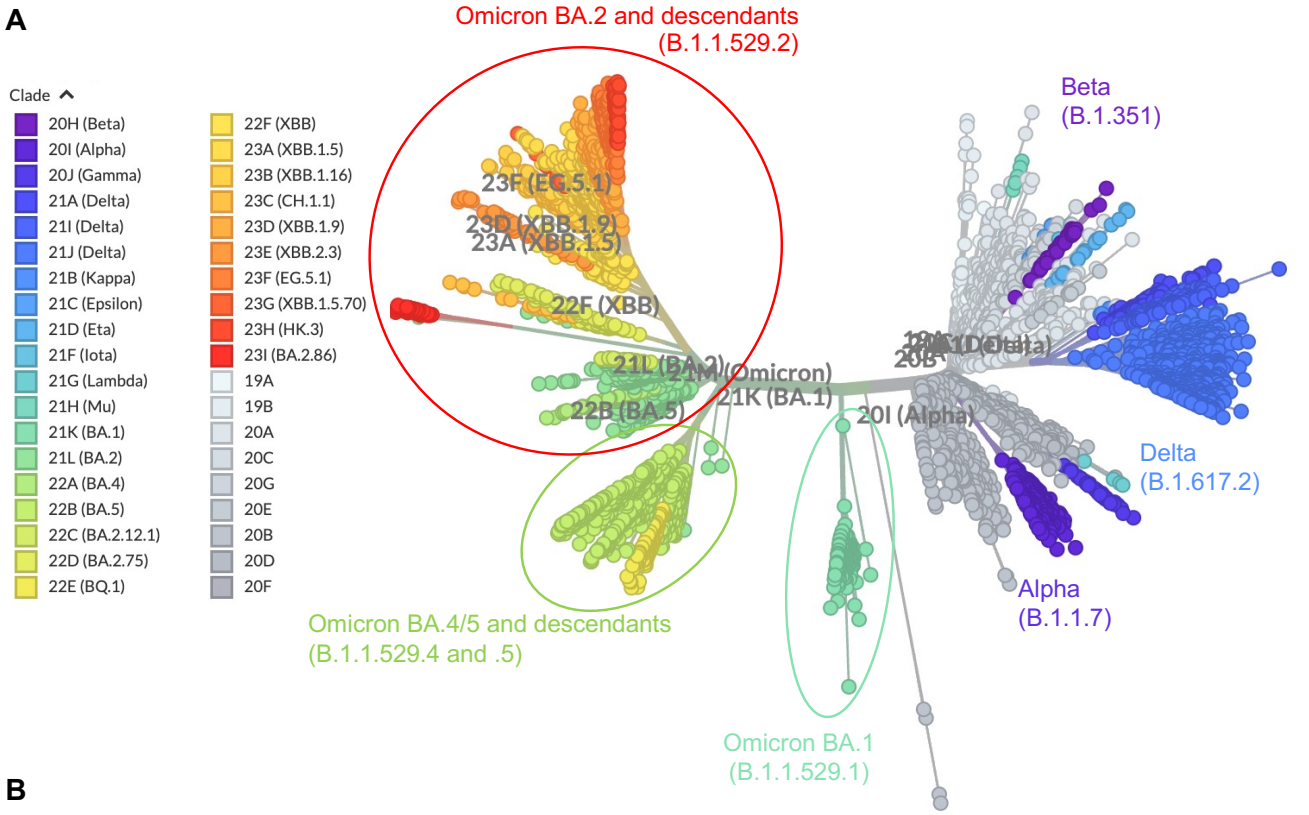
A
Omicron BA.2 and descendants
(B.1.1.529.2)
Clade
20H (Beta)
20I (Alpha)
20J (Gamma)
21A (Delta)
21I (Delta)
21J (Delta)
21B (Kappa)
21C (Epsilon)
21D (Eta)
21F (Iota)
21G (Lambda)
21H (Mu)
21K (BA.1)
21L (BA.2)
22A (BA.4)
22B (BA.5)
22C (BA.2.12.1)
22D (BA.2.75)
22E (BQ.1)
22F (XBB)
23A (XBB.1.5)
23B (XBB.1.16)
23C (CH.1.1)
23D (XBB.1.9)
23E (XBB.2.3)
23F (EG.5.1)
23G (XBB.1.5.70)
23H (HK.3)
23I (BA.2.86)
19A
19B
20A
20C
20G
20E
20B
20D
20F
23F (EG.5.1)
23D (XBB.1.9)
23A (XBB.1.5)
22F (XBB)
21L (BA.2)
21M (Omicron)
21K (BA.1)
22B (BA.5)
20I (Alpha)
Beta
(B.1.351)
Delta
(B.1.617.2)
Alpha
(B.1.1.7)
Omicron BA.4/5 and descendants
(B.1.1.529.4 and .5)
Omicron BA.1
(B.1.1.529.1)

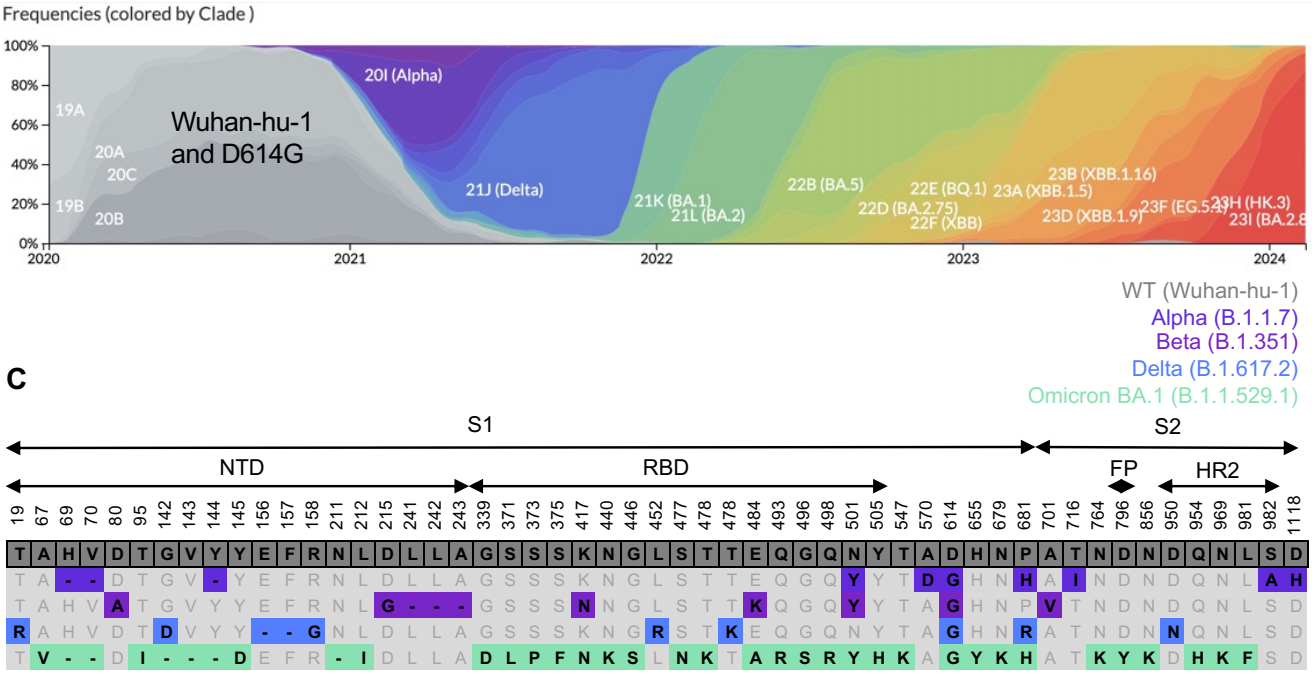
B
Frequencies (colored by Clade)
100%
80%
60%
40%
20%
0%
2020
2021
2022
2023
2024
19A
19B
20A
20B
20C
Wuhan-hu-1
and D614G
20I (Alpha)
21J (Delta)
21K (BA.1)
21L (BA.2)
22B (BA.5)
22D (BA.2.75)
22E (BQ.1)
22F (XBB)
23A (XBB.1.5)
23B (XBB.1.16)
23D (XBB.1.9)
23F (EG.5.1)
23H (HK.3)
WT (Wuhan-hu-1)
Alpha (B.1.1.7)
Beta (B.1.351)
Delta (B.1.617.2)
Omicron BA.1 (B.1.1.529.1)

C
S1
S2
NTD
RBD
FP
HR2
19 67 69 70 80 95 142 143 144 145 156 157 158 211 212 215 241 242 243 339 371 373 375 417 440 446 452 477 478 478 484 493 496 498 501 505 547 570 614 655 679 681 701 716 764 796 856 950 954 969 981 982 1118
T A H V D T G V Y Y E F R N L D L L A G S S S K N G L S T T E Q G Q N Y T A D H N P A T N D N D Q N L S D
T A - - D T G V - Y E F R N L D L L A G S S S K N G L S T T E Q G Q Y Y T D G H N H A I N D N D Q N L A H
T A H V A T G V Y Y E F R N L G - - - G S S S N N G L S T K Q G Q Y Y T A G H N P V T N D N D Q N L S D
R A H V D T D V Y Y - - G N L D L L A G S S S K N G R S T K E Q G Q N Y T A G H N R A T N D N N Q N L S D
T V - - D I - - - D E F R - I D L L A D L P F N K S L N K T A R S R Y H K A G Y K H A T K Y K D H K F S D

Figure 1.2.3: *SARS-CoV-2 variants of concern.* ***A.*** *Phylogenetic tree of all SARS-CoV-2 sequences submitted to GISAID between 22/12/2019 to 13/02/2024 (rooted on Wuhan-hu-1) coloured by Nextstrain clade (19A to 23I with corresponding WHO Greek names for VOCs or Pango lineages names).* ***B.*** *For the same time period, the prevalence for each variant is given by the frequency of submitted sequences. A and B are from the Nextstrain dashboard (https://nextstrain.org/ncov/gisaid/global/all-time* (Hadfield et al., 2018)*, consulted on 13/02/2024).* ***C.*** *List of point mutation found in the Alpha (B.1.1.7), Beta (B.1.351), Delta (B.1.617.2) and Omicron BA.1 (B.1.1.529.1) variants compared to WT (Wuhan-hu-1) with the amino acid number above each amino acid single letter code. Regions of the spike protein are annotated above.*

1.2.4. Vaccines.

At the start of the pandemic, no licensed vaccines existed for any human coronaviruses. Rapid sequencing of the SARS-CoV-2 genome led to the immediate repurposing of previously optimised vaccine platforms for accelerated vaccine development. Firstly, an adenovirus vectored vaccine using the modified chimpanzee adenovirus vector ChAdOx1 developed by the University of Oxford had already shown immunogenicity and protection against MERS-CoV in several animal models with a single dose (Alharbi et al., 2019; van Doremalen et al., 2020; Munster et al., 2017). The chimpanzee adenovirus is modified to avoid replication of the virus which can then be used as a vector to deliver the gene of interest into a cell, which can then be transcribed into mRNA and finally translated into the protein of interest. Additionally, ChAdOx1 was chosen so that a minimum amount of antibodies against the vector (due to cross-reactivity between human and simian adenovirus) would be produced (Dicks et al., 2012). However, no vaccine using ChAdOx1 was yet licensed for use in humans at the start of 2020. In collaboration with Astra-Zeneca, the ChAdOx1 platform was used to deliver a full-length codon-optimised SARS-CoV-2 spike based on the Wuhan-hu-1 SARS-CoV-2 isolate. By the summer of 2020, phase 1/2 in-human trial results showed that two doses of ChAdOX-1 nCoV-19 (now known as AZD1222) were safe and that all participants were able to produce a neutralising response (Folegatti et al., 2020). In December 2020, phase 2/3 results showed that two doses of AZD1222 had an overall efficacy against symptomatic COVID-19 disease of 70.4% (Voysey et al., 2021). AZD1222 was approved for use in the UK in January 2021 on a two-dose schedule spaced each by 8-12 weeks. Other adenoviral vector-based vaccines for SARS-CoV-2 include Ad26.COV2.S from Janssen (Sadoff et al., 2021) which was approved for use in the UK in May 2021 and Sputnik V/ Gam-COVID-Vac which was mostly used in Russia (Logunov et al., 2021).

Similarly, vaccines using messenger RNA (mRNA) were being developed for other diseases prior to 2020 and this technology was adapted for use against SARS-CoV-2. An mRNA vaccine packages the mRNA of interest inside a lipid envelope. The mRNA is specially optimised so that all the uridine bases are replaced by pseudo-uridine bases to avoid innate immune sensing which would prevent vaccine efficacy (Karikó et al., 2005, 2008). The incorporation of pseudo-uridines still allows for the translation of the mRNA by the ribosome to produce the protein of interest. Both

adenoviral vector-based and mRNA vaccines lead to the same act of protein production, processing, and presentation on MCHs. Presentation on MHC can then directly or indirectly lead to the activation of B and T cells. At the start of 2020, no mRNA vaccine was licensed for use in humans. From early 2020 both Pfizer-BioNTech and Moderna designed new mRNA vaccines to include a codon-optimised spike protein based on Wuhan-hu-1 in their respective proprietary lipid envelopes. In Autumn 2020, phase 1 in-human trial results for Pfizer-BioNTech's BNT162b2 (Walsh et al., 2020) and Moderna's mRNA-1273 (Jackson et al., 2020) showed an acceptable safety profile and the production of neutralising antibodies for all participants after two doses of these mRNA vaccines. In phase 2/3 trials, two doses of BNT162b2 (Polack et al., 2020) led to a vaccine efficacy of 95% against SARS-CoV-2 infection whilst two doses of mRNA-1273 (Baden et al., 2021) led to a vaccine efficacy of 94.1% against symptomatic SARS-CoV-2 infection. BNT162b2 was approved for use in early December 2020 in the UK whilst mRNA-1273 was approved for use in early January 2021. Both vaccines were administered on a two-dose schedule spaced by 3 weeks which was then changed to a 12-week interval in the UK to accelerate vaccine uptake and match it to AZD1222's schedule (JCVI, 2021a).

More traditional vaccine platforms like inactivated vaccines have also been used against SARS-CoV-2 using a whole inactivated SARS-CoV-2 virus via serial passage in Vero cells and inactivation with beta-propiolactone for Sinopharm/ BBIBP-CorV (Xia et al., 2021), BBV152/Covaxin (Ella et al., 2021), CoronaVac/Sinovac (Tanriover et al., 2021) and Valneva (Lazarus et al., 2022). Only Valneva was approved for use in the UK, whilst the others were widely used in Asia, Africa and South America. Subunit vaccines were also designed using a stabilised spike protein by Novavax/ NVX-CoV2373 (Heath et al., 2021) or Sanofi-GSK (Sridhar et al., 2022) were also approved for use in the UK in 2022.

The three vaccines which were received by the participants in this thesis were AZD1222, BNT162b2 and mRNA-1273. In the UK vaccination started in December 2020 for prioritised groups first (healthcare workers, elderly, immunocompromised) and extended to the general population from June 2021 (JCVI, 2022). Rapid uptake had a measurable impact on COVID-19 disease and death (***Figure 1.2.4***). From the autumn of 2021 onwards an additional third vaccine dose of any mRNA vaccines was recommended for the general population to keep up with novel variants.

Comparison of real-world data has shown that there are slight differences in the quality of antibody, B and T cell responses produced, with mRNA vaccines outperforming adenoviral-vector-based vaccines (Hensley et al., 2022; Klemis et al., 2022; Röltgen et al., 2020; Zhang et al., 2022b) although heterologous AZD1222 plus mRNA vaccination performed as well as any two-dose of mRNA vaccination (Klemis et al., 2022; Pozzetto et al., 2021). Antibody, B cells and spike-specific T cell responses are generally inferior in inactivated vaccines compared to mRNA vaccines (Röltgen et al., 2020; Zuo et al., 2022) but can elicit T cell responses specific for other SARS-CoV-2 proteins (Lim et al., 2022). This highlights the potential benefit of including T cell targets in vaccines. In a mice vaccination study, mRNA vaccination including N alongside spike provided better protection against reinfection and higher quality T cell and humoral responses (Hajnik et al., 2022). Another important factor is that all licensed vaccines so far are delivered intra-muscularly in the deltoid, and therefore fail to provide the same amount of mucosal-derived immune responses seen with natural infection (Azzi et al., 2022; Tang et al., 2022).

Finally, all of these first-generation SARS-CoV-2 vaccines were based on the SARS-CoV-2 Wuhan-hu-1 spike. By the time most of the population had been vaccinated, novel variants were circulating as seen in ***Figure 1.2.3***. Since, bivalent mRNA vaccines including WT and an Omicron variant vaccine (BA.1, BA.4/5 or XBB.1.5) have been designed and have shown higher neutralising titres against Omicron variants than WT-based vaccines (Chalkias et al., 2022; Lee et al., 2023). Updated bivalent vaccines are now the preferred vaccine choice in the UK (JCVI, 2023).

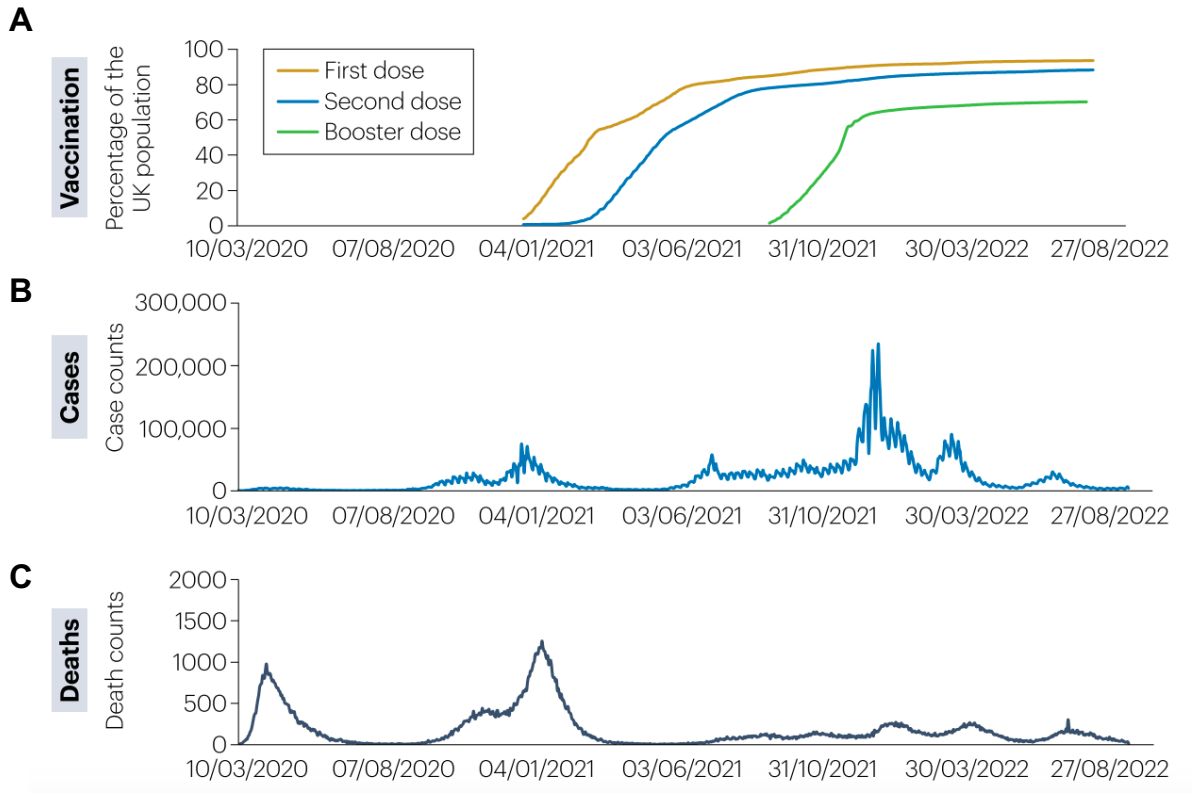

Figure 1.2.4: *Impact of vaccination in the COVID-19 pandemic in the UK*. ***A.*** *Percentage of UK population who received their 1st, 2nd or booster (i.e., 3rd) SARS-CoV-2 vaccine dose over time.* ***B.*** *SARS-CoV-2 cases or* ***C.*** *death counts in the UK over time (data from the https://coronavirus.data.gov.uk/ dashboard). Of interest, this timeline englobes the whole recruitment period relevant to this thesis (the first participant in the convalescent cohort in Chapter 3 was recruited on 23/07/2020 and the last participant in the vaccine cohort in Chapters 4, 5 and 6 was recruited on 25/03/2022). This figure is adapted from* (Carabelli et al., 2023).

1.2.5. Antibody responses to SARS-CoV-2 infection and vaccination

The main neutralising antibody target of SARS-CoV-2 is spike (Brouwer et al., 2020; Ju et al., 2020; Piccoli et al., 2020; Shi et al., 2020; Shrock et al., 2020; Zost et al., 2020) as it situated directly on the surface of the virus, as seen with other coronaviruses (Cao et al., 2010; Huang et al., 2020; Mou et al., 2013). Most antibodies are directed towards the S1 subunit, particularly the RBD (Amanat et al., 2021; Barnes et al., 2020; Brouwer et al., 2020; Ju et al., 2020; Liu et al., 2021; Piccoli et al., 2020; Shi et al., 2020; Zost et al., 2020) and NTD domains (Amanat et al., 2021; Liu et al., 2021; McCallum et al., 2021; Voss et al., 2021). In general, this will lead to a neutralising antibody response that functions by blocking directly or indirectly the interaction between the RBD and ACE2. As S2 is less accessible, there are fewer neutralising antibodies targeted against it (Liu et al., 2021; Piccoli et al., 2020; Pinto et al., 2021; Voss et al., 2021). In this case. S2 targeting antibodies won't neutralise via ACE-2 blocking but by potentially interfering with the membrane fusion. However, S2 is better conserved throughout the different variants and across hCoVs, which has led to continued interest in finding and directing the neutralising responses to S2 for pan-coronavirus protection (Ng et al., 2022). Additionally, a large portion of the binding antibody responses is directed against N, as seen with SARS-CoV-1 (Leung et al., 2004) and SARS-CoV-2 (Shrock et al., 2020), due to the abundance and low glycosylation of N in coronaviruses (Krokhin et al., 2003). Throughout the COVID-19 pandemic, antibodies against N have been a useful marker to serologically distinguish infection from vaccination. As all the licenced COVID-19 vaccines rely on spike, only individuals with prior SARS-CoV-2 infection should have SARS-CoV-2 N-specific antibodies, which has made N a popular antigen-target for clinical testing and surveillance. However, only clinical commercial assays are capable of discriminating between anti-N antibodies raised by SARS-CoV-2 infection and those from prior seasonal coronavirus exposures. Moreover, nowadays this strategy is less reliable as most of the population has gained anti-N immunity through breakthrough infections (Harker et al., 2023).

In the context of a first encounter with SARS-CoV-2, IgG-specific binding antibodies against SARS-CoV-2 spike, appear after 10-15 days and peak around a month post-symptom onset (Iyer et al., 2020; Seow et al., 2020). An early report demonstrated waning after three months (Seow et al., 2020), although later reports suggested that

binding and neutralising antibodies can still be detected up to eight-month post-SARS-CoV-2 infection (Cohen et al., 2021; Dan et al., 2021). Both IgA and IgM-spike-specific antibodies peaked and waned earlier than IgG-specific antibodies, with IgGs making up the majority of the spike-specific antibody response after 15 days (Guo et al., 2020; Iyer et al., 2020; Long et al., 2020; Okba et al., 2020; Röltgen et al., 2020; Seow et al., 2020). After COVID-19 vaccination, IgA and IgM antibodies and MBCs can be detected following vaccination (Goel et al., 2021b, 2021a; Kardava et al., 2022) although like with infection, IgG-specific binding antibodies form the immunodominant portion of the responses (Cohen et al., 2021; Dan et al., 2021; Goel et al., 2021b, 2021a; Long et al., 2020; Seow et al., 2020). Curiously, it has been noted that the mucosal response driven by IgA and IgM after vaccination in individuals who had a prior history of SARS-CoV-2 infection is lower than after infection. This is likely due to the change of tissue site (respiratory mucosae in infection to the deltoid muscle in vaccination), which further polarises the response towards IgG (Azzi et al., 2022; Sheikh-Mohamed et al., 2022; Smith et al., 2021; Tang et al., 2022). Within IgG, IgG1 and IgG3 dominate the spike-specific responses after infection (Yates et al., 2021) and vaccination (Farkash et al., 2021; Irrgang et al., 2022). Expansion of the IgG4 compartment after the 3rd dose has been observed, the causes of which are poorly understood (Irrgang et al., 2022).

In addition to binding, the basis of a protective response against SARS-CoV-2 infection includes the presence of neutralising antibodies against the spike protein (Gilbert et al., 2022; Lumley et al., 2021). The Moderna clinical vaccine trial established a correlate of protection with a neutralising antibody titre of at least 1:100 equivalent to 91% vaccine efficacy against infection (Gilbert et al., 2022). Development of a neutralising response happens slightly later than the production of binding IgG-specific antibodies in infection (Cohen et al., 2021; Dan et al., 2021; Seow et al., 2020) and vaccination (Goel et al., 2021b, 2021a; Zhang et al., 2022b). A history of previous SARS-CoV-2 infection has been shown to increase binding and neutralisation responses compared to a SARS-CoV-2 naïve individual after vaccination (Bates et al., 2022; Krammer et al., 2021; Reynolds et al., 2021, 2022a). Repeated vaccination has been shown to improve binding and neutralising responses in SARS-CoV-2 naïve individuals and to a lesser extent in individuals with prior infection (also referred to as hybrid immunity) (Goel et al., 2021b, 2021a; Zhang et al., 2022b). Indeed, individuals

with hybrid immunity more quickly attain a maximal threshold or ceiling of how much binding/neutralising antibodies can be produced, although ultimately SARS-CoV-2 naïve individuals will reach this endpoint with more vaccine doses (Srivastava et al., 2024). Without re-exposure through infection or vaccination, the best estimate is that the antibody response can persist for at least 6-8 months (Cohen et al., 2021; Dan et al., 2021; Wheatley et al., 2021). On the other hand, antibody responses induced via vaccination after three doses appear to be more stable and long-lasting, although titres are expected to be reduced against novel variants (Srivastava et al., 2024).

1.2.6. Heterogeneity and the impact of variants on the antibody responses to SARS-CoV-2.

Antibody responses to SARS-CoV-2 can be heterogeneous in terms of duration or neutralisation titres depending on inter-individual characteristics. Older age was found to be associated with lower serological responses and disease outcomes in infection (Jeffery-Smith et al., 2022; Rydyznski Moderbacher et al., 2020). This pattern of lower neutralising responses in the elderly was also confirmed following vaccination (Collier et al., 2021b). Higher COVID-19 disease severity has been consistently associated with higher titres of binding and neutralising antibodies than in mild disease most likely due to higher antigen burden with uncontrolled replication not due to pathogenic effects of antibodies (Chen et al., 2020; Lucas et al., 2021; Rees-Spear et al., 2021; Seow et al., 2020; Wang et al., 2020). Interestingly, in the most severe disease cases, some studies reported that deceased COVID-19 patients had lower antibody titres compared to ICU survivors (Garcia-Beltran et al., 2021; Lucas et al., 2021). This lack of sufficient antibody titres may explain the lack of viral clearance often seen in deceased individuals (Wang et al., 2020) which then potentiates an already overwhelmed immune system leading to systemic organ failure and ultimately death. In these severe cases, it is hard to pick apart how much of this high level of antibodies is protective. One hypothesis is that individuals with severe disease make the ‘wrong’ kind of antibodies, which may participate in detrimental over-immune activation (Bastard et al., 2020, 2021). There is evidence that severe cases produced antibodies with higher levels of SHM than milder cases (Schultheiß et al., 2020) and had reduced repertoire diversity (Kotagiri et al., 2022) which may underline ongoing clonal expansion of non-beneficial antibodies. In general, delayed antibody production was

associated with death in severe COVID (Lucas et al., 2021), and inversely, early development of an antibody responses was found to be protective against mortality (De Vito et al., 2022).

As seen in **section 1.2.3**, most variants were less effectively neutralised by sera from individuals vaccinated with WT spike vaccines due to changes in the spike antigen in the variant. This phenomenon is thought of as “original antigenic sin” or immune imprinting which is the idea that an individual’s immune response is largely shaped by the first exposure to any given pathogen. This can potentially affect what kind of antibodies are produced upon re-exposure with the same pathogen/or variant of said pathogen. Originally, this was described in the context of influenza (Davenport and Henessy, 1956; Davenport et al., 1953), where there is preferential back-boosting of antibodies induced during someone’s first encounter with influenza (Fonville et al., 2014). Renewed interest in this concept came after the emergence of Omicron where it became clear that some degree of immune imprinting was visible in individuals who experienced a first infection after vaccination where the antibody response was still mostly directed against WT rather than Omicron (Buckner et al., 2022; Reynolds et al., 2021; Röltgen et al., 2022). The inverse was also true where individuals who had been infected with Omicron variants only, without any prior vaccination, had markedly reduced titres against WT (Yisimayi et al., 2023). The effect of immune imprinting appears to not be absolute and to be diminished with further re-infection with increasing antigenic distance (Schiepers et al., 2023a, 2023b; Yisimayi et al., 2023).

1.2.7. Convergent/public antibody responses in SARS-CoV-2.

Convergent antibody responses or public antibodies are named based on their similarity. This phenomenon of shared receptor use between individuals has long been described for T cell receptor (TCR). This was first described in the context of influenza (Forgacs et al., 2021; Jackson et al., 2014; Krause et al., 2011), but it has been observed to a limited degree in HIV (Setliff et al., 2018), in Ebola (Ehrhardt et al., 2019) and other viruses (Abu-Shmais et al., 2023; Shrock et al., 2023; Yang et al., 2021a). Before the observation of public antibodies in influenza, they were thought to be quasi-impossible due to the sheer diversity of potential antibodies produced by VDJ recombination and SHM. As much as 0.95% of the antibody repertoire is shared between any given pair of individuals, with public antibodies generally having lower

levels of SHM and shorter CDRH3s (Briney et al., 2019). Public antibodies are generally defined on the basis of using the same IGHV gene and IGHJ gene, having the same CDRH3 length and a high degree of similarity across the IGHV gene and CDRH3.

However, public antibodies have been repeatedly observed after SARS-CoV-2 infection (Galson et al., 2020; Kotagiri et al., 2022; Nielsen et al., 2020; Robbiani et al., 2020; Voss et al., 2021; Yang et al., 2021a) and vaccination (Chen et al., 2021; Lima et al., 2022). For SARS-CoV-2 public antibodies there was a preferential usage towards IGHV1-58 (Abu-Shmais et al., 2023; Robbiani et al., 2020), IGHV1-69 (Abu-Shmais et al., 2023; Chen et al., 2021; Lima et al., 2022), IGHV3-30/3-30-3 (Abu-Shmais et al., 2023; Chen et al., 2021; Lima et al., 2022; Robbiani et al., 2020) and IGHV4-59 (Abu-Shmais et al., 2023; Chen et al., 2021). Many SARS-CoV-2 public antibodies can actively participate in neutralising responses (Chen et al., 2021; Raybould et al., 2021; Robbiani et al., 2020; Yuan et al., 2020). This recurrent observation is probably biased by the high level of research interest on SARS-CoV-2 which has provided enough depth to identify public antibodies. However, it is notable that SARS-CoV-2 can sensitively be neutralised by public antibodies with minimal SHM from the germline VDJ encoded in the naïve B cell. A recent study by Shrock et al. (2023) has proposed that public antibodies arise because of their germline sequences being poised to bind a given amino acid with one of their CDRs. This effectively is a path of least resistance to antibody generation where from germline some antibodies can readily bind a given target and can then hone their avidity for this target with fewer rounds of affinity maturation.

1.2.8. B cell responses to SARS-CoV-2.

The literature reviewed in this section was generated in the same timeframe as the experimental work described in **Chapter 5**, but now provides key insights to better understand this topic. Given antibody titres eventually wane after infection or vaccination, spike-specific MBCs can provide a more long-lived immune response after antigen exposure, as shown after infection (Cohen et al., 2021; Dan et al., 2021; Wang et al., 2021b; Wheatley et al., 2021). Plasmablast are the earliest detected spike-specific B cell population after 5-10 days post-infection/vaccination (Kardava et al., 2022; Pape et al., 2021; Sokal et al., 2021) and are then replaced by a more long-

lived population of spike-specific MBCs (Cohen et al., 2021; Dan et al., 2021a; Goel et al., 2021b, 2021a; Kardava et al., 2022; Pape et al., 2021; Sokal et al., 2021). Plasmablasts are found to be elevated and persistent in severe COVID-19 (Dugan et al., 2021; Sokal et al., 2021; Woodruff et al., 2020). Some studies have highlighted that a large portion of the plasmablasts are not targeting spike (Dugan et al., 2021; Kardava et al., 2022). This suggests that increased plasmablast numbers are due to both higher levels of antigen due to uncontrolled infection potentiated by overall immune hyperactivation. However, it is unclear how many plasmablasts will participate in the establishment of long-lived ASCs. Overall, it has been observed that severe COVID-19 disease was associated with more extrafollicular B cell responses with higher levels of atypical MBCs (Ogega et al., 2021; Oliviero et al., 2020; Woodruff et al., 2020). However, atypical MBCs are part of a normal MBC response to SARS-CoV-2 infection (Ogega et al., 2021; Oliviero et al., 2020; Pušnik et al., 2022; Woodruff et al., 2020; Zurbuchen et al., 2023) and vaccination (Pape et al., 2021; Pušnik et al., 2022; Zurbuchen et al., 2023). In time, the MBC response focuses away from atypical and towards generating a steady-state pool of MBC comprised of resting MBCs and intermediate MBCs poised to be recalled upon re-exposure (Buckner et al., 2022).

Akin to the kinetics of the antibody response, hybrid immunity led to higher frequencies of spike-specific MBCs than in SARS-CoV-2 naïve (Andreano et al., 2021; Goel et al., 2021b, 2021a; Mazzoni et al., 2021, 2022; Reynolds et al., 2021). Breakthrough infection only modestly increased levels of spike-specific MBCs past the 2nd vaccine dose (Terreri et al., 2022), which mirrors the maximal titre effect seen with antibodies. Regardless of SARS-CoV-2 status, spike-specific MBCs induced by vaccination showed cross-reactivity against variants of concern (Goel et al., 2021a). Additional vaccination with a bivalent vaccine containing an Omicron spike (Alsoussi et al., 2023) or Omicron breakthrough infection (Weber et al., 2023), showed the recall of cross-reactive MBCs that could neutralise Omicron. MBCs cross-reactive for Omicron were generated from encounters with WT with these MBCs hardly maturing upon recall after exposure to Omicron (Weber et al., 2023). Overall, one Omicron infection or vaccination only generated low levels of spike-specific MBCs only specific for Omicron (Alsoussi et al., 2023; Weber et al., 2023; Yisimayi et al., 2023). Two Omicron breakthroughs increased Omicron-only MBC frequency (Yisimayi et al., 2023),

highlighting that MBCs may be less prone to immune imprinting than serum (Schiepers et al., 2023a, 2023b).

For SARS-CoV-2 naïve individuals, despite the lack of mucosal delivery, IgA and IgM -specific MBCs were detectable shortly after the 1st vaccine dose, with an additional vaccine dose skewing the spike-specific MBC response towards IgG+ MBCs (Kardava et al., 2022). Whereas individuals with prior-SARS-CoV-2 infection already showed a preference for IgG+ spike-specific MBCs after the 1st vaccine dose (Goel et al., 2021b, 2021a; Pape et al., 2021; Pušnik et al., 2022). Overall, this translated to preferential use of IgG1 and IgG3 for spike-specific MBCs after infection (Hartley et al., 2020; Zurbuchen et al., 2023) and after two vaccine doses (Amanat et al., 2021; Irrgang et al., 2022).

1.2.9. Other cell-specific responses to SARS-CoV-2.

T cells play an important role in the response to SARS-CoV-2 infection/vaccination by promoting viral clearance and coordinating the adaptive immune response, altogether this provides an added layer of immune-mediated protection on top of antibodies and B cells. Crucially, a CD4 T cell response is also required in concert to provide help to B cells and result in the production of antibody responses. Following, SARS-CoV-2 infection, SARS-CoV-2 specific T cells can target not only the spike protein but other structural proteins (M, N, E) and non-structural proteins (ORF1-10) (Grifoni et al., 2020). Akin to antibodies, early and broad T cell responses have been associated with reduced COVID-19 disease severity (Grifoni et al., 2020; Rydyznski Moderbacher et al., 2020; Tan et al., 2021). In addition, a study (Swadling et al., 2022) demonstrated the presence of T cells specific for proteins within the RTC, most likely developed by previous hCoV infections, which could prevent the establishment of infection before the development of an antibody response. Indeed, T cells can target well-conserved epitopes not available for recognition by antibodies which can add another layer of resilience to the immune response in the face of emerging variants. This means that cross-protective pre-existing CD8 T cells from hCoVs may mediate early viral clearance (Braun et al., 2020; Tan et al., 2021).

Spike-specific memory T cells can still be observed after 6-8 month-post SARS-CoV-2 infection (Cohen et al., 2021; Poon et al., 2021) and after vaccination (Goel et al., 2021a). Functional CD8+ spike-specific T cells will be detected earlier than CD4+ T

cells, from one week post-vaccination (Oberhardt et al., 2021). Post-vaccination, CD4 and CD8 T cells specific for spike are boosted after each dose, although the magnitude of the response does not improve with subsequent doses (Nayrac et al., 2022; Oberhardt et al., 2021; Zhang et al., 2022b). As with humoral/B cell responses, hybrid immunity confers higher frequencies of CD4/CD8 spike-specific T cells than SARS-CoV-2 vaccination alone (Mazzoni et al., 2021; Nayrac et al., 2022). In contrast to the lower binding and neutralising antibody titres seen against emerging variants, spike-specific T cell responses CD4+ and CD8+ responses stimulated by vaccination were cross-reactive with unchanged magnitude against a range of emerging variants (Liu et al., 2022a; Tarke et al., 2022). As discussed in **section 1.2.4**, all licensed vaccines in the UK will induce spike-specific T cells only, adding non-spike targets in future vaccines may provide added protection from T cells by stimulating T cell response towards these non-spike epitopes.

1.3. Human Immunodeficiency Virus-1

1.3.1. HIV-1 emergence and lifecycle.

A string of cases (Centers for Disease Control and Prevention (U.S.), 1981; Gottlieb et al., 1981; Masur et al., 1981) of Pneumocystis carinii pneumonia in 'previously healthy young gay men' in the summer of 1981 in California, a bacterial infection normally found in immunosuppressed individuals, provided the first hint of what would become known as acquired immunodeficiency syndrome (AIDS). In addition to the presence of opportunistic infections (e.g. Pneumocystis, Kaposi's sarcoma), AIDS was characterised by ongoing lymphopenia (Murray et al., 1984; Stahl et al., 1982). The pattern of transmissions (sexual/blood-borne) in men who have sex with men, intravenous drug users or haemophiliacs quickly pointed towards an infectious aetiology. The causal agent of AIDS was then identified with the isolation of a retrovirus now known as human immunodeficiency virus-1 (HIV-1) by two teams of researchers (Barré-Sinoussi et al., 1983; Gallo et al., 1984; Popovic et al., 1984). Since the beginning of the HIV pandemic, roughly 85 million people have been infected with HIV and 40 million have died. In 2022, 39 million people are currently living with HIV (PLWH), and 630,000 PLWH have died. The face of the HIV pandemic has also changed with early 50% of new infections being in women (United Nations Programme on HIV/AIDS (UNAIDS), 2023).

The best available evidence suggests that HIV-1 emerged through a zoonosis event from a chimpanzee's simian immunodeficiency virus (SIV) in the present-day Democratic Republic of Congo in the 1930s (Faria et al., 2014). Another HIV exists, HIV-2 which similarly emerged through zoonosis of a SIV from sooty mangabeys but only represents a minority of infections outside of Africa. There is extraordinary diversity across the different strains of HIV, in Europe and North America most HIV infections are attributable to HIV-1, group M (clade B) with group M (clade C) infections predominating in Africa although much greater diversity is found there (reviewed in (Sharp and Hahn, 2011)). Throughout the rest of this thesis, HIV-1 is referred to as simply HIV for simplicity.

HIV is an enveloped lentivirus of the *Retroviridae* family, with a genome of roughly 9.6kb. The genome of HIV encodes three major structural genes (*gag*, *pol*, and *env*), with *pol* encoding the required enzyme for the viral lifecycle (reverse transcriptase,

integrase and protease), and six accessory proteins (*tat*, *rev*, *nef*, *vif*, *vpu* and *vpr*). Briefly, HIV can enter any cells which have the CD4 receptor on their surface, traditionally these are CD4+ T cells, via interaction between CD4 and Env (Dalgleish et al., 1984). Further interaction with one of two co-receptors (CCR5 or CXCR4) (Deng et al., 1996; Feng et al., 1996) will trigger a chain of events leading to membrane fusion and entry of the capsid within the cytoplasm. Within the capsid, reverse transcription of the viral genome will be mediated by reverse transcriptase enzyme (encoded by *pol*). Lack of error-proofing in the activity of reverse transcriptase will lead to the wide genetic diversity found in HIV (Mansky and Temin, 1995). In an optimal infection, the capsid will then enter the nucleus before uncoating to prevent innate sensing of the viral genome (Burdick et al., 2020; Zila et al., 2021). within the nucleus, the now fully reverse-transcribed DNA can integrate within the host genome using integrase (also encoded by *pol*). The integrated viral DNA will then be transcribed into mRNA as part of the host's and translated into the different viral proteins. Integration of the viral DNA into the host's DNA in quiescent T cells allows for the establishment of latency where the viral DNA is effectively 'invisible' to the immune system and to anti-retroviral treatment (ART) (reviewed in (Dahabieh et al., 2015)). Translated proteins and transcribed mRNA will then be packaged into a new virion which will then be released. Further maturation of the virion will then proceed with cleavage of gag and pol into their mature forms by protease (also encoded by *pol*). Most of the different steps of the HIV replication lifecycle can be blocked by ART (***Figure 1.3.1***).

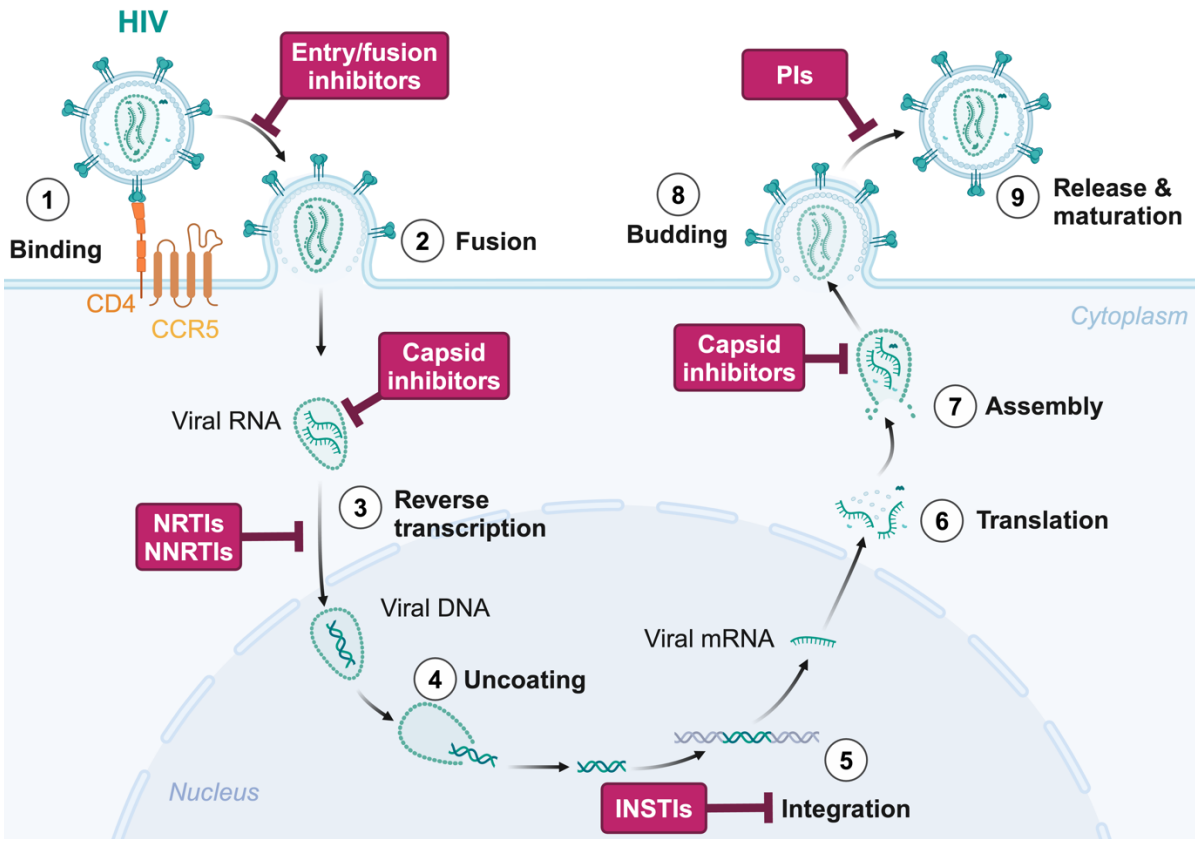

Figure 1.3.1: *HIV replication cycle. The HIV virion first binds to CD4 (1) and then utilises the coreceptor to mediate membrane fusion (2). Within the capsid, the process of reverse transcription of the viral RNA into DNA begins (3). The capsid then enters the nucleus and begins uncoating (4), this reveals the fully reverse-transcribed viral DNA which can then integrate into the host genome (5). Viral mRNA will be translated into proteins (6), which will then be assembled alongside the mRNA (7) to form a new HIV virion (8) which will be released and mature further (9). This cycle can be stopped at different steps using ART (different classes of drugs are highlighted in pink). ART can target enzyme activity: reverse transcriptase with NRTIs (nucleoside reverse transcriptase inhibitor)/NNRTIs (non-nucleoside reverse transcriptase inhibitor), integrase with INSTIs (integrase nuclear strand transfer inhibitors) or protease with PIs (protease inhibitors). ART can also block protein activity with entry/fusion inhibitors blocking CCR5 or the interaction between Env and CCR5 and capsid inhibitors with triggering HIV capsid uncoating/assembly. Diagram created with biorender.com.*

1.3.2. T cells, immune reconstitution and ART treatment.

The persistent presence of virus leads to the triggering of inflammation via innate sensing or by adaptive cells' secretion of pro-inflammatory cytokines, skewing the immune system towards a permanent inflammatory/antiviral mode. Viraemia acts as an 'initial insult' to the immune system leading to more or less reversible changes to T and B cell function as discussed below.

Early evidence immediately recognised that HIV was associated with lower levels of CD4+ T cells and CD4 T cell dysfunction (Lane et al., 1985; Murray et al., 1984; Stahl et al., 1982). It was then understood that the main target of HIV infection is CD4 T cells, with CD4 used as an entry receptor for HIV (Dalgleish et al., 1984). In general, there is a direct link between high levels of viraemia and low levels of CD4 T cells, which is associated with worse HIV outcomes (Mellors et al., 1997). Additionally, it has been shown that the risk of opportunistic infections was decreased in PLWH with higher CD4 counts (Ledergerber et al., 1999; Mocroft et al., 2007, 2013). There is evidence that HIV-specific CD4 T cells are preferentially infected, which further restricts the HIV-specific immune response (Douek et al., 2002). Infected T cells will then be destroyed upon virus exit from the infected cells which will further reduce the pool of CD4 T cells available. This reduction will therefore reduce the pool of possible TCRs (Heather et al., 2015), which limits cognate T cell help for B cells (more detail on the impact of HIV on B cells is discussed in **sections 1.3.3** and **1.3.4**). Additionally, death of HIV-infected CD4 T cells triggers the release of inflammatory cytokines which further reinforces the overall inflammatory state of HIV infection (Doitsh et al., 2014). In contrast to the reduction of CD4+ T cells, numbers of Tfh are preserved during chronic untreated HIV due to ongoing inflammation driven by viraemia (Lindqvist et al., 2012). However, these remaining Tfh may not be able to provide adequate help to B cells (Cubas et al., 2013) as they may play a more regulatory than helper role (Miles et al., 2015) which further exacerbates HIV-mediated B cell dysfunction. Tfh dysfunction was still preeminent in treated PLWH (Cubas et al., 2015). CD4 T cells can naturally reside within lymphoid tissue, therefore infection of CD4 T cells by HIV will lead to a state of general inflammation in lymphoid tissue and lymphadenopathy (Biancotto et al., 2007) which in turn leads to loss of tissue architecture via fibrosis, loss of CD4 T cells number and loss of GC function (Schacker et al., 2002). Excessive lymphoid fibrosis leads to lower effectiveness of ART (Schacker et al., 2005) and

vaccination in PLWH (Kityo et al., 2018). Similar processes of over-inflammation and loss of tissue architecture can be seen in the gut due to HIV antigen persistence (Estes et al., 2008). Once lymph node architecture is lost, this cannot be reversed even with successful ART (Sanchez et al., 2015).

An indicator of HIV disease is a skewed ratio of CD4 to CD8 T cells towards less CD4 helper T cells and more cytotoxic CD8 T cells. Indeed, CD8+ T cells are still present and functional and can help control the infection in the first instance (Borrow et al., 1994; Walker et al., 1988, 1986). To this effect, many efforts have been made to curate the CD8-response for HIV viral control (reviewed in (Collins et al., 2020)).

The first approved treatment for HIV was zidovudine/AZT, a re-purposed cancer drug which was effective at blocking the activity of reverse transcriptase as a nucleoside reverse transcriptase inhibitor (NRTI) (Fischl et al., 1987). AZT was both ineffective after a couple of years of treatment as the virus developed resistance mutations and was not well tolerated. In the mid-1990s the development of protease inhibitors (PI) combined with two NRTI, a combination referred to as HAART (highly active anti-retroviral therapy) was proved to be highly efficacious at maintaining viral load suppression (Gulick et al., 1997; Hammer et al., 1997). HAART (now mostly referred to simply as ART) has become the gold standard for HIV treatment and commonly also includes non-nucleoside reverse transcriptase inhibitor (NNRTI) and integrase inhibitors. Without treatment, there is an initial acute phase of HIV where CD4+ T cell count will plummet whilst viral load surges. This will then re-equilibrate naturally towards a viral set point i.e., equilibrium between CD4+ T cells and viraemia (Deeks et al., 2004; Mellors et al., 1997), partly mediated by CD8+ T cells viral control (Borrow et al., 1994). This state of chronic infection can be maintained without treatment for several years without severe disease although the immune system is being progressively damaged. With time, untreated HIV infection will lead to the development of AIDS. Whilst there is heterogeneity among individuals, roughly 50% of PLWH not on ART are expected to develop AIDS after 10 years of living with HIV (Rutherford et al., 1990). In contrast, with treatment, the viral load decreases to an undetectable level and AIDS can be prevented as long as treatment is maintained. However, CD4 T cells frequency and function are only partially restored depending on how early ART was initiated (Korencak et al., 2019; Le et al., 2013; The Antiretroviral Therapy (ART) Cohort Collaboration, 2003) (***Figure 1.3.2***). Indeed, the START and

TEMPRANO trials indicated the long-term benefit of starting ART even if CD4 counts were above 500 cells/μL rather than the <350 CD4 T cells/μL cut-off previously used (Lundgren et al., 2023; The INSIGHT START Study Group, 2015; The TEMPRANO ANRS 12136 Study Group, 2015) (***Figure 1.3.2***). Immediate initiation of ART upon HIV diagnosis is now the official guidance in the UK (British HIV Association, 2015). It is now understood that PLWH with continued ART adherence have undetectable viral loads have zero chance of passing it on to another person (Rodger et al., 2019). Despite this highly effective treatment, HIV remains a lifelong chronic infection with no functional cure bar a handful of individuals cured through complete reconstitution of their immune system by CCR5Δ32 stem cell/bone marrow transplant (Allers et al., 2011; Dickter et al., 2024; Gupta et al., 2019; Hsu et al., 2023; Jensen et al., 2023).

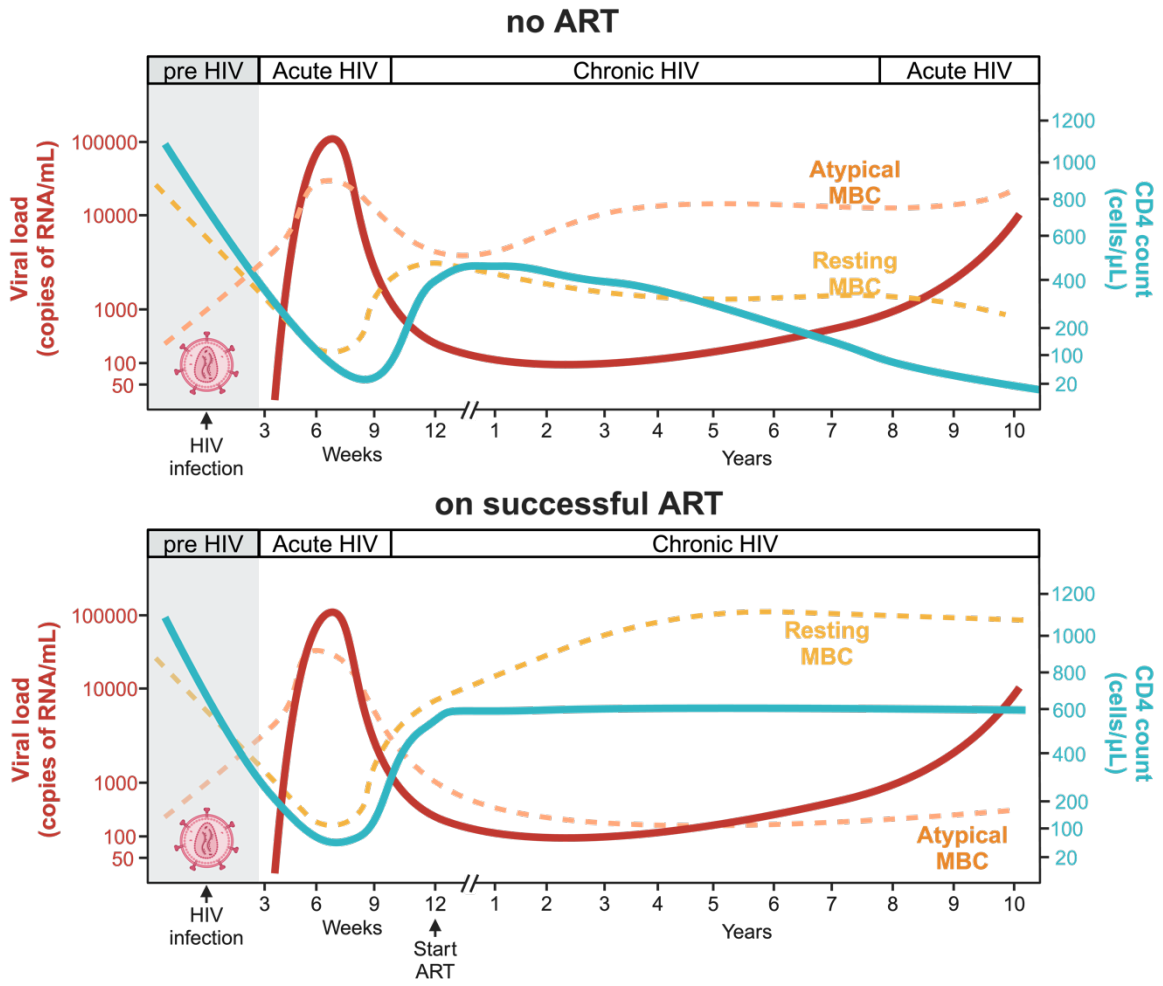

Figure 1.3.2: *Model of immune reconstitution on ART. Schematic of the dynamics of viral load (copies of RNA/mL – in red), CD4 T cell count (cells/μL – in blue) and of the frequency of resting (yellow) and atypical (orange) MBC without ART and with successful ART treatment. Diagram created with biorender.com.*

1.3.3. HIV-specific antibody responses in PLWH.

In the acute phase of HIV infection, the first antibodies targeting HIV's Env protein can be detected after ~13 days after the first detection of viraemia (Tomaras et al., 2008). These early antibodies mostly target non-neutralising epitopes on Env, and therefore fail to control viraemia (Tomaras et al., 2008). It is only after several months that neutralising antibodies against the autologous virus can be detected and this early neutralising activity can influence viral evolution (Richman et al., 2003; Wei et al., 2003),. In general, production of cross-reactive neutralising antibodies with a high degree of breadth is very rare, with only 10-30% of PLWH making cross-neutralising antibodies and 1-10% being able to make broadly neutralising antibodies (bnAbs) (reviewed in (McCoy and McKnight, 2017)) i.e. antibodies which can neutralise at least 30-99% of HIV pseudoviruses included in a cross-clade neutralisation panel with relatively high potency (reviewed in (Griffith and McCoy, 2021)). In the majority of PLWH, their HIV-specific antibody repertoire is mostly made up of non-neutralising antibodies, with no bnAbs and where most of the neutralising antibodies generated quickly become obsolete due to escape by the autologous virus (Bar et al., 2012). Generation of bnAbs is a rare event amongst PLWH because of the sheer viral diversity of HIV sequences at the population and individual level and the lack of understanding of which events within the host's immune system-HIV interaction lead to their generation. Efforts to recapitulate bnAbs development by immunisation have yielded mixed results (reviewed in (Haynes et al., 2023)). However, evidence has shown that passive transfer of a combination of monoclonal bnAbs in non-bnAb-producing PLWH led to suppression of viraemia without ART for a median of 5 months (Mendoza et al., 2018). Of note, PLWH who produce bnAbs often fail to control their own virus and have high viraemia (Gray et al., 2011). This suggests that chronic encounters with antigen are necessary to produce cross-protective neutralising responses. On the other hand, long-term non-progressors or elite controllers rarely produce bnAbs, and their ability to control their viraemia is mostly associated with protective HLA alleles and strong HIV-specific CD8 T cell responses (González et al., 2018), reviewed in (Rutishauser and Trautmann, 2022). In all cases, bnAbs represent the best antibody response that natural HIV infection can generate and a better understanding of bnAbs development will be needed to generate a successful vaccine against HIV.

1.3.4. The BCR repertoire in PLWH.

Overall, antibody maturation and development are perturbed in chronic HIV. Early reports hinted at some form of antibody dysfunction with the consistent observation of elevated IgG or hypergammaglobulinemia (Lane et al., 1983; Masur et al., 1981; Siegal et al., 1981; Stahl et al., 1982; Terpstra et al., 1989). IgGs in hypergammaglobulinemia are mostly non-HIV specific and produced by naïve B cells (De Milito et al., 2004; Wang et al., 1999), many of these IgGs are poly-specific for host antigens and may further potentiate T cell-mediated immune dysfunction (Wang et al., 1999). The acute phase of HIV antibody response is associated with a higher proportion of HIV-specific IgG3 antibodies (Yates et al., 2011). As discussed in **section 1.1.3**, class-switching operates in a consecutive manner of where each isotype gene sits in the locus: IgG3 antibodies are first produced after IgM, then IgG1 and so on with further isotypes being selected where more B cell stimulation occurs. This enrichment of IgG3 in the HIV-specific response suggests a lower level of affinity maturation. In support of this, atypical/CD27- MBCs expressing IgG3 are common in HIV (Kardava et al., 2014; Knox et al., 2017) and their generation has been associated with a GC-independent response (Budeus et al., 2015).

Most of the understanding of the BCR repertoire of PLWH has focused on bnAbs and other HIV-specific antibodies, and therefore in the absence of treatment. It is well-accepted that bnAbs present a high level of SHM and have longer CDRH3s than non-bnAbs (Griffith and McCoy, 2021). Env-specific BCRs were found to be enriched within atypical MBCs, with these BCRs being less somatically hyper-mutated than those of resting MBCs. This lower level of SHM is associated with inferior neutralisation capacity (Meffre et al., 2016). Considering non-specific antibodies, it was shown that PLWH who were unable to produce bnAbs and were not on treatment had less mutated IgG BCRs than HIV-negative controls whereas IgM BCRs showed no difference (Roskin et al., 2020). Additionally, BCRs from PLWH generally had longer CDRH3 and their repertoire was formed of larger clonal expansion (Roskin et al., 2020). Further to this, PLWH with a late start of ART had a BCR repertoire made up of larger clonal expansion compared to early ART starters when looking at bulk BCR in the HIV-infected gut (Planchais et al., 2023). Both studies (Planchais et al.,

2023; Roskin et al., 2020) reported higher usage of IGHV4-34 in PLWH compared to HIV-negative controls or in late versus early ART starters, which is associated with autoreactive responses. It is important to bear in mind that both studies looked at BCRs without knowing their specificity. HIV-specific BCRs included in these two studies likely make up only a small portion of the sampled BCRs if any, this suggests that chronic HIV also disturb the normal generation of non-HIV-specific BCRs.

1.3.5. B cell defects in PLWH.

HIV infection has a profound, lifelong impact on the immune system beyond simply infecting CD4+ T cells. The B cell compartment of the immune system is no exception to this with many studies showing defects in different subtypes of B cells responding to HIV or other pathogens compared to responses in the absence of chronic infection (reviewed in (Moir and Fauci, 2013, 2017)) (***Figure 1.3.2***). Early reports which highlighted T cell defects concurrently described a reduction in the quantity and quality of B cells (Lane et al., 1983; Schnittman et al., 1986; Stahl et al., 1982; Terpstra et al., 1989).

This is clearly associated with the loss of CD4 helper cells in general which has widespread ramifications on the integrity of the adaptive immune response. In the case of B cells, the lack of functional Tfh directly impacts the ability of PLWH to form successful GCs (Cubas et al., 2013). However, ongoing B cell dysfunction in PLWH cannot be sorely caused by the quantitative and qualitative defect of CD4 T cells. Just as the presence of viruses drives the T cell dysfunction, viraemia has a direct effect on B cell homeostasis as illustrated by the detection of B cell dysfunction prior to detectable T cell loss (Terpstra et al., 1989). Another piece of evidence is as described in **section 1.3.2**, the loss of lymphoid tissue architecture which also has a profound impact on GC response and therefore B cell response. Perhaps the most important clue that HIV infection directly impacts B cell function is that the start of ART, and therefore suppression of viraemia without immediate recovery of CD4 T cell counts, reverts many of the changes in MBC dysfunction (Fogli et al., 2012; Pensieroso et al., 2013). Similarly, PLWH on ART will downregulate the expression of ISGs on their B cells compared to untreated PLWH (Moir et al., 2004). In general, B cells are less responsive to T cell help in the presence of virus, which is recovered with the initiation of ART (Moir et al., 2003).

However, a hallmark of B cell defects in HIV is the abnormal and persistent high frequency of atypical (see **section 1.1.4.**, often described tissue-like in the HIV literature) CD21- CD27- memory B cells (MBCs) and increased activated CD21- CD27+ MBCs (Moir et al., 2008a). This hallmark is seen in viraemic individuals and is seldom present in such proportions in HIV-negative individuals outside of acute infection and vaccination settings (as discussed in **sections 1.1.4** and **1.2.7**). In untreated HIV atypical and activated MBC cells reportedly form the majority of HIV-directed B cell responses (Kardava et al., 2014; Moir et al., 2008a) but there are more of these dysfunctional subsets than antigen-specific cells by a substantial margin. Dysfunction from these MBC subsets may be due to increased apoptosis in $CD21^{lo}$ CD10- activated B cells, which suggests that atypical MBCs may represent a dead-end for MBC differentiation (Ho et al., 2006). Precursors to MBCs are also affected as there are increased frequencies of CD10+ transitional B cells in PLWH with active viraemia but not in aviraemic PLWH (Malaspina et al., 2006). Additionally, naïve (sometimes referred to as intermediate memory if CD10 and/or IgD is excluded) CD21+ CD27- memory B cells, were also found to be increased in PLWH on ART compared to HIV-negative controls (Moir et al., 2008b, 2010; Pensieroso et al., 2013). Increased frequencies of these precursors to MBCs suggest that in the presence of virus, immature/naïve MBCs are less able to further differentiate into resting MBCs. In balance with this accumulation of immature/naïve B cells, as HIV infection progresses, studies have found less circulating CD21+ CD27+ resting MBCs (De Milito et al., 2001; Moir et al., 2010; Titanji et al., 2006), which normally constitute the bulk of the steady-state MBC response. Thus, it seems likely that B cell defects in HIV would affect the maintenance of humoral immunity against other pathogens. This disturbed B cell (excess of atypical MBCs, less resting MBCs) phenotype was still present following the initiation of ART (Pensieroso et al., 2013), with early initiation after diagnosis having a greater effect on recovering a normalised frequency of resting MBCs compared to later initiation (Moir et al., 2010). In the context of HIV infection, plasmablasts are only elevated with active viraemia and are found in normal proportion in PLWH on ART (Buckner et al., 2013; Moir et al., 2010). Additionally, the excess of plasmablasts in uncontrolled viraemia may be auto-reactive (Liao et al., 2017). Interestingly, only a small proportion of the plasmablast population is actually HIV-specific (Buckner et al., 2013). Therefore, it has been hypothesised that this increase of plasmablast in viraemic HIV infection is not driven by HIV antigen but by the

inflammatory environment seen in HIV viraemia ((Moir et al., 2004; Stacey et al., 2009).

Much of this early literature showed these defects in viraemic individuals or shortly after the start of treatment. However, as guidelines for ART treatment have changed towards immediate ART initiation upon diagnosis, the current immunological context for PLWH nowadays after perhaps years on ART is different. Prior studies have shown that even after the initiation of ART, defects in the B cell compartment are only partly restored (Moir et al., 2008b, 2010; Pensieroso et al., 2009, 2013). However, different histories of ART adherence and viraemic relapse throughout an individual's life with HIV could also complicate the impact of chronic HIV on B cells and the immune system at large. Nonetheless, B cell homeostasis is disrupted in PLWH, even following successful ART. The exact causes of this disruption and the impact on non-HIV immune responses are not fully understood. This thesis aims to probe how this HIV-mediated perturbation of the MBC phenotype of PLWH affects the functionality of PLWH's B cells and antibodies in the context of another immune stimulus, here SARS-CoV-2 vaccination or infection.

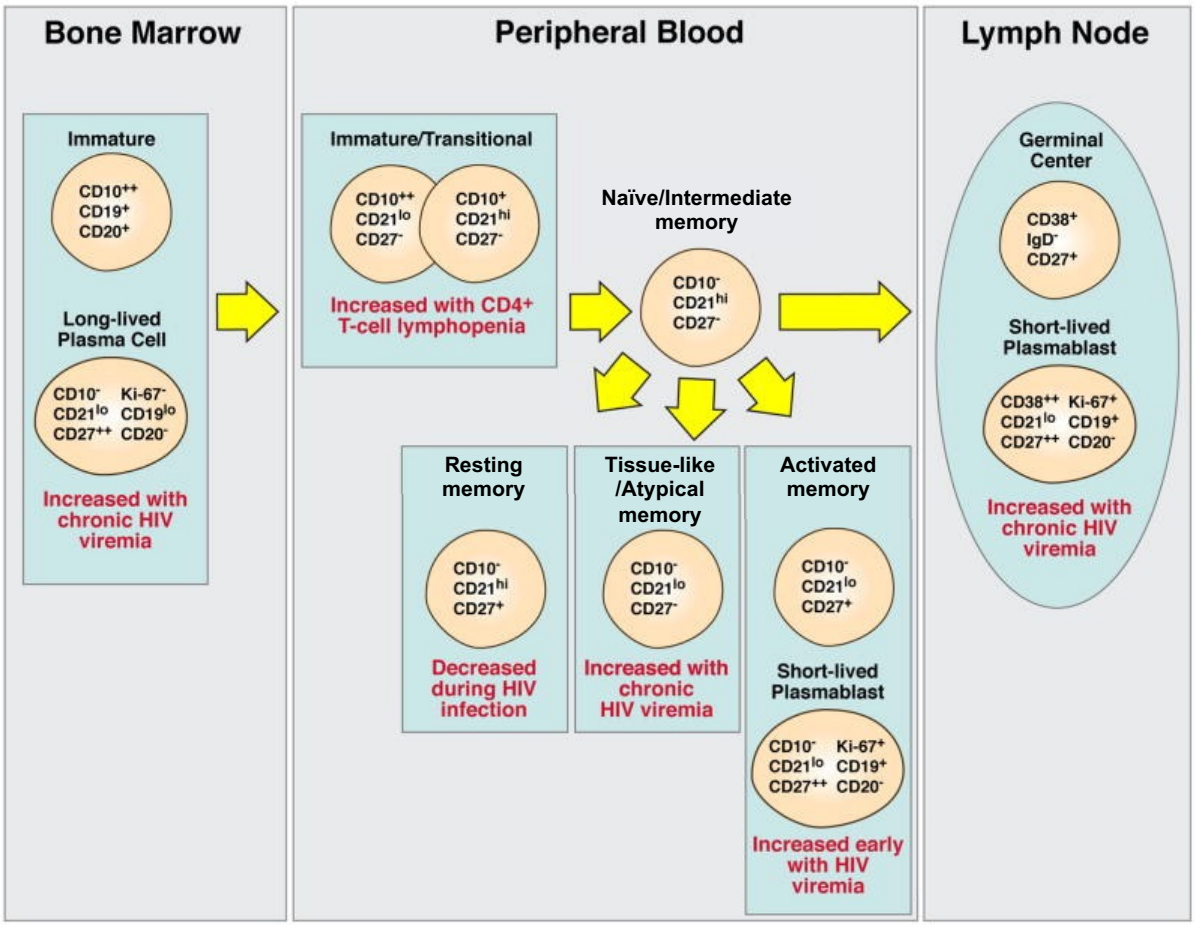

Figure 1.3.4: *Summary of B cell dysfunction in chronic HIV. Schematic of the different major types of B cells influenced by the presence of HIV and/or active viraemia according to their tissue and the different markers that can be used to identify them. Adapted from* (Moir and Fauci, 2017).

1.3.6. Responses to vaccines in PLWH.

The immune dysfunction seen in PLWH in the T and B cell compartment naturally leads to poorer serological outcomes following routine vaccinations. This fits with the original description of opportunistic infections in PLWH. Timing of ART initiation is also key in developing successful vaccine responses. Indeed, infants that initiated ART within their first year of life made better vaccine responses against a range of childhood vaccinations like measles or tetanus compared to late starters (Pensieroso et al., 2009). This was confirmed in adult PLWH, where PLWH who had received measles vaccination pre-HIV infection retained those responses years after vaccination (Wallace et al., 1994) but many PLWH vaccinated post-HIV acquisition lost antibodies against measles already after 1 year (Belaunzarán-Zamudio et al., 2009). This suggests that either preventing viraemia-induced MBC dysfunction and/or reducing it alongside T cell restoration with ART prior to vaccination could improve protective vaccine responses.

Inferior serological response after a full course of hepatitis B vaccination (e.g. low levels of anti-HBsAg antibodies or non-response) have been described in PLWH (Cruciani et al., 2009). Likewise, after influenza vaccination, PLWH make worse serological responses compared to age-matched HIV-negative controls (George et al., 2015) and have lower levels of cross-reactive MBCs between strains (Wheatley et al., 2016). A study (Cagigi et al., 2014) found that lower serological responses to influenza could directly be associated with higher frequencies of DN B cells (IgD- CD27-) in both PLWH and HIV-negative controls, the wider DN B cell subset includes atypical MBCs as described above in **section 1.1.4**.

Similar outcomes of qualitatively and quantitatively poorer vaccine responses in the elderly population (reviewed in (Crooke et al., 2019)) have led to the observation that chronic HIV infection leads to premature immunosenescence and can be thought of as a model for immune ageing (Nasi et al., 2017). Older age is associated with poorer MBC responses to influenza vaccination in the general population(George et al., 2015; Lambert et al., 2012), and this immunosenescence phenotype was exacerbated in PLWH (George et al., 2015; Pallikkuth et al., 2018). Underlying immune dysregulation in other cellular compartments, such as lower CD4 count, is also associated with lower levels of protective antibody responses after vaccination against influenza and

tetanus, which rely on the presentation of T-cell-dependent antigen (Kroon et al., 1994). In the same study, responses to the T-cell independent pneumococcal vaccine were similar between PLWH and HIV-negative controls regardless of CD4 count suggesting B cell dysfunction may be overcome in PLWH by some vaccines. However, this response may not be as long-lived as the response seen in HIV-negative controls as demonstrated by another study assessing antibody waning after the pneumococcal vaccine (Hung et al., 2010). Broadly, a meta-analysis found that vaccination responses after 5 years were systematically lower in PLWH compared to the general population (Kernéis et al., 2014). Overall, these serological defects are reflected in differential vaccination guidance for PLWH such as an additional (or higher) dose and accelerated schedule recommended by BHIVA for hepatitis B vaccination (BHIVA, 2015) or prioritised vaccination for PLWH during the UK's COVID-19 vaccination rollout (JCVI, 2022).

1.3.7. Impact of SARS-CoV-2 infection and vaccination in PLWH.

The emergence of SARS-CoV-2 led to the immediate concern as to how immunocompromised groups would fare against this novel pathogen. Available data on the rate of infection in PLWH compared to HIV-negative controls now shows that HIV-positive status did not result in an increased risk for SARS-CoV-2 infection (Charre et al., 2020; Huang et al., 2021; Park et al., 2022). One potential caveat to this is that early in the SARS-CoV-2 pandemic PLWH were asked to shield (BHIVA, 2020; BHIVA and Terrence Higgins Trust, 2020) which may have artificially lowered their SARS-CoV-2 infection risk.

On the other hand, large population studies consistently reported increased risk of mortality from COVID-19 for PLWH in general (Bertagnolio et al., 2022; Bhaskaran et al., 2021; Boulle et al., 2021; Brown et al., 2022; Geretti et al., 2021; Tesoriero et al., 2021; Yang et al., 2021b) and some reported a more modest increased risk of severe COVID-19 disease (Bertagnolio et al., 2022; Tesoriero et al., 2021; Yang et al., 2021b; Yendewa et al., 2021). As expected, most of these studies reported that these adverse outcomes were worsened for PLWH with active viraemia and/or low CD4 counts and/or lack of ART (Bertagnolio et al., 2022; Boulle et al., 2021; Dandachi et al., 2021; Hoffmann et al., 2021; Kassanjee et al., 2023; Nomah et al., 2021; Tesoriero et al., 2021; Wit et al., 2023; Yang et al., 2021b; Yendewa et al., 2021). One study highlighted

that COVID-19 disease severity was worse during the B.1.351 wave compared to the WT wave for PLWH as it may have further exacerbated the inherent CD4 lymphopenia in PLWH (Karim et al., 2021). Some smaller cohort studies reported no increased risk of death and severe COVID-19 disease in cohorts of PLWH with well-controlled HIV due to ART (Inciarte et al., 2020; Möller et al., 2023). Disparities in these findings can be attributed to differences in the proportion of PLWH on suppressive treatment or conversely with active viraemia and/or low CD4 counts included in these studies depending on geographical location, differences in shielding guidance from country to country, or lack of adjusting for comorbidities, smoking, socio-economic status and other social determinant of health tightly linked with COVID-19 disease and outcome.

Immunological studies of SARS-CoV-2 infection including that which forms **Chapter 3** of this thesis (Alrubayyi et al., 2021) have shown that SARS-CoV-2 infection is immunogenic enough to overcome any residual immune dysfunction with PLWH and HIV-negative controls making similar antibody and spike-specific T cell responses (Alcaide et al., 2022; Alrubayyi et al., 2021; Donadeu et al., 2022; Hwa et al., 2023; Motsoeneng et al., 2023; Snyman et al., 2022). There is some evidence that PLWH with lower CD4 count or active viraemia make slightly inferior responses than HIV-negative controls which is discussed at greater length in the discussion section of **Chapter 3**.

Upon vaccine rollout, PLWH were included in priority groups 4 and 6 for earlier COVID-19 vaccination than the general population and JCVI advised to invite this patient group for a 4th booster dose (JCVI, 2022). Successful immunological responses to vaccination were contingent on a minimum amount of CD4 T cells as described in **Chapter 4** of this thesis (Touizer et al., 2021). This was reflected in wider PLWH populations where PLWH with lower CD4 count made worse antibody responses against SARS-CoV-2 vaccination than those who had higher CD4 count (Jedicke et al., 2022; Marchitto et al., 2023; Matveev et al., 2023; Nault et al., 2022; Noe et al., 2021; Søndergaard et al., 2023; Zhou et al., 2023). When comparing to HIV-negative controls, there was heterogeneity in the findings with some studies, including the work described in **Chapter 4** of this thesis (Touizer et al., 2023) finding that PLWH made worse antibody response post-vaccination (Antinori et al., 2022; Bessen et al., 2022; Heftdal et al., 2022; Hensley et al., 2022; Jedicke et al., 2022; Levy et al., 2021; Madhi et al., 2021b; Matveev et al., 2023; Nault et al., 2022; Spinelli et al., 2021; Tuttle et al.,

2023), and some studies which found equivalent antibody responses between PLWH and HIV-negative controls (Brumme et al., 2022; Frater et al., 2021; Lapointe et al., 2023a, 2023b; Lombardi et al., 2022; Ogbe et al., 2022; Polvere et al., 2023; Verburgh et al., 2023; Vergori et al., 2022; Woldemeskel et al., 2022). These findings are discussed at greater length in the discussion section of **Chapter 4**. Finally, there is a paucity of data investigating the quality and phenotype of the MBC response to SARS-CoV-2 in PLWH which again is discussed in the discussion section of **Chapter 5**. Ultimately, it appears that PLWH may require additional vaccine doses to make fully equivalent responses to HIV-negative controls, as suggested by recent studies which suggest that PLWH were more likely than HIV-negative controls to experience Omicron variant mediated breakthrough infections (Coburn et al., 2022; Yang et al., 2024).

1.4. Aim & Hypothesis

Chronic HIV infection leads to some degree of permanent B cell dysfunction which persists to varying degrees even with ART. In turn, this may lead to differences in how B cells are able to mount a successful antibody response to infection or vaccination due to differences in the functionality and phenotypes of B cells responding. At the time of starting this project, many studies had characterised the different B cell defects in PLWH and the serological defect seen post-vaccination in PLWH but no study had precisely linked how this cellular defect affected the production of an efficient serological response compared to HIV-negative controls. To answer this, my PhD thesis studied a cohort of PLWH and HIV-negative control participants who were sampled around their SARS-CoV-2 infection and vaccination. Overall this thesis aims to answer the following research questions:

1. Do B cells responding in PLWH have a different functional capacity? More specifically, is there any difference in the quantity and quality of the binding and neutralising titres made by PLWH, compared to HIV-negative controls after SARS-CoV-2 infection (**Chapter 3**) and vaccination (**Chapter 4**). This was achieved by using semi-quantitative ELISA and pseudovirus neutralisation.

2. Do B cells responding in PLWH have a different phenotype? In particular, this was achieved by investigating the phenotype of the entire or 'global' B cell response and the spike-specific B cell response by multiparameter flow cytometry (**Chapter 5**).

3. Do responding B cells encode less functional antibodies? Finally, the last aim of this thesis was to sequence BCRs from PLWH and HIV-negative controls post-vaccination (**Chapter 6**) to better understand how the overall B cell dysfunction may impact PLWH's ability to recall their antibody repertoire and produce affinity-mature antibodies.

2. Methods

2.1. Study cohort sampling & ethics.

The protocols and study documents for the clinical sampling were approved by the local Research Ethics Committee (REC) Berkshire (REC 16/SC/0265, Jenner II study, Chief Investigator Dimitra Peppa) and South Central - Hampshire B (REC 19/SC/0423, Vaccines in Chronic Infection study, Chief Investigator Laura McCoy). All subjects enrolled in both studies provided written informed consent. Both studies complied with all relevant ethical regulations for work with human participants and conformed to the Helsinki Declaration principles and Good Clinical Practice (GCP) guidelines. All participants were recruited at the Mortimer Market Centre for Sexual Health and HIV Research (London, UK) or at the Ian Charleson Day Centre at the Royal Free Hospital (London, UK).

2.1.1. Convalescent cohort.

As part of a prospective, observational longitudinal cohort study (Jenner II), 47 HIV-negative controls and 35 PLWH were recruited on the basis of a prior confirmed or suspected SARS-CoV-2 infection during the convalescent phase of infection. These participants were recruited between the 23rd of July 2020 and the 5th of November 2020. PBMCs and plasma (or serum) were collected for each participant although there was only access to plasma/serum for this study. In total, 55 participants (24 PLWH and 31 HIV-negative) declared having had a lab-confirmed SARS-CoV-2 infection during the first wave of the pandemic. Confirmation of SARS-CoV-2 infection was accessed independently from this study via real-time polymerase chain reaction (RT-PCR), Roche/Abbot serological assays or lateral flow tests. The other 27 participants (23 PLWH and 4 HIV-negative controls) had a suspected SARS-CoV-2 infection either due to reported close contact with confirmed cases and/or COVID-19 symptoms but did not have access to testing. To validate the different SARS-CoV-2-specific serological assays, 22 participants (18 PLWH and 4 HIV-negative controls) who were sampled pre-COVID-19 pandemic (July 2016 – November 2019) as part of the Jenner II study were included. Additionally, through this same study, there was access to one participant with a history of a prior SARS-CoV-1 infection.

For each participant, limited clinical information was recorded and/or made available to the research team, this included days since symptom onset (DPSO) for participants with lab-confirmed and suspected SARS-CoV-2 infection, gender, age, ethnicity, and severity of COVID-19 disease (based on the WHO progression scale (Marshall et al., 2020)). All recruited PLWH had undetectable viral loads and were currently on ART. For PLWH, there was access to a recent CD4 count (cells/μL) and CD4:CD8 ratio measured as part of their routine clinical care. The clinical characteristics of participants are summarized in ***Table 3.2***.

2.1.2. Vaccination cohort.

As part of two prospective, observational longitudinal cohort studies (VCI - Vaccine in Clinical Infection and Jenner II), 64 HIV-negative controls and 111 PLWH were recruited. Participants were sampled longitudinally throughout their COVID-19 vaccination regimen for plasma or serum and PBMCs. Participants received a mix of available COVID-19 vaccination (Pfizer-BioNTech's BNT162b2; Moderna's mRNA-1273 or Astra-Zeneca's AZD1222) depending on what was available to them at the time according to the JCVI guidelines (JCVI, 2022). Not every participant was sampled at all timepoints. Timepoints are defined as follows:

- Baseline: sampled before any COVID-19 vaccination.
- Post 1st vaccine dose: sampled ≥12 days following the 1st dose of approved COVID-19 vaccination.
- Post 2nd vaccine dose: sampled between 7 and 70 days following the 2nd dose of approved COVID-19 vaccination.
- Pre 3rd vaccine dose: sampled ≥70 days following the 2nd dose of approved COVID-19 vaccination.
- Post 3rd vaccine dose: sampled >7 days following the 3rd dose (or 1st booster) of approved COVID-19 vaccination.

These time cut-offs were chosen to both to allow the development of a de-novo (or recall) immune response following each vaccination and in the case of the pre-3rd vaccine dose timepoint to best evaluate waning (Cohen et al., 2021; Dan et al., 2021; Goel et al., 2021a; Levin et al., 2021; Seow et al., 2020).

At each visit, participants were asked to report any history of SARS-CoV-2 infection. Between vaccinations, 10 participants in total declared a breakthrough infection: 3 provided pre 3rd vaccine dose samples, 6 post 3rd vaccine dose samples and 1 provided both pre and post 3rd vaccine dose samples.

For each participant, limited clinical information was recorded and/or made available to the research team, this included days since last vaccination, prior history of SARS-CoV-2 infection, gender, age, and ethnicity. All recruited PLWH had undetectable viral loads and were currently on ART. For PLWH, there was access to a recent CD4 count (cells/μL) and CD4:CD8 ratio measured as part of their routine clinical care. The clinical characteristics of participants and a full breakdown of how many participants from which group are included at which timepoint are summarized in ***Tables 4.3.1*** and ***4.3.2***.

2.2. Blood processing

Approximately, 60mL of blood was collected per participant in heparin-coated tubes. PBMCs were isolated from whole blood via density-gradient sedimentation. Whole blood was first collected by centrifugation for 5 min at 800g with a high braking speed to efficiently separate the plasma from blood. The plasma was then directly aliquoted and stored at -80ºC for future use. The remaining blood was diluted 1:1 with either 1X phosphate-buffered saline (PBS) or Roswell Park Memorial Institute media (RPMI) and layered onto 15ml of Ficoll (Cytiva) subjected to centrifugation for 20min at 800g without brake. The PBMC layer was then collected in a separate tube and topped with 1X PBS or RPMI to achieve a volume of 50mL and was then collected via centrifugation for 10 min at 400g. Finally, the washed PBMCs were counted in 10mL of 1X PBS or RPMI using trypan blue exclusion either manually or using an Automated Cell Counter (BioRad). PBMCs were aliquoted in a cryovial at $1x10^6$ cells/mL in a cryo-preserving solution made of foetal bovine serum (FBS; Gibco) supplemented with 10% dimethylsulfoxide (DMSO; Sigma). Cryopreserved PBMC were then stored at -80ºC overnight in a MrFrosty and then stored in LN2 for long-term storage.

2.3. Enzyme-linked immunosorbent assays (ELISA).

2.3.1. S1 and N semiquantitative ELISAs

This assay was set up previously in our lab by Luke Muir (Muir et al., 2021; O'Nions et al., 2021; Rees-Spear et al., 2021), based on assays developed in collaboration with the groups of Katie Doores (KCL) and George Kassiotis (Francis Crick Institute) (Ng et al., 2020; Pickering et al., 2020). In a 96-half-well NUNCMaxisorp plate (Nalgene), three columns were coated overnight at 4°C with 25 µl of goat anti-human F(ab)'2 (1:1000) in 1X PBS to generate an internal standard curve, whilst the other nine columns were coated with the 25µl antigen of interest, here purified SARS-CoV-2 WT S1 protein or N protein (a kind gift from Peter Cherepanov, Francis Crick Institute (Ng et al., 2020)) at 3 µg/ml in 1X PBS. The next day, plates were washed with PBS-T (0.05% Tween in 1X PBS) four times and blocked for 1h at room temperature (RT) with assay buffer (5% milk powder in PBS-T). Assay buffer was then removed and 25 µl of the participant's plasma at dilutions from 1:50−1:10000 in assay buffer was added to the antigen-coated wells in duplicate. Serial dilutions of known concentrations of IgG were added to the F(ab)'2 IgG-coated wells in triplicate starting from a concentration of 1000 ng/mL. After 2 h of incubation at RT, the assay plates were washed four times with PBS-T. Finally, 25 µl of alkaline phosphatase (AP)-conjugated goat anti-human IgG (Jackson ImmunoResearch) at a 1:1000 dilution in assay buffer was added to each well and incubated for 1h at RT. Plates were then washed six times with PBS-T, and 25 µl of AP substrate (Sigma Aldrich) was added. Optical density (OD) was measured using a MultiskanFC (ThermoFisher) plate reader at 405 nm. Each serum dilution was carried out in duplicate, the average OD was taken to interpolate S1 and N-specific IgG titres (µg/mL) from the IgG standard curve using a 4PL regression curve-fitting model on GraphPad Prism (GraphPad). Samples where no detectable binding was detected were assigned an arbitrary concentration of 0.2 µg/mL for visualisation.

2.3.2. Total IgG ELISAs

To measure total IgG levels in plasma, a 96-half-well NUNCMaxisorp plate was entirely coated overnight at 4°C with 25 µl of goat anti-human F(ab)'2 (1:1000). As above, plates were washed four times in PBS-T and blocked for 1h at RT in assay

buffer. 25µl of serial dilutions of patient plasma (1:100 to $1:10^7$) were added in duplicates to the plate alongside known concentrations of IgG in triplicates. After 2h of incubation at RT, plates were washed four times with PBS-T and 25 µl AP-conjugated goat anti-human IgG (1:1000 in assay buffer) added to each well and incubated for 1h at room temperature. Plates were then washed with PBS-T six times, and 25 µl of AP substrate was added. ODs were measured using a MultiskanFC plate reader at 405 nm. Each serum dilution was carried out in duplicate, the average OD was used to interpolate total IgG titres (mg/mL) from the IgG standard curve using a 4PL regression curve-fitting model on GraphPad Prism.

2.4. IgG purification

As all the PLWH participants in this study were on ART, the remaining ART in their plasma interfered with the lentivirus-based pseudotype neutralization assay. To mitigate this, IgG was purified from plasma using a 96-well protein G spin plate (Pierce). The plate was first washed by addition of 200µL per well of 1X PBS, placed in a collection plate and subjected to centrifugation at 1000g for 1 min, discarding the flowthrough from the collection plate. 180µL of plasma per sample was then added alongside 20µL of 10X PBS to each well containing protein G resin and left to incubate on a shaker at RT for 30 min to capture plasma IgG. The plate was then placed in a clean collection plate and subjected to centrifugation at 1000g for 1 min. The plasma flowthrough was then reapplied to the same wells of the protein G spin plate for an extra 30 min incubation at RT on a plate shaker. Afterwards, it was placed in a clean collection plate and subjected to centrifugation at 1000g for 1 min and flowthrough discarded. Each well of the protein G spin plate was then washed thrice with 200µL of 1X PBS as above. To elute the captured IgG, 200µL of 0.1M glycine (pH=2-3) was added to each well of the protein G spin plate, which was placed onto a fresh collection plate containing 20µL of 2M Tris (pH=7.5-9) in each well. The collection/protein G spin plate was then subjected to centrifugation at 1000g for 1 min, and the combined glycine/Tris eluate containing IgG was reapplied to the wells of the protein G plate and subjected to centrifugation again at 1000g for 1 min. To remove Tris/Glycine buffer from the purified IgG, the eluate was placed in a 0.5mL 50KD concentrator (Pierce) alongside 200µL of 1X PBS and subjected to centrifugation at 10000g for 10 min in a table-top microfuge and discarding the flowthrough. The purified IgG was then washed by adding 400µL of 1X PBS to the upper chamber of the concentrator and subjected

to centrifugation at 2500g for 10 min in a table-top microfuge then discarding the flowthrough, this was repeated twice to wash any remaining elution buffer. Finally, the membrane of the upper chamber of the concentrator was washed with 150µL of 1X PBS to collect the purified IgG for quantification (mg/mL) by measuring absorbance at 280nm on a Nanodrop (ThermoFischer). The entire volume of purified IgG was then filtered sterile using a 0.22µm PDVF hydrophilic membrane filter plate (Corning) and stored at 4°C for further use.

2.5. Cell Culture

HeLa-ACE2 cells (a kind gift from James Voss, The Scripps Research Institute) and HEK-293T cells were cultured in complete DMEM (Dulbecco's Modified Eagle's Medium (Gibco) supplemented with 10% FBS and 50µg/ml penicillin-streptomycin) at 37°C with 5% CO2. Adherent cells were split every 2-3 days using 0.25% trypsin-ethylene diamine tetra acetic acid (EDTA; Gibco).

HEK-293F cells were cultured in Freestyle™ 293 Expression Medium (Gibco) at 37°C in a shaking incubator with 5% CO2. Suspension cells were split every 3 days.

2.6. Pseudovirus neutralisation

2.6.1. Pseudovirus plasmid transformation and preparation.

The plasmids used to generate pseudoviruses were p8.91, an HIV-1 gag/pol packaging plasmid; pCSLW an HIV-1 luciferase reporter vector plasmid (Grehan et al., 2015; Wright et al., 2008; Zufferey et al., 1997, 1998) and a plasmid containing the SARS-CoV-1 or 2 spikes of interest, either WT SARS-CoV-2, B.1.1.7 or Omicron BA.1 (Lechmere et al., 2022; Rees-Spear et al., 2021; Seow et al., 2020). Plasmids were transformed using 10-beta chemically competent *E. coli* cells (NEB). First, the plasmid DNA of interest was mixed at a ratio of 1:10 ratio of DNA to competent cells. The DNA/cells mixture was then incubated for 30 min on ice, followed by heat shocking at 42ºC for 30 sec and another 5 min incubation on ice. The transformed cells were then further diluted into 5mL of Luria-Bertani (LB) broth (10g of Miller LB Broth powder (Fischer Scientific) mixed into 400mL of ddH20, autoclaved before use) and left to incubate at 30ºC degrees at 220 rotation per minute (RPM) for 1h in a shaking incubator. After incubation, the transformed cells were plated onto LB agar plates (15g of Miller LB Agar powder (Invitrogen) mixed into 400ml ddH20, autoclaved before use)

supplemented with 100 µg/mL ampicillin (Sigma). The agar plates were then incubated overnight at 30ºC. The next day, single colonies were picked and grown into 5mL of LB broth containing 100 µg/mL ampicillin to incubate overnight at 30ºC degrees at 220RPM in a shaking incubator. The following day, DNA could directly be extracted from the transformed cell culture using a QIAprep Spin Miniprep Kit (QIAGEN) according to the manufacturer's instruction or glycerol stocks were prepared using an equal volume of transformed cell culture to 80% glycerol which was stored at -80ºC for future large-scale DNA extraction.

For large-scale DNA extraction, cultures of 2µL of a glycerol stock into 5mL of LB broth supplemented with 100 µg/mL of ampicillin were grown at 30ºC degrees at 220RPM overnight in a shaking incubator. These cultures were then upscaled into 200mL of LB broth supplemented with 100 µg/mL of ampicillin and grown again at 30ºC degrees at 220RPM overnight in a shaking incubator. The next day, DNA could directly be extracted from the transformed cell culture using a QIAGEN Plasmid Maxi Kit (QIAGEN) according to the manufacturer's instructions.

2.6.2. Pseudovirus production and titration.

This assay was set up previously in collaboration with the group of Katie Doores (O'Nions et al., 2021; Rees-Spear et al., 2021; Seow et al., 2020). In a T75 flask, $3x10^6$ HEK-293T cells were seeded in 10mL of complete DMEM. The next day, the following transfection mix was prepared: 1 mL of Optimem (Gibco); 90 µL of PEI-max (1mg/mL); 10 µg of p8.91 HIV-1 gag/pol packaging plasmid and of pCSLW HIV-1 luciferase reporter vector plasmid and 5 µg of the SARS-CoV-2 spike plasmid of interest. The transfection mix was left to incubate for 20 min before being added to the seeded HEK-293T cells and then left to incubate at 37ºC with 5%CO2 for 72h before being collected and filtered through a 0.45 mm filter (Millipore). The pseudovirus preparations were then frozen down at -80ºC for future use. A small aliquot was kept to titrate the pseudovirus preparation. Briefly, the pseudovirus preparation was serially diluted in complete DMEM in a 96-well white plate (ThermoFischer). Then, 100µL of HeLA-ACE-2 cells (at a $1x10^5$ cells/mL concentration) were added to each well, and the plate was incubated for 72h at 37ºC with 5%CO2. After the incubation, the supernatant was aspirated, and cells were lysed using 1X luciferase buffer (10X buffer: 33g of 25M Glycylglycine (Sigma), 37g of MgSO4 heptahydrate (Sigma) and 18.8g EGTA

tetrasodium (Sigma) mixed in 900mL ddH20 with 100mL of Triton X-100, adjust pH=7.8 with 5M NaOH (Sigma)). BrightGlo luciferase substrate (Promega) was then added for a final concentration of 1:20 in 1X luciferase buffer, and relative light unit (RLU) values were read on a Glomax (Promega) or BioTek Synergy H1 (Agilent) plate reader. The dilution of a given pseudovirus preparation to be used in neutralisation assays was chosen by having at least 150,000 RLU (relative light units) or an RLU which was at least 20x over the background (cells-only wells). Alternatively, the pseudovirus preparation could be used neat directly in an assay.

2.6.3. Pseudovirus neutralisation assays.

Neutralisation assays were performed in a 96-well white plate by adding either duplicate serial dilutions of neat plasma in complete DMEM starting at 1:50 for HIV-negative samples or the appropriate starting dilution explained further for samples from PLWH. Compared to the amount of total IgG present in neat plasma calculated in **section 2.4**, the IgG purification protocol can either concentrate or more likely, dilute the amount of IgG that is found in the purified output. As such, to make sure to add an equivalent in a neutralisation assay amount of purified IgG compared to the original total IgG amount found in neat plasma, the following calculation was used. Instead of a starting serial dilution of 1:50 as is standard with neat plasma, the new starting serial dilution is calculated for either 200 or 400µg/mL of purified IgG based on the total IgG amount in neat plasma (ideally as close to 1:50 as possible):

$$New\ starting\ dilution = \frac{Total\ IgG\ in\ neat\ plasma\ (mg/mL)}{200\ or\ 400\mu g/mL}$$

This then allows to know which is more appropriate between 200 or 400µg/ml and calculate the volume of purified IgG needed to add for this new starting dilution:

$$Volume\ of\ purified\ IgG = \frac{Final\ volume\ of\ well}{\frac{Amount\ of\ purified\ IgG\ (mg/mL)}{200\ or\ 400\mu g/mL\ \times 2}}$$

To the plasma serial dilution is added the appropriate amount of filtered pseudovirus and then incubated for 1h at 37°C 5% CO2 before adding 10,000 HeLa-ACE2 cells in 100µL per well. After a 72h incubation at 37°C 5%CO2, the supernatant is aspirated, and cells are lysed. BrightGlo luciferase substrate is then added, and RLU values are read on a Glomax or BioTek Synergy H1 plate reader. Each serum dilution was carried

out in duplicate. RLU readouts were used to calculate the reciprocal inhibitory dilution at which 50% of the virus activity is neutralised by plasma (ID_{50}) for each sample on GraphPad Prism as described previously (Montefiori, 2009). Samples with no detectable neutralising activity were assigned an arbitrary ID_{50} of 1:20 for visualisation.

2.7. Live neutralisation

All the live neutralisation assays were carried out by Pehuén Pereyra Gerber (University of Cambridge) as described previously (Bergamaschi et al., 2021; Gerber et al., 2022; van der Klaauw et al., 2023). The SARS-CoV-2 virus used in this study was SARS-CoV-2/human/Liverpool/REMRQ0001/2020, which was an early WT isolate of SARS-CoV-2, a kind gift from Ian Goodfellow (University of Cambridge, UK), isolated by Lance Turtle (University of Liverpool, UK) and David Matthews and Andrew Davidson (University of Bristol, UK) (Daly et al., 2020; Patterson et al., 2020). HEK293T-ACE2-30F-PLP2 reporter cells (clone B7) expressing SARS-CoV-2 Papain-like protease-activatable circularly permuted firefly luciferase (FFluc) were seeded in 96-well plates. The next day, SARS-CoV-2 viral stock (multiplicity of infection (MOI) = 0.01) was pre-incubated with a 3-fold dilution series of each sample for 2h at 37ºC, then added to the cells. Before use, the plasma was heat-inactivated at 56ºC for 30min. 16h post-infection, cells were lysed in BrightGlo Luciferase Buffer (Promega) diluted 1:1 with 1X PBS and 1%NP-40, and FFluc activity was measured by luminometry. Experiments were conducted in duplicate. To obtain neutralizing antibody titres at 50% inhibition (NT_{50}), titration curves were plotted as FFluc vs log (serum dilution), then analysed by using a 4PL regression curve-fitting model on GraphPad Prism. Samples with no detectable neutralising activity were assigned an arbitrary NT_{50} of 1:20.

2.8. Protein production for spike and RBD

2.8.1. Transfection

To produce biotinylated spike or RBD protein, HEK-293F were seeded at $1x10^6$ cells/mL in an Erlenmeyer flask. The next day, a transfection mix was prepared (for 200ml of cells) of 72µg of spike-Avi-His or RBD-Avi-His plasmid, 18µg of BirA plasmid into 11mL of Optimen alongside 2mL of PEI-Max. All plasmids were designed and previously validated by Katie Doores' laboratory (Graham et al., 2021; Seow et al., 2020). The spike plasmid was optimised to stabilise the expressed spike in a pre-

fusion conformation by including four glycine and two proline residues at the furin cleavage site. The transfection mix was left to incubate for 20 min before being added to the 293F cells alongside 3mL of 10mM biotin and left to incubate at 37°C 5% CO2 for 7 days before being harvested for purification.

2.8.2. His GraviiTap purification of spike and RBD proteins.

The following work was carried out at 4°C to protect the integrity of the produced protein. The harvested supernatant from transfected cells was filtered through a 0.45µm unit imidazole (Sigma) to achieve a final concentration of 20mM, before being placed in a His GraviTap (Cytiva) column to drip through. The column was then washed with 20mM imidazole. To elute the captured protein an elution buffer of 500mM imidazole was used. The eluted protein was then concentrated with a 100KD concentrator (Merck) and washed with 1X PBS to remove excess buffer before quantification using a Nanodrop.

2.8.3. Size exclusion chromatography.

The purified biotinylated protein produced was further purified through size exclusion chromatography using an AKTApure system (Cytiva) with a Superdex 200 Increase 10/300 GL column (Sigma) by Sarah Griffith to select for fractions containing trimeric Spike or monomeric RBD protein which were then pooled together and concentrated.

2.9. Memory B cell flow cytometry phenotyping

This flow cytometry panel was first optimised by Anna Jeffery-Smith (Jeffery-Smith et al., 2022). To assess the phenotype of B cells, previously cryopreserved aliquots of $10x10^6$ PBMCs were quickly thawed in 10mL of 1X PBS and collected by centrifugation for 15 min at 600g. They were then counted manually or with an automated cell counter to assess cell recovery. At least $5x10^6$ cells in 200µL were plated for the main panel (***Table 2.9***) and any leftover cells in 200µl were plated for the fluorescence minus one (FMO) panel which did not include the spike and RBD bait stains. With each run, the PBMCs from the same participant were run each time to assess any potential inter-assay variability. For the main panel, tetramer baits were prepared as follows and incubated for 30 min protected from the light at 4°C before use:

Protein	Fluorophore	1X PBS
1µg purified biotinylated spike	1µl streptavidin-conjugated APC	7µl
1µg purified biotinylated spike	0.5µl streptavidin-conjugated APC	7.5µl
0.5µg purified biotinylated spike	1µl streptavidin-conjugated BV421	8µl

Plated cells were then stained 50µL of the following panel for 30 min whilst covered to prevent photobleaching:

Marker	Fluorophore	Reference	Dilution
IgG	FITC	BD #560952	5:100
Live/Dead	UV	Invitrogen #L23105	2:1000
CD19	BV786	BD #740968	2:100
CD27	BUV395	BD #563815	1:100
IgD	PE-Cy7	BD #561314	1:100
IgM	APC-Cy7	BioLegend #314520	1:100
CD20	AF700	BD #560631	1:100
CD21	BV711	BD #563163	1:100
CD38	PE-dazzle	BD #562288	0.5:100
CD3	BV510	BioLegend #317332	0.5:100
CD14	BV510	BioLegend #301842	0.5:100
RBD (biotinylated)	BV421-streptavidin	BioLegend #405226	2:100
Spike (biotinylated)	PE-streptavidin	Agilent #PJRS25-1	2:100
Spike (biotinylated)	APC-streptavidin	Agilent #PJ25S	2:100

Table 2.9: *Staining panel for MBC phenotyping.*

Stained PBMCs were then washed 1X PBS before being fixed in 70µL of CytoFix/Perm (BD) and kept at 4°C before acquisition. Compensation controls were prepared according to the manufacturer's instructions using anti-mouse Ig/κ CompBeads (BD). Samples were acquired on an LSR-Fortessa (BD) flow cytometer. Data was analysed (see ***Figure 5.2*** for gating strategy) on FlowJo v10 (FlowJo). For further analysis of the phenotype of spike-specific MBCs, analysis was limited to samples for which at least 50 cells were characterised as CD19+ CD20+ $CD38^{lo/-}$ IgD- spike-PE+ spike-APC+ as previously defined (Jeffery-Smith et al., 2022).

2.10. Spike-specific B cell sorting.

2.10.1. Staining PBMCs for spike-specific sorting.

This panel adapted the B cell phenotyping panel in **section 2.9** and another sorting-based panel used previously by the lab (Griffith et al., 2024). Cryopreserved aliquots of $10x10^6$ PBMCs were quickly thawed into 15mL of complete DMEM and collected

by centrifugation for 5 min at 300g at 4ºC. Media was then removed, and cells were resuspended into 1mL of complete DMEM. Cells were split into $9x10^6$ for staining and $1x10^6$ to prepare dry pellets (see **section 2.12.1**). With each run, the PBMCs from the same participant were run each time to assess any potential inter-assay variability and to create an unstained control for compensation and mock control where the full stain panel in ***Table 2.10.1*** was included but PBS was conjugated with the streptavidin stains rather than biotinylated proteins to assess any background fluorescence. The $9x10^6$ cells included for staining were further collected by centrifugation for 5 min at 300g at 4ºC. The cells were then resuspended in 200µL of 1X PBS with 0.5µL of live-dead Zombie Aqua™ Fixable Viability (BioLegend) and incubated at RT protected from the light for 20 min. After the incubation, 1mL of complete DMEM was added to the cells to quench any excess live-dead stain, and the cells were collected again for 5 min at 300g at RT. The cells were then further washed in 1mL of 1X PBS by centrifugation for 5 min at 300g at RT before being resuspended in the 100µL of 1X PBS including all the stains shown in ***Table 2.10.1*** and incubated for a further 30 min at RT protected from the light. Bait stains were prepared as in **section 2.9**. Finally, the stained cells were washed twice with 5mL of 1X PBS by centrifugation for 5 min at 300g at RT before a final resuspension in 1.6mL of 1X PBS by pushing the cell suspension through the 35µM filter cap of a polystyrene sorting tube (FischerScientific). The stained cells were kept at 4ºC until acquisition on a FACSAria Fusion (BD) flow cytometer. Before sorting, 10,000 events were acquired to assess MBC phenotype. For each participant, CD4- CD19+ IgG+ (or IgM+) double-positive spike-specific B cells were sorted into lysis buffer (see **section 2.10.2**). First, a full plate with 1 spike-specific IgG+ B cell per well was sorted (with the last column left blank for negative controls). If there were any remaining cells 100 spike-specific IgG+ or IgM+ B cells per well were sorted. To prevent RNA degradation of the now lysed cells, each sorted plate was quickly subjected to centrifugation at 8000g and snap frozen by submerging the plate into dry ice and stored at -80ºC until further use. BCRs were amplified from sorted plates containing a single cell per well using the pipeline described in **section 2.11** whilst amplification of BCR for sorted plates containing 100 cells per well is described in **section 2.12**.

Marker	Fluorophore	Reference	Dilution
CD19	BV786	BD #740968	2:100
CD21	PE-Cy7	BD #561374	1:100
CD27	BV421	BD #562514	2:100
CD4(dump)	BV510	BD #562971	2:100
IgG	FITC	BD #560952	5:100
IgM	APC-Cy7	BioLegend #314520	1:100
Live dead	Aqua	Biolegend #423101	
Spike (biotinylated)	PE-streptavidin	Agilent #PJRS25-1	2:100
Spike (biotinylated)	APC-streptavidin	Agilent #PJ25S	2:100

Table 2.10.1: *Staining panel for spike-specific MBC sorting.*

2.10.2. Lysis plate preparation for sorted cells.

For plates which received a single cell, lysis buffer plates were prepared before sorting by adding 0.5µL of RNAse OUT (Invitrogen), 5µL of First Strand Superscript III Buffer (Invitrogen), 1.25µL of 0.1M Dithiothreitol (DTT, Invitrogen) and 0.125µL of IGEPAL (Sigma) into ddH20 for a total volume of 25µL per well. For plates which received 100 cells, lysis buffer plates were prepared before sorting by adding 1µL of RNAse OUT and 0.45µL of IGEPAL into ddH20 for a total volume of 15µL per well.

2.11. Single-cell PCR pipeline

2.11.1. cDNA generation and nested PCR steps for sorted single spike-specific B cells.

To reverse transcribe the RNA of cells lysed during sorting, 3µL of random hexamer primers at 150ng/µL (GeneLink), 2µL of 10µM deoxyribonucleotides triphosphate (dNTPs) (Invitrogen) and 0.5µL of First Strand Superscript III Reverse Transcriptase (Invitrogen) were mixed in ddH20 for a total volume of 6µL and were added to each well containing a single sorted cell. cDNA was amplified from RNA by using the conditions outlined in the cDNA program in ***Table 2.11.1*** in a Mastercycler nexus gradient thermocycler (Eppendorf). As random hexamers primers will non-specifically amplify any RNA into cDNA, further rounds of nested polymerase chain reactions (PCRs) were needed to amplify the BCR's heavy chain VDJ region. For the first round of PCR, 0.17µL each of 10mM dNTPs, H1 forward and reverse primer mix, alongside 0.86µL of 10X HotStarTaq buffer (Qiagen) and 0.04µL of HotStarTaq DNA polymerase were mixed in ddH20 for a total volume of 6.32µL which was added to each well of a

new plate alongside 2.5µL of cDNA template. The H1 forward and reverse primers mixes will respectively amplify upstream of the different IGVH leader regions and within the IgG constant region (Tiller et al., 2008). The conditions for this first nested PCR are outlined in the PCR1 program in ***Table 2.11.1***. For the second round of PCR, 0.17µL each of 10mM dNTPs, H2 forward and reverse primer mix, alongside 0.86µL of 10X HotStarTaq buffer and 0.04µL of HotStarTaq DNA polymerase were mixed in ddH20 for a total volume of 6.32µL which was added to each well of a new plate alongside 2.5µL of PCR1 template. Again, the H2 forward and reverse primer mixes are designed to be further upstream within the IGHV leader region and the IgG constant region than PCR1. The conditions for this second nested PCR are outlined in the PCR2 program in ***Table 2.11.1***. Before the final PCR step, each PCR2 well was topped up to 10µL with ddH20. For the third round of PCR, 0.25µL each of 10mM dNTPs, HGibF mix and 1399 reverse primer, 1.25µL of 10X high-fidelity Platinum Taq buffer (Invitrogen), 0.5µL of 50mM MgSO4 and 0.1µL of high-fidelity Platinum Taq DNA polymerase were mixed in ddH20 for a total volume of 10.5µL which was added to each well of a new plate alongside 2.5µL of PCR2 template. This final PCR added enough overhangs on the side of the leader and constant regions to allow for sequencing. The conditions for this second nested PCR are outlined in the PCR2 program in ***Table 2.11.1***. All primers were used at a concentration of 10 µM and are described in ***Table 2.11.2***.

cDNA program - single cell				
Group	**Temperature (°C)**	**Time**	**Cycle count**	**Purpose**
1	42	10 min	1	Initial Denaturation
2	25	10 min	1	Incubation
3	50	60 min	1	Reverse transcription
4	95	5 min	1	Enzyme inactivation
5	4	∞	1	Final store

PCR1 program - single cell				
Group	**Temperature (°C)**	**Time**	**Cycle count**	**Purpose**
1	95	5 min	1	Initial Denaturation
2	94	30 sec	50	Cycle Denaturation
	50	30 sec		Cycle Annealing
	72	1 min		Cycle Extension
3	72	1 min	1	Final extension
4	4	∞	1	Final store

PCR2 program - single cell				
Group	**Temperature (°C)**	**Time**	**Cycle count**	**Purpose**
1	95	5 min	1	Initial Denaturation
2	94	30 sec	50	Cycle Denaturation
	55	30 sec		Cycle Annealing
	72	1 min		Cycle Extension
3	72	1 min	1	Final extension
4	4	∞	1	Final store

PCR3 program - single cell				
Group	**Temperature (°C)**	**Time**	**Cycle count**	**Purpose**
1	94	2 min	1	Initial Denaturation
2	94	30 sec	40	Cycle Denaturation
	55	30 sec		Cycle Annealing
	68	1 min		Cycle Extension
3	68	2 min	1	Final extension
4	4	∞	1	Final store

Table 2.11.1: *PCR conditions for amplification of the BCR's heavy chain VDJ region from single sorted cells.*

Step	Primer (or mix) name	Sequence	Description
cDNA	Random hexamers	NNNNNN	Randomly binds any 6 bp combination.
PCR1	H1F mix (FWD)	ACAGGTGCCCACTCCCAGGTGCAG	Anneals to VH1 leader sequence.
		AAGGTGTCCAGTGTGARGTGCAG	Anneals to VH3 leader sequence.
		CCCAGATGGGTCCTGTCCCAGGTGCAG	Anneals to VH4 and 6 leader sequence.
		CAAGGAGTCTGTTCCGAGGTGCAG	Anneals to VH5 leader sequence.
	H1R (REV)	GGAAGGTGTGCACGCCGCTGGTC	Anneals to a conserved portion of IgGs' CH1.
PCR2	H2F mix (FWD)	CTGCAACCGGTGTACATTCCGAGGTGCAGCTGGTGCAG	Further nested within the VH1 and 5 leader sequences.
		CTGCAACCGGTGTACATTCTGAGGTGCAGCTGGTGGAG	Further nested within the VH3 leader sequence.
		CTGCAACCGGTGTACATTCCCAGGTGCAGCTGCAGGAG	Further nested within the VH4 leader sequence.
		CTGCAACCGGTGTACATTCTGAGGTGCAGCTGTTGGAG	Further nested within the VH3-23 leader sequence.
		CTGCAACCGGTGTACATTCCCAGGTGCAGCTACAGCAGTG	Further nested within the VH3-34 leader sequence.
	H2R mix (REV)	GTTCGGGGAAGTAGTCCTTGAC	Further nested in IgG CH1.
PCR3	HGibF mix (FWD)	CATCCTTTTTCTAGTAGCAACTGCAACCGGTGTACATTCTsArGTGCAGCTGkTGGAG	Anneals to the VH3 leader sequence and add overhang for Gibson cloning.
		CATCCTTTTTCTAGTAGCAACTGCAACCGGTGTACATTCCsAGGTyCAGCTGGTrCAG	Anneals to the VH1 leader sequence and add overhang for Gibson cloning.
		CATCCTTTTTCTAGTAGCAACTGCAACCGGTGTACATTCCCAGsTrCAGCTGCAGsAG	Anneals to the VH4 leader sequence and add overhang for Gibson cloning.
		CATCCTTTTTCTAGTAGCAACTGCAACCGGTGTACATTCCCAGGTGCAGCTACAGCAGTG	Anneals to the VH4-34 leader sequence and add overhang for Gibson cloning.
	1399 (REV)	GGAGTTCAGACGTGTGCTCTGTCCTTGACCAGGCAGCCCAG	Anneals within IgG CH1 + add an overhang to help with sequencing
Sequencing	PT056 (REV)	GGAGTTCAGACGTGTGCTCT	Anneals to overhang in 1399 for sequencing
	1423 (FWD)	CTAGTAGCAACTGCAACCGG	Anneals in Gibson overhang present in all HGibF primers.

Table 2.11.2: *Primers for the single-cell sequencing pipeline.*

2.11.2. Agarose gel quality control (QC) check.

After PCR3, each well was topped up to 50µL with ddH20, and 5µL of each well was used to be run on a 2% agarose E-gel (Thermo) to visualise the presence of amplified VDJ region. Any well with a 300-500 base pair (bp) band was carried forward for Sanger sequencing.

2.11.3. Sanger sequencing.

Sequences generated with the single-cell PCR pipeline were sent for sequencing using Azenta/Genewiz 96-well plates barcode services. 7.5ul of PCR3 product was added to each well alongside 2.5ul of either reverse (PT056) or forward primer (1423). This strategy for sequencing from the forward and reverse end was chosen to maximise sequence quality due to the relatively short number of bp between the start of the sequencing read and the regions of interest (start of V gene or end of J gene).

2.12. Bulk-cell PCR pipeline.

This pipeline considered cells from 3 different sources: (1) from 100 sorted spike-specific B cells (post 3rd dose – spike-specific), (2) from dry pellets (post 3rd dose – bulk) or (3) from cells which were previously thawed due to a mechanical failure of the LN2 tank (baseline, post 1st and post 2nd vaccine – all bulk).

2.12.1. Dry pellet preparation.

When thawing PBMCs for sorting (as described in **section 2.10**), 1 million PBMCs were reserved for bulk BCR sequencing. For this, each $10x10^6$ cell aliquot of PBMCs was resuspended in 1mL of complete DMEM, 100µL were aliquoted in a new Eppendorf and subjected to centrifugation for 1 min at 2500g in a table-top microfuge. All the liquid was removed whilst taking care not to disturb the cell pellet, and the Eppendorf containing the dry pellet was immediately submerged in a bucket filled with dry ice to snap-freeze the cell pellet. These dry pellets were stored at -80ºC for further usage.

2.12.2. RNA extraction for dry pellets and previously thawed cells.

PBMCs which were previously thawed in the LN2 failure were quickly thawed again in a waterbath and were directly collected by centrifugation for 30 sec at 10,000g. All the

supernatant was removed whilst taking care not to disturb the cell pellet. From that moment, akin to the dry pellets described in **section 2.12.1**, standard RNA extraction was performed using an RNeasy Mini Kit (QIAGEN). As the exact number of cells contained in the pellet of previously thawed cells or the dry pellets was technically unknown, a volume of 700µL of RLT buffer was chosen based on the manufacturer's recommendations. RNA extraction proceeded by following the RNeasy Mini Kit instructions. RNA was eluted into 32µL of ddH20, and the concentration of RNA was measured using a Nanodrop.

2.12.3. cDNA generation and nested PCR steps for 100 sorted spike-specific B cells and previously thawed cells.

To generate cDNA for 100 sorted single spike-specific B cells and from previously-thawed cells, 3µL of random hexamer primers at 150ng/µL, alongside 0.2µL of 10mM dNTPs, 1.25µL of 0.1M DTT, 5µL of 5X First Strand buffer (Invitrogen) and 0.25µL of First Strand Superscript IV Reverse Transcriptase (Invitrogen) in ddH20 for a total volume of 10.75µL was added to each well containing 100 sorted spike-specific B cells. For the previously-thawed cells, the same mastermix was created with the addition of 0.5µL of RNAseOUT, which was added to reactions containing 1µg of RNA extracted in **section 2.12.2**. The cDNA was amplified by using the conditions outlined in the cDNA program in ***Table 2.12.3***. For the first round of nested PCR, 0.5µL each of 10mM dNTPs, H1 forward primer mix and either 1389 or H1 reverse primer, 2.5µL of 10X HotStarTaq buffer and 0.13µL of HotStarTaq DNA polymerase were mixed in ddH20 for a total volume of 22.53µL which was added to each well of a new plate alongside 2.5µL of cDNA template. The H1 reverse primer will specifically amplify BCRs using IgG as described above whilst the 1389 primer was designed to amplify within the IgM constant region. The conditions for this first nested PCR are outlined in the PCR1 program in ***Table 2.12.3***. PCR1 products were cleaned using AMPure DNAClean XP beads (Beckman-Coulter) to remove any remaining primers, primer dimers or buffer salt. For this 30µL of beads were added to each well and washed twice with 80% Ethanol, the beads were then air dried for 5 min before the bead-bound purified DNA was eluted using 50µL of ddH20. For the second round of nested PCR, 0.5µL each of 10mM dNTPs, H2F-R1 forward primer mix and either 1367 or 1369 reverse primer, alongside 2.5µL of 10X HotStarTaq buffer and 0.13µL of HotStarTaq

DNA polymerase were mixed in ddH20 for a total volume of 22.53µL which was added to each well of a new plate alongside 2.5µL of purified PCR1 template. Here, the H2F-R1 forward primer mix is based on H2F with the added read 1 (R1) site necessary for Illumina-based next-generation sequencing (NGS), whilst 1367 and 1369 respectively amplify the IgG or IgM constant region whilst introducing the necessary read 2 (R2) site for Illumina-based NGS. The conditions for this second nested PCR are outlined in the PCR2 program in in ***Table 2.12.3***. Again, the PCR2 product was cleaned using AMPure DNAClean XP beads as described above. Of note, the different number of cycles in the PCR1 and 2 programs for the 100 sorted cells versus previously-thawed cells was done to account that fundamentally there was a difference in input i.e., 100 B cells versus an unknown number of cells (but likely greater than 100). Indeed, over-amplification of DNA can lead to more PCR-induced replication errors. All primers were used at a concentration of 10 µM and are described in ***Table 2.12.5.2***.

cDNA program - 100 cells/previously thawed cells				
Group	**Temperature (°C)**	**Time**	**Cycle count**	**Purpose**
1	42	10 min	1	Initial Denaturation
2	25	10 min	1	Incubation
3	50	60 min	1	Reverse transcription
4	95	5 min	1	Enzyme inactivation
5	4	∞	1	Final store

PCR1 program - 100 cells/previously-thawed cells				
Group	**Temperature (°C)**	**Time**	**Cycle count**	**Purpose**
1	95	5 min	1	Initial Denaturation
2	94	30 sec	25 for 100 cells, 15 for previously-thawed cells	Cycle Denaturation
	50	30 sec		Cycle Annealing
	72	1 min		Cycle Extension
3	72	1 min	1	Final extension
4	4	∞	1	Final store

PCR2 program - 100 cells/previously-thawed cells				
Group	**Temperature (°C)**	**Time**	**Cycle count**	**Purpose**
1	95	5 min	1	Initial Denaturation
2	94	30 sec	25 for 100 cells, 15 for previously-thawed cells	Cycle Denaturation
	55	30 sec		Cycle Annealing
	72	1 min		Cycle Extension
3	72	1 min	1	Final extension
4	4	∞	1	Final store

Table 2.12.3: *PCR conditions for amplification of the BCR's heavy chain VDJ region from 100 sorted spike-specific B cells and previously thawed cells.*

2.12.4. cDNA generation and nested PCR steps for dry pellets.

To generate cDNA from the RNA extracted from dry pellets from **section 2.12.1**, 1µg of extracted RNA was mixed with 0.25µL of primer PT020, 0.5µL of 10mM dNTPs and 2µL of ddH20 and incubated at 65ºC for 5 min to facilitate annealing of PT020 to its target, the constant region of IgG. After this incubation step, 5µL of 5X First Strand buffer, 1.25µL of 0.1M DTT, 0.5µL of First Strand Superscript IV Reverse Transcriptase and 0.5µL of RNAseOUT were added to each well. PT020 will specifically allow for the amplification of RNA containing the IgG constant region. Additionally, PT020 adds the R2 site needed for Illumina NGS and provides a 13bp unique molecular identifier (UMI) to each RNA molecule for downstream error correction (Aird et al., 2011). The first cDNA program was then run (***Table 2.12.4***). Then, 1µL of RNase H was added to each well to remove any remaining RNA and the

second cDNA program was run (***Table 2.12.4***). After this, the produced cDNA was purified using AMPure DNAClean XP beads as described above. For the first round of nested PCR, 25µL of 2X Q5 mastermix (NEB), 1µL of H1 forward primer mix and 2.5µL of PT056 reverse primer were mixed in ddH20 for a total volume of 30µL which was added to each well of a new plate alongside 30µL of purified cDNA template. The PT056 primer is designed to anneal to the R2 site introduced by PT020. After this, the PCR1 product was purified using AMPure DNAClean XP beads as described above. For the second round of nested PCR, 25µL of 2X Q5 mastermix (NEB), 1µL of H2F-R1 forward primer mix and 2.5µL of PT056 reverse primer were mixed in ddH20 for a total volume of 30µL which was added to each well of a new plate alongside 30µL of purified PCR1 template. After this, the PCR2 product was purified using AMPure DNAClean XP beads as described above. The conditions for both nested PCR are outlined in the PCR1 program in in ***Table 2.12.4***. All primers were used at a concentration of 10 µM and are described in ***Table 2.12.5.2***.

cDNA program 1 - dry pellets				
Group	**Temperature (°C)**	**Time**	**Cycle count**	**Purpose**
1	50	45 min	1	Reverse transcription
2	80	10 min	1	Enzyme inactivation
3	4	∞	1	Final store

cDNA program 2 - dry pellets				
Group	**Temperature (°C)**	**Time**	**Cycle count**	**Purpose**
1	37	20 min	1	RNA digestion
2	4	∞	1	Final store

PCR1 and PCR2 program - dry pellets				
Group	**Temperature (°C)**	**Time**	**Cycle count**	**Purpose**
1	98	50 sec	1	Initial denaturation
2	98	10 sec	15	Cycle denaturation
	68	20 sec		Cycle Annealing
	72	20 sec		Cycle Extension
3	72	3 min	1	Final Extension
4	4	∞	1	Final Store

Table 2.12.4: *PCR conditions for amplification of the BCR's heavy chain VDJ region from dry pellets.*

2.12.5. *Barcode indexing.*

To identify which sequence came from which participant and which timepoint, all the samples were given unique barcodes as follows. 8 primers (PT501.3-PT508.3) were designed to anneal to the R1 site introduced previously and added the P5 flow cell adapter needed for sequencing on an Illumina MiSeq and a unique 8bp barcode. Similarly, 12 primers (PT701.2-PT712.2) were designed to anneal to the R2 site introduced previously, added the P7 flow cell adapter needed for sequencing on an Illumina MiSeq, and a unique 8bp barcode. In total, this meant that 96 unique barcode combinations could be used in a given Illumina MiSeq run. 20µM stocks of each 96 combinations of indexing barcodes were first produced. To index all purified PCR2 products produced in **section 2.12.3-4**, 25µL of 2X Q5 Mastermix and 2.5µL of any 20µM indexing barcodes were added to 22.5µL of purified PCR2 product. The conditions for this final PCR are detailed in ***Table 2.12.5.1***. The indexing PCR products were further purified with AMPure DNAClean XP beads as described above.

Indexing PCR program - 100 cells/previously thawed cells/dry pellets				
Group	**Temperature (°C)**	**Time (s)**	**Cycle count**	**Purpose**
1	98	50	1	Initial Denaturation
2	98	10	9 (touchdown, decrease by 0.5°C per cycle)	Cycle Denaturation
	72 - 68	20		Cycle Annealing
	72	20		Cycle Extension
3	98	10	22 for 100 cells, 10 for previously thawed cells/dry pellets	Cycle Denaturation
	68	20		Cycle Annealing
	72	20		Cycle Extension
3	72	120	1	Final extension
4	10	Inf	1	Final store

Table 2.12.5.1: *PCR conditions for the final indexing PCR.*

Step	Primer (or mix) name	Sequence	Description	Pipeline
cDNA	Random hexamers	NNNNNN	Randomly binds any 6 bp combination.	Bulk (non-UMI)
	PT020	GGAGTTCAGACGTGTGCTCTTCCGATCTNNNNNNNNNNNNNNGCCAGGGGGAAGACCGATGGG	Capture IgG, and add UMI and R2 site.	Bulk (with UMI)
PCR1	H1F mix (FWD)	ACAGGTGCCCACTCCCAGGTGCAG	Anneals to VH1 leader sequence.	Bulk (both)
		AAGGTGTCCAGTGTGARGTGCAG	Anneals to VH3 leader sequence.	
		CCCAGATGGGTCCTGTCCCAGGTGCAG	Anneals to VH4 and 6 leader sequence.	
		CAAGGAGTCTGTTCCGAGGTGCAG	Anneals to VH5 leader sequence.	
	H1R (REV)	GGAAGGTGTGCACGCCGCTGGTC	Anneals to a conserved portion of IgGs' CH1.	Bulk (non-UMI)
	1389 (REV)	GGAAGGAAGTCCTGTGCGAGGC	Anneals to a portion of IgM's CH1.	
	PT056 (REV)	GGAGTTCAGACGTGTGCTCT	Anneals to R2 site introduced by PT020.	Bulk (with UMI)
PCR2	H2F-R1 mix (FWD)	CTACACTCTTTCCCTACACGACGCTCTTCCGATCTGAGGTGCAGCTGGTGCAG	Further nested within the VH1 and 5 leader sequences, adds R1 site.	Bulk (both)
		CTACACTCTTTCCCTACACGACGCTCTTCCGATCTGAGGTGCAGCTGGTGGAG	Further nested within the VH3 leader sequence, adds R1 site.	
		CTACACTCTTTCCCTACACGACGCTCTTCCGATCTCAGGTGCAGCTGCAGGAG	Further nested within the VH4 leader sequence, adds R1 site.	
		CTACACTCTTTCCCTACACGACGCTCTTCCGATCTGAGGTGCAGCTGTTGGAG	Further nested within the VH3-23 leader sequence, adds R1 site.	
		CTACACTCTTTCCCTACACGACGCTCTTCCGATCTCAGGTGCAGCTACAGCAG	Further nested within the VH3-34 leader sequence, adds R1 site.	
	1367 (REV)	GGAGTTCAGACGTGTGCTCTTCCGATCTGCCAGGGGGAAGACCGATGGG	Further nested in IgG CH1, adds R2 site.	Bulk (non-UMI)
	1369 (REV)	GGAGTTCAGACGTGTGCTCTTCCGATCTCCGACGGGGAATTCTCACAGGAGACGAGGGGGAAAAG	Further nested in IgM CH1, adds R2 site.	
	PT056 (REV)	GGAGTTCAGACGTGTGCTCT	Anneals to R2 site introduced by PT020.	Bulk (with UMI)
PCR3	PT074 (FWD)	AATGATACGGCGACCACCGAGATCTACACTCTTTCCCTACACGACG	i5 primer without barcode: add **P5** flow cell adapter and can anneal to the **R1** site.	Bulk (with UMI)
	PT501.3 (FWD)	AATGATACGGCGACCACCGAGATCTACACTAGATCGCTCTTTCCCTACACGACG	i5 primers: add **P5** flow cell adapter, a unique **barcode** and can anneal to the **R1** site.	Bulk (non-UMI)
	PT502.3 (FWD)	AATGATACGGCGACCACCGAGATCTACACCTCTCTATTCTTTCCCTACACGACG		

	PT503.3 (FWD)	AATGATACGGCGACCACCGAGA TCTACACTATCCTCTTCTTTCCC TACACGACG		
	PT504.3 (FWD)	AATGATACGGCGACCACCGAGA TCTACACAGAGTAGATCTTTCCC TACACGACG		
	PT505.3 (FWD)	AATGATACGGCGACCACCGAGA TCTACACGTAAGGAGTCTTTCCC TACACGACG		
	PT506.3 (FWD)	AATGATACGGCGACCACCGAGA TCTACACACTGCATATCTTTCCC TACACGACG		
	PT507.3 (FWD)	AATGATACGGCGACCACCGAGA TCTACACAAGGAGTATCTTTCCC TACACGACG		
	PT508.3 (FWD)	AATGATACGGCGACCACCGAGA TCTACACCTAAGCCTTCTTTCCC TACACGACG		
	PT701.2 (REV)	CAAGCAGAAGACGGCATACGAG ATTCGCCTTAGTGACTGGAGTTC AGACGTGTGCTCT	i5 primers: add **P7** flow cell adapter, a unique **barcode** and can anneal to the **R2** site.	Bulk (both)
	PT702.2 (REV)	CAAGCAGAAGACGGCATACGAG ATCTAGTACGGTGACTGGAGTT CAGACGTGTGCTCT		
	PT703.2 (REV)	CAAGCAGAAGACGGCATACGAG ATTTCTGCCTGTGACTGGAGTTC AGACGTGTGCTCT		
	PT704.2 (REV)	CAAGCAGAAGACGGCATACGAG ATGCTCAGGAGTGACTGGAGTT CAGACGTGTGCTCT		
	PT705.2 (REV)	CAAGCAGAAGACGGCATACGAG ATAGGAGTCCGTGACTGGAGTT CAGACGTGTGCTCT		
	PT706.2 (REV)	CAAGCAGAAGACGGCATACGAG ATCATGCCTAGTGACTGGAGTTC AGACGTGTGCTCT		
	PT707.2 (REV)	CAAGCAGAAGACGGCATACGAG ATGTAGAGAGGTGACTGGAGTT CAGACGTGTGCTCT		
	PT708.2 (REV)	CAAGCAGAAGACGGCATACGAG ATCCTCTCTGGTGACTGGAGTTC AGACGTGTGCTCT		
	PT709.2 (REV)	CAAGCAGAAGACGGCATACGAG ATAGCGTAGCGTGACTGGAGTT CAGACGTGTGCTCT		
	PT710.2 (REV)	CAAGCAGAAGACGGCATACGAG ATCAGCCTCGGTGACTGGAGTT CAGACGTGTGCTCT		
	PT711.2 (REV)	CAAGCAGAAGACGGCATACGAG ATTGCCTCTTGTGACTGGAGTTC AGACGTGTGCTCT		
	PT712.2 (REV)	CAAGCAGAAGACGGCATACGAG ATTCCTCTACGTGACTGGAGTTC AGACGTGTGCTCT		

Table 2.12.5.2: *Primers for the bulk sequencing pipeline. Bulk non-UMI: 100 sorted spike-specific B cells and previously thawed samples; Bulk UMI: dry pellets.*

2.12.6. NGS MiSeq Sequencing.

The indexed BCR libraries prepared in section 2.12.5, were further quantified using the Qubit 1X dsDNA high-sensitivity kit (Invitrogen) and Tapestation D5000 reagents (Agilent) as per the manufacturer's instructions. All samples were pooled in an equimolar manner to produce a final library with a concentration of 2nM. The pooled BCR libraries were submitted, sequenced and demultiplexed by UCL Genomics using an Illumina MiSeq Kit v3 (600 cycles) (Illumina). The length of read 1 was 325bp, of 8bp each for the i5 and i7 index read, and of 275bp for read 2. The library was loaded at a concentration of 10pM and spiked with 20% PhiX to account for the overall similarity between the target regions (all heavy chain VDJ regions).

2.13. Bioinformatic analysis.

2.13.1. Low throughput BCR library preparation and quality control.

The paired sequences generated from single spike-specific BCRs sequenced in **section 2.11.3** were assembled using the sangeranalayseR package (Chao et al., 2021) in R. This required the use of ab1 files from the forward and reverse read of each set of single cells sequences. The trimming method used was M2 with the following settings: M2CutoffQualityScore = 20, M2SlidingWindowSize = 10, baseNumPerRow = 100, heightPerRow =200 and signalRatioCutoff = 0.98. From this, contiguous sequences using the forward and reverse reads were generated and manually inspected for quality control: any contiguous sequences (or forward/reverse read) with an overall Phred score <20 was discarded and any degenerate base (signalling a mismatch in base calling at a given bp between the forward and reverse read) was replaced by the base call of the forward or reverse read which had the highest Phred score. FASTQ files were created for each participant and imported into the high-performance computer (HPC) environment (UCL Myriad High Performance Computing Facility) for further analysis.

2.13.2. High throughput BCR library preparation and quality control.

The demultiplexed FASTQ files generated after NGS in **section 2.12** were directly imported into the HPC environment for quality control. The BCR libraries generated

with and without UMIs were processed using the pRESTO tool from the Immcantation framework (Vander Heiden et al., 2014).

For sequences produced without UMIs (**section 2.12.3**), the R1 and R2 reads were first assembled using the AssemblePairs.py script, low quality assembled reads (Phred score <20) were then filtered out with FilterSeq.py script. Any sequence matching the forward and reverse primers used was then removed with the MaskPrimers.py script. All identical sequences (which could share at least 20 non-called 'N' bp) were collapsed into a single sequence using the CollapseSeq.py script. To filter out PCR sequencing artefacts, any collapsed sequence created in the previous step which had been read (i.e., sequenced) less than 10 times was filtered out with the SplitSeq.py script. This cut-off is higher to account for the lack of UMIs.

For sequences produced with UMIs (**section 2.12.4**), R1 and R2 reads were first checked for low-quality reads (Phred score <20) which were then filtered out with FilterSeq.py script. As above, reverse and forward primers were removed with MaskPrimers.py. Using the UMI, any R1 and R2 reads using the same UMI were annotated with the UMI used using the PairSeq.py script and were then aligned within each UMI group using AlignSets.py. A consensus sequence was then built for each UMI group using the BuildConsensus.py script with the following settings: --prcons 0.6 --maxerror 0.1 --maxgap 0.5. The PairSeq.py script was run again on these consensus sequences to confirm that UMI were matched. Finally, any identical consensus sequences were collapsed into a single sequence using the CollapseSeq.py script, and any collapsed sequence created in the previous step which had been read less than twice was filtered out with the SplitSeq.py script.

2.13.3. Clonal assignment, gene usage and somatic hypermutation.

FASTQ files produced in **section 2.13.2** after the SplitSeq.py script or in **section 2.13.1** were annotated using the Change-O tool from the Immcantation framework (Gupta et al., 2015). First, IgBLAST was run on each FASTQ file with the AssignGenes.py script and was then converted into a tab-delimited file with MakeDb.py. All sequences with incomplete VDJ assignments or non-productive rearrangements were removed with the ParseDb.py script. Clonal lineage assignment was then either assigned within each participant (single hierarchical clustering), within each combination of participant and timepoint (single hierarchical clustering) or by

considering all participants together (complete hierarchical clustering) using the DefineClones.py script. Clonal lineages were assigned based on sharing an identical IGVH and IGJH gene call, identical CDRH3 length, and 90% AA identity in CDRH3. Finally, germline sequences were assigned for each clonal lineage using the CreateGermlines.py script.

Any clonal lineage was considered public if it contained two or more clones from different participants or if it contained a clone which had an exact CDRH3 match with a known public clone contained in the CoV-AbDab repository (Raybould et al., 2021) (https://opig.stats.ox.ac.uk/webapps/covabdab/, the database was accessed on the 31st of January 2024).

For analysis, IGVH gene usage was inferred using the countGenes function in the alakazam R package from the Immcantation framework (Gupta et al., 2015; Stern et al., 2014). This allows to consider V gene usage for each clonal lineage as a proportion of the overall repertoire of a given donor. To measure levels of SHM, the number of mutations in the entire VDJ was considered for each sequence using the observedMutations function in the SHazaM R package from the Immcantation framework (Gupta et al., 2015). The mean mutation count was then reported per clonal lineage by averaging the number of mutations found in all members of a lineage.

2.13.4. Diversity measurements.

Diversity was first considered as the number of clonal families as a proportion of a given participant's repertoire. Other metrics commonly used to measure clonal diversity within a BCR repertoire are the Shannon and Simpson indexes (Shannon and Weaver, 1949; Simpson, 1949). Each gives different weight to the importance of the abundance of rare clonal lineages (few members) versus more commonly sampled clonal lineages (many members) alongside the total number of clonal lineages that can be detected within a repertoire (species richness). Shannon's and Simpson's index were calculated for each participant's repertoire using the vegan R package (Dixon, 2003). To better account for the variety of possible structure of a BCR repertoire, the Hill diversity index (Hill, 1973) can be used to generate a diversity profile curve (Greiff et al., 2015) for each group where the frequency and number of clonal lineages are weighted by any value of q. The diversity curve was then calculated using 500 bootstrap replicates. With q increasing, more weight is given to the contribution of

larger clones towards diversity. With q=1 equivalent to Shannon's index and q=2 equivalent to Simpson's index. Generally higher q values will give more importance to evenness (i.e., many clonal lineages of the same size and therefore of bigger sizes) whilst lower q values give more weight to rarer clonal lineages when measuring the diversity of a given repertoire. As suggested by (Gupta et al., 2015; Stern et al., 2014), the repertoire for each group was sub-sampled to include the same numbers of BCR sequences in each repertoire before assigning clonal lineages and generating diversity curves.

2.14. Statistics

All statistical analyses were carried out in GraphPad Prism 9.0 or within the R environment using the rstatix package. All tests were two-tailed. Mann- Whitney U-test (MWU) was used to compare unpaired, non-parametric data whilst Wilcoxon matched-pairs sign rank test (Wilcoxon) was used to compare paired, non-parametric data. Non-parametric Spearman's correlation test was used for correlation analysis between two or more sets of data. Where appropriate, the median for each group was shown. Statistical significance in the figures is shown as p-value>0.05 (*); >0.01 (**); >0.001 (***) and >0.0001 (****). For Spearman's rank correlation coefficient, on top of significance, correlations were considered weak, modest or strong depending on the following criteria: weak correlation: -0.4<r<0.4; modest correlation: 0.4<r<0.6 or -0.4<r<-0.6 or strong correlation: r>0.6 or r<-0.6.

3. Humoral responses to SARS-CoV-2 infection in PLWH

3.1. Summary

Historically, serological responses to vaccines and infection have been observed to be worse in PLWH than in HIV-negative controls (see **section 1.3.6** for a more detailed discussion). The exact nature of this defect can be hard to unpick from complex vaccination and/or infection histories frequently found in seasonal pathogens such as influenza. The COVID-19 pandemic provided us with the unique opportunity to study humoral responses to a novel pathogen in PLWH. Indeed, pre-existing immunity against SARS-CoV-2 was limited (see **section 1.2.1** for more detailed discussion), making it easier to link immune stimuli and HIV status to serological output.

As discussed in **section 1.3.6**, an increased risk of COVID-19 mortality, and potentially severity, was identified for PLWH, especially for those with low CD4 count and/or active viraemia. Concurrently, studies of severe COVID-19 reported overall lymphopenia in individuals (Diao et al., 2020; Tan et al., 2020), which could further potentiate infection risk in PLWH with pre-existing lymphopenia. In early 2020 in the UK, guidance advised that on top of the general social distancing measure in place for the general population, PLWH with extreme immune dysfunction (CD4 count <200 cells/μL or recent opportunistic infection) and other immunocompromised patient groups should shield (BHIVA, 2020; BHIVA and Terrence Higgins Trust, 2020). Therefore, at the time of this study, more information on the quality of immune responses post-SARS-CoV-2 infection was needed.

Thus, the main aim of this chapter was to assess the quantitative and qualitative serological responses of PLWH to SARS-CoV-2 infection. For this HIV-negative controls and PLWH were recruited shortly after the first wave of the COVID-19 pandemic. As such, most of this recruitment period overlapped with various national restrictions on participants' ability to access clinical diagnostic tools which meant that there was a mix of participants with suspected and lab-confirmed SARS-CoV-2 infection. First, IgG binding titres to S1 and N were measured to both verify the self-reported/clinical data where available and to highlight any potential differences between PLWH and HIV-negative controls. Then, neutralisation titres were measured against the circulating strain at the time, SARS-CoV-2 Wuhan-hu1 (WT), the SARS-CoV-2 B.1.1.7 variant and also historic SARS-CoV-1 to assess the breadth of the

responses in both groups. Part of the work presented here was published in November 2021 in Nature Communications (Alrubayyi et al., 2021) as part of a larger immunological characterisation of the response to SARS-CoV-2 infection in PLWH.

3.2. Cohort design.

A total of 82 individuals (47 PLWH and 35 HIV-negative controls) were sampled between July and November 2020 (see **Methods – section 2.1.1** for more details). This study (Jenner II) was approved by the local Research Ethics Committee (REC) - Berkshire (REC 16/SC/0265).

Participants were recruited based on self-declaration of either suspected or lab-confirmed SARS-CoV-2 infection. Lab-confirmed infections meant the participants had independently accessed outside diagnostic tools such as RT-PCR, Roche/Abbot serological assays or lateral flow tests. Suspected SARS-CoV-2 infection participants reported close contact with confirmed cases and/or COVID-19 symptoms but did not have access to testing. When stratifying by HIV status, 24 PLWH and 31 HIV-negative controls had a lab-confirmed diagnosis whilst 23 PLWH and 4 HIV-negative controls had suspected SARS-CoV-2 infections. Additionally, 22 individuals who were sampled pre-pandemic (July 2016 – November 2019) were included for the further optimisation of our S1 and N IgG-specific assays (which had been previously established by our lab (Muir et al., 2021; O'Nions et al., 2021; Rees-Spear et al., 2021)) in the context of PLWH. In this cohort, we also had access to one HIV-negative individual who had a history of previous SARS-CoV-1 infection. For each participant, limited clinical information was recorded and/or made available to the research team, this included days since symptom onset (DPSO), gender, age, ethnicity, and where applicable COVID-19-related hospitalisation status, CD4 count and CD4:CD8 ratio. All PLWH recruited had undetectable viral loads and were currently on ART treatment. For SARS-CoV-2 seropositive participants (those positive for S1 and N IgG-specific antibodies), the median CD4 count was 560 cells/μL and the median CD4:CD8 ratio was 0.84. Most of the cohort reported mild COVID-19 disease (based on the WHO clinical progression scale (Marshall et al., 2020)). Overall, four participants had asymptomatic SARS-CoV-2 infections (PLWH=2 and HIV-negative controls=2) and 42 participants had symptomatic infections that did not require hospitalisation (PLWH=20 and HIV-negative controls=22). 4/29 HIV-negative controls and 8/30 PLWH required hospitalisation following their SARS-CoV-2 infection. All 12 hospitalised participants scored 4-5 on the WHO progression scale (Marshall et al., 2020) i.e., moderate COVID-19 disease requiring hospitalisation (with the maximum intervention being

oxygen mask therapy). No participant in this cohort required ICU-level support or died following COVID-19 disease in the timeframe of the study.

		HIV-			HIV+		
		Pre-pandemic	Suspected SARS-CoV-2	Confirmed SARS-CoV-2	Pre-pandemic	Suspected SARS-CoV-2	Confirmed SARS-CoV-2
	N=	4	4	31	18	23	24
Serology	Seronegative (S1- N-)	4	1	0	14	12	1
	Seropositive (S1+ N+)	0	0	29	0	7	23
	Seropositive for N only	0	3	1	3	4	0
	Seropositive for S1 only	0	0	1	1	0	0

for seropositive (S1+ N+) participants only

		HIV-	HIV+
N=		29	30
% female		0.52	0.2
% Ethnic minorities (excl. white minorities)		0.41	0.4
Median age (range)		42 (26-65)	51 (30-73)
Median DPSO (range)		146 (101-220)	158 (46-232)
COVID-19 severity	Asymptomatic	2	2
	Non-hospitalised	22	20
	Hospitalised	4	8
Median CD4 cell count (range)		-	560 (133-1110)
Median CD4:CD8 ratio (range)		-	0.84 (0.17-2.54)
HIV viral load (viral copies/mL)		-	Undetectable (<50)

Table 3.2*: Characteristics and demographic information for the convalescent cohort. Demographic information shown here was obtained as described in* Alrubayyi et al. (2021)*, as part of the Jenner II study (REC 16/SC/0265). All hospitalised (n=12) individuals presented with moderate disease requiring hospitalisation (score 4-5 on the WHO clinical progression scale* (Marshall et al., 2020)*).*

3.3. Combined S1 and N antibody detection indicates previous SARS-CoV-2 infections.

To assess serological responses post-SARS-CoV-2 infection in a convalescent cohort an assay was needed to quantify SARS-CoV-2 specific antibody responses. As discussed in **section 1.2.5**, the spike protein represents the immunodominant portion of the SARS-CoV-2 antibody binding response. Beside spike, the structural protein N is the other main target of anti-coronaviruses antibodies and is widely used in diagnostics akin to the p24 antigen in HIV, potentially due to its large abundance within the virus (Leung et al., 2004; Shrock et al., 2020). Additionally, during the timeframe of this study there was a focus on understanding IgG-specific binding responses as anti-SARS-CoV-2 antibodies had been recently described to be the dominant portion of the antibody response over IgA and IgM roughly 15 days after infection (Cohen et al., 2021; Dan et al., 2021; Long et al., 2020; Seow et al., 2020).

The assay presented here is based on ELISA assays developed in collaboration with the groups of Katie Doores and George Kassiotis to detect the presence of spike-specific (or its subdomain S1 or RBD) and N-specific antibodies (Ng et al., 2020; Pickering et al., 2020). This initial assay was designed to differentiate between cross-reactive/background reactivity and 'true' responses to COVID-19 with a high degree of specificity and validated against a wide range of clinical samples and commercially available serological assays. This included a large cohort of pre-pandemic samples alongside samples from COVID-19 ICU patients. With this combined S and N ELISA assay alone, all COVID-19 patients were correctly detected as being seropositive for both anti-N and anti-spike IgG antibodies with no false positives in 320 pre-2020 samples (Pickering et al., 2020). The change from using the whole spike in the original assay (Pickering et al., 2020) to the S1 subunit can be explained by the higher level of specificity given by S1-targeting antibodies rather than whole spike-targeting antibodies which can also include epitopes within the more conserved S2 region that cross-react with pre-existing hCoV antibodies as seen in (Ng et al., 2020). Additionally, S1 contains the RBD domain which is the main target of neutralising antibodies (Greaney et al., 2021; Piccoli et al., 2020). Both the S1 and N proteins used here were produced at the Francis Crick Institute by Peter Cherepanov's lab. This assay was then further optimised and validated in our lab to quantitatively measure amounts of

IgG against S1 and N (rather than the initial seropositive/seronegative readout) by Luke Muir (Muir et al., 2021; O'Nions et al., 2021; Rees-Spear et al., 2021).

To validate this assay for use with PLWH, 22 samples from pre-pandemic individuals were included (4 HIV-negative controls, 18 PLWH). These participants were recruited as part of the Jenner II cohort between 2016 and 2019 and had no known history of previous SARS-CoV-1 infection. The presence of S1-specific IgGs was largely limited to individuals with lab-confirmed (53/55 participants) or suspected (7/27 participants) SARS-CoV-2 infection bar one pre-pandemic sample who had very low levels of S1-specific IgGs (0.29µg/mL). The data in ***Figure 3.3A*** is consistent with the original optimisation of this ELISA as described by (Pickering et al., 2020), where all COVID-19 patient samples were positive for spike-specific IgGs but 4/320 pre-pandemic samples were also seropositive for spike and only 1 for RBD. Similarly, in (Ng et al., 2020), all 156 patients with a history of SARS-CoV-2 infection had spike-specific IgGs, while only 16/302 of SARS-CoV-2 naïve individuals were seropositive for spike. Here, pre-existing cross-reactivity to spike was greatly reduced because it measured S1-specific IgG rather than the whole spike.

As per (Pickering et al., 2020), to help differentiate pre-existing cross-reactive hCoV antibodies from those indicating SARS-CoV-2 infection, the samples were also tested for reactivity against N. The presence of N-specific IgGs was detected in most of the lab-confirmed SARS-CoV-2 infection participants (53/55) and over half of the suspected SARS-CoV-2 infection participants (14/27). Additionally, three pre-pandemic participants and the only participant with a history of previous SARS-CoV-1 infection had detectable N-specific IgGs (***Figure 3.3B***). As seen in ***Figure 1.2.1***, N is conserved throughout the different hCoVs whereas there is a larger amount of diversity within the spike protein of SARS-CoV-2, especially in the S1 subunit ***Figure 1.2.1*** *and* ***1.2.2***. As such, the cross-reactive N-only antibody response in the pre-pandemic samples can potentially be attributed to hCoV anti-N antibodies reactivity, as demonstrated in other studies (Guo et al., 2020; Ng et al., 2020; Pickering et al., 2020; Wang et al., 2020).

Crucially, as previously seen in (Pickering et al., 2020), combined detection of spike-specific IgG (or RBD-specific IgG) and N-specific IgG provided the highest assay sensitivity and specificity to detect SARS-CoV-2 infection-mediated immunity from

background compared to detection of spike, RBD or N-specific IgG only (Ng et al., 2020; Pickering et al., 2020). Only participants in the lab-confirmed SARS-CoV-2 infection participants (52/55) and in the suspected SARS-CoV-2 infection participants (7/27) group had titres for S1-specific IgG and N-specific IgGs (***Figure 3.3C***). Overall, there was a significant correlation between S1-IgG specific titres and N-IgG specific titres across all samples (***Figure 3.3C***). For the seven participants in the suspected group who were seropositive for S1 and N, based on the prior systematic validation of the assay they likely had SARS-CoV-2 infection but either did not have access to testing at the time or their infections were asymptomatic. Similarly, 3/53 participants were seronegative for S1 or N in this assay despite a previous lab-confirmed diagnosis: one seronegative for both antigens, one seronegative for N only and one for S1 only. This discordance could be explained by several reasons: a false-positive from their outside lab diagnosis or errors in self-reporting. However, most likely they had antibody titres below the limit of detection of this assay (0.25µg/mL) because they had a mild SARS-CoV-2 infection and their antibodies had waned by the time of sampling which was on average in August/September of 2020. Indeed, one of the three individuals who were seronegative for S1 or N was asymptomatic.

Overall, this semi-quantitative ELISA assay allowed to sensitively detect SARS-CoV-2-specific antibodies from cross-reactive immunity by using the combined detection of S1-specific and N-specific IgG antibodies.

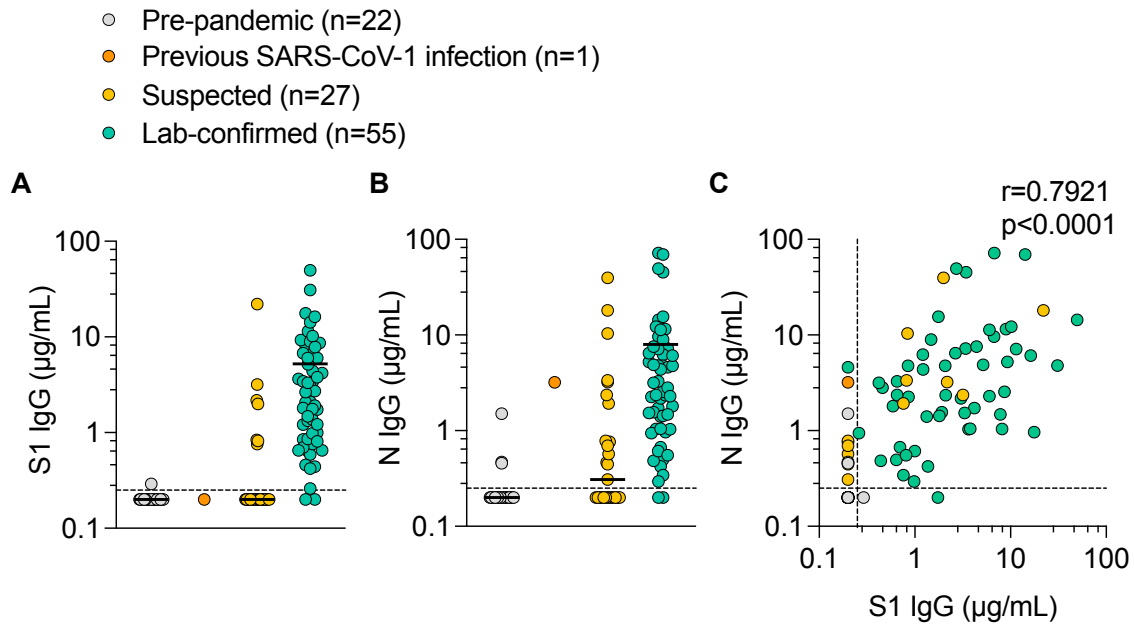

Figure 3.3*: A semi-quantitative ELISA against N and S1 IgG-specific antibodies can delineate between SARS-CoV-2 infection and previous cross-reactive hCoV responses. IgG-specific antibody titres (µg/mL) against SARS-CoV-2 S1 for* ***A.*** *and against N for* ***B.*** *measured by semi-quantitative ELISA stratified my exposure status (pre-pandemic – grey; previous SARS-CoV-1 infection – orange; suspected SARS-CoV-2 infection – yellow; lab-confirmed SARS-CoV-2 infection – mint).* ***C.*** *Correlation between S1 IgG-specific and N IgG-specific antibody titres (µg/mL). Statistical test: Spearman's rank correlation coefficient. For A-C, data points are representative of n=2 experimental repeats performed in duplicate, is shown the median for each group, dotted line represents the limit of detection of the assay (0.25 µg/mL IgG). Where no binding was detected, data points were assigned a titre of 0.2 µg/mL for visualisation.*

3.4. Similar levels of SARS-CoV-2 specific binding antibodies in PLWH and HIV-negative controls at a convalescent timepoint

As seen in **3.3**, only individuals seropositive for both S1 and N were considered to have had a SARS-CoV-2 infection. Therefore, 29 HIV-negative participants and 30 PLWH were included in the following analysis to assess SARS-CoV-2 specific antibody responses at a convalescent timepoint.

First, there was no significant difference between PLWH and HIV-negative controls in terms of their mean IgG-specific binding antibody titres against S1 (***Figure 3.4A-B***) or N (***Figure 3.4B***). There was a modest (0.4>r>0.6) but significant association between S1 and N IgG-specific binding antibody titres for the HIV-negative group, whilst this association was weaker (r<0.4) and non-significant for the PLWH group (***Figure 3.4C***). There was no clear association between the strength of binding to either S1 or N and the number of days post-symptom onset regardless of HIV status (***Figure 3.4D-E***). This may be due to the specific timeframe of the study. Samples were collected between 46 and 232 days post-symptom onset, which is a wide range and may have been too late to evaluate potential differences in the early induction of the antibody response, and too variable/early to determine clear antibody waning as reported elsewhere (Seow et al., 2020).

Effectively, these results show that there was no difference in the titres of S1-specific or N-specific IgGs between PLWH and HIV-negative controls. Reassuringly there was no apparent antibody waning in the PLWH group and the time of sampling was mostly representative of the stable phase of SARS-CoV-2 antibody kinetics (Cohen et al., 2021; Dan et al., 2021). However, the presence of neutralizing antibodies acts as the actual functional indicator of a protective response against re-infection and disease in humans rather than just binding antibodies (Feng et al., 2021; Gilbert et al., 2022). Therefore, I next assessed the neutralising of PLWH and HIv-negative controls after SARS-CoV-2 infection.

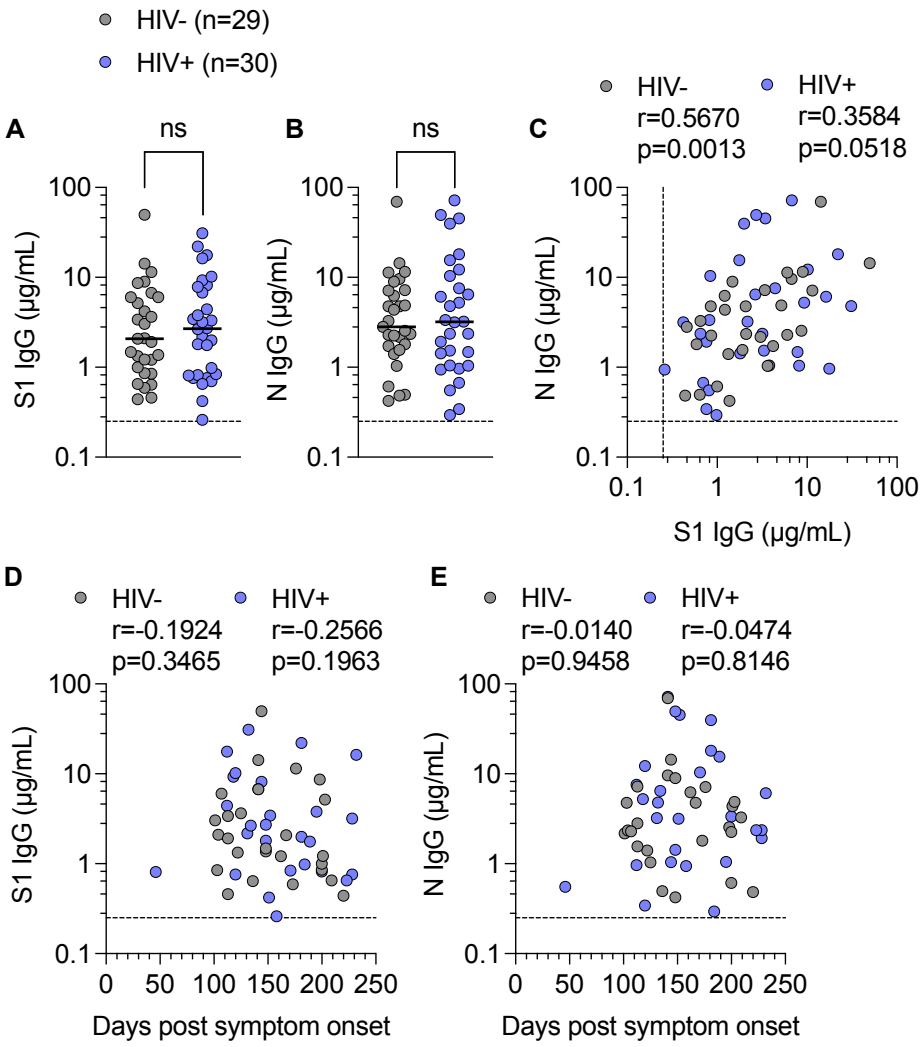

***Figure 3.4**: PLWH and HIV-negative controls have similar titres of S1 and N IgG-specific antibody titres following SARS-CoV-2 infection. IgG-specific antibody titres (µg/mL) against SARS-CoV-2 S1 for **A.** and against N for **B.** measured by semi-quantitative ELISA stratified my HIV status (HIV- – grey; HIV+ – blue). **C.** Correlation between S1 IgG-specific and N IgG-specific antibody titres (µg/mL) for the HIV- and HIV+ group. **D.** Correlation between S1 IgG-specific antibody titres (µg/mL) or **E.** N IgG-specific antibody titres (µg/mL) and days post symptom onset for the HIV- and HIV+ group. For A-E, data points are representative of n=2 experimental repeats performed in duplicate, is shown the median for each group, dotted line represents the limit of detection of the assay (0.25 µg/mL IgG). Where no binding was detected, samples were assigned a titre of 0.2 µg/mL for visualisation. Statistical test: MWU for A-B and Spearman's rank correlation for C-E.*

3.5. Optimisation of pseudovirus assay for the detection of SARS-CoV-2 neutralising antibodies.

To assess neutralisation antibody responses against SARS-CoV-2, the assay used here was first optimised in collaboration with Dr Katie Doores' group (Seow et al., 2020). This assay was based on historic lentiviral-based pseudovirus assays (Grehan et al., 2015; Wright et al., 2008; Zufferey et al., 1997, 1998). Pseudovirus-based assays are routinely used to test neutralisation instead of live-virus-based assays as they present the neutralising antigen in a viral context without any infection risk. Additionally, this removes the challenge of maintaining sequence fidelity when growing stocks by propagating viral isolates as for pseudoviruses molecular clones are used and propagated by single-round transfection. Another advantage of pseudovirus assays is that their superior safety profile means they can be performed at BSL-2 making these assays much more accessible for a wide variety of labs (Bentley et al., 2015; Li et al., 2018). Importantly, many studies have shown a robust correlation between pseudovirus and live neutralisation assays across many viruses (Cantoni et al., 2023).

Pseudoviruses were generated by transfecting 293T cells with an HIV packaging plasmid (p8.91), a firefly-luciferase reporter plasmid (CSLW) and a plasmid expressing the viral glycoprotein of choice (***Figure 3.5A***). In the context of SARS-CoV-2 neutralising responses, the main target is the spike protein, as it is readily available on the surface of SARS-CoV-2 viruses rather than N (Brouwer et al., 2020; Ju et al., 2020; Piccoli et al., 2020; Shi et al., 2020; Shrock et al., 2020; Zost et al., 2020). ACE-2 was the first receptor recognized to be essential for SARS-CoV-2 entry into human cells, with ACE-2 being widely expressed across different human tissues (Li et al., 2020). Briefly, the SARS-CoV-2 spike directly interacts with ACE-2 via its RBD to mediate viral fusion (Walls et al., 2020; Wrapp et al., 2020). To model SARS-CoV-2 infection in-vitro, this assay uses HeLa cells transduced to stably express the ACE-2 receptor (Rogers et al., 2020), rendering them permissible to infection. In this model, pseudovirus particles expressing SARS-CoV-2 spike on their surfaces can freely enter HeLa target cells by binding to ACE-2. Following entry, the pseudovirus will complete its viral replication cycle which will lead to the expression of the luciferase reporter gene encoded by the CSLW plasmid. Luciferase expression is then measured by RLU and used as a surrogate readout for successful infection (***Figure 3.5D***). Plasma

containing neutralising antibodies that bind epitopes on the spike protein, mostly within S1 will either directly or indirectly interfere with the binding between RBD and ACE-2 and/or viral fusion and thus block infection of the target cells by SARS-CoV-2. In turn, this will prevent the expression of luciferase by the PV, and the overall reduction of the luciferase readout can be quantified as a measure of neutralisation activity (***Figure 3.5C***).

In the context of our PLWH cohort, all patients were treated with ART. Thus, the participants' plasma may contain drugs which directly target the different steps of the HIV lifecycle (see ***Figure 1.3.1***). However, the pseudoviruses used in this assay are based on a lentiviral backbone: the packaging plasmid p8.91 directly encodes proteins (reverse transcriptase, integrase, and protease) that are targeted by ART drugs recommended in the UK (Waters et al., 2022). Therefore, the presence of ART blocks luciferase expression (***Figure 3.5D***) and leads to a reduction of the luciferase readout which is undistinguishable from antibody-mediated neutralisation. This ART-mediated interference in neutralisation assays has previously been documented, with the literature implicating both PIs and NRTI or NNRTI for this false-positive neutralisation (De La Torre-Tarazona et al., 2023; Sarzotti-Kelsoe et al., 2014).

Therefore, to distinguish ART interference from 'true' antibody-mediated neutralisation, a pseudovirus expressing the envelope protein of Murine Leukaemia Virus (MLV) was used (***Figure 3.5A***). This is because MLV doesn't infect humans, thus no humans have specific MLV antibodies and therefore neutralisation cannot be antibody-mediated. Therefore, any neutralising activity seen against it cannot be attributed to antibodies reacting against MLV Env, but rather here to ART-mediated neutralisation of the lentiviral backbone (***Figure 3.5D***). Initially, the use of a VSV-based pseudovirus instead of the lentivirus-based backbone was trialled to remove the ART-mediated neutralisation, based on previously validated VSV-based PV assays (Condor Capcha et al., 2021; Whitt, 2010). However, this method did not yield consistent infectious stock titres that would have enabled assay-to-assay reproducibility and given the urgency to provide information to PLWH on the functionality of their antibody responses an alternative method was pursued. Specifically, polyclonal IgG was purified out from the plasma of all PLWH, which effectively gave an ART-free fraction to use in the pseudovirus assay. For this, participant plasma was incubated with protein G resin to positively select for IgG while

any other non-specific proteins and ART drugs were washed out with PBS. Finally, the bound IgG was eluted and concentrated (***Figure 3.5E***). Due to extensive washing and concentrating steps, this process can lead to dilution or concentration of the IgG compared to the original amount present in the un-purified plasma. To account for this potential difference, the amount of total IgG was measured in the original plasma and in the purified IgG fraction using a total IgG ELISA. This allowed the same amount of purified IgG to be added to each assay well as would have been the case if unmodified plasma had been used. After I IgG purification of the plasma of PLWH, any previous "neutralisation" of MLV PV due to ART interference was removed (***Figure 3.5E***). Thus, after IgG purification, any neutralisation seen against a SARS-CoV-2 pseudovirus could be solely due to the presence of SARS-CoV-2-specific neutralising antibodies rather than due to a mix of SARS-CoV-2-specific neutralising antibodies and of ART interference (***Figure 3.5F***). Overall, this PV system coupled with IgG purification allowed the detection of neutralising antibodies specific to SARS-CoV-2 in both HIV-negative controls and PLWH.

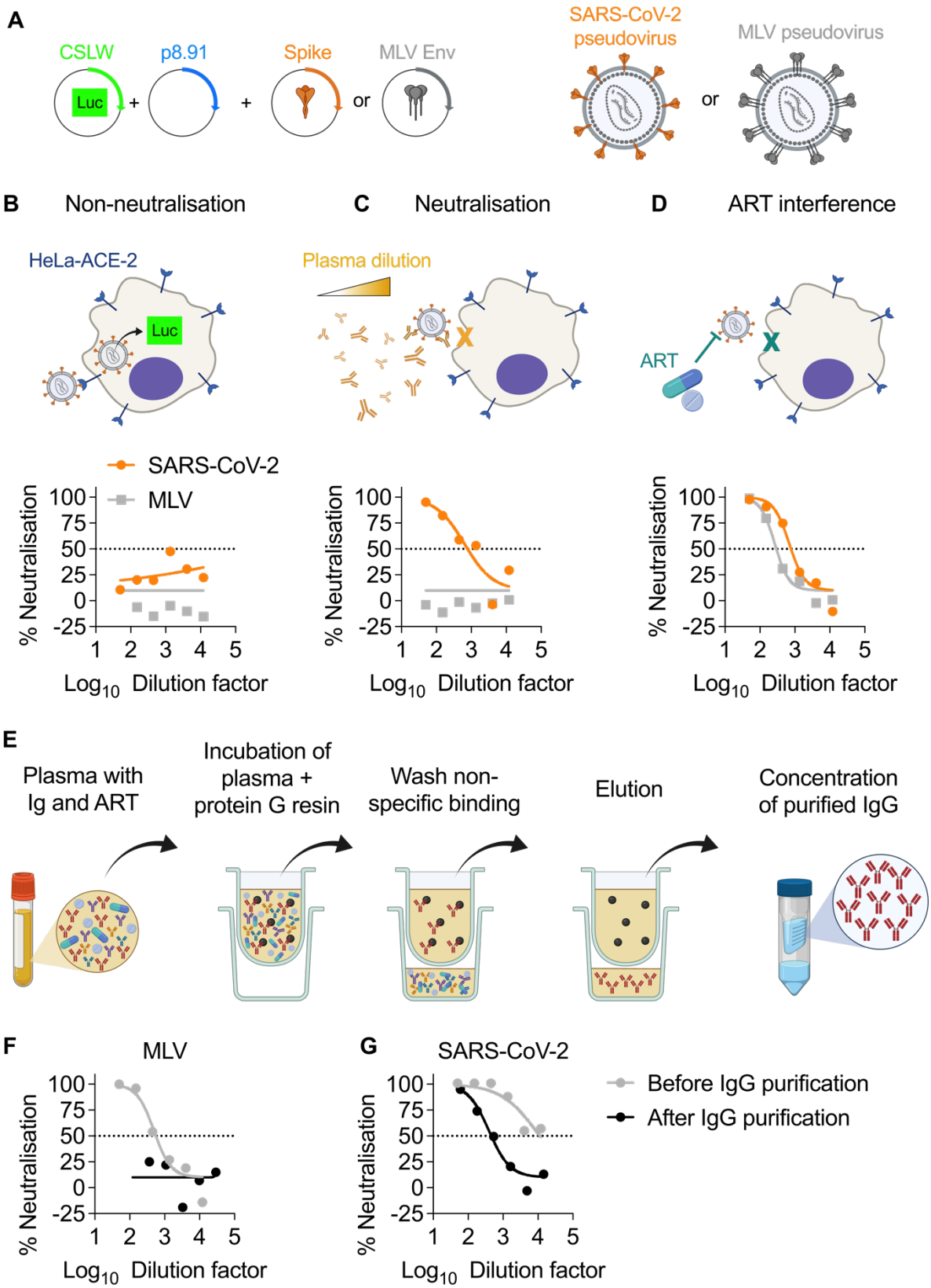
A
CSLW
p8.91
Spike
MLV Env
Luc
+
+
or
SARS-CoV-2 pseudovirus
or
MLV pseudovirus
B Non-neutralisation
C Neutralisation
D ART interference
HeLa-ACE-2
Luc
Plasma dilution
ART
SARS-CoV-2
MLV
% Neutralisation
100
75
50
25
0
-25
1 2 3 4 5
Log10 Dilution factor
E
Plasma with Ig and ART
Incubation of plasma + protein G resin
Wash non-specific binding
Elution
Concentration of purified IgG
F
MLV
G
SARS-CoV-2
Before IgG purification
After IgG purification

***Figure 3.5**: Optimisation of a pseudovirus assay for the detection of SARS-CoV-2 antibodies in PLWH. **A.** Schematic of the 3-plasmid system needed for the production of pseudovirus (PV) particles **B.** Schematic of no neutralising activity: there are no neutralising antibodies against the PV, therefore the PV can infect the cell and luciferase activity is detected. (top). Neutralisation curves from serial dilution of one donor's plasma showing no neutralisation against SARS-CoV-2 PV or MLV PV (bottom). **C.** Schematic of neutralisation: infection of HeLa-ACE-2 cells by the PV is blocked by the presence of neutralising antibodies (top). Neutralisation curves from serial dilution of one donor's plasma showing neutralisation against SARS-CoV-2 PV (orange) but not MLV PV (grey) (bottom). **D.** Schematic of ART interference: due to the presence of ART in the donor's plasma blocking the PV from completing its replication cycle within the cell, and thus blocking luciferase expression (top). Neutralisation curves from serial dilution of one donor's plasma showing neutralisation against both SARS-CoV-2 PV or MLV PV (bottom). **E.** Schematic of the purification of IgG from plasma containing all Ig isotype and ART using protein G resin. Negative controls (**F.** MLV) and positive virus (**G.** SARS-CoV-2) control curves for and pseudovirus neutralisation after serial dilution of one donor's plasma with (black) and without IgG purification (grey).*

3.6. Equivalent titres of WT neutralising antibodies in PLWH and HIV-negative controls after SARS-CoV-2 infection.

Using the pseudovirus neutralisation and IgG purification assay described in ***Figure 3.5***, neutralising antibody titres against SARS-CoV-2 WT were measured for PLWH and HIV-negative controls. Only participants who were seropositive for both S1 and N were tested. This is due to the high confidence that these participants had experienced SARS-CoV-2 infection as described in ***Figure 3.3.*** Additionally, the correlation between binding and neutralising titres suggested it was highly unlikely to mount a detectable neutralising response in the absence of a detectable binding response as seen in other studies (Cohen et al., 2021; Gaebler et al., 2021; Seow et al., 2020).

As this cohort was infected during the first wave of the pandemic in 2020 with collection ending in early November 2020, the pseudovirus used here contains the spike protein of SARS-CoV-2 WT, as based on the Wuhan-Hu-1 isolate (Wu et al., 2020)). Wuhan-Hu-1 was the relevant circulating strain up until April 2020, when the D614G mutation became dominant (Korber et al., 2020). Of note, this single-point mutation only very subtly increased susceptibility to neutralisation but conferred an infectivity advantage (Weissman et al., 2021). Additionally, the Wuhan-Hu-1 isolate formed the basis of contemporaneous assays and all first-generation COVID-19 vaccines (Baden et al., 2021; Folegatti et al., 2020; Polack et al., 2020). Therefore, using Wuhan-Hu-1 as WT represented the most relevant choice for both comparison to other studies studying SARS-CoV-2 infection and to compare any difference in the neutralising responses mounted after infection compared to SARS-CoV-2 vaccination.

As seen with binding titres of S1 and N IgG-specific antibodies, there was no difference in levels of neutralising antibody titres between PLWH and HIV-negative controls (***Figure 3.6A***). Similarly to the binding data, there was no significant link between neutralising titres and the number of days post-symptom onset (***Figure 3.6B***). Although this cohort was only sampled at one timepoint, this suggests that for both PLWH and HIV-negative controls, neutralising titres remained stable during the timeframe of this study. Neutralising titres against WT correlated modestly with both S1 and N binding antibody titres (***Figure 3.6C-D***). Other studies have reported stronger associations between binding, especially to spike, and neutralisation titres (Cohen et al., 2021; Seow et al., 2020; Wang et al., 2020). The modest but significant correlations seen here, especially for S1-specific IgG ($r<0.4$), may have been

strengthened with more uniform timing of sampling, as it has been suggested that binding antibody titres wane more rapidly than neutralising titres (Iyer et al., 2020).

Altogether, this data showed that at a convalescent timepoint PLWH and HIV-negative produced similar neutralising titres against SARS-CoV-2 WT. This suggests that infection with SARS-CoV-2 is immunogenic enough to overcome any immune defect related to chronic HIV infection in PLWH on ART. Although this was a reassuring piece of data for the HIV community at large, it was paramount to understand how the neutralising responses of PLWH would cope with new COVID-19 surges driven by novel variants.

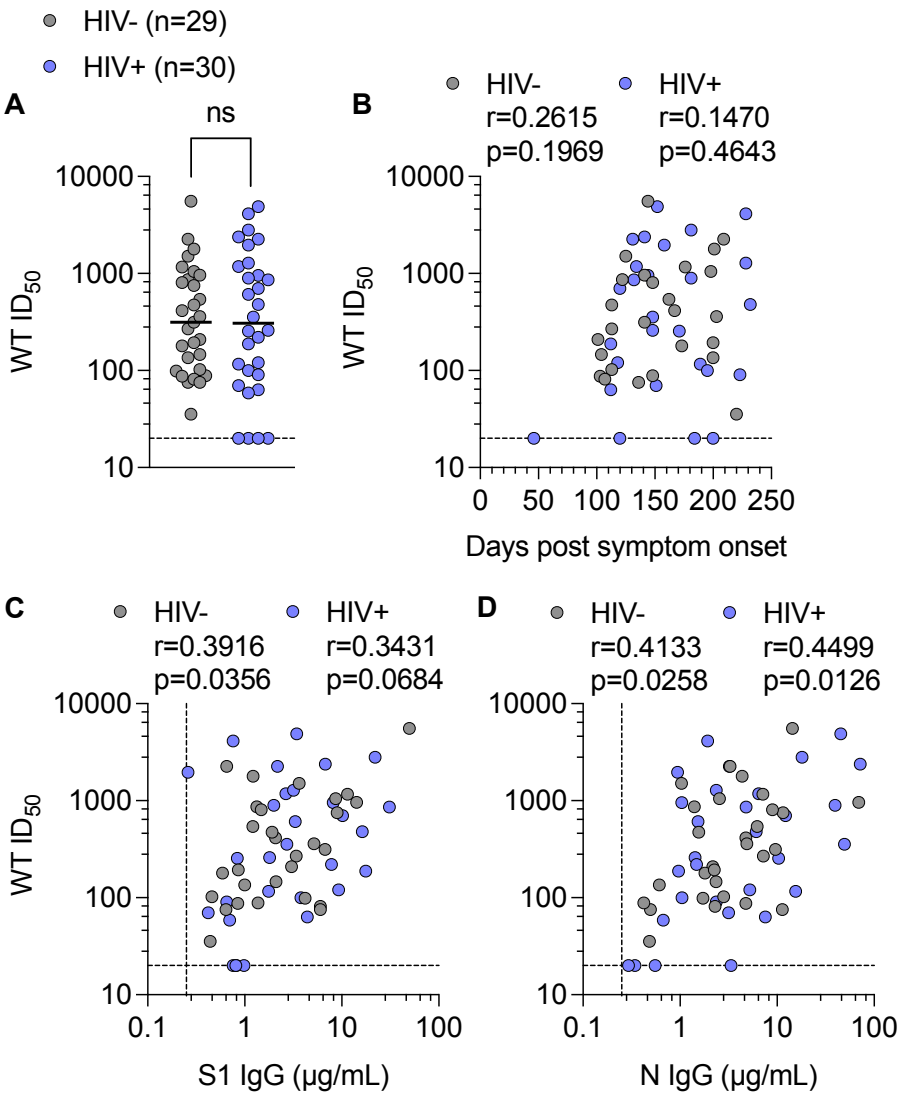

***Figure 3.6**: PLWH and HIV-negative controls have similar titres of neutralizing antibodies against SARS-CoV-2 WT following SARS-CoV-2 infection. **A.** SARS-CoV-2 WT (Wuhan-1) pseudovirus neutralising reciprocal 50% inhibitory titres (ID_{50}) in PLWH (blue) and HIV-negative controls (grey). Each data point represents the mean of n=2 experimental repeats performed in duplicate; the median is shown for each group. **B.** Correlation between SARS-CoV-2 WT neutralising antibody titres (ID_{50}) and days since symptom onset or **C.** S1 IgG-specific antibody titres (µg/mL) or **D.** N IgG-specific antibody titres (µg/mL) for the HIV- and HIV+ group. For A-D, the dotted line represents the limit of detection of the assay: 0.25 µg/mL IgG or ID_{50}=20. Where no neutralisation was detected, samples were assigned an ID_{50} of 20 for visualisation. Statistical test: MWU for A and Spearman's rank correlation for B-D.*

3.7. Convalescent donors, regardless of HIV status, have lower neutralising activity to the SARS-CoV-2 B.1.1.7 variant and to SARS-CoV-1.

Thus far, binding and neutralising responses to SARS-CoV-2 WT were equivalent between PLWH and HIV-negative controls. When this work was done (circa January-February 2021), the B.1.1.7 variant (discussed in **section 1.2.3**) had just arisen and became the dominant variant in the UK and in other parts of the world. At the time, this led to growing concern as to how WT-mediated antibodies, whether by infection in the first wave of the pandemic as seen in this cohort or by vaccination, would cope with this new more antigenically diverse challenge. This concern was particularly exacerbated for immune-compromised populations like PLWH where it was unclear if their neutralising response would be sufficiently broad to neutralise this new variant or future arising variants. To address this question, neutralising titres against the B.1.1.7 variant were measured. Additionally, neutralising titres against the other pandemic betacoronavirus SARS-CoV-1 were assessed to use as a model of how neutralising responses would cope with an even more antigenically distinct virus. Compared to SARS-CoV-2 WT, the B.1.1.7 variant contains six mutations in the S1 domain and three mutations in the S2 domain.

Only individuals who were seropositive for both S1 and N and with WT ID_{50}>150 were assessed for neutralisation breadth. This was because given the pseudovirus assay starts at a dilution of 1:50, samples with ID_{50} values between 50 and 150 can only neutralise (defined as >50% reduction in virus) at the lowest plasma dilution. It was thus hypothesized these weak titres would be unlikely to offer cross-protection against B.1.1.7 or SARS-CoV-1. This decision was guided by the small reduction in neutralisation titres observed against B.1.1.7 (Collier et al., 2021a) and the previously observed large amount of reduction in neutralisation caused by SARS-CoV-1 (Brouwer et al., 2020; Lv et al., 2020; Rees-Spear et al., 2021; Robbiani et al., 2020; Stamatatos et al., 2021; Wang et al., 2023).

Here, PLWH and HIV-negative individuals made comparable neutralising titres against the B.1.1.7 variant of SARS-CoV-2 (***Figure 3.7A***) and against SARS-CoV-1 (***Figure 3.7B***). However, there was a significant decrease in the neutralising response against the B.1.1.7 variant compared to SARS-CoV-2 WT for both PLWH and HIV-negative controls. Similarly, as anticipated both groups made significantly reduced neutralising titres against SARS-CoV-1 compared to SARS-CoV-2 WT (***Figure 3.7C***). Importantly,

the magnitude of the drop in the neutralisation against B.1.1.7 was minimal as compared to that against SARS-CoV-1. For the B.1.1.7 variant, the median fold reduction in ID_{50} was 1.4 for PLWH and 1.5 for HIV-negative controls compared to WT. In contrast, for SARS-CoV-1, the median fold reduction in ID_{50} was of 7.5 for PLWH and 5.4 for HIV-negative controls compared to WT. Two HIV-negative controls and three PLWH participants lost all neutralisation activity but 47% for PLWH and 45% for HIV-negative controls had ID_{50}<100. For neutralisation assays, it is commonly accepted that a reduction in neutralisation titres of less than 3-fold is indistinguishable from assay-to-assay variation and therefore only a fold-change greater than three is considered a real drop or gain in neutralising function (Rees-Spear et al., 2021).

Overall, there was no difference in the breadth of the neutralising responses between PLWH and HIV-negative controls after SARS-CoV-2 infection. The reduction in neutralising titres was consistent with antigenic distance. Neutralisation from WT to B.1.1.7 was mostly consistent for both groups. However, in both groups, nearly half of the participants had ID_{50}<100 against SARS-CoV-1, this highlights that there is heterogeneity in responses even after SARS-CoV-2 infection and as such it is key to understand how this will translate to new emerging variants in SARS-CoV-2 naïve PLWH and HIV-negative controls.

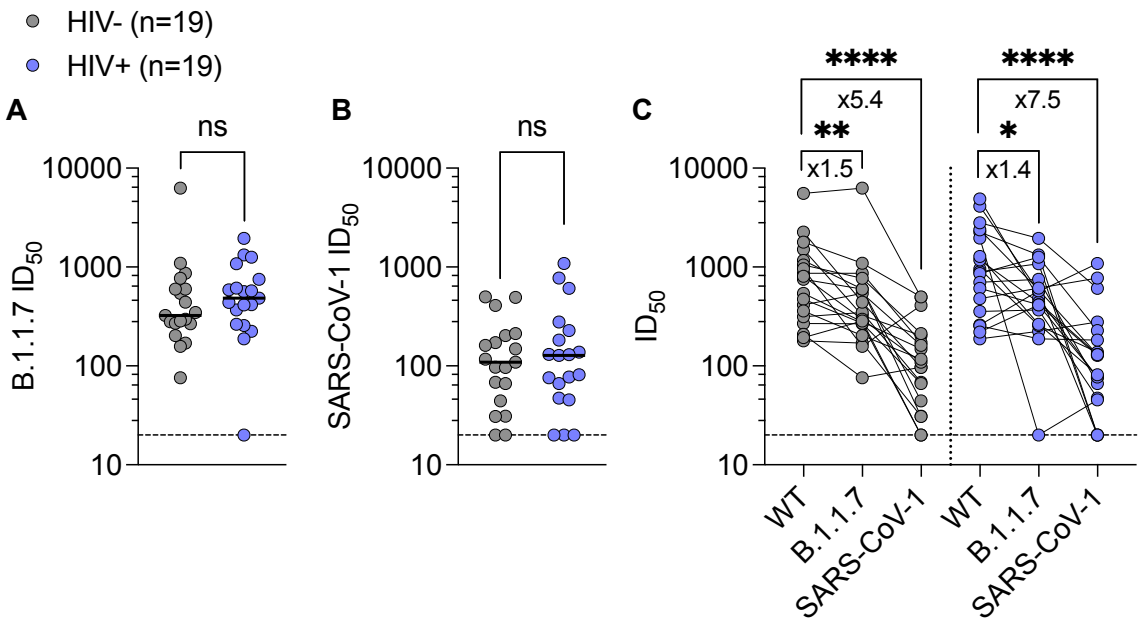

***Figure 3.7**: PLWH and HIV-negative controls have similar titres of neutralising antibodies against SARS-CoV-2 WT following SARS-CoV-2 infection. **A.** SARS-CoV-1 pseudovirus neutralising titres (ID_{50}) in PLWH (blue) and HIV-negative controls (grey). **B.** SARS-CoV-2 B.1.1.7 variant pseudovirus neutralising titres (ID_{50}) in PLWH and HIV-negative controls. **C.** Comparison of SARS-CoV-2 WT, B.1.1.7 variant and SARS-CoV-1 ID_{50}. Median fold decrease from WT to either B.1.1.7 or SARS-CoV-1 is shown for each group. For A-C, each data point represents the mean of n=2 experimental repeats performed in duplicate, the median is shown for each group. The dotted line represents the limit of detection of the assay (ID_{50}=20). Where no neutralisation was detected, samples were assigned an ID_{50} of 20. Statistical test: MWU for A-B and Wilcoxon's matched pair rank test for C.*

3.8. No association between SARS-CoV-2 specific antibody titres and CD4 count or CD4:CD8 ratio.

Although there was no difference in binding or neutralising titres of PLWH compared to HIV-negative controls, using clinical indicators of immune reconstitution like CD4 count and CD4:CD8 ratio can be useful to highlight any differences in responses within the PLWH group (n=30). As seen in the binding and neutralisation data in the previous figures, there is heterogeneity in the titres produced within the PLWH group which may be related to any differences in immune reconstitution.

However, there was no significant correlation (all p=n.s and r<0.4) between S1 IgG-specific titres or SARS-CoV-2 WT neutralising antibodies and either CD4 counts or CD4:CD8 ratios (***Figure 3.7A-D***). Importantly, there is not one single cut-off value for what constitutes a 'low' CD4 count, but of note, only 3/30 individuals in this cohort had CD4 counts under 350 cells/μL which is frequently used as a threshold for incomplete immune reconstitution. This highlights that our cohort is mostly composed of well-recovered PLWH, with a median CD4 count of 560 cells/μL (133-1110) and a median CD4:CD8 ratio is 0.84 (0.17-2.54) (as seen in ***Table 3.2***).

Overall, this suggests that in these well-treated PLWH, the remaining level of T cell-mediated dysfunction did not explain the heterogeneity in binding and neutralising titres seen in PLWH. Effectively, the large immune stimuli that SARS-CoV-2 infection provided enabled these well-treated PLWH to make similar humoral responses to HIV-negative controls following SARS-CoV-2 infection.

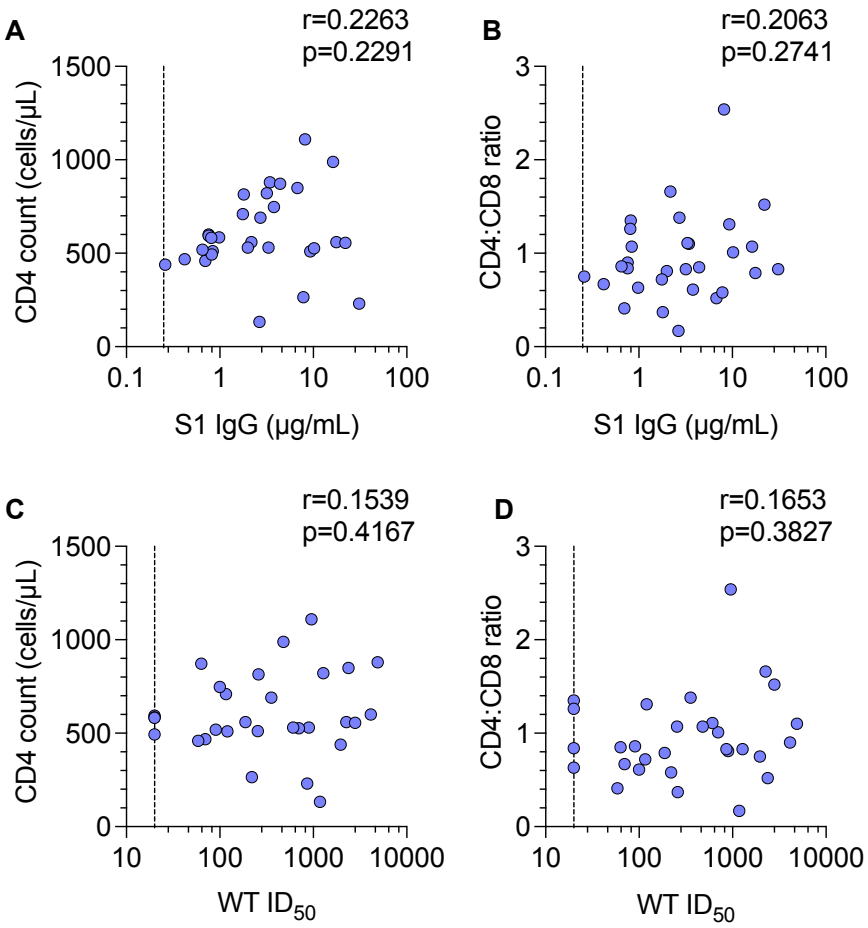

Figure 3.8*: No association between SARS-CoV-2 specific antibody titres and CD4 count or CD4:CD8 ratio*. ***A.*** *Correlation between S1 IgG-specific antibody titres (µg/mL) and CD4 count (cells/µL) or* ***B.*** *CD4:CD8 ratio in PLWH (blue).* ***C.*** *Correlation between S1 IgG-specific antibody titres (µg/mL) and CD4 count (cells/µL) or* ***D.*** *CD4:CD8 ratio in PLWH. For A-D, the dotted line represents the limit of detection of the assay: 0.25 µg/mL IgG or ID_{50}=20. Where no neutralisation was detected, samples were assigned an ID_{50} of 20. Statistical test: Spearman's rank correlation.*

3.9. Discussion

This study allowed for the evaluation of humoral responses post-SARS-CoV-2 infection in PLWH and HIV-negative controls at a convalescent timepoint. To identify SARS-CoV-2 cases, this study relied at first on either outside 'lab-confirmed' diagnosis or self-reported 'suspected' diagnosis of SARS-CoV-2. The 'suspected' group comprised individuals who did not have access to testing at the time but had good reason to suspect a potential SARS-CoV-2 infection. Using, the semi-quantitative assay presented in ***Figure 3.3***, SARS-CoV-2 status was confirmed using the co-presence of S1-specific and N-specific IgG antibodies. Combined detection of N and spike/RBD offered the highest level of specificity and sensitivity for delineating SARS-CoV-2 infection from background cross-reactivity due to hCoV-mediated immunity. Five months after SARS-CoV-2 infection there was no difference in the level of binding antibodies to S1 or N between PLWH and HIV-negative (***Figure 3.4***). Similarly, there was no difference in the level of neutralising antibodies against SARS-CoV-2 WT (***Figure 3.6***). Overall, binding and neutralising antibodies correlated well together. Development of N-specific IgG antibodies alongside S1-specific antibodies post-SARS-CoV-2 infection is consistent with other contemporaneous reports (Algaissi et al., 2020; Harris et al., 2021; Piccoli et al., 2020; To et al., 2020). The lack of longitudinal samples limited the assessment of waning in binding or neutralisation responses. The timing of sampling seen in this cohort mostly represented the stable phase of antibody kinetics with no apparent waning in PLWH or HIV-negative controls' neutralising and binding antibodies. In most individuals, neutralising titres can still be detected after six months post-infection (Chia et al., 2021; Cohen et al., 2021; Dan et al., 2021; Gaebler et al., 2021), which fits with this cohort being sampled roughly five-month post-infection. However, some immunocompromised populations have been observed to lose neutralisation activity already after five months post-infection (Jeffery-Smith et al., 2022). Reassuringly, even the lower end of neutralising titres seen in this cohort (ID_{50}<100) can still confer protection (Corbett et al., 2020; Gilbert et al., 2022).

An important aspect of the work presented here is the context in which it was done. Succinctly, all the work shown here on S1 and N-specific binding and neutralisation against WT was done between October 2020 and December 2020, with the work done on neutralisation against SARS-CoV-1 and B.1.1.7 in January-February 2021. At the time, the literature on COVID-19 and HIV was limited to case studies dealing with

treatment management and small population studies dealing with the increased risk (or not) of adverse COVID-19 outcomes. There was a paucity of data characterising the serological outcome post-SARS-CoV-2 infection in PLWH. This became more urgent with the emergence of SARS-CoV-2 variants like B.1.1.7 or B.1.351 in South Africa where there is a high HIV burden. Concurrent with this work, there were reports of ongoing viral evolution within immunocompromised hosts (Clark et al., 2021; Kemp et al., 2021), which have since been reported in several PLWH throughout the pandemic (Cele et al., 2022; Maponga et al., 2023; Riddell et al., 2022). This led to the growing concern that SARS-CoV-2 infections in severely immunocompromised PLWH could lead to new variants generation.

Therefore, it was particularly relevant to assess if the neutralising responses of PLWH seen at this convalescent timepoint would cope with emerging variants. In the case of this cohort, the participant's immunity was trained against the WT virus, therefore using B.1.1.7 and SARS-CoV-1 to probe neutralisation abilities was useful to differentiate between narrow and broad neutralising responses. There was no difference in the level of neutralising antibodies made by PLWH and HIV-negative controls against either the B.1.1.7 variant or SARS-CoV-1 at that point. The reduction in neutralisation from WT to B.1.1.7 was small and similar in both groups. This is concordant with the small number of mutations (nine) found in B.1.1.7. On the other hand, the reduction in neutralisation was more pronounced for SARS-CoV-1 as it represented an even more antigenically diverse challenge. Obviously, SARS-CoV-1 is altogether a different virus to SARS-CoV-2 albeit there is 78% of sequence similarity between the two spike proteins (Lewitus et al., 2023). At the time, SARS-CoV-1 was a compelling model to assess how well WT-induced neutralisation could protect from future emerging variants. Previous work by our lab and others showed that the neutralising activity of SARS-CoV-2-specific monoclonal antibodies (Brouwer et al., 2020; Rees-Spear et al., 2021; Robbiani et al., 2020; Stamatatos et al., 2021) or plasma from SARS-CoV-2 convalescent donors (Lv et al., 2020; Stamatatos et al., 2021; Wang et al., 2023) had highly variable activity and could be completely abrogated against SARS-CoV-1. Of note, plasma from COVID-19-infected individuals tested against the whole SARS-CoV-1 spike had similar binding abilities but most binding was abrogated when looking only at the S1 domain (Cohen et al., 2021; Okba et al., 2020; Piccoli et al., 2020; Song et al., 2021). Interestingly, plasma from SARS-

CoV-1 survivors appeared to be much more able to bind to the SARS-CoV-2 spike, although neutralisation activity against SARS-CoV-2 was reduced compared to SARS-CoV-1 (Lv et al., 2020; Wang et al., 2023). Studies (Collier et al., 2021a; Greaney et al., 2021; Rees-Spear et al., 2021; Starr et al., 2021) have highlighted that although the mutations found in B.1.1.7, SARS-CoV-1 or other variants can be enough to abrogate binding for monoclonal antibodies it was more likely to see a reduction in neutralisation rather than a complete loss of function or a change in binding with polyclonal plasma. On this basis, binding against spike-specific for B.1.1.7 or SARS-CoV-1 was not measured. Altogether, this showed that after SARS-CoV-2 infection, both PLWH and HIV-negative controls were able to cope with the same level of breadth (***Figure 3.7***). Obviously, this convalescent timepoint only represented a snapshot of the response made by PLWH and HIV-negative controls, with unknown heterogeneity in the severity of their initial infection due to lack of sampling/restricted access to testing. Re-sampling closer to the point of B.1.1.7 emergence and spread would have been more useful to investigate potential protective cross-reactivity and how this may have been limited by antibody waning. Further to this, Gilbert et al. (2022) reported vaccine efficacy (as protecting against infection) of 91% with an ID_{50} of 100 against WT, which here, all participants achieved for B.1.1.7 bar two. Additionally, the presence of neutralising antibody titres against WT at that stage was found to warrant some level of protection as seen in a study (Lumley et al., 2021) which found a lower risk of re-infection in individuals who had a prior SARS-CoV-2 infection during the first wave of the pandemic compared to those who did not. This highlights that the immunity provided by a first WT infection may have been enough to protect against re-infection for most participants. For this cohort, reinfections with WT, B.1.1.7 or any subsequent variants were monitored as part of the vaccine arm of this study (see **Chapter 4**), but the number of reinfections was too low to have statistical power to assess the difference in risk of reinfections between PLWH and HIV-negative controls. Additionally, most participants started receiving vaccination in early 2021 which rendered impossible the assessment of long-term memory response to SARS-CoV-2 infection.

Overall, the lack of difference in both neutralising and binding titres suggests that SARS-CoV-2 infection provided enough immune stimulation to overcome any residual immune dysfunction in PLWH and allowed them to make similar responses to HIV-

negative controls. The data shown in this chapter was published as a joint first author paper which detailed serological and T cell responses in PLWH compared to HIV-negative participants, pre-printed in February 2021 and published fully in November 2021 (Alrubayyi et al., 2021).

Does HIV-mediated immune dysfunction impact the generation of an antibody response post-SARS-CoV-2 infection?

In this study, there was no overall link between HIV-mediated T cell dysfunction as measured by CD4 count and CD4:CD8 ratio and serological output (***Figure 3.8***). This fits with the reports that emerged after the conclusion of this study showing that PLWH with 'high' CD4 counts (>350) did not have an increased risk for adverse COVID-19 outcomes (discussed in **section 1.3.7**). It is important to note this finding in the context of this cohort, where the PLWH could be considered 'well treated' from a clinical standpoint i.e., all on treatment, all with undetectable viral load and 90% with a CD4 count >350 cells/μL (see ***Table 3.2***). It can be hypothesized that in the lower range of CD4 counts, there is a direct link between CD4 count and the development of a functional antibody response. However, once above a certain threshold of CD4 cells/μL, the relationship between antibody development and the amount of CD4+ T cells is likely no longer linear. The finding that neither binding nor neutralising antibody titres correlated with CD4 count of CD4:CD8 ratio in this cohort mostly highlights that most of the cohort had 'enough' CD4s to not impact the production of antigen-specific antibodies. No other study stratified their PLWH group by CD4 count to explore this question but of note when stratifying by viral suppression, PLWH with active viraemia had lower levels of SARS-CoV-2 specific antibodies (Hwa et al., 2023; Khan et al., 2022). Rather than a low CD4 count, two studies suggested that lack of ART and active viraemia were detrimental to the generation of a successful antibody response against SARS-CoV-2 (Donadeu et al., 2022; Hwa et al., 2023). Other studies with similar well-treated cohorts of PLWH found no difference in the antibody titres of PLWH compared to HIV-negative controls (Alcaide et al., 2022; Donadeu et al., 2022; Hwa et al., 2023; Motsoeneng et al., 2023; Snyman et al., 2022). Observations from other published studies that are in disagreement with the results presented here can be explained by the recruitment of PLWH cohort with lower CD4 count and/or with active viraemia (Khan et al., 2022; Spinelli et al., 2021a). Interestingly, in another study where the magnitude of the humoral response in PLWH after infection was also

similar to that of HIV-negative controls, the investigators found that early induction of antibodies (one-week post-hospital admission) was delayed in PLWH compared to HIV-negative controls (Motsoeneng et al., 2023). In our cohort, there was no access to samples during the early development to assess the issue of the early kinetics of the responses. Moreover, the study reported by Motsoeneng et al. (2023) recruited PLWH who required hospital admission i.e., score>4 on the WHO scale used here, whereas very few of our cohort were hospitalised. It is therefore hard to say if these results would translate to a cohort where most PLWH had mild COVID-19 infections.

Due to the low number of participants requiring hospitalisation in this cohort, and no participants being classified as having had severe disease (≥6 on the WHO clinical progression scale), it was not possible to assess any links between humoral responses and severity in PLWH. There are consistent reports of increased risk of mortality after SARS-CoV-2 infections for PLWH as a whole, but the literature is less unanimous on the increased risk of COVID-19 severity. However, there is a growing consensus on the link between lower immune reconstitution in PLWH and a higher risk of severe COVID-19 and mortality as discussed in **section 1.3.7**. As discussed in more detail in **section 1.2.5-6**, patients with severe COVID-19 disease often have higher binding antibody titres against spike and N than those with mild disease (Chen et al., 2020; Lucas et al., 2021; Rees-Spear et al., 2021; Seow et al., 2020; Wang et al., 2020). This is presumably due to higher antigen burden during severe disease, with the caveat that individuals who had died following severe disease had lower antibody titres (Aydillo et al., 2021; Lucas et al., 2021). This pattern did hold for PLWH, where hospitalised PLWH produced higher antibody titres than PLWH with mild COVID-19 (Donadeu et al., 2022; Schuster et al., 2022).

Considering how well PLWH respond to challenges with other viruses beyond SARS-CoV-2, few studies have focused on measuring serological output after infection and rather have focused on serological output post-vaccination. One small study investigating 2009 H1N1 pandemic influenza humoral responses found that PLWH compared to HIV-negative controls made similar IgG, but lower IgM titres 14 days post-infection (Sansonetti et al., 2014). The literature on vaccine responses (reviewed in **section 1.3.6**) shows that PLWH, especially those with continued immune dysfunction, make inferior antibody responses than HIV-negative controls to many routine vaccinations such as influenza, hepatitis B or tetanus vaccines. The lack of

difference in antibody responses seen in this chapter compared to the insights of the vaccine literature can be explained by the difference in the nature of the immune stimuli provided by an infection versus vaccination. Here, the lack of relationship between HIV status and serological output seen here may be attributable to the strength of the immune stimuli received by infection with SARS-CoV-2. This likely allowed the PLWH in this cohort to overcome any residual immune dysfunction to build this equivalent humoral response.

Alongside the serological data presented here, characterisation of the SARS-CoV-2 specific T cell response was published (Alrubayyi et al., 2021). This showed that there were no differences in the magnitude of T cell-specific responses against spike or other SARS-CoV-2 proteins between PLWH and HIV-negative controls. SARS-CoV-2-specific T cell responses overall correlated with SARS-CoV-2 specific neutralising titres highlighting the cooperation between the T and B cell compartments. Overall PLWH with better T cell mediated immune reconstitution had stronger SARS-CoV-2-specific T cell responses. This data was echoed by other studies which showed that other well-treated PLWH made comparable SARS-CoV-2 specific T cell responses (Donadeu et al., 2022; Nkosi et al., 2022). However, PLWH with ongoing viraemia had a lower magnitude of SARS-CoV-2-specific T CD4+ cell responses which in turn led to poorer cross-recognition of subsequent variants (Nkosi et al., 2022).

Overall limitations.

I did not have access to PBMC samples for this convalescent cohort and therefore did not investigate any difference in the generation and phenotype of antigen-specific memory B cell responses in PLWH post SARS-CoV-2 infection. So far only two studies have provided insights into this question (Donadeu et al., 2022; Krause et al., 2022). The available data mirrored the serological insights of this chapter, with PLWH and HIV-negative controls making similar amounts of spike-specific MBCs (Donadeu et al., 2022; Krause et al., 2022). Thus, the best evidence so far shows that although antibodies wane, spike-specific MBCs are maintained for up to six-month post-SARS-CoV-2 infection in HIV-negative controls (Cohen et al., 2021; Dan et al., 2021; Wang et al., 2021b; Wheatley et al., 2021). It will be key to determine how this translates to PLWH with heterogeneous levels of immune reconstitution.

Neutralisation against live viruses was not measured as pseudoviruses are excellent surrogate assays (Cantoni et al., 2023) although this is explored in **Chapter 4**. Verifying the neutralisation data with live virus assays which were at that stage less developed and accessible, would not have allowed the timely publication of this data. A drawback to the method presented in ***Figure 3.6*** is the additional IgG purification required to measure neutralising antibodies in PLWH. Although great care was taken to account for the potential over or under-dilution of the PLWH samples compared to the HIV-negative by adding equivalent amounts of IgG after total IgG quantification, the fact is that samples from PLWH and HIV-negative were fundamentally handled differently which may have introduced variation. A potential limitation of the IgG purification is that neutralisation measured for PLWH will only account for IgG-mediated neutralisation compared to HIV-negative neutralisation. After SARS-CoV-2 infection, IgA and IgM have been shown to be part of the early neutralising response (Gasser et al., 2021; Hale et al., 2022; Pušnik et al., 2022; Sterlin et al., 2021) although IgG-specific antibody responses are the immunodominant portion of the response and form the majority of serum Ig (Cohen et al., 2021; Dan et al., 2021; Long et al., 2020; Seow et al., 2020). Here, after IgG purification in PLWH, any of these IgA or IgM neutralising antibodies would have been lost although it is hard to say how much of these IgA/IgM neutralising antibodies would be present in the first place at this convalescent timepoint. Similarly, only IgG-specific binding titres were measured. Participants were recruited around 46 days post-symptom onset at the earliest and up to 273 days post-symptom onset at the latest. This limited our ability to assess the acute serological response against IgA or IgM in almost all participants as these responses would have waned in the timeframe of this study (Seow et al., 2020). In general, IgM antibodies account for roughly 5% of the antibodies found in peripheral blood whilst IgA accounts for roughly 15% (Gasser et al., 2021; Wang et al., 2021c). These individuals have an additional level of humoral immunity provided by IgA, which is known to be an important part of the post-SARS-CoV-2 infection mucosal response alongside IgM which could not be addressed due to the lack of mucosal samples. IgA and IgM S1 and N-specific titres peak earlier than IgGs (Guo et al., 2020; Iyer et al., 2020; Long et al., 2020; Okba et al., 2020; Röltgen et al., 2020; Seow et al., 2020). Reassuringly, two studies highlighted that the development and titres of IgA and IgM-specific responses were similar in PLWH and HIV-negative controls over a period of 6 months post SARS-CoV-2 infection (Alcaide et al., 2022; Snyman et al., 2022).

Finally, this cohort only represents a snapshot of the serological responses, with variation in the recruitment timing from one month to nearly seven months post-symptom onset. Sampling more uniformly around either a month or five post symptoms onset might have allowed to more confidently assess either the peak neutralisation and binding responses or convalescent responses.

Chapter conclusions.

Altogether the data in the chapter support the idea that well-treated PLWH can make similar serological responses to HIV-negative controls after SARS-CoV-2 infection. This was caveated by several factors: at the time SARS-CoV-2 was a novel pathogen for the entire cohort therefore neither PLWH nor HIV-negative controls could rely on previous recall immunity. Here, the *de novo* B cell response of PLWH appears to be equally efficient to HIV-negative at providing humoral-level protection. Additionally, PLWH in this cohort were all well-treated and mostly experienced mild COVID-19 disease. Therefore, this cohort neither represented the full spectrum of HIV-mediated dysfunction or COVID-19 severity. The long-term evaluation of the strength and quality of the post-SARS-CoV-2 infection responses in PLWH was quickly limited by the rapid distribution of COVID-19 vaccines. Therefore, I next characterised how this prior infection-mediated immunity affected the serological responses of PLWH post-vaccination and how it compared to serological responses made by infection-naïve PLWH.

4. Humoral responses to SARS-CoV-2 vaccination in PLWH

4.1. Summary

Shortly after the study of SARS-CoV-2 infection responses in PLWH was completed as described in **Chapter 3**, the first COVID-19 vaccines were licensed in the UK and given from the 8th of December 2020 onward. This allowed for the unique opportunity to systematically characterise the humoral responses made by PLWH against what at the time was a vaccine against a novel pathogen, SARS-CoV-2. Indeed, PLWH were prioritised for early vaccination regardless of age (JCVI, 2022), based on historical data showing lower serological output following vaccination due to potential immune dysfunction. As such there was an urgent need to understand if HIV status would impact SARS-CoV-2 vaccination outcomes.

The main aim of this chapter was to assess the quantitative and qualitative serological responses of PLWH to SARS-CoV-2 vaccination following the initial two-vaccine dose vaccine course. The work then expanded to investigate responses after a booster or 3rd vaccine dose. As part of the Vaccine in Chronic Infection / Jenner II studies (see **section 2.1** for details), 111 PLWH and 64 HIV-negative participants in total were sampled from December 2020 until March 2022 before and after 1, 2 and 3 doses of COVID-19 vaccines. Each group had a mix of SARS-CoV-2 naïve participants and of participants with prior SARS-CoV-2 infection. To characterise the humoral responses following vaccination, IgG binding titres against S1 and neutralisation titres were measured against the strain on which the initially licenced vaccines were based, SARS-CoV-2 Wuhan-hu1 (WT). Finally, to further ascertain the breadth of the response in both groups, neutralising titres against the SARS-CoV-2 variant Omicron BA.1 were measured.

The data presented in **section 4.2** was published as part of a case report in June 2021 (Touizer et al., 2021), most of the data presented in the rest of this chapter was published as part of a wider study on humoral, B and T cell responses to SARS-CoV-2 vaccination in January 2023 (Touizer et al., 2023) (this work was first pre-printed in November 2022).

4.2. Failure to seroconvert following 2 vaccine doses of COVID-19 vaccination in a participant with advanced HIV.

Alongside the known increased risk of opportunistic infections, it has been clear throughout the HIV pandemic that PLWH with advanced HIV have poorer vaccination outcomes compared to the general population and to PLWH without advanced HIV as discussed in **section 1.3.5**.

On the 18th of January 2021, an individual with advanced HIV attended the Mortimer Market Centre clinic and was recruited to the Jenner II study. At that time, this participant was a late presenter with profound immune dysfunction with a CD4 count of 20 cells/μL, a CD4:CD8 ratio of 0.03, high viraemia (831,764 viral copies/ml) and was not on ART (***Figure 4.2A-B***). Simultaneous with recruitment, ART and prophylaxis against opportunistic infections were started right away. However, before sampling, this participant had already received two vaccine doses of BNT162b2 mRNA vaccines due to potential occupational exposure. This vaccination course was carried on the original schedule, where the second vaccine dose was administered 24 days after the first vaccine dose, not following the extended schedule later implemented in the UK. The participant did not declare or have clinically validated prior SARS-CoV-2 infection, nor was there evidence they contracted it during the study period.

This first sample was obtained 40 days after the 1st vaccine dose and 16 days after the 2nd vaccine dose. At this point, the participant had not seroconverted (S1-specific IgG titres<0.6μg/mL; undetectable neutralising antibody titres against WT and Omicron BA.1) (***Figure 4.2C-D***). This failure to seroconvert was observed despite having received two vaccine doses of BNT162b2, which is highly unlikely to happen in the general population in whom this vaccine is very immunogenic (Goel et al., 2021b; Krammer et al., 2021; Sahin et al., 2021) and was a marked contrast to HIV-negative controls already collected in our studies post vaccination at the time of sampling (Touizer et al., 2021). A second sample was obtained 68 days after the 1st vaccine dose, at which point the participant had an undetectable viral load, but still had a CD4 count of 70 cells/μL and a CD4: CD8 ratio of 0.08. Similarly, there was still no measurable sign of seroconversion.

After these two vaccine doses but before the administration of a 3rd vaccine dose on day 224 post 1st vaccine dose, the participant gave further samples on days 124, 154

and 204. Owing to ART-mediated viral suppression (which commenced at the first sample timepoint at day 40), the immune system of the participant continued to rapidly recover with CD4 counts of 160, 160 and 190 cells/μL respectively and CD4:CD8 ratio of 0.07, 0.07 and 0.09 (***Figure 4.2A-B***). Despite this immune restitution, the S1-specific IgG binding titres post-vaccination were only barely detectable (0.93, 0.61 and <0.6 μg/mL respectively) and there were still no detectable neutralising antibodies against SARS-CoV-2 WT or Omicron BA.1 (***Figure 4.2C-D***).

Finally, after 224 days after the 1st vaccine dose, the participant received an additional 3rd vaccine dose of BNT162b2. When sampled 15 days post 3rd vaccine dose (day 239), the participant produced a strong humoral response with an S1-specific IgG binding titre of 169.35 μg/mL, neutralising antibody titre of 1473 against WT and of 1799 against Omicron BA.1 (***Figure 4.2C-D***). At the point of the 3rd vaccination, the participant had started ART nearly seven months prior and had a CD4 count of 200 along a CD4:CD8 ratio of 0.13, which although still low, is within the range of values seen in PLWH on suppressive ART who are immune reconstituted. Importantly, the spike-specific antibody response seen here is in a range that reflects the recall responses seen from the 2nd vaccine dose onward rather than a *de novo* response (as seen in ***Figures 4.4A*** and ***4.5A***). This suggests that despite little humoral response after two vaccine doses, some memory B cells were generated and were likely recalled after the 3rd vaccine dose to contribute to the serum response observed at this final timepoint.

The first description of this case study included the first two samples and additional data on the lack of SARS-CoV-2 T-cell specific responses and was published in June 2021 in Lancet HIV (Touizer et al., 2021). The complete picture presented here agrees with the main conclusion of that publication that profound immune dysfunction due to ongoing HIV viraemia can prevent an individual from robustly seroconverting after two vaccine doses of mRNA vaccination against COVID-19. However, we also found evidence for a level of B cell response before the third vaccine dose. More importantly, rapid initiation of ART at 40 days after the initial vaccination and an additional 3rd vaccine dose once the participant had recovered more immune function allowed for a strong humoral response comparable to the one seen post 3rd vaccine dose in SARS-CoV-2 naïve participants with or without HIV. This shows the potential benefit of waiting for immune reconstitution or revaccinating after COVID-19 initial vaccination

which is similar to the situation observed in cases of B-cell related immune dysfunction (Pinder et al., 2023; Prendecki et al., 2021; Zonozi et al., 2023). Moreover, this initial case suggested it may be important to investigate humoral responses to COVID-19 vaccination in the PLWH population at large to better understand how immune dysfunction can affect vaccine responses.

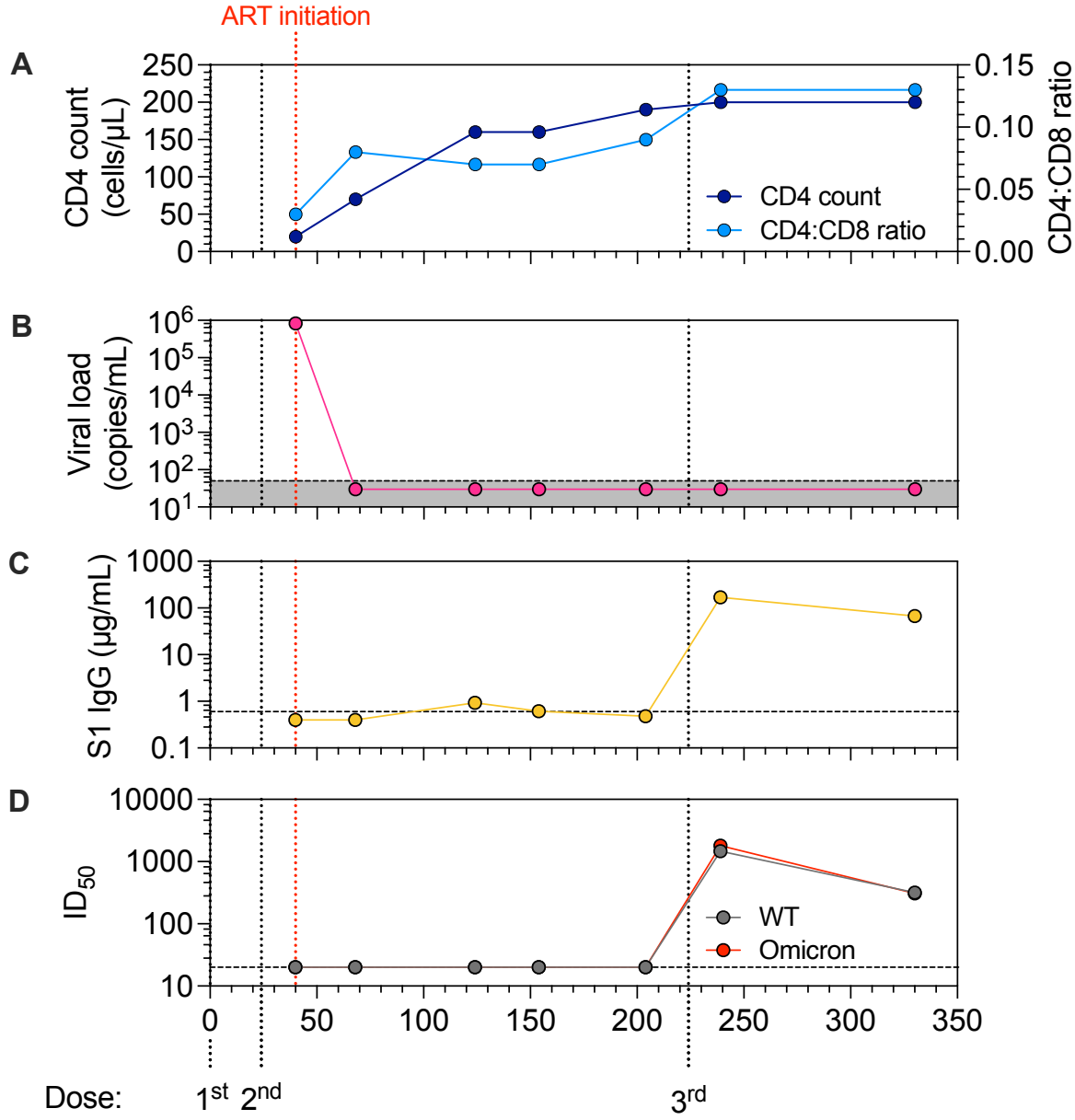

Figure 4.2*: Failure to seroconvert following 2 vaccine doses of COVID-19 vaccination in a participant with advanced HIV*. ***A.*** *CD4 count (cells/µL) and CD4:CD8 ratio;* ***B.*** *HIV viral load (copies of RNA/mL);* ***C.*** *S1-specific IgG (µg/mL) and* ***D.*** *SARS-CoV-2 WT (Wuhan-hu1) or Omicron BA.1 pseudovirus neutralising reciprocal 50% inhibitory titres (ID_{50}) for the index patient over time. 1st vaccine dose was given at day 0, 2nd vaccine dose at day 24 and 3rd vaccine dose at day 224. The dotted lines represent the limit of detection of the assays (for B. viral load<50 copies/mL, for C. 0.6µg/mL of IgG and for D. ID_{50}=20). Where no binding was detected, samples were assigned a titre of 0.4 µg/mL and where no neutralisation was detected, samples were assigned an ID_{50} of 20 for visualisation.*

4.3. Vaccination cohort design.

In concert with the observation that seroconversion in response to vaccination was not achieved in the absence of ART, we sought to collect samples from PLWH on suppressive medication and uninfected controls. To this end, a total of 111 PLWH and 64 HIV-negative individuals were recruited as part of either the VCI or Jenner II studies between November 2020 and March 2022 around their COVID-19 vaccination. Due to the fast-paced nature of the COVID-19 vaccine roll-out, participants were recruited in a longitudinal manner to maximise sampling around the defined timepoints in **section 2.1.2**, but where this was not possible participants were also recruited after any number of vaccine doses. As such the results presented in this chapter should be considered as a collection of cross-sectional samples for each timepoint unless specified.

Briefly, samples were collected at the following timepoints: baseline, post 1st vaccine dose (at least >12 days post 1st vaccine dose), post 2nd vaccine dose (between 7-70 days post 2nd vaccine dose), pre 3rd vaccine dose (at least >70 days post 2nd vaccine dose) and post 3rd vaccine dose (at least >7 days post 3rd vaccine dose). These timing parameters were set to allow for enough time after each vaccine dose to evaluate the induction of a *de novo* humoral response or in the case of the pre 3rd vaccine dose timepoint to evaluate waning (Goel et al., 2021a; Levin et al., 2021; Seow et al., 2020). All PLWH recruited had undetectable viral loads and were currently on ART treatment. For the SARS-CoV-2 naïve PLWH, the median CD4 count was 601 cells/μL and the median CD4:CD8 ratio was 0.74. For PLWH with prior SARS-CoV-2, the median CD4 count was 560 cells/μL and the median CD4:CD8 ratio was 0.93.

To infer SARS-CoV-2 status (prior infection or naïve), participants were systematically asked about any previous positive test/infection at sampling. Additionally, I found that S1-specific IgG titres and neutralising antibodies against WT were clearly in a very different range in the case of vaccination plus infection (as seen in ***Figure 4.4C-D*** and ***4.5C-D***) as per other independent reports (Bates et al., 2022; Krammer et al., 2021; Reynolds et al., 2021, 2022a). This added another level of confidence in identifying potential asymptomatic infection. In contrast to the previous chapter, N-specific IgG titres were not generated, mainly because the difference in S1-specific IgG titres between those who reported prior infection and those who did not was robust and in line with the literature showing a clear demarcation between individuals with and

without prior infection after vaccination. Moreover, N-specific ELISAs were not performed due to cross-reactivity with seasonal coronaviruses rendering this assay not discriminatory unless used in conjunction with a spike ELISA (as originally described in (Pickering et al., 2020)), and the joint approach was nullified by the seroconversion triggered by vaccination. However, due to self-reporting and lack of clinical surveillance particularly in PLWH (many of the HIV-negative controls recruited were healthcare workers), minimal data existed on the exact timing of prior infection and/or the infecting variant. Over the course of the study, 10 participants declared a breakthrough infection: 3 provided pre 3rd vaccine dose samples, 6 post 3rd vaccine dose samples and 1 provided both pre and post 3rd vaccine dose samples. It is important to note that this study was not powered to study breakthrough infection and only a handful of these occurred and are described in detail later and signposted throughout the figures only for information.

	HIV- (n=64)		HIV+ (n=111)	
	SARS-CoV-2 naïve (n=27)	prior SARS-CoV-2 (n=37)	SARS-CoV-2 naïve (n=66)	prior SARS-CoV-2 (n=45)
	Clinical parameters			
% Female	76%	41%	8%	18%
% Ethnic minorities (excl. white minorities)	26%	24%	22%	44%
Median age (range)	33 (21-65)	41(23-66)	53 (22-93)	49 (26-73)
HIV viral load (viral copies/mL)	-	-	Undetectable (<50)	Undetectable (<50)
Median CD4 count (range)	-	-	601 (22-1360)	560 (200-1229)
Median CD4:CD8 ratio (range)	-	-	0.74 (0.07-3.05)	0.93 (0.37-2.55)
Diabetes	-	1	1	3
Hypertension/ Cardiovascular disease	-	3	6	6
Renal disease	-	-	5	1
Liver disease	-	-	3	2
Respiratory disease	-	1	3	1
Weakened immune system inc. cancer/transplant	-	-	7	1
Advanced HIV/ Hepatitis B co-infection	-	-	5	-
Other	-	-	Splenectomy, Sarcoidosis, Chylous Ascites	Splenectomy

***Table 4.3.1**: Demographic information for the vaccine cohort. Demographic data was reported upon recruitment as described in **section 2.1.2**.*

	HIV- (n=64)		HIV+ (n=111)	
	SARS-CoV-2 naïve (n=27)	prior SARS-CoV-2 (n=37)	SARS-CoV-2 naïve (n=66)	prior SARS-CoV-2 (n=45)
	Timepoints			
	Baseline			
N=	15	11	19	17
	post 1st vaccine dose			
N=	17	28	31	32
Median days post-1st vaccine dose (range)	14 (12-74)	19 (12-60)	20 (12-102)	22(13-82)
Vaccine (AZ | Moderna | Pfizer)	3 | 2 | 12	3 | 1 | 24	19 | 2 | 10	21 | 0 | 11
	post 2nd vaccine dose			
N=	18	25	30	24
Median days post-2nd vaccine dose (range)	39 (23-67)	26 (15-68)	20 (7-48)	21 (9-52)
Vaccine (AZ | Moderna | Pfizer)	3 | 3 | 12	2 | 1 | 23	17 | 1 | 12	12 | 0 | 12
	pre 3rd vaccine dose			
N=	21	26	39	16
Median days post-2nd vaccine dose (range)	129 (75-258)	129 (76-236)	125 (72-218)	119 (86-317)
Vaccine (AZ | Moderna | Pfizer)	-	-	-	-
	post 3rd vaccine dose			
N=	14	25	34	16
Median days post-3rd vaccine dose (range)	21 (13-43)	43 (18-129)	40 (9-149)	64(7-125)
Vaccine (AZ | Moderna | Pfizer)	0 | 3 | 12	0 | 2 | 23	1 | 2 | 32	1 | 0 | 15

***Table 4.3.2**: Breakdown of participants' vaccination history at each timepoint for the vaccine cohort. The participants recruited in this cohort were sampled with a mixed longitudinal and cross-sectional approach, meaning different numbers of participants were sampled at the different timepoint as indicated in this table. The definition for the timepoints is described in **section 2.1.2**. AZ= AZD1222; Moderna=mRNA-1273 and Pfizer= BNT162b2.*

4.4. Lower levels of binding S1 antibodies in SARS-CoV-2 naïve PLWH compared to HIV-negative control.

As seen with responses to SARS-CoV-2 infection, antibodies against spike, particularly against the S1 subunit, are associated with protection against SARS-CoV-2 reinfection (Gilbert et al., 2022; Lumley et al., 2021). Moreover, in the UK all licenced COVID-19 vaccines target the induction of a spike-specific response by delivering the spike protein either via a viral vectored envelope or via mRNA to be translated *in vivo*. All the participants in this cohort received either AstraZeneca's AZD1222, Pfizer-BioNTech's BNT16b2 or Moderna's mRNA-1273 or a mix of these vaccines. As such the first proof of a successful vaccine response was to measure the level of binding IgG antibodies against S1 using a semiquantitative ELISA.

In the SARS-CoV-2 naïve group (***Figure 4.4A***), PLWH and HIV-negative participants produced similar S1-specific IgG titres after 1 and 2 vaccine doses of COVID-19 vaccines, although there was a non-significant trend towards lower titres in PLWH. At the pre-3rd vaccine timepoint, SARS-CoV-2 naïve PLWH produced significantly lower S1-specific IgG titres compared to SARS-CoV-2 naïve HIV-negative controls, despite similar sampling intervals (both groups were recruited at a median of 129 days post-2nd vaccine dose). This suggests that the waning of the binding antibodies after the 2nd vaccine dose was more rapid in the PLWH group. Following the 3rd vaccine dose, SARS-CoV-2 naïve PLWH continued to have significantly lower S1-specific IgG titres compared to SARS-CoV-2 naïve HIV-negative controls. Seroconversion was 100% at all timepoints for all HIV-negative participants with prior infection from baseline onward. For the SARS-CoV-2 naïve HIV-negative controls, 94% seroconverted after the 1st vaccine dose and 100% after the 2nd vaccine dose, they then maintained seropositivity for S1 throughout the study (***Figure 4.4A***). As such, it is particularly notable to see that two SARS-CoV-2 naïve PLWH did not seroconvert even after 3 vaccine doses and two SARS-CoV-2 naïve PLWH achieved very low titres of 0.72 and 0.83 µg/mL respectively despite maintaining viral suppression on ART.

In the group with prior SARS-CoV-2 (***Figure 4.4B***), there was no significant difference between the S1-specific IgG titres made by PLWH compared to HIV-negative controls at any timepoint. This observation fits with the binding data seen in **section 3.4** and hints that regardless of HIV status, SARS-CoV-2 infection is enough to provide strong S1-specific IgG titres in PLWH equivalent to those in HIV-negative controls regardless

of any residual immune dysfunction. Indeed, HIV-negative controls (***Figure 4.4C***) and PLWH (***Figure 4.4D***) with prior SARS-CoV-2 made significantly higher S1-specific IgG titres than their SARS-CoV-2 naïve counterparts. Each vaccine dose showed a benefit for SARS-CoV-2 naïve participants regardless of HIV status, with binding titres rising, whereas titres from participants with prior SARS-CoV-2 infection seemed to have plateaued already after 1 vaccine dose. Of note, the magnitude of the differences between the SARS-CoV-2 naïve and experienced group did decrease with additional vaccine doses. As seen in ***Figure 4.4C***, three vaccine doses in HIV-negative SARS-CoV-2 naïve individuals were enough to 'catch up' to those with prior SARS-CoV-2 infection, although this was not true for the PLWH group (***Figure 4.4D***). This clear difference in the titres following vaccination alone or by hybrid immunity (vaccination plus infection) has been widely reported in the general population (Bates et al., 2022; Krammer et al., 2021; Reynolds et al., 2021, 2022a).

At the pre 3rd dose timepoint, 4 samples were from participants who experienced breakthrough infection post 2nd vaccine dose (1 PLWH, 3 HIV-negative controls). At the post 3rd dose timepoint, 4 samples were from participants who experienced breakthrough infection post 2nd vaccine dose (4 HIV-negative controls) and 3 were from participants who experienced breakthrough infection post 3rd vaccine dose (3 PLWH). No formal sequencing was done to assess which variant strain may have been the cause of these breakthrough infections, but the timing of the post 2nd vaccine dose infections coincided with the Delta (B.1.617.2) wave of Summer 2021 in the UK whilst the post 3rd vaccine dose infections coincided with the Omicron (BA.1/BA.2) wave in the UK. 5/8 post 2nd vaccine dose breakthrough cases happened in participants with previous WT/Alpha SARS-CoV-2 infection. Overall, these numbers are too low to make any meaningful comparisons, but it seems that participants with breakthrough infections (highlighted in red in the figures) produced similar S1-specific IgG titres to those who experienced SARS-CoV-2 infections before vaccination.

Overall, these data show that although binding titres against S1 were similar between PLWH and HIV-negative controls with prior experience of SARS-CoV-2 infection, SARS-CoV-2 naïve PLWH did struggle more than their HIV-negative control counterparts to maintain their S1-specific titres after the initial two-dose vaccine course. Similarly, they had lower binding responses after three vaccine doses, although the third vaccine dose provided an added level of stimulation which rescued

the pronounced waning seen particularly in SARS-CoV-2 naïve PLWH at the pre-3rd timepoint.

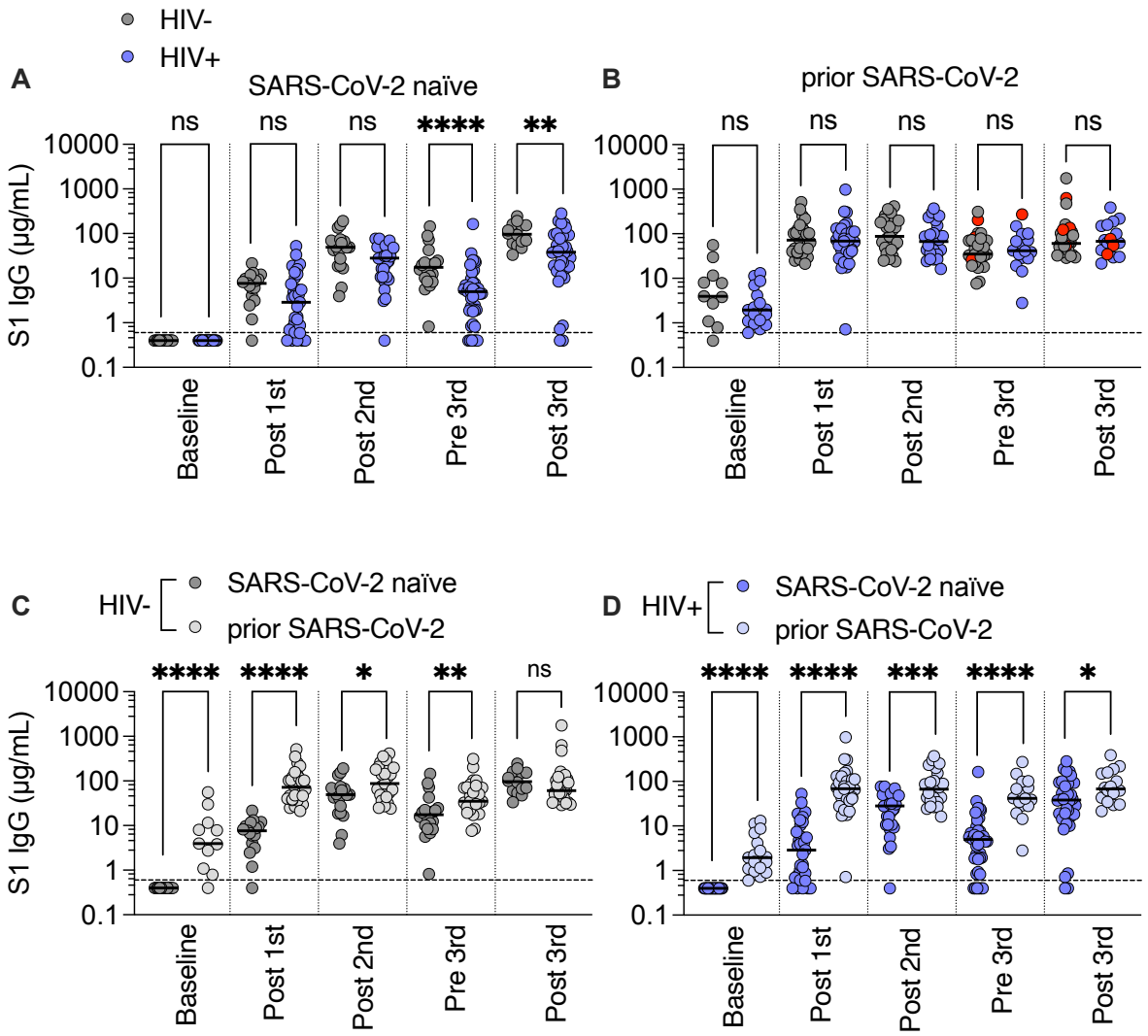

***Figure 4.4**: Lower levels of binding S1 antibodies in SARS-CoV-2 naïve PLWH compared to HIV-negative control. IgG-specific antibody titres (µg/mL) against SARS-CoV-2 S1 for **A.** SARS-CoV-2 naïve participants and **B.** participants with prior SARS-CoV-2 infection stratified by timepoint and HIV status (HIV-negative controls – grey; PLWH – blue; breakthrough infection - red). IgG-specific antibodies titre against SARS-CoV-2 S1 for **C.** HIV-negative controls and **D.** PLWH stratified by timepoint and SARS-CoV-2 experience. For A-D, data points are representative of n=2 experimental repeats performed in duplicate, is shown the median for each group, the dotted line represents the limit of detection of the assay (0.6 µg/mL IgG). N numbers for each group are equivalent to those seen in **Table 4.3.2**. Where no binding was detected, samples were assigned a titre of 0.4 µg/mL. Statistical test: MWU.*

4.5. Lower levels of WT neutralisation in PLWH across all timepoints, regardless of previous COVID-19 infection.

After assessing binding to S1, neutralising antibodies against the SARS-CoV-2 Wuhan-Hu-1 strain were measured using a pseudovirus assay as described in ***Figure 3.5***. During the timeframe of this study, all participants received 'first-generation' COVID-19 vaccines which were designed based on the Wuhan-Hu-1 strain, making the use of SARS-CoV-2 Wuhan-Hu-1 pseudovirus (WT) the most relevant readout of an effective vaccine response.

In the SARS-CoV-2 naïve arm of the cohort, PLWH systematically produced lower neutralising titres against SARS-CoV-2 WT compared to HIV-negative controls (***Figure 4.5A*** and ***E-F***). This difference was already striking after the 1st vaccine dose where the median ID_{50} was of 1:20 for PLWH and 1:127 for HIV-negative controls, translating to more than 71% of PLWH producing a seronegative or non-neutralising response compared to 18% of HIV-negative controls. Similarly, neutralising antibody titres from PLWH waned faster after the initial two-dose vaccine course shown by the lower levels seen at the pre-3rd vaccine dose timepoint (median WT ID_{50} of 1:30 compared to 1:302 in HIV-negative). Reassuringly, neutralising titres were increased both for HIV-negative and PLWH post 3rd vaccine dose. The upper range of responses seen in PLWH after the 3rd vaccine dose is similar to the one seen in HIV-negative controls meaning that a proportion of PLWH are able to make a 'normal' response. However, there is an overall reduction at the population level is due to the PLWH with lower responses who may be the individuals with residual immune dysfunction.

Unlike with S1-specific binding titres, PLWH with prior SARS-CoV-2 infection also made lower WT neutralising antibody titres compared to HIV-negative controls after each timepoint (***Figure 4.5B***). This may indicate that although PLWH with prior infection-based immunity mount equally strong binding responses, re-exposure through vaccination broadens the neutralising response more in HIV-negative controls than in PLWH. Despite this difference, all PLWH and all HIV-negative controls with prior SARS-CoV-2 infection had detectable neutralising antibody titres and maintained them throughout the timeframe of this study (***Figure 4.5G-H***). As with S1, participants with breakthrough infections (coloured in red in ***Figure 4.5B***) had heterogeneous neutralising titres against WT. Of note, PLWH with prior SARS-CoV-2 infection had significantly lower neutralisation titres against WT than HIV-negative controls at

baseline (***Figure 4.5B***). This appears to contradict the lack of difference seen at a convalescent timepoint (***Figure 3.6***). Although both sets of samples are post-SARS-CoV-2 infection only, on average the data in ***Figure 4.5B*** represents participants who had an initial infection either during the first wave of the pandemic (spring 2020) or second wave (autumn 2020-winter 2021). In other words, there is a longer interval between infection and sampling in this figure than in ***Figure 3.6***. Effectively, this result may indicate that waning is more pronounced in PLWH than HIV-negative although there was not enough overlap between the participants in the convalescent cohort and in the vaccination cohort to statistically test this hypothesis.

As reported with S1-specific IgG binding antibodies, participants with prior SARS-CoV-2 infection had significantly higher titres of neutralising titres against WT, regardless of HIV status, at all timepoints up until 3rd vaccine dose. After this last vaccination, in both the PLWH and HIV-negative control group, neutralisation titres against WT were similar regardless of SARS-CoV-2 status (***Figure 4.5C-D***). The results from ***Figure 4.5D*** show that PLWH can make highly potent neutralising titres when given the correct stimuli, here either infection plus one vaccination or three vaccinations alone. Obviously, SARS-CoV-2 infection, its accompanying illness and risk of long-term complications is never a desirable outcome in any individual, but here it conceptually provides a model of what a highly immunogenic stimulus can achieve in individuals with immune dysfunction. Specifically, in PLWH with prior SARS-CoV-2, all participants bar one achieved neutralisation titres against WT greater than 1:100 after the 1st vaccine dose and maintained them, which according to Gilbert et al., (2022) provides 91% vaccine efficacy against infection with WT.

Finally, the differences in neutralisation potency between PLWH and controls after the 3rd vaccine dose in the SARS-CoV-2 naïve arm of the cohort were validated by Nicholas Matheson's lab at Cambridge using a live virus assay (Gerber et al., 2022). To closely model the WT pseudovirus assay used, a live virus (SARS-CoV-2/human/Liverpool/REMRQ0001/2020) isolated early in the first wave of the pandemic was used in this assay. This was pursued because of the striking differences observed in neutralisation post-vaccination as opposed to the equivalence in titres found in **Chapter 3**. There was a strong correlation ($r>0.6$) between live and pseudovirus-based neutralising titres for these samples (***Figure 4.5I***). Using this live virus approach there was still a decrease in neutralising titres in SARS-CoV-2 naïve PLWH compared

to HIV-negative controls at the 3rd vaccine dose. While the decrease was no longer significant (***Figure 4.5J***), importantly the same individuals in both the pseudovirus and the live neutralisation assay were found to be negative (***Figure 4.5I***). The absolute increase in titres from pseudovirus WT ID_{50} to live virus NT_{50} was equivalent in both groups (***Figure 4.5K***).

Overall, PLWH made lower neutralising titres against the SARS-CoV-2 WT strain than HIV-negative controls, regardless of timepoint and prior SARS-CoV-2 infection. Reassuringly, PLWH with prior SARS-CoV-2 infection all produced a detectable neutralising response after the 1st vaccine dose and maintained high titres throughout the study showing that PLWH can produce a satisfactory humoral response after a strong immunogenic stimulus of infection plus vaccination. To further understand the functionality of the neutralisation response seen in PLWH post-SARS-CoV-2 vaccination, I next assessed how well PLWH's neutralisation responses could cope with a more antigenically diverse variant like Omicron BA.1.

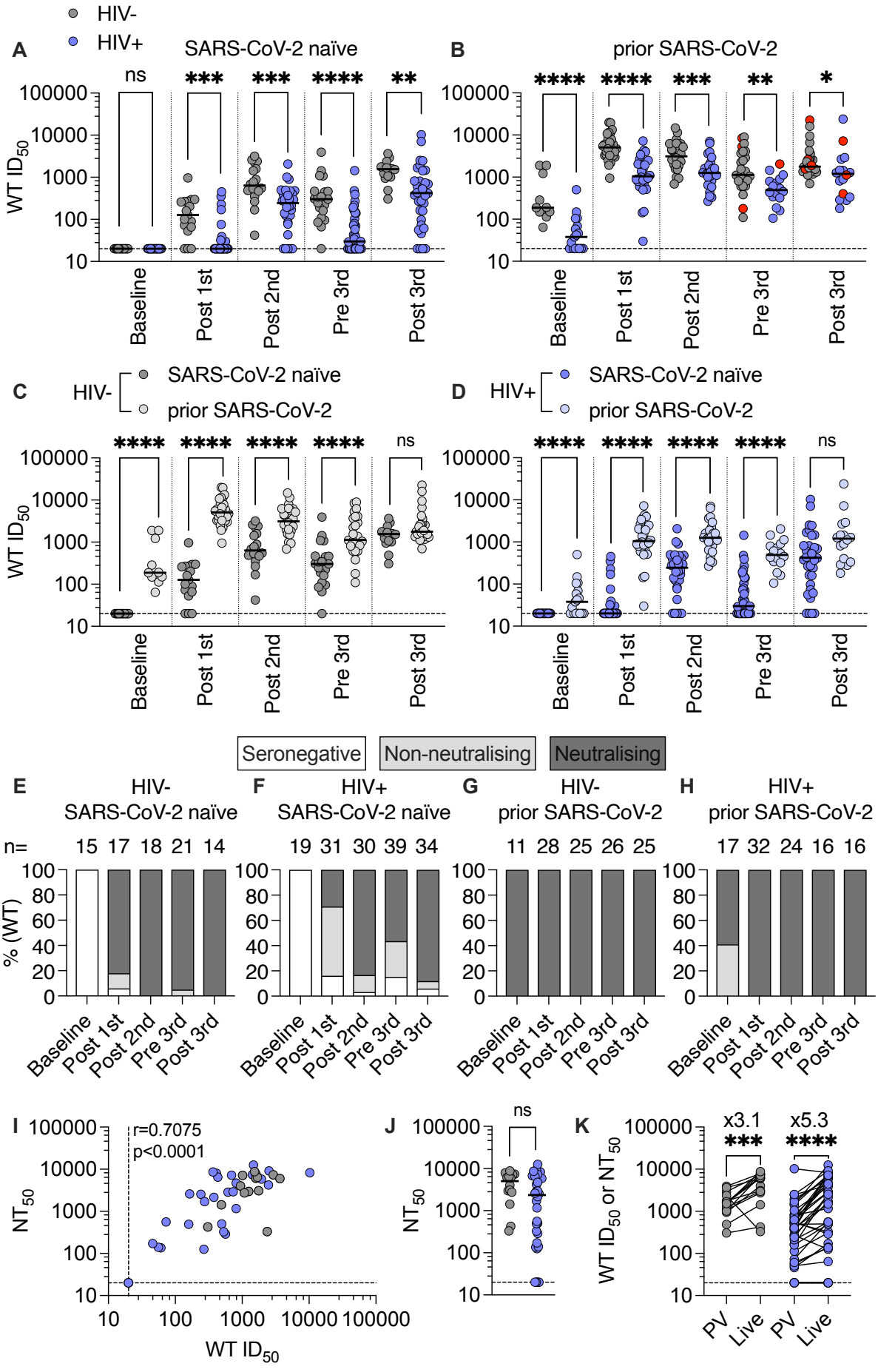
HIV-
HIV+
A
SARS-CoV-2 naïve
B
prior SARS-CoV-2
WT ID50
Baseline
Post 1st
Post 2nd
Pre 3rd
Post 3rd
C
HIV-
SARS-CoV-2 naïve
prior SARS-CoV-2
D
HIV+
Seronegative
Non-neutralising
Neutralising
E
HIV-
SARS-CoV-2 naïve
F
HIV+
SARS-CoV-2 naïve
G
HIV-
prior SARS-CoV-2
H
HIV+
prior SARS-CoV-2
n= 15 17 18 21 14
19 31 30 39 34
11 28 25 26 25
17 32 24 16 16
% (WT)
I
r=0.7075
p<0.0001
NT50
WT ID50
J
K
x3.1
x5.3
WT ID50 or NT50
PV
Live

***Figure 4.5**: Lower levels of neutralising antibodies in PLWH against SARS-CoV-2 WT across all timepoints, regardless of previous COVID-19 infection. SARS-CoV-2 WT (Wuhan-hu1) pseudovirus neutralising reciprocal 50% inhibitory titres (ID_{50}) for **A.** SARS-CoV-2 naïve participants and **B.** participants with prior SARS-CoV-2 infection stratified by timepoint and HIV status (HIV-negative controls – grey; PLWH – blue; breakthrough infection - red). SARS-CoV-2 WT neutralising titres for **C.** HIV-negative controls and **D.** PLWH stratified by timepoint and SARS-CoV-2 experience. **E-H.** Percentage of individuals in each group with either seronegative response (binding S1-specific IgG titres <0.6µg/mL), non-neutralising responses (detectable S1-specific IgG but WT ID_{50}<20) or neutralising responses. **I.** Correlation of SARS-CoV-2 WT neutralising titres with live virus titres at the 3rd vaccine dose against an early SARS-CoV-2 isolate (SARS-CoV-2/human/Liverpool/REMRQ0001/2020). for PLWH (n=32 – 2 samples were not available at the time) and HIV-negative controls (n=14). **J.** Live virus titres at the 3rd vaccine dose stratified by HIV status. **K.** Comparison between pseudovirus-based (PV) neutralisation titres (WT ID50) and live virus-based neutralisation titres (WT NT50). The median fold increase from PV to Live is shown for each group. For A-D, data points are representative of n=2 experimental repeats performed in duplicate, is shown the median for each group, dotted line represents the limit of detection of the assay (ID_{50}=20). For I-K, NT50 titres represent a single experimental repeat performed in triplicate, is shown the median for each group, dotted line represents the limit of detection of the assay (NT_{50}=20). For A-H, N numbers for each group are equivalent to those seen in **Table 4.3.2**. Where no neutralisation was detected, samples were assigned an ID_{50} or NT_{50} of 20. Statistical test: MWU for A-D and J, Spearman's rank correlation for I and Wilcoxon's matched pair rank test for K.*

4.6. Limited breadth of the neutralising response to the Omicron BA.1 variant in PLWH.

During the recruitment period of this study, many variants (see **section 1.2.3** for details) emerged which posed various questions as to the efficacy of vaccines. Omicron BA.1 or B.1.1.529.1 was first detected in November 2021 and quickly became the dominant circulant strain in the UK followed by the closely related BA.2 strain. For this study, this coincided with the period when most of the participants received their 3rd vaccine dose. Most of the dominant strains emerging since then have been classified as subvariants or sub-subvariants of Omicron (UKHSA, 2023b). Omicron (BA.1) presented a substantial change from the previously widely circulating VOCs with 36 individual non-synonymous amino acid changes in spike to 10 each for B.1.1.7, B.1.351 and B.1.617.2 (see ***Figure 1.2.3***). This led to growing concern that immunity gained from vaccines or previous non-Omicron infection may not be sufficiently broad to prevent infection, with several reports showing escape from neutralisation for monoclonal antibodies (Andreano et al., 2022; Cameroni et al., 2021; Cao et al., 2022; Planas et al., 2021) and an overall 22 to 43 fold-change reduction in neutralising titres in polyclonal plasma after two vaccine doses (Cameroni et al., 2021; Cele et al., 2021b; Garcia-Beltran et al., 2022; Liu et al., 2022a; Planas et al., 2021). This potential lack of breadth was particularly relevant for patient groups with known defects in neutralisation of the WT virus, for example, PLWH as shown in ***Figure 4.5***. As such, this analysis focused on differences in neutralising antibody titres against the 'ancestral strain of Omicron, BA.1.

As seen with WT, SARS-CoV-2 naïve PLWH made lower response compared to SARS-CoV-2 naïve HIV-negative controls at all timepoints (***Figure 4.6A***). After the 1st and 2nd vaccine dose, most PLWH lacked the breadth needed to neutralise Omicron BA.1. Overall, Omicron BA.1 posed a greater challenge to SARS-CoV-2 naïve participants with 53% of HIV-negative and 94% of PLWH not managing to produce a neutralising response after the 1st vaccine dose. After two doses, 77% of SARS-CoV-2 naïve PLWH were still not producing neutralising responses against Omicron BA.1 as compared to 100% of SARS-CoV-2 naïve HIV-negative controls. It was only after the 3rd vaccine dose that more than 50% of SARS-CoV-2 naïve PLWH achieved a neutralising response against Omicron BA.1. In contrast, at this point all SARS-CoV-

2 naïve HIV-negative controls produced neutralising titres against Omicron BA.1 greater than 1:100 (***Figure 4.6A*** and ***E-F***).

In the arm of the cohort who had previously experienced SARS-CoV-2, the trend towards significantly decreased Omicron BA.1 neutralisation titres in PLWH compared to HIV-negative controls was also seen after one and two vaccine doses. Although, at the pre and post 3rd vaccine dose timepoint, the decrease was no longer significant and equivalent titres were observed (***Figure 4.6B***). However, 31% of PLWH and 4% of HIV-negative controls with a history of SARS-CoV-2 infection lost detectable neutralising antibodies against BA.1 at the pre 3rd vaccine timepoint (***Figure 4.6G-H***). By contrast, this loss in neutralisation activity was never seen against WT (see ***Figure 4.5***). Reassuringly, 84% of PLWH with prior SARS-CoV-2 produced a neutralising response against Omicron BA.1 after the 1st vaccine dose and 96% did so after the 2nd vaccine dose showing that broad responses against SARS-CoV-2 are possible in PLWH (***Figure 4.6G-H***). As seen previously, participants with breakthrough infections (coloured in red in ***Figure 4.6B***) had neutralising titres against Omicron BA.1 spanning the whole range of their respective groups. As expected, participants with prior SARS-CoV-2 infections mounted higher Omicron neutralisation titres than SARS-CoV-2 naïve participants, regardless of HIV status, with the difference lessening after the 3rd vaccine dose (***Figure 4.6C-D***).

Overall, the defect seen in SARS-CoV-2 neutralisation in PLWH compared to HIV-negative controls was exacerbated against Omicron BA.1. These results highlight the benefit of a 3rd vaccine dose overall for SARS-CoV-2 naïve individuals, especially for PLWH, many of whom had little neutralising responses against Omicron after the original two-dose vaccine course. The overall lower level of neutralisation against Omicron as compared to WT, especially after the 2nd vaccine dose was partially normalised after the 3rd vaccine dose. Altogether these data highlight that the serological defect in PLWH is not only quantitative but also qualitative with decreased breadth against a more antigenically diverse variant like Omicron BA.1. To further understand the qualitative defect of the serological response of PLWH I evaluated the kinetics of their neutralising response.

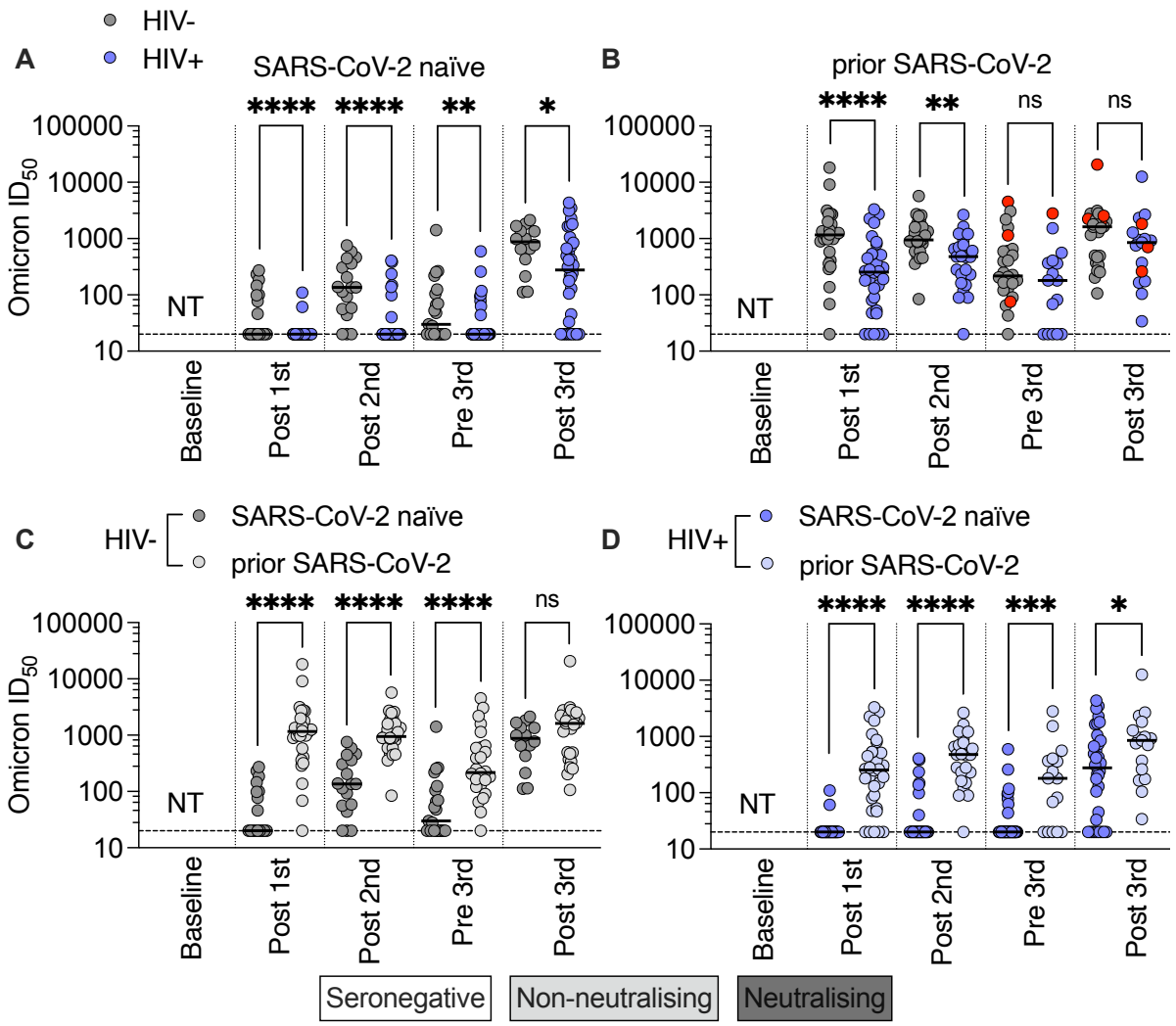
HIV-
HIV+
A
SARS-CoV-2 naïve
B
prior SARS-CoV-2
Omicron ID50
NT
Baseline
Post 1st
Post 2nd
Pre 3rd
Post 3rd
****
**
*
ns
C
HIV-
SARS-CoV-2 naïve
prior SARS-CoV-2
D
HIV+
***
Seronegative
Non-neutralising
Neutralising

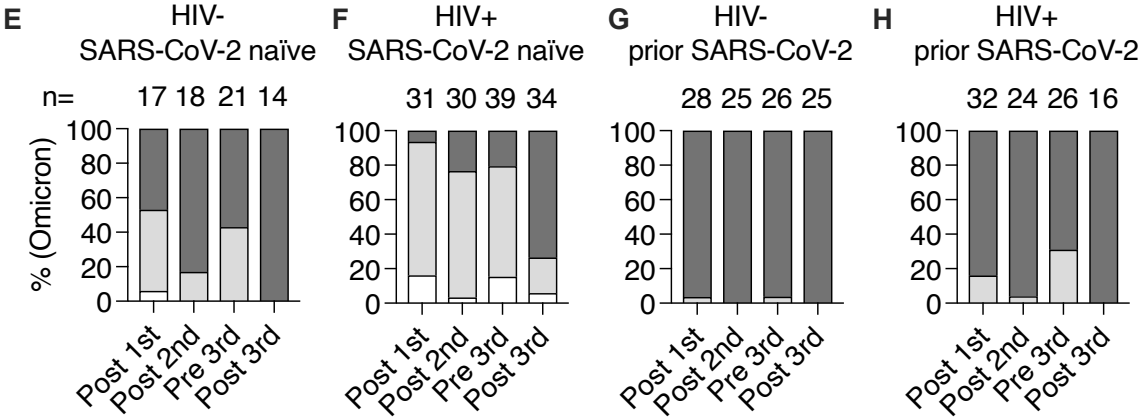
E
HIV-
SARS-CoV-2 naïve
F
HIV+
SARS-CoV-2 naïve
G
HIV-
prior SARS-CoV-2
H
HIV+
prior SARS-CoV-2
n=
17 18 21 14
31 30 39 34
28 25 26 25
32 24 26 16
% (Omicron)
Post 1st
Post 2nd
Pre 3rd
Post 3rd

***Figure 4.6**: Lower levels of neutralising antibodies in PLWH against SARS-CoV-2 Omicron BA.1 across all timepoints, regardless of previous COVID-19 infection. SARS-CoV-2 Omicron (BA.1) pseudovirus neutralising titres (ID_{50}) for **A.** SARS-CoV-2 naïve participants and **B.** participants with prior SARS-CoV-2 infection stratified by timepoint and HIV status (HIV-negative controls – grey; PLWH – blue; breakthrough infection - red). SARS-CoV-2 Omicron (BA.1) neutralising titres for **C.** HIV-negative controls and **D.** PLWH stratified by timepoint and SARS-CoV-2 experience. **E-H.** Percentage of individuals in each group with either seronegative response (binding S1-specific IgG titres <0.6µg/mL), non-neutralising responses (detectable S1-specific IgG but Omicron ID_{50}<20) or neutralising responses. For A-D, data points are representative of n=2 experimental repeats performed in duplicate, is shown the median for each group, dotted line represents the limit of detection of the assay (ID_{50}=20). N numbers for each group are equivalent to those seen in **Table 4.3.2**. Where no neutralisation was detected, samples were assigned an ID_{50} of 20. Statistical test: MWU.*

4.7. Production of a neutralising response is delayed in PLWH.

So far, PLWH made lower titres of binding and neutralising antibodies than HIV-negative controls and their neutralising response had less breadth. I hypothesised that antibody kinetics may differ in PLWH and therefore explain the quantitative and qualitative defects described in the previous section. To test this, I selected 53 PLWH and 44 HIV-negative participants who provided a sample at the post 1st vaccine dose timepoint and at least one other longitudinal sample.

In the SARS-CoV-2 naïve groups (***Figure 4.8A-B***), two neutralising trajectories were observed. First, participants who produced a detectable neutralising response after their 1st vaccine dose were deemed 'standard' neutralisers. Secondly, those termed 'delayed' neutralisers had failed to produce a neutralising response after their 1st vaccine dose and required at least two or more vaccine doses to produce a neutralising response. In the SARS-CoV-2 naïve HIV-negative controls, most participants (14/17) were defined as standard neutralisers with only 3/17 defined as delayed neutralisers (***Figure 4.8A***). Despite this delayed neutraliser status, all participants achieved neutralisation after two vaccine doses. However, in SARS-CoV-2 naïve PLWH (***Figure 4.8B***), 21/30 participants were defined as delayed neutralisers, with 4/20 not achieving neutralisation after two vaccine doses and 4/15 still unable to produce a neutralisation response after three vaccine doses. Effectively, this continuous delay in producing a detectable neutralising response was strongly enriched in SARS-CoV-2 naïve PLWH. This phenomenon of delayed neutralisation was completely absent when participants had a prior SARS-CoV-2 infection (***Figure 4.8C-D***), then all participants were classified as standard neutralisers.

When looking at how the timing of neutralisation mapped to S1-specific binding response the trends were muted but broadly similar. SARS-CoV-2 naïve PLWH with delayed neutralisation produced significantly lower binding titres compared to standard neutralisers after the 1st vaccine dose (***Figure 4.8F***). However, for SARS-CoV-2 naïve HIV-negative controls (***Figure 4.8E***), the delayed neutralisation group was not large enough to make any meaningful conclusions. Moreover, for timepoints after the 2nd vaccine dose, there was no difference in binding titres. Of note, while lower average levels of binding in those with delayed neutralisation, there was still heterogeneity in the range of S1-specific IgG titres in PLWH and HIV-negative participants within this group after the 1st vaccine dose. This suggests that some of

the participants with delayed neutralisation were making large amounts of spike-specific antibodies but not the 'right' kind i.e., ones which can neutralise SARS-CoV-2 pseudovirus.

Importantly the delay in neutralisation observed in SARS-CoV-2 naïve participants, was not an artefact due to differences in the timing of sampling as both delayed and standard neutralisers were sampled at an equivalent time since the 1st vaccine dose (***Figure 4.8H***). Similarly, PLWH with a delayed neutralisation phenotype did not differ by CD4 count (***Figure 4.8H***) or CD4:CD8 ratio (***Figure 4.8I***) to PLWH with a standard neutralisation phenotype. This suggests that this delay in the development of a neutralisation response wasn't directly associated with a lack of T-cell help due to T-cell-related immune dysfunction.

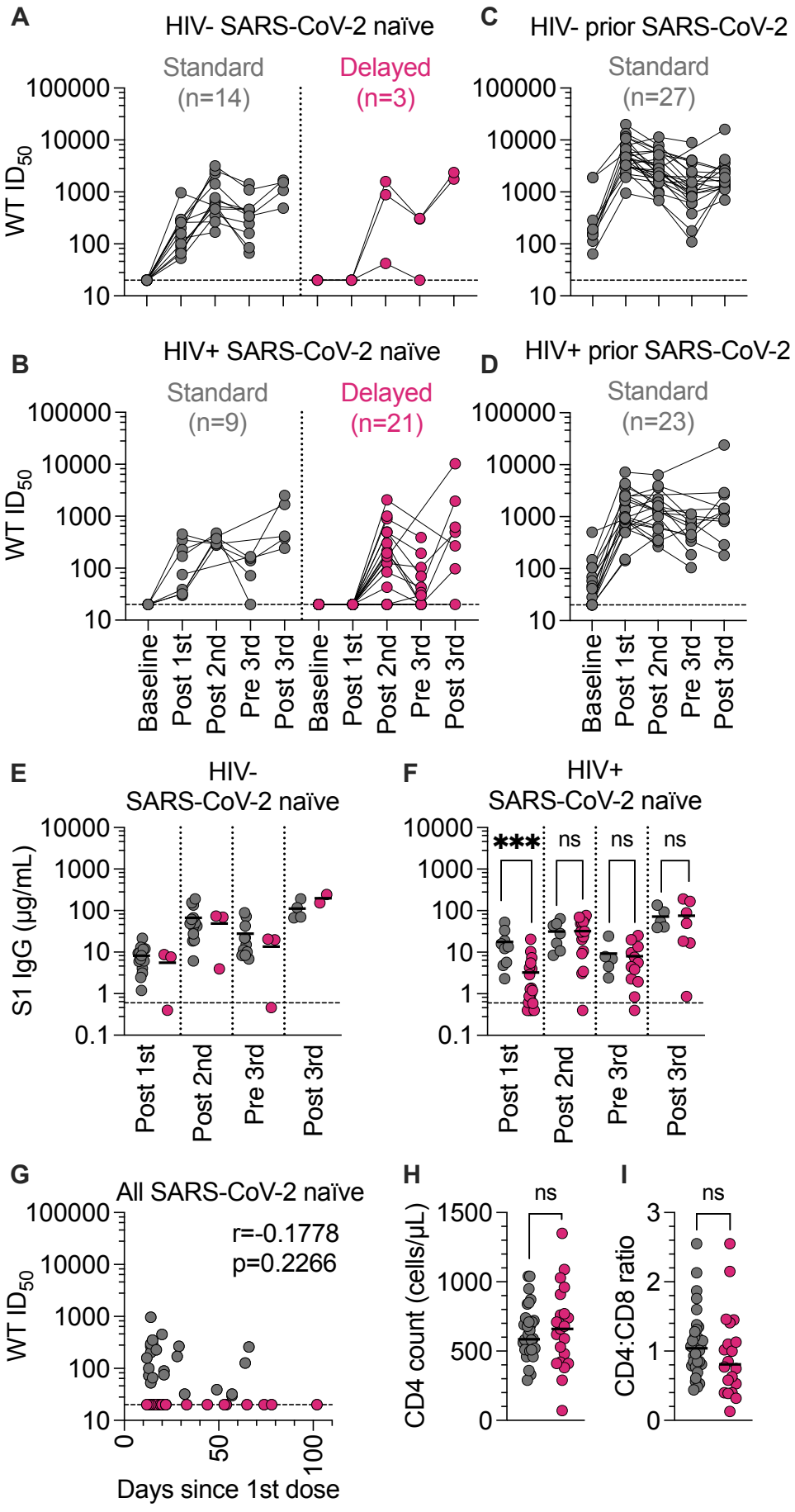
A
HIV- SARS-CoV-2 naïve
Standard (n=14)
Delayed (n=3)
C
HIV- prior SARS-CoV-2
Standard (n=27)
B
HIV+ SARS-CoV-2 naïve
Standard (n=9)
Delayed (n=21)
D
HIV+ prior SARS-CoV-2
Standard (n=23)
WT ID50
100000
10000
1000
100
10
Baseline
Post 1st
Post 2nd
Pre 3rd
Post 3rd
E
HIV- SARS-CoV-2 naïve
F
HIV+ SARS-CoV-2 naïve
S1 IgG (µg/mL)
10000
1000
100
10
1
0.1
***
ns
G
All SARS-CoV-2 naïve
r=-0.1778
p=0.2266
0
50
100
Days since 1st dose
H
CD4 count (cells/µL)
1500
1000
500
0
I
CD4:CD8 ratio
3
2
1
0

***Figure 4.7**: Production of a neutralising response is delayed in PLWH. Longitudinal SARS-CoV-2 WT neutralising antibody titres (ID_{50}) for participants with at least a post 1st vaccine dose sample and another longitudinal sample in **A.** SARS-CoV-2 naïve HIV-negative controls; **B.** SARS-CoV-2 naïve PLWH; **C.** HIV-negative controls with prior SARS-CoV-2 infection and **D.** PLWH with prior SARS-CoV-2 infection, stratified by standard (grey) or delayed (magenta) neutralising profile. Participants were classified as having 'standard' neutralisation if they produced neutralising antibodies from 1st vaccine dose onwards, if they did not produce neutralising antibodies they were classified as 'delayed.' **E.** S1 IgG-specific antibody titres (µg/mL) in SARS-CoV-2 naïve HIV-negative controls or in **F.** SARS-CoV-2 naïve PLWH stratified by standard or delayed neutralising profile. **G.** Correlation between days since 1st vaccine dose and WT ID_{50} titres for all 1st vaccine dose timepoint in all SARS-CoV-2 naïve participants stratified by standard (n=23) or delayed (n=24) neutralising profile. **H.** CD4 counts (cells/µL) and **I.** CD4:CD8 ratio in PLWH stratified by standard (n=32) or delayed (n=21) neutralising profile. N numbers for each group are indicated above each graph for A-D, E is equivalent to A, F to B. For A-G, data points are representative of n=2 experimental repeats performed in duplicate, is shown the median for each group, the dotted line represents the limit of detection of the assay (ID_{50}=20 or 0.6µg/mL IgG). Where no binding was detected, samples were assigned a titre of 0.4 µg/mL and where no neutralisation was detected, samples were assigned an ID_{50} of 20. Statistical test: MWU.*

4.8. Binding and neutralising responses are predictive of one another.

To further understand why PLWH make inferior antibody responses to HIV-negative controls despite similar immune stimulation, correlations between binding and neutralising responses after vaccination were calculated.

As seen in **Chapter 3**, S1-specific IgG binding antibodies correlated well with neutralising antibodies against the relevant SARS-CoV-2 WT strain (***Figure 4.8A-D***). In all four groups, the strongest correlations between S1-specific IgG and WT ID_{50} were seen after at least two vaccine doses, whereas after one vaccine dose, the correlations were only significant for the two groups of PLWH (***Figure 4.8B*** and ***D***). This may reflect that after one vaccine dose, some HIV-negative individuals have a greater ability to produce high levels of neutralising antibodies despite having modest amounts of binding antibodies. However, this was not observed in the PLWH studied, demonstrating a stricter relationship between binding and neutralisation titres in this group. S1-specific IgG antibodies correlated strongly with Omicron BA.1 ID_{50} titres (***Figure 4.7E-H***). Importantly, although vaccination-mediated neutralisation was decreased against Omicron BA.1 (***Figure 4.6)***, neutralising antibodies only represent a fraction of total S1 binding antibodies (Brouwer et al., 2020; Rees-Spear et al., 2021). Of note, each Spearman's rank correlation r value for Omicron BA.1 was weaker than those seen with WT (***Figure 4.8I***). This is likely because the S1 used here is from the WT strain and as such is lacking the 30 changes found in the Omicron BA.1 meaning any antibodies that are only specific to the Omicron BA.1 S1 are not accounted for here. Despite this, a study showed that there was no notable difference in the levels binding against the WT spike compared to the Omicron BA.1 spike, even in SARS-CoV-2 naïve participants (Hornsby et al., 2023). Therefore, one likely explanation for the weaker correlation is that the S1-specific IgG titres reflect a wide range of epitopes on the WT spike which can be bound by polyclonal sera, but these epitopes may now be inadequate for neutralisation of variants like Omicron BA.1. Indeed, decrease in neutralisation titres from WT to Omicron BA.1 mapped to epitopes in highly mutated regions like RBD as seen in other studies (Cao et al., 2023; Liu et al., 2022a).

As both PLWH and HIV-negative controls had coordinated binding and neutralising responses I set out to characterise whether there were differences in the proportion of the antibody response that was neutralising in PLWH and HIV-negative controls.

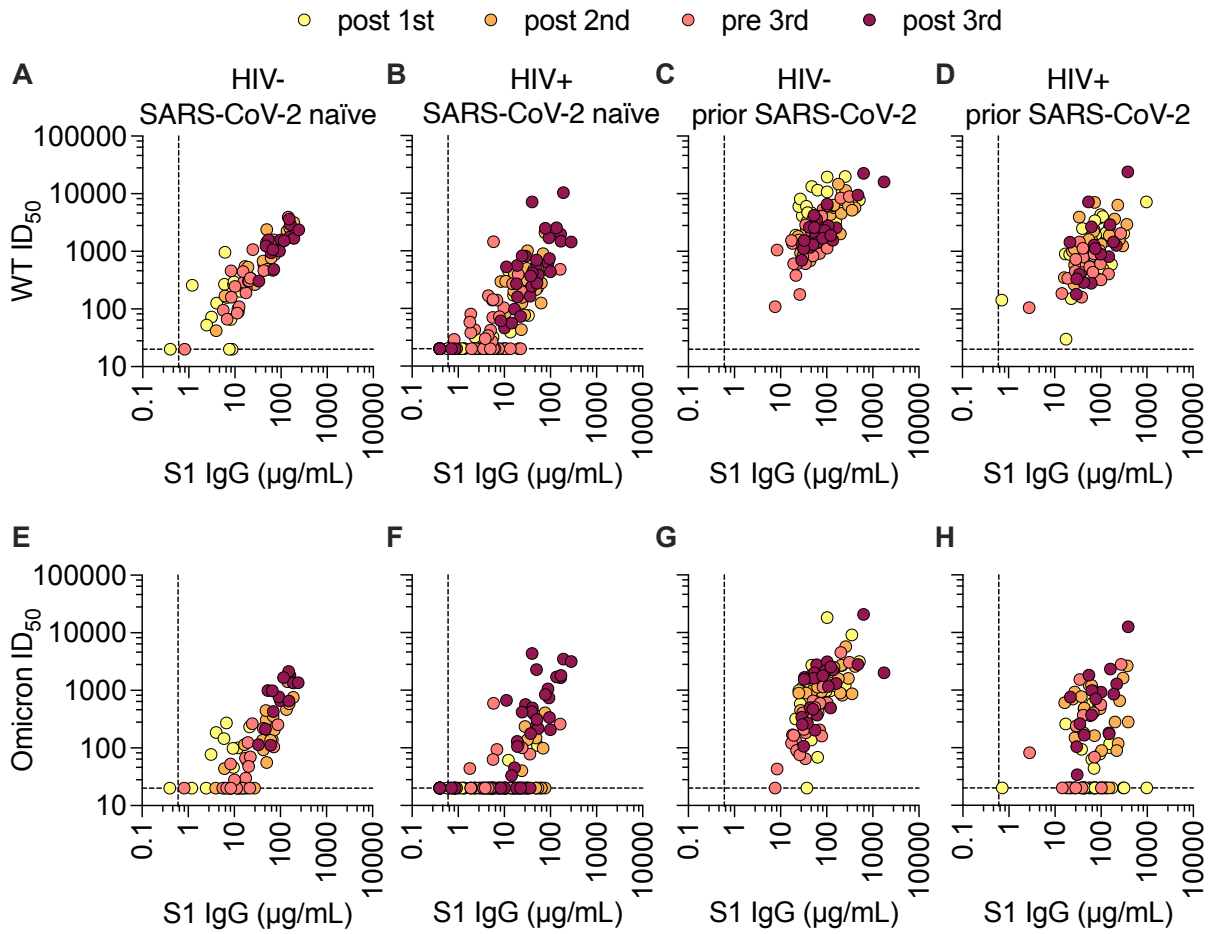

I

		for *WT ID*$_{50}$	SARS-CoV-2 naïve				prior SARS-CoV-2			
			post 1st	post 2nd	pre 3rd	post 3rd	post 1st	post 2nd	pre 3rd	post 3rd
HIV-	Spearman's r		0.2826	**0.7936**	**0.8221**	**0.7538**	0.2983	**0.7869**	**0.7292**	**0.7131**
	P-value		0.2708	**<0.0001**	**<0.0001**	**0.0027**	0.1231	**<0.0001**	**<0.0001**	**<0.0001**
HIV+	Spearman's r		**0.6625**	**0.6914**	**0.5733**	**0.8091**	**0.5205**	**0.5504**	0.3882	**0.5059**
	P-value		**<0.0001**	**<0.0001**	**0.0001**	**<0.0001**	**0.0023**	**0.0053**	0.1382	**0.0479**

		for *Omicron ID*$_{50}$	SARS-CoV-2 naïve				prior SARS-CoV-2			
			post 1st	post 2nd	pre 3rd	post 3rd	post 1st	post 2nd	pre 3rd	post 3rd
HIV-	Spearman's r		0.1805	**0.836**	**0.7777**	**0.6835**	**0.6208**	**0.6477**	**0.8113**	**0.6238**
	P-value		0.4862	**<0.0001**	**<0.0001**	**0.0088**	**0.0004**	**0.0005**	**<0.0001**	**0.0009**
HIV+	Spearman's r		0.3557	0.3988	**0.44**	**0.7879**	0.02582	-0.09959	**0.4389**	**0.6324**
	P-value		**0.0496**	**0.0291**	**0.0051**	**<0.0001**	0.876	0.6434	**0.0908**	**0.0101**

***Figure 4.8**: Binding and neutralising responses are predictive of one another. Correlation between SARS-CoV-2 WT neutralising antibody titres (ID_{50}) and S1 IgG-specific antibody titres (µg/mL) for **A.** SARS-CoV-2 naïve HIV-negative controls; **B.** HIV-negative controls with prior SARS-CoV-2 infection; **C.** SARS-CoV-2 naïve PLWH and **D.** PLWH with prior SARS-CoV-2 infection, stratified by timepoint. **E-H.** Equivalent to A-D for neutralising antibody titres against Omicron. **I.** Results of the statistical test (Spearman's rank correlation) for A-H, bolded values are significant ($p<0.05$ or $-0.4<r<0.4$). N numbers for each group are equivalent to those seen in **Table 4.3.2**. For A-H, data points are representative of n=2 experimental repeats performed in duplicate, is shown the median for each group, the dotted line represents the limit of detection of the assay: 0.25 µg/mL IgG or ID_{50}=20. Where no binding was detected, samples were assigned a titre of 0.4 µg/mL and where no neutralisation was detected, samples were assigned an ID_{50} of 20.*

4.9. PLWH require more binding antibodies to produce neutralisation titres than HIV-negative controls.

Previously, our group showed that patients with severe COVID-19 illness required a higher amount of polyclonal S1-specific IgG to make an equivalent neutralising response than patients with mild illness (Rees-Spear et al., 2021). This showed that despite their high binding titres, a larger proportion of the antibody response of severe COVID-19 patients compared to mild patients was either not targeting neutralising epitopes or the individual antibodies made were less potently neutralising. Here, this analysis was redeployed to understand the balance between neutralising and non-neutralising antibodies in PLWH. This was based on data in **sections 4.4** to **4.7** showing lower quantitative (less binding and neutralising antibodies) and poorer qualitative (lower breadth towards variants, delayed neutralising response) antibody responses after SARS-CoV-2 vaccination compared to HIV-negative controls. For this analysis, seronegative participants were excluded as they have neither binding nor neutralisation antibodies.

SARS-CoV-2 naïve PLWH made significantly more binding S1-specific IgG antibodies relative to the amount of neutralising antibodies they made against WT compared to HIV-negative controls. This was true at each timepoint until the 3rd vaccine dose, where there was no difference (***Figure 4.9A***). For PLWH with prior SARS-CoV-2 this significant trend towards having more binding antibodies relative to the amount of neutralising antibodies compared to HIV-negative controls held true after every single timepoint (***Figure 4.9B***).

This highlights the antibody response of many PLWH to SARS-CoV-2 vaccination is fundamentally less efficient than the one made by HIV-negative controls. Specifically, a larger proportion of the response in PLWH is either targeting non-neutralising epitopes or is less able to potently neutralise. This could be due to either making a higher proportion of very similar antibodies directed towards poorly immunogenic epitopes on spike, or a relative lack of SHM and clonal expansion in PLWH. Epitope mapping of the binding response of PLWH and sequencing of SARS-CoV-2 specific BCR could allow to understand what kind of defect leads to less efficacious antibody response by PLWH, the latter of which will be explored in **Chapter 6**.

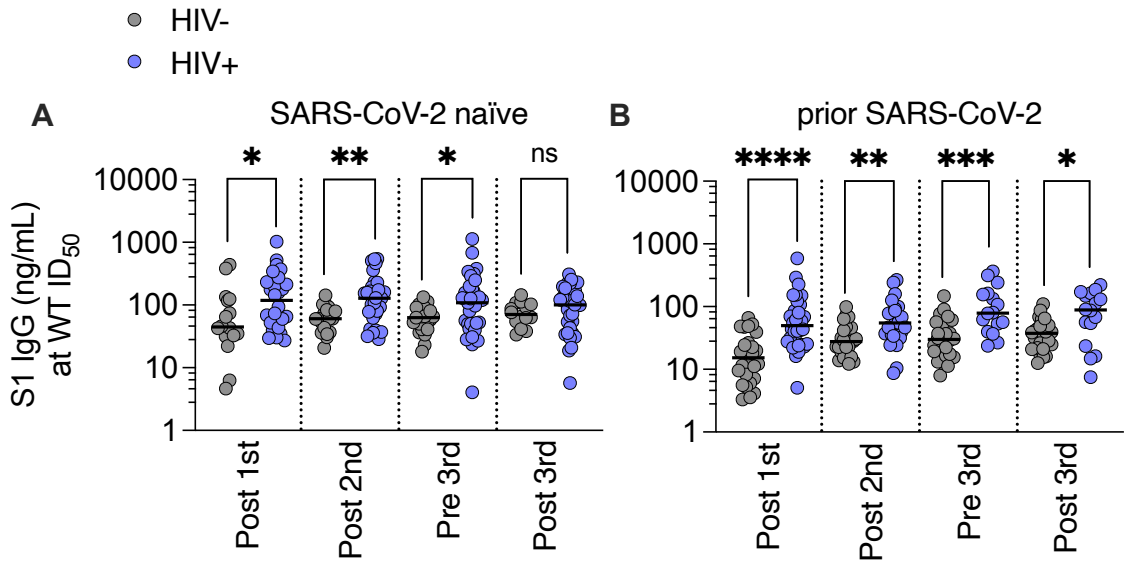

Figure 4.9: *PLWH require more binding antibodies to produce neutralisation titres than HIV-negative controls. Amount of S1 IgG-specific antibody titres (ng/mL) at ID_{50} against SARS-CoV-2 WT in* ***A.*** *SARS-CoV-2 naïve and* ***B.*** *prior SARS-CoV-2 participants stratified by timepoint and HIV status (HIV-negative controls – grey; PLWH – blue). For A and B, is shown the median for each group. Statistical test: MWU.*

4.10. Differences in vaccine platforms do not explain the serological defect seen in PLWH.

Participants in this study received a mix of vaccines due to the UK-wide vaccine rollout via a mixture of primary care providers, drop-in clinics and occupational health clinics This resulted in some disparities in the vaccine types received by the participants. For example, in the HIV-negative arm of the cohort, many of the participants were healthcare workers, and as such started their initial vaccine course earlier than the rest of the population. This meant that many of these healthcare workers were vaccinated before AZD1222 (AstraZeneca) was approved for use in the UK. Similarly, some participants in the HIV-negative control group, which overall skewed slightly younger, were only eligible for vaccination after April 2021, when JCVI recommended that the use of AZD1222 be limited to those over 40 years old (JCVI, 2021b). As discussed in **section 1.2.4**, as the vaccination rollout was underway, larger studies explored the differences in immunogenicity between the vaccine platforms. However, this study was not designed to assess differences in vaccine platforms or power for it. Regardless, to address this nonetheless important question, the following analysis shows neutralising data for participants who received a full course of mRNA vaccines i.e., any mix of BNT16b2 (Pfizer-BioNTech) and mRNA-1273 (Moderna).

When analysing mRNA vaccine recipients only there was still a significant reduction in neutralising titres against SARS-CoV-2 WT for SARS-CoV-2 naïve PLWH at each timepoint compared to HIV-negative controls (***Figure 4.10A***). Similarly, PLWH with prior SARS-CoV-2 still produced significantly lower neutralising titres than HIV-negative controls at each timepoint (***Figure 4.10B***). While there were not sufficient numbers of AZD1222 recipients across all arms to perform the analysis independently, that the mRNA vaccine-only data matches the results for the total cohort suggests the vaccine regimen was not the driving feature in the lower responses observed in PLWH. A large prospective cohort study of PLWH in the Netherlands compared vaccine platform (AZD1222, BNT16b2, mRNA-1273 and Janssen's Ad26.COV2.S) and binding antibody response and found that differences in vaccine platform did not impact the overall finding of lower binding titres in PLWH compared to HIV-negative controls (Hensley et al., 2022).

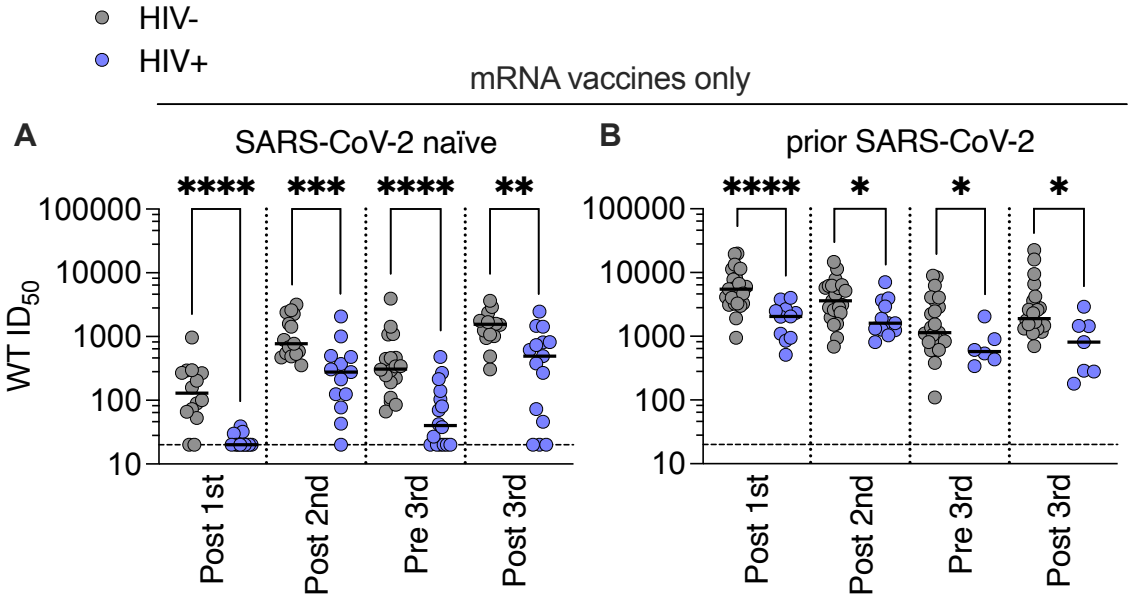

***Figure 4.10**: Differences in vaccine platform do not explain the serological defect seen in PLWH. SARS-CoV-2 WT pseudovirus neutralising titres (ID_{50}) for **A.** SARS-CoV-2 naïve participants and **B.** participants with prior SARS-CoV-2 infection who received only mRNA-based vaccines (Pfizer-BioNTech BNT162b2 or Moderna mRNA-1273) stratified by timepoint and HIV status (HIV-negative controls – grey; PLWH – blue). N numbers for each group are equivalent to those seen in **Table 4.3.2**. For A and B, is shown the median for each group, the dotted line represents the limit of detection of the assay: ID_{50}=20. Where no neutralisation was detected, samples were assigned an ID_{50} of 20. Statistical test: MWU.*

4.11. No clear association between CD4 count, CD4:CD8 ratio and serological output following vaccination.

As described in **Chapter 3**, differences in vaccine response in PLWH are often attributed to T cell-specific immune dysfunction, with many studies highlighting that PLWH with low CD4 count and lower CD4:CD8 ratio make poorer serological response following vaccination (discussed in **section 1.3.6**). In the case of extreme T cell-specific immune dysfunction, as seen in **section 4.2**, SARS-CoV-2-specific humoral responses were limited until some degree of T cell-specific immune reconstitution was achieved and the participant was provided with an additional vaccine dose. However, as detailed in ***Table 4.3.1***, with the exclusion of the individual described in **section 4.2**, all of the PLWH in this study were on ART and had undetectable viral loads. This cohort represented a range of T cell immune reconstitution, although most PLWH could be considered well-treated, with a median CD4 count of 601 and 560 cells/μL for the SARS-CoV-2 naïve and prior SARS-CoV-2 group respectively. This provided the opportunity to address how T cell-mediated immune dysfunction in PLWH affected their serological output post-SARS-CoV-2 vaccination in this well-treated cohort.

At least one set of CD4 counts and CD4:CD8 ratios were available for each PLWH in our cohort, although there was variation in how much time had elapsed since the clinical measurement and the study timepoint. This was deemed acceptable as reportedly once treatment is started and viral suppression is achieved, CD4+ counts will recover rapidly and will stay stable over time with continued ART adherence (Lundgren et al., 2023; Mocroft et al., 2007). Notwithstanding this caveat, there was no significant correlation between CD4 count and neutralising titres against SARS-CoV-2 WT in SARS-CoV-2 naïve PLWH (***Fig.4.11A***). Similarly, there was no significant correlation between the CD4:CD8 ratio and neutralising titres against SARS-CoV-2 WT in SARS-CoV-2 naïve PLWH (***Fig.4.11C***) after the 1st and 2nd vaccine doses. However, the post 3rd vaccine dose timepoint showed a significant but weak ($r<0.4$) correlation between higher CD4:CD8 ratios and higher titres of neutralisation antibodies.

Finally, there was no significant association at any timepoint between CD4 counts (***Fig.4.11B***) or CD4:CD8 ratios (***Fig.4.11D***) and neutralising antibody titres against SARS-CoV-2 WT for PLWH with prior SARS-CoV-2. Again, these participants all

produced high neutralisation titres overall due to the highly immunogenic stimuli provided by a SARS-CoV-2 infection, which may have negated any effect of T cell-mediated immune dysfunction.

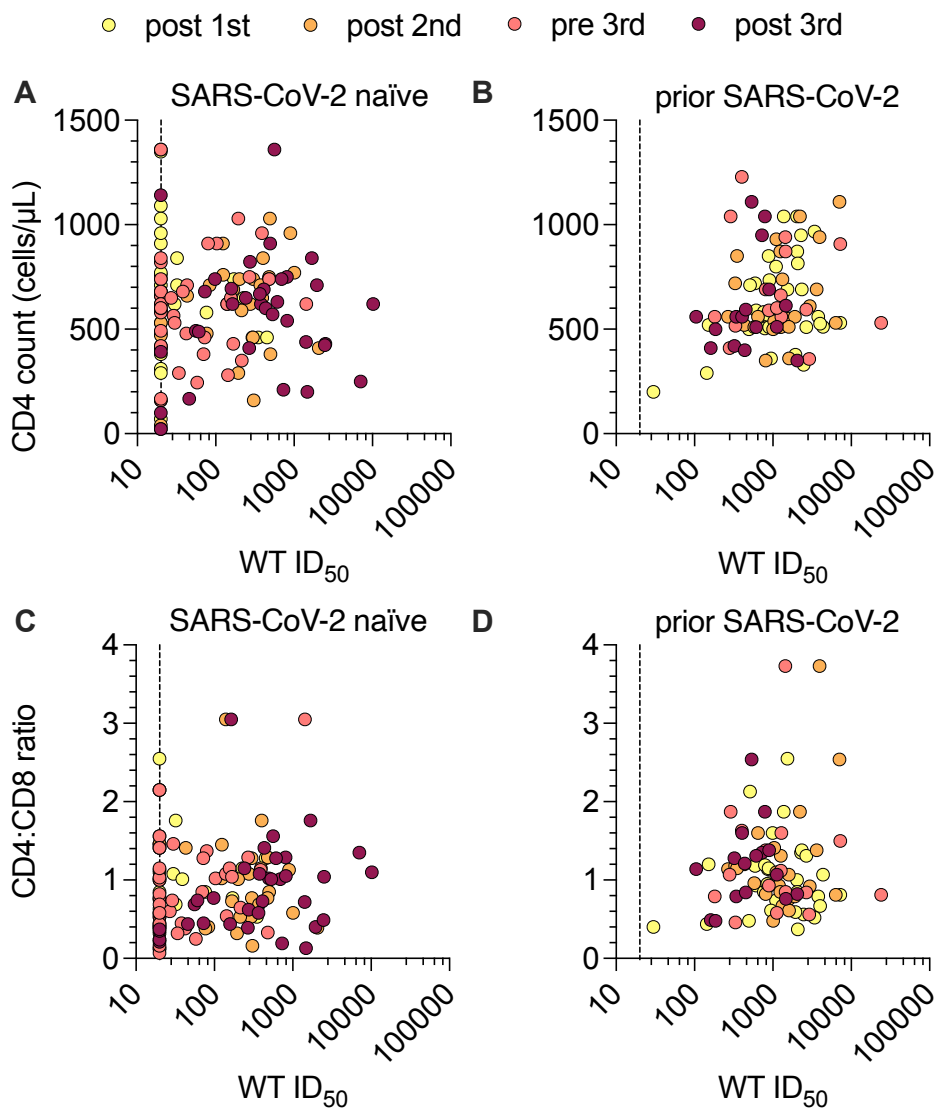

E

		HIV+ SARS-CoV-2 naïve				HIV+ prior SARS-CoV-2			
		post 1st	post 2nd	pre 3rd	post 3rd	post 1st	post 2nd	pre 3rd	post 3rd
CD4 count	Spearman's r	-0.0162	0.1660	0.1864	0.0740	0.2118	0.2777	0.2714	-0.0074
	P-value	0.9309	0.3806	0.2559	0.6773	0.2445	0.1889	0.3083	0.9805
CD4:CD8 ratio	Spearman's r	0.1634	-0.1000	0.1438	0.3978	-0.0262	0.0191	0.2118	-0.0677
	P-value	0.3884	0.6057	0.3891	**0.0198**	0.8868	0.9293	0.4298	0.8051

***Figure 4.11**: No clear association between CD4 count, CD4:CD8 ratio and serological output following vaccination. Correlation between SARS-CoV-2 WT neutralising antibody titres (ID_{50}) and CD4 count (cells/μL) for **A.** SARS-CoV-2 naïve PLWH and **B.** PLWH with prior SARS-CoV-2 infection. Correlation between SARS-CoV-2 WT neutralising antibody titres (ID_{50}) and CD4:CD8 ratio for **B.** SARS-CoV-2 naïve PLWH and **C.** PLWH with prior SARS-CoV-2 infection. **E.** Results of statistical test (Spearman's rank correlation) for A-D, bolded values are significant ($p<0.05$ or $-0.4<r<0.4$). N numbers for each group are equivalent to those seen in **Table 4.3.2**. For A-D, the dotted line represents the limit of detection of the assay: $ID_{50}=20$. Where no neutralisation was detected, samples were assigned an ID_{50} of 20. Statistical test: Spearman's rank correlation.*

4.12. Discussion

To what extent are there lower antibody responses post-vaccination in PLWH?

This study provided cross-sectional insights into the humoral responses made by PLWH (and HIV-negative controls) with or without a prior history of SARS-CoV-2 infection after on, two or three doses of COVID-19 vaccines.

S1-specific IgG binding titres served as a first indication of seroconversion after each vaccine dose of COVID-19 vaccine. For the SARS-CoV-2 naïve arm of the cohort, PLWH produced equivalent S1-specific IgG binding titres to HIV-negative controls after the 1st and 2nd vaccine doses, but responses were lower before the 3rd vaccine dose. This suggested that binding responses may wane more rapidly in PLWH. In turn, S1-specific IgG binding titres were still lower in SARS-CoV-2 naïve PLWH after the 3rd vaccine dose. This indicates that the 3rd vaccine dose did not provide the same benefit in PLWH, with PLWH experiencing less efficient recall and therefore failing to increase their binding antibody responses. Importantly, there was no difference in S1-specific binding IgG titres between PLWH and HIV-negative controls with prior SARS-CoV-2 infection at any timepoint. For the neutralising responses, there was a much more marked difference between PLWH and HIV-negative controls: PLWH produced lower titres of neutralising antibodies against SARS-CoV-2 WT than HIV-negative controls at each timepoint, regardless of prior SARS-CoV-2 infection (***Figure 4.5***). These data highlight that binding responses are more readily achieved by PLWH, but the more functional and protective response provided by neutralising antibodies (Corbett et al., 2020; Gilbert et al., 2022) is harder to attain for PLWH. Indeed, there is an important overall qualitative defect in the humoral responses made by PLWH. Specifically, most SARS-CoV-2 naïve PLWH required three vaccine doses to neutralise the more antigenically distinct variant Omicron BA.1, when 83% of the SARS-CoV-2 naïve HIV-negative cohort could readily neutralise Omicron BA.1 after two vaccine doses. For WT, the range of neutralising response seen in SARS-CoV-2 naïve HIV-negative controls and PLWH was equivalent to their counterparts with previous SARS-CoV-2 infections after three vaccine doses. Overall, it appeared that the 3rd vaccine dose provided the necessary boost in SARS-CoV-2 naïve participants to overcome the more pronounced waning seen at the pre 3rd vaccine dose timepoint. Practically, this was very relevant as the 3rd vaccine rollout happened contemporaneously with a peak of breakthrough infections due to Omicron BA.1 and BA.2 in well-vaccinated

populations during the northern hemisphere winter season (2021-2022) (Elliott et al., 2022). The benefit seen here from the 3rd dose is in line with many other studies showing increased titres after the 3rd dose in the general population (Buckner et al., 2022; Garcia-Beltran et al., 2022; Willett et al., 2022), in various immunocompromised groups (Fendler et al., 2022; Pinder et al., 2023; Tauzin et al., 2022) and in other studies with PLWH (Bessen et al., 2022; Corma-Gómez et al., 2023; Fidler et al., 2023; Marchitto et al., 2023; Tuttle et al., 2023). Still, after the 3rd vaccine dose, 12% of SARS-CoV-2 naïve PLWH had still not produced a neutralising response and thus would have benefitted from a 4th vaccine dose sooner than the general population.

To a large extent, the 3rd vaccine dose seemed to be a 'sweet spot' i.e., very efficient at rescuing waning titres in SARS-CoV-2 naïve participants and at broadening the responses towards more antigenically diverse variants despite at this point WT spike still being the main vaccine antigen. This could be explained by the more prolonged interval between the 2nd and 3rd vaccination than between the 1st and 2nd vaccine doses for most participants, which might allow for further rounds of somatic hypermutation and selection and amplification of more diverse B cell clones. Studies on immune imprinting have suggested that a 3rd vaccine dose broadens the repertoire of a SARS-CoV-2 naïve individual to a greater extent than those with pre-Omicron infections (Buckner et al., 2022). The causal variant of the first infection shapes disproportionately the subsequent vaccination-induced response akin to the concept of 'original antigenic sin' (Buckner et al., 2022; Reynolds et al., 2021; Röltgen et al., 2022).

Importantly, the development of a neutralising response for SARS-CoV-2 naïve PLWH was frequently delayed and required a larger amount of IgG antibodies to achieve similar neutralising activity as HIV-negative controls (***Figure 4.7***). This higher number of participants with delayed neutralisation within the SARS-CoV-2 naïve PLWH group further builds on data in this chapter suggesting there is both a qualitative and quantitative defect in the neutralising response of PLWH. Here, only one timepoint was available between the 1st and 2nd dose and therefore this only represents a snapshot of this important period of the neutralisation response development. Without extended longitudinal sampling between the first two doses, it is impossible to say if the delayed neutralisation phenotype seen here can only be remediated by an extra dose in delayed participants. Alternatively, the delay seen may be apparent only

because the production of neutralising antibodies had not been detected yet but would be before the administration of a second dose. Only one other study looked at the kinetics of neutralisation in PLWH (Motsoeneng et al., 2023) and found a similar delay in the induction of a neutralising response in PLWH compared to HIV-negative controls after SARS-CoV-2 infection but only observed this delay in binding response after vaccination with AZD1222 (AstraZeneca).

Another aspect of the qualitative defect in the post-vaccination antibody response of PLWH is that they required more binding antibodies to generate the same amount of neutralising titres as HIV-negative controls (***Figure 4.9***), This meant a focus towards less functional SARS-CoV-2-specific antibodies. Instead of quickly generating neutralising antibodies that confer protection, the GCs of PLWH are busy making non-neutralising antibodies.

How does hybrid immunity affect the neutralisation responses of PLWH?

This study also compared PLWH and HIV-negative controls with and without a history of prior SARS-CoV-2 infection. The latter distinction was made based on a self-declaration at the time of sampling from each participant (sometimes after clinical confirmation) and supported by detecting S1-specific antibodies at baseline to pick up any asymptomatic infections. Additionally, systematic measurement of N-specific antibodies could have provided another layer of certainty to detect any breakthrough infections. Access was sought to clinically available commercial N ELISA assays which use proprietary blocking peptides to remove seasonal coronavirus cross-reactivity, however, UCL's legal team failed to reach a contractual agreement with the UCLH diagnostic lab within a viable time frame which prevented this analysis. However, with that caveat, the results from this chapter show that hybrid immunity (vaccination plus infection) increased all serological outputs in HIV-negative controls but also in PLWH. This is agreement in the wider literature where hybrid immunity has been shown to produce larger serological responses than vaccination or infection alone (Bates et al., 2022; Krammer et al., 2021; Reynolds et al., 2021, 2022a). This may be due to the added layer of protection provided by the mucosae in infection (Azzi et al., 2022; Smith et al., 2021), the larger viral burden leading to more antigenic stimulation or the synergistic aspect of the innate immune system, stimulated by the presence of a whole virus – rather than spike protein only in the case of vaccines –

which will trigger an overall immune response (reviewed in (Sievers et al., 2023)) that can feed back into the humoral arm of the adaptive immune system.

The lower levels of neutralisation in SARS-CoV-2 naïve participants (regardless of HIV status) seen with WT were also more pronounced when assessing activity against Omicron BA.1. There was still a large decrease in Omicron BA.1 titres compared to WT titres in the two groups who had experienced prior SARS-CoV-2 infection. This highlights that even strongly immunogenic hybrid immunity can be limited in breadth when a new variant is not part of the original exposure. At that time neither group had been immunologically educated by Omicron BA.1 through infection or vaccination. As such both the prior SARS-CoV-2 and SARS-CoV-2 naïve group's pool of neutralising antibodies was mostly comprised of strain-specific antibodies and in lower proportion some antibodies which randomly had a greater breadth and thus the ability to neutralise Omicron BA.1. Therefore, the only difference in the two groups was that prior SARS-CoV-2 had more neutralising antibodies overall rather than antibodies which are better able to neutralise Omicron BA.1. This fits with the idea of immune imprinting, where neutralisation is directed to whichever strain one is infected/vaccinated with, as highlighted in some studies (Cao et al., 2022, 2023; Reynolds et al., 2022b).

Despite the advantages of hybrid immunity, PLWH still maintained lower responses than their HIV-negative counterparts with a similar infection history. Although these responses were notably higher than those produced by SARS-CoV-2 naïve PLWH or even SARS-CoV-2 naïve HIV-negative controls. This highlights that with sufficient immunogenic stimulation, PLWH can make adequate responses. Many immunocompromised groups, like the elderly (Collier et al., 2021b), have a similarly wide range of SARS-CoV2 vaccine responses and in these populations, it is also poorly understood why humoral responses are reduced compared to the general population.

How much immune stimulation do PLWH require to mount a vaccination response resilient to emerging variants?

The data in this chapter could not offer any conclusive data on breakthrough infections. Although the data shown in ***Figure 4.6*** may suggest that PLWH will struggle more than HIV-negative controls to make protective titres against emerging variants with

greater antigenic distance from WT, which was recapitulated by other studies (Bessen et al., 2022; Corma-Gómez et al., 2023; Fidler et al., 2023; Marchitto et al., 2023; Tuttle et al., 2023). Supporting this idea, a prospective study in the US found a slightly increased rate of breakthrough infection for PLWH overall compared to HIV-negative controls, especially in PLWH with lower CD4 count (<500 cells/μL) and/or those who had not received a 3rd vaccine dose (Coburn et al., 2022; Yang et al., 2024). This trend towards higher risk of breakthrough infections and severe disease was also recapitulated in a UK retrospective study that showed that even fully vaccinated (≥3 vaccine doses) highly immunocompromised individuals like PLWH with untreated advanced HIV still experienced more severe forms of COVID-19 infection (Evans et al., 2023). These results therefore suggest that PLWH and other immunocompromised groups require more immunogenic vaccines. Better vaccines for PLWH in the context of SARS-CoV-2 vaccination have so far meant additional doses.

Since the autumn 2022-spring 2023 (outside of the timeframe of this study), individuals with a weakened immune system including PLWH were invited to receive a 4th COVID-19 vaccine dose in the UK (JCVI, 2023). Limited data is available on the efficacy of a 4th vaccine dose in PLWH (Cheung et al., 2023; Lamacchia et al., 2022), but it may have proved favourable for PLWH who still had not produced neutralising antibodies after three vaccine doses or more widely, to maintain high and cross-protective neutralising titres against arising variants (Cheung et al., 2023; Regev-Yochay et al., 2022). However, any benefit (or not) would be hard to unpick considering the prior impact of potential infections as most individuals in the UK would have reported at least one COVID-19 infection by the time of the 4th vaccine dose.

The ideal vaccine may need to mimic the immunogenic effect of a real SARS-CoV-2 infection without increasing the risk of side effects. The obvious strategy of using a live-attenuated may not be appropriate for these immunocompromised populations where live-attenuated vaccines like the yellow fever vaccine are contraindicated (JCVI, 2024) due to the risk of severe side effects (Lindsey et al., 2008). Additionally, these vaccines may also have reduced efficacy altogether compared to the general population (Avelino-Silva et al., 2016; Veit et al., 2009, 2018). Similarly, inactivated virus vaccines against SARS-CoV-2 have been used more widely in China, with PLWH making poorer humoral responses than HIV-negative controls (Ao et al., 2022; Cai et al., 2022; Huang et al., 2022; Lv et al., 2023). Realistically, mRNA vaccines have

provided a great compromise between overall efficacy and safety profile, higher dosage in any given dose to increase immunogenicity coupled with additional yearly doses for PLWH and other immunocompromised groups may help improve their serological responses to SARS-CoV-2 vaccination.

The results presented throughout this chapter have shown that overall PLWH produce an inferior SARS-CoV-2 vaccine serum response compared to HIV-negative controls (less seroconversion, less binding, less and narrower neutralising, delayed response). This is in agreement with the pre-existing literature finding that PLWH make poorer vaccine responses (El Chaer and El Sahly, 2019; Kernéis et al., 2014; Pallikkuth et al., 2018) and with the wider literature on immunocompromised patient groups in the context of SARS-CoV-2 vaccination (Barnes et al., 2023; Bergman et al., 2021). Although this may cause concern for the efficacy of vaccination in PLWH, these lower serological outputs may be enough for protection against severe disease outcomes, as seen in Gilbert et al., (2022), where a WT ID_{50} titre of 100 was enough to provide protection against WT infection of 91% against severe disease.

How does this data fit with the wider HIV and COVID-19 vaccination literature?

Akin to the data on HIV status and humoral responses to SARS-CoV-2 infection discussed in ***Chapter 3***, the literature on HIV status and responses to SARS-CoV-2 vaccination responses is very varied. One point of contention is that to date no study compares humoral responses to vaccination between PLWH and HIV-negative controls and includes all of the criteria needed to answer this question in the most confident manner. Specifically, strict longitudinal sampling with fixed intervals after each vaccine dose, within a large group of PLWH and HIV-negative controls, comprehensive simultaneous HIV clinical parameters and then evaluation by extensive serological testing (binding and pseudovirus or live-based neutralising assays). The study presented in this chapter is no exception to this, particularly due to the nature of the longitudinal sampling because each timepoint represents a mix of longitudinal and cross-sectional sampling. However, my study does provide unique insights from the 1st to the 3rd vaccine dose, with a longitudinal sub-cohort showing alterations in the kinetics of neutralisation and data on the impact of a previous SARS-CoV-2 infection on PLWH's vaccination response, which was frequently lacking in other studies.

Considering studies which only included vaccine platforms licenced in the UK, the evidence can be divided into studies which found a difference in humoral responses to SARS-CoV-2 vaccination between PLWH and HIV-negative controls (Antinori et al., 2022; Bessen et al., 2022; Heftdal et al., 2022; Hensley et al., 2022; Jedicke et al., 2022; Levy et al., 2021; Madhi et al., 2021b; Matveev et al., 2023; Nault et al., 2022; Spinelli et al., 2021a; Tuttle et al., 2023), and the studies which did not (Brumme et al., 2022; Frater et al., 2021; Lapointe et al., 2023a, 2023b; Lombardi et al., 2022; Ogbe et al., 2022; Polvere et al., 2023; Verburgh et al., 2023; Vergori et al., 2022; Woldemeskel et al., 2022). These studies vary on whether they included PLWH with detectable viral loads, the number of PLWH with ongoing immune dysfunction (CD4 counts under 200-350 cells/μL, history of AIDS-defining condition etc), age-matching and sex-matching to controls or geographical location. Moreover, some studies actively adjusted for these parameters in their conclusions while others did not.

For the studies that agreed with the findings of this chapter, some purposefully included a wide range of immune reconstitution in PLWH to address the role of CD4 counts in vaccine responses (Antinori et al., 2022; Heftdal et al., 2022; Hensley et al., 2022; Matveev et al., 2023; Spinelli et al., 2021b), whilst some concordant studies included mostly suppressed PLWH (Bessen et al., 2022; Levy et al., 2021; Madhi et al., 2021b; Tuttle et al., 2023). Two studies focused on responses in older participants (Matveev et al., 2023; Tuttle et al., 2023). Out of these studies, some did not include pseudovirus or live virus-based assay, which is a limitation when considering the qualitative antibody function: Nault et al. (2022) noted lower binding in PLWH after the 1st vaccine dose, and two other studies showed lower binding after the 2nd vaccine dose of any mRNA or viral vectored vaccines (Hensley et al., 2022; Spinelli et al., 2021b). Another two studies found a similar binding response between SARS-CoV-2 naïve PLWH and HIV-negative controls whilst neutralisation titres were decreased after the 2nd vaccine dose of AZD1222 (Madhi et al., 2021b) or of BNT16b2 (Heftdal et al., 2022). Many studies observed both decreased binding and neutralising titres after the 1st vaccine dose (Jedicke et al., 2022; Matveev et al., 2023) or after the 2nd vaccine dose (Antinori et al., 2022; Bessen et al., 2022; Jedicke et al., 2022; Tuttle et al., 2023). Only one study included data after the 3rd vaccine dose and saw both lower binding and neutralising (Bessen et al., 2022).

In the studies that did not agree with the findings of this chapter, some did not provide live or pseudovirus-based neutralisation data comparing titres of PLWH versus HIV-negative controls which as discussed is a major limitation for antibody functionality (Frater et al., 2021; Lombardi et al., 2022; Ogbe et al., 2022; Woldemeskel et al., 2022). Some of these studies also had very small numbers of participants with 12 PLWH and 17 HIV-negative controls (Woldemeskel et al., 2022), or only 8 SARS-CoV-2 naïve HIV-negative controls (Lombardi et al., 2022). As the biggest difference shown in this chapter between PLWH and HIV-negative controls is apparent when looking at neutralisation, some of these studies, which only included binding data do not fundamentally disagree with this chapter's findings and simply do not cover the same antibody output. The set of studies from the AZD1222 clinical trials (Frater et al., 2021; Ogbe et al., 2022) reported on the same cohort which included only SARS-CoV-2 naïve participants who had received AZD1222 and followed them until 6 months after the 2nd vaccine dose. Of these studies, Woldemeskel et al. (2022) showed no difference in binding titres up to 17 days after the 2nd vaccine dose and Polvere et al. (2023) showed no difference in binding responses following the 1st and 2nd vaccine dose (up to 6 months post 2nd vaccine dose). For studies that did include neutralisation data, a cohort study with a wide range of CD4 count (Vergori et al., 2022) found similar levels of binding or neutralising titres between SARS-CoV-2 naïve PLWH and HIV-negative controls after the 3rd vaccine dose. Additionally, a set of studies (Brumme et al., 2022; Lapointe et al., 2023a, 2023b), followed up a cohort of well-controlled SARS-CoV-2 naïve PLWH (median CD4 count=710 cells/μL, IQR (525-935)) and HIV-negative participants after the one, two and three vaccine dose of a mix of mRNA based and viral-vectored vaccines. They found lower levels of binding and neutralising titres against WT and Omicron variants and faster waning in SARS-CoV-2 naïve PLWH compared to HIV-negative controls in line with our findings. However, their findings were no longer significant once adjusting for age and socio-economic factors. Finally, in a cohort of well-controlled PLWH (median CD4 count= 690 cells/μL, IQR(515–930)), there were no differences in the binding or neutralisation responses of PLWH compared to HIV-negative controls around 60 days after the 2nd vaccine dose, regardless of prior SARS-CoV-2 infection (Verburgh et al., 2023). As the cohort of PLWH/HIV-negative controls in this study is fairly similar to the one included in this Chapter, it is curious that the conclusion at this timepoint do not match this Chapter's where waning was more pronounced in PLWH (***Figure 4.3-5***).

Consistently, the strongest association between lowered neutralising or binding titres after any vaccine doses in PLWH was found where the study population had lower levels of immune reconstitution. PLWH with substantially lowered CD4 counts (generally defined as either <200 or <350 cells/μL) were shown to have lower serological output and seroconversion (Antinori et al., 2022; Corma-Gómez et al., 2023; Hassold et al., 2022; Lu et al., 2023; Marchitto et al., 2023; Søndergaard et al., 2023; Zhou et al., 2023) whilst some studies did not (Lombardi et al., 2022; Vergori et al., 2022). Compared to these studies, this Chapter's cohort had few PLWH representing the lower end of CD4 counts, with only 13/111 PLWH with CD4 count below 350 cells/μL and 20/111 PWLH with CD4 counts between 350 and 500 cells/μL. As such, it is not surprising to see that neither the CD4 count nor CD4:CD8 ratio correlated well with serological output at any of the timepoints (***Figure 4.8***). However, loss of CD4+ T cells during untreated HIV infections or in cases of extreme immune dysfunction poses a huge constraint on the humoral responses of PLWH, as exemplified by the case study in ***Figure 4.2.*** This fits with the hypothesis that once a certain threshold of T-cell mediated immune reconstitution, the linear relationship between CD4 count and humoral response breaks down. The heterogeneity of serological responses seen in PLWH following SARS-CoV-2 vaccination in this chapter cannot solely be explained by T-cell mediated dysfunction.

Altogether, this conflicting evidence highlights the heterogeneity of responses to SARS-CoV-2 vaccination within the PLWH group. Overall, the difference seen in binding responses between PLWH and HIV-negative controls may not be apparent until the 3rd dose as in our study. For neutralisation titres, the evidence is influenced by the heterogeneity of PLWH as a group where different individuals can have vastly different levels of immune reconstitution, comorbidities, demographic characteristics like age or ethnicity and other social determinants of health which can be hard to adjust for in a real-world setting. Overall, the most vulnerable PLWH with lower levels of immune reconstitution tended to produce lower serological response after COVID-19 vaccination and as such may require more vaccine doses to produce equivalent responses. In virally suppressed PLWH with better immune reconstitution, lower serological output seen post-SARS-CoV-2 vaccination can still be observed for reasons which are not yet fully understood.

One unique characteristic of the cohort presented in this chapter, compared to these other published studies, is that it was predominantly made up of participants who were vaccinated on the extended interval vaccine schedule with both mRNA- and viral vectored-based vaccines platform rather than the shorter interval schedule. The cohort in this chapter was recruited in the UK, where the vaccine schedule for the mRNA vaccines was quickly modified in January 2021 to mirror the schedule of the vectored vaccine AZD1222. This increased the interval between the 1st and 2nd vaccine doses to >12 weeks (JCVI, 2021a) rather than the 3-4 weeks recommended by the vaccine manufacturer (Baden et al., 2021; Polack et al., 2020). For this Chapter's cohort, this meant that 91% of post 2nd vaccine dose, 91.5% of pre 3rd vaccine dose and 90% of post 3rd vaccine dose participants received their 2nd vaccine dose on the extended interval schedule (>6-24 weeks between vaccine dose, with a median of 10 weeks). As the PITCH study demonstrated, this long schedule proved to be beneficial and led to increased serological and cellular outputs (Payne et al., 2021). It could be hypothesised that in the PLWH studied herein, the beneficial recall mechanisms that lead to higher antibody response after a longer interval schedule may not be fully equivalent to those seen in the HIV-negative participants thus leading to the defect seen in this study compared to the other studies which did not find any differences after the 3rd vaccine dose.

Alongside this work, T-cell-specific responses following vaccination were measured by our collaborator, Aljawharah Alrubayyi (Touizer et al., 2023). These data showed that T cells specific for WT or Omicron peptide pools were present in comparable amounts between PLWH and HIV-negative controls, after the 1st, 2nd or 3rd dose, regardless of prior SARS-CoV-2 infection. After the 2nd dose, some of the PLWH with lower serological output, defined here as those with neutralisation titres lower than 1:150 against WT, could still mount detectable SARS-CoV-2-specific T-cell responses. In this subgroup, these lower serological responses were weakly associated with a lower frequency of circulating CD3+ CD4+ CXCR5+ CXCR3+ T_{FH} cells. Although T_{FH} cells are primarily found in primary immune tissue within germinal centres, circulating or peripheral T_{FH} have been described (He et al., 2013), with CXCR3+ circulating T_{FH} correlating well with neutralising antibody titres after COVID-19 infection (Zhang et al., 2021). Overall, this highlighted that T cell-specific immunity may provide an added barrier of immune protection when antibody responses are lower in PLWH.

Unfortunately, we had limited availability of samples to fully address how defective T_{FH} responses may have affected the lower serological responses seen in PLWH throughout this Chapter at all timepoints.

Overall limitations.

The conclusions of this chapter are most strongly limited by the mostly cross-sectional recruitment strategy. Systematic sampling of the same individuals at each timepoint would have accorded greater confidence in the strengths of the association between positive HIV status and poorer humoral responses to SARS-CoV-2 vaccination.

Additionally, comparison with live virus neutralisation data in ***Figure 4.5*** highlighted that the pseudovirus assay used here may marginally decreased the titres, although this decrease was similar in PLWH and HIV-negative controls. Pseudovirus-based assays have been shown before to be more sensitive at distinguishing differences in the lower range of neutralisation than live virus-based assays (Cantoni et al., 2023; Khoury et al., 2020), this may be due to the inherent abilities of live viruses to quickly infect cells compared to pseudovirus and thus saturate the assay and preventing the detection of low levels of neutralisation. Additionally, they have been used extensively to understand humoral correlates of protection after vaccination (Atti et al., 2022; Gilbert et al., 2022). Re-running all timepoints using a live virus assay or with consistent IgG purification would allow to add another level of confidence in any differences seen between PLWH and HIV-negative controls. However, here, the greatest additional information would have been provided by longitudinal surveillance data of infection to assess if the reduction in neutralisation seen translated to an increased risk of breakthrough infection in PLWH.

Another potential caveat to the results from this cohort is that they were vaccinated according to the UK-wide organised COVID-19 vaccine rollout, which therefore led to differences in the vaccine platform used between the different groups. Although both mRNA-based and viral-vectored-based vaccines are effective and very immunogenic (Baden et al., 2021; Polack et al., 2020; Voysey et al., 2021; Walsh et al., 2020), there were some differences in amount of binding/neutralising antibodies produced (Hensley et al., 2022; Klemis et al., 2022; Röltgen et al., 2022; Wilhelm et al., 2022). Importantly, the neutralisation defect seen in this chapter in PLWH was still apparent

when controlling for differences in vaccine platform which shows that there is a real biological difference due to HIV status which is not yet understood.

Chapter conclusions

The data presented in this chapter suggests that PLWH fundamentally struggles to make quantitatively and qualitatively equivalent antibody responses to SARS-CoV-2 vaccination compared to HIV-negative controls. Binding and neutralising antibody titres were lower, neutralising responses were delayed and showed less breadth in PLWH. This trend towards lower responses in PLWH still held true in participants who had experienced prior SARS-CoV-2 infections. To further understand if these lower serological outputs were the consequence of the well-known defect seen in the memory B cell compartment of PLWH due to their HIV-associated immune dysfunction, I then set on characterising the global and antigen-specific memory B cell responses in this cohort.

5. Memory B cell responses to SARS-CoV-2 vaccination in PLWH

5.1. Summary

SARS-CoV-2-specific antibodies wane to a lower steady state after several months unless re-exposure occurs (i.e., re-vaccination or infection) as observed in most other infections. Therefore, in the early stages of the pandemic after spike-specific antibody levels had waned, spike-specific MBCs, alongside T cells, remained as a line of defence against re-infection by being able to produce a new wave of antibodies upon re-exposure (Cohen et al., 2021; Dan et al., 2021; Wang et al., 2021b; Wheatley et al., 2021). Thus, I wanted to investigate the SARS-CoV-2 specific MBC response between PLWH and HIV-negative controls after vaccination/infection. Moreover, given the deficiencies in neutralization seen after vaccination in PLWH were not clearly associated with differences in peripheral CD4 T cell counts (**Chapter 4**), the next step was to establish if there was a link with differences in MBC populations. This issue was of particular interest as there is a well-documented perturbation in the phenotype of MBCs in PLWH, even after ART initiation (discussed in **section 1.3.4**). Therefore, this chapter aimed to understand if this inherent perturbation of B cell phenotype in PLWH contributed to the lower quality and quantity of the serological output described in **Chapter 4**.

This chapter used a previously optimised flow cytometry panel (Jeffery-Smith et al., 2022) to characterise global and spike-specific MBC responses in PLWH and HIV-negative controls. This work initially focused on understanding responses after the 1st vaccine dose, to probe how *de novo* responses to vaccination may differ in PLWH compared to HIV-negative individuals. The next stage was to investigate how recall responses after the 3rd vaccine dose may lead to the generation of an inadequate MBC response in PLWH. A limitation of the work described in this chapter was the relatively low number of PBMC samples available for flow cytometry analysis as compared to the serum samples studied in **Chapter 4**. This was due to a mechanical LN2 failure and the loss of 64% of the PBMC samples collected alongside each serum sample. Despite this unfortunate setback, the findings of this chapter were published as part of a wider study on humoral, B and T cell responses to SARS-CoV-2 vaccination in January 2023 (Touizer et al., 2023) (this work was first pre-printed in November 2022).

5.2. Cohort design and flow gating strategy

To characterise the B cells in this cohort of PLWH and HIV-negative controls, an extensive flow cytometry panel was used to identify different subsets of B cells and spike-specific B cells using biotinylated spike protein pre-incubated with fluorescently conjugated streptavidin. This panel was first optimised and published in collaboration with our lab (Jeffery-Smith et al., 2022) by Anna Jeffery-Smith (UCL) to analyse B cell responses following SARS-CoV-2 infection in care-home residents and staff.

A flow cytometry gating strategy was used to define the different populations of B cells of interest (***Figure 5.2***). In brief, total B cells were considered to be CD19+ CD4- CD14-, within this population plasmablasts were identified as $CD20^{lo}$ $CD38^{hi}$ and non-plasmablasts B cells as CD20 + $CD38^{lo/-}$. Only class-switched B cells (IgD-) were considered when gating the different MBC subtypes: activated MBCs (CD21- CD27+), resting MBCs (CD21+ CD27+), intermediate MBCs (CD21+ CD27-) and atypical MBCs (CD21- CD27-). Within any of the MBC subtypes, isotype was inferred using IgG or IgM. Similarly, antigen-specific MBCs were identified as those that were double positive for spike baits (Jeffery-Smith et al., 2022). They were then defined as RBD-specific or as RBD-non-specific using an RBD bait, as discussed in **Methods 2.8-9**.

One important limitation of phenotyping antigen-specific MBCs is their rarity compared to other PBMC populations. For example, when considering all the samples run in this study, the median frequency of spike-specific MBCs was 1.4% of total MBCs, which was equivalent to a median of 224 cells for an aliquot of $10x10^6$ PBMCs. This makes sub-phenotyping of spike-specific cells (isotype usage, RBD specificity etc.) potentially difficult. Therefore, as previously described (Jeffery-Smith et al., 2022), sub-phenotyping on spike-specific MBCs was only performed where at least 50 cells were present in the parent gate.

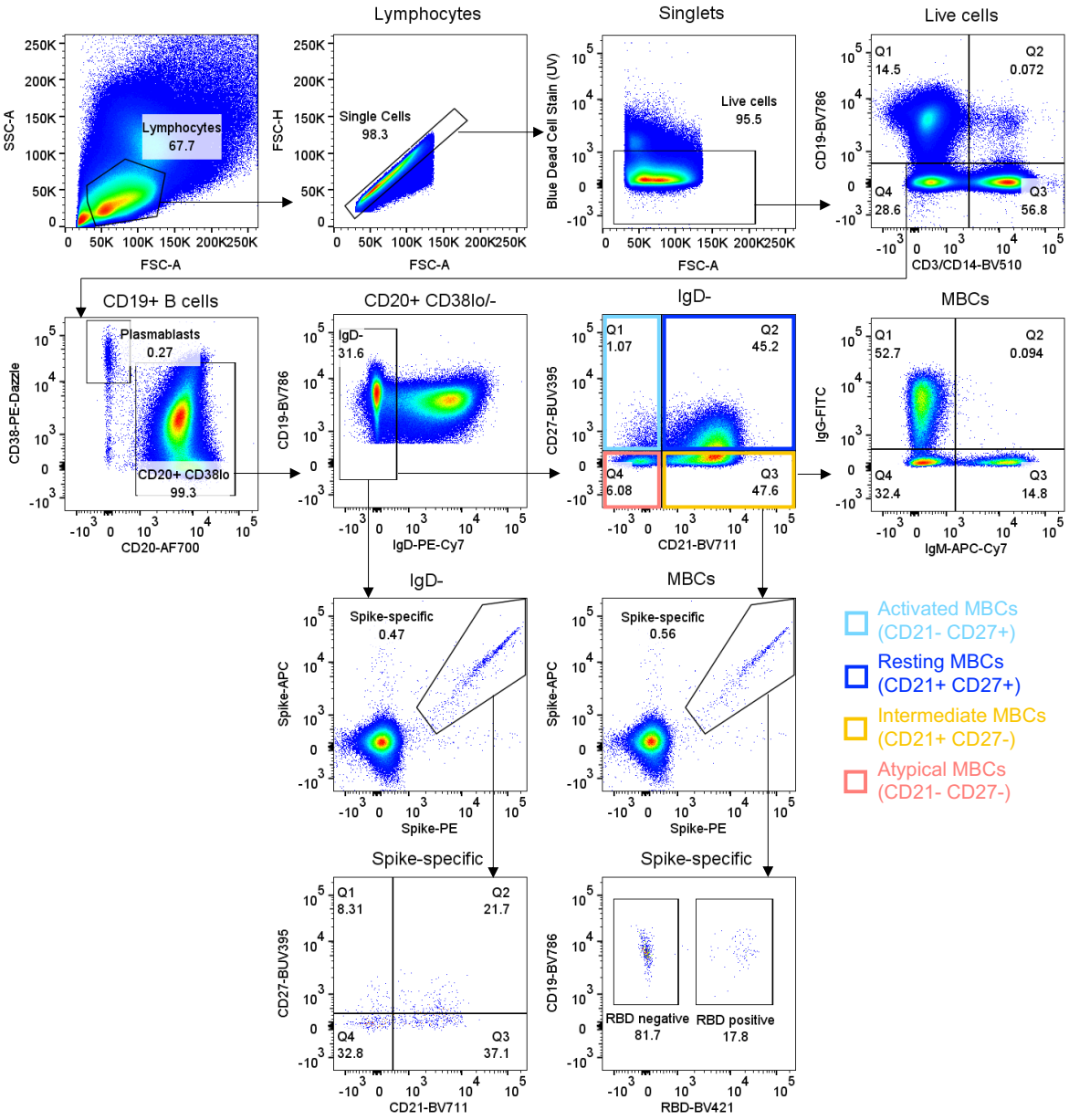
Lymphocytes
Singlets
Live cells
SSC-A
Lymphocytes
67.7
FSC-A
FSC-H
Single Cells
98.3
Blue Dead Cell Stain (UV)
Live cells
95.5
CD19-BV786
CD3/CD14-BV510
Q1
14.5
Q2
0.072
Q4
28.6
Q3
56.8
CD19+ B cells
CD38-PE-Dazzle
Plasmablasts
0.27
CD20+ CD38lo
99.3
CD20-AF700
CD20+ CD38lo/-
IgD-
31.6
IgD-PE-Cy7
IgD-
CD27-BUV395
CD21-BV711
Q1
1.07
Q2
45.2
Q4
6.08
Q3
47.6
MBCs
IgG-FITC
IgM-APC-Cy7
Q1
52.7
Q2
0.094
Q4
32.4
Q3
14.8
IgD-
Spike-APC
Spike-specific
0.47
Spike-PE
MBCs
Spike-specific
0.56
Spike-specific
CD27-BUV395
CD21-BV711
Q1
8.31
Q2
21.7
Q4
32.8
Q3
37.1
Spike-specific
CD19-BV786
RBD-BV421
RBD negative
81.7
RBD positive
17.8
Activated MBCs
(CD21- CD27+)
Resting MBCs
(CD21+ CD27+)
Intermediate MBCs
(CD21+ CD27-)
Atypical MBCs
(CD21- CD27-)

Figure 5.2: *B cell phenotyping flow cytometry gating strategy. Total PBMCs were first gated to identify lymphocytes using SSC and FSC, then on single cells using FSC-H and FSC-A, then on live cells using Blue live/dead cell stain (UV), then on B cells using CD19-BV786+ expression whilst excluding CD3/CD14-BV510+ cells. Within B cells, plasmablasts were gated as CD20-AF700^{lo} CD38-PE-Dazzle^{hi} and non-plasmablasts B cells as CD20-AF700+ CD38-PE-Dazzle$^{lo/-}$. Naïve B cells were excluded using IgD-PE-Cy7 to gate on class-switched MBCs. CD21-BV711 and CD27-BUV395 were used to gate on the different MBCs subsets: activated MBCs (CD21- CD27+), resting MBCs (CD21+ CD27+), intermediate MBCs (CD21+ CD27-) and atypical MBCs (CD21- CD27-). Then, the isotype was inferred on any B cell population by using IgG-FITC and IgM-APC-Cy7. Spike-specificity was identified for any given B cell population by using biotinylated spike protein pre-incubated with streptavidin-PE and streptavidin-APC. Furthermore, biotinylated RBD protein pre-incubated with streptavidin was used to distinguish RBD from non-RBD specific spike B cells for further epitope mapping by differentiating between RBD-specific and RBD-non-specific B cells using RBD-strep-BV421.*

5.3. Ongoing disruption in *de novo* memory B cell response after the 1st vaccine dose.

5.3.1. Prior infection gives an advantage in the generation of a robust spike-specific MBC response.

As highlighted in **section 1.2.1**, there is a degree of pre-existing immunity to SARS-CoV-2 due to exposure to other hCoVs. This naturally translated into the presence of MBCs induced by prior hCoV infections which can cross-react with SARS-CoV-2 spike in flow cytometry, as seen in other studies (Dan et al., 2021; Goel et al., 2021b, 2021a; Jeffery-Smith et al., 2022; Mazzoni et al., 2021). To account for this background reactivity, a positive detection threshold of 0.1% dual positive spike-specific MBCs was used based on previous analysis of levels of spike-specific MBCs in pre-pandemic samples by Anna Jeffery-Smith (Jeffery-Smith et al., 2022). Thus, in this study, the use of two spike proteins independently labelled with different fluorophores allows for the confident detection of a spike-specific MBC response (>0.1%) after the 1st vaccine dose regardless of prior SARS-CoV-2 (***Figure 5.3.1A***). By contrast, the baseline sample in ***Figure 5.3.1A*** has less than 0.1% spike-specific MBCs, highlighting the difference between the level of cross-reactivity seen in the general population pre-COVID-19 infection/vaccination and the response after vaccination alone.

Spike is the main target of the SARS-CoV-2-specific antibody response and the sole antigen in most vaccines (discussed in **section 1.2.4**). It has been previously shown that infection and vaccination produce spike-specific MBCs in proportion to serological responses (Cohen et al., 2021; Dan et al., 2021; Goel et al., 2021b, 2021a). In line with this, in my study, the frequency of spike-specific MBCs correlated strongly ($p<0.05$, $r>0.4$) with binding S1-specific IgG titres for both HIV-negative controls and PLWH (***Figure 5.3.1B***). Although, interestingly, two participants (one HIV-negative control and one PLWH, both SARS-CoV-2 naïve) had a frequency of more than 0.1% spike-specific MBCs despite having no detectable serum binding titres at the same timepoint. Similarly, the frequency of spike-specific MBCs correlated strongly with both WT and Omicron BA.1 neutralising titres for both HIV-negative controls and PLWH, with a stronger correlation for WT than Omicron BA.1 (***Figure 5.3.1C-D***). Out of the three serological parameters, binding antibody titres showed the strongest association with the frequency of spike-specific MBC. Overall, these findings fit with the broader

literature showing that individuals who mount strong titres against SARS-CoV-2 after vaccination or infection also tend to have higher frequencies of spike-specific MBCs (Andreano et al., 2021; Goel et al., 2021b, 2021a; Mazzoni et al., 2022; Reynolds et al., 2021).

As expected, a history of SARS-CoV-2 infection before the 1st vaccine dose resulted in higher frequencies of spike-specific MBCs after vaccination, regardless of HIV status (***Figure 5.3.1E***). The effect seen here is fairly small, due to the low number of participants analysed but this observation was recapitulated in other studies (Andreano et al., 2021; Goel et al., 2021b, 2021a; Mazzoni et al., 2021, 2022; Reynolds et al., 2021). Overall, while there was a trend to lower frequencies of spike-specific MBCs in PLWH compared to HIV-negative controls, there was no significant difference regardless of prior SARS-CoV-2 infection (***Figure 5.3.1B***). However, the lower than originally planned number of participants weakens this observation (15 PLWH, with 11 SARS-CoV-2 naïve and 4 with prior SARS-CoV-2). Similarly, there is a trend towards a lower frequency of RBD-specific MBCs in SARS-CoV-2 naïve participants compared to participants with a history of SARS-CoV-2 infection but given the very small numbers no clear conclusions can be drawn. (***Figure 5.3.1F***). Specifically, only 3 data points are presented out of 15 SARS-CoV-2 naïve participants because it was not possible to perform sub-gating to determine RBD reactivity in the other samples as there were too few spike-specific cells as described in **section 5.2**. Thus, based on the samples available for analysis at this time point, the lower serum titres reported in **Chapter 4** in PLWH cannot be conclusively attributed to lower levels of spike-specific or RBD-specific MBC.

Next, I considered differences in the plasmablast response, as these cells are linked to the rapid rise in serum antibodies post-infection or vaccination. There were no differences in the frequency of plasmablast between PLWH and HIV-negative controls (not shown). However, when grouping by SARS-CoV-2 infection status, SARS-CoV-2 naïve participants had significantly higher frequencies of plasmablasts compared to participants with prior SARS-CoV-2 infection (***Figure 5.3.1G***). This may underline that the plasmablast response of participants with prior SARS-CoV-2 infection waned more rapidly than the response from SARS-CoV-2 naïve participants, as it was a recall rather than a de novo response.

Altogether the data in ***Figure 5.3.1***. highlight that participants with prior SARS-CoV-2 infection have an advantage in mounting strong antigen-specific B cell responses compared to SARS-CoV-2 naïve participants. There is a trend towards lower numbers of antigen-specific B cells in PLWH after one vaccine dose although this does not reach significance. However, given the significantly lower serological output observed in PLWH in the previous chapter and the relatively small difference in numbers of spike-specific MBCs between the two groups, I next investigated global B cell phenotypes known to be disrupted in chronic HIV and their association to serological output.

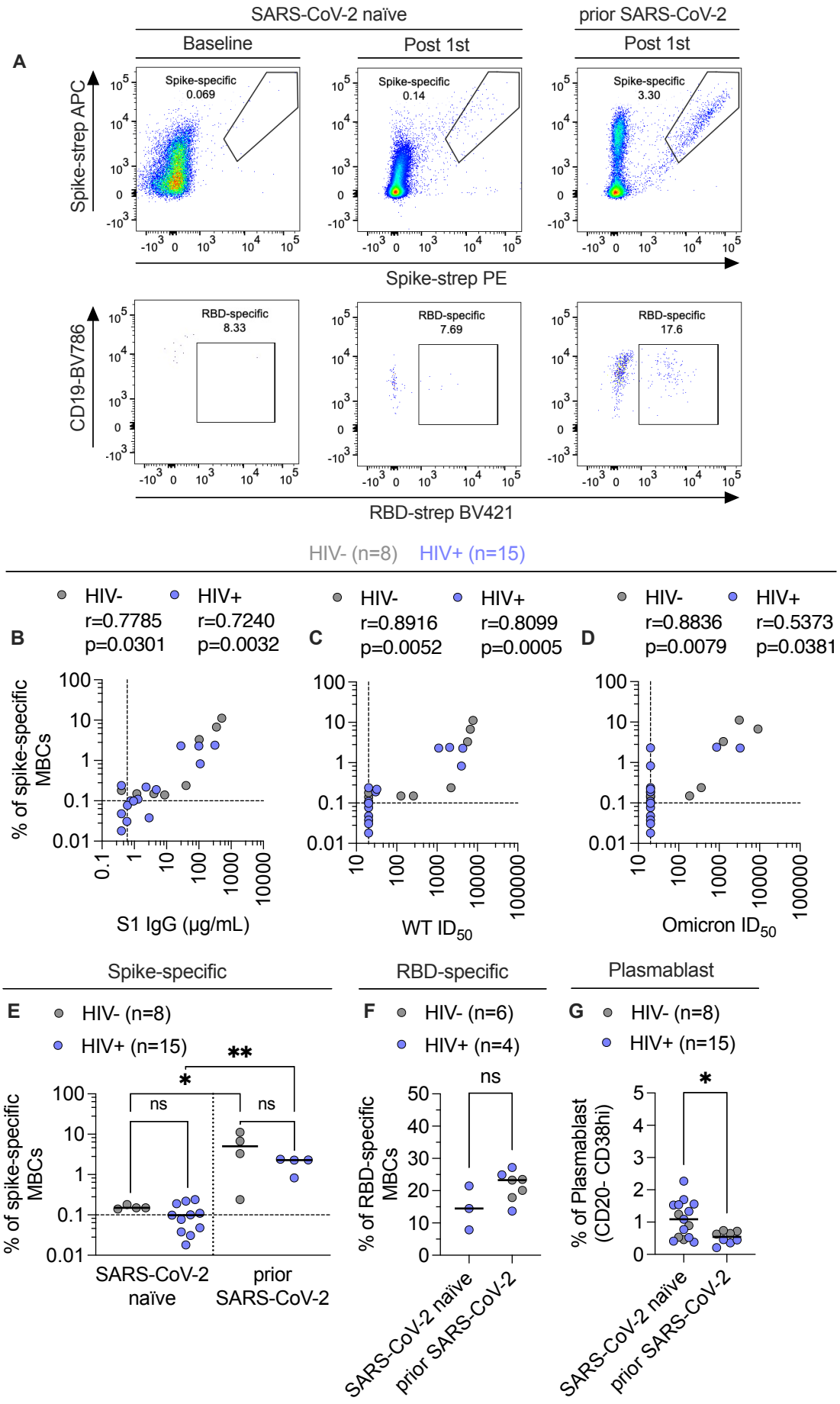
A
SARS-CoV-2 naïve
prior SARS-CoV-2
Baseline
Post 1st
Post 1st
Spike-specific 0.069
Spike-specific 0.14
Spike-specific 3.30
Spike-strep APC
Spike-strep PE
RBD-specific 8.33
RBD-specific 7.69
RBD-specific 17.6
CD19-BV786
RBD-strep BV421
HIV- (n=8) HIV+ (n=15)
B
HIV- r=0.7785 p=0.0301
HIV+ r=0.7240 p=0.0032
% of spike-specific MBCs
S1 IgG (µg/mL)
C
HIV- r=0.8916 p=0.0052
HIV+ r=0.8099 p=0.0005
WT ID50
D
HIV- r=0.8836 p=0.0079
HIV+ r=0.5373 p=0.0381
Omicron ID50
Spike-specific
RBD-specific
Plasmablast
E
HIV- (n=8)
HIV+ (n=15)
ns
ns
SARS-CoV-2 naïve
prior SARS-CoV-2
F
HIV- (n=6)
HIV+ (n=4)
ns
% of RBD-specific MBCs
G
HIV- (n=8)
HIV+ (n=15)
% of Plasmablast (CD20- CD38hi)

Figure 5.3.1: *Prior infection gives an advantage in the generation of a robust spike-specific MBC response.* ***A.*** *Representative gating of spike-specific MBC on CD19+ CD20+ CD38$^{lo/-}$ IgD- excluding CD21+ CD27- (top) and RBD-specific B cells on spike-specific B cells (bottom) for baseline and post 1st dose samples (in a SARS-CoV-2 naïve participant and a prior SARS-CoV-2 participant).* ***B.*** *Correlation between frequency of spike-specific MBC (as a % of the parent population, CD19+ CD20+ CD38$^{lo/-}$ IgD- excluding CD21+ CD27-) after the 1st vaccine dose and S1 IgG-specific antibody titres (µg/mL) or* ***C.*** *SARS-CoV-2 WT neutralising antibody titres (ID$_{50}$) or* ***D.*** *SARS-CoV-2 Omicron BA.1 neutralising antibody titres (ID$_{50}$).* ***E.*** *Frequency of spike-specific MBCs after 1 dose stratified by HIV and SARS-CoV-2 status.* ***F.*** *Frequency of RBD-specific MBCs (as a % of the parent population, spike-specific MBCs) after 1 dose stratified by HIV and SARS-CoV-2 status.* ***G.*** *Frequency of Plasmablasts (CD19+ CD20- CD38hi) as a % of the parent population (total CD19+ B cells), after the 1st vaccine dose, stratified by HIV status. For A-D, dotted line represents the limit of detection of the assay: 0.25 µg/mL IgG or ID$_{50}$=20, or the limit of sensitivity for the detection of spike-specific MBCs (0.1%), based on previous optimisation using baseline samples* (Jeffery-Smith et al., 2022; Touizer et al., 2023)*. For E-G, is shown the median for each group. Statistical test: Spearman's rank correlation for B-D, MWU for E-G.*

5.3.2. *Perturbed global memory B cell phenotypes are associated with a delay in the development of neutralisation.*

It has long been observed that the global MBC compartment of PLWH is perturbed, even after the start of ART (discussed in **section 1.3.4**) and as seen in other chronic (and acute) infections, in autoimmunity or even ageing. One aspect of this B cell disruption is that PLWH have higher levels of atypical MBCs, whose exact role is not well-understood, although it has been noted that they may be less able to respond to soluble antigens and more 'exhausted' as discussed in **section 1.1.4**. In turn, PLWH have fewer resting MBCs, which are thought of as the 'classical' long-term MBC. To illustrate this dynamic an example of the skewing of MBC phenotypes in PLWH is illustrated in ***Figure 5.3.2A***. As described above there was no significant difference between the total number of spike-specific MBCs in SARS-CoV-2 naïve PLWH compared to controls, but this group most frequently displayed a delayed neutralisation phenotype (see ***Figure 4.7***). Therefore, I hypothesised they may have more HIV-associated global B cell perturbation and thus poorer quality antibody responses. Specifically, I thought there may be more atypical MBCs in those who were slower to develop neutralisation.

Firstly, I observed there was a non-significant trend towards lower frequencies of resting MBCs (CD21+ CD27+) in PLWH. Similarly, there was a non-significant trend towards increased atypical MBCs (CD21- CD27-) compared to HIV-negative controls after the 1st vaccine dose (***Figure 5.3.2B***). However, stratifying samples by neutralisation phenotype revealed a clearer association between serological output and MBC profile. Specifically, participants with delayed neutralisation after the 1st vaccine dose had significantly lower frequencies of spike-specific MBCs than those with standard development of neutralisation (***Figure 5.3.2C***), in agreement with the neutralisation data of **Chapter 4**. This contrasts with the lack of difference in the frequency of spike-specific MBCs seen in ***Figure 5.3.1*** between PLWH and HIV-negative overall. This suggests that there is heterogeneity within the PLWH group in their ability to make spike-specific MBC. It is important to note that although PLWH were over-represented in the delayed neutralisation group, the standard neutralisation group was made up of equal numbers of PLWH and HIV-negative controls. Moreover, the delay in the development of a neutralisation response after the 1st vaccine dose was significantly associated with higher levels of activated MBCs (CD21- CD27+) and

atypical MBCs, and a reduction in the levels of resting MBCs (***Figure 5.3.2D***). Indeed, levels of resting MBCs were positively correlated with higher titres of neutralising antibodies after the 1st vaccine dose (***Figure 5.3.2E***). Similarly, levels of atypical MBCs were associated with lower titres of neutralising antibodies (***Figure 5.3.2F***). In addition, participants with a delayed neutralisation phenotype had significantly higher levels of plasmablasts (CD20- $CD38^{hi}$) (***Figure 5.3.2G***).

Overall, after the 1st vaccine dose antigen-specific and MBC responses fell into two distinct patterns, which were more strongly associated with the ability of participants to rapidly produce a neutralising response than HIV status. However, most individuals with a delayed neutralisation response were PLWH. Specifically, delayed neutralisers produced fewer spike-specific MBCs and exhibited a global MBC phenotype with more atypical MBCs, fewer resting MBCs and more plasmablasts.

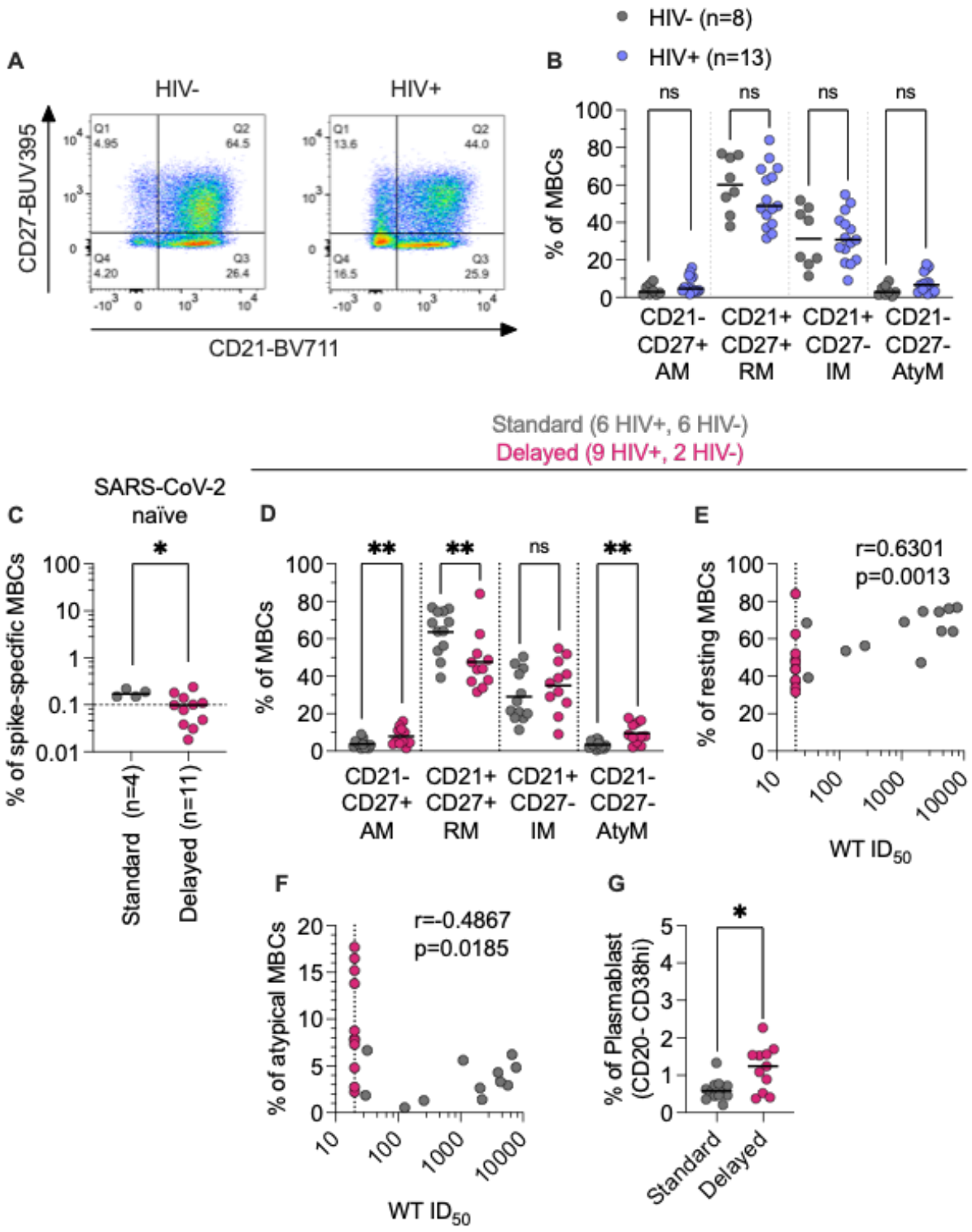
A
HIV-
HIV+
CD27-BUV395
CD21-BV711
Q1 4.95
Q2 64.5
Q4 4.20
Q3 26.4
Q1 13.6
Q2 44.0
Q4 16.5
Q3 25.9
B
HIV- (n=8)
HIV+ (n=13)
% of MBCs
ns
CD21- CD27+ AM
CD21+ CD27+ RM
CD21+ CD27- IM
CD21- CD27- AtyM
Standard (6 HIV+, 6 HIV-)
Delayed (9 HIV+, 2 HIV-)
C
SARS-CoV-2 naïve
% of spike-specific MBCs
Standard (n=4)
Delayed (n=11)
D
% of MBCs
E
% of resting MBCs
r=0.6301
p=0.0013
WT ID50
F
% of atypical MBCs
r=-0.4867
p=0.0185
WT ID50
G
% of Plasmablast (CD20- CD38hi)
Standard
Delayed

Figure 5.3.2**: Perturbed global memory B cell phenotypes are associated with a delay in the development of neutralisation.* ***A. *Representative gating of the different MBC subsets on CD19+ CD20+ CD38$^{lo/-}$ IgD- in a typical HIV-negative control (left) and PLWH (right).* ***B.*** *Frequency of each MBCs subset (as a % of the parent population, CD19+ CD20+ CD38$^{lo/-}$ IgD- excluding CD21+ CD27-): CD21- CD27+ activated MBCs (AM), CD21+ CD27+ resting MBCs (RM), CD21+ CD27- intermediate MBCs (IM) and CD21- CD27- atypical MBCs (AtyM) after the 1st vaccine dose, stratified by HIV status.* ***C.*** *Frequency of spike-specific MBCs (as a % of the parent population, CD19+ CD20+ CD38$^{lo/-}$ IgD- excluding CD21+ CD27-) after 1st vaccine dose stratified by standard (n=4) or delayed (n=11) neutralisation status in the SARS-CoV-2 naïve group.* ***D.*** *Frequency of each MBCs subset after the 1st vaccine dose, stratified by standard or delayed neutralisation status.* ***E.*** *Correlation between SARS-CoV-2 WT neutralising antibody titres (ID_{50}) and frequency of resting MBCs or* ***F.*** *frequency of atypical MBCs.* ***E.*** *Frequency of Plasmablasts (CD19+ CD20- CD38hi) as a % of the parent population (total CD19+ B cells), after the 1st vaccine dose, stratified by HIV status. For A-D and G, is shown the median for each group. For C, dotted line represents the limit of sensitivity for the detection of spike-specific MBCs (0.1%) or ID_{50}=20. Statistical test: MWU for A-D and G, Spearman's rank correlation for E-F.*

5.3.3. <u>No difference in isotype usage after the 1st vaccine dose.</u>

To further understand the generation of a *de novo* MBC response I assessed if the global B cell perturbation in the delayed neutralisation group was underpinned by differential isotype usage. In the panel presented here, the only isotype stained for were IgD, IgM and IgG which did not allow to directly identify IgA B cells.

First, there was no overall difference in the total amount of IgG+ MBCs, IgM+ MBCs or IgG- IgM- (which were most likely IgA+) MBCs when stratifying by HIV status (***Figure 5.3.3A***). In agreement with a previous observation by the Moir group (Kardava et al., 2018), PLWH had higher frequencies of IgG+ IgM+ cells (***Figure 5.3.3A***). In PLWH, IgG+ IgM+ B cells have been described mainly in viraemic individuals. Rather than suggesting that a B cell is expressing both IgG and IgM BCRs on its surface, or a flow cytometry artefact, these cells have been shown to be IgM+ B cells coated with soluble IgG3 (Kardava et al., 2018). As isotype usage was mostly similar between PLWH and HIV-negative controls (***Figure 5.3.3A***), both groups were pooled together to assess the impact of prior SARS-CoV-2 infection on isotype use. There was both a non-significant trend towards less IgG+ MBCs and a non-significant trend towards more IgM+ MBCs in the SARS-CoV-2 naïve group compared to the prior SARS-CoV-2 infection group (***Figure 5.3.3B***). This fits with the broader literature (Cohen et al., 2021; Goel et al., 2021b, 2021a; Kardava et al., 2022) that shows that at first *de novo* responses involve more IgM+ than IgG+ MBCs. Finally, for the different neutralisation phenotypes, there was no difference in the frequencies of any of the isotypes tested between the delayed and standard neutralising groups (***Figure 5.3.3C***). Due to low numbers of spike-specific MBCs in each donor after the 1st vaccine dose, it was not possible to analyse any differences in isotype usage in spike-specific MBCs.

Altogether these data suggest that the binding and neutralisation defect seen in the delayed neutralising group after the 1st vaccine dose is not due to any inherent issue with class-switching in B cells. Rather, it seems that the main difference in MBC class-switching is between recall responses upon vaccination after prior infection versus *de novo* responses after the 1st vaccination. In light of the data shown throughout **section 5.3**, it seems that there is heterogeneity in the early MBC responses after one SARS-CoV-2 vaccine dose independent of HIV status, albeit with PLWH more commonly having weaker responses. Specifically, the lower frequency of spike-specific MBC and

ongoing perturbation in the global MBC compartment was more pronounced in participants with delayed neutralisation, who are more frequently PLWH. As seen in **Chapter 4**, serological differences between PLWH and HIV-negative controls persisted past the *de novo* response seen after the 1st vaccine controls and were observed even after three vaccine doses. Therefore, to understand why this was the case I next investigated the spike-specific and global MBC responses in PLWH and HIV-negative controls at this later timepoint.

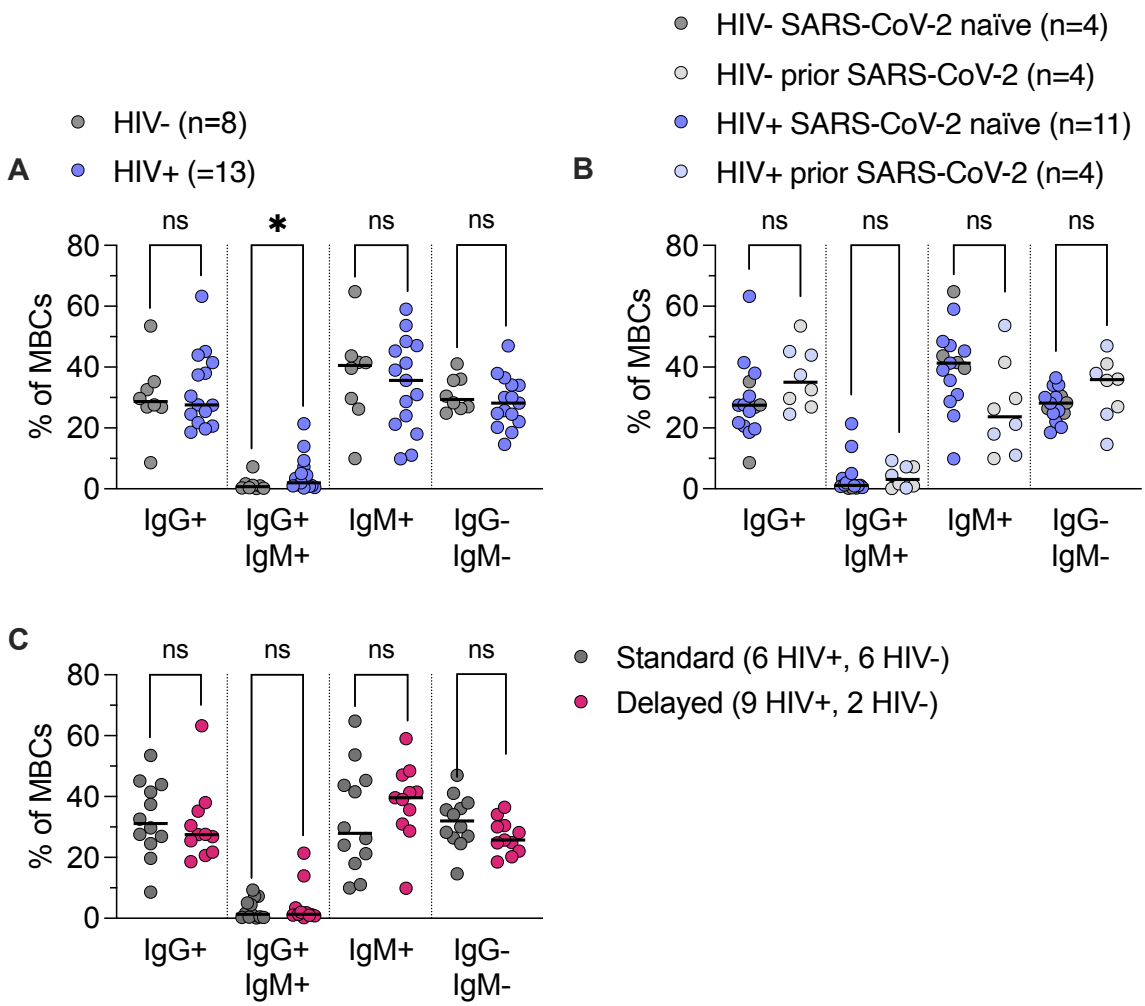

Figure 5.3.3: *No difference in isotype usage after the 1st vaccine dose. Frequency of different isotypes in MBCs (as a % of the parent population, CD19+ CD20+ CD38lo/- IgD-): IgG+, IgG+ IgM+ (composed of IgM+ B cells coated with secreted IgG3, as characterised in* (Kardava et al., 2018)*, IgM+ cells and IgG- IgM- (likely IgA+) after 1 dose stratified by* ***A.*** *HIV status or* ***B.*** *SARS-CoV-2 status or* ***C.*** *Standard and delayed neutralisation status. For A-C, is shown the median for each group. Statistical test: MWU.*

5.4. B cell disruption after the 3rd vaccine dose underpins a limited recall response in PLWH.

5.4.1. Similar levels of spike-specific MBCs between PLWH and HIV-negative controls regardless of prior infection.

The data in **Chapter 4** showed that PLWH produced lower binding responses, lower neutralising responses and had less neutralisation breadth than their HIV-negative counterparts despite having also received three vaccine doses. Additionally, serological waning was more marked in PLWH, specifically before the 3rd vaccine dose where in 3-4 months neutralising antibody titres against WT had waned by a median of 11.6-fold for SARS-CoV-2 naïve and 2.5-fold for PLWG with prior SARS-CoV-2 compared to immediately after the 2nd dose. Serological titres were then boosted after the 3rd vaccine dose to achieve broader titres, for example against Omicron BA.1. However, this boosting after the 3rd vaccine dose still resulted in lower binding and neutralisation titres in PLWH compared to HIV-negative controls, with a number of PLWH failing to neutralise (as seen in ***Figures 4.4***, ***4.5*** and ***4.6***). I hypothesized that this defect may be explained by the less efficient recall and overall lower numbers of spike-specific MBCs in PLWH after the 3rd vaccine dose.

Fortunately, in contrast with **section 5.3**, fewer samples were lost in the LN2 failure from the post 3rd vaccine dose timepoint. Therefore, to investigate how the 3rd vaccine dose affected the B cell response, 28 samples from HIV-negative controls (SARS-CoV-2 naïve =13 and prior SARS-CoV-2 infection =15) and 32 samples from PLWH (SARS-CoV-2 naïve =20 and prior SARS-CoV-2 infection =12) were run on the B cell phenotyping flow cytometry panel described in **section 5.2**. Importantly the intervals between vaccine doses two and three were similar between the different groups (***Figure 5.4.1***). Therefore, any remaining defects in the MBC response could not be solely attributed to differences in vaccination timing.

However, there were no differences in the frequency of spike-specific MBCs between PLWH and HIV-negative controls, regardless of prior SARS-CoV-2 infection. Similarly, there was no difference between the SARS-CoV-2 naïve group and the prior SARS-CoV-2 group (***Figure 5.4.1A***). This data contrasts with the findings of **Chapter 4** where lower neutralising responses were still seen after the 3rd vaccine dose in PLWH and in the SARS-CoV-2 naïve group overall. It also contrasts with the results in **section**

5.3 showing a correlation between the level of spike-specific MBCs and serum neutralisation after the 1st vaccine dose (***Figure 5.3B-D***). Helpfully, at this later timepoint within the spike-specific MBC compartments, all bar 2 SARS-CoV-2 naïve PLWH had sufficient spike-specific MBCs to further evaluate RBD-specific responses (as explained in **sections 2.9** and **5.2**). However, there was no difference in RBD-specific MBC frequencies when stratifying by HIV status so this also does not explain why the serum titres, particularly neutralisation titres are lower in PLWH (***Figure 5.4.1B***). Therefore, these data reject my original hypothesis that the serological defect can be explained by overall lower numbers of spike-specific MBCs in PLWH after the 3rd vaccine dose. Furthermore, this data suggests that there is a disconnect between the serological output and the amount of spike-specific or RBD-specific MBC after three doses, where PLWH can make as many antigen-specific MBC as HIV-negative controls only their function and/or the function of the antibodies encoded is inferior. Interestingly, SARS-CoV-2 naïve HIV-negative controls had significantly higher frequencies of RBD-specific MBCs than HIV-negative controls with prior SARS-CoV-2 (***Figure 5.4.1B***). This indicates that participants first infected with SARS-CoV-2 reach this maximal threshold or "ceiling" for RBD-specific MBCs earlier, whereas SARS-CoV-2 naïve participants can still improve that aspect of their response, as described by Buckner et al., (2022). This is also consistent with the observation from an HIV-negative cohort that the 3rd vaccine dose preferentially induced the formation and maturation of new clonal families targeting less conserved regions of RBD in SARS-CoV-2 naïve (Muecksch et al., 2022).

Although the amount of spike-specific B cells was no longer delineated by whether individuals had prior SARS-CoV-2 infection nor by HIV status, all serological parameters still significantly correlated with the frequency of spike-specific MBCs (***Figure 5.4.2C-E***). The strength of each correlation was weaker than those seen after the 1st vaccine dose for binding S1-specific IgG titres and neutralisation titres against WT and Omicron BA.1 (***Figure 5.4.2C-D***). Unfortunately, due to the loss of most PBMCs from the earlier timepoints, there was no opportunity to longitudinally assess within participants the building of the spike-specific MBC response with each additional dose. As a proxy, correlations between the time since the 1st vaccine dose and the frequency of spike-specific MBCs were assessed (***Figure 5.4.1F-I***). These correlations suggested that the 1st and 2nd vaccine doses helped to produce higher

frequencies of spike-specific MBCs for SARS-CoV-2 naïve participants, whilst the 3rd vaccine dose only maintained the frequency of spike-specific MBCs (***Figure 5.4.1F-G***). For participants who had had a SARS-CoV-2 infection prior to vaccination, the frequencies of spike-specific MBCs stayed within the same range with each dose suggesting each additional vaccine dose only maintained the already strong spike-specific MBCs response seen from the 1st vaccine dose rather than boosting the frequency further (***Figure 5.4.1H-I***).

Altogether the data in this figure suggests that after the 3rd vaccine dose (a) PLWH have 'caught up' to HIV-negative controls in terms of levels of spike-specific MBCs and (b) SARS-CoV-2 naïve participants have 'caught up' with those individuals who had prior SARS-CoV-2. Although there is still a link between the quantity of spike-specific MBCs and the development of a broad neutralising response the spike-specific MBC response of most participants has plateaued. Therefore, the remaining serological difference after the 3rd vaccine dose is not a simple product of having fewer spike-specific MBCs, just as seen after the 1st vaccine dose. This suggests that potentially the serological defect seen in PLWH could be compensated by further affinity maturation of pre-existing spike-specific MBCs rather than the production of more spike-specific MBCs. Therefore, to understand what may underpin the lower serological output, the B cell phenotypes of the spike-specific MBCs were investigated.

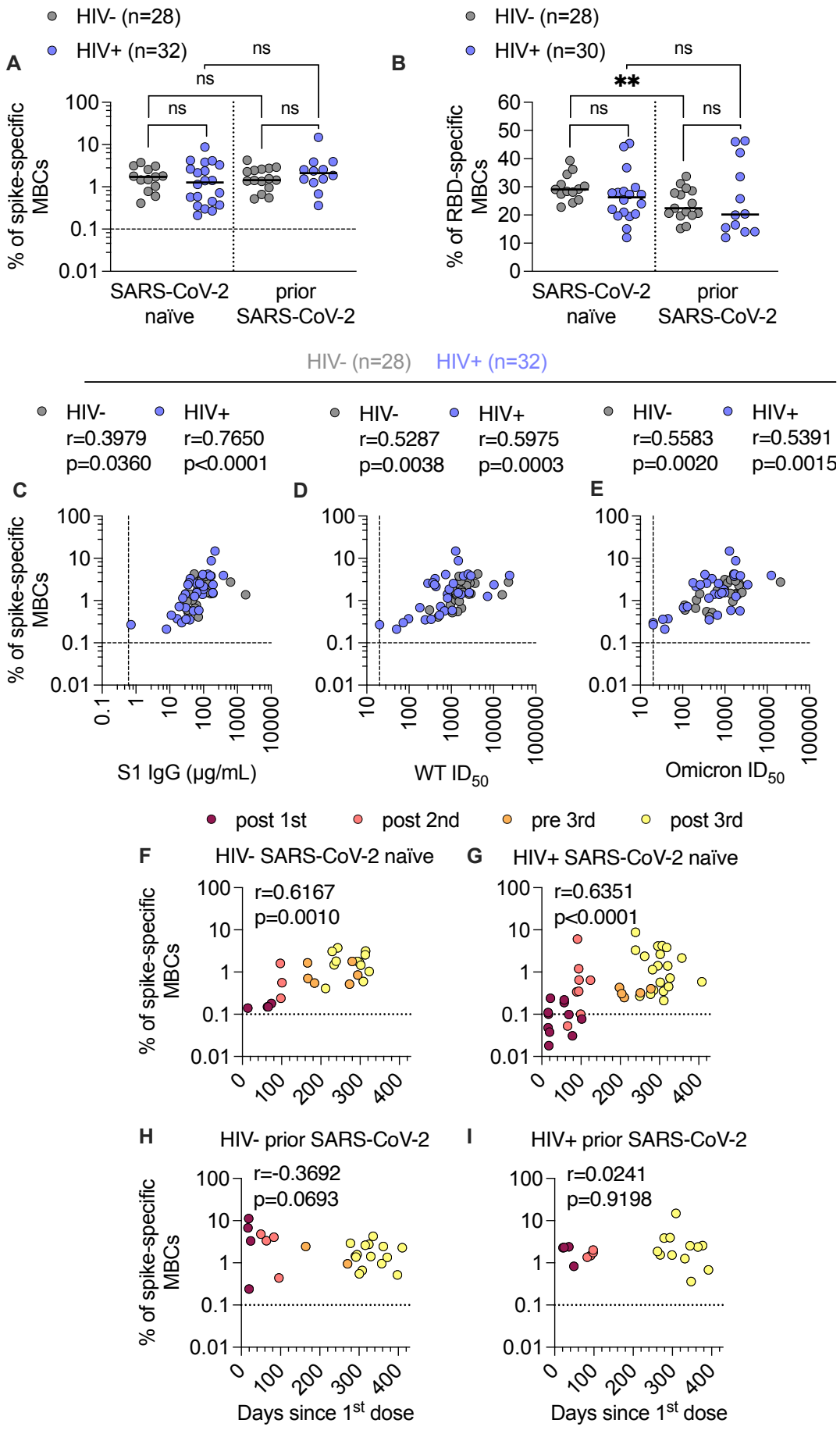
A
HIV- (n=28)
HIV+ (n=32)
ns
ns
ns
ns
% of spike-specific MBCs
100
10
1
0.1
0.01
SARS-CoV-2 naïve
prior SARS-CoV-2
B
HIV- (n=28)
HIV+ (n=30)
ns
**
ns
ns
% of RBD-specific MBCs
60
50
40
30
20
10
0
SARS-CoV-2 naïve
prior SARS-CoV-2
HIV- (n=28) HIV+ (n=32)
HIV- r=0.3979 p=0.0360
HIV+ r=0.7650 p<0.0001
HIV- r=0.5287 p=0.0038
HIV+ r=0.5975 p=0.0003
HIV- r=0.5583 p=0.0020
HIV+ r=0.5391 p=0.0015
C
D
E
% of spike-specific MBCs
S1 IgG (µg/mL)
WT ID50
Omicron ID50
post 1st
post 2nd
pre 3rd
post 3rd
F
HIV- SARS-CoV-2 naïve
r=0.6167
p=0.0010
G
HIV+ SARS-CoV-2 naïve
r=0.6351
p<0.0001
H
HIV- prior SARS-CoV-2
r=-0.3692
p=0.0693
I
HIV+ prior SARS-CoV-2
r=0.0241
p=0.9198
% of spike-specific MBCs
Days since 1st dose
Days since 1st dose

Figure 5.4.1: *Similar levels of spike-specific MBCs between PLWH and HIV-negative controls regardless of prior infection.* ***A.*** *Frequency of spike-specific MBCs (as a % of the parent population, CD19+ CD20+ CD38$^{lo/-}$ IgD- excluding CD21+ CD27-) after 3 doses stratified by HIV and SARS-CoV-2 status.* ***B.*** *Frequency of RBD-specific MBCs (as a % of the parent population, spike-specific MBCs) after 3 doses stratified by HIV and SARS-CoV-2 status.* ***C.*** *Correlation between frequency of spike-specific MBCs after 3 doses and S1 IgG-specific antibody titres (µg/mL);* ***D.*** *SARS-CoV-2 WT neutralising antibody titres (ID_{50}) or* ***E.*** *SARS-CoV-2 Omicron BA.1 neutralising antibody titres (ID_{50}).* ***F.*** *Correlation between frequency of spike-specific MBCs and days since 1st dose, stratified by timepoint for SARS-CoV-2 naïve HIV-negative controls;* ***G.*** *HIV-negative controls with prior SARS-CoV-2 infection;* ***H.*** *SARS-CoV-2 naïve PLWH and* ***I.*** *PLWH with prior SARS-CoV-2 infection. The median interval between the 2nd and 3rd vaccine dose for the SARS-CoV-2 naïve PLWH group was 186 days, 212 days for the SARS-CoV-2 naïve HIV-negative controls group, 192 days for the PLWH with prior SARS-CoV-2 infection group and 192 days for the HIV-negative controls with prior SARS-CoV-2 infection group. For A and C-I, the dotted line represents the limit of detection of the assay: 0.25 µg/mL IgG or ID_{50}=20, or the limit of sensitivity for the detection of spike-specific MBCs (0.1%). For A-B, is shown the median for each group. Statistical test: MWU for A-B, Spearman's rank correlation for C-I.*

5.4.2. *The inherent global memory B cell dysfunction is still present after the 3rd vaccine dose in PLWH but is lessened in the spike-specific memory B cells.*

Analysis of the *de novo* response seen after the 1st vaccine dose highlighted that perturbations in the MBC phenotype were apparent in participants with a delayed neutralisation response, a group which was mostly comprised of PLWH. Moreover, this group had markedly lower spike-specific MBCs. However, as seen in ***Figure 5.4.1***, after the 3rd vaccine dose regardless of HIV status, there was no longer a striking difference in the number of spike-specific MBCs between individuals with or without a history of SARS-CoV-2 which was significant after the 1st vaccine dose. This was despite there being persistent differences in the serum titres observed between PLWH and HIV-negative individuals, and between those with/without a history of SARS-CoV-2. As such, it was important to further assess if these differences in serological outcome could be explained by differences in the phenotype, and therefore quality, of global and spike-specific MBCs.

After the 3rd vaccine dose, PLWH showed the same perturbations in the global MBC phenotype described in **section 1.3.4**, with significantly lower frequencies of resting MBCs and significantly higher frequencies of atypical and intermediate MBCs (***Figure 5.4.2A***). As seen after the 1st vaccine dose, there was no difference in the frequency of plasmablasts between PLWH and HIV-negative controls. On the other hand, there was no longer a difference in the frequency of plasmablasts between the SARS-CoV-2 naïve group and prior SARS-CoV-2 infection groups (***Figure 5.4.2B***). This can be rationalised by considering that the response in the SARS-CoV-2 naïve group is now also a recall response. Within the spike-specific MBC compartment, there were no significant differences in the frequency of each MBC subset between PLWH and HIV-negative controls. However, there was a non-significant trend towards decreased resting MBCs and increased atypical MBCs in PLWH (***Figure 5.4.2C***).

This suggests that the MBC perturbations in the global MBC compartment in HIV (fewer resting, more atypical and intermediate) may limit the amount and the efficiency of high-quality B cells available to respond to further antigenic stimulation. Interestingly, despite this perturbation in the number of resting versus atypical MBCs in the global compartment in PLWH, there was minimal difference in the balance of these two phenotypes in spike-specific B cells between PLWH and HIV-negative

participants. This suggests that spike-specific MBCs are not getting “stuck” in the atypical phenotype and rather the impact of increased global atypical MBC on serological output is indirect. As opposed to previous hypotheses that, for example, pathogen-specific MBCs in chronic infection are more frequently atypical and as such fail to produce soluble antibodies as much as other MBCs (Burton et al., 2018; Meffre et al., 2016). To further understand which aspect of the MBC response may contribute to the differential serology response between PLWH and HIV-negative controls, I assessed isotype use in global and spike-specific MBCs to investigate if improper class-switching participated in the serology defect after the 3rd vaccine dose.

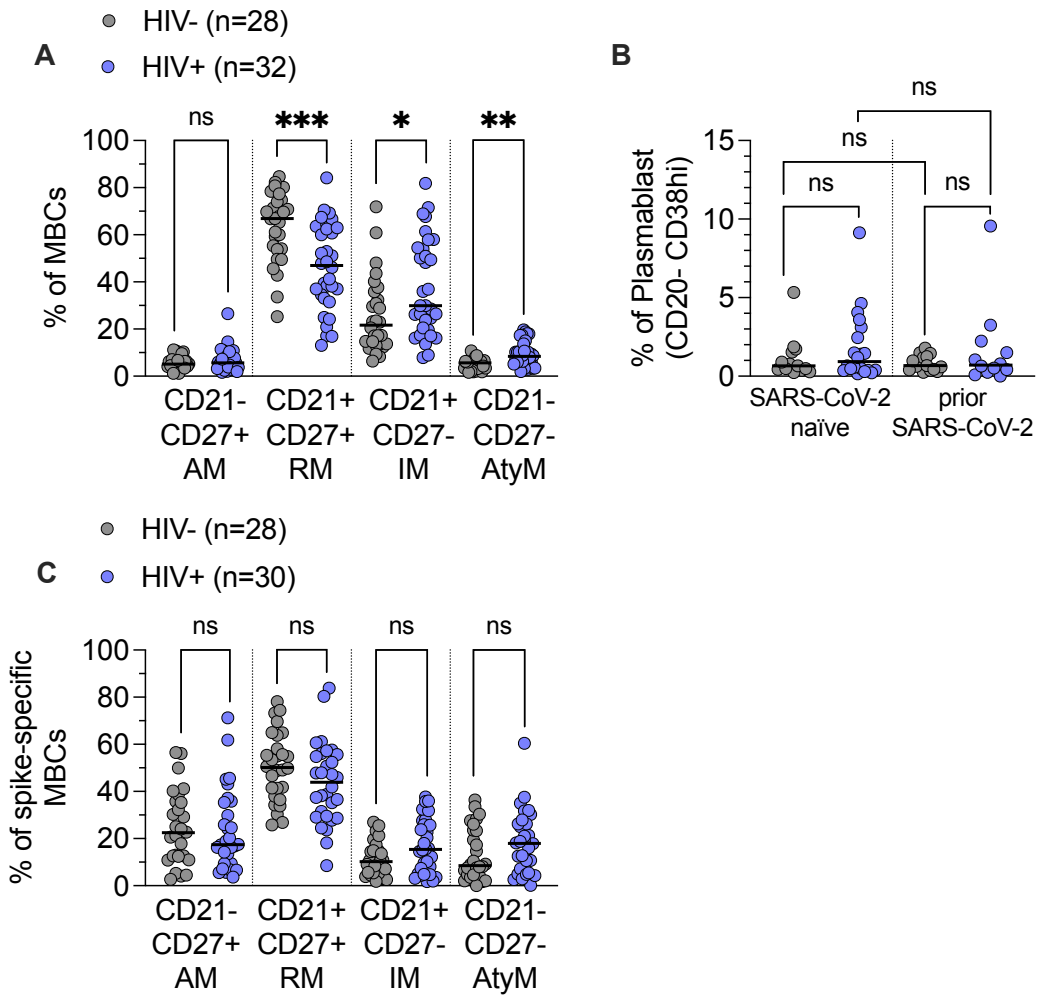

Figure 5.4.2: *The inherent global memory B cell dysfunction is still present after the 3rd vaccine dose in PLWH but is lessened in the spike-specific memory B cells.* ***A.*** *Frequency of each MBC subset in MBCs (as a % of the parent population, CD19+ CD20+ CD38lo/- IgD-): CD21- CD27+ activated MBCs (AM), CD21+ CD27+ resting MBCs (RM), CD21+ CD27- intermediate MBCs (IM) and CD21- CD27- atypical MBCs (AtyM) after 3 doses, stratified by HIV status.* ***B.*** *Frequency of Plasmablasts (CD19+ CD20- CD38hi) as a % of the parent population (total CD19+ B cells), after 3 doses, stratified by HIV status and prior history of SARS-CoV-2.* ***C.*** *Frequency of each MBC subsets in spike-specific MBCs (as a % of the parent population, CD19+ CD20+ CD38lo/- IgD- spike-specific): CD21- CD27+ activated MBCs (AM), CD21+ CD27+ resting MBCs (RM), CD21+ CD27- intermediate MBCs (IM) and CD21- CD27- atypical MBCs (AtyM) after 3 doses, stratified by HIV status. For A-C, is shown the median for each group. Statistical test: MWU.*

5.4.3. *Higher expression of IgM in spike-specific MBCs of PLWH reflects a maturity defect.*

As shown in ***Figure 5.4.2A*** after the 3rd vaccine dose, the global MBC compartment of PLWH was skewed towards more atypical MBCs and fewer resting MBCs compared to HIV-negative controls and this was accompanied by lower serological outputs. However, this skewed phenotype was attenuated within the spike-specific MBC compartment suggesting it doesn't directly limit the production of anti-spike antibodies and does not fully explain the lower serological response in PLWH. Given the overall dominance of IgG isotype use over IgM within spike-specific MBCs is the normal endpoint of a successful response to SARS-CoV-2 infection or vaccination (Hartley et al., 2020; Zurbuchen et al., 2023). I hypothesised that in PLWH, class-switching of spike-specific MBC may be disrupted by the overall MBC dysfunction and in turn explain the serological defect.

In the global MBC compartment, akin to the post 1st vaccine dose, there were no significant differences in the frequencies of IgG+, IgM+ or IgG- IgM- (likely IgA+) MBCs between PLWH and HIV-negative controls after the 3rd vaccine dose (***Figure 5.4.3A***). Of note, there is little overlap between the participants included in the post 1st and post 3rd vaccine dose cohorts due to the limited availability of samples. Interestingly, with this slightly different cohort of PLWH, I did not observe the small increase in IgG+ IgM+ in PLWH seen in ***Figure 5.3.3A*** after the 3rd vaccine dose (***Figure 5.4.3A***). Strikingly, within the spike-specific MBC compartment, PLWH had significantly lower frequencies of IgG+ spike-specific MBC and in turn, significantly higher frequencies of IgM+ spike-specific MBC (***Figure 5.4.3B***). These data highlight that although there were no inherent differences in the global class-switching of MBCs between PLWH and HIV-negative controls, the spike-specific MBCs in PLWH were less frequently class-switched to IgG after the 3rd vaccine dose. This difference in the isotype use of MBCs in PLWH may directly shrink the pool of MBCs able to be recalled after each re-exposure to produce high-affinity IgG which are most strongly associated with neutralisation. Therefore, this observation that spike-specific MBC in PLWH appear to be less mature is consistent with the finding that serologically they produce less highly affinity-matured antibodies with sufficient breadth to neutralise antigenically distinct variants.

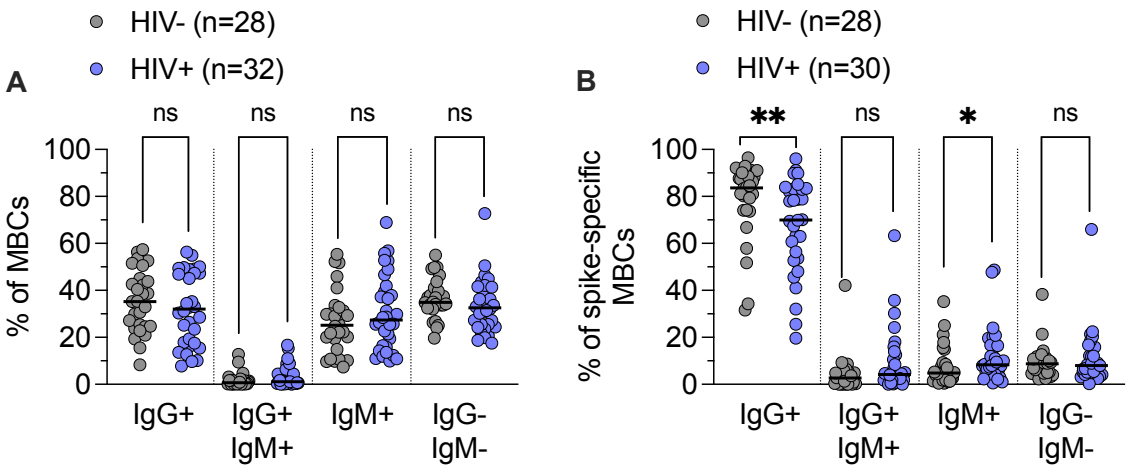

Figure 5.4.3: *Higher expression of IgM in spike-specific MBCs of PLWH reflects a maturity defect.* ***A.*** *Frequency of different isotypes in MBCs (as a % of the parent population, CD19+ CD20+ CD38$^{lo/-}$ IgD-): IgG+, IgG+ IgM+, IgM+ cells and IgG- IgM- after 3 doses stratified by HIV status.* ***B.*** *Frequency of different isotypes in spike-specific MBCs (as a % of the parent population, CD19+ CD20+ CD38$^{lo/-}$ IgD- spike-specific): IgG+, IgG+ IgM+, IgM+ cells and IgG- IgM- after 3 doses stratified by HIV status. For A-B, is shown the median for each group. Statistical test: MWU.*

5.5. No association between MBC dysfunction and CD4 count or CD4:CD8 ratio.

Finally, it was important to understand if any of the different changes in B cell phenotype seen in PLWH could be linked to their underlying HIV-mediated T cell dysfunction that may not have been fully corrected despite suppressive ART. After the 1st vaccine dose, there was no association between frequencies of spike-specific MBCs and CD4 count (cells/μL) or CD4:CD8 ratio in PLWH (***Figure 5.5A-B***). As highlighted in ***Figure 5.3.1***, the main driver of high spike-specific MBC frequencies in PLWH after the 1st vaccine dose was prior SARS-CoV-2 infection rather than differences in T cell immune reconstitution. Similarly, there was no association between the frequency of spike-specific MBCs and CD4 count (cells/μL) or CD4:CD8 ratio in PLWH after the 3rd vaccine dose (***Figure 5.5E-F***). In this regard, it is important to note that this cohort was mostly comprised of well-treated PLWH, and there were only 2 and 3 participants with CD4 counts under 350 cells/μL after the 1st and 3rd vaccine dose respectively. In individuals with lower T cell reconstitution, the situation is likely different. For example, two studies found that PLWH with CD4 counts under 200 cells/μL produced similar frequencies of spike-specific MBCs to PLWH with better T cell immune reconstitution after the 2nd (Ao et al., 2022; Lu et al., 2023) and 3rd vaccine dose (Lu et al., 2023). Additionally, there was no clear association between the frequencies of resting MBCs and CD4 counts (***Figure 5.5C*** and ***G***) or with the frequencies of atypical MBCs and CD4 counts (***Figure 5.5D*** and ***H***) in PLWH after the 1st or 3rd vaccine dose. Overall, these data do not support the idea that ongoing global and antigen-specific MBC disruption is driven solely by T cell-mediated dysfunction in this cohort of well-treated PLWH.

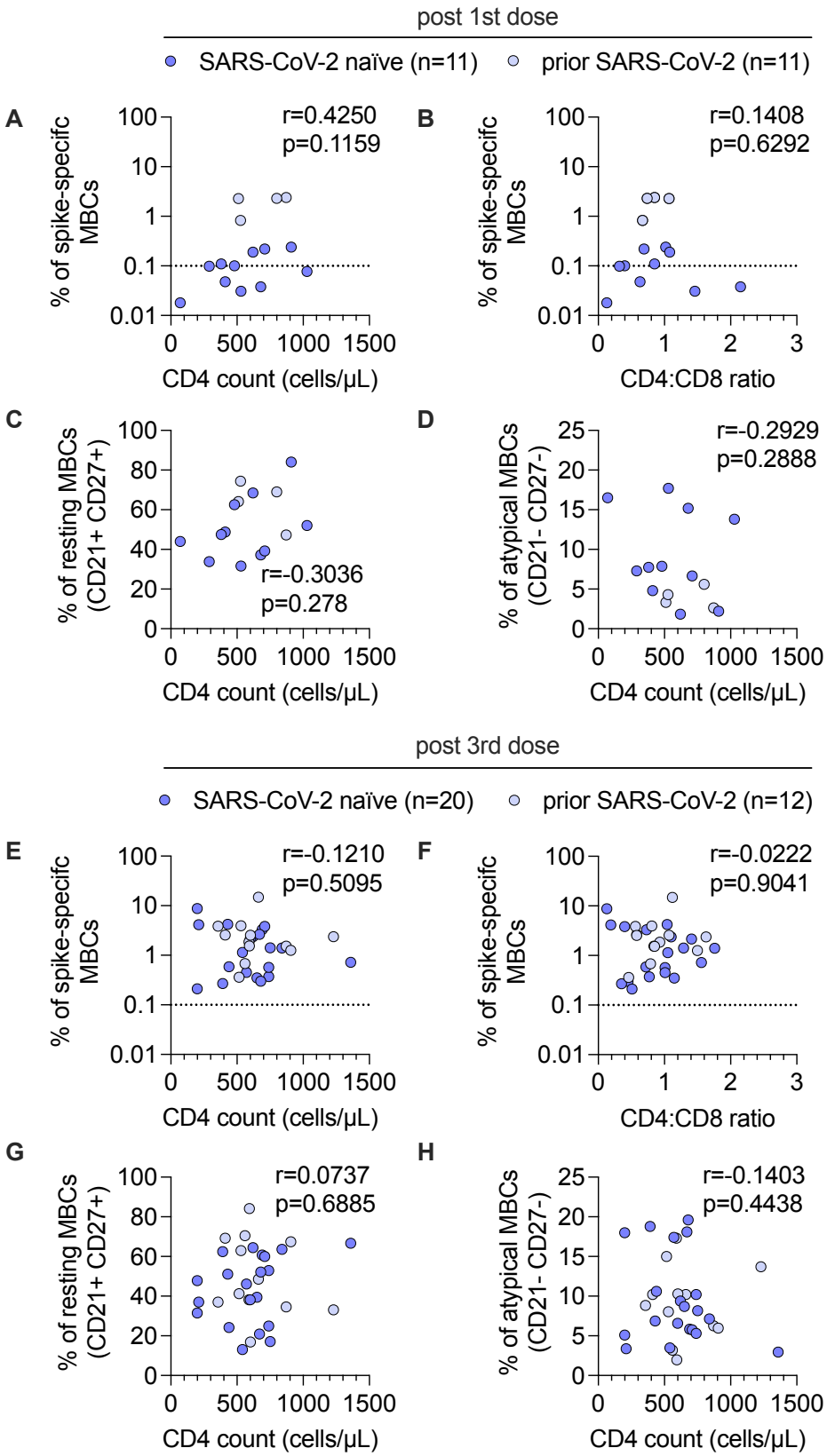
post 1st dose
SARS-CoV-2 naïve (n=11)
prior SARS-CoV-2 (n=11)
A
% of spike-specifc MBCs
r=0.4250
p=0.1159
CD4 count (cells/µL)
B
% of spike-specifc MBCs
r=0.1408
p=0.6292
CD4:CD8 ratio
C
% of resting MBCs (CD21+ CD27+)
r=-0.3036
p=0.278
CD4 count (cells/µL)
D
% of atypical MBCs (CD21- CD27-)
r=-0.2929
p=0.2888
CD4 count (cells/µL)
post 3rd dose
SARS-CoV-2 naïve (n=20)
prior SARS-CoV-2 (n=12)
E
% of spike-specifc MBCs
r=-0.1210
p=0.5095
CD4 count (cells/µL)
F
% of spike-specifc MBCs
r=-0.0222
p=0.9041
CD4:CD8 ratio
G
% of resting MBCs (CD21+ CD27+)
r=0.0737
p=0.6885
CD4 count (cells/µL)
H
% of atypical MBCs (CD21- CD27-)
r=-0.1403
p=0.4438
CD4 count (cells/µL)

Figure 5.5: *No association between MBC dysfunction and CD4 count or CD4:CD8 ratio. Correlation between frequency of spike-specific MBCs (as a % of the parent population, CD19+ CD20+ CD38$^{lo/-}$ IgD- excluding CD21+ CD27-) and* ***A.*** *CD4 count (cells/μL) and* ***B.*** *CD4:CD8 ratio after the 1st vaccine dose in PLWH, stratified by COVID-19 status.* ***C.*** *Correlation between CD4 count (cells/μL) frequency of CD21+ CD27+ resting MBCs and* ***D.*** *frequency of CD21- CD27- atypical MBCs after the 1st vaccine dose in PLWH, stratified by COVID-19 status.* ***E-H.*** *Equivalent to A-D after the 3rd vaccine dose. For A-B and E-F, dotted line represents the limit of sensitivity for the detection of spike-specific MBCs (0.1%). Statistical test: Spearman's rank correlation.*

5.6. Discussion

Underlying MBC dysfunction underpins the generation of a defective neutralisation response.

In summary, this chapter provided insights into the generation of memory and spike-specific B cell responses in PLWH after the 1st vaccine dose which allowed investigation into the formation of *de novo* MBC responses. This was followed by investigating the ability of PLWH to mount a recall MBC response after the 3rd vaccine dose. Immediately, there was a clear boosting effect where prior infection had occurred, presumably due to hybrid immunity (discussed in **section 1.2.8**) after the 1st dose. Specifically, participants with prior SARS-CoV-2 infection produced higher numbers of spike and RBD-specific MBCs than the SARS-CoV-2 naïve participants. This held true regardless of HIV status, which fits with the idea that the serological defect seen in PLWH can be overcome with highly immunogenic stimulation as discussed in **Chapters 3** and **4**. As binding to RBD is associated with potent neutralisation, participants with prior history of SARS-CoV-2 infection (who produce higher neutralising titres) had higher frequencies of RBD-specific MBCs as seen in other studies (Goel et al., 2021b, 2021a). However, in this chapter, due to the limited number of samples available after the 1st dose, it was unclear if overall, PLWH produced fewer spike-specific MBCs than HIV-negative controls (***Figure 5.3.1***). More convincingly, the delayed neutralisation phenotype described in **Chapter 4** (seen in many PLWH and fewer HIV-negative controls), was associated with lower frequencies of spike-specific B cells. Furthermore, delayed neutralisers had a skewed MBC phenotype with higher atypical MBCs and fewer resting MBCs, as described predominantly for PLWH with chronic viremia and lacking immune reconstitution in the wider literature (Kardava et al., 2014; Moir et al., 2008a, 2010; Pensieroso et al., 2013). Coupled with higher levels of plasmablasts, this phenotype may indicate that in delayed neutralisers the perturbation of MBC phenotypes directly limits the production of a timely neutralising response (***Figure 5.3.2***). Akin to plasma cells, plasmablasts have reduced expression of their surface BCR (Ellebedy et al., 2016). It is unclear how their increased presence early on after the 1st vaccine dose will impact the generation of a useful long-lived ASCs response, as many of these early plasmablasts were not spike-specific after the 1st vaccine dose (Kardava et al., 2022) and may be binding to irrelevant epitopes for neutralising antibody generation (Dugan et al., 2021). This may

also indicate that participants with a delayed neutralisation phenotype have a slower induction of their B cell response with the characteristic post-antigen exposure induction of plasmablasts is seen at this timepoint (delayed neutralisers were sampled at a median of 20 days post 1st vaccine dose, ***Figure 5.3.2***) rather than earlier as it would be expected. Indeed, in the context of SARS-CoV-2, other studies have reported that plasmablasts were found at the highest level during the early B cell response (~5-10 days) post-infection/vaccination and rapidly decreased with the development of more long-lived memory or antigen-secreting cells (Kardava et al., 2022; Pape et al., 2021; Sokal et al., 2021). Alternatively, the responding B cells of delayed neutralisers may somehow get 'stuck' resulting in high numbers of non-neutralising plasmablasts rather than differentiating into long-lived and more diverse sets of MBCs and plasma cells. This higher number of plasmablasts may reflect a higher contribution of the extrafollicular pathway (see **section 1.1.4** for details), away from the canonical GC pathway which is mainly thought to lead to neutralising responses.

Finally, there was no difference in global isotype use of MBCs between PLWH and HIV-negative controls. After the 1st vaccination, the only factor that influenced isotype use was prior SARS-CoV-2 infection. 'True' *de novo* responders i.e., SARS-CoV-2 naïve participants produced less IgG+ MBCs after their 1st vaccine dose (***Figure 5.3.3***). One limitation of the work in **section 5.3** is that due to the low number of events in the spike-specific MBC gate, it was not possible to do any sub-gating on this population. This meant I wasn't able to meaningfully characterise the MBC phenotype or isotype usage of spike-specific cells after the 1st vaccine dose.

After the 3rd dose, the greater levels of spike-specific MBCs due to hybrid immunity from prior SARS-CoV-2 infection had tapered off, regardless of HIV status. This suggests that three vaccine doses had effectively 'maxed out' the amount of spike-specific MBC that could be made in both PLWH and HIV-negative controls. Therefore, the capacity of the serological response to develop was not limited by the number of spike-specific MBCs at this point as there were still significant serological differences at that timepoints between the four groups. I propose that these serological differences are due to differences in the quality and functionality of these spike-specific MBCs rather than quantity, and in turn that this MBC quality may be influenced by global changes in MBC phenotypes (***Figure 5.4.1***). The data presented here is in agreement

with the literature, with two studies showing that after the 2nd vaccine dose, there was no difference in the frequency of spike-specific MBC between SARS-CoV-2 naïve PLWH and HIV-negative controls (Ao et al., 2022; Polvere et al., 2023). Another study also reported no difference in levels of spike-specific MBCs between PLWH and HIV-negative controls after the 3rd vaccine dose (Matveev et al., 2023). Moreover, two studies found that there was a marked increase in the frequencies of spike-specific MBC in SARS-CoV-2 naïve PLWH after the 3rd dose (Jongkees et al., 2023; Lu et al., 2023).

There was still a marked difference in the overall MBC phenotype between PLWH and HIV-negative controls after the 3rd vaccine dose. PLWH still had fewer resting MBCs and more atypical and intermediate MBCs, although this MBC perturbation was less pronounced in the spike-specific compartment and did not reach significance (***Figure 5.4.2***). This data mirrors the increase in spike-specific atypical B cells and the decrease in resting/switched MBC reported in PLWH after the 2nd vaccine dose in other studies published concurrently with this work (Ao et al., 2022; Polvere et al., 2023). In PLWH receiving inactivated SARS-CoV-2 vaccines, a longitudinal study (Lu et al., 2023) showed that the frequencies of every subset of spike-specific MBC stayed stable in a timeframe englobing post 2nd and 3rd vaccine dose. Therefore, the slight differences in the phenotype of spike-specific MBCs in PLWH may have been already apparent after the 1st dose if sufficient samples had been available to analyse. Altogether, in my data, the imbalance between frequencies of atypical and resting MBCs is associated with the reduced quantity and quality of the neutralisation responses after three doses of SARS-CoV-2 vaccination although how mechanistically this occurs is unclear. It could be global MBC phenotype perturbation limits the numbers of high-quality MBCs available to participate in future GC reactions and differentiate into long-lived ASC upon re-exposure. In addition, excess of atypical MBCs may be less able to respond to antigens as described previously (Moir et al., 2008a) and lead to weaker spike-specific MBC response. Indeed, it has been reported that following SARS-CoV-2 vaccination and infection in HIV-negative individuals, atypical MBCs were rarely the precursor of resting MBCs but rather formed an alternative pathway (Lopes de Assis et al., 2023; Zurbuchen et al., 2023). Excess of atypical MBCs seen here may break the well-established cycle of early induction of

CD21- MBCs before the dominance of CD21+ CD27+ resting MBCs seen in normal post-SARS-CoV-2 infection/vaccination response (Buckner et al., 2022).

Whilst overall numbers of IgG+ and IgM+ MBCs were similar between PLWH and HIV-negative controls, this was not true within the spike-specific MBC compartment. The spike-specific MBC response of PLWH skewed towards higher usage of IgM and less IgG compared to HIV-negative controls (***Figure 5.4.3***). Excess IgM+ spike-specific MBCs might represent MBCs which were not able to or failed to class-switch to IgG, hence curtailing the utility of these antibodies in the serum response, as IgG antibodies should make up roughly 80% of the serum (Gasser et al., 2021; Wang et al., 2021c). Indeed, after SARS-CoV-2 infection and vaccination, long-lived MBC responses consist mostly of IgG+ MBCs (Goel et al., 2021b, 2021a; Kardava et al., 2022; Turner et al., 2021). In some studies of SARS-CoV-2 naïve individuals after the 1st vaccine dose (where the response was truly *de novo*) a higher usage of IgA and IgM in spike-specific MBCs was seen in the first instance (Goel et al., 2021b, 2021a; Kardava et al., 2022), with additional vaccine dose skewing the spike-specific MBC response towards IgG. Whereas it was reported that in individuals with a prior history of SARS-CoV-2 infection, the spike-specific MBC response already showed a preference for IgG+ spike-specific MBCs after the 1st vaccine dose as it included *de novo* and recalled MBCs (Goel et al., 2021b, 2021a; Pušnik et al., 2022). Additionally, it must be noted that PLWH have hypergammaglobulinemia i.e., higher levels of IgG in the first place (see **section 1.3.4**), which is driven by higher titres of IgG1 and IgG3 (Buckner et al., 2013). Interestingly, IgG3 are preferentially used by atypical MBCs and therefore may play a role in the overall MBC disruption in PLWH (Kardava et al., 2018). Taking all of this into account, the abundance of IgM+ spike-specific MBCs after the 3rd vaccine dose in PLWH is unusual and suggests that PLWH's spike-specific response may have lower levels of affinity maturation and thus be less able to produce a neutralising response.

Finally, the differences in frequencies of spike-specific, atypical, and resting MBCs in PLWH were not influenced by T cell mediated dysfunction. This highlights that although ART is successful at recovering much T cell immunity in PLWH, there is still a heterogeneity in MBC function and phenotype in PLWH which is associated here with poorer serological outcomes. The observations of no association between resting MBCs and CD4 counts may seem surprising as the prototypical phenotype of MBC

disruption seen in HIV is exacerbated in early HIV infection when PLWH are not yet on ART and thus have lower CD4 counts (Moir et al., 2008b; Pensieroso et al., 2013). Lack of ART is often associated with lower CD4 count and overall T cell dysfunction, but it seems that MBC disruption is driven rather by active viraemia than lack of CD4+ T cells (Fogli et al., 2012; Pensieroso et al., 2013). This fits with two important observations shown in this thesis: (1) Once a certain threshold of CD4+ T cells and antigenic stimulation is reached, as seen in SARS-CoV-2 vaccination ***Figure 4.2***, antigen-specific humoral and the B cell response is 'turned on'. For example, in this thesis PLWH sampled after the 3rd vaccine dose had a wide range of CD4 counts (200-1360 cells/μL) and yet managed to make similar spike-specific responses; (2) The presence of atypical MBCs seems to be driven either directly or indirectly by active viraemia, or inflammation associated to viraemia as exemplified by the increase seen shortly after acute SARS-CoV-2 infection/vaccination or their permanent presence in chronic HIV infection.

Atypical MBCs: friend or foe?

It is important to bear in mind, that atypical MBCs have recently been acknowledged to be part of a normal post-infection or vaccination response (Carr et al., 2023; Sutton et al., 2021; Zurbuchen et al., 2023). Their exact role and origins in these responses are still unclear. The best evidence shows that they are increased by active viraemia in acute and chronic infections (Fogli et al., 2012; Krause et al., 2022; Moir et al., 2008a; Pensieroso et al., 2013; Woodruff et al., 2020). In SARS-CoV-2 infection it has been highlighted that the early MBC response is dominated by CD21- MBC i.e., atypical and activated MBC (Ogega et al., 2021; Oliviero et al., 2020; Pape et al., 2021; Pušnik et al., 2022; Woodruff et al., 2020; Zurbuchen et al., 2023). The presence of atypical MBC is exacerbated in severe COVID-19 disease (Ogega et al., 2021; Oliviero et al., 2020; Woodruff et al., 2020). This suggests that ongoing viral infection and therefore antigen deposition is creating a feedback loop where atypical MBCs are induced as long as the infection is not cleared. CD21- B cells will progressively disappear in the convalescent phase of infection where in turn, resting MBC and intermediate MBC will dominate (de Campos-Mata et al., 2021; Zurbuchen et al., 2023). This was still true within the spike-specific compartment in HIV-negative controls (Ogega et al., 2021; Pape et al., 2021; Pušnik et al., 2022; Zurbuchen et al., 2023). For PLWH, the already higher frequencies of atypical MBC were exacerbated

with severe presentation of COVID-19, this further translated into higher titres of spike-specific atypical MBC as well (Krause et al., 2022). After SARS-CoV-2 infection and vaccination in HIV-negative individuals (Zurbuchen et al., 2023) found that spike-specific atypical MBC may actually have an increased capacity for antigen presentation, although this may not result in more beneficial T cell help as this increased function has been previously associated with auto-reactivity (Reincke et al., 2020). However, another study found that higher levels of IgD- CD27- B cells co-expressing CD137, were associated with broader variant neutralising in SARS-CoV-2 vaccination (Carr et al., 2023).

The early induction of atypical MBC in viral infection may serve different roles: (1) atypical MBCs actively participate in the anti-viral activity of the immune system or (2) they are a by-product of viral-mediated inflammation which would therefore explain their persistence in chronic infections and what has been described as an exhausted-like phenotype. In the past few years, studies (Reyes et al., 2023; Sutton et al., 2021) have proposed that within CD21- CD27- atypical MBCs there are several subtypes (or at the very least functional roles) which can be delineated by their surface expression of CD11c, Tbet or CXCR3 and their differential gene expression of genes associated with antigen presentation or interferon signalling. These different subtypes seem to differ in their ability to secrete antibodies, present antigens to T cells and overall level of 'exhaustion'. Therefore, I hypothesise that the healthy atypical response seen in early/acute response to viral infections may be driven by the atypical MBCs with increased ability for antigen presentation and antibody secretion which further facilitate viral clearance by the adaptive immune system. On the other hand, persistent infections lead to over-inflammation and over-accumulation of atypical MBCs which may be skewed towards the more exhausted subtype of atypical at this point and direct MBCs away from the classical resting phenotype.

How does this data fit with the wider HIV and COVID-19 vaccination B cell literature?

There is still a paucity of data on memory and antigen-specific B cell response in PLWH following SARS-CoV-2 infection and vaccination. At the point when this chapter's data was first published (November 2022), no other study had looked at spike-specific MBC response in PLWH after the 1st vaccine dose. The data now available broadly fits with the results presented in this chapter. A study of SARS-CoV-

2 naïve PLWH showed that immediately after receiving two doses of inactivated vaccines, PLWH produced slightly inferior frequencies of spike-specific MBCs compared to HIV-negative controls (Ao et al., 2022). This difference had disappeared 3 months after the 2nd vaccine dose (Ao et al., 2022). In the same manner, in a study focusing on responses ~5 months after the 2nd mRNA vaccine dose (Polvere et al., 2023), there was no difference in the frequency of RBD-specific MBC between SARS-CoV-2 naïve PLWH and HIV-negative controls. After the 3rd vaccine dose, levels of spike-specific MBC were similar between PLWH and HIV-negative controls (Matveev et al., 2023). Two studies (Jongkees et al., 2023; Lu et al., 2023) also showed the benefit of a 3rd dose in PLWH in generating a stronger spike-specific MBC response. Both studies did not have an HIV-negative group for comparison, and therefore it is still debatable if there are any differences as compared to HIV-negative participants in terms of the development kinetics of spike-specific MBCS after the 3rd vaccine dose. Akin to the data shown in ***Figure 5.4.3***, other studies have shown the phenotype of spike-specific MBCs was skewed towards fewer resting and more atypical MBC in PLWH after the 2nd vaccine dose (Ao et al., 2022; Polvere et al., 2023). All of these studies included SARS-CoV-2 naïve donors only and as such there is no equivalent MBC data on the impact of hybrid immunity in PLWH to that presented in this thesis. The only data available is following SARS-CoV-2 infection only, where PLWH also achieved similar levels of spike-specific MBCs to HIV-negative controls (Krause et al., 2022).

Limitations due to the lack of available samples.

Due to circumstances outside of our control, most PBMC samples collected for this project were lost in October 2021 in an LN2 failure, with very limited samples remaining available compared to corresponding plasma samples characterised in **Chapters 3** and **4**. The timing of the LN2 failure meant that most of our cohort, like the general UK population, had already received at least two vaccine doses and therefore there was no real possibility to re-recruit a similar cohort. Therefore, efforts focused on maximising the collection of samples around the 3rd vaccine dose to compensate for this event. The bulk of lost samples were from early timepoints: 76% of baseline, 80% of post 1st, 86% of post 2nd and 68% of pre 3rd vaccine dose samples were lost. Effectively, this meant that only 23 samples (8 HIV-negative controls and 15 PLWH) after the 1st vaccine dose, 19 samples (7 HIV-negative controls and 12 PLWH) after

the 2nd vaccine dose, 13 samples (8 HIV-negative controls and 5 PLWH) were assessed in this chapter whereas and 60 samples (28 HIV-negative controls and 32 PLWH) were available for analysis after the 3rd vaccine dose.

Due to low sample availability after the 2nd dose or before the 3rd vaccine dose, the analysis focused on understanding how immediate *de novo* responses formed after the 1st vaccine dose and how these responses were maintained/improved after 'recall' i.e., after the 3rd vaccine dose. Additionally, this meant that the data in this chapter is strictly cross-sectional. Availability of longitudinal samples at each timepoint, across PLWH and HIV-negative controls, would have allowed for better assessment of how each additional dose affected the amount and the type of spike-specific MBC made across these groups at an individual level. For example, to understand why some individual PLWH made good neutralising responses after the 1st dose when so many others didn't, as seen in ***Figure 4.7***, it would have been interesting to assess if there were any inherent differences to their B cell phenotype at baseline. Importantly, pronounced waning was seen before the 3rd vaccine dose in ***Figure 4.4-6***, and analysis of PBMC from these individuals before and after the 3rd vaccine dose would have allowed to potentially investigate which MBC subsets helped produce the characteristically higher titres seen after the 3rd dose. However, while the PBMC samples for these timepoints were rendered unviable for flow cytometry analysis by the LN2 failure, we found it was possible to extract RNA. Therefore, in the next chapter sequencing of the BCR, including IgM+ spike-specific BCR was performed in an attempt to address some of the outstanding questions.

Chapter conclusions.

The data shown in this chapter directly builds on the previous chapter's observations of lower binding, lower and delayed neutralisation, and restricted neutralisation breadth in PLWH after SARS-CoV-2 vaccination. Here, delayed neutralisation was associated with the perturbed MBC phenotype commonly seen in PLWH of higher levels of atypical MBCs and lower levels of resting MBCs. The lower quantity and breadth of neutralisation still observed after the 3rd dose in PLWH was not reflected in the quantity of spike-specific MBC but was associated with both higher levels of global atypical MBCs and fewer resting MBCs which may limit the pool of available MBCs that can respond to antigen. Furthermore, there were fewer IgG+ spike-specific MBCs

in PLWH than in HIV-negative controls. Altogether this shows that despite generating sufficient quantities of antigen-specific cells after three vaccine doses, PLWH struggle to make the kind of high-quality affinity matured antibodies seen in HIV-negative controls. This highlights the need to understand at a clonal level the kind of SARS-CoV2 antibodies made in PLWH.

6. Modulation of the B cell receptor repertoire post SARS-CoV-2 vaccination in PLWH

6.1. Summary

Throughout this thesis so far, I have shown that in a cohort of PLWH, there was a marked quantitative and qualitative defect in the serological output after each dose of COVID-19 vaccination. Even after three vaccine doses, PLWH made lower binding and neutralising responses with less breadth. Despite this, PLWH had as many spike-specific MBCs as HIV-negative controls, although IgM usage was higher. Therefore, I hypothesised that the overall imbalance in the global MBC phenotype and the higher frequencies of IgM+ spike-specific MBCs in PLWH could reflect a fundamental difference in the way PLWH are able to make antibodies against other pathogens. To address whether the defect in antibody responses in PLWH is associated with improper recall responses and thus inadequate affinity maturation, I characterised the BCR repertoires of PLWH and HIV-negative controls. VDJ regions were amplified by PCR for NGS from participants in both groups, with and without a prior history of SARS-CoV-2 infection, after all vaccine doses. This allowed the characterisation of any potential difference in V gene usage, SHM, clonal relationships and overall diversity between PLWH and HIV-negative controls after SARS-CoV-2 vaccination and how it related to the lower serological output and MBC imbalance seen previously. The bulk BCR repertoire was sequenced at all timepoints for the chosen participants but spike-specific BCRs were sequenced only after the 3rd vaccine dose due to sample availability. Although only available at one timepoint, based on prior work (Bonsignori et al., 2016) spike-specific BCRs sequenced after the 3rd vaccine dose theoretically could be used to identify spike-specific clones at the previous timepoints within the bulk repertoire. Similarly, the bulk repertoires were filtered to identify public spike-specific clones (see **section 1.2.7** for more details), which have been widely documented in SARS-CoV-2 infection (Galson et al., 2020; Kotagiri et al., 2022; Nielsen et al., 2020; Robbiani et al., 2020; Voss et al., 2021; Yang et al., 2021a) and vaccination (Chen et al., 2021; Lima et al., 2022).

6.2. Sub-study design and sorting strategy for BCR sequencing

In this chapter, the BCR repertoires of 20 participants in total were characterised from the wider vaccination cohort described in **Chapter 4** and **5**. Specifically, 10 PLWH and 10 HIV-negative controls were studied, with both groups comprising 5 participants who were SARS-CoV-2 naïve and 5 who had a prior history of SARS-CoV-2 infection. The participants in this sub-study had titres of S1-specific IgG antibodies (***Fig.6.2.1A-B***), neutralising antibodies against SARS-CoV-2 WT (***Fig.6.2.1C-D)*** and Omicron BA.1 (***Fig.6.2.1E-F)*** which were mostly representative of those seen in their wider corresponding groups. Specifically, stronger binding and neutralisation titres were seen where prior SARS-CoV-2 infection had occurred, and weaker neutralisation was seen in PLWH as compared to HIV-negative controls with the same SARS-CoV-2 history.

For each participant, BCR libraries were generated from baseline, post 1st, post 2nd and post 3rd vaccine dose samples (***Figure 6.2.2***). The baseline, post 1st and post 2nd vaccine dose samples were used to amplify total VDJ sequences and generate bulk IgG and IgM BCR libraries for each participant. This approach was the only feasible choice from RNA extracted from the available non-viable cells (due to accidental thawing during the LN2 mechanical failure). In contrast, for the post 3rd vaccine dose samples, 10x10^6 viable PBMC aliquots for each donor were available and as such could be used to generate spike-specific IgG and IgM libraries after sorting (see **Methods 2.10-2.12** for details). Prior to staining, 1 x10^6 PBMCs were reserved to generate bulk IgG BCR libraries for the post 3rd vaccine dose timepoint.

Finally, to sort spike-specific MBCs a gating strategy (***Figure 6.2.3***) was adapted from previous work in our lab by Luke Muir and Sarah Griffith alongside the one presented in **section 5.2**. Briefly, this was used to sort 1 cell or alternatively, 100 CD19+ CD4- IgG+ or IgM+ spike-specific cells were sorted in each well. Both IgG and IgM spike-specific BCR were amplified to further understand any issues with the quality of class-switched antibodies in PLWH. This dual approach of sorting either 1 or 100 spike-specific B cells was chosen to maximise the amount of antigen-specific B cells that could be sorted from a unique 10 x10^6 PBMC vials and enable the extensive downstream processing for 20 participants. A BCR sequencing-only approach was preferred due to the technical limitations of single-cell BCR sequencing platforms like 10x. Specifically, there are limitations in regard to antigen-specific cells as any antigen-

specific population is incredibly rare, as seen in ***Figure 5.4.1A***, where the median frequency of spike-specific MBCs for all groups was 1.5% in total MBCs. Practically this can mean anywhere between 20 and 4383 spike-specific B cells can be obtained from a $10x10^6$ PBMCs vial. As 10x requires a minimum of 10,000 cells, more vials of cells would have been needed (which were not available) to sort enough spike-specific B cells or pooling all donors together would have been required. However, at the time this work was carried out it was not technically possible to both stain for antigen-specific B cells and individually barcode each donor via cell hashing as the hashing process interferes with the antigen-specific labelling. Another point of interest was that albeit being far more labour-intensive, the downstream pipeline used to sequence VDJs from antigen-specific sorted IgG+ single cells was at that time fully optimised in our lab (McCoy and Burton, 2017), whereas the bulk antigen-specific strategy was effectively novel, hence I prioritised acquiring one plate of IgG+ spike-specific single cells and then acquired any remaining spike-specific B cells with the 100 cells per well mixed IgG/IgM approach.

Overall, the sorting and sequencing strategy summarised in ***Figure 6.2.1*** yielded a bulk BCR library for each donor for the baseline, post 1st, post 2nd and post 3rd vaccine dose timepoints and a spike-specific BCR library for each donor at the post 3rd vaccine dose timepoint.

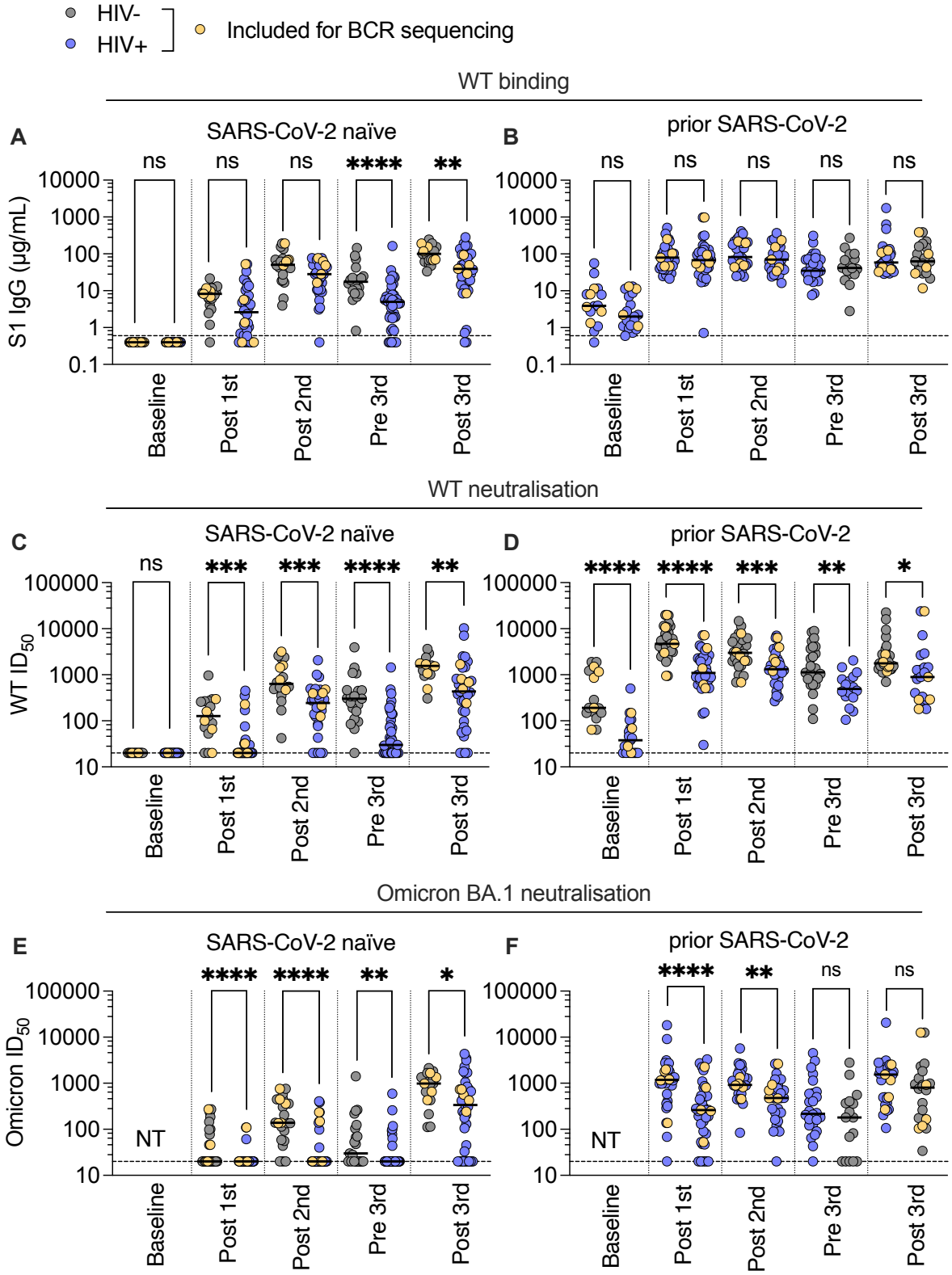
HIV-
HIV+
Included for BCR sequencing
WT binding
A
SARS-CoV-2 naïve
B
prior SARS-CoV-2
S1 IgG (µg/mL)
ns
ns
ns
****
**
ns
ns
ns
ns
ns
10000
1000
100
10
1
0.1
Baseline
Post 1st
Post 2nd
Pre 3rd
Post 3rd
WT neutralisation
C
SARS-CoV-2 naïve
D
prior SARS-CoV-2
WT ID50
ns
***
***
****
**
****
****
***
**
*
100000
10000
1000
100
10
Baseline
Post 1st
Post 2nd
Pre 3rd
Post 3rd
Omicron BA.1 neutralisation
E
SARS-CoV-2 naïve
F
prior SARS-CoV-2
Omicron ID50
****
****
**
*
****
**
ns
ns
NT
NT
100000
10000
1000
100
10
Baseline
Post 1st
Post 2nd
Pre 3rd
Post 3rd

***Figure 6.2.1**: Participants included for BCR sequencing demonstrate representative binding and neutralisation abilities. IgG-specific antibody titres (µg/mL) against SARS-CoV-2 S1 for **A.** SARS-CoV-2 naïve participants and **B.** participants with prior SARS-CoV-2 infection stratified by timepoint and HIV status (HIV-negative controls – grey; PLWH). Throughout the figure, the participants whose BCRs were sequenced for this project are highlighted in yellow. **C.** SARS-CoV-2 WT (Wuhan-hu1) pseudovirus neutralising reciprocal 50% inhibitory titres (ID_{50}) for SARS-CoV-2 naïve participants and **D.** participants with prior SARS-CoV-2 infection stratified by timepoint and HIV status. **E-F.** Equivalent to C-D for Omicron BA.1. The dotted lines represent the limit of detection of the assays (for B. viral load<50 copies/mL, for C. 0.6µg/mL of IgG and for D. ID_{50}=20). Where no binding was detected, samples were assigned a titre of 0.4 µg/mL and where no neutralisation was detected, samples were assigned an ID_{50} of 20 for visualisation. Statistical test: MWU.*

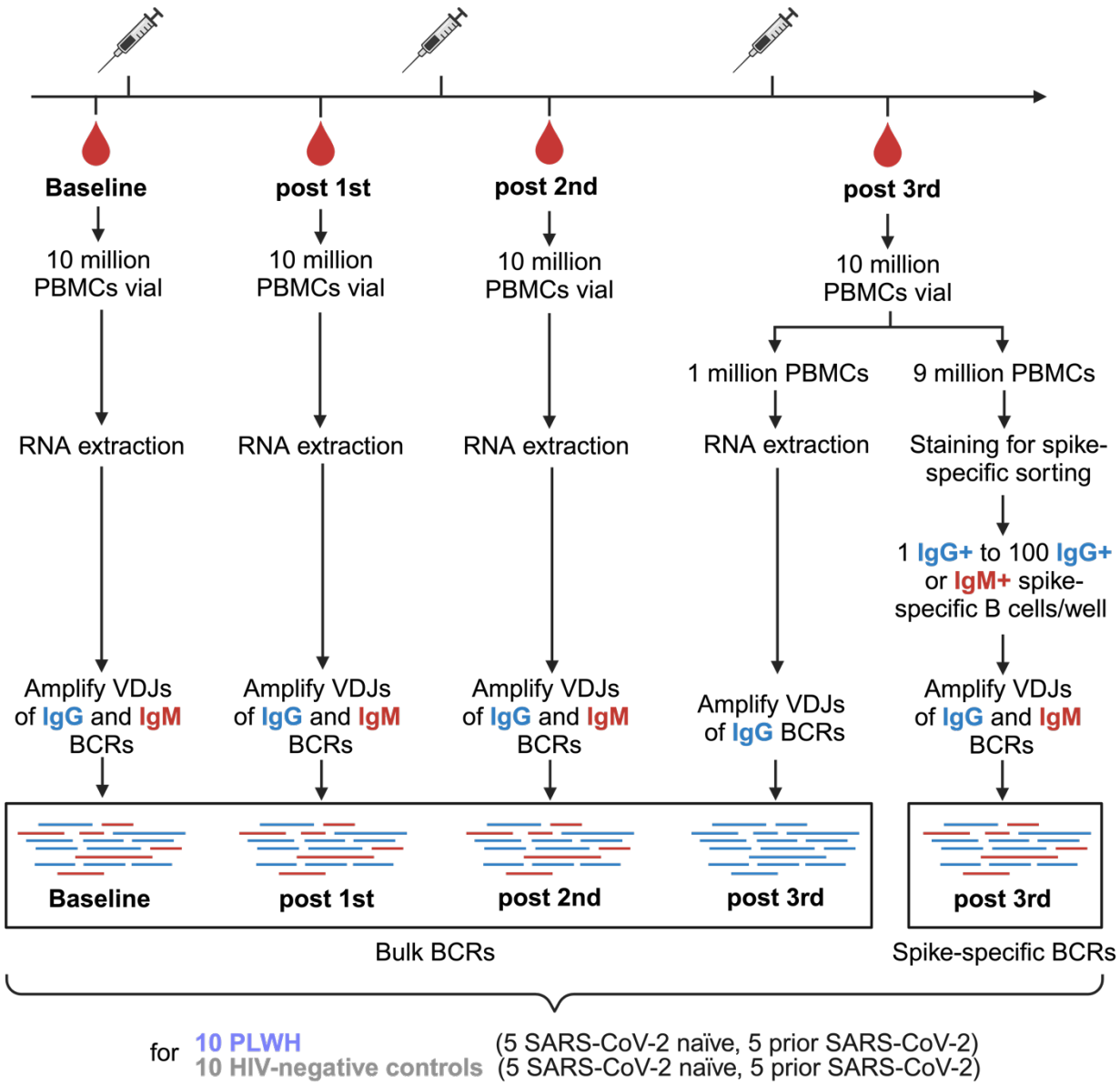

Figure 6.2.2: *Schematic of BCR sequencing strategy. From the baseline, post 1st and post 2nd vaccine dose timepoints, 1x10 million PBMCs vial was used to generate a bulk library of IgG and IgM BCRs per timepoint. For the post 3rd vaccine dose timepoint, 1x10 million PBMCs vial was divided to generate a bulk library of IgG BCRs and a library of spike-specific IgG and IgM BCRs.*

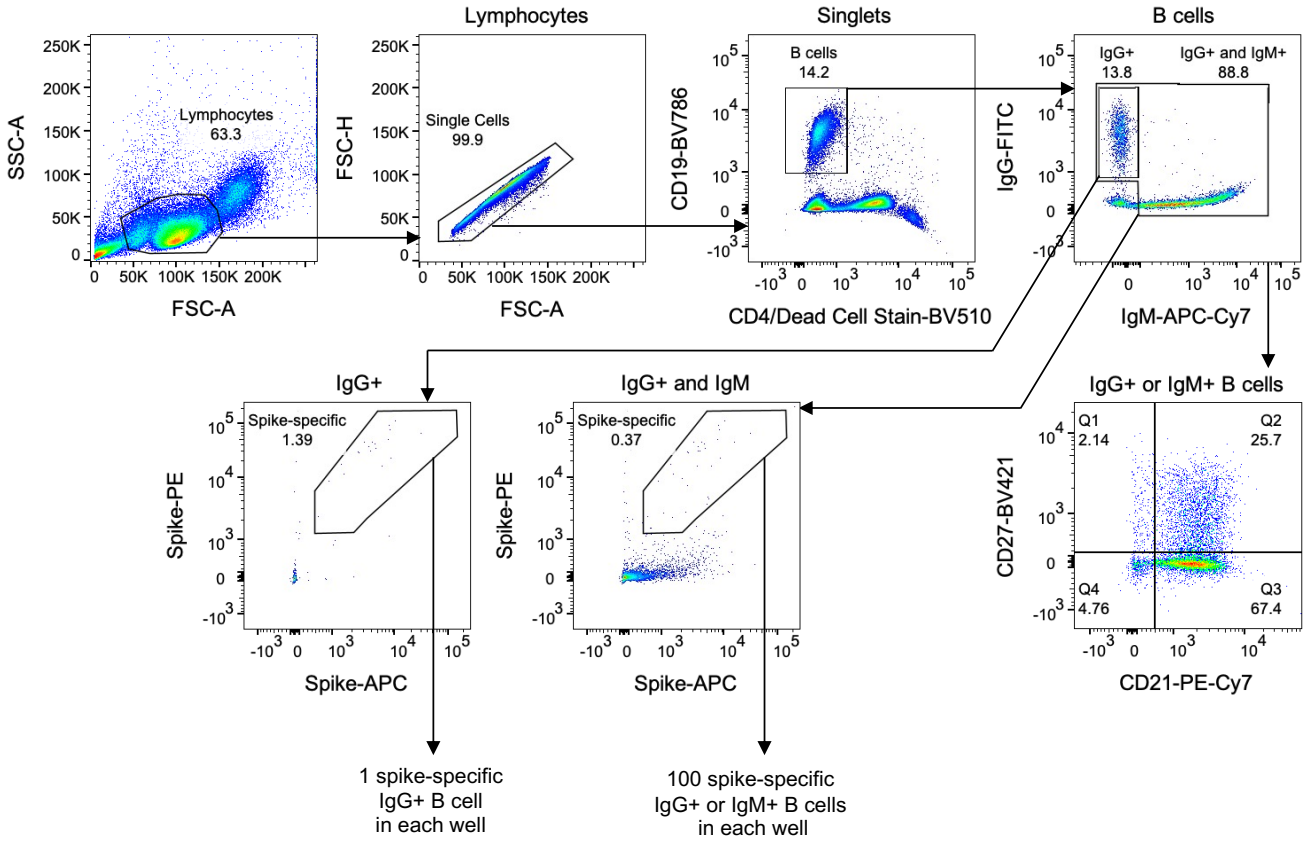

Figure 6.2.3: *Gating strategy for spike-specific B cell sorting. Total PBMCs were first gated to identify lymphocytes using SSC and FSC, then on single cells using FSC-H and FSC-A, and then on B cells using CD19-BV786+ expression whilst excluding CD4/Aqua live/dead cell stain-BV510+ cells. To sort for antigen-specific B cells, either IgG-FITC+ only B cells were selected or any cells within a gate including IgG-FITC+ and IgM-APC-Cy7+ B cells. Spike-specificity was identified for any of these two gates by using biotinylated spike protein pre-incubated with streptavidin-PE and streptavidin-APC as described in* ***section 5.2****. 1 or 100 spike-specific CD19+ CD4- IgG+ or IgM+ B cells were sorted in each well. Additionally, B cell phenotype on any isotype can be inferred by using CD21-PE-Cy7 and CD27-BV421 to gate on the different MBCs subsets: activated MBCs (CD21- CD27+), resting MBCs (CD21+ CD27+), intermediate/naïve MBCs (CD21+ CD27-) and atypical/transitional MBCs (CD21- CD27-). Due to constraints in how many fluorophores could be included in this sorting panel, IgD was not used to exclude naïve MBCs, as such any IgM+ sorted could effectively be a naïve B cell expressing both IgD and IgM on its surface.*

6.3. NGS pipeline output.

Prepared BCR libraries were designed to include the entire VDJ region of the heavy chain with some overlap into the constant region of the heavy chain to identify which isotype was used by a given BCR sequence. Each sequence was flanked by adapters to allow for amplification and sequencing by an Illumina MiSeq and barcoded to identify the donor and timepoint it came from. Alternatively, the libraries were sequenced using Sanger sequencing for BCRs coming from single cells. Sequencing reads from the Illumina MiSeq or from Sanger sequencing were processed and quality controlled (QC) via pResto (Vander Heiden et al., 2014) or sangeranalyseR (Chao et al., 2021), then using ChangeO (Gupta et al., 2015) to assign gene usage and infer clonality and germline assignment, as detailed in **Methods 2.13**.

Due to inherent differences in the type and quality of samples between individuals, there were variations in the number of sequences obtained per group and per timepoint. In total, 56,378 unique BCRs were sequenced with 16,725 of these BCRs coming from spike-specific MBCs sorted at the post 3rd vaccine dose timepoint. The numbers of BCR sequences retrieved and which passed QC at the baseline, post 1st, post 2nd and post 3rd vaccine dose bulk timepoints were all broadly equivalent (***Figure 6.3A***). The first three bulk timepoints' BCR repertoire were generated from 10x10^6 PBMCs whilst the post 3rd dose bulk timepoint's BCR repertoire was generated from 1x10^6 PBMCs. This suggests that the accidental thawing of the first three timepoints (baseline, post 1st, and post 2nd vaccine dose) artificially reduced by ten-fold the amount of B cells available, this is in line with the level of viability assessed of the accidentally thawed PBMCs by flow cytometry (5-10%).

As described in **section 1.1.2**, one B cell can give rise to many progeny B cells following sequential rounds of clonal expansion and SHM within the GC, with each progeny B cell having a unique but related BCR sequence within the same clonal family. As such, to better understand B cell repertoire dynamics it is highly relevant to identify within a repertoire which unique BCRs are part of the same clonal lineage. Many strategies can be used to identify members or clones of a distinct clonal lineage, which are generally based on the idea that it is unlikely that two unrelated B cells would share a similar CDRH3 sequence as this part of the antibody that is mostly encoded during VDJ recombination i.e., before clonal expansion (Chen et al., 2010; Gupta et al., 2017; Zhou and Kleinstein, 2019). In my study two or more BCRs were considered

part of the same clonal lineage if they used the same IGHV and IGHJ gene, had the same CDRH3 length and shared 90% amino acid identity within their CDRH3. Using this definition, clonal lineages were assigned for each combination of donor and timepoint (***Figure 6.3B***). In total, 35,623 distinct clonal lineages were identified with 4491 of these lineages being identified as spike-specific as they came from sorted spike-specific MBCs (***Figure 6.3C***). At that point, to identify more putative spike-specific BCRs, all the BCR sequences were re-clustered together across all timepoint/ all donors to identify additional clonally-related BCRs from earlier timepoints which were part of any spike-specific clonal lineages from the post 3rd dose spike-specific clonal lineages.

A

		# of sequences					
		Baseline	Post 1st	Post 2nd	Post 3rd	Post 3rd - spike-specific	TOTAL
HIV-	SARS-CoV-2 naïve	2018	2359	2475	2955	8062	17869
	prior SARS-CoV-2 infection	2233	1977	2442	5486	3683	15821
HIV+	SARS-CoV-2 naïve	2247	2232	3374	1237	1395	10485
	prior SARS-CoV-2 infection	2860	2000	3171	587	3585	12203
	TOTAL	9358	8568	11462	10265	16725	56378

B

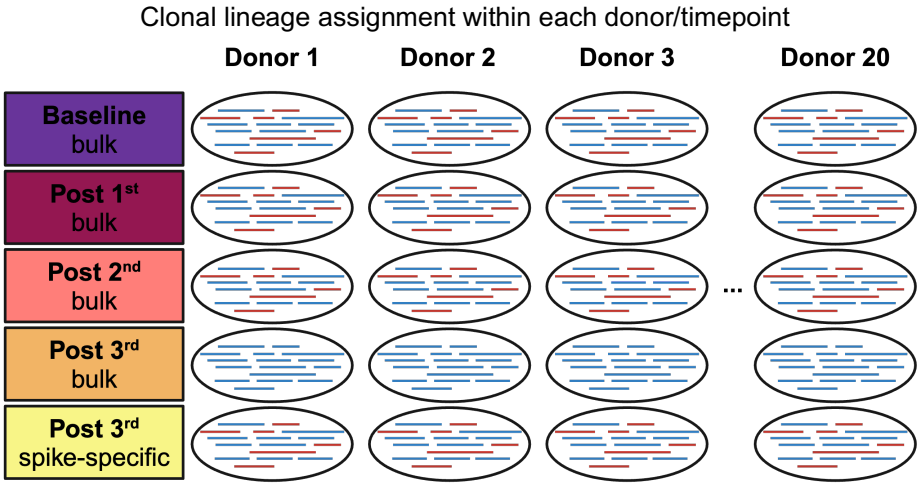

C

		# of clonal lineages					
		Baseline	Post 1st	Post 2nd	Post 3rd	Post 3rd - spike-specific	TOTAL
HIV-	SARS-CoV-2 naïve	1887	2136	2247	1822	1919	10011
	prior SARS-CoV-2 infection	2060	1698	2157	2124	971	9010
HIV+	SARS-CoV-2 naïve	1964	2033	3014	548	544	8103
	prior SARS-CoV-2 infection	2558	1699	2968	217	1057	8499
	TOTAL	8469	7566	10386	4711	4491	35623

Figure 6.3: *Retrieval of BCR sequences and distinct clonal lineages across all timepoints and groups.* ***A.*** *Table showing how many BCR sequences were obtained in each group at each timepoint.* ***B.*** *Clonal lineage assignment strategy to identify clonal lineages within each combination of donor and timepoints.* ***B.*** *Table showing how many distinct clonal lineages are present in each group at each timepoint.*

6.4. Limited clonal overlap between early bulk BCR repertoires and spike-specific BCR was observed at the final timepoint.

To further understand how recall responses were built upon in PLWH, spike-specific BCRs obtained from cells sorted after the 3rd vaccine dose were used here to identify related spike-specific BCRs in the previous timepoints (baseline, post 1st and post 2nd vaccine dose) where no BCR-specificity data could be generated. Conceptually, this works on the assumption that some BCRs in the bulk timepoints belong to the same clonal lineage as a post 3rd vaccine dose spike-specific BCR (***Figure 6.4A***). This is effectively a way to identify a 'needle in a haystack' as the BCRs sequenced from the bulk timepoints could have any antigen-specificity not just spike-specific which from flow analysis only make up 1.5% of total MBCs. The BCR repertoire obtained from PBMCs at any given timepoint should sample circulating B cells which are representative of the overall diversity found in most primary lymphoid tissue (Meng et al., 2017). This approach of looking into bulk repertoires to find additional antigen-specific BCRs using known antigen-specific BCRs from a different timepoint has been successfully used in the past (Galson et al., 2016; Lopes de Assis et al., 2023; Montague et al., 2021; Phad et al., 2022; Turner et al., 2020).

Using this re-clustering strategy (***Figure 6.4A***), 35,421 clonal lineages were identified. Overall, amongst all donors, 342 clonal lineages were shared between at least two timepoints. However, only 54 clonal lineages out of 342 were shared between the post 3rd vaccine dose timepoint and at least one of the bulk timepoints. This means only these 54 clones from the bulk repertoire timepoints can be considered spike-specific. (***Figure 6.4B***). Additionally, this meant that 99% of clonal lineages identified in this study were restricted to one timepoint. Rather than a biological observation, this low number of clonal lineages shared across time is most likely due to the low numbers of BCRs available from the earlier bulk timepoints in the first place. Indeed, many studies which longitudinally investigated the spike-specific BCR repertoire found overlap across several timepoints (Goel et al., 2021b; Lopes de Assis et al., 2023; Paschold et al., 2022; Sokal et al., 2023). In this case, using PBMCs whose diversity has not been artificially lowered due to error or more ideally sorting for spike-specific MBCs at earlier timepoints would have been a far more efficacious strategy to identify clonal lineages shared between timepoints. As so few spike-specific clones were identified in total, clonality with public spike-specific antibodies was considered next.

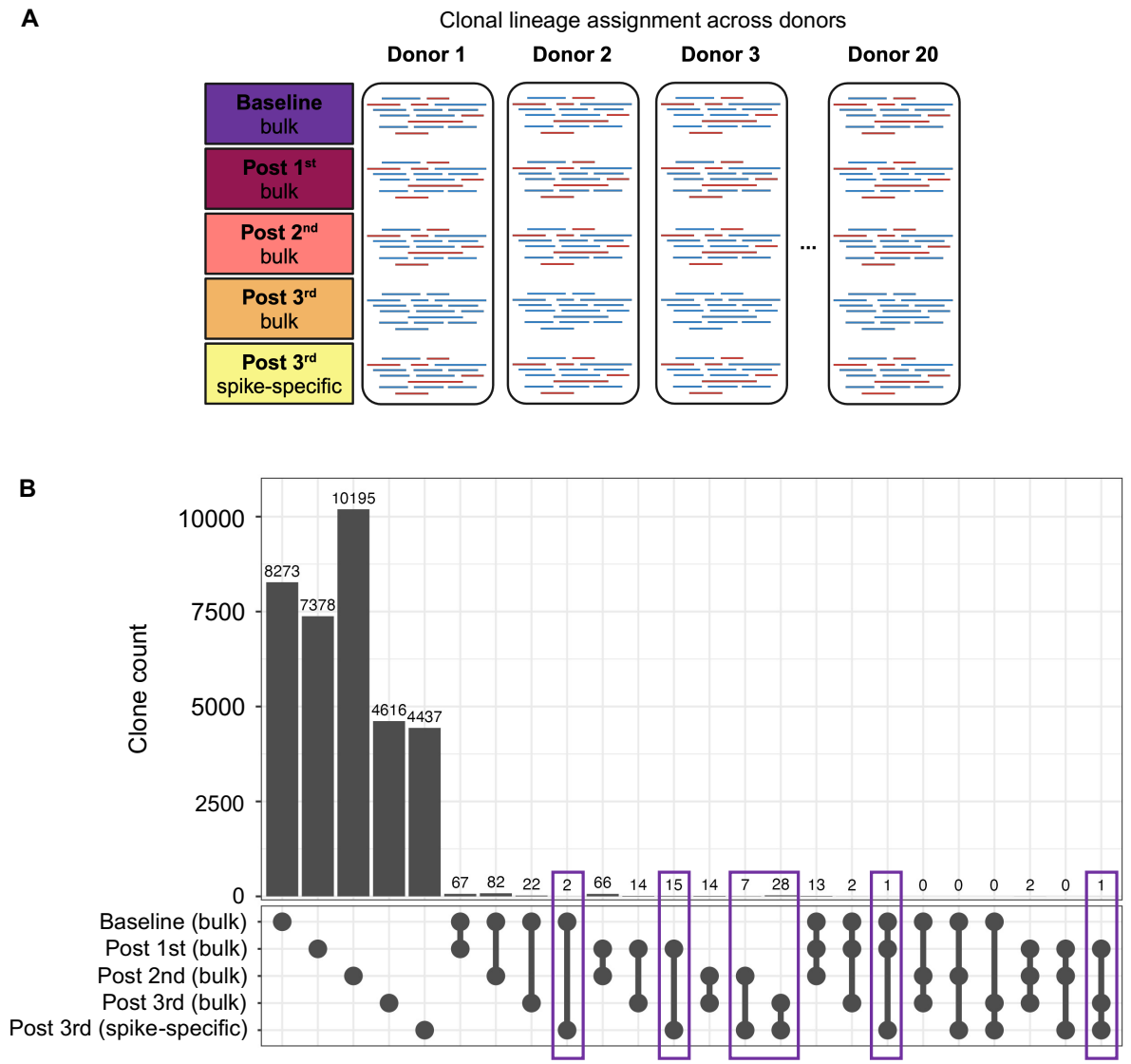

Figure 6.4: *Limited clonal overlap between bulk and spike-specific timepoints*. ***A.*** *Clonal lineage assignment strategy to identify spike-specific BCRs shared between timepoints.* ***B.*** *Upset plot showing how many clonal lineages include clones from different timepoints. Bars represent the number of clonal lineages which overlap between one or more timepoints. Vertical lines connecting points highlight which timepoints have overlapping clonal lineages for any given combination. Highlighted in the purple boxes are timepoint combinations for which at least one clonal lineage includes a clone which is present in the post 3rd vaccine dose spike-specific and includes a clone which is present in a bulk timepoint.*

6.5. Higher frequency of public clonal lineages in HIV-negative controls than in PLWH.

Public antibodies or convergent antibodies have been widely described in the context of SARS-CoV-2 infection and vaccination (see **section 1.2.7** for more details). To identify more spike-specific BCRs, I used a repository of identified SARS-CoV-2 specific public clones, the CoV-AbDab (Raybould et al., 2021). Any clone and therefore clonal lineage were considered public if it was found in more than one donor in my study. Alternatively, any clonal lineage identified in my study where one of its clones was found to have an exact CDRH3 amino acid match to a known public antibody in the CoV-AbDab was also considered public (***Figure 6.5A***).

This allowed for the identification of 781 spike-specific public clonal lineages in my study data. These were not found uniformly between the different timepoints. Most of the spike-specific public clones (n=731) were found in the post 3rd vaccine dose timepoint, either as part of clones already known to be spike-specific as they were sorted for antigen reactivity or within the bulk repertoire (***Figure 6.5A***). Of note, out of the 258 public clonal lineages identified from bulk sequencing of the SARS-CoV-2 naïve HIV-negative control group after the 3rd vaccine dose (***Figure 6.5A***), 255 of these clonal lineages came from one donor. Inspection of these 255 different clonal lineages did not reveal any pattern that could explain why so many public clonal lineages were identified in this one donor at that timepoint but not in others. Another interesting feature is that 3 public clonal lineages were found in SARS-CoV-2 naïve participants at baseline (***Figure 6.5A***). Of note, these lineages were all substantially mutated, with a median divergence of 5.6% from germline in their IGHV gene compared to 3.2.% across all public spike-specific clones. The significance of this difference in distance to germline is hard to interpret as there were so few instances of public clonal lineages at baseline in the first place. There are two likely explanations as to why spike-specific clonal lineages could be detected before any vaccination/infections. Firstly, these lineages may be cross-reactive for other hCoVs, secondly, that many spike-specific public clones have been described to be very close to germline or naïve configuration (Nielsen et al., 2020; Shrock et al., 2023; Voss et al., 2021). Only one of these lineages (#1018) was identified as public via the CoV-AbDab. The public antibody linked to this lineage 1018 has shown the ability to weakly bind HKU1, SARS-CoV-1 and SARS-CoV-2 (Raybould et al., 2021; Wec et al., 2020)

further highlighting that hCoV-induced antibodies may have participated in the vaccine response of SARS-CoV-2 naïve participants as suggested by other studies of BCR repertoire response post-SARS-CoV-2 vaccination (Amanat et al., 2021; Sokal et al., 2021).

Out of the 4491 clonal lineages identified at the post 3rd dose spike-specific timepoint, only 464 were public (***Figure 6.5B***). This suggests that studies (Kotagiri et al., 2022; Paschold et al., 2022) which identify spike-specific BCRs solely using known public antibodies are missing the vast majority of the spike-specific response which is private. There are also meaningful differences between the public versus private clonal lineages, as seen in ***Figure 6.5C***, public clonal lineages tended to be significantly closer to germline than private clonal lineages.

As the main hypothesis was that HIV may affect the way recall happens, it was hypothesised that public antibody generation and/or selection may be different in PLWH. After the 3rd vaccine dose, there was a non-significant trend towards a higher frequency of public clonal lineages in the repertoire of HIV-negative controls than in the repertoire of PLWH (***Figure 6.5D***). Additionally, the frequency of public clonal lineages was in a similar range between the SARS-CoV-2 naïve and the prior SARS-CoV-2 groups. This suggests that antigenic stimulation by SARS-CoV-2 infection and vaccination can equally result in the development of public antibodies. In general, public antibodies can directly mediate neutralising responses (Chen et al., 2021; Raybould et al., 2021; Robbiani et al., 2020; Yuan et al., 2020) and therefore can provide a spike-specific response which is easily attainable in virtue of being close to germline VDJ configuration. Lower frequencies of the public antibodies in PLWH may consequently reflect an aberrant GC response or selection mechanism. In total, counting the extra clonal lineages which were identified as spike-specific in the bulk post 3rd dose timepoint (as they were either public or shared with the spike-specific sorted BCRs), a total of 4755 distinct spike-specific clonal lineages were identified after the 3rd vaccine dose and were used for the subsequent analyses.

A

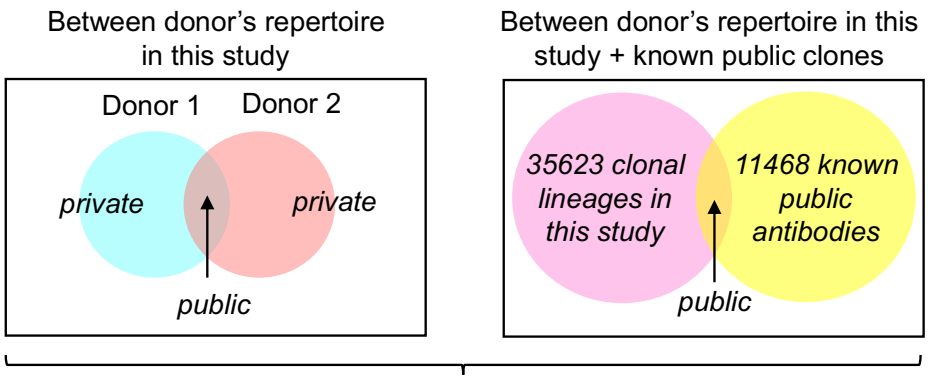

# of spike-specific public clonal lineages

		Baseline bulk	Post 1st bulk	Post 2nd bulk	Post 3rd bulk	Post 3rd spike-specific
HIV-	SARS-CoV-2 naïve	2	31	0	258*	225
	prior SARS-CoV-2 infection	2	5	1	2	106
HIV+	SARS-CoV-2 naïve	1	2	3	3	39
	prior SARS-CoV-2 infection	1	1	1	4	94

* 255 from one donor

B

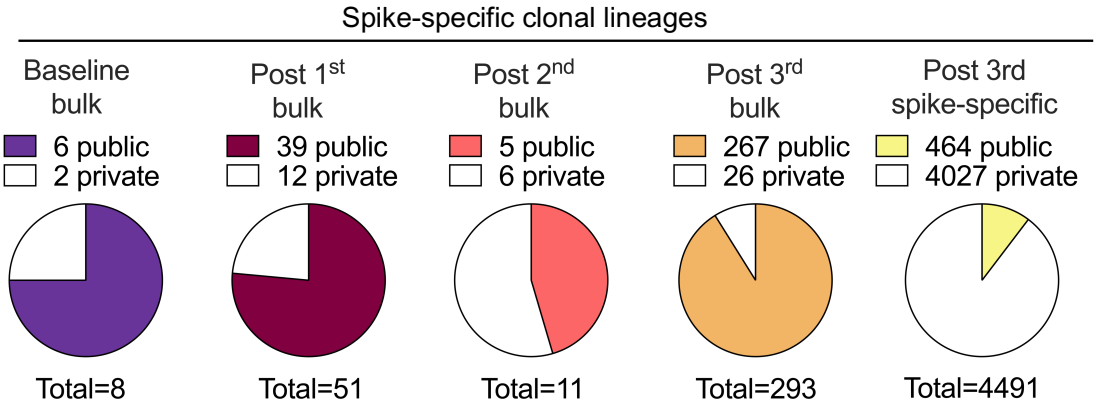

Post 3rd vaccine dose - spike-specific clonal lineages

C

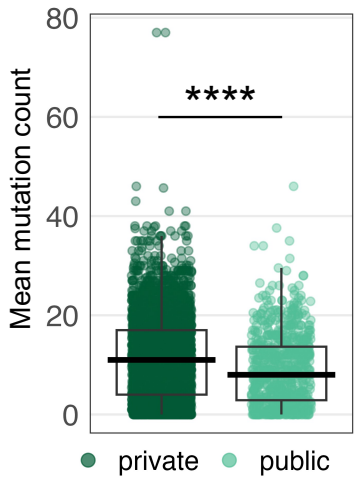

D

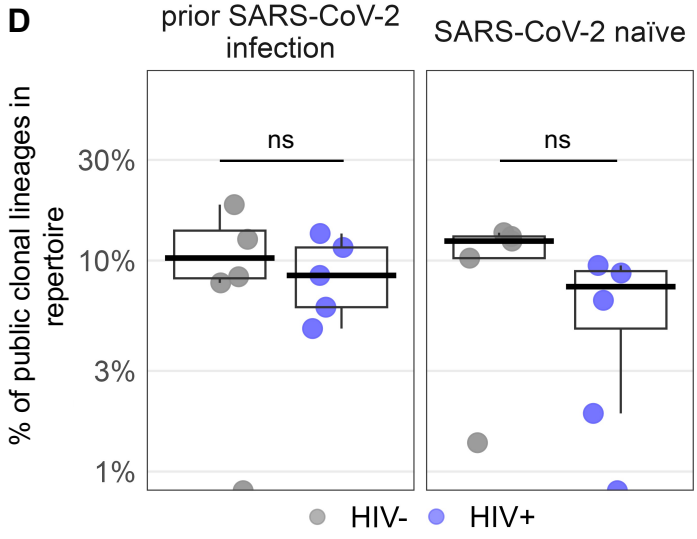

Figure 6.5: *Trend towards higher frequency of public clonotypes in HIV-negative controls than in PLWH.* ***A.*** *Spike-specific public clones were identified either as any clone found in >2 donors in this study or using the CoV-AbDab* (Raybould et al., 2021)*. The table illustrates how many spike-specific public clones were identified at each timepoint for each group based on HIV status and prior history of SARS-CoV-2 infection.* ***B.*** *Pie chart for each timepoint showing how many spike-specific clonal families were identified as either public or private.* ***C.*** *Mean numbers of mutations (both silent and replacement mutation) were measured in the entire VDJ for each spike-specific clonal lineage after the 3rd vaccine dose, stratified by whether they were private or public.* ***D.*** *Frequency of spike-specific public clones in the repertoire of each donor after the 3rd vaccine dose, stratified by HIV status and prior history of SARS-CoV-2 infection. For C-D, is shown the median for each group. Statistical test: MWU.*

6.6. PLWH participants included for BCR sequencing have normalised MBC phenotype.

During the sorting of spike-specific MBCs for BCR repertoire sequencing, 10,000 events were captured to understand the overall MBC phenotype of these participants after the 3rd vaccine dose. The previously optimised sorting panel did not include IgD to exclude naïve B cells. Therefore, in this analysis, true class-switched cells were defined as IgG+ as the majority of IgM+ cells recorded would most likely also have expressed IgD and be naïve not MBC. Interestingly, overall, the classical MBC perturbation phenotype seen in **Chapter 5** was not represented with these participants, although there was still a slight trend towards more atypical MBCs in PLWH (***Figure 6.6.2A)*** and this trend may have failed to reach significance given only 10 participants were included in each group or due to the altered flow cytometry panel. For IgM+ B cells, there were also no significant differences in the frequency of the different phenotypes between PLWH and HIV-negative control (***Figure 6.6.2B)***. Finally, as seen in ***Figure 5.4.3A*** there was no difference in isotype usage between PLWH and HIV-negative controls at the global B cell level. It was not possible to assess isotype usage within the spike-specific population to recapitulate (or not) the findings from ***Figure 5.4.3B***. The participants in this sub-study were less representative of the wider cohort in terms of MBC output overall. As the primary purpose of this experiment was to sort antigen-specific MBCs rather than phenotyping, I then went on to measure more discrete features of these participants' BCR repertoire.

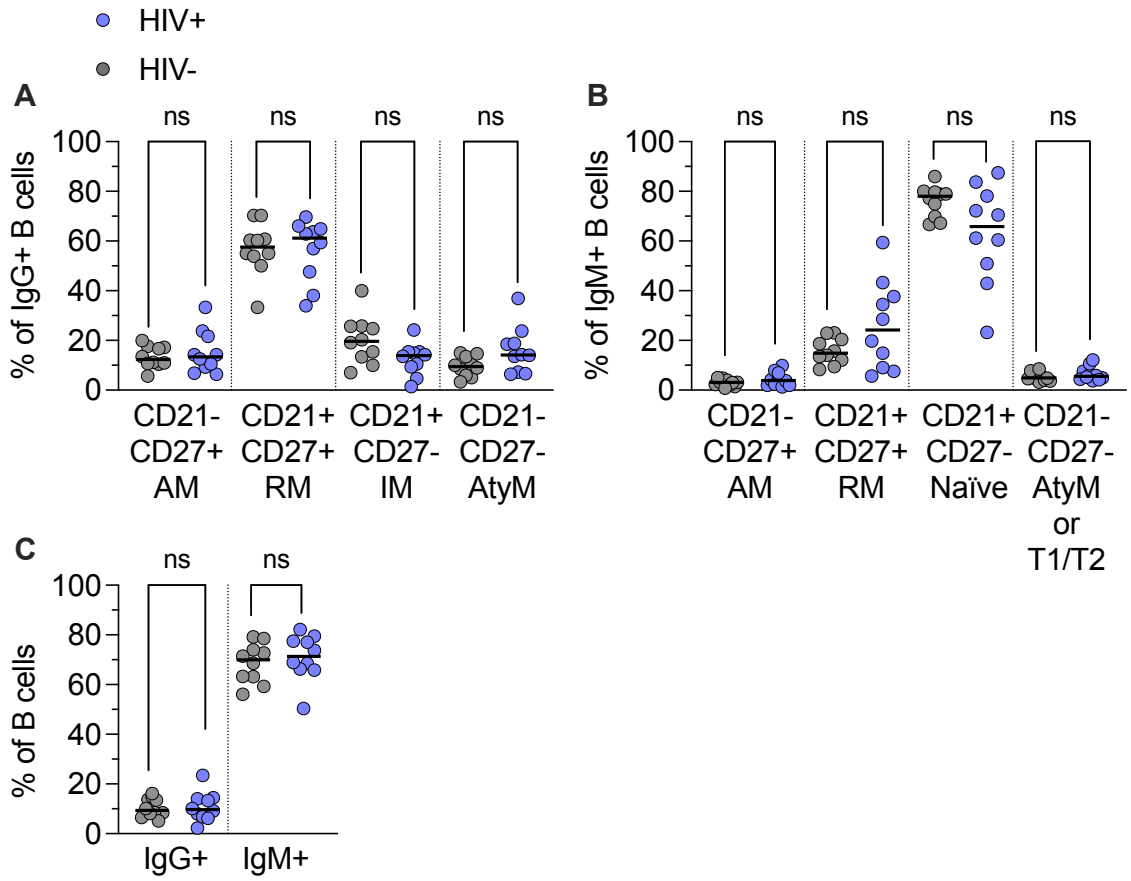

Figure 6.6: *PLWH participants included for BCR sequencing have normalised MBC phenotype.* ***A.*** *Frequency of each MBCs subset as a % of the parent population, CD19+ IgG+ or* ***B.*** *CD19+ IgM+: CD21- CD27+ activated MBCs (AM), CD21+ CD27+ resting MBCs (RM), CD21+ CD27- intermediate MBCs (IM)/naïve B cells and CD21- CD27- atypical MBCs (AtyM)/Transitional T1/T2 B cells in the participants included for BCR sequencing after the 3rd vaccine dose, stratified by HIV status.* ***C.*** *Frequency of different isotypes in CD19+ B cells in the participants included for BCR sequencing after the 3rd vaccine dose, stratified by HIV status. For A-C, is shown the median for each group. Statistical test: MWU.*

6.7. V gene usage differs between spike-specific clones and non-specific clones.

To first characterise the BCR repertoire of PLWH and HIV-negative controls after vaccination their V gene usage was assessed. V gene usage was weighted by considering usage per clonal lineage within a given donor's repertoire using the countGenes function within the alakazam package (Gupta et al., 2015).

As described in **section 1.1.5**, the most commonly used V gene family in humans is IGHV3 and the most commonly used IGHV3 gene is IGHV3-23 (Brezinschek et al., 1995; Volpe and Kepler, 2008). Indeed, the most prevalent IGHV for the four bulk timepoints was IGHV3-23 (***Figure 6.7.1A***). On the other hand, spike-specific clonal lineages from the post 3rd vaccine dose timepoint had a preferential usage of other V genes like IGHV1-69 and IGHV3-30 over IGHV3-23 (***Figure 6.7.1A***) This is also the case for public clonal lineages which preferentially used IGHV1-69, IGHV3-30, IGHV1-18 and IGHV1-46 (***Figure 6.7.2B***). Favoured usage of these specific V genes has been widely reported in the SARS-CoV-2 BCR repertoire literature (see **section 1.2.7**). Overall, there was no clear difference in the usage of the different V gene families according to HIV status or prior history of SARS-CoV-2 infection, although a small increase in IGHV3 usage was seen in SARS-CoV-2 naïve PLWH compared to SARS-CoV-2 naïve PLWH (***Figure 6.7.2***).

Differential V usage in the SARS-CoV-2 spike-specific response can be explained by the idea that different V genes will provide slightly different backbones which may pose different constraints on the antibody shape, directly impacting the spatial relationship between the CDRH3 (which directs most of the binding) and the epitope on the target antigen (Fernández-Quintero et al., 2020; Shrock et al., 2023). No BCRs using IGHV2 were identified, this was because the primers used to amplify VDJs were based on the standard set of primers for human monoclonal antibody cloning (Tiller et al., 2008) which was then found to not be able to successfully amplify most IGHV2 genes (Kreer et al., 2020; Tiller et al., 2008). As discussed in **section 1.1.5**, IGHV2 is one of the more rarely used V gene families and therefore this oversight is probably not significant in the context of these results. Altogether, IGHV usage is only one aspect of the antibody response, more discrete measures are needed to understand the dynamics of the BCR repertoire.

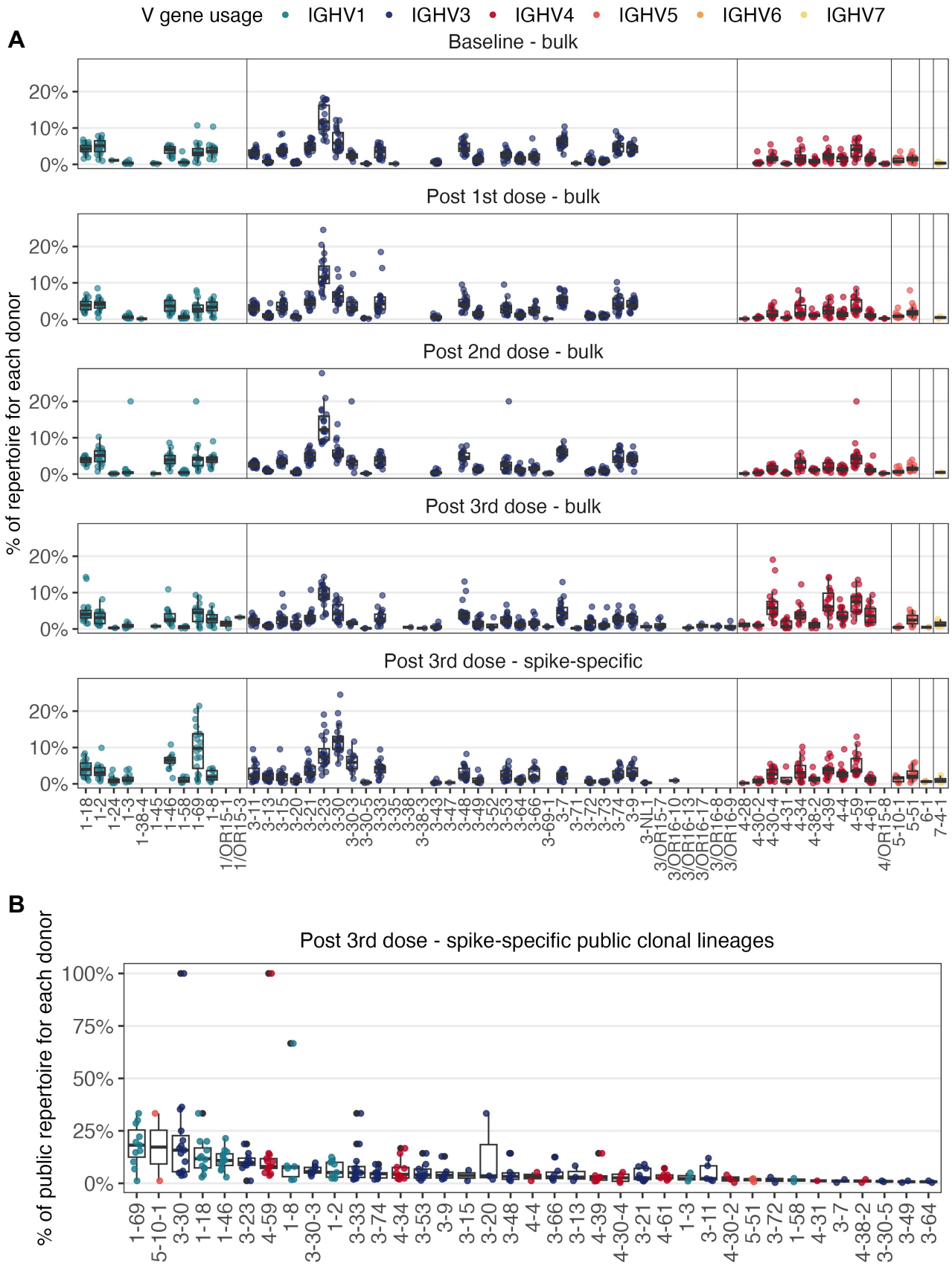
A
V gene usage
IGHV1
IGHV3
IGHV4
IGHV5
IGHV6
IGHV7
Baseline - bulk
Post 1st dose - bulk
Post 2nd dose - bulk
Post 3rd dose - bulk
Post 3rd dose - spike-specific
% of repertoire for each donor
20%
10%
0%
1-18
1-2
1-24
1-3
1-38-4
1-45
1-46
1-58
1-69
1-8
1/OR15-1
1/OR15-3
3-11
3-13
3-15
3-20
3-21
3-23
3-30
3-30-3
3-30-5
3-33
3-35
3-38
3-38-3
3-43
3-47
3-48
3-49
3-52
3-53
3-64
3-66
3-69-1
3-7
3-71
3-72
3-73
3-74
3-9
3-NL1
3/OR15-7
3/OR16-10
3/OR16-13
3/OR16-17
3/OR16-8
3/OR16-9
4-28
4-30-2
4-30-4
4-31
4-34
4-38-2
4-39
4-4
4-59
4-61
4/OR15-8
5-10-1
5-51
6-1
7-4-1
B
Post 3rd dose - spike-specific public clonal lineages
% of public repertoire for each donor
100%
75%
50%
25%
0%
1-69
5-10-1
3-30
1-18
1-46
3-23
4-59
1-8
3-30-3
1-2
3-33
3-74
4-34
3-53
3-9
3-15
3-20
3-48
4-4
3-66
3-13
4-39
4-30-4
3-21
4-61
1-3
3-11
4-30-2
5-51
3-72
1-58
4-31
3-7
4-38-2
3-30-5
3-49
3-64

Figure 6.7.1: *V gene usage differs between spike-specific BCRs and non-specific BCRs.* ***A.*** *Percentage of clonal families within a donor's repertoire using a given IGHV gene, stratified by timepoint.* ***B.*** *Percentage of spike-specific public clones within a donor's repertoire using a given IGHV gene after the 3rd vaccine dose, ranked by usage. Gene usage is coloured by V gene family. For A-B, the median is shown for each V gene.*

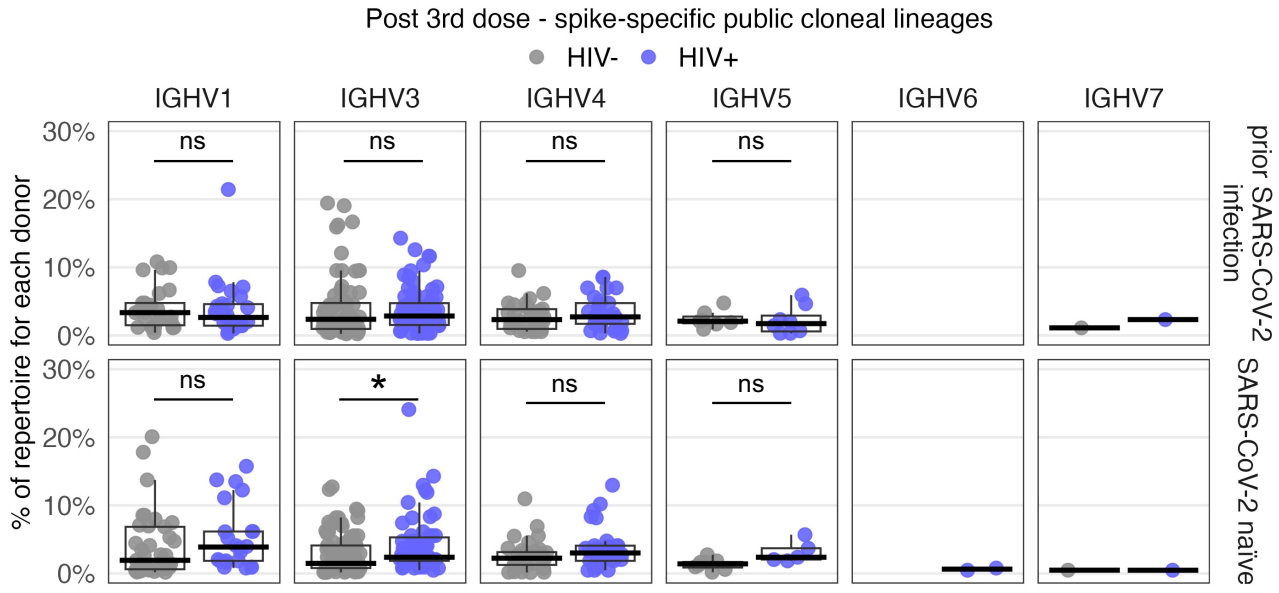

Figure 6.7.2: *PLWH and HIV-negative controls have the same V gene usage in their spike-specific BCR repertoire.* *Percentage of clonal families within a donor's repertoire using a given V gene family, stratified by HIV status and prior history of SARS-CoV-2 infection. The median is shown for each group. Statistical test: MWU.*

6.8. Aberrant somatic hypermutation in PLWH.

To assess potential differences in affinity maturation after the 3rd vaccine dose, levels of SHM were measured using the observedMutations function of alakazam, which counts the number of mutations found in the entire VDJ compared to germline. Mutation counts were reported as the mean number of mutations found in a given clonal lineage.

In the non-spike-specific post 3rd vaccine dose repertoire (***Figure 6.8A***), levels of SHM in IgG+ BCRs were equivalent between SARS-CoV-2 naïve PLWH and HIV-negative controls whilst SHM was slightly elevated in PLWH with prior SARS-CoV-2 infection compared to their HIV-negative counterparts. In the bulk post 3rd vaccine dose dry pellets, no IgM+ BCRs were amplified therefore it was not possible to assess the background level of SHM in the IgM+ BCRs of PLWH. I next focused on the level of SHM in spike-specific clonal lineages identified either by antigen sorting or by close relation to known public spike-reactive BCRs. SARS-CoV-2 naïve PLWH had a significantly higher mutation count in their spike-specific IgG+ BCRs but a significantly lower mutation count in their spike-specific IgM+ BCRs than HIV-negative controls. On the other hand, PLWH with prior SARS-CoV-2 infection also had significantly higher numbers of mutations in their spike-specific IgG+, albeit to a lower extent than the SARS-CoV-2 naïve group, and in their IgM+ BCR (***Figure 6.8B***). In the context of the lower levels of spike-specific IgG+ MBCs seen in ***Figure 5.4.3*** with an overall lower serological response in PLWH still present the 3rd vaccine dose this suggests that the higher levels of SHM in IgG+ BCRs in SARS-CoV-2 naïve PLWH may not be beneficial. This observation was also a departure from equivalence across the non-specific BCR repertoires between the two SARS-CoV-2 naïve groups (***Figure 6.8A***). Here, in spike-specific BCRs, PLWH may over-focus on producing a few highly affinity maturated IgG+ BCRs which may not actually have neutralising activity, explaining how this counter-intuitive observation could result in an inadequate neutralising response compared to HIV-negative controls. In contrast, the lower level of mutation in IgG+ BCRs of HIV-negative controls may be spread across multiple different BCRs with a higher proportion of neutralising clones. Overall, this data highlights that more SHM doesn't fully guarantee a better serological response in the context of SARS-CoV-2 vaccination, and it is therefore important to consider the diversity of the response at the repertoire level and which clones are/aren't neutralising.

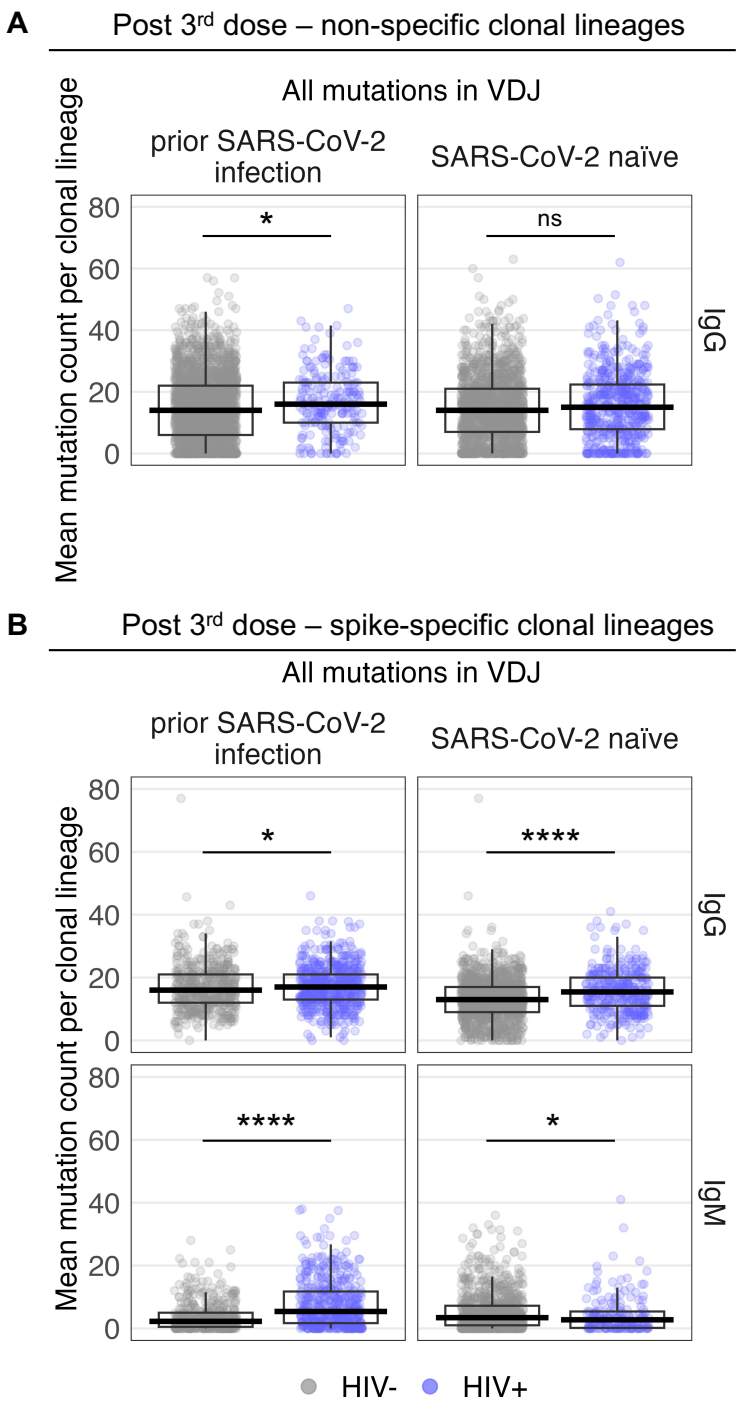

Figure 6.8: *Aberrant somatic hypermutation in PLWH. Mean numbers of mutations (both silent and replacement mutation) were measured in the entire VDJ for each* ***A.*** *non-specific clonal lineage and* ***B.*** *spike-specific clonal lineages after the 3rd vaccine dose, stratified by isotype usage and HIV status and prior history of SARS-CoV-2 infection. For A and B is shown the median for each group. Statistical test: MWU.*

6.9. Lower levels of repertoire diversity in the spike-specific repertoire of SARS-CoV-2 naïve PLWH.

As previously observed there was a difference in the amount of IgG and IgM used in the spike-specific compartment of PLWH at a cell surface phenotype level (**Chapter 5**) coupled with the aberrant SHM seen in the previous section, I hypothesised that the BCR repertoire of PLWH may be less diverse. An important aspect of a given BCR repertoire is its diversity i.e., how many different clonal lineages are present in the repertoire and how many members does each clonal lineage has. Several measures of diversity have been proposed to quantify repertoire diversity each giving different weight to the number and the size of distinct clonal lineage within an individual's repertoire (see **Methods section 2.13.4**).

The most crude measure of diversity can be seen in how many distinct clonal lineages make up the repertoire. Here, the frequency of each clonal lineage is given as how many clones are found in a given lineage compared to how many clones are found in the entire spike-specific repertoire of a given donor. For spike-specific clones after the 3rd vaccine dose, each clonal lineage, which used either IgG or IgM, contributed on average to a significantly larger proportion of the overall spike-specific BCR repertoire of SARS-CoV-2 naïve PLWH than SARS-CoV-2 naïve HIV-negative controls (***Figure 6.9A***). Effectively, this means that in SARS-CoV-2 naïve individuals the spike-specific repertoire of HIV-negative controls was made up of more distinct clonal lineages than that of PLWH. For both PLWH and HIV-negative controls with prior SARS-CoV-2 infection there was no difference in the contribution of IgG and IgM clonal lineages to the overall spike-specific repertoire (***Figure 6.9A***). As the effect on diversity was similar for IgG and IgM BCRs, all clonal lineages regardless of isotype usage were grouped for the next analysis. It is difficult to decide what diversity should look like in a BCR repertoire. Is a truly diverse repertoire an even repertoire i.e., each clonal lineage has a similar number of clones or is a truly diverse repertoire one where a maximal number of clonal lineages are present, regardless of their potential difference in size? To try to capture these different BCR repertoire architectures, a diversity profile based on Hill's index can be used (Greiff et al., 2015; Hill, 1973). With each q value increasing, more and more weight is given to larger clonal lineages in their contribution to the overall diversity. Using this method the diversity profiles were equivalent for the prior SARS-CoV-2 infection HIV-negative controls and PLWH

groups (***Figure 6.9B***). On the other hand, there was a marked difference in the diversity profile of the two SARS-CoV-2 naïve groups where the HIV-negative control group repertoires were more diverse than those of the PLWH group (***Figure 6.9C***). When considering diversity in each participant's repertoire individually, there was a non-significant trend towards lower Shannon and Simpson indexes for SARS-CoV-2 naïve PLWH compared to their HIV-negative counterparts (***Figure 6.9D-E***). Again, significance was hard to reach as each group only comprised five donors.

Overall, the lower diversity seen in the SARS-CoV-2 naïve PLWH group but not in PLWH with prior SARS-CoV-2 infection fits with the serology data from **Chapter 4** where PLWH with prior SARS-CoV-2 achieved far greater binding and neutralisation than SARS-CoV-2 naïve PLWH. In these PLWH with a history of SARS-CoV-2, the lack of adequate diversity in the spike-specific BCR repertoire of PLWH was potentially compensated by a highly immunogenic stimulus in the form of a SARS-CoV-2 infection enabling a more diverse response despite any intrinsic immune limitations imposed by living with HIV.

Post 3rd dose – spike-specific clonal lineages

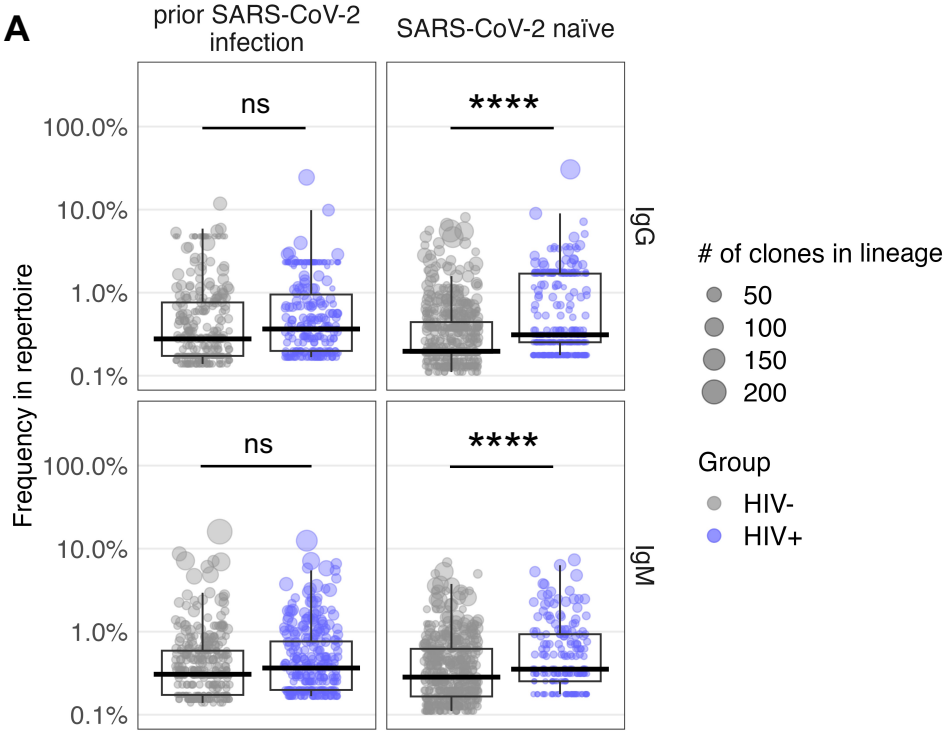

Post 3rd dose – spike-specific clonal lineages (all isotypes)

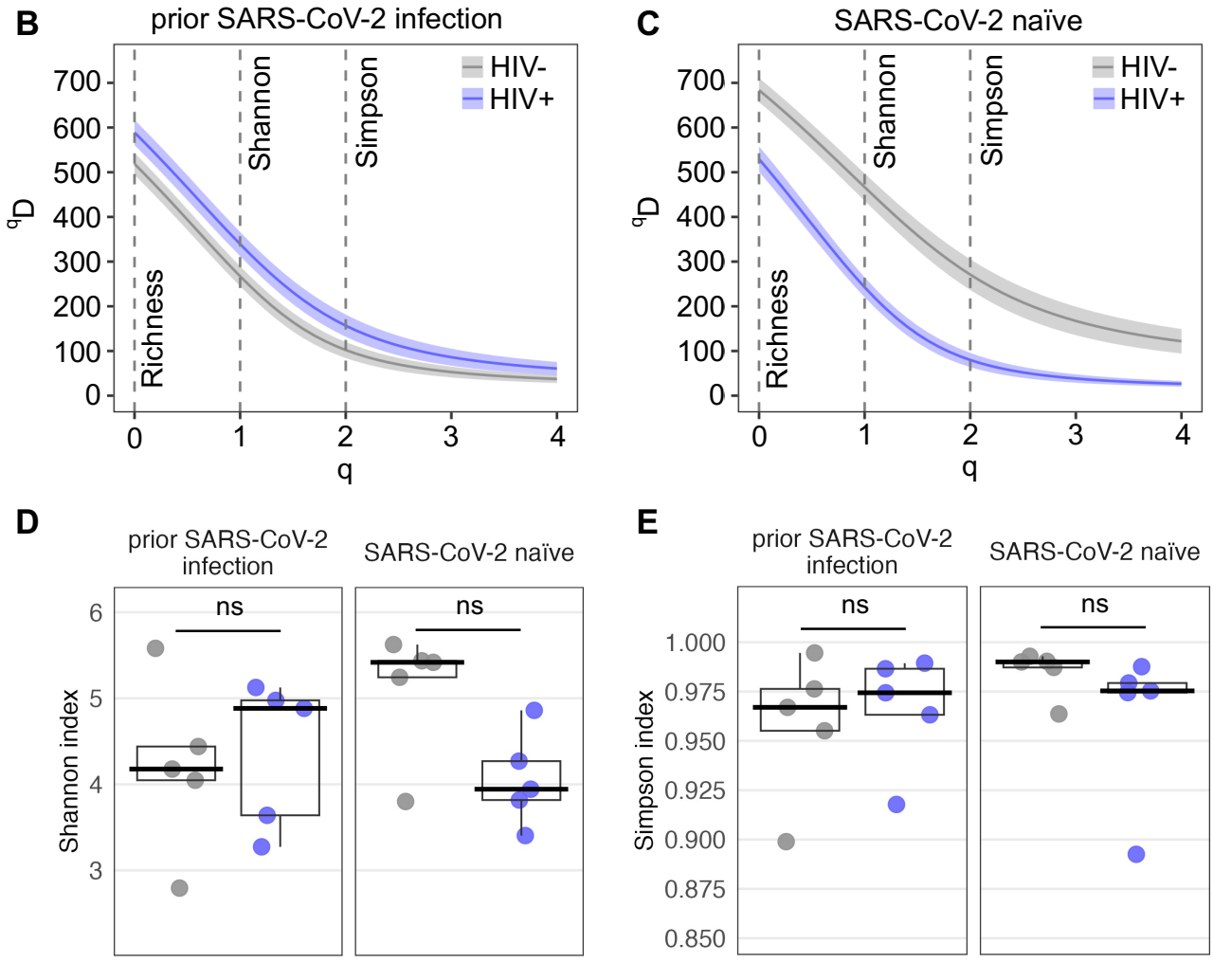

Figure 6.9: *Lower levels of diversity in SARS-CoV-2 naïve PLWH.* ***A.*** *Frequency in repertoire for each spike-specific clonal lineages after the 3rd vaccine dose, stratified by isotype usage and HIV status and prior history of SARS-CoV-2 infection.* ***B.*** *Diversity profile using Hill's index calculated using the alphaDiversity function of alakazam, for the prior SARS-CoV-2 infection group or* ***C.*** *the SARS-CoV-2 naïve group.* ***D.*** *Shannon index value and* ***E.*** *Simpson index value for each donor in each group. For A and D-E is shown the median for each group. For C-D, each group was randomly sub-sampled to include the same number of BCR sequences to account for differences in sequencing depth as advised by* (Gupta et al., 2015; Stern et al., 2014)***.*** *The diversity curve was then calculated using 500 bootstrap replicates. The shaded portion of the curve represents the 95% confidence interval. Statistical test: MWU for A and D-E. To account for differences in the size of the groups for A, which is important when measuring diversity, statistical tests were calculated after 10 random repeated sampling which included 150 clonal lineages per group each time.*

6.10. Higher diversity is associated with better serological output.

Finally, to understand how clonality, diversity or affinity maturation affected serological output, a correlation matrix using Spearman's correlation coefficient was calculated between the different serological parameters (binding and neutralisation titres), frequency of the different MBC phenotype and the different repertoire features (***Figure 6.10***). As the binding and neutralising data obtained considered mostly IgG (S1-specific binding titres are IgG only, neutralisation for PLWH was measured post IgG purification), only clonal lineages which were spike-specific and used IgG were considered as I hypothesised that these clonal lineages are the most likely to have an impact on the IgG serological response assessed.

Both diversity indexes (Simpson and Shannon) were significantly and strongly associated with higher S1-specific IgG binding titres (Spearman's r=0.681 and r=0.722 respectively). Similarly, the Simpson and Shannon indexes had a significant albeit more modest association with higher WT neutralising titres (r=0.525 and r=0.559 respectively) and Omicron BA.1 neutralising titres (r=0.574 and r=0.617 respectively) at the same timepoint. Additionally, higher frequency of public antibodies was also weakly associated with higher neutralising titres against WT and Omicron BA.1 (r=0.475 and 0.444 respectively). Overall, this reflects that regardless of HIV status, greater spike-specific BCR repertoire diversity is associated with stronger binding and neutralising titres. Interestingly, despite their lower level of SHM, the development of public antibodies was also positively associated with a neutralising response which suggests that in the context of SARS-CoV-2, the right kind of germline-like antibodies may be enough for an effective serological response. Of note, all these significant correlations between higher diversity indexes and higher serological output parameters became non-significant when considering IgM+ clonal lineages only. This suggests that the lack of diversity in the IgG compartment of PLWH is what is driving the lower serological response measured in **Chapter 4**.

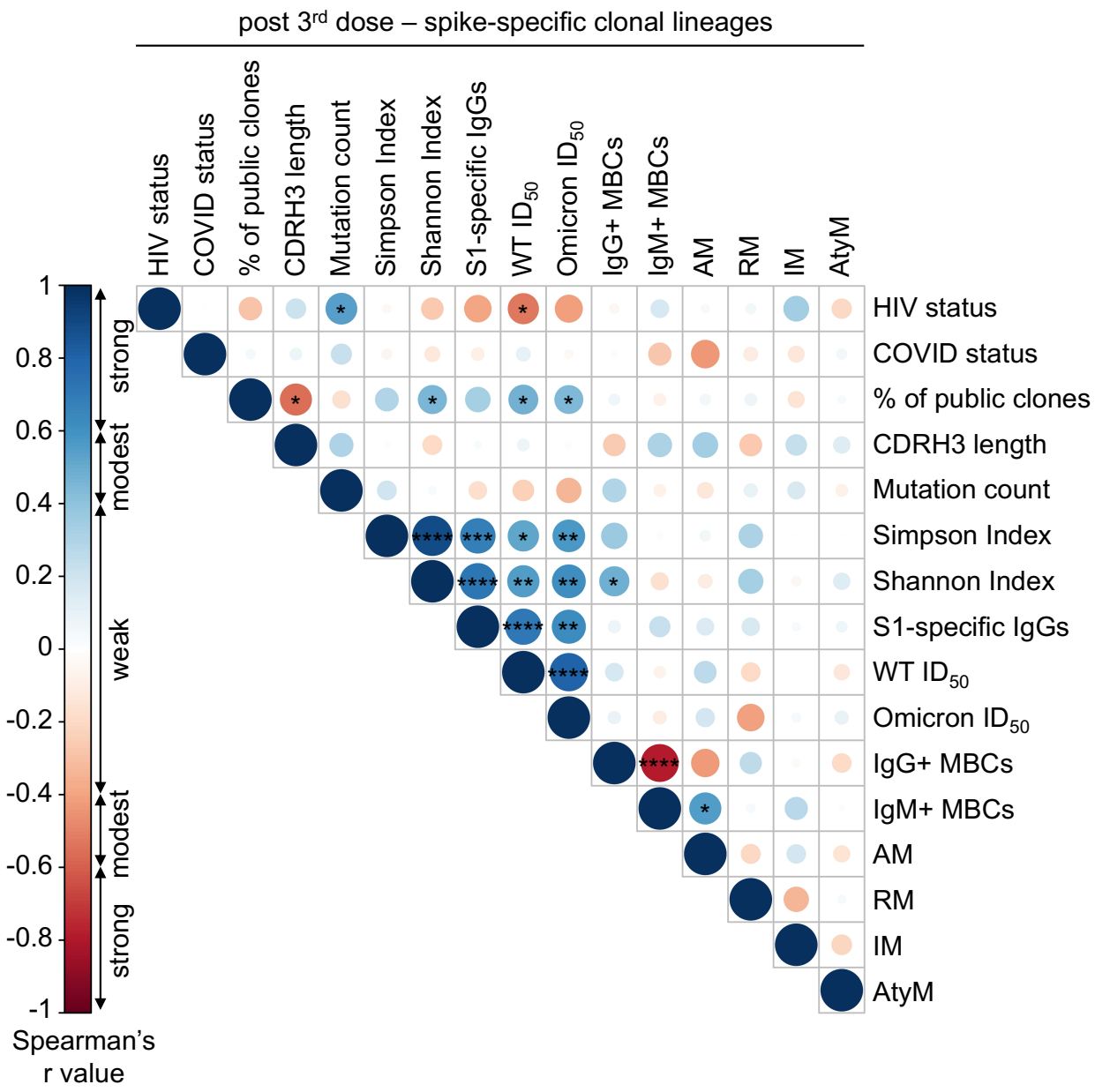

Figure 6.10: *Higher diversity is associated with better serological output. Correlation matrix between BCR-related parameters (frequency of public clones in the repertoire, mean CDRH3 length, mean mutation count for the entire VDJ, Simpson and Shannon index per donor) for spike-specific IgG+ clonal lineages only and serological (S1-specific IgG titres, WT and Omicron BA.1 neutralising titres) and MBC output (frequency of IgG+ or IgM+ MBCs, activated (AM), resting (RM), intermediate (IM) or atypical (AtyM) MBCs) after the 3rd vaccine dose. The size and colour of the circles correspond to the strength of the correlation (Spearman's r value), for any significant correlation, the p-value is indicated (p>0.05 = *; >0.01 = **; >0.001 = *** and >0.0001 = ****).*

6.11. Discussion

Lack of appropriate diversity in PLWH underpins lower serological response.

The results in this chapter show that it was possible to generate high-quality BCR repertoire data using bulk and spike-specific sorted cells. However, there was little overlap between the clonal lineages found at different bulk timepoints and those known to be spike-specific due to antigen-specific sorting. Ideally, directly sorting spike-specific MBCs from each timepoint would have been the most effective way to assess the spike-specific BCR repertoire after each vaccine dose and how many of the spike-specific clones were recalled and further affinity matured after each dose. Unfortunately, there were no viable cells available at these timepoints, only RNA to amplify bulk BCRs. In total, 4755 distinct spike-specific clonal lineages were identified after the 3rd vaccine dose using direct spike-specific sorting or because these lineages were part of known public clones. However, there was a trend towards lower frequencies of public antibodies in the repertoire of PLWH. When considering V gene usage, there was no difference between PLWH and HIV-negative controls. After the 3rd vaccine dose, the spike-specific IgG+ BCR repertoire of SARS-CoV-2 naïve PLWH was hypermutated whilst the IgM+ BCR repertoire was hypomutated. Additionally, the spike-specific BCR repertoire of SARS-CoV-2 naïve PLWH was less diverse than the repertoire of HIV-negative controls. This lack of diversity was lessened in PLWH with prior SARS-CoV-2 infection. Overall focussed affinity maturation in non-neutralising clones and lower spike-specific diversity may explain the serological defects in PLWH observed in the previous chapters that will now be discussed in detail.

As seen throughout the COVID-19 literature, public antibodies are part of a normal response to SARS-CoV-2 infection and vaccination and can be neutralising. Although most of the spike-specific BCR repertoire is private after the 3rd vaccine dose, public antibodies, which are less mutated than private antibodies, may reflect an efficient spike-specific response which requires fewer rounds of affinity maturation. The fact that PLWH may be less able to make these public antibodies or at least to make them in lower proportions likely reflects a fundamental issue in the formation of GC response in PLWH. Moreover, this may be underpinned by the overall increase in SHM in the IgG+ spike-specific BCR of SARS-CoV-2 naïve PLWH and to a lesser extent, PLWH with prior SARS-CoV-2 infection. In this case, the GC reaction of PLWH may directly overlook the generation of more germline-like antibodies for the production of highly

mutated BCRs. Counterintuitively there is no guarantee that highly mutated BCRs are the most adept at virus neutralisation because as per all antigens they are selected in the GC for better binding, not neutralisation. Certain epitopes on viral entry proteins such as spike can be non-neutralising regardless of the degree of affinity that they are targeted with (Sokal et al., 2022), and such non-neutralising epitopes are actually the majority target in the SARS-CoV-2 antibody response (Brouwer et al., 2020). It can be hypothesised that these highly mutated IgG+ may all target similar epitopes which in turn may be either be non-neutralising or are easily evaded by emerging variants. Effectively, the response is overly-focused on making hyper-mutated IgG BCRs from clones that were initially selected which prevents PLWH from attaining the level of diversity/breadth seen in HIV-negative controls. This may represent a negative cycle where more SHM is seen in PLWH because they keep re-recruiting the same IgG+ BCRs for further rounds of GC maturation, rather than new naïve B cells which in turn would have lower levels of SHM and should be the main GC recruits in recall/secondary GCs (Mesin et al., 2020). In the context of SARS-CoV-2, this may mean that the preferential recruitment of pre-existing clones which underpins some of the imprinting effect seen with WT vs Omicron (Sokal et al., 2023; Yisimayi et al., 2023) is exacerbated in PLWH. PLWH recruit too few naïve clones compared to HIV-negative controls, their BCR response therefore stays focused on their primary exposure against WT which would explain the lower levels of breadth seen against Omicron BA.1 in ***Chapter 4***. On the other hand, the IgM+ spike-specific BCRs of SARS-CoV-2 naïve PLWH were less mutated than those of their HIV-negative counterparts. In light of the data from ***Chapter 5***, where PLWH made more IgM+ spike-specific MBC than HIV-negative counterparts, this suggests that IgM+ MBCs may exit the GC early without attaining adequate levels of affinity maturation or class-switching to IgG to better support serum neutralisation hence the over-abundance of these cells in PLWH. The IgM MBCs that are therefore left to be recalled are of poorer quality but likely higher affinity than naïve B cells. This means these IgM MBCs should get more T cell help and potentially become ASCs making inadequate IgM antibodies of poor quality when it would be more advantageous to focus on engaging naïve B cells which could lead to a more diverse response.

In PLWH with prior SARS-CoV-2 infection, SHM was higher across both IgG and IgM BCRs than in HIV-negative controls. In this scenario, the elevated SHM may also

reflect the same mechanism of over-focusing on hyper-mature IgG+ BCR in PLWH without any clear benefit. In all cases, it is difficult to pick apart what level of SHM/which clones arise due to the differences in severity of infection versus those triggered by vaccination versus systemic alterations in antibody selection due to the impact of chronic but suppressed HIV. The impact of HIV on the non-HIV-specific BCR repertoire is poorly understood. According to Roskin et al. (2020), there is no difference in the level of SHM for IgM BCRs between viraemic PLWH and HIV-negative controls whilst IgG BCRs were found to be slightly less mutated than in HIV-negative controls. This was partially recovered for PLWH who started ART early (Planchais et al., 2023). Another aspect to consider is that the BCR repertoire in the blood is representative of what exists and what has been produced throughout each exposure to infection and vaccination, not just the most recent spike exposure. It can therefore be hypothesised that these hyper-mutated IgM and IgG seen in PLWH with prior SARS-CoV-2 infection may have been generated after the initial SARS-CoV-2 infection. Studies of post-COVID-19 infection have suggested that hyper-mutation of the spike-specific BCR repertoire was associated with more severe disease (Kuri-Cervantes et al., 2020; Schultheiß et al., 2020; Woodruff et al., 2022), however, this could be explained by more severe disease associating with higher antigen burden which would driver greater SHM.

Finally, different measures of diversity showed that the overall spike-specific repertoire of SARS-CoV-2 naïve PLWH was less diverse than the spike-specific repertoire of SARS-CoV-2 naïve HIV-negative controls. In my study, greater repertoire diversity in IgG+ BCR was associated with better binding and neutralising response overall and higher frequencies of public clones. Altogether, this builds towards a model (***Figure 6.11***) where global B cell disruption affects what kind of MBCs are able to participate in de novo and recall GC reactions. In PLWH following vaccination alone, I propose this leads to over-representation of IgM+ spike-specific MBCs which may be of poorer quality. In the meantime, the few IgG+ spike-specific MBCs that are generated are focused towards continued affinity maturation rather than additional recruitment of IgG clones allowing the diversification of the IgG response, potentially at the expense of making a more useful response which would include public antibodies. In turn, this leads to a spike-specific IgG binding and neutralising response which is less able to target the right epitopes that are key for a resilient polyclonal response in PLWH. There

is potentially more neutralisation capacity in the IgM compartment for PLWH but this is limited at the systemic level as IgM+ antibodies only represent ~5% of the circulating antibodies in the blood (Gasser et al., 2021).

A final unanswered question is how exactly does the global MBC dysfunction seen in PLWH alter how *de novo* and recall GC spike-specific responses proceed? Crucially whether the presence of altered peripheral MBC subsets is directly leading to altered GCs or if it is the consequence of HIV-driven changes in GC perturbation in PLWH? More mechanistic studies of the role of over-represented MBCs subtypes in PLWH like atypical MBCs are needed to understand their function and their output at the BCR level. These studies should ideally recapitulate the GC formation and the potential perturbation of GC architecture seen in chronic HIV, as discussed in **section 1.3.2**.

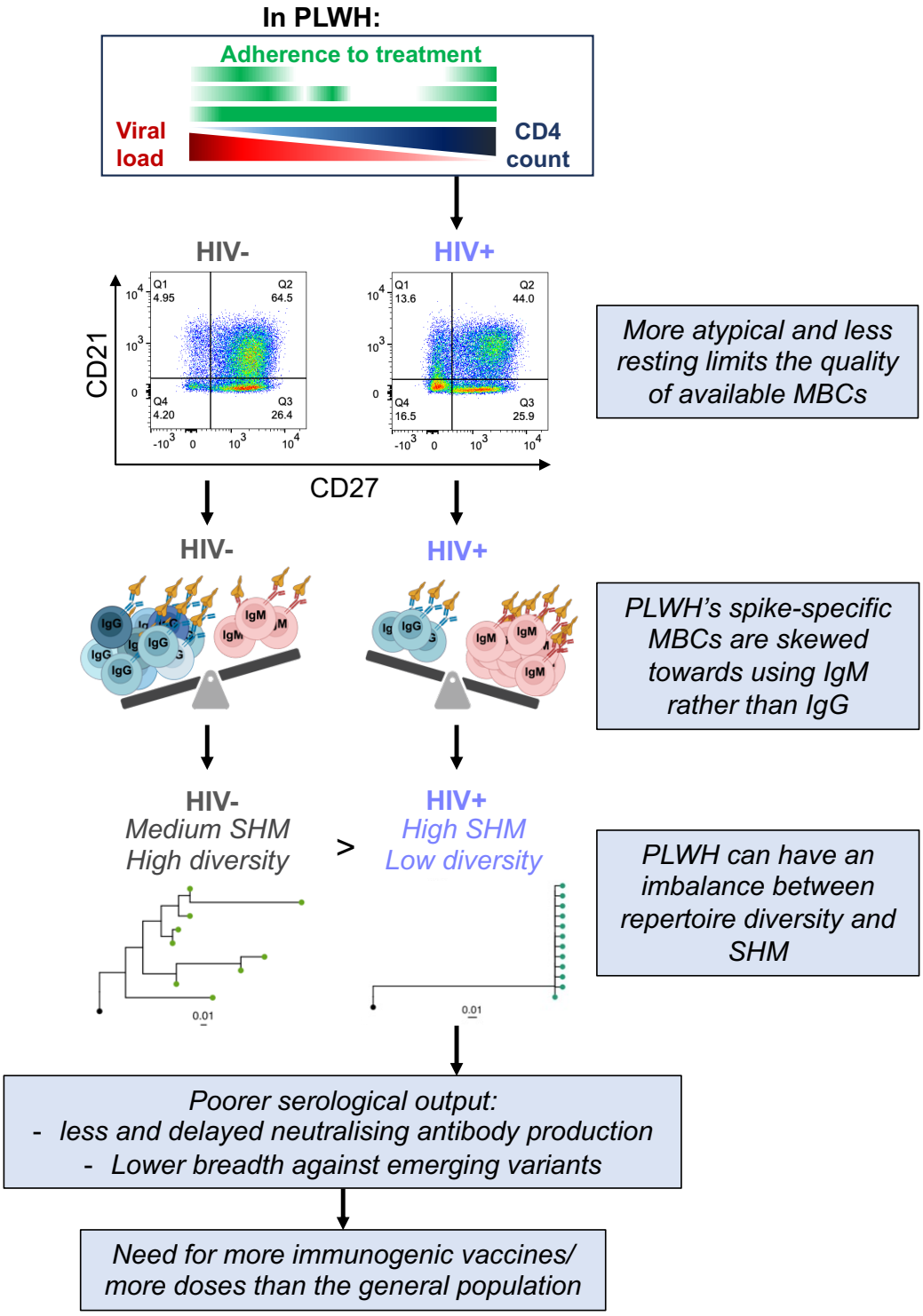

Figure 6.11: *Model of the impact of chronic HIV infection on the MBC and BCR repertoire. PLWH with have different clinal histories which may lead to ongoing B cell dysfunction. This then limits the pool of MBCs which are able to participate in GC reactions after infection/vaccination. PLWHs are therefore less able to make a diverse BCR response and hyper-focus on making a few highly mutated BCRs which underpins lower serological responses.*

Limitations and future work.

Due to technical difficulties adapting the bulk NGS library preparation method developed by Peter Thomas for the requirement of this project, UMIs were not included in the original bulk sequencing strategy (used to sequence baseline, post 1st, post 2nd and spike-specific post 3rd vaccine dose timepoints) and only used to amplify BCRs from the post 3rd vaccine dose bulk timepoint. UMIs help correct for any sequencing artefacts during NGS sequencing (Aird et al., 2011). To correct for the lack of UMIs, a more stringent criterion for the number of reads that could proceed in the pipeline was applied. However, this means that the non-UMI timepoints may include artificially generated mutations which cannot be corrected.

Due to the low viability of the cells due to the LN2 failure, there was no possibility to sort for spike-specific MBC at the earlier timepoints. This also reduced the amount of bulk BCRs that could be recovered in these vials as described in **section 6.4**. Access to more viable cells would have allowed to better understand how the spike-specific BCR repertoire was built over time in PLWH versus HIV-negative controls. Additionally, it would have been interesting to select different SARS-CoV-2 naïve PLWH donors. For example, equal numbers of participants with a delayed or a standard neutralisation profile (as seen in **Chapter 4)** to assess how these different neutralisation phenotypes were reflected in the BCR repertoire over time but insufficient numbers of these participants donated PBMCs after the 3rd vaccine. Another limitation of this work is that there was no information on the phenotype of the spike-specific sorted cells. Again, this would have required a greater number of PBMCs to start with to obtain meaningful numbers of spike-specific B cells with the different MBC phenotypes. However, it could be key to understanding which, if any, MBC subtype is lacking in diversity and is responsible for the inadequate affinity maturation seen in PLWH.

The sequencing strategy used here focused on sequencing the heavy chains of BCRs only as this is sufficient to address most BCR dynamics. Large-scale production and characterisation of monoclonal antibodies based on paired heavy and light chains can be very time-consuming and expensive. However, it would be interesting to produce and map the epitope of the highly mutated IgG+ spike-specific BCRs seen in SARS-CoV-2 naïve PLWH to measure if they are either worse, or at least less broad, in terms

of neutralisation capacity than IgG+ BCR from these same individuals with a lower level of SHM or those sorted from HIV-negative individuals. Alternatively, using an Omicron-spike bait alongside the WT-spike bait used here to sort Omicron-specific versus WT-specific MBCs could have provided more information on the breadth of the BCR sequenced.

Conclusions

Whilst the end of **Chapter 5** highlighted there is an issue with class-switching in PLWH: more IgM+ spike-specific MBCs, here the data highlights there is an added issue with the affinity maturation of the spike-specific response for PLWH. Moreover, the BCR repertoire of PLWH is of lower diversity. Potentially the issue with recall in PLWH is two-fold: overabundant IgM+ MBCs are of poor quality whilst the relatively few IgG+ MBCs are highly mutated towards less useful, most likely non-neutralising epitopes and the IgG+ MBC repertoire is not sufficiently diverse. This leads to the poorer and less resilient serological responses seen in **Chapter 4**. However, these issues were reduced with an immunogenic enough antigenic stimulation for the PLWH with prior SARS-CoV-2 infection hinting that B cell dysfunction can be overcome with the right stimuli.

7. Discussion

7.1. Results summary.

The aim of this thesis was to investigate the impact of chronic HIV on the ability of PLWH to form an effective antibody and B cell response to other infections and vaccination. In this thesis, these were SARS-CoV-2 infection and vaccination. In the first result chapter (***Chapter 3***), binding and neutralisation responses were measured in a cohort of convalescent PLWH and HIV-negative controls who had been infected with a novel pathogen, SARS-CoV-2, during the first wave of the COVID-19 pandemic. Binding and neutralising responses were of similar quality and quantity between PLWH and HIV-negative controls. This was the first piece of evidence that a SARS-CoV-2 infection provides a highly immunogenic stimulus that can overcome HIV-mediated dysfunction. This data represented the first characterisation of the antibody response of PLWH post-SARS-CoV-2 infection (Alrubayyi et al., 2021).

Then, I processed and analysed samples from a cohort of 111 PLWH and 64 HIV-negative controls which were sampled around sequential SARS-CoV-2 vaccination doses to measure their antibody response (**Chapter 4**) and their memory B cell response (**Chapter 5**). Immediately, it became clear that (a) prior SARS-CoV-2 conferred an advantage after each dose compared to the SARS-CoV-2 naïve group regardless of HIV status, and (b) that PLWH on average made lower binding and neutralising antibody responses after each dose. Indeed, even when prior SARS-CoV-2 infection provided a boost for post-vaccination response, most PLWH consistently made quantitatively and qualitatively lower responses than their HIV-negative control counterparts. This was particularly pronounced in the SARS-CoV-2 naïve PLWH, who were more likely to have a delayed neutralising response after the 1st vaccine dose compared to HIV-negative controls and generally needed at least three doses to be able to neutralise antigenically diverse variants like Omicron BA.1. This delayed neutralising responses was particularly associated with both lower frequencies of spike-specific MBCs and the MBC dysfunction characteristic of PLWH (more atypical and less resting MBCs). After three doses of SARS-CoV-2 vaccination, despite a lower serological output still being observed in PLWH, there was no difference in the frequency of spike-specific MBCs. However, there was still a marked increase in the level of atypical global MBCs and a decrease in resting global MBCs, which was less

pronounced in the spike-specific compartment. Moreover, PLWH had an excess of spike-specific MBCs using IgM rather than IgG compared to HIV-negative controls. This suggests that the serology defect observed in PLWH may be partly due to the lower level of IgG+ spike-specific MBCs. The insights gained from the serological and MBC characterisation of post-SARS-CoV-2 vaccination responses presented in this thesis were also published (Touizer et al., 2021, 2023).

Finally, to further investigate the impact of MBC dysfunction on effective antibody repertoire generation, the vaccine cohort was sub-sampled to 5 participants in each group to longitudinally assess changes in BCR repertoire after each dose of SARS-CoV-2 vaccination (**Chapter 6**). This revealed that paradoxically, the IgG+ BCRs of SARS-CoV-2 naïve PLWH are more mutated compared to those of HIV-negative controls whilst the IgM+ BCRs of SARS-CoV-2 naïve PLWH are less mutated than HIV-negative controls. Additionally, the BCR repertoire of SARS-CoV-2 naïve PLWH was less clonally diverse, which was associated with negative serological outcomes. This implies that the overabundant IgM+ spike-specific MBCs in PLWH have not undergone enough affinity maturation whilst the more highly mutated IgG+ BCRs in this group are not diverse enough in terms of different clonal families, which is likely compounded by a focus within spike-specific antibodies on non-neutralising epitopes (Brouwer et al., 2020). Altogether, the vaccination response in many PLWH is limited by residual MBC dysfunction which associates with aberrant affinity maturation and inadequate diversity of the spike-specific BCR repertoire thus leading to the poorer serological outcomes observed. However, without mechanistic studies on the function of atypical MBCs, it is unclear how the perturbation in the global phenotype affects the antigen-specific responses and the changes in BCR repertoire observed. Importantly, the findings above consider the majority response across PLWH as compared to HIV-negative controls but there was a high degree of heterogeneity in the antibody and B cell response, with some individuals having a B cell/antibody/repertoire profile more similar to that of most HIV-negative participants. The causes of this heterogeneity are not fully understood but would be of great interest to unpick to help promote better responses in those whose antibody responses underperform.

7.2. Overall limitations of this thesis.

Due to the presence of ART in PLWH's plasma, as described in **section 3.5**, the IgG in PLWH had to be purified to remove any ART that interfered with the neutralisation assay. A consequence of IgG purification is that the IgM portion of PLWH's plasma was not considered when measuring neutralisation. In the blood, IgM-specific for S1 is only measurable post-infection during a relatively short timeframe post-infection (Cohen et al., 2021; Dan et al., 2021; Long et al., 2020; Seow et al., 2020). Notably, IgM constitutes normally only 5% of total serum and so is unlikely to make a major contribution to serum neutralisation. However, IgM antibodies isolated from convalescent individuals have been shown to contribute to the neutralising response (Gasser et al., 2021; Hale et al., 2022). Moreover, in the context of vaccination, the contribution of IgM to the spike-specific binding response is hard to measure as IgM make a smaller portion of the post-vaccination response (unpublished data from our lab, (Faliti et al., 2023)) due to the lack of mucosal-mediated responses. This is also supported by the dominance of IgG+ spike-specific MBCs over IgM+ in healthy participants post-vaccination (Goel et al., 2021b, 2021a; Kardava et al., 2022; Turner et al., 2021). As IgM+ spike-specific MBCs are over-represented in the peripheral blood of PLWH it raises the question of whether IgM could in this population play a more important role in the binding and neutralising response of PLWH after SARS-CoV-2 vaccination than in HIV-negative controls. As the serological output of PLWH was poorer than those of HIV-negative controls, this suggests that IgM+ spike-specific MBCs, which failed to class-switch to IgG, provide a spike-specific IgM response which is functionally inferior to IgG although this could not be measured. The IgG purification strategy precluded assessment of the IgM component, for this using a live virus neutralisation assay would have allowed to circumvent this issue and more confidently assess the entire IgG and IgM neutralisation contribution. I hypothesise that this potentially neutralising IgM response only represents a minor part of the useful serum response and is likely not as resilient to novel variants.

More generally, an important limitation of the work presented in this thesis is the lack of longitudinal sampling. As the post-vaccination cohort was a mix of cross-sectional and longitudinal sampling, not enough participants from the different groups came back at each timepoints to properly compare the impact of each dose across timepoints. Additionally, that many PBMC samples were lost in the LN2 failure entirely

precluded the analysis of the MBC response of participants across timepoints. These samples would have been key to understanding if the heterogeneity in serological responses (e.g., delayed versus standard neutralisers) seen in the PLWH cohort was underpinned by inherent differences in MBC dysfunction at baseline and how it evolved with subsequent doses. This loss of these samples also prevented the efficient identification of spike-specific BCRs at the baseline, post 1st and 2nd vaccine dose (as discussed in **section 6.4**), which therefore did not allow to fully address if and how the recall of previously generated BCRs was defective in PLWH.

7.3. Perspectives.

7.3.1. What is needed for a working B cell response?

The relationship between a working antibody and MBC response and the amount of CD4 T cells seems to be strictly linear in extreme cases of immune dysfunction as seen in our case report where a participant with advanced HIV failed to respond to two doses of SARS-CoV-2 vaccination (see **section 4.2** and (Touizer et al., 2021)). Based on this and the wider literature I propose that once a certain threshold of CD4 T cells is reached, there is enough T cell help for B cell to achieve their normal function. In the case of chronic HIV infection, ART treatment helps to recover higher CD4 counts normally to above >350 cells/μL. What level of CD4 T cell is recovered depends on the initial viral set point and timing of treatment, and this is also true of the reversal of B cell disruption seen in early HIV (discussed in **section 1.3.2-5**). Despite that, some PLWH on ART with CD4 count >350 cells/μL in this study still struggled to make equivalent titres to HIV-negative controls. Effectively, B cells in some PLWH appear unable to respond appropriately whereas other PLWHs produce similar serological output to HIV-negative controls. I hypothesise that this is likely due to differences in the initial 'viral insult' experienced which has a direct effect on the phenotype and function of MBC. Potentially, in individuals who do not fully reconstitute their B cell function this 'viral insult' leads to persistent inflammation and ISG induction (Moir et al., 2004), loss of GC architecture (Schacker et al., 2002) or inadequate T cell help (Moir et al., 2003) leading to some form of permanent immune scarring. This all leads to a vicious cycle of more inflammation, excess of atypical MBCs, inadequate antibody feedback and in turn lower serological outcomes. As discussed in **section 1.3.2-5**, early intervention to prevent HIV viraemia with early to immediate initiation of ART can

successfully reduce or prevent B and T-cell mediated dysfunction. However, some PLWH did not start ART immediately after diagnosis (i.e., most PLWH diagnosed before 2015 in the UK) or where the diagnosis was substantially later than acquisition. This applies to the bulk of a cohort like the one studied in this thesis who were predominantly diagnosed before 2015. For these individuals, a better understanding of the development and accumulation of atypical MBCs and their function could lead to potential immunomodulation strategies to 'bring back' PLWH's MBC towards homeostasis.

7.3.2. What does an effective clonal response look like?

This thesis provides important insights into the impact of HIV on the immune response of PLWH against other pathogens. The results shown here dissect the specific immune response to either SARS-CoV-2 infection or vaccination, but I hypothesise that the fundamental insights of this thesis can be applied to most other infections/vaccinations. This is highly relevant for PLWH as untreated HIV historically leads to uncommon opportunistic infections and they generally make lower responses seen after vaccination against influenza, tetanus or hepatitis B in PLWH (discussed in **section 1.3.6**). It may be that the serological responses to other vaccines in PLWH are similarly associated with persistent MBC phenotype perturbation, lower levels of IgG+ antigen-specific MBCs or restricted BCR repertoire diversity as seen in SARS-CoV-2-vaccination. Alternatively, these may be general features of the B cell response of PLWH to 'less' immunogenic stimuli whereas 'more' immunogenic like SARS-CoV-2 infection can overcome underlying B cell dysfunction. Here, SARS-Cov-2 infection is more immunogenic as it allows the generation of B and T cell responses to other proteins than spike and the triggering of the innate response which can then potentiate the adaptive response and generally delivers a higher 'dose' of antigen than a discrete vaccination. Evidence into the response of PLWH post-viral infection is scarce although in line with the results of this thesis, there is a study showing that post-H1N1 pdm09 influenza infection responses were similar between PLWH and HIV-negative controls (Sansonetti et al., 2014) whilst responses of PLWH were inferior post-vaccination to same strain (Cagigi et al., 2014; George et al., 2015). When considering differences in immunogenicity in vaccination only, the attenuated Mpox vaccine, which still contains the viral genome and many viral proteins, PLWH made similar serological

responses to HIV-negative controls and did not have global MBC perturbation (unpublished data from our lab, (Mazzotta et al., 2024)), further highlighting the capacity of some PLWH in making adequate response with the right immunogenic stimulus.

Even if further studies could elucidate how common these features are in the post-vaccination response of PLWH, it would be hard to assess when looking at a given infection or vaccination which will be immunogenic enough to overcome any underlying B cell dysfunction. Invariably, first encounter matters: in this study infection primed PLWH to be able to overcome some level of inherent HIV-mediated immune dysfunction. The problem was that the secondary encounter with antigen via vaccination was not enough. In contrast, most HIV-negative controls effectively built upon their primary response via recall or responded *de novo* sufficiently to improve their serological response as recall response should mostly involve naïve B cells (Mesin et al., 2020). In some cases, PLWH produced elevated titres via this recall response to their secondary antigen encounter, but this increase was not equivalent to the improvement seen in HIV-negative controls. Whether infection rather than vaccination as a secondary or tertiary antigen encounter would have overcome the antibody/B cell defects in SARS-CoV-2 naïve PLWH observed is unclear as this cohort did not have sufficient numbers of re-infections to assess the impact of breakthrough infections and no other study published so far has answered this question.

Importantly, a high level of affinity maturation in individual BCRs is not sufficient for an effective clonal response and consequently for a better serological response. For targets that may naturally be harder to recognise such as those recognised by HIV bnAbs, which can involve recessed epitopes and glycans (reviewed in (Griffith and McCoy, 2021)), germline or antibodies with low mutation levels are not enough and extremely high SHM is often necessary. However, this has not been the case for SARS-CoV-2, where successful neutralising antibodies display comparatively lower SHM (Barnes et al., 2020; Brouwer et al., 2020; Pinto et al., 2020; Robbiani et al., 2020; Rogers et al., 2020). Overall, it appears that to neutralise pathogens like SARS-CoV-2, where natural immunity is incredibly successful at clearing infection, achieving high repertoire diversity is much more important than high SHM, whereas for pathogens which are harder to neutralise, like with HIV and bnAbs, achieving high SHM is also essential.

Immune imprinting data for SARS-CoV-2 antibody responses suggests that primary encounter shapes the secondary (and tertiary) responses disproportionately, especially in the case of infection as the primary encounter (Buckner et al., 2022; Reynolds et al., 2021; Röltgen et al., 2022). In light of this, it would be interesting to see if PLWH were subjected to the same imprinting effect and what the impact of this is when a more restricted spike-specific BCR repertoire is generated. As the IgG+ BCR response seen in PLWH is less diverse, this may be a feature of imprinting where highly mutated IgG+ clones get re-recruited to GCs rather than naïve B cells which could theoretically target different epitopes and diversify the BCR repertoire. Overall, my data in PLWH and current reports on the general population (Muecksch et al., 2022; Sokal et al., 2023; Weber et al., 2023; Yisimayi et al., 2023) suggest incremental increases in diversity towards as many neutralising epitopes as possible seem to be the effective path towards the most resilient antibody responses against SARS-CoV-2. It will be of great interest to see how the importance of repertoire diversity varies across different pathogens where there are/aren't germline or antibodies with low mutation levels that can effectively neutralise.

7.3.3. What does this study tell us about the kind of vaccines PLWH and other immunocompromised populations need?

The impact of chronic HIV on the immune system of PLWH has many similarities to the impact of ageing on the immune system of HIV-negative donors, and as such can be considered as a model of premature immune ageing and immunosenescence (Nasi et al., 2017). For example, in a cohort of older individuals (>70 years old), lower neutralising responses were similarly associated with increased levels of atypical MBCs (Ferreira et al., 2023). This is particularly relevant in the UK, where the population of PLWH is ageing which will inevitably compound their risk of lower vaccine response. More generally, although the causes vary, many immune-related diseases lead to a similar B cell phenotype as in PLWH. Insights gained from this cohort can therefore inform vaccine requirements across a wider spectrum of human biology.

Specifically for SARS-CoV-2, there are several approaches to improving vaccine responses in at-risk groups such as other immunocompromised patients and the elderly. First, increasing the variety of immunogens in the vaccine to produce

bivalent/trivalent vaccines (as is now recommended in current vaccination guidelines (JCVI, 2023)) will allow participants to educate their MBC against a wide array of SARS-CoV-2 variants, which can give a head start to vaccine recipients against novel variants whilst limiting immune imprinting. Strategic boosting with temporally relevant antigens may be beneficial to re-educate the immune system of patients who have undergone immune depletion due to chemotherapy or transplantation. Without sequencing the BCRs and epitope mapping the polyclonal responses of PLWH and immunocompromised groups it is difficult to say how well this strategy will diversify their response. A conceptual variant of this strategy is to make a pan-coronavirus vaccine, which would hopefully be variant-proof by targeting conserved regions of spike, for example within S2 (see ***Figure 1.2.2*** and **section 1.2.5**). The major advantage of this would be in controlling SARS-CoV-2 spread and hence new variant generation alongside limiting any emerging new coronavirus, but it could theoretically also prevent hCoV-mediated common cold. Part of such a strategy could be to include a wider range of targets which are not B cell-mediated by adding in T cell-mediated epitopes in the hope of potentiating B-T cell responses. These vaccines may be of interest to patient groups receiving B cell depletion therapy but who still make efficient T cell-specific responses (Zonozi et al., 2023). For PLWH with effective T cell reconstitution, this strategy may help overcome any residual B cell dysfunction although the HIV-mediated loss of TCR diversity (Heather et al., 2015) could limit the efficacy of this strategy. An alternative strategy is to simply give a higher dose or repeated doses to increase the immunogenicity of the vaccines, as is the case with repeated and higher doses of hepatitis B vaccination in PLWH (Chaiwarith et al., 2019; Psevdos et al., 2010). In the UK, updated bivalent vaccines have now been in use for two years for at-risk groups (JCVI, 2023), and they have been shown to improve variant-specific responses in immunocompromised populations (Solera et al., 2023).

A mixed approach of repeated and higher doses, updated to provide immunity against temporally relevant variants which can both induce B and T cell responses is probably the ideal vaccine solution for PLWH and other immunocompromised groups. Additionally, offering vaccination to the general population and not just at-risk groups will benefit the latter by reducing the circulation of SARS-CoV-2. In a more pragmatic manner, the best vaccine is the one that can be easily manufactured, licenced and

distributed, even in resource-poor settings where the population may carry other comorbidities putting them at higher risk of severe COVID-19 disease.

References

Abu-Raddad, L.J., Chemaitelly, H., and Butt, A.A. (2021). Effectiveness of the BNT162b2 Covid-19 Vaccine against the B.1.1.7 and B.1.351 Variants. New England Journal of Medicine *385*, 187–189. https://doi.org/10.1056/NEJMC2104974/SUPPL_FILE/NEJMC2104974_DISCLOSURES.PDF.

Abu-Shmais, A.A., Vukovich, M.J., Wasdin, P.T., Suresh, Y.P., Rush, S.A., Gillespie, R.A., Sankhala, R.S., Choe, M., Joyce, M.G., Kanekiyo, M., et al. (2023). Convergent Sequence Features of Antiviral B Cells. BioRxiv 2023.09.06.556442. https://doi.org/10.1101/2023.09.06.556442.

Aird, D., Ross, M.G., Chen, W.S., Danielsson, M., Fennell, T., Russ, C., Jaffe, D.B., Nusbaum, C., and Gnirke, A. (2011). Analyzing and minimizing PCR amplification bias in Illumina sequencing libraries. Genome Biol *12*, R18. https://doi.org/10.1186/GB-2011-12-2-R18.

Alcaide, M.L., Nogueira, N.F., Salazar, A.S., Montgomerie, E.K., Rodriguez, V.J., Raccamarich, P.D., Barreto, I.T., McGaugh, A., Sharkey, M.E., Mantero, A.M., et al. (2022). A Longitudinal Analysis of SARS-CoV-2 Antibody Responses Among People With HIV. Front Med (Lausanne) *9*, 1–8. https://doi.org/10.3389/fmed.2022.768138.

Aldridge, R.W., Lewer, D., Beale, S., Johnson, A.M., Zambon, M., Hayward, A.C., and Fragaszy, E. (2020). Seasonality and immunity to laboratory-confirmed seasonal coronaviruses (HCoV-NL63, HCoV-OC43, and HCoV-229E): results from the Flu Watch cohort study. Wellcome Open Res *5*, 52. https://doi.org/10.12688/wellcomeopenres.15812.1.

Algaissi, A., Alfaleh, M.A., Hala, S., Abujamel, T.S., Alamri, S.S., Almahboub, S.A., Alluhaybi, K.A., Hobani, H.I., Alsulaiman, R.M., AlHarbi, R.H., et al. (2020). SARS-CoV-2 S1 and N-based serological assays reveal rapid seroconversion and induction of specific antibody response in COVID-19 patients. Sci Rep *10*. https://doi.org/10.1038/S41598-020-73491-5.

Alharbi, N.K., Qasim, I., Almasoud, A., Aljami, H.A., Alenazi, M.W., Alhafufi, A., Aldibasi, O.S., Hashem, A.M., Kasem, S., Albrahim, R., et al. (2019). Humoral

Immunogenicity and Efficacy of a Single Dose of ChAdOx1 MERS Vaccine Candidate in Dromedary Camels. Sci Rep *9*, 1–11. https://doi.org/10.1038/s41598-019-52730-4.

Allen, C.D.C., Ansel, K.M., Low, C., Lesley, R., Tamamura, H., Fujii, N., and Cyster, J.G. (2004). Germinal center dark and light zone organization is mediated by CXCR4 and CXCR5. Nat Immunol *5*, 943–952. https://doi.org/10.1038/ni1100.

Allers, K., Hütter, G., Hofmann, J., Loddenkemper, C., Rieger, K., Thiel, E., and Schneider, T. (2011). Evidence for the cure of HIV infection by CCR5Δ32/Δ32 stem cell transplantation. Blood *117*, 2791–2799. https://doi.org/10.1182/BLOOD-2010-09-309591.

Allman, D., Li, J., and Hardy, R.R. (1999). Commitment to the B Lymphoid Lineage Occurs before DH-JH Recombination. J Exp Med *189*, 735. https://doi.org/10.1084/JEM.189.4.735.

Allman, D., Wilmore, J.R., and Gaudette, B.T. (2019). The Continuing Story of T-cell Independent Antibodies. Immunol Rev *288*, 128. https://doi.org/10.1111/IMR.12754.

Alrubayyi, A., Gea-Mallorquí, E., Touizer, E., Hameiri-Bowen, D., Kopycinski, J., Charlton, B., Fisher-Pearson, N., Muir, L., Rosa, A., Roustan, C., et al. (2021). Characterization of humoral and SARS-CoV-2 specific T cell responses in people living with HIV. Nat Commun *12*, 1–16. https://doi.org/10.21203/rs.3.rs-309746/v1.

Alsoussi, W.B., Malladi, S.K., Zhou, J.Q., Liu, Z., Ying, B., Kim, W., Schmitz, A.J., Lei, T., Horvath, S.C., Sturtz, A.J., et al. (2023). SARS-CoV-2 Omicron boosting induces de novo B cell response in humans. Nature *617*, 592–598. https://doi.org/10.1038/s41586-023-06025-4.

Amanat, F., Thapa, M., Lei, T., Ahmed, S.M.S., Adelsberg, D.C., Carreño, J.M., Strohmeier, S., Schmitz, A.J., Zafar, S., Zhou, J.Q., et al. (2021). SARS-CoV-2 mRNA vaccination induces functionally diverse antibodies to NTD, RBD, and S2. Cell *184*, 3936-3948.e10. https://doi.org/10.1016/j.cell.2021.06.005.

Amanna, I.J., Carlson, N.E., and Slifka, M.K. (2007). Duration of Humoral Immunity to Common Viral and Vaccine Antigens. New England Journal of Medicine *357*, 1903–1915.

https://doi.org/10.1056/NEJMOA066092/SUPPL_FILE/NEJM_AMANNA_1903SA1.PDF.

Ambegaonkar, A.A., Kwak, K., Sohn, H., Manzella-Lapeira, J., Brzostowski, J., and Pierce, S.K. (2020). Expression of inhibitory receptors by B cells in chronic human infectious diseases restricts responses to membrane-associated antigens. Sci Adv *6*. https://doi.org/10.1126/SCIADV.ABA6493.

Anderson, E.M., Goodwin, E.C., Verma, A., Arevalo, C.P., Bolton, M.J., Weirick, M.E., Gouma, S., McAllister, C.M., Christensen, S.R., Weaver, J.E., et al. (2021). Seasonal human coronavirus antibodies are boosted upon SARS-CoV-2 infection but not associated with protection. Cell *184*, 1858-1864.e10. https://doi.org/10.1016/j.cell.2021.02.010.

Andreano, E., Paciello, I., Piccini, G., Manganaro, N., Pileri, P., Hyseni, I., Leonardi, M., Pantano, E., Abbiento, V., Benincasa, L., et al. (2021). Hybrid immunity improves B cells and antibodies against SARS-CoV-2 variants. Nature *600*, 530–535. https://doi.org/10.1038/s41586-021-04117-7.

Andreano, E., Paciello, I., Marchese, S., Donnici, L., Pierleoni, G., Piccini, G., Manganaro, N., Pantano, E., Abbiento, V., Pileri, P., et al. (2022). Anatomy of Omicron BA.1 and BA.2 neutralizing antibodies in COVID-19 mRNA vaccinees. Nat Commun *13*, 1–8. https://doi.org/10.1038/s41467-022-31115-8.

Antinori, A., Cicalini, S., Meschi, S., Bordoni, V., Lorenzini, P., Vergori, A., Lanini, S., De Pascale, L., Matusali, G., Mariotti, D., et al. (2022). Humoral and Cellular Immune Response Elicited by mRNA Vaccination Against Severe Acute Respiratory Syndrome Coronavirus 2 (SARS-CoV-2) in People Living With Human Immunodeficiency Virus Receiving Antiretroviral Therapy Based on Current CD4 T-Lymphocyte Co. Clinical Infectious Diseases *75*, E552–E563. https://doi.org/10.1093/cid/ciac238.

Ao, L., Lu, T., Cao, Y., Chen, Z., Wang, Y., Li, Z., Ren, X., Xu, P., Peng, M., Chen, M., et al. (2022). Safety and immunogenicity of inactivated SARS-CoV-2 vaccines in people living with HIV. Emerg Microbes Infect *11*, 1126. https://doi.org/10.1080/22221751.2022.2059401.

Atti, A., Insalata, F., Carr, E.J., Otter, A.D., Castillo-Olivares, J., Wu, M., Harvey, R., Howell, M., Chan, A., Lyall, J., et al. (2022). Antibody correlates of protection from

SARS-CoV-2 reinfection prior to vaccination: A nested case-control within the SIREN study. Journal of Infection *85*, 545–556. https://doi.org/10.1016/J.JINF.2022.09.004.

Avelino-Silva, V.I., Miyaji, K.T., Mathias, A., Costa, D.A., De Carvalho Dias, J.Z., Lima, S.B., Simoes, M., Freire, M.S., Caiaffa-Filho, H.H., Hong, M.A., et al. (2016). CD4/CD8 Ratio Predicts Yellow Fever Vaccine-Induced Antibody Titers in Virologically Suppressed HIV-Infected Patients. J Acquir Immune Defic Syndr (1988) *71*, 189–195. https://doi.org/10.1097/QAI.0000000000000845.

Aydillo, T., Rombauts, A., Stadlbauer, D., Aslam, S., Abelenda-Alonso, G., Escalera, A., Amanat, F., Jiang, K., Krammer, F., Carratala, J., et al. (2021). Immunological imprinting of the antibody response in COVID-19 patients. Nat Commun *12*. https://doi.org/10.1038/s41467-021-23977-1.

Azzi, L., Dalla Gasperina, D., Veronesi, G., Shallak, M., Ietto, G., Iovino, D., Baj, A., Gianfagna, F., Maurino, V., Focosi, D., et al. (2022). Mucosal immune response in BNT162b2 COVID-19 vaccine recipients. EBioMedicine *75*, 103788. https://doi.org/10.1016/J.EBIOM.2021.103788/ATTACHMENT/6FF19417-4923-4409-A08A-031D0F1CC704/MMC1.PDF.

Baden, L.R., El Sahly, H.M., Essink, B., Kotloff, K., Frey, S., Novak, R., Diemert, D., Spector, S.A., Rouphael, N., Creech, C.B., et al. (2021). Efficacy and Safety of the mRNA-1273 SARS-CoV-2 Vaccine. New England Journal of Medicine *384*, 403–416. https://doi.org/10.1056/NEJMOA2035389/SUPPL_FILE/NEJMOA2035389_DATA-SHARING.PDF.

Bar, K.J., Tsao, C. yen, Iyer, S.S., Decker, J.M., Yang, Y., Bonsignori, M., Chen, X., Hwang, K.K., Montefiori, D.C., Liao, H.X., et al. (2012). Early Low-Titer Neutralizing Antibodies Impede HIV-1 Replication and Select for Virus Escape. PLoS Pathog *8*, 1002721. https://doi.org/10.1371/JOURNAL.PPAT.1002721.

Barnes, C.O., Jette, C.A., Abernathy, M.E., Dam, K.M.A., Esswein, S.R., Gristick, H.B., Malyutin, A.G., Sharaf, N.G., Huey-Tubman, K.E., Lee, Y.E., et al. (2020). SARS-CoV-2 neutralizing antibody structures inform therapeutic strategies. Nature *588*, 682–687. https://doi.org/10.1038/s41586-020-2852-1.

Barnes, E., Goodyear, C.S., Willicombe, M., Gaskell, C., Siebert, S., I de Silva, T., Murray, S.M., Rea, D., Snowden, J.A., Carroll, M., et al. (2023). SARS-CoV-2-specific

immune responses and clinical outcomes after COVID-19 vaccination in patients with immune-suppressive disease. Nat Med *29*, 1760–1774. https://doi.org/10.1038/s41591-023-02414-4.

Barré-Sinoussi, F., Chermann, J.C., Rey, F., Nugeyre, M.T., Chamaret, S., Gruest, J., Dauguet, C., Axler-Blin, C., Vézinet-Brun, F., Rouzioux, C., et al. (1983). Isolation of a T-lymphotropic retrovirus from a patient at risk for acquired immune deficiency syndrome (AIDS). Science *220*, 868–871. https://doi.org/10.1126/SCIENCE.6189183.

Basso, K., Klein, U., Niu, H., Stolovitzky, G.A., Tu, Y., Califano, A., Cattoretti, G., and Dalla-Favera, R. (2004). Tracking CD40 signaling during germinal center development. Blood *104*, 4088–4096. https://doi.org/10.1182/BLOOD-2003-12-4291.

Bastard, P., Rosen, L.B., Zhang, Q., Michailidis, E., Hoffmann, H.H., Zhang, Y., Dorgham, K., Philippot, Q., Rosain, J., Béziat, V., et al. (2020). Autoantibodies against type I IFNs in patients with life-threatening COVID-19. Science *370*. https://doi.org/10.1126/SCIENCE.ABD4585/SUPPL_FILE/ABD4585_MDAR-REPRODUCIBILITYCHECKLIST.PDF.

Bastard, P., Gervais, A., Voyer, T. Le, Rosain, J., Philippot, Q., Manry, J., Michailidis, E., Hoffmann, H.H., Eto, S., Garcia-Prat, M., et al. (2021). Autoantibodies neutralizing type I IFNs are present in ~ 4% of uninfected individuals over 70 years and account for ~ 20% of COVID-19 deaths. Sci Immunol *6*. https://doi.org/10.1126/SCIIMMUNOL.ABL4340.

Bates, T.A., McBride, S.K., Leier, H.C., Guzman, G., Lyski, Z.L., Schoen, D., Winders, B., Lee, J.Y., Lee, D.X., Messer, W.B., et al. (2022). Vaccination before or after SARS-CoV-2 infection leads to robust humoral response and antibodies that effectively neutralize variants. Sci Immunol *7*, 8014. https://doi.org/10.1126/SCIIMMUNOL.ABN8014/SUPPL_FILE/SCIIMMUNOL.ABN8014_MDAR_REPRODUCIBILITY_CHECKLIST.ZIP.

Bayati, A., Kumar, R., Francis, V., and McPherson, P.S. (2021). SARS-CoV-2 infects cells after viral entry via clathrin-mediated endocytosis. J Biol Chem *296*. https://doi.org/10.1016/J.JBC.2021.100306.

Belaunzarán-Zamudio, P.F., García-León, M.L., Wong-Chew, R.M., Villasís-Keever, A., Cuellar-Rodríguez, J., Mosqueda-Gómez, J.L., Muñoz-Trejo, T., Escobedo, K.,

Santos, J.I., Ruiz-Palacios, G.M., et al. (2009). Early loss of measles antibodies after MMR vaccine among HIV-infected adults receiving HAART. Vaccine *27*, 7059–7064. https://doi.org/10.1016/J.VACCINE.2009.09.063.

Bentley, E.M., Mather, S.T., and Temperton, N.J. (2015). The use of pseudotypes to study viruses, virus sero-epidemiology and vaccination. Vaccine *33*, 2955. https://doi.org/10.1016/J.VACCINE.2015.04.071.

Bergamaschi, L., Mescia, F., Turner, L., Hanson, A.L., Kotagiri, P., Dunmore, B.J., Ruffieux, H., de Sa, A., Huhn, O., Morgan, M.D., et al. (2021). Longitudinal analysis reveals that delayed bystander CD8+ T cell activation and early immune pathology distinguish severe COVID-19 from mild disease. Immunity *54*, 1257-1275.e8. https://doi.org/10.1016/J.IMMUNI.2021.05.010.

Bergman, P., Blennow, O., Hansson, L., Mielke, S., Nowak, P., Chen, P., Söderdahl, G., Österborg, A., Smith, C.I.E., Wullimann, D., et al. (2021). Safety and efficacy of the mRNA BNT162b2 vaccine against SARS-CoV-2 in five groups of immunocompromised patients and healthy controls in a prospective open-label clinical trial. EBioMedicine *74*, 103705. https://doi.org/10.1016/J.EBIOM.2021.103705.

Bertagnolio, S., Thwin, S.S., Silva, R., Nagarajan, S., Jassat, W., Fowler, R., Haniffa, R., Reveiz, L., Ford, N., Doherty, M., et al. (2022). Clinical features of, and risk factors for, severe or fatal COVID-19 among people living with HIV admitted to hospital: analysis of data from the WHO Global Clinical Platform of COVID-19. Lancet HIV *9*, e486–e495. https://doi.org/10.1016/S2352-3018(22)00097-2.

Bessen, C., Plaza-Sirvent, C., Simsek, A., Bhat, J., Marheinecke, C., Urlaub, D., Bonowitz, P., Busse, S., Schumann, S., Blanco, E.V., et al. (2022). Impact of SARS-CoV-2 vaccination on systemic immune responses in people living with HIV. Front Immunol *13*, 1049070. https://doi.org/10.3389/FIMMU.2022.1049070.

Bhaskaran, K., Rentsch, C.T., MacKenna, B., Schultze, A., Mehrkar, A., Bates, C.J., Eggo, R.M., Morton, C.E., Bacon, S.C.J., Inglesby, P., et al. (2021). HIV infection and COVID-19 death: a population-based cohort analysis of UK primary care data and linked national death registrations within the OpenSAFELY platform. Lancet HIV *8*, e24–e32. https://doi.org/10.1016/S2352-3018(20)30305-2.

BHIVA (2015). BHIVA guidelines on the use of vaccines in HIV-positive adults 2015.

BHIVA (2020). COVID-19 & shielding: advice for HIV clinicians, GPs and people living with HIV.

BHIVA, and Terrence Higgins Trust (2020). COVID-19 risk for people with HIV - 7 August 2020.

Biancotto, A., Grivel, J.C., Iglehart, S.J., Vanpouille, C., Lisco, A., Sieg, S.F., Debernardo, R., Garate, K., Rodriguez, B., Margolis, L.B., et al. (2007). Abnormal activation and cytokine spectra in lymph nodes of people chronically infected with HIV-1. Blood *109*, 4272. https://doi.org/10.1182/BLOOD-2006-11-055764.

Blutt, S.E., and Conner, M.E. (2013). The Gastrointestinal Frontier: IgA and Viruses. Front Immunol *4*. https://doi.org/10.3389/FIMMU.2013.00402.

Ten Boekel, E., Melchers, F., and Rolink, A.G. (1998). Precursor B Cells Showing H Chain Allelic Inclusion Display Allelic Exclusion at the Level of Pre-B Cell Receptor Surface Expression. Immunity *8*, 199–207. https://doi.org/10.1016/S1074-7613(00)80472-0.

Bonsignori, M., Zhou, T., Sheng, Z., Chen, L., Gao, F., Joyce, M.G., Ozorowski, G., Chuang, G.Y., Schramm, C.A., Wiehe, K., et al. (2016). Maturation Pathway from Germline to Broad HIV-1 Neutralizer of a CD4-Mimic Antibody. Cell *165*, 449–463. https://doi.org/10.1016/j.cell.2016.02.022.

Borrow, P., Lewicki, H., Hahn, B.H., Shaw, G.M., and Oldstone, M.B. (1994). Virus-specific CD8+ cytotoxic T-lymphocyte activity associated with control of viremia in primary human immunodeficiency virus type 1 infection. J Virol *68*, 6103–6110. https://doi.org/10.1128/jvi.68.9.6103-6110.1994.

Boulle, A., Davies, M.A., Hussey, H., Ismail, M., Morden, E., Vundle, Z., Zweigenthal, V., Mahomed, H., Paleker, M., Pienaar, D., et al. (2021). Risk Factors for Coronavirus Disease 2019 (COVID-19) Death in a Population Cohort Study from the Western Cape Province, South Africa. Clinical Infectious Diseases *73*, E2005–E2015. https://doi.org/10.1093/cid/ciaa1198.

Braun, J., Loyal, L., Frentsch, M., Wendisch, D., Georg, P., Kurth, F., Hippenstiel, S., Dingeldey, M., Kruse, B., Fauchere, F., et al. (2020). SARS-CoV-2-reactive T cells in

healthy donors and patients with COVID-19. Nature *587*, 270–274. https://doi.org/10.1038/s41586-020-2598-9.

Brezinschek, H.P., Brezinschek, R.I., and Lipsky, P.E. (1995). Analysis of the heavy chain repertoire of human peripheral B cells using single-cell polymerase chain reaction. The Journal of Immunology *155*, 190–202. https://doi.org/10.4049/JIMMUNOL.155.1.190.

Briney, B., Inderbitzin, A., Joyce, C., and Burton, D.R. (2019). Commonality despite exceptional diversity in the baseline human antibody repertoire. Nature *566*, 393–397. https://doi.org/10.1038/s41586-019-0879-y.

Brouwer, P.J.M., Caniels, T.G., van der Straten, K., Snitselaar, J.L., Aldon, Y., Bangaru, S., Torres, J.L., Okba, N.M.A., Claireaux, M., Kerster, G., et al. (2020). Potent neutralizing antibodies from COVID-19 patients define multiple targets of vulnerability. Science *369*, 643–650. https://doi.org/10.1126/science.abc5902.

Brown, A.E., Croxford, S.E., Nash, S., Khawam, J., Kirwan, P., Kall, M., Bradshaw, D., Sabin, C., Miller, R.F., Post, F.A., et al. (2022). COVID-19 mortality among people with diagnosed HIV compared to those without during the first wave of the COVID-19 pandemic in England. HIV Med *23*, 90–102. https://doi.org/10.1111/hiv.13167.

Brumme, Z.L., Mwimanzi, F., Lapointe, H.R., Cheung, P.K., Sang, Y., Duncan, M.C., Yaseen, F., Agafitei, O., Ennis, S., Ng, K., et al. (2022). Humoral immune responses to COVID-19 vaccination in people living with HIV receiving suppressive antiretroviral therapy. NPJ Vaccines *7*. https://doi.org/10.1038/S41541-022-00452-6.

Buckner, C.M., Moir, S., Ho, J., Wang, W., Posada, J.G., Kardava, L., Funk, E.K., Nelson, A.K., Li, Y., Chun, T.-W., et al. (2013). Characterization of Plasmablasts in the Blood of HIV-Infected Viremic Individuals: Evidence for Nonspecific Immune Activation. J Virol *87*, 5800–5811. https://doi.org/10.1128/jvi.00094-13.

Buckner, C.M., Kardava, L., El Merhebi, O., Narpala, S.R., Serebryannyy, L., Lin, B.C., Wang, W., Zhang, X., Lopes de Assis, F., Kelly, S.E.M., et al. (2022). Interval between prior SARS-CoV-2 infection and booster vaccination impacts magnitude and quality of antibody and B cell responses. Cell *185*, 4333-4346.e14. https://doi.org/10.1016/j.cell.2022.09.032.

Budeus, B., De Reynoso, S.S., Przekopowitz, M., Hoffmann, D., Seifert, M., Küppers, R., and Rajewsky, K. (2015). Complexity of the human memory B-cell compartment is determined by the versatility of clonal diversification in germinal centers. Proc Natl Acad Sci U S A *112*, E5281–E5289. https://doi.org/10.1073/PNAS.1511270112/-/DCSUPPLEMENTAL.

Burdick, R.C., Li, C., Munshi, M.H., Rawson, J.M.O., Nagashima, K., Hu, W.S., and Pathak, V.K. (2020). HIV-1 uncoats in the nucleus near sites of integration. Proc Natl Acad Sci U S A *117*, 5486–5493. https://doi.org/10.1073/pnas.1920631117.

Burton, A.R., Pallett, L.J., McCoy, L.E., Suveizdyte, K., Amin, O.E., Swadling, L., Alberts, E., Davidson, B.R., Kennedy, P.T.F., Gill, U.S., et al. (2018). Circulating and intrahepatic antiviral B cells are defective in hepatitis B. J Clin Invest *128*, 4588–4603. https://doi.org/10.1172/JCI121960.

Burton, A.R., Guillaume, S.M., Foster, W.S., Wheatley, A.K., Hill, D.L., Carr, E.J., and Linterman, M.A. (2022). The memory B cell response to influenza vaccination is impaired in older persons. Cell Rep *41*. https://doi.org/10.1016/j.celrep.2022.111613.

Cagigi, A., Rinaldi, S., Di Martino, A., Concetta Manno, E., Zangari, P., Aquilani, A., Cotugno, N., Nicolosi, L., Villani, A., Bernardi, S., et al. (2014). Premature immune senescence during HIV-1 vertical infection relates with response to influenza vaccination. Journal of Allergy and Clinical Immunology *133*, 592-594.e1. https://doi.org/10.1016/j.jaci.2013.07.054.

Cai, S., Liao, G., Yu, T., Gao, Q., Zou, L., Zhang, H., Xu, X., Chen, J., Lu, A., Wu, Y., et al. (2022). Immunogenicity and safety of an inactivated SARS-CoV-2 vaccine in people living with HIV: A cross-sectional study. J Med Virol *94*, 4224. https://doi.org/10.1002/JMV.27872.

Cameroni, E., Bowen, J.E., Rosen, L.E., Saliba, C., Zepeda, S.K., Culap, K., Pinto, D., VanBlargan, L.A., De Marco, A., di Iulio, J., et al. (2021). Broadly neutralizing antibodies overcome SARS-CoV-2 Omicron antigenic shift. Nature *602*, 664–670. https://doi.org/10.1038/s41586-021-04386-2.

de Campos-Mata, L., Tejedor Vaquero, S., Tachó-Piñot, R., Piñero, J., Grasset, E.K., Arrieta Aldea, I., Rodrigo Melero, N., Carolis, C., Horcajada, J.P., Cerutti, A., et al. et al. (2021). SARS-CoV-2 sculpts the immune system to induce sustained virus-specific

naïve-like and memory B-cell responses. Clin Transl Immunology *10*. https://doi.org/10.1002/CTI2.1339.

Cantoni, D., Wilkie, C., Bentley, E.M., Mayora-Neto, M., Wright, E., Scott, S., Ray, S., Castillo-Olivares, J., Heeney, J.L., Mattiuzzo, G., et al. (2023). Correlation between pseudotyped virus and authentic virus neutralisation assays, a systematic review and meta-analysis of the literature. Front Immunol *14*, 1–12. https://doi.org/10.3389/fimmu.2023.1184362.

Cao, Y., Yang, R., Lee, I., Zhang, W., Sun, J., Wang, W., and Meng, X. (2021). Characterization of the SARS-CoV-2 E Protein: Sequence, Structure, Viroporin, and Inhibitors. Protein Science *30*, 1114–1130. https://doi.org/10.1002/pro.4075.

Cao, Y., Wang, J., Jian, F., Xiao, T., Song, W., Yisimayi, A., Huang, W., Li, Q., Wang, P., An, R., et al. (2022). Omicron escapes the majority of existing SARS-CoV-2 neutralizing antibodies. Nature *602*, 657–663. https://doi.org/10.1038/s41586-021-04385-3.

Cao, Y., Jian, F., Wang, J., Yu, Y., Song, W., Yisimayi, A., Wang, J., An, R., Chen, X., Zhang, N., et al. (2023). Imprinted SARS-CoV-2 humoral immunity induces convergent Omicron RBD evolution. Nature *614*, 521–529. https://doi.org/10.1038/s41586-022-05644-7.

Cao, Z., Liu, L., Du, L., Zhang, C., Jiang, S., Li, T., and He, Y. (2010). Potent and persistent antibody responses against the receptor-binding domain of SARS-CoV spike protein in recovered patients. Virol J *7*, 299. https://doi.org/10.1186/1743-422X-7-299.

Carabelli, A.M., Peacock, T.P., Thorne, L.G., Harvey, W.T., Hughes, J., de Silva, T.I., Peacock, S.J., Barclay, W.S., de Silva, T.I., Towers, G.J., et al. (2023). SARS-CoV-2 variant biology: immune escape, transmission and fitness. Nat Rev Microbiol *21*, 162–177. https://doi.org/10.1038/s41579-022-00841-7.

Carr, E.J., Townsley, H., Wu, M.Y., Wilkinson, K.A., Hobson, P.S., Levi, D., Namjou, S., Mears, H. V, Hobbs, A., Ragno, M., et al. (2023). Dichotomy of neutralizing antibody, B cell and T cell responses to SARS-CoV-2 vaccination and protection in healthy adults. BioRxiv 2023.05.24.541920. .

Carrasco, Y.R., and Batista, F.D. (2007). B Cells Acquire Particulate Antigen in a Macrophage-Rich Area at the Boundary between the Follicle and the Subcapsular Sinus of the Lymph Node. Immunity *27*, 160–171. https://doi.org/10.1016/J.IMMUNI.2007.06.007.

Carsetti, R., Köhler, G., and Lamers, M.C. (1995). Transitional B cells are the target of negative selection in the B cell compartment. J Exp Med *181*, 2129. https://doi.org/10.1084/JEM.181.6.2129.

Catalan, N., Selz, F., Imai, K., Revy, P., Fischer, A., and Durandy, A. (2003). The Block in Immunoglobulin Class Switch Recombination Caused by Activation-Induced Cytidine Deaminase Deficiency Occurs Prior to the Generation of DNA Double Strand Breaks in Switch μ Region. The Journal of Immunology *171*, 2504–2509. https://doi.org/10.4049/JIMMUNOL.171.5.2504.

Cele, S., Gazy, I., Jackson, L., Hwa, S.H., Tegally, H., Lustig, G., Giandhari, J., Pillay, S., Wilkinson, E., Naidoo, Y., et al. (2021a). Escape of SARS-CoV-2 501Y.V2 from neutralization by convalescent plasma. Nature *593*, 142. https://doi.org/10.1038/S41586-021-03471-W.

Cele, S., Jackson, L., Khoury, D.S., Khan, K., Moyo-Gwete, T., Tegally, H., San, J.E., Cromer, D., Scheepers, C., Amoako, D.G., et al. (2021b). Omicron extensively but incompletely escapes Pfizer BNT162b2 neutralization. Nature *602*, 654–656. https://doi.org/10.1038/s41586-021-04387-1.

Cele, S., Karim, F., Lustig, G., San, J.E., Hermanus, T., Tegally, H., Snyman, J., Moyo-Gwete, T., Wilkinson, E., Bernstein, M., et al. (2022). SARS-CoV-2 prolonged infection during advanced HIV disease evolves extensive immune escape. Cell Host Microbe *30*, 154-162.e5. https://doi.org/10.1016/j.chom.2022.01.005.

Centers for Disease Control and Prevention (U.S.) (1981). Pneumocystis Pneumonia — Los Angeles (MMWR June 5, 1981). Morbidity and Mortality Weekly Report *30*, 250–252. .

El Chaer, F., and El Sahly, H.M. (2019). Vaccination in the Adult Patient Infected with HIV: A Review of Vaccine Efficacy and Immunogenicity. American Journal of Medicine *132*, 437–446. https://doi.org/10.1016/j.amjmed.2018.12.011.

Chaiwarith, R., Praparattanapan, J., Kotarathititum, W., Wipasa, J., Chaiklang, K., and Supparatpinyo, K. (2019). Higher rate of long-term serologic response of four double doses vs. standard doses of hepatitis B vaccination in HIV-infected adults: 4-year follow-up of a randomised controlled trial. AIDS Res Ther *16*, 33. https://doi.org/10.1186/S12981-019-0249-8.

Chalkias, S., Harper, C., Vrbicky, K., Walsh, S.R., Essink, B., Brosz, A., McGhee, N., Tomassini, J.E., Chen, X., Chang, Y., et al. (2022). A Bivalent Omicron-Containing Booster Vaccine against Covid-19. N Engl J Med *387*, 1279–1291. https://doi.org/10.1056/NEJMOA2208343.

Chandler, J.C., Bevins, S.N., Ellis, J.W., Linder, T.J., Tell, R.M., Jenkins-Moore, M., Root, J.J., Lenoch, J.B., Robbe-Austerman, S., DeLiberto, T.J., et al. (2021). SARS-CoV-2 exposure in wild white-tailed deer (Odocoileus virginianus). Proc Natl Acad Sci U S A *118*, e2114828118. https://doi.org/10.1073/PNAS.2114828118/SUPPL_FILE/PNAS.2114828118.SD01.CSV.

Chao, K.H., Barton, K., Palmer, S., and Lanfear, R. (2021). sangeranalyseR: Simple and Interactive Processing of Sanger Sequencing Data in R. Genome Biol Evol *13*. https://doi.org/10.1093/GBE/EVAB028.

Charre, C., Icard, V., Pradat, P., Brochier, C., Lina, B., Chidiac, C., and Cotte, L. (2020). Coronavirus disease 2019 attack rate in HIV-infected patients and in preexposure prophylaxis users. AIDS *34*, 1765. https://doi.org/10.1097/QAD.0000000000002639.

Chen, E.C., Gilchuk, P., Zost, S.J., Suryadevara, N., Winkler, E.S., Cabel, C.R., Binshtein, E., Chen, R.E., Sutton, R.E., Rodriguez, J., et al. (2021). Convergent antibody responses to the SARS-CoV-2 spike protein in convalescent and vaccinated individuals. Cell Rep *36*, 109604. https://doi.org/10.1016/J.CELREP.2021.109604.

Chen, Y., Tong, X., Li, Y., Gu, B., Yan, J., Liu, Y., Shen, H., Huang, R., and Wu, C. (2020). A comprehensive, longitudinal analysis of humoral responses specific to four recombinant antigens of SARS-CoV-2 in severe and non-severe COVID-19 patients. PLoS Pathog *16*. https://doi.org/10.1371/JOURNAL.PPAT.1008796.

Chen, Z., Collins, A.M., Wang, Y., and Gata, B.A. (2010). Clustering-based identification of clonally-related immunoglobulin gene sequence sets. Immunome Res *6*, S4. https://doi.org/10.1186/1745-7580-6-S1-S4.

Cherukuri, A., Cheng, P.C., and Pierce, S.K. (2001). The Role of the CD19/CD21 Complex in B Cell Processing and Presentation of Complement-Tagged Antigens. The Journal of Immunology *167*, 163–172. https://doi.org/10.4049/JIMMUNOL.167.1.163.

Cheung, P.K., Lapointe, H.R., Sang, Y., Ennis, S., Mwimanzi, F., Speckmaier, S., Barad, E., Dong, W., Liang, R., Simons, J., et al. (2023). SARS-CoV-2 live virus neutralization after four COVID-19 vaccine doses in people with HIV receiving suppressive antiretroviral therapy. AIDS *37*, F11–F18. https://doi.org/10.1097/QAD.0000000000003519.

Chia, W.N., Zhu, F., Le Bert, N., Tan, C.W., Tiu, C.B., Zhang, J.B., L Tham, C.Y., Kunasegaran, K.B., H Low MPH, J.G., Bertoletti, A., et al. (2021). Dynamics of SARS-CoV-2 neutralising antibody responses and duration of immunity: a longitudinal study. Lancet Microbe *2*, e240–e249. https://doi.org/10.1016/S2666-5247(21)00025-2.

Choi, Y.S., Kageyama, R., Eto, D., Escobar, T.C., Johnston, R.J., Monticelli, L., Lao, C., and Crotty, S. (2011). ICOS Receptor Instructs T Follicular Helper Cell versus Effector Cell Differentiation via Induction of the Transcriptional Repressor Bcl6. Immunity *34*, 932–946. https://doi.org/10.1016/J.IMMUNI.2011.03.023.

Chothia, C., Lesk, A.M., Tramontano, A., Levitt, M., Smith-Gill, S.J., Air, G., Sheriff, S., Padlan, E.A., Davies, D., Tulip, W.R., et al. (1989). Conformations of immunoglobulin hypervariable regions. Nature *342*, 877–883. https://doi.org/10.1038/342877a0.

Clark, S.A., Clark, L.E., Pan, J., Coscia, A., McKay, L.G.A., Shankar, S., Johnson, R.I., Brusic, V., Choudhary, M.C., Regan, J., et al. (2021). SARS-CoV-2 evolution in an immunocompromised host reveals shared neutralization escape mechanisms. Cell *184*, 2605-2617.e18. https://doi.org/10.1016/j.cell.2021.03.027.

Coburn, S.B., Humes, E., Lang, R., Stewart, C., Hogan, B.C., Gebo, K.A., Napravnik, S., Edwards, J.K., Browne, L.E., Park, L.S., et al. (2022). Analysis of Postvaccination Breakthrough COVID-19 Infections among Adults with HIV in the United States. JAMA Netw Open *5*, E2215934. https://doi.org/10.1001/jamanetworkopen.2022.15934.

Cohen, K.W., Linderman, S.L., Moodie, Z., Czartoski, J., Lai, L., Mantus, G., Norwood, C., Nyhoff, L.E., Edara, V.V., Floyd, K., et al. (2021). Longitudinal analysis shows durable and broad immune memory after SARS-CoV-2 infection with persisting antibody responses and memory B and T cells. Cell Rep Med *2*. https://doi.org/10.1016/j.xcrm.2021.100354.

Collier, D.A., De Marco, A., Ferreira, I.A.T.M., Meng, B., Datir, R.P., Walls, A.C., Kemp, S.A., Bassi, J., Pinto, D., Silacci-Fregni, C., et al. (2021a). Sensitivity of SARS-CoV-2 B.1.1.7 to mRNA vaccine-elicited antibodies. Nature *593*, 136–141. https://doi.org/10.1038/s41586-021-03412-7.

Collier, D.A., Ferreira, I.A.T.M., Kotagiri, P., Datir, R.P., Lim, E.Y., Touizer, E., Meng, B., Abdullahi, A., Baker, S., Dougan, G., et al. (2021b). Age-related immune response heterogeneity to SARS-CoV-2 vaccine BNT162b2. Nature *596*, 417–422. https://doi.org/10.1038/s41586-021-03739-1.

Collins, C., Tsui, F.W.L., and Shulman, M.J. (2002). Differential activation of human and guinea pig complement by pentameric and hexameric IgM. Eur J Immunol *32*, 1802–1810. https://doi.org/10.1002/1521-4141(200206)32:6<1802::AID-IMMU1802>3.0.CO;2-C.

Collins, D.R., Gaiha, G.D., and Walker, B.D. (2020). CD8+ T cells in HIV control, cure and prevention. Nat Rev Immunol *20*, 471–482. https://doi.org/10.1038/s41577-020-0274-9.

Colonna-Romano, G., Bulati, M., Aquino, A., Pellicanò, M., Vitello, S., Lio, D., Candore, G., and Caruso, C. (2009). A double-negative (IgD−CD27−) B cell population is increased in the peripheral blood of elderly people. Mech Ageing Dev *130*, 681–690. https://doi.org/10.1016/J.MAD.2009.08.003.

Condor Capcha, J.M., Lambert, G., Dykxhoorn, D.M., Salerno, A.G., Hare, J.M., Whitt, M.A., Pahwa, S., Jayaweera, D.T., and Shehadeh, L.A. (2021). Generation of SARS-CoV-2 Spike Pseudotyped Virus for Viral Entry and Neutralization Assays: A 1-Week Protocol. Front Cardiovasc Med *7*, 618651. https://doi.org/10.3389/fcvm.2020.618651.

Cooper M, Peterson R, and Good R (1965). Delineation of the Thymic and Bursal Lymphoid Systems in the Chicken. Nature *205*, 143–146. .

Corbett, K.S., Flynn, B., Foulds, K.E., Francica, J.R., Boyoglu-Barnum, S., Werner, A.P., Flach, B., O'Connell, S., Bock, K.W., Minai, M., et al. (2020). Evaluation of the mRNA-1273 Vaccine against SARS-CoV-2 in Nonhuman Primates. New England Journal of Medicine *383*, 1544–1555. https://doi.org/10.1056/NEJMOA2024671/SUPPL_FILE/NEJMOA2024671_DISCLOSURES.PDF.

Corma-Gómez, A., Fernández-Fuertes, M., Viñuela, L., Domínguez, C., Santos, M., Fuentes-López, A., Rojas, A., Fernández-Pérez, N., Martín-Carmona, J., Serrano-Conde, E., et al. (2023). Reduced neutralizing antibody response to SARS-CoV-2 vaccine booster dose in people living with HIV with severe immunosuppression. J Med Virol *95*, 1–8. https://doi.org/10.1002/jmv.28602.

Crooke, S.N., Ovsyannikova, I.G., Poland, G.A., and Kennedy, R.B. (2019). Immunosenescence and human vaccine immune responses. Immunity & Ageing *16*, 1–16. https://doi.org/10.1186/s12979-019-0164-9.

Cruciani, M., Mengoli, C., Serpelloni, G., Lanza, A., Gomma, M., Nardi, S., Rimondo, C., Bricolo, F., Consolaro, S., Trevisan, M.T., et al. (2009). Serologic response to hepatitis B vaccine with high dose and increasing number of injections in HIV infected adult patients. Vaccine *27*, 17–22. https://doi.org/10.1016/J.VACCINE.2008.10.040.

Cubas, R., van Grevenynghe, J., Wills, S., Kardava, L., Santich, B.H., Buckner, C.M., Muir, R., Tardif, V., Nichols, C., Procopio, F., et al. (2015). Reversible Reprogramming of Circulating Memory T Follicular Helper Cell Function during Chronic HIV Infection. The Journal of Immunology *195*, 5625–5636. https://doi.org/10.4049/JIMMUNOL.1501524.

Cubas, R.A., Mudd, J.C., Savoye, A.L., Perreau, M., Van Grevenynghe, J., Metcalf, T., Connick, E., Meditz, A., Freeman, G.J., Abesada-Terk, G., et al. (2013). Inadequate T follicular cell help impairs B cell immunity during HIV infection. Nat Med *19*, 494–499. https://doi.org/10.1038/nm.3109.

Cui, X., and Meek, K. (2007). Linking double-stranded DNA breaks to the recombination activating gene complex directs repair to the nonhomologous end-joining pathway. Proc Natl Acad Sci U S A *104*, 17046. https://doi.org/10.1073/PNAS.0610928104.

Cyster, J.G., Ansel, K.M., Reif, K., Ekland, E.H., Hyman, P.L., Tang, H.L., Luther, S.A., and Ngo, V.N. (2000). Follicular stromal cells and lymphocyte homing to follicles. Immunol Rev *176*, 181–193. https://doi.org/10.1034/J.1600-065X.2000.00618.X.

Dahabieh, M.S., Battivelli, E., and Verdin, E. (2015). Understanding HIV Latency: The Road to an HIV Cure. Annu Rev Med *66*, 407. https://doi.org/10.1146/ANNUREV-MED-092112-152941.

Dai, D., Gu, S., Han, X., Ding, H., Jiang, Y., Zhang, X., Yao, C., Hong, S., Zhang, J., Shen, Y., et al. (2024). The transcription factor ZEB2 drives the formation of age-associated B cells. Science *383*, 413–421. https://doi.org/10.1126/SCIENCE.ADF8531/SUPPL_FILE/SCIENCE.ADF8531_MDAR_REPRODUCIBILITY_CHECKLIST.PDF.

Dalgleish, A.G., Beverley, P.C.L., Clapham, P.R., Crawford, D.H., Greaves, M.F., and Weiss, R.A. (1984). The CD4 (T4) antigen is an essential component of the receptor for the AIDS retrovirus. Nature *312*, 763–767. https://doi.org/10.1038/312763a0.

Daly, J.L., Simonetti, B., Klein, K., Chen, K.E., Williamson, M.K., Antón-Plágaro, C., Shoemark, D.K., Simón-Gracia, L., Bauer, M., Hollandi, R., et al. (2020). Neuropilin-1 is a host factor for SARS-CoV-2 infection. Science *370*, 861–865. https://doi.org/10.1126/SCIENCE.ABD3072/SUPPL_FILE/ABD3072_REPRODUCIBILITYCHECKLIST.PDF.

Dan, J.M., Mateus, J., Kato, Y., Hastie, K.M., Yu, E.D., Faliti, C.E., Grifoni, A., Ramirez, S.I., Haupt, S., Frazier, A., et al. (2021). Immunological memory to SARS-CoV-2 assessed for up to 8 months after infection. Science *371*, eabf4063. https://doi.org/10.1126/science.abf4063.

Dandachi, D., Geiger, G., Montgomery, M.W., Karmen-Tuohy, S., Golzy, M., Antar, A.A.R., Llibre, J.M., Camazine, M., Santiago, A.D. De, Carlucci, P.M., et al. (2021). Characteristics, Comorbidities, and Outcomes in a Multicenter Registry of Patients With Human Immunodeficiency Virus and Coronavirus Disease 2019. Clinical Infectious Diseases *73*, E1964–E1972. https://doi.org/10.1093/cid/ciaa1339.

Davenport, F.M., and Henessy, A. V. (1956). A serologic recapitulation of past experiences with influenza A; antibody response to monovalent vaccine. J Exp Med *104*, 85–97. https://doi.org/10.1084/jem.104.1.85.

Davenport, F.M., Henessy, A. V., and Francis, T. (1953). Epidemiologic and immunologic significance of age distribution of antibody to antigenic variants of influenza virus. J Exp Med *98*, 641–656. https://doi.org/10.1084/jem.98.6.641.

Davies, N.G., Jarvis, C.I., van Zandvoort, K., Clifford, S., Sun, F.Y., Funk, S., Medley, G., Jafari, Y., Meakin, S.R., Lowe, R., et al. (2021a). Increased mortality in community-tested cases of SARS-CoV-2 lineage B.1.1.7. Nature 2021 593:7858 *593*, 270–274. https://doi.org/10.1038/s41586-021-03426-1.

Davies, N.G., Jarvis, C.I., van Zandvoort, K., Clifford, S., Sun, F.Y., Funk, S., Medley, G., Jafari, Y., Meakin, S.R., Lowe, R., et al. (2021b). Increased mortality in community-tested cases of SARS-CoV-2 lineage B.1.1.7. Nature *593*, 270. https://doi.org/10.1038/S41586-021-03426-1.

Davis, H.E., McCorkell, L., Vogel, J.M., and Topol, E.J. (2023). Long COVID: major findings, mechanisms and recommendations. Nat Rev Microbiol *21*, 133–146. https://doi.org/10.1038/s41579-022-00846-2.

Deeks, S.G., Kitchen, C.M.R., Liu, L., Guo, H., Gascon, R., Narváez, A.B., Hunt, P., Martin, J.N., Kahn, J.O., Levy, J., et al. (2004). Immune activation set point during early HIV infection predicts subsequent CD4+ T-cell changes independent of viral load. Blood *104*, 942–947. https://doi.org/10.1182/BLOOD-2003-09-3333.

Deng, H.K., Liu, R., Ellmeier, W., Choe, S., Unutmaz, D., Burkhart, M., Di Marzio, P., Marmon, S., Sutton, R.E., Mark Hill, C., et al. (1996). Identification of a major co-receptor for primary isolates of HIV-1. Nature *381*, 661–666. https://doi.org/10.1038/381661a0.

Diao, B., Wang, C., Tan, Y., Chen, X., Liu, Y., Ning, L., Chen, L., Li, M., Liu, Y., Wang, G., et al. (2020). Reduction and Functional Exhaustion of T Cells in Patients With Coronavirus Disease 2019 (COVID-19). Front Immunol *11*, 1–7. https://doi.org/10.3389/fimmu.2020.00827.

Dicks, M.D.J., Spencer, A.J., Edwards, N.J., Wadell, G., Bojang, K., Gilbert, S.C., Hill, A.V.S., and Cottingham, M.G. (2012). A Novel Chimpanzee Adenovirus Vector with Low Human Seroprevalence: Improved Systems for Vector Derivation and Comparative Immunogenicity. PLoS One *7*, 40385. https://doi.org/10.1371/JOURNAL.PONE.0040385.

Dickter, J.K., Aribi, A., Cardoso, A.A., Gianella, S., Gendzekhadze, K., Li, S., Feng, Y., Chaillon, A., Laird, G.M., Browning, D.L., et al. (2024). HIV-1 Remission after Allogeneic Hematopoietic-Cell Transplantation. New England Journal of Medicine *390*, 669–671. https://doi.org/10.1056/NEJMC2312556.

Dixon, P. (2003). VEGAN, A Package of R Functions for Community Ecology. Source: Journal of Vegetation Science *14*, 927–930. .

Dogan, I., Bertocci, B., Vilmont, V., Delbos, F., Mégret, J., Storck, S., Reynaud, C.A., and Weill, J.C. (2009). Multiple layers of B cell memory with different effector functions. Nat Immunol *10*, 1292–1299. https://doi.org/10.1038/ni.1814.

Doi, H., Tanoue, S., and Kaplan, D.E. (2014). Peripheral CD27-CD21- B-cells represent an exhausted lymphocyte population in hepatitis C cirrhosis. Clinical Immunology *150*, 184–191. https://doi.org/10.1016/j.clim.2013.12.001.

Doitsh, G., Galloway, N.L.K., Geng, X., Yang, Z., Monroe, K.M., Zepeda, O., Hunt, P.W., Hatano, H., Sowinski, S., Muñoz-Arias, I., et al. (2014). Cell death by pyroptosis drives CD4 T-cell depletion in HIV-1 infection. Nature *505*, 509–514. https://doi.org/10.1038/nature12940.

Donadeu, L., Tiraboschi, J.M., Scévola, S., Torija, A., Meneghini, M., Jouve, T., Favà, A., Calatayud, L., Ardanuy, C., Cidraque, I., et al. (2022). Long-lasting adaptive immune memory specific to SARS-CoV-2 in convalescent coronavirus disease 2019 stable people with HIV. AIDS *36*, 1373–1382. https://doi.org/10.1097/QAD.0000000000003276.

van Doremalen, N., Haddock, E., Feldmann, F., Meade-White, K., Bushmaker, T., Fischer, R.J., Okumura, A., Hanley, P.W., Saturday, G., Edwards, N.J., et al. (2020). A single dose of ChAdOx1 MERS provides protective immunity in rhesus macaques. Sci Adv *6*. https://doi.org/10.1126/sciadv.aba8399.

Douek, D.C., Brenchley, J.M., Betts, M.R., Ambrozak, D.R., Hill, B.J., Okamoto, Y., Casazza, J.P., Kuruppu, J., Kunstman, K., Wolinsky, S., et al. (2002). HIV preferentially infects HIV-specific CD4+ T cells. Nature *417*, 95–98. https://doi.org/10.1038/417095a.

Drosten, C., Günther, S., Preiser, W., van der Werf, S., Brodt, H.-R., Becker, S., Rabenau, H., Panning, M., Kolesnikova, L., Fouchier, R.A.M., et al. (2003). Identification of a Novel Coronavirus in Patients with Severe Acute Respiratory Syndrome. New England Journal of Medicine *348*, 1967–1976. https://doi.org/10.1056/nejmoa030747.

Dugan, H.L., Stamper, C.T., Li, L., Changrob, S., Asby, N.W., Halfmann, P.J., Zheng, N.Y., Huang, M., Shaw, D.G., Cobb, M.S., et al. (2021). Profiling B cell immunodominance after SARS-CoV-2 infection reveals antibody evolution to non-neutralizing viral targets. Immunity *54*, 1290-1303.e7. https://doi.org/10.1016/j.immuni.2021.05.001.

Ehrhardt, G.R.A., Hsu, J.T., Gartland, L., Leu, C.M., Zhang, S., Davis, R.S., and Cooper, M.D. (2005). Expression of the immunoregulatory molecule FcRH4 defines a distinctive tissue-based population of memory B cells. Journal of Experimental Medicine *202*, 783–791. https://doi.org/10.1084/jem.20050879.

Ehrhardt, G.R.A., Hijikata, A., Kitamura, H., Ohara, O., Wang, J.Y., and Cooper, M.D. (2008). Discriminating gene expression profiles of memory B cell subpopulations. Journal of Experimental Medicine *205*, 1807–1817. https://doi.org/10.1084/jem.20072682.

Ehrhardt, S.A., Zehner, M., Krähling, V., Cohen-Dvashi, H., Kreer, C., Elad, N., Gruell, H., Ercanoglu, M.S., Schommers, P., Gieselmann, L., et al. (2019). Polyclonal and convergent antibody response to Ebola virus vaccine rVSV-ZEBOV. Nat Med *25*, 1589–1600. https://doi.org/10.1038/s41591-019-0602-4.

Ella, R., Reddy, S., Blackwelder, W., Potdar, V., Yadav, P., Sarangi, V., Aileni, V.K., Kanungo, S., Rai, S., Reddy, P., et al. (2021). Efficacy, safety, and lot-to-lot immunogenicity of an inactivated SARS-CoV-2 vaccine (BBV152): interim results of a randomised, double-blind, controlled, phase 3 trial. The Lancet *398*, 2173–2184. https://doi.org/10.1016/S0140-6736(21)02000-6.

Ellebedy, A.H., Jackson, K.J.L., Kissick, H.T., Nakaya, H.I., Davis, C.W., Roskin, K.M., McElroy, A.K., Oshansky, C.M., Elbein, R., Thomas, S., et al. (2016). Defining antigen-specific plasmablast and memory B cell subsets in human blood after viral infection or vaccination. Nat Immunol *17*, 1226–1234. https://doi.org/10.1038/ni.3533.

Elliott, P., Bodinier, B., Eales, O., Wang, H., Haw, D., Elliott, J., Whitaker, M., Jonnerby, J., Tang, D., Walters, C.E., et al. (2022). Rapid increase in Omicron infections in England during December 2021: REACT-1 study. Science *375*, 1406–1411. https://doi.org/10.1126/SCIENCE.ABN8347/SUPPL_FILE/SCIENCE.ABN8347_SM.PDF.

Elsner, R.A., and Shlomchik, M.J. (2020). Germinal Center and Extrafollicular B Cell Responses in Vaccination, Immunity, and Autoimmunity. Immunity *53*, 1136–1150. https://doi.org/10.1016/j.immuni.2020.11.006.

Estes, J., Baker, J. V., Brenchley, J.M., Khoruts, A., Barthold, J.L., Bantle, A., Reilly, C.S., Beilman, G.J., George, M.E., Douek, D.C., et al. (2008). Collagen Deposition Limits Immune Reconstitution in the Gut. J Infect Dis *198*, 456. https://doi.org/10.1086/590112.

Evans, J.G., Chavez-Rueda, K.A., Eddaoudi, A., Meyer-Bahlburg, A., Rawlings, D.J., Ehrenstein, M.R., and Mauri, C. (2007). Novel Suppressive Function of Transitional 2 B Cells in Experimental Arthritis. The Journal of Immunology *178*, 7868–7878. https://doi.org/10.4049/jimmunol.178.12.7868.

Evans, R.A., Dube, S., Lu, Y., Yates, M., Arnetorp, S., Barnes, E., Bell, S., Carty, L., Evans, K., Graham, S., et al. (2023). Impact of COVID-19 on immunocompromised populations during the Omicron era: insights from the observational population-based INFORM study. The Lancet Regional Health - Europe *35*, 100747. https://doi.org/10.1016/j.lanepe.2023.100747.

Faliti, C.E., Anam, F.A., Cheedarla, N., Woodruff, M.C., Usman, S.Y., Runnstrom, M.C., Van, T.T.P., Kyu, S., Ahmed, H., Morrison-Porter, A., et al. (2023). Poor immunogenicity upon SARS-CoV-2 mRNA vaccinations in autoimmune SLE patients is associated with pronounced EF-mediated responses and anti-BAFF/Belimumab treatment. MedRxiv 1–13. https://doi.org/10.1101/2023.06.08.23291159.

Faria, N.R., Rambaut, A., Suchard, M.A., Baele, G., Bedford, T., Ward, M.J., Tatem, A.J., Sousa, J.D., Arinaminpathy, N., Pépin, J., et al. (2014). The early spread and epidemic ignition of HIV-1 in human populations. Science *346*, 56–61. https://doi.org/10.1126/science.1256739.

Farkash, I., Feferman, T., Cohen-Saban, N., Avraham, Y., Morgenstern, D., Mayuni, G., Barth, N., Lustig, Y., Miller, L., Shouval, D.S., et al. (2021). Anti-SARS-CoV-2 antibodies elicited by COVID-19 mRNA vaccine exhibit a unique glycosylation pattern. Cell Rep *37*, 110114. https://doi.org/10.1016/J.CELREP.2021.110114.

Fendler, A., Shepherd, S.T.C., Au, L., Wu, M., Harvey, R., Schmitt, A.M., Tippu, Z., Shum, B., Farag, S., Rogiers, A., et al. (2022). Omicron neutralising antibodies after third COVID-19 vaccine dose in patients with cancer. The Lancet *399*, 905–907. https://doi.org/10.1016/S0140-6736(22)00147-7.

Feng, S., Phillips, D.J., White, T., Sayal, H., Aley, P.K., Bibi, S., Dold, C., Fuskova, M., Gilbert, S.C., Hirsch, I., et al. (2021). Correlates of protection against symptomatic and asymptomatic SARS-CoV-2 infection. Nat Med *27*, 2032–2040. https://doi.org/10.1038/S41591-021-01540-1.

Feng, Y., Broder, C.C., Kennedy, P.E., and Berger, E.A. (1996). HIV-1 Entry Cofactor: Functional cDNA Cloning of a Seven-Transmembrane, G Protein-Coupled Receptor. Science *272*, 872–877. https://doi.org/10.1126/SCIENCE.272.5263.872.

Fernández-Quintero, M.L., Pomarici, N.D., Math, B.A., Kroell, K.B., Waibl, F., Bujotzek, A., Georges, G., and Liedl, K.R. (2020). Antibodies exhibit multiple paratope states influencing VH–VL domain orientations. Commun Biol *3*, 1–14. https://doi.org/10.1038/s42003-020-01319-z.

Ferrante, A., Beard, L., and Feldman, R. (1990). IgG subclass distribution of antibodies to bacterial and viral antigens. Pediatr Infect Dis J *9*, 516–524. .

Ferreira, I.A.T.M., Lee, C.Y.C., Foster, W.S., Abdullahi, A., Dratva, L.M., Tuong, Z.K., Stewart, B.J., Ferdinand, J.R., Guillaume, S.M., Potts, M.O.P., et al. (2023). Atypical B cells and impaired SARS-CoV-2 neutralization following heterologous vaccination in the elderly. Cell Rep *42*, 112991. https://doi.org/10.1016/J.CELREP.2023.112991.

Fidler, S., Fox, J., Tipoe, T., Longet, S., Tipton, T., Abeywickrema, M., Adele, S., Alagaratnam, J., Ali, M., Aley, P.K., et al. (2023). Booster Vaccination Against SARS-CoV-2 Induces Potent Immune Responses in People With Human Immunodeficiency Virus. Clinical Infectious Diseases *76*, 201–209. https://doi.org/10.1093/cid/ciac796.

Fischl, M.A., Richman, D.D., Grieco, M.H., Gottlieb, M.S., Volberding, P.A., Laskin, O.L., Leedom, J.M., Groopman, J.E., Mildvan, D., Schooley, R.T., et al. (1987). The Efficacy of Azidothymidine (AZT) in the Treatment of Patients with AIDS and AIDS-Related Complex. New England Journal of Medicine *317*, 185–191. https://doi.org/10.1056/NEJM198707233170401.

Fogli, M., Torti, C., Malacarne, F., Fiorentini, S., Albani, M., Izzo, I., Giagulli, C., Maggi, F., Carosi, G., and Caruso, A. (2012). Emergence of exhausted B cells in asymptomatic HIV-1-infected patients Naïve for HAART is related to reduced immune surveillance. Clin Dev Immunol *2012*. https://doi.org/10.1155/2012/829584.

Folegatti, P.M., Ewer, K.J., Aley, P.K., Angus, B., Becker, S., Belij-Rammerstorfer, S., Bellamy, D., Bibi, S., Bittaye, M., Clutterbuck, E.A., et al. (2020). Safety and immunogenicity of the ChAdOx1 nCoV-19 vaccine against SARS-CoV-2: a preliminary report of a phase 1/2, single-blind, randomised controlled trial. The Lancet *0*. https://doi.org/10.1016/S0140-6736(20)31604-4.

Fonville, J.M., Wilks, S.H., James, S.L., Fox, A., Ventresca, M., Aban, M., Xue, L., Jones, T.C., Le, N.M.H., Pham, Q.T., et al. (2014). Antibody landscapes after influenza virus infection or vaccination. Science *346*, 996–1000. https://doi.org/10.1126/science.1256427.

Forgacs, D., Abreu, R.B., Sautto, G.A., Kirchenbaum, G.A., Drabek, E., Williamson, K.S., Kim, D., Emerling, D.E., and Ross, T.M. (2021). Convergent antibody evolution and clonotype expansion following influenza virus vaccination. PLoS One *16*, e0247253. https://doi.org/10.1371/JOURNAL.PONE.0247253.

Förster, R., Schubel, A., Breitfeld, D., Kremmer, E., Renner-Müller, I., Wolf, E., and Lipp, M. (1999). CCR7 coordinates the primary immune response by establishing functional microenvironments in secondary lymphoid organs. Cell *99*, 23–33. https://doi.org/10.1016/S0092-8674(00)80059-8.

Foss, S., Jonsson, A., Bottermann, M., Watkinson, R., Lode, H.E., McAdam, M.B., Michaelsen, T.E., Sandlie, I., James, L.C., and Andersen, J.T. (2022). IgG3 hinge dependent enhancement of intracellular antiviral immunity. Sci Immunol *7*, eabj1640. https://doi.org/10.1126/SCIIMMUNOL.ABJ1640.

Frater, J., Ewer, K.J., Ogbe, A., Pace, M., Adele, S., Adland, E., Alagaratnam, J., Aley, P.K., Ali, M., Ansari, M.A., et al. (2021). Safety and immunogenicity of the ChAdOx1 nCoV-19 (AZD1222) vaccine against SARS-CoV-2 in HIV infection: a single-arm substudy of a phase 2/3 clinical trial. Lancet HIV *0*. https://doi.org/10.1016/S2352-3018(21)00103-X.

Gaebler, C., Wang, Z., Lorenzi, J.C.C., Muecksch, F., Finkin, S., Tokuyama, M., Cho, A., Jankovic, M., Schaefer-Babajew, D., Oliveira, T.Y., et al. (2021). Evolution of antibody immunity to SARS-CoV-2. Nature *591*, 639–644. https://doi.org/10.1038/s41586-021-03207-w.

Galanti, M., Birger, R., Ud-Dean, M., Filip, I., Morita, H., Comito, D., Anthony, S., Freyer, G.A., Ibrahim, S., Lane, B., et al. (2019). Longitudinal active sampling for respiratory viral infections across age groups. Influenza Other Respir Viruses *13*, 226–232. https://doi.org/10.1111/irv.12629.

Galli, S.J., and Tsai, M. (2012). IgE and mast cells in allergic disease. Nat Med *18*, 693. https://doi.org/10.1038/NM.2755.

Gallo, R.C., Salahuddin, S.Z., Popovic, M., Shearer, G.M., Kaplan, M., Haynes, B.F., Palker, T.J., Redfield, R., Oleske, J., Safai, B., et al. (1984). Frequent detection and isolation of cytopathic retroviruses (HTLV-III) from patients with AIDS and at risk for AIDS. Science *224*, 500–503. https://doi.org/10.1126/SCIENCE.6200936.

Galson, J.D., Trück, J., Clutterbuck, E.A., Fowler, A., Cerundolo, V., Pollard, A.J., Lunter, G., and Kelly, D.F. (2016). B-cell repertoire dynamics after sequential hepatitis B vaccination and evidence for cross-reactive B-cell activation. Genome Med *8*, 1–13. https://doi.org/10.1186/S13073-016-0322-Z/FIGURES/7.

Galson, J.D., Schaetzle, S., Bashford-Rogers, R.J.M., Raybould, M.I.J., Kovaltsuk, A., Kilpatrick, G.J., Minter, R., Finch, D.K., Dias, J., James, L.K., et al. (2020). Deep Sequencing of B Cell Receptor Repertoires From COVID-19 Patients Reveals Strong Convergent Immune Signatures. Front Immunol *11*, 605170. https://doi.org/10.3389/fimmu.2020.605170.

Gao, X., Shen, Q., Roco, J.A., Dalton, B., Frith, K., Mee, C., Munier, L., Ballard, F.D., Wang, K., Kelly, H.G., et al. (2024). Zeb2 drives the formation of CD11c + atypical B

cells to sustain germinal centers that control persistent infection. Sci Immunol *9*, 4748. https://doi.org/10.1126/SCIIMMUNOL.ADJ4748.

Garcia-Beltran, W.F., Lam, E.C., Astudillo, M.G., Yang, D., Miller, T.E., Feldman, J., Hauser, B.M., Caradonna, T.M., Clayton, K.L., Nitido, A.D., et al. (2021). COVID-19-neutralizing antibodies predict disease severity and survival. Cell *184*, 476-488.e11. https://doi.org/10.1016/j.cell.2020.12.015.

Garcia-Beltran, W.F., St. Denis, K.J., Hoelzemer, A., Lam, E.C., Nitido, A.D., Sheehan, M.L., Berrios, C., Ofoman, O., Chang, C.C., Hauser, B.M., et al. (2022). mRNA-based COVID-19 vaccine boosters induce neutralizing immunity against SARS-CoV-2 Omicron variant. Cell *185*, 457-466.e4. https://doi.org/10.1016/j.cell.2021.12.033.

Gasser, R., Cloutier, M., Prévost, J., Fink, C., Ducas, É., Ding, S., Dussault, N., Landry, P., Tremblay, T., Laforce-Lavoie, A., et al. (2021). Major role of IgM in the neutralizing activity of convalescent plasma against SARS-CoV-2. Cell Rep *34*, 108790. https://doi.org/10.1016/J.CELREP.2021.108790.

Gatto, D., Wood, K., and Brink, R. (2011). EBI2 Operates Independently of but in Cooperation with CXCR5 and CCR7 To Direct B Cell Migration and Organization in Follicles and the Germinal Center. The Journal of Immunology *187*, 4621–4628. https://doi.org/10.4049/JIMMUNOL.1101542.

Gay, D., Saunders, T., Camper, S., and Weigert, M. (1993). Receptor editing: An approach by autoreactive B cells to escape tolerance. Journal of Experimental Medicine *177*, 999–1008. https://doi.org/10.1084/jem.177.4.999.

Van Gent, D.C., Ramsden, D.A., and Gellert, M. (1996). The RAG1 and RAG2 proteins establish the 12/23 rule in V(D)J recombination. Cell *85*, 107–113. https://doi.org/10.1016/S0092-8674(00)81086-7.

George, V.K., Pallikkuth, S., Parmigiani, A., Alcaide, M., Fischl, M., Arheart, K.L., and Pahwa, S. (2015). HIV infection Worsens Age-Associated Defects in Antibody Responses to Influenza Vaccine. J Infect Dis *211*, 1959. https://doi.org/10.1093/INFDIS/JIU840.

Gerber, P.P., Duncan, L.M., Greenwood, E.J.D., Marelli, S., Naamati, A., Teixeira-Silva, A., Crozier, T.W.M., Gabaev, I., Zhan, J.R., Mulroney, T.E., et al. (2022). A

protease-activatable luminescent biosensor and reporter cell line for authentic SARS-CoV-2 infection. PLoS Pathog *18*, e1010265. https://doi.org/10.1371/JOURNAL.PPAT.1010265.

Geretti, A.M., Stockdale, A.J., Kelly, S.H., Cevik, M., Collins, S., Waters, L., Villa, G., Docherty, A., Harrison, E.M., Turtle, L., et al. (2021). Outcomes of Coronavirus Disease 2019 (COVID-19) Related Hospitalization among People with Human Immunodeficiency Virus (HIV) in the ISARIC World Health Organization (WHO) Clinical Characterization Protocol (UK): A Prospective Observational Study. Clinical Infectious Diseases *73*, E2095–E2106. https://doi.org/10.1093/cid/ciaa1605.

Ghafari, M., Hall, M., Golubchik, T., Ayoubkhani, D., House, T., MacIntyre-Cockett, G., Fryer, H.R., Thomson, L., Nurtay, A., Kemp, S.A., et al. (2024). Prevalence of persistent SARS-CoV-2 in a large community surveillance study. Nature 1–8. https://doi.org/10.1038/s41586-024-07029-4.

Gilbert, P.B., Montefiori, D.C., McDermott, A.B., Fong, Y., Benkeser, D., Deng, W., Zhou, H., Houchens, C.R., Martins, K., Jayashankar, L., et al. (2022). Immune correlates analysis of the mRNA-1273 COVID-19 vaccine efficacy clinical trial. Science *375*, 43–50. https://doi.org/10.1126/science.abm3425.

Gitlin, A.D., Mayer, C.T., Oliveira, T.Y., Shulman, Z., Jones, M.J.K., Koren, A., Nussenzweig, M.C., and Edu, N. (2015). T cell help controls the speed of the cell cycle in germinal center B cells. Science *349*, 643–646. https://doi.org/10.1126/science.aac4919.

Glick, B., Chang, T.S., and Jaap, R.G. (1956). The Bursa of Fabricius and Antibody Production. Poult Sci *35*, 224–225. https://doi.org/10.3382/PS.0350224.

Goel, R.R., Painter, M.M., Apostolidis, S.A., Mathew, D., Meng, W., Rosenfeld, A.M., Lundgreen, K.A., Reynaldi, A., Khoury, D.S., Pattekar, A., et al. (2021a). mRNA vaccines induce durable immune memory to SARS-CoV-2 and variants of concern. Science *374*. https://doi.org/10.1126/science.abm0829.

Goel, R.R., Apostolidis, S.A., Painter, M.M., Mathew, D., Pattekar, A., Kuthuru, O., Gouma, S., Hicks, P., Meng, W., Rosenfeld, A.M., et al. (2021b). Distinct antibody and memory B cell responses in SARSCoV-2 naïve and recovered individuals following mRNA vaccination. Sci Immunol *6*, 1–19. https://doi.org/10.1126/sciimmunol.abi6950.

Golinski, M.L., Demeules, M., Derambure, C., Riou, G., Maho-Vaillant, M., Boyer, O., Joly, P., and Calbo, S. (2020). CD11c+ B Cells Are Mainly Memory Cells, Precursors of Antibody Secreting Cells in Healthy Donors. Front Immunol *11*, 1–16. https://doi.org/10.3389/fimmu.2020.00032.

González, N., McKee, K., Lynch, R.M., Georgiev, I.S., Jimenez, L., Grau, E., Yuste, E., Kwong, P.D., Mascola, J.R., and Alcamí, J. (2018). Characterization of broadly neutralizing antibody responses to HIV-1 in a cohort of long term non-progressors. PLoS One *13*. https://doi.org/10.1371/JOURNAL.PONE.0193773.

Goodnow, C.C., Crosbie, J., Adelstein, S., Lavoie, T.B., Smith-Gill, S.J., Brink, R.A., Pritchard-Briscoe, H., Wotherspoon, J.S., Loblay, R.H., Raphael, K., et al. (1988). Altered immunoglobulin expression and functional silencing of self-reactive B lymphocytes in transgenic mice. Nature *334*, 676–682. https://doi.org/10.1038/334676a0.

Gottlieb, M.S., Schroff, R., Schanker, H.M., Weisman, J.D., Fan, P.T., Wolf, R.A., and Saxon, A. (1981). Pneumocystis carinii Pneumonia and Mucosal Candidiasis in Previously Healthy Homosexual Men . New England Journal of Medicine *305*, 1425–1431. https://doi.org/10.1056/NEJM198112103052401.

Graham, C., Seow, J., Huettner, I., Khan, H., Kouphou, N., Acors, S., Winstone, H., Pickering, S., Galao, R.P., Dupont, L., et al. (2021). Neutralization potency of monoclonal antibodies recognizing dominant and subdominant epitopes on SARS-CoV-2 Spike is impacted by the B.1.1.7 variant. Immunity *54*, 1–14. https://doi.org/10.1016/j.immuni.2021.03.023.

Gray, E.S., Madiga, M.C., Hermanus, T., Moore, P.L., Kurt Wibmer, C., Tumba, N.L., Werner, L., Mlisana, K., Sibeko, S., Williamson, C., et al. (2011). The Neutralization Breadth of HIV-1 Develops Incrementally over Four Years and Is Associated with CD4 T Cell Decline and High Viral Load during Acute Infection. J Virol *85*, 4828–4840. https://doi.org/10.1128/JVI.00198-11.

Greaney, A.J., Loes, A.N., Crawford, K.H.D., Starr, T.N., Malone, K.D., Chu, H.Y., and Bloom, J.D. (2021). Comprehensive mapping of mutations in the SARS-CoV-2 receptor-binding domain that affect recognition by polyclonal human plasma

antibodies. Cell Host Microbe *29*, 463-476.e6. https://doi.org/10.1016/j.chom.2021.02.003.

Grehan, K., Ferrara, F., and Temperton, N. (2015). An optimised method for the production of MERS-CoV spike expressing viral pseudotypes. MethodsX *2*, 379–384. https://doi.org/10.1016/j.mex.2015.09.003.

Greiff, V., Bhat, P., Cook, S.C., Menzel, U., Kang, W., and Reddy, S.T. (2015). A bioinformatic framework for immune repertoire diversity profiling enables detection of immunological status. Genome Med *7*, 1–15. https://doi.org/10.1186/S13073-015-0169-8/TABLES/1.

Griffith, S.A., and McCoy, L.E. (2021). To bnAb or Not to bnAb: Defining Broadly Neutralising Antibodies Against HIV-1. Front Immunol *12*. https://doi.org/10.3389/FIMMU.2021.708227/FULL.

Griffith, S., Muir, L., Suchanek, O., Hope, J., Pade, C., Gibbons, J.M., Tuong, Z.K., Fung, A., Touizer, E., Rees-Spear, C., et al. (2024). Preservation of memory B cell homeostasis in an individual producing broadly neutralising antibodies against HIV-1. BioRxiv https://doi.org/10.1101/2024.02.05.578789.

Grifoni, A., Weiskopf, D., Ramirez, S.I., Smith, D.M., Crotty, S., and Sette, A. (2020). Targets of T Cell Responses to SARS-CoV-2 Coronavirus in Humans with COVID-19 Disease and Unexposed Individuals. Cell https://doi.org/10.1016/j.cell.2020.05.015.

Gulick, R.M., Mellors, J.W., Havlir, D., Eron, J.J., Gonzalez, C., McMahon, D., Richman, D.D., Valentine, F.T., Jonas, L., Meibohm, A., et al. (1997). Treatment with Indinavir, Zidovudine, and Lamivudine in Adults with Human Immunodeficiency Virus Infection and Prior Antiretroviral Therapy. New England Journal of Medicine *337*, 734–739. https://doi.org/10.1056/nejm199709113371102.

Guo, L., Ren, L., Yang, S., Xiao, M., Chang, D., Yang, F., Dela Cruz, C.S., Wang, Y., Wu, C., Xiao, Y., et al. (2020). Profiling Early Humoral Response to Diagnose Novel Coronavirus Disease (COVID-19). Clin Infect Dis *71*, 778–785. https://doi.org/10.1093/CID/CIAA310.

Gupta, N.T., Vander Heiden, J.A., Uduman, M., Gadala-Maria, D., Yaari, G., and Kleinstein, S.H. (2015). Change-O: a toolkit for analyzing large-scale B cell

immunoglobulin repertoire sequencing data. Bioinformatics *31*, 3356–3358. https://doi.org/10.1093/BIOINFORMATICS/BTV359.

Gupta, N.T., Adams, K.D., Briggs, A.W., Timberlake, S.C., Vigneault, F., and Kleinstein, S.H. (2017). Hierarchical Clustering Can Identify B Cell Clones with High Confidence in Ig Repertoire Sequencing Data. The Journal of Immunology *198*, 2489–2499. https://doi.org/10.4049/jimmunol.1601850.

Gupta, R.K., Abdul-Jawad, S., McCoy, L.E., Mok, H.P., Peppa, D., Salgado, M., Martinez-Picado, J., Nijhuis, M., Wensing, A.M.J., Lee, H., et al. (2019). HIV-1 remission following CCR5Δ32/Δ32 haematopoietic stem cell transplantation. Nature *568*, 244. https://doi.org/10.1038/S41586-019-1027-4.

Hadfield, J., Megill, C., Bell, S.M., Huddleston, J., Potter, B., Callender, C., Sagulenko, P., Bedford, T., and Neher, R.A. (2018). Nextstrain: real-time tracking of pathogen evolution. Bioinformatics *34*, 4121–4123. https://doi.org/10.1093/BIOINFORMATICS/BTY407.

Hajnik, R.L., Plante, J.A., Liang, Y., Alameh, M.G., Tang, J., Bonam, S.R., Zhong, C., Adam, A., Scharton, D., Rafael, G.H., et al. (2022). Dual spike and nucleocapsid mRNA vaccination confer protection against SARS-CoV-2 Omicron and Delta variants in preclinical models. Sci Transl Med *14*, 1–15. https://doi.org/10.1126/scitranslmed.abq1945.

Hale, M., Netland, J., Chen, Y., Thouvenel, C.D., Smith, K.N., Rich, L.M., Vanderwall, E.R., Miranda, M.C., Eggenberger, J., Hao, L., et al. (2022). IgM antibodies derived from memory B cells are potent cross-variant neutralizers of SARS-CoV-2. J Exp Med *219*. https://doi.org/10.1084/JEM.20220849.

Hammer, S.M., Squires, K.E., Hughes, M.D., Grimes, J.M., Demeter, L.M., Currier, J.S., Eron, J.J., Feinberg, J.E., Balfour, H.H., Deyton, L.R., et al. (1997). A Controlled Trial of Two Nucleoside Analogues plus Indinavir in Persons with Human Immunodeficiency Virus Infection and CD4 Cell Counts of 200 per Cubic Millimeter or Less. New England Journal of Medicine *337*, 725–733. https://doi.org/10.1056/nejm199709113371101.

Hardy, R.R., Carmack, C.E., Shinton, S.A., Kemp, J.D., and Hayakawa, K. (1991). Resolution and characterization of pro-B and pre-pro-B cell stages in normal mouse bone marrow. J Exp Med *173*, 1213. https://doi.org/10.1084/JEM.173.5.1213.

Harker, S., James, S.E., Murphy, J., Davies, B., Moore, C., Tennant, B.P., Geen, J., and Thomas, D. (2023). Serosurveillance of SARS-CoV-2 in Welsh Blood Donors: Establishment of the surveillance system and results up to November 2022. Eurosurveillance *28*, 1. https://doi.org/10.2807/1560-7917.ES.2023.28.19.2200473.

Harris, R.J., Whitaker, H.J., Andrews, N.J., Aiano, F., Amin-Chowdhury, Z., Flood, J., Borrow, R., Linley, E., Ahmad, S., Stapley, L., et al. (2021). Serological surveillance of SARS-CoV-2: Six-month trends and antibody response in a cohort of public health workers. J Infect *82*, 162. https://doi.org/10.1016/J.JINF.2021.03.015.

Hartley, G.E., Edwards, E.S.J., Aui, P.M., Varese, N., Stojanovic, S., McMahon, J., Peleg, A.Y., Boo, I., Drummer, H.E., Hogarth, P.M., et al. (2020). Rapid generation of durable B cell memory to SARS-CoV-2 spike and nucleocapsid proteins in COVID-19 and convalescence. Sci Immunol *5*. https://doi.org/10.1126/sciimmunol.abf8891.

Hassold, N., Brichler, S., Ouedraogo, E., Leclerc, D., Carroue, S., Gater, Y., Alloui, C., Carbonnelle, E., Bouchaud, O., Mechai, F., et al. (2022). Impaired antibody response to COVID-19 vaccination in advanced HIV infection. AIDS *36*, F1–F5. https://doi.org/10.1097/QAD.0000000000003166.

Havervall, S., Marking, U., Svensson, J., Greilert-Norin, N., Bacchus, P., Nilsson, P., Hober, S., Gordon, M., Blom, K., Klingström, J., et al. (2022). Anti-Spike Mucosal IgA Protection against SARS-CoV-2 Omicron Infection. New England Journal of Medicine *387*, 1333–1336. https://doi.org/10.1056/NEJMC2209651/SUPPL_FILE/NEJMC2209651_DISCLOSURES.PDF.

Haynes, B.F., Wiehe, K., Borrow, P., Saunders, K.O., Korber, B., Wagh, K., McMichael, A.J., Kelsoe, G., Hahn, B.H., Alt, F., et al. (2023). Strategies for HIV-1 vaccines that induce broadly neutralizing antibodies. Nat Rev Immunol *23*, 142–158. https://doi.org/10.1038/s41577-022-00753-w.

He, J., Tsai, L.M., Leong, Y.A., Hu, X., Ma, C.S., Chevalier, N., Sun, X., Vandenberg, K., Rockman, S., Ding, Y., et al. (2013). Circulating precursor CCR7loPD-1hi CXCR5+

CD4+ T cells indicate tfh cell activity and promote antibody responses upon antigen reexposure. Immunity *39*, 770–781. https://doi.org/10.1016/j.immuni.2013.09.007.

Heath, P.T., Galiza, E.P., Baxter, D.N., Boffito, M., Browne, D., Burns, F., Chadwick, D.R., Clark, R., Cosgrove, C., Galloway, J., et al. (2021). Safety and Efficacy of NVX-CoV2373 Covid-19 Vaccine. New England Journal of Medicine *385*, 1172–1183. https://doi.org/10.1056/NEJMOA2107659/SUPPL_FILE/NEJMOA2107659_DATA-SHARING.PDF.

Heather, J.M., Best, K., Oakes, T., Gray, E.R., Roe, J.K., Thomas, N., Friedman, N., Noursadeghi, M., and Chain, B. (2015). Dynamic Perturbations of the T-Cell Receptor Repertoire in Chronic HIV Infection and following Antiretroviral Therapy. Front Immunol *6*. https://doi.org/10.3389/FIMMU.2015.00644.

Heftdal, L.D., Knudsen, A.D., Hamm, S.R., Hansen, C.B., Møller, D.L., Pries-Heje, M., Fogh, K., Hasselbalch, R.B., Jarlhelt, I., Pérez-Alós, L., et al. (2022). Humoral response to two doses of BNT162b2 vaccination in people with HIV. J Intern Med *291*, 513. https://doi.org/10.1111/JOIM.13419.

Vander Heiden, J.A., Yaari, G., Uduman, M., Stern, J.N.H., O'connor, K.C., Hafler, D.A., Vigneault, F., and Kleinstein, S.H. (2014). pRESTO: a toolkit for processing high-throughput sequencing raw reads of lymphocyte receptor repertoires. Bioinformatics *30*, 1930–1932. https://doi.org/10.1093/BIOINFORMATICS/BTU138.

Hensley, K.S., Jongkees, M.J., Geers, D., GeurtsvanKessel, C.H., Mueller, Y.M., Dalm, V.A.S.H., Papageorgiou, G., Steggink, H., Gorska, A., Bogers, S., et al. (2022). Immunogenicity and reactogenicity of SARSCoV-2 vaccines in people living with HIV in the Netherlands: A nationwide prospective cohort study. PLoS Med *19*, e1003979. https://doi.org/10.1371/journal.pmed.1003979.

Hess, J., Werner, A., Wirth, T., Melchers, F., Jäck, H.M., and Winkler, T.H. (2001). Induction of pre-B cell proliferation after de novo synthesis of the pre-B cell receptor. Proc Natl Acad Sci U S A *98*, 1745–1750. https://doi.org/10.1073/pnas.98.4.1745.

Hill, M.O. (1973). Diversity and Evenness: A Unifying Notation and Its Consequences. Ecology *54*, 427–432. https://doi.org/10.2307/1934352.

Ho, J., Moir, S., Malaspina, A., Howell, M.L., Wang, W., DiPoto, A.C., O'Shea, M.A., Roby, G.A., Kwan, R., Mican, J.A.M., et al. (2006). Two overrepresented B cell populations in HIV-infected individuals undergo apoptosis by different mechanisms. Proc Natl Acad Sci U S A *103*, 19436–19441. https://doi.org/10.1073/pnas.0609515103.

Hoffmann, C., Casado, J.L., Härter, G., Vizcarra, P., Moreno, A., Cattaneo, D., Meraviglia, P., Spinner, C.D., Schabaz, F., Grunwald, S., et al. (2021). Immune deficiency is a risk factor for severe COVID-19 in people living with HIV. HIV Med *22*, 372–378. https://doi.org/10.1111/HIV.13037.

Hoffmann, M., Kleine-Weber, H., and Pöhlmann, S. (2020). A Multibasic Cleavage Site in the Spike Protein of SARS-CoV-2 Is Essential for Infection of Human Lung Cells. Mol Cell *78*, 779-784.e5. https://doi.org/10.1016/j.molcel.2020.04.022.

Holla, P., Dizon, B., Ambegaonkar, A.A., Rogel, N., Goldschmidt, E., Boddapati, A.K., Sohn, H., Sturdevant, D., Austin, J.W., Kardava, L., et al. (2021). Shared transcriptional profiles of atypical B cells suggest common drivers of expansion and function in malaria, HIV, and autoimmunity. Sci Adv *7*, 8384–8410. https://doi.org/10.1126/SCIADV.ABG8384/SUPPL_FILE/SCIADV.ABG8384_TABLES.

Hornsby, H., Nicols, A.R., Longet, S., Liu, C., Tomic, A., Angyal, A., Kronsteiner, B., Tyerman, J.K., Tipton, T., Zhang, P., et al. (2023). Omicron infection following vaccination enhances a broad spectrum of immune responses dependent on infection history. Nat Commun *14*, 1–16. https://doi.org/10.1038/s41467-023-40592-4.

Hou, Y.J., Okuda, K., Edwards, C.E., Martinez, D.R., Asakura, T., Dinnon, K.H., Kato, T., Lee, R.E., Yount, B.L., Mascenik, T.M., et al. (2020a). SARS-CoV-2 Reverse Genetics Reveals a Variable Infection Gradient in the Respiratory Tract. Cell *182*, 429. https://doi.org/10.1016/J.CELL.2020.05.042.

Hou, Y.J., Chiba, S., Halfmann, P., Ehre, C., Kuroda, M., Dinnon, K.H., Leist, S.R., Schäfer, A., Nakajima, N., Takahashi, K., et al. (2020b). SARS-CoV-2 D614G variant exhibits efficient replication ex vivo and transmission in vivo. Science *370*, 1464–1468. https://doi.org/10.1126/science.abe8499.

Hsu, J., Van Besien, K., Glesby, M.J., Pahwa, S., Coletti, A., Warshaw, M.G., Petz, L., Moore, T.B., Chen, Y.H., Pallikkuth, S., et al. (2023). HIV-1 remission and possible cure in a woman after haplo-cord blood transplant. Cell *186*, 1115-1126.e8. https://doi.org/10.1016/J.CELL.2023.02.030.

Huang, A.T., Garcia-Carreras, B., Hitchings, M.D.T., Yang, B., Katzelnick, L.C., Rattigan, S.M., Borgert, B.A., Moreno, C.A., Solomon, B.D., Trimmer-Smith, L., et al. (2020). A systematic review of antibody mediated immunity to coronaviruses: kinetics, correlates of protection, and association with severity. Nat Commun *11*. https://doi.org/10.1038/S41467-020-18450-4.

Huang, J., Xie, N., Hu, X., Yan, H., Ding, J., Liu, P., Ma, H., Ruan, L., Li, G., He, N., et al. (2021). Epidemiological, Virological and Serological Features of Coronavirus Disease 2019 (COVID-19) Cases in People Living With Human Immunodeficiency Virus in Wuhan: A Population-based Cohort Study. Clinical Infectious Diseases *73*, E2086–E2094. https://doi.org/10.1093/cid/ciaa1186.

Huang, X., Yan, Y., Su, B., Xiao, D., Yu, M., Jin, X., Duan, J., Zhang, X., Zheng, S., Fang, Y., et al. (2022). Comparing Immune Responses to Inactivated Vaccines against SARS-CoV-2 between People Living with HIV and HIV-Negative Individuals: A Cross-Sectional Study in China. Viruses *14*, 277. https://doi.org/10.3390/V14020277/S1.

Hung, C.C., Chang, S.Y., Su, C.T., Chen, Y.Y., Chang, S.F., Yang, C.Y., Liu, W.C., Wu, C.H., and Chang, S.C. (2010). A 5-year longitudinal follow-up study of serological responses to 23-valent pneumococcal polysaccharide vaccination among patients with HIV infection who received highly active antiretroviral therapy. HIV Med *11*, 54–63. https://doi.org/10.1111/j.1468-1293.2009.00744.x.

Hwa, S.H., Snyman, J., Bernstein, M., Ganga, Y., Cele, S., Muema, D., Tan, C.W., Khan, K., Karim, F., Hanekom, W., et al. (2023). Association Between Human Immunodeficiency Virus Viremia and Compromised Neutralization of Severe Acute Respiratory Syndrome Coronavirus 2 Beta Variant. Journal of Infectious Diseases *227*, 211–220. https://doi.org/10.1093/infdis/jiac343.

Inciarte, A., Gonzalez-Cordon, A., Rojas, J., Torres, B., De Lazzari, E., De La Mora, L., Martinez-Rebollar, M., Laguno, M., Callau, P., Gonzalez-Navarro, A., et al. (2020). Clinical characteristics, risk factors, and incidence of symptomatic coronavirus disease

2019 in a large cohort of adults living with HIV: A single-center, prospective observational study. AIDS *34*, 1775–1780. https://doi.org/10.1097/QAD.0000000000002643.

Irrgang, P., Gerling, J., Kocher, K., Lapuente, D., Steininger, P., Habenicht, K., Wytopil, M., Beileke, S., Schäfer, S., Zhong, J., et al. (2022). Class switch towards non-inflammatory, spike-specific IgG4 antibodies after repeated SARS-CoV-2 mRNA vaccination. Sci Immunol https://doi.org/10.1126/SCIIMMUNOL.ADE2798.

Iyer, A.S., Jones, F.K., Nodoushani, A., Kelly, M., Becker, M., Slater, D., Mills, R., Teng, E., Kamruzzaman, M., Garcia-Beltran, W.F., et al. (2020). Persistence and decay of human antibody responses to the receptor binding domain of SARS-CoV-2 spike protein in COVID-19 patients. Sci Immunol *5*. https://doi.org/10.1126/SCIIMMUNOL.ABE0367/SUPPL_FILE/ABE0367_TABLE_S4.XLSX.

Jackson, K.J.L., Liu, Y., Roskin, K.M., Glanville, J., Hoh, R.A., Seo, K., Marshall, E.L., Gurley, T.C., Moody, M.A., Haynes, B.F., et al. (2014). Human responses to influenza vaccination show seroconversion signatures and convergent antibody rearrangements. Cell Host Microbe *16*, 105–114. https://doi.org/10.1016/j.chom.2014.05.013.

Jackson, L.A., Anderson, E.J., Rouphael, N.G., Roberts, P.C., Makhene, M., Coler, R.N., McCullough, M.P., Chappell, J.D., Denison, M.R., Stevens, L.J., et al. (2020). An mRNA Vaccine against SARS-CoV-2 — Preliminary Report. New England Journal of Medicine *383*, 1920–1931. https://doi.org/10.1056/NEJMOA2022483/SUPPL_FILE/NEJMOA2022483_DATA-SHARING.PDF.

Jaffe, D.B., Shahi, P., Adams, B.A., Chrisman, A.M., Finnegan, P.M., Raman, N., Royall, A.E., Tsai, F.N., Vollbrecht, T., Reyes, D.S., et al. (2022). Functional antibodies exhibit light chain coherence. Nature *611*, 352–357. https://doi.org/10.1038/s41586-022-05371-z.

JCVI (2021a). Optimising the COVID-19 vaccination programme for maximum short-term impact - 26 January 2021.

JCVI (2021b). Use of the AstraZeneca COVID-19 (AZD1222) vaccine: updated JCVI statement - 7 May 2021.

JCVI (2022). COVID-19 Greenbook chapter 14a - 28 February 2022.

JCVI (2023). A guide to the COVID-19 spring booster 2023 (Updated 26 April 2023).

JCVI (2024). Greenbook Chapter 35: Yellow fever - February 2024.

Jedicke, N., Stankov, M. V., Cossmann, A., Dopfer-Jablonka, A., Knuth, C., Ahrenstorf, G., Ramos, G.M., and Behrens, G.M.N. (2022). Humoral immune response following prime and boost BNT162b2 vaccination in people living with HIV on antiretroviral therapy. HIV Med *23*, 558–563. https://doi.org/10.1111/HIV.13202.

Jeffery-Smith, A., Burton, A.R., Lens, S., Rees-Spear, C., Davies, J., Patel, M., Gopal, R., Muir, L., Aiano, F., Doores, K.J., et al. (2022). SARS-CoV-2–specific memory B cells can persist in the elderly who have lost detectable neutralizing antibodies. Journal of Clinical Investigation *132*. https://doi.org/10.1172/JCI152042.

Jenks, S.A., Cashman, K.S., Boss, J.M., Lund, F.E., and Correspondence, I.S. (2018). Distinct Effector B Cells Induced by Unregulated Toll-like Receptor 7 Contribute to Pathogenic Responses in Systemic Lupus Erythematosus The properties of SLE DN2 B cells stem from distinct transcriptional networks. Immunity *49*, 725–739. https://doi.org/10.1016/j.immuni.2018.08.015.

Jensen, B.E.O., Knops, E., Cords, L., Lübke, N., Salgado, M., Busman-Sahay, K., Estes, J.D., Huyveneers, L.E.P., Perdomo-Celis, F., Wittner, M., et al. (2023). In-depth virological and immunological characterization of HIV-1 cure after CCR5Δ32/Δ32 allogeneic hematopoietic stem cell transplantation. Nat Med *29*, 583. https://doi.org/10.1038/S41591-023-02213-X.

Jongkees, M.J., Geers, D., Hensley, K.S., Huisman, W., GeurtsvanKessel, C.H., Bogers, S., Gommers, L., Papageorgiou, G., Jochems, S.P., den Hollander, J.G., et al. (2023). Immunogenicity of an Additional mRNA-1273 SARS-CoV-2 Vaccination in People With HIV With Hyporesponse After Primary Vaccination. Journal of Infectious Diseases *227*, 651–662. https://doi.org/10.1093/infdis/jiac451.

Ju, B., Zhang, Q., Ge, J., Wang, R., Sun, J., Ge, X., Yu, J., Shan, S., Zhou, B., Song, S., et al. (2020). Human neutralizing antibodies elicited by SARS-CoV-2 infection. Nature *584*, 115–119. https://doi.org/10.1038/s41586-020-2380-z.

Kabat, E.A., and Wu, T.T. (1991). Identical V region amino acid sequences and segments of sequences in antibodies of different specificities. Relative contributions of VH and VL genes, minigenes, and complementarity-determining regions to binding of antibody-combining sites. The Journal of Immunology *147*, 1709–1719. https://doi.org/10.4049/jimmunol.147.5.1709.

Karasuyama, H., Rolink, A., and Melchers, F. (1993). A complex of glycoproteins is associated with VpreB/λ5 Surrogate Light Chain on the Surface of μ Heavy Chain-negative Early Precursor B Cell Lines. Journal of Experimental Medicine *178*, 469–478. https://doi.org/10.1084/jem.178.2.469.

Kardava, L., Moir, S., Shah, N., Wang, W., Wilson, R., Buckner, C.M., Santich, B.H., Kim, L.J.Y., Spurlin, E.E., Nelson, A.K., et al. (2014). Abnormal B cell memory subsets dominate HIV-specific responses in infected individuals. Journal of Clinical Investigation *124*, 3252–3262. https://doi.org/10.1172/JCI74351.

Kardava, L., Sohn, H., Youn, C., Austin, J.W., Wang, W., Buckner, C.M., Justement, J.S., Melson, V.A., Roth, G.E., Hand, M.A., et al. (2018). IgG3 regulates tissue-like memory B cells in HIV-infected individuals. Nat Immunol *19*, 1001–1012. https://doi.org/10.1038/s41590-018-0180-5.

Kardava, L., Rachmaninoff, N., Lau, W.W., Buckner, C.M., Trihemasava, K., Blazkova, J., de Assis, F.L., Wang, W., Zhang, X., Wang, Y., et al. (2022). Early human B cell signatures of the primary antibody response to mRNA vaccination. Proc Natl Acad Sci U S A *119*. https://doi.org/10.1073/PNAS.2204607119/-/DCSUPPLEMENTAL.

Karikó, K., Buckstein, M., Ni, H., and Weissman, D. (2005). Suppression of RNA recognition by Toll-like receptors: The impact of nucleoside modification and the evolutionary origin of RNA. Immunity *23*, 165–175. https://doi.org/10.1016/j.immuni.2005.06.008.

Karikó, K., Muramatsu, H., Welsh, F.A., Ludwig, J., Kato, H., Akira, S., and Weissman, D. (2008). Incorporation of Pseudouridine Into mRNA Yields Superior

Nonimmunogenic Vector With Increased Translational Capacity and Biological Stability. Mol Ther *16*, 1833. https://doi.org/10.1038/MT.2008.200.

Karim, F., Gazy, I., Cele, S., Zungu, Y., Krause, R., Bernstein, M., Khan, K., Ganga, Y., Rodel, H., Mthabela, N., et al. (2021). HIV status alters disease severity and immune cell responses in beta variant sars-COV-2 infection wave. Elife *10*, 1–19. https://doi.org/10.7554/eLife.67397.

Kassanjee, R., Davies, M.A., Ngwenya, O., Osei-Yeboah, R., Jacobs, T., Morden, E., Timmerman, V., Britz, S., Mendelson, M., Taljaard, J., et al. (2023). COVID-19 among adults living with HIV: correlates of mortality among public sector healthcare users in Western Cape, South Africa. AIDS *26*, 26104. https://doi.org/10.1002/jia2.26104.

Kemp, S.A., Collier, D.A., Datir, R.P., Ferreira, I.A.T.M., Gayed, S., Jahun, A., Hosmillo, M., Rees-Spear, C., Mlcochova, P., Lumb, I.U., et al. (2021). SARS-CoV-2 evolution during treatment of chronic infection. Nature *592*, 277–282. https://doi.org/10.1038/s41586-021-03291-y.

Kernéis, S., Launay, O., Turbelin, C., Batteux, F., Hanslik, T., and Boëlle, P.Y. (2014). Long-term immune responses to vaccination in HIV-infected patients: A systematic review and meta-analysis. Clinical Infectious Diseases *58*, 1130–1139. https://doi.org/10.1093/cid/cit937.

Khan, K., Lustig, G., Bernstein, M., Archary, D., Cele, S., Karim, F., Smith, M., Ganga, Y., Jule, Z., Reedoy, K., et al. (2022). Immunogenicity of Severe Acute Respiratory Syndrome Coronavirus 2 (SARS-CoV-2) Infection and Ad26.CoV2.S Vaccination in People Living With Human Immunodeficiency Virus (HIV). Clinical Infectious Diseases *75*, E857–E864. https://doi.org/10.1093/cid/ciab1008.

Khoury, D.S., Wheatley, A.K., Ramuta, M.D., Reynaldi, A., Cromer, D., Subbarao, K., O'Connor, D.H., Kent, S.J., and Davenport, M.P. (2020). Measuring immunity to SARS-CoV-2 infection: comparing assays and animal models. Nat Rev Immunol *20*, 727. https://doi.org/10.1038/S41577-020-00471-1.

Kim, C.C., Baccarella, A.M., Bayat, A., Pepper, M., and Fontana, M.F. (2019). FCRL5 + Memory B Cells Exhibit Robust Recall Responses. Cell Rep *27*, 1446-1460.e4. https://doi.org/10.1016/J.CELREP.2019.04.019.

Kim, I.J., Lee, Y. ho, Khalid, M.M., Chen, I.P., Zhang, Y., Ott, M., and Verdin, E. (2023). SARS-CoV-2 protein ORF8 limits expression levels of Spike antigen and facilitates immune evasion of infected host cells. Journal of Biological Chemistry *299*, 104955. https://doi.org/10.1016/j.jbc.2023.104955.

Kityo, C., Makamdop, K.N., Rothenberger, M., Chipman, J.G., Hoskuldsson, T., Beilman, G.J., Grzywacz, B., Mugyenyi, P., Ssali, F., Akondy, R.S., et al. (2018). Lymphoid tissue fibrosis is associated with impaired vaccine responses. J Clin Invest *128*, 2763–2773. https://doi.org/10.1172/JCI97377.

van der Klaauw, A.A., Horner, E.C., Pereyra-Gerber, P., Agrawal, U., Foster, W.S., Spencer, S., Vergese, B., Smith, M., Henning, E., Ramsay, I.D., et al. (2023). Accelerated waning of the humoral response to COVID-19 vaccines in obesity. Nat Med *29*, 1146. https://doi.org/10.1038/S41591-023-02343-2.

Klein, U., Rajewsky, K., and Küppers, R. (1998). Human Immunoglobulin (Ig)M+IgD+ Peripheral Blood B Cells Expressing the CD27 Cell Surface Antigen Carry Somatically Mutated Variable Region Genes: CD27 as a General Marker for Somatically Mutated (Memory) B Cells. J Exp Med *188*, 1679. https://doi.org/10.1084/JEM.188.9.1679.

Klemis, V., Schmidt, T., Schub, D., Mihm, J., Marx, S., Abu-Omar, A., Ziegler, L., Hielscher, F., Guckelmus, C., Urschel, R., et al. (2022). Comparative immunogenicity and reactogenicity of heterologous ChAdOx1-nCoV-19-priming and BNT162b2 or mRNA-1273-boosting with homologous COVID-19 vaccine regimens. Nat Commun *13*. https://doi.org/10.1038/S41467-022-32321-0.

Knox, J.J., Buggert, M., Kardava, L., Seaton, K.E., Eller, M.A., Canaday, D.H., Robb, M.L., Ostrowski, M.A., Deeks, S.G., Slifka, M.K., et al. (2017). T-bet+ B cells are induced by human viral infections and dominate the HIV gp140 response. JCI Insight *2*. https://doi.org/10.1172/JCI.INSIGHT.92943.

Kondo, M., Weissman, I.L., and Akashi, K. (1997). Identification of clonogenic common lymphoid progenitors in mouse bone marrow. Cell *91*, 661–672. https://doi.org/10.1016/S0092-8674(00)80453-5.

Korber, B., Fischer, W.M., Gnanakaran, S., Yoon, H., Theiler, J., Abfalterer, W., Hengartner, N., Giorgi, E.E., Bhattacharya, T., Foley, B., et al. (2020). Tracking

Changes in SARS-CoV-2 Spike: Evidence that D614G Increases Infectivity of the COVID-19 Virus. Cell *182*, 812. https://doi.org/10.1016/J.CELL.2020.06.043.

Korencak, M., Byrne, M., Richter, E., Schultz, B.T., Juszczak, P., Ake, J.A., Ganesan, A., Okulicz, J.F., Robb, M.L., De Los Reyes, B., et al. (2019). Effect of HIV infection and antiretroviral therapy on immune cellular functions. JCI Insight *4*. https://doi.org/10.1172/JCI.INSIGHT.126675.

Kotagiri, P., Mescia, F., Rae, W.M., Bergamaschi, L., Tuong, Z.K., Turner, L., Hunter, K., Gerber, P.P., Hosmillo, M., Hess, C., et al. (2022). B cell receptor repertoire kinetics after SARS-CoV-2 infection and vaccination. Cell Rep *38*. https://doi.org/10.1016/J.CELREP.2022.110393.

Krammer, F., Srivastava, K., Alshammary, H., Amoako, A.A., Awawda, M.H., Beach, K.F., Bermúdez-González, M.C., Bielak, D.A., Carreño, J.M., Chernet, R.L., et al. (2021). Antibody Responses in Seropositive Persons after a Single Dose of SARS-CoV-2 mRNA Vaccine. New England Journal of Medicine *384*, 1372–1374. https://doi.org/10.1056/nejmc2101667.

Krause, J.C., Tsibane, T., Tumpey, T.M., Huffman, C.J., Briney, B.S., Smith, S.A., Basler, C.F., and Crowe, J.E. (2011). Epitope-Specific Human Influenza Antibody Repertoires Diversify by B Cell Intraclonal Sequence Divergence and Interclonal Convergence. The Journal of Immunology *187*, 3704–3711. https://doi.org/10.4049/jimmunol.1101823.

Krause, R., Snyman, J., Shi-Hsia, H., Muema, D., Karim, F., Ganga, Y., Ngoepe, A., Zungu, Y., Gazy, I., Bernstein, M., et al. (2022). HIV skews the SARS-CoV-2 B cell response toward an extrafollicular maturation pathway. Elife *11*. https://doi.org/10.7554/ELIFE.79924.

Kreer, C., Döring, M., Lehnen, N., Ercanoglu, M.S., Gieselmann, L., Luca, D., Jain, K., Schommers, P., Pfeifer, N., and Klein, F. (2020). openPrimeR for multiplex amplification of highly diverse templates. J Immunol Methods *480*, 112752. https://doi.org/10.1016/J.JIM.2020.112752.

Krokhin, O., Li, Y., Andonov, A., Feldmann, H., Flick, R., Jones, S., Stroeher, U., Bastien, N., Dasuri, K.V.N., Cheng, K., et al. (2003). Mass spectrometric

characterization of proteins from the SARS virus: a preliminary report. Mol Cell Proteomics *2*, 346–356. https://doi.org/10.1074/mcp.M300048-MCP200.

Kroon, F.P., Van Dissel, J.T., De Jong, J.C., and Van Furth, R. (1994). Antibody response to influenza, tetanus and pneumococcal vaccines in HIV-seropositive individuals in relation to the number of CD4+ lymphocytes. AIDS *8*, 469–476. https://doi.org/10.1097/00002030-199404000-00008.

Kuri-Cervantes, L., Pampena, M.B., Meng, W., Rosenfeld, A.M., Ittner, C.A.G., Weisman, A.R., Agyekum, R.S., Mathew, D., Baxter, A.E., Vella, L.A., et al. (2020). Comprehensive mapping of immune perturbations associated with severe COVID-19. Sci Immunol *5*. https://doi.org/10.1126/SCIIMMUNOL.ABD7114.

Kurosaki, T., Kometani, K., and Ise, W. (2015). Memory B cells. Nat Rev Immunol *15*, 149–159. https://doi.org/10.1038/nri3802.

De La Torre-Tarazona, E., González-Robles, A., Cascajero, A., Jiménez, P., Miró, J.M., Sánchez-Palomino, S., Alcamí, J., Buzón, M.J., and García-Pérez, J. (2023). Treatment with integrase inhibitors alters SARS-CoV-2 neutralization levels measured with HIV-based pseudotypes in people living with HIV. J Med Virol *95*. https://doi.org/10.1002/jmv.28543.

Lamacchia, G., Salvati, L., Kiros, S.T., Mazzoni, A., Vanni, A., Capone, M., Carnasciali, A., Farahvachi, P., Lagi, F., Di Lauria, N., et al. (2022). Fourth Dose of mRNA COVID-19 Vaccine Transiently Reactivates Spike-Specific Immunological Memory in People Living with HIV (PLWH). Biomedicines *10*, 3261. https://doi.org/10.3390/BIOMEDICINES10123261/S1.

Lambert, N.D., Ovsyannikova, I.G., Pankratz, V.S., Jacobson, R.M., and Poland, G.A. (2012). Understanding the immune response to seasonal influenza vaccination in older adults: a systems biology approach. Expert Rev Vaccines *11*, 985. https://doi.org/10.1586/ERV.12.61.

Landau, N.R., Schatz, D.G., Rosa, M., and Baltimore, D. (1987). Increased frequency of N-region insertion in a murine pre-B-cell line infected with a terminal deoxynucleotidyl transferase retroviral expression vector. Mol Cell Biol *7*, 3237. https://doi.org/10.1128/MCB.7.9.3237.

Lane, H.C., Masur, H., Edgar, L.C., Whalen, G., Rook, A.H., and Fauci, A.S. (1983). Abnormalities of B-Cell Activation and Immunoregulation in Patients with the Acquired Immunodeficiency Syndrome. New England Journal of Medicine *309*, 453–458. https://doi.org/10.1056/nejm198308253090803.

Lane, H.C., Depper, J.M., Greene, W.C., Whalen, G., Waldmann, T.A., and Fauci, A.S. (1985). Qualitative Analysis of Immune Function in Patients with the Acquired Immunodeficiency Syndrome. New England Journal of Medicine *313*, 79–84. https://doi.org/10.1056/nejm198507113130204.

Lapointe, H.R., Mwimanzi, F., Cheung, P.K., Sang, Y., Yaseen, F., Speckmaier, S., Barad, E., Moran-Garcia, N., Datwani, S., Duncan, M.C., et al. (2023a). Antibody response durability following three-dose coronavirus disease 2019 vaccination in people with HIV receiving suppressive antiretroviral therapy. AIDS *37*, 709–721. https://doi.org/10.1097/QAD.0000000000003469.

Lapointe, H.R., Mwimanzi, F., Cheung, P.K., Sang, Y., Yaseen, F., Umviligihozo, G., Kalikawe, R., Speckmaier, S., Moran-Garcia, N., Datwani, S., et al. (2023b). People With Human Immunodeficiency Virus Receiving Suppressive Antiretroviral Therapy Show Typical Antibody Durability After Dual Coronavirus Disease 2019 Vaccination and Strong Third Dose Responses. In Journal of Infectious Diseases, (Oxford University Press), pp. 838–849.

Lau, D., Lan, L.Y.L., Andrews, S.F., Henry, C., Rojas, K.T., Neu, K.E., Huang, M., Huang, Y., DeKosky, B., Palm, A.K.E., et al. (2017). Low CD21 expression defines a population of recent germinal center graduates primed for plasma cell differentiation. Sci Immunol *2*. https://doi.org/10.1126/SCIIMMUNOL.AAI8153.

Lazarus, R., Querton, B., Corbic Ramljak, I., Dewasthaly, S., Jaramillo, J.C., Dubischar, K., Krammer, M., Weisova, P., Hochreiter, R., Eder-Lingelbach, S., et al. (2022). Immunogenicity and safety of an inactivated whole-virus COVID-19 vaccine (VLA2001) compared with the adenoviral vector vaccine ChAdOx1-S in adults in the UK (COV-COMPARE): interim analysis of a randomised, controlled, phase 3, immunobridging trial. Lancet Infect Dis *22*, 1716–1727. https://doi.org/10.1016/S1473-3099(22)00502-3.

Le, T., Wright, E.J., Smith, D.M., He, W., Catano, G., Okulicz, J.F., Young, J.A., Clark, R.A., Richman, D.D., Little, S.J., et al. (2013). Enhanced CD4+ T-Cell Recovery with Earlier HIV-1 Antiretroviral Therapy. New England Journal of Medicine *368*, 218–230. https://doi.org/10.1056/NEJMOA1110187/SUPPL_FILE/NEJMOA1110187_DISCLOSURES.PDF.

Le, T.L., Kim, T.H., and Chaplin, D.D. (2008). Intraclonal Competition Inhibits the Formation of High-Affinity Antibody-Secreting Cells. The Journal of Immunology *181*, 6027–6037. https://doi.org/10.4049/jimmunol.181.9.6027.

Lechmere, T., Snell, L.B., Graham, C., Seow, J., Shalim, Z.A., Charalampous, T., Alcolea-Medina, A., Batra, R., Nebbia, G., Edgeworth, J.D., et al. (2022). Broad Neutralization of SARS-CoV-2 Variants, Including Omicron, following Breakthrough Infection with Delta in COVID- 19-Vaccinated Individuals. MBio *13*. https://doi.org/10.1128/mbio.03798-21.

Ledergerber, B., Egger, M., Erard, V., Weber, R., Hirschel, B., Furrer, H., Battegay, M., Vernazza, P., Bernasconi, E., Opravil, M., et al. (1999). AIDS-Related Opportunistic Illnesses Occurring After Initiation of Potent Antiretroviral Therapy: The Swiss HIV Cohort Study. JAMA *282*, 2220–2226. https://doi.org/10.1001/JAMA.282.23.2220.

Lee, I.T., Cosgrove, C.A., Moore, P., Bethune, C., Nally, R., Bula, M., Kalra, P.A., Clark, R., Dargan, P.I., Boffito, M., et al. (2023). Omicron BA.1-containing mRNA-1273 boosters compared with the original COVID-19 vaccine in the UK: a randomised, observer-blind, active-controlled trial. Lancet Infect Dis *23*, 1007–1019. https://doi.org/10.1016/S1473-3099(23)00295-5.

Lee, S.K., Rigby, R.J., Zotos, D., Tsai, L.M., Kawamoto, S., Marshall, J.L., Ramiscal, R.R., Chan, T.D., Gatto, D., Brink, R., et al. (2011). B cell priming for extrafollicular antibody responses requires Bcl-6 expression by T cells. Journal of Experimental Medicine *208*, 1377–1388. https://doi.org/10.1084/jem.20102065.

Lefranc, M.P., and Lefranc, G. (2023). Antibody Sequence and Structure Analyses Using IMGT®: 30 Years of Immunoinformatics. Methods in Molecular Biology *2552*, 3–59. https://doi.org/10.1007/978-1-0716-2609-2_1/FIGURES/16.

Lesley, R., Xu, Y., Kalled, S.L., Hess, D.M., Schwab, S.R., Shu, H.B., and Cyster, J.G. (2004). Reduced Competitiveness of Autoantigen-Engaged B Cells due to Increased Dependence on BAFF. Immunity *20*, 441–453. https://doi.org/10.1016/S1074-7613(04)00079-2.

Leston, M., Elson, W., Ordóñez-Mena, J.M., Kar, D., Whitaker, H., Joy, M., Roberts, N., Hobbs, F.D.R., and de Lusignan, S. (2024). Disparities in COVID-19 mortality amongst the immunosuppressed: A systematic review and meta-analysis for enhanced disease surveillance. Journal of Infection *88*, 106110. https://doi.org/10.1016/J.JINF.2024.01.009.

Leung, D.T.M., Tam, F.C.H., Ma, C.H., Chan, P.K.S., Cheung, J.L.K., Niu, H., Tam, J.S.L., and Lim, P.L. (2004). Antibody Response of Patients with Severe Acute Respiratory Syndrome (SARS) Targets the Viral Nucleocapsid. J Infect Dis *190*, 379–386. https://doi.org/10.1086/422040.

Levin, E.G., Lustig, Y., Cohen, C., Fluss, R., Indenbaum, V., Amit, S., Doolman, R., Asraf, K., Mendelson, E., Ziv, A., et al. (2021). Waning Immune Humoral Response to BNT162b2 Covid-19 Vaccine over 6 Months. New England Journal of Medicine *385*, e84. https://doi.org/10.1056/NEJMOA2114583/SUPPL_FILE/NEJMOA2114583_DATA-SHARING.PDF.

Levy, I., Wieder-Finesod, A., Litchevsky, V., Biber, A., Indenbaum, V., Olmer, L., Huppert, A., Mor, O., Goldstein, M., Levin, E.G., et al. (2021). Immunogenicity and safety of the BNT162b2 mRNA COVID-19 vaccine in people living with HIV-1. Clinical Microbiology and Infection *27*, 1851. https://doi.org/10.1016/J.CMI.2021.07.031.

Lewitus, E., Bai, H., and Rolland, M. (2023). Design of a pan-betacoronavirus vaccine candidate through a phylogenetically informed approach. Sci Adv *9*. https://doi.org/10.1126/sciadv.abq4149.

Li, H., Borrego, F., Nagata, S., and Tolnay, M. (2016). Fc Receptor–like 5 Expression Distinguishes Two Distinct Subsets of Human Circulating Tissue–like Memory B Cells. The Journal of Immunology *196*, 4064–4074. https://doi.org/10.4049/JIMMUNOL.1501027.

Li, M., Li, L., Zhang, Y., and Wang, X. (2020). An Investigation of the Expression of 2019 Novel Coronavirus Cell Receptor Gene ACE2 in a Wide Variety of Human Tissues. Infect Dis Poverty *9(1)*, 1–7. .

Li, Q., Liu, Q., Huang, W., Li, X., and Wang, Y. (2018). Current status on the development of pseudoviruses for enveloped viruses. Rev Med Virol *28*. https://doi.org/10.1002/rmv.1963.

Liao, H., Yu, Y., Li, S., Yue, Y., Tao, C., Su, K., and Zhang, Z. (2017). Circulating plasmablasts from chronically human immunodeficiency virus-infected individuals predominantly produce polyreactive/autoreactive antibodies. Front Immunol *8*, 1691. https://doi.org/10.3389/fimmu.2017.01691.

Lim, J.M.E., Hang, S.K., Hariharaputran, S., Chia, A., Tan, N., Lee, E.S., Chng, E., Lim, P.L., Young, B.E., Lye, D.C., et al. (2022). A comparative characterization of SARS-CoV-2-specific T cells induced by mRNA or inactive virus COVID-19 vaccines. Cell Rep Med *3*. https://doi.org/10.1016/J.XCRM.2022.100793.

Lima, N.S., Musayev, M., Johnston, T.S., Wagner, D.A., Henry, A.R., Wang, L., Yang, E.S., Zhang, Y., Birungi, K., Black, W.P., et al. (2022). Primary exposure to SARS-CoV-2 variants elicits convergent epitope specificities, immunoglobulin V gene usage and public B cell clones. Nat Commun *13*, 1–14. https://doi.org/10.1038/s41467-022-35456-2.

Lindqvist, M., Van Lunzen, J., Soghoian, D.Z., Kuhl, B.D., Ranasinghe, S., Kranias, G., Flanders, M.D., Cutler, S., Yudanin, N., Muller, M.I., et al. (2012). Expansion of HIV-specific T follicular helper cells in chronic HIV infection. J Clin Invest *122*, 3271. https://doi.org/10.1172/JCI64314.

Lindsey, N.P., Schroeder, B.A., Miller, E.R., Braun, M.M., Hinckley, A.F., Marano, N., Slade, B.A., Barnett, E.D., Brunette, G.W., Horan, K., et al. (2008). Adverse event reports following yellow fever vaccination. Vaccine *26*, 6077–6082. https://doi.org/10.1016/J.VACCINE.2008.09.009.

Liu, D., Xu, H., Shih, C., Wan, Z., Ma, X., Ma, W., Luo, D., and Qi, H. (2015). T-B-cell entanglement and ICOSL-driven feed-forward regulation of germinal centre reaction. Nature *517*, 214–218. https://doi.org/10.1038/nature13803.

Liu, J., Chandrashekar, A., Sellers, D., Barrett, J., Jacob-Dolan, C., Lifton, M., McMahan, K., Sciacca, M., VanWyk, H., Wu, C., et al. (2022a). Vaccines elicit highly conserved cellular immunity to SARS-CoV-2 Omicron. Nature *603*, 493–496. https://doi.org/10.1038/s41586-022-04465-y.

Liu, X., Zhao, Y., and Qi, H. (2022b). T-independent antigen induces humoral memory through germinal centers. Journal of Experimental Medicine *219*. https://doi.org/10.1084/JEM.20210527/212958.

Liu, Y., Soh, W.T., Kishikawa, J. ichi, Hirose, M., Nakayama, E.E., Li, S., Sasai, M., Suzuki, T., Tada, A., Arakawa, A., et al. (2021). An infectivity-enhancing site on the SARS-CoV-2 spike protein targeted by antibodies. Cell *184*, 3452-3466.e18. https://doi.org/10.1016/j.cell.2021.05.032.

Liu, Y., Liu, J., Johnson, B.A., Xia, H., Ku, Z., Schindewolf, C., Widen, S.G., An, Z., Weaver, S.C., Menachery, V.D., et al. (2022c). Delta spike P681R mutation enhances SARS-CoV-2 fitness over Alpha variant. Cell Rep *39*, 110829. https://doi.org/10.1016/J.CELREP.2022.110829.

Löffert, D., Ehlich, A., Müller, W., and Rajewsky, K. (1996). Surrogate light chain expression is required to establish immunoglobulin heavy chain allelic exclusion during early B cell development. Immunity *4*, 133–144. https://doi.org/10.1016/S1074-7613(00)80678-0.

Logunov, D.Y., Dolzhikova, I. V., Shcheblyakov, D. V., Tukhvatulin, A.I., Zubkova, O. V., Dzharullaeva, A.S., Kovyrshina, A. V., Lubenets, N.L., Grousova, D.M., Erokhova, A.S., et al. (2021). Safety and efficacy of an rAd26 and rAd5 vector-based heterologous prime-boost COVID-19 vaccine: an interim analysis of a randomised controlled phase 3 trial in Russia. The Lancet *397*, 671–681. https://doi.org/10.1016/S0140-6736(21)00234-8.

Lombardi, A., Butta, G.M., Donnici, L., Bozzi, G., Oggioni, M., Bono, P., Matera, M., Consonni, D., Ludovisi, S., Muscatello, A., et al. (2022). Anti-spike antibodies and neutralising antibody activity in people living with HIV vaccinated with COVID-19 mRNA-1273 vaccine: a prospective single-centre cohort study. The Lancet Regional Health - Europe *13*, 100287. https://doi.org/10.1016/J.LANEPE.2021.100287.

Long, Q.X., Liu, B.Z., Deng, H.J., Wu, G.C., Deng, K., Chen, Y.K., Liao, P., Qiu, J.F., Lin, Y., Cai, X.F., et al. (2020). Antibody responses to SARS-CoV-2 in patients with COVID-19. Nat Med *26*, 845–848. https://doi.org/10.1038/s41591-020-0897-1.

Lopes de Assis, F., Hoehn, K.B., Zhang, X., Kardava, L., Smith, C.D., El Merhebi, O., Buckner, C.M., Trihemasava, K., Wang, W., Seamon, C.A., et al. (2023). Tracking B cell responses to the SARS-CoV-2 mRNA-1273 vaccine. Cell Rep *42*, 112780. https://doi.org/10.1016/J.CELREP.2023.112780.

Lopez Bernal, J., Andrews, N., Gower, C., Gallagher, E., Simmons, R., Thelwall, S., Stowe, J., Tessier, E., Groves, N., Dabrera, G., et al. (2021). Effectiveness of Covid-19 Vaccines against the B.1.617.2 (Delta) Variant. New England Journal of Medicine *385*, 585–594. https://doi.org/10.1056/NEJMOA2108891/SUPPL_FILE/NEJMOA2108891_DISCLOSURES.PDF.

Lu, L., and Osmond, D.G. (1997). Apoptosis during B lymphopoiesis in mouse bone marrow. The Journal of Immunology *158*, 5136–5145. https://doi.org/10.4049/JIMMUNOL.158.11.5136.

Lu, T., Chen, Z., Cao, Y., Ao, L., Li, Z., Gu, X., Ren, X., Wang, Y., Zhang, G., Xiang, D., et al. (2023). Dynamic immunogenicity after primary and booster inactivated SARS-CoV-2 vaccination in people living with HIV: A longitudinal observational study. J Med Virol *95*, e28730. https://doi.org/10.1002/JMV.28730.

Lucas, C., Klein, J., Sundaram, M.E., Liu, F., Wong, P., Silva, J., Mao, T., Oh, J.E., Mohanty, S., Huang, J., et al. (2021). Delayed production of neutralizing antibodies correlates with fatal COVID-19. Nat Med *27*, 1178–1186. https://doi.org/10.1038/s41591-021-01355-0.

Lumley, S.F., O'Donnell, D., Stoesser, N.E., Matthews, P.C., Howarth, A., Hatch, S.B., Marsden, B.D., Cox, S., James, T., Warren, F., et al. (2021). Antibody Status and Incidence of SARS-CoV-2 Infection in Health Care Workers. New England Journal of Medicine *384*, 533–540. https://doi.org/10.1056/NEJMOA2034545/SUPPL_FILE/NEJMOA2034545_DISCLOSURES.PDF.

Lundgren, J.D., Babiker, A.G., Sharma, S., Grund, B., Phillips, A.N., Matthews, G., Kan, V.L., Aagaard, B., Abo, I., Alston, B., et al. (2023). Long-Term Benefits from Early Antiretroviral Therapy Initiation in HIV Infection. NEJM Evidence *2*. https://doi.org/10.1056/EVIDOA2200302.

Lv, H., Wu, N.C., Tsang, O.T.Y., Yuan, M., Perera, R.A.P.M., Leung, W.S., So, R.T.Y., Chan, J.M.C., Yip, G.K., Chik, T.S.H., et al. (2020). Cross-reactive Antibody Response between SARS-CoV-2 and SARS-CoV Infections. Cell Rep *31*, 107725. https://doi.org/10.1016/J.CELREP.2020.107725.

Lv, Z., Lv, S., Li, Q., Xia, Y., Feng, Z., Zhang, H., Yang, H., Wu, Z., Zou, N., Mo, Q., et al. (2023). A third (booster) dose of the inactivated SARS-CoV-2 vaccine elicits immunogenicity and T follicular helper cell responses in people living with HIV. Front Immunol *14*, 1–10. https://doi.org/10.3389/fimmu.2023.1264160.

Madhi, S.A., Baillie, V., Cutland, C.L., Voysey, M., Koen, A.L., Fairlie, L., Padayachee, S.D., Dheda, K., Barnabas, S.L., Bhorat, Q.E., et al. (2021a). Efficacy of the ChAdOx1 nCoV-19 Covid-19 Vaccine against the B.1.351 Variant. New England Journal of Medicine *384*, 1885–1898. https://doi.org/10.1056/NEJMOA2102214/SUPPL_FILE/NEJMOA2102214_DATA-SHARING.PDF.

Madhi, S.A., Koen, A.L., Izu, A., Fairlie, L., Cutland, C.L., Baillie, V., Padayachee, S.D., Dheda, K., Barnabas, S.L., Bhorat, Q.E., et al. (2021b). Safety and immunogenicity of the ChAdOx1 nCoV-19 (AZD1222) vaccine against SARS-CoV-2 in people living with and without HIV in South Africa: an interim analysis of a randomised, double-blind, placebo-controlled, phase 1B/2A trial. Lancet HIV *8*, e568–e580. https://doi.org/10.1016/S2352-3018(21)00157-0.

Mäkelä, O., Rouslahti, E., and Seppälä, I.J.T. (1970). Affinity of IgM and IgG antibodies. Immunochemistry *7*, 917–932. https://doi.org/10.1016/0019-2791(70)90053-4.

Malaspina, A., Moir, S., Ho, J., Wang, W., Howell, M.L., O'Shea, M.A., Roby, G.A., Rehm, C.A., Mican, J.A.M., Chun, T.W., et al. (2006). Appearance of immature/transitional B cells in HIV-infected individuals with advanced disease:

Correlation with increased IL-7. Proc Natl Acad Sci U S A *103*, 2262. https://doi.org/10.1073/PNAS.0511094103.

Malone, B., Urakova, N., Snijder, E.J., and Campbell, E.A. (2022). Structures and functions of coronavirus replication–transcription complexes and their relevance for SARS-CoV-2 drug design. Nat Rev Mol Cell Biol *23*, 21–39. https://doi.org/10.1038/s41580-021-00432-z.

Mansky, L.M., and Temin, H.M. (1995). Lower In Vivo Mutation Rate of Human Immunodeficiency Virus Type 1 than That Predicted from the Fidelity of Purified Reverse Transcriptase †. J Virol *69*, 5087–5094. .

Maponga, T.G., Jeffries, M., Tegally, H., Sutherland, A., Wilkinson, E., Lessells, R.J., Msomi, N., Van Zyl, G., De Oliveira, T., and Preiser, W. (2023). Persistent Severe Acute Respiratory Syndrome Coronavirus 2 Infection With accumulation of mutations in a patient with poorly controlled Human Immunodeficiency Virus infection. Clinical Infectious Diseases *76*, e522–e525. https://doi.org/10.1093/CID/CIAC548.

Marchitto, L., Chatterjee, D., Ding, S., Gendron-Lepage, G., Tauzin, A., Boutin, M., Benlarbi, M., Medjahed, H., Sylla, M., Lanctôt, H., et al. (2023). Humoral Responses Elicited by SARS-CoV-2 mRNA Vaccine in People Living with HIV. Viruses 2023, Vol. 15, Page 2004 *15*, 2004. https://doi.org/10.3390/V15102004.

Marshall, J.C., Murthy, S., Diaz, J., Adhikari, N., Angus, D.C., Arabi, Y.M., Baillie, K., Bauer, M., Berry, S., Blackwood, B., et al. (2020). A minimal common outcome measure set for COVID-19 clinical research. Lancet Infect Dis *20*, e192–e197. https://doi.org/10.1016/S1473-3099(20)30483-7.

Masur, H., Michelis, M.A., Greene, J.B., Onorato, I., Vande Stouwe, R.A., Holzman, R.S., Wormser, G., Brettman, L., Lange, M., Murray, H.W., et al. (1981). An Outbreak of Community-Acquired Pneumocystis carinii Pneumonia. New England Journal of Medicine *305*, 1431–1438. https://doi.org/10.1056/nejm198112103052402.

Matveev, V.A., Mihelic, E.Z., Benko, E., Budylowski, P., Grocott, S., Lee, T., Korosec, C.S., Colwill, K., Stephenson, H., Law, R., et al. (2023). Immunogenicity of COVID-19 vaccines and their effect on HIV reservoir in older people with HIV. IScience *26*. https://doi.org/10.1016/j.isci.2023.107915.

Mazzoni, A., Lauria, N. Di, Maggi, L., Salvati, L., Vanni, A., Capone, M., Lamacchia, G., Mantengoli, E., Spinicci, M., Zammarchi, L., et al. (2021). First-dose mRNA vaccination is sufficient to reactivate immunological memory to SARS-CoV-2 in subjects who have recovered from COVID-19. J Clin Invest *131*. https://doi.org/10.1172/JCI149150.

Mazzoni, A., Vanni, A., Spinicci, M., Lamacchia, G., Kiros, S.T., Rocca, A., Capone, M., Di Lauria, N., Salvati, L., Carnasciali, A., et al. (2022). SARS-CoV-2 infection and vaccination trigger long-lived B and CD4+ T lymphocytes with implications for booster strategies. J Clin Invest *132*. https://doi.org/10.1172/JCI157990.

Mazzotta, V., Lepri, A.C., Matusali, G., Cimini, E., Piselli, P., Aguglia, C., Lanini, S., Colavita, F., Notari, S., Oliva, A., et al. (2024). Immunogenicity and reactogenicity of modified vaccinia Ankara pre-exposure vaccination against mpox according to previous smallpox vaccine exposure and HIV infection: prospective cohort study. EClinicalMedicine *68*, 102420. https://doi.org/10.1016/j.eclinm.2023.102420.

McCallum, M., De Marco, A., Lempp, F.A., Tortorici, M.A., Pinto, D., Walls, A.C., Beltramello, M., Chen, A., Liu, Z., Zatta, F., et al. (2021). N-terminal domain antigenic mapping reveals a site of vulnerability for SARS-CoV-2. Cell *184*, 2332-2347.e16. https://doi.org/10.1016/J.CELL.2021.03.028.

McCoy, L.E., and Burton, D.R. (2017). Identification and specificity of broadly neutralizing antibodies against HIV. Immunol Rev *275*, 11–20. https://doi.org/10.1111/imr.12484.

McCoy, L.E., and McKnight, A. (2017). Lessons learned from humoral responses of HIV patients. Curr Opin HIV AIDS *12*, 195–202. https://doi.org/10.1097/COH.0000000000000361.

Mcheyzer-Williams, L.J., Milpied, P.J., Okitsu, S.L., and Mcheyzer-Williams, M.G. (2015). Switched-memory B cells remodel B cell receptors within secondary germinal centers. Nat Immunol *16*, 296. https://doi.org/10.1038/NI.3095.

McMichael, T.M., Currie, D.W., Clark, S., Pogosjans, S., Kay, M., Schwartz, N.G., Lewis, J., Baer, A., Kawakami, V., Lukoff, M.D., et al. (2020). Epidemiology of Covid-19 in a Long-Term Care Facility in King County, Washington. New England Journal of Medicine *382*, 2005–2011.

https://doi.org/10.1056/NEJMOA2005412/SUPPL_FILE/NEJMOA2005412_DATA-SHARING.PDF.

Meffre, E., Louie, A., Bannock, J., Kim, L.J.Y., Ho, J., Frear, C.C., Kardava, L., Wang, W., Buckner, C.M., Wang, Y., et al. (2016). Maturational characteristics of HIV-specific antibodies in viremic individuals. JCI Insight *1*, :e84610. https://doi.org/10.1172/jci.insight.84610.

Mehr, R., Shannon, M., and Litwin, S. (1999). Models for Antigen Receptor Gene Rearrangement. I. Biased Receptor Editing in B Cells: Implications for Allelic Exclusion. The Journal of Immunology *163*, 1793–1798. .

Melamed, D., Benschop, R.J., Cambier, J.C., and Nemazee, D. (1998). Developmental Regulation of B Lymphocyte Immune Tolerance Compartmentalizes Clonal Selection from Receptor Selection. Cell *92*, 173–182. https://doi.org/10.1016/S0092-8674(00)80912-5.

Mellors, J.W., Muñoz, A., Giorgi, J. V., Margolick, J.B., Tassoni, C.J., Gupta, P., Kingsley, L.A., Todd, J.A., Saah, A.J., Detels, R., et al. (1997). Plasma viral load and CD4+ lymphocytes as prognostic markers of HIV-1 infection. Ann Intern Med *126*, 946–954. https://doi.org/10.7326/0003-4819-126-12-199706150-00003.

Mendoza, P., Gruell, H., Nogueira, L., Pai, J.A., Butler, A.L., Millard, K., Lehmann, C., Suárez, I., Oliveira, T.Y., Lorenzi, J.C.C., et al. (2018). Combination therapy with anti-HIV-1 antibodies maintains viral suppression. Nature *561*, 479. https://doi.org/10.1038/S41586-018-0531-2.

Meng, B., Kemp, S.A., Papa, G., Datir, R., Ferreira, I.A.T.M., Marelli, S., Harvey, W.T., Lytras, S., Mohamed, A., Gallo, G., et al. (2021). Recurrent emergence of SARS-CoV-2 spike deletion H69/V70 and its role in the Alpha variant B.1.1.7. Cell Rep *35*, 109292. https://doi.org/10.1016/j.celrep.2021.109292.

Meng, W., Zhang, B., Schwartz, G.W., Rosenfeld, A.M., Ren, D., Thome, J.J.C., Carpenter, D.J., Matsuoka, N., Lerner, H., Friedman, A.L., et al. (2017). An atlas of B-cell clonal distribution in the human body. Nat Biotechnol *35*, 879–886. https://doi.org/10.1038/nbt.3942.

Mesin, L., Schiepers, A., Ersching, J., Barbulescu, A., Cavazzoni, C.B., Angelini, A., Okada, T., Kurosaki, T., and Victora, G.D. (2020). Restricted Clonality and Limited Germinal Center Reentry Characterize Memory B Cell Reactivation by Boosting. Cell *180*, 92. https://doi.org/10.1016/J.CELL.2019.11.032.

Miles, B., Miller, S.M., Folkvord, J.M., Kimball, A., Chamanian, M., Meditz, A.L., Arends, T., McCarter, M.D., Levy, D.N., Rakasz, E.G., et al. (2015). Follicular regulatory T cells impair follicular T helper cells in HIV and SIV infection. Nat Commun *6*, 1–16. https://doi.org/10.1038/ncomms9608.

De Milito, A., Mörch, C., Anders Sönnerborg, A., and Chiodi, F. (2001). Loss of memory (CD27) B lymphocytes in HIV-1 infection. AIDS *15*, 957–964. https://doi.org/10.1097/00002030-200105250-00003.

De Milito, A., Nilsson, A., Titanji, K., Thorstensson, R., Reizenstein, E., Narita, M., Grutzmeier, S., Sönnerborg, A., and Chiodi, F. (2004). Mechanisms of hypergammaglobulinemia and impaired antigen-specific humoral immunity in HIV-1 infection. Blood *103*, 2180–2186. https://doi.org/10.1182/BLOOD-2003-07-2375.

Mlcochova, P., Kemp, S.A., Dhar, M.S., Papa, G., Meng, B., Ferreira, I.A.T.M., Datir, R., Collier, D.A., Albecka, A., Singh, S., et al. (2021). SARS-CoV-2 B.1.617.2 Delta variant replication and immune evasion. Nature *599*, 114. https://doi.org/10.1038/S41586-021-03944-Y.

Mocroft, A., Phillips, A., Gatell, J., Ledergerber, B., Fisher, M., Clumeck, N., Losso, M., Lazzarin, A., Fatkenheuer, G., and Lundgren, J. (2007). Normalisation of CD4 counts in patients with HIV-1 infection and maximum virological suppression who are taking combination antiretroviral therapy: an observational cohort study. Lancet *370*, 407–413. https://doi.org/10.1016/S0140-6736(07)60948-9.

Mocroft, A., Furrer, H.J., Miro, J.M., Reiss, P., Mussini, C., Kirk, O., Abgrall, S., Ayayi, S., Bartmeyer, B., Braun, D., et al. (2013). The incidence of AIDS-defining illnesses at a current CD4 count ≥200 cells/μL in the post-combination antiretroviral therapy era. Clinical Infectious Diseases *57*, 1038–1047. https://doi.org/10.1093/cid/cit423.

Moir, S., and Fauci, A.S. (2013). Insights Into B Cells And Hiv-Specific B-Cell Responses In Hiv-Infected Individuals. Immunol Rev *254*, 207–224. https://doi.org/10.1111/IMR.12067.

Moir, S., and Fauci, A.S. (2017). B-cell responses to HIV infection. Immunol Rev *275*, 33–48. https://doi.org/10.1111/imr.12502.

Moir, S., Ogwaro, K.M., Malaspina, A., Vasquez, J., Donoghue, E.T., Hallahan, C.W., Liu, S., Ehler, L.A., Planta, M.A., Kottilil, S., et al. (2003). Perturbations in B cell responsiveness to CD4+ T cell help in HIV-infected individuals. Proc Natl Acad Sci U S A *100*, 6057. https://doi.org/10.1073/PNAS.0730819100.

Moir, S., Malaspina, A., Pickeral, O.K., Donoghue, E.T., Vasquez, J., Miller, N.J., Krishnan, S.R., Planta, M.A., Turney, J.F., Justement, J.S., et al. (2004). Decreased survival of B cells of HIV-viremic patients mediated by altered expression of receptors of the TNF superfamily. Journal of Experimental Medicine *200*, 587–599. https://doi.org/10.1084/jem.20032236.

Moir, S., Ho, J., Malaspina, A., Wang, W., DiPoto, A.C., O'Shea, M.A., Roby, G., Kottilil, S., Arthos, J., Proschan, M.A., et al. (2008a). Evidence for HIV-associated B cell exhaustion in a dysfunctional memory B cell compartment in HIV-infected viremic individuals. Journal of Experimental Medicine *205*, 1797–1805. https://doi.org/10.1084/jem.20072683.

Moir, S., Malaspina, A., Ho, J., Wang, W., DiPoto, A.C., O'Shea, M.A., Roby, G., Mican, J.A.M., Kottilil, S., Chun, T.W., et al. (2008b). Normalization of B cell counts and subpopulations after antiretroviral therapy in chronic HIV disease. Journal of Infectious Diseases *197*, 572–579. https://doi.org/10.1086/526789.

Moir, S., Buckner, C.M., Ho, J., Wang, W., Chen, J., Waldner, A.J., Posada, J.G., Kardava, L., O'Shea, M.A., Kottilil, S., et al. (2010). B cells in early and chronic HIV infection: Evidence for preservation of immune function associated with early initiation of antiretroviral therapy. Blood *116*, 5571–5579. https://doi.org/10.1182/blood-2010-05-285528.

Möller, I.K., Gisslén, M., Wagner, P., Sparén, P., and Carlander, C. (2023). COVID-19 hospitalization outcomes in adults by HIV status; a nation-wide register-based study. HIV Med *24*, 1045–1055. https://doi.org/10.1111/hiv.13515.

Montague, Z., Lv, H., Otwinowski, J., DeWitt, W.S., Isacchini, G., Yip, G.K., Ng, W.W., Tsang, O.T.Y., Yuan, M., Liu, H., et al. (2021). Dynamics of B cell repertoires and

emergence of cross-reactive responses in patients with different severities of COVID-19. Cell Rep *35*. https://doi.org/10.1016/J.CELREP.2021.109173.

Montefiori, D.C. (2009). Measuring HIV neutralization in a luciferase reporter gene assay. Methods in Molecular Biology *485*, 395–405. https://doi.org/10.1007/978-1-59745-170-3_26/FIGURES/26_1_978-1-59745-170-3.

Motsoeneng, B.M., Manamela, N.P., Kaldine, H., Kgagudi, P., Hermanus, T., Ayres, F., Makhado, Z., Moyo-Gwete, T., van der Mescht, M.A., Abdullah, F., et al. (2023). Despite delayed kinetics, people living with HIV achieve equivalent antibody function after SARS-CoV-2 infection or vaccination. Front Immunol *14*, 1–12. https://doi.org/10.3389/fimmu.2023.1231276.

Mou, H., Raj, V.S., van Kuppeveld, F.J.M., Rottier, P.J.M., Haagmans, B.L., and Bosch, B.J. (2013). The Receptor Binding Domain of the New Middle East Respiratory Syndrome Coronavirus Maps to a 231-Residue Region in the Spike Protein That Efficiently Elicits Neutralizing Antibodies. J Virol *87*, 9379–9383. https://doi.org/10.1128/jvi.01277-13.

Muecksch, F., Wang, Z., Cho, A., Gaebler, C., Ben Tanfous, T., DaSilva, J., Bednarski, E., Ramos, V., Zong, S., Johnson, B., et al. (2022). Increased memory B cell potency and breadth after a SARS-CoV-2 mRNA boost. Nature *607*, 128–134. https://doi.org/10.1038/s41586-022-04778-y.

Muir, L., Jaffer, A., Rees-Spear, C., Gopalan, V., Chang, F.Y., Fernando, R., Vaitkute, G., Roustan, C., Rosa, A., Earl, C., et al. (2021). Neutralizing Antibody Responses After SARS-CoV-2 Infection in End-Stage Kidney Disease and Protection Against Reinfection. Kidney Int Rep https://doi.org/10.1016/j.ekir.2021.03.902.

Munnink, B.B.O., Sikkema, R.S., Nieuwenhuijse, D.F., Molenaar, R.J., Munger, E., Molenkamp, R., Van Der Spek, A., Tolsma, P., Rietveld, A., Brouwer, M., et al. (2021). Transmission of SARS-CoV-2 on mink farms between humans and mink and back to humans. Science *371*, 172–177. https://doi.org/10.1126/SCIENCE.ABE5901/SUPPL_FILE/ABE5901_OUDE_MUNNINK_TABLE_S1.PDF.

Munster, V.J., Wells, D., Lambe, T., Wright, D., Fischer, R.J., Bushmaker, T., Saturday, G., Van Doremalen, N., Gilbert, S.C., De Wit, E., et al. (2017). Protective

efficacy of a novel simian adenovirus vaccine against lethal MERS-CoV challenge in a transgenic human DPP4 mouse model. NPJ Vaccines *2*, 28. https://doi.org/10.1038/S41541-017-0029-1.

Muramatsu, M., Sankaranand, V.S., Anant, S., Sugai, M., Kinoshita, K., Davidson, N.O., and Honjo, T. (1999). Specific Expression of Activation-induced Cytidine Deaminase (AID), a Novel Member of the RNA-editing Deaminase Family in Germinal Center B Cells. Journal of Biological Chemistry *274*, 18470–18476. https://doi.org/10.1074/JBC.274.26.18470.

Muramatsu, M., Kinoshita, K., Fagarasan, S., Yamada, S., Shinkai, Y., and Honjo, T. (2000). Class Switch Recombination and Hypermutation Require Activation-Induced Cytidine Deaminase (AID), a Potential RNA Editing Enzyme. Cell *102*, 553–563. https://doi.org/10.1016/S0092-8674(00)00078-7.

Murray, H.W., Rubin, B.Y., Masur, H., and Roberts, R.B. (1984). Impaired Production of Lymphokines and Immune (Gamma) Interferon in the Acquired Immunodeficiency Syndrome. New England Journal of Medicine *310*, 883–889. https://doi.org/10.1056/nejm198404053101404.

Nasi, M., De Biasi, S., Gibellini, L., Bianchini, E., Pecorini, S., Bacca, V., Guaraldi, G., Mussini, C., Pinti, M., and Cossarizza, A. (2017). Ageing and inflammation in patients with HIV infection. Clin Exp Immunol *187*, 44–52. https://doi.org/10.1111/cei.12814.

Nault, L., Marchitto, L., Goyette, G., Tremblay-Sher, D., Fortin, C., Martel-Laferrière, V., Trottier, B., Richard, J., Durand, M., Kaufmann, D., et al. (2022). Covid-19 vaccine immunogenicity in people living with HIV-1. Vaccine *40*, 3633–3637. https://doi.org/10.1016/J.VACCINE.2022.04.090.

Nayrac, M., Dubé, M., Sannier, G., Nicolas, A., Marchitto, L., Tastet, O., Tauzin, A., Brassard, N., Lima-Barbosa, R., Beaudoin-Bussières, G., et al. (2022). Temporal associations of B and T cell immunity with robust vaccine responsiveness in a 16-week interval BNT162b2 regimen. Cell Rep *39*. https://doi.org/10.1016/J.CELREP.2022.111013.

Nemazee, D. (2017). Mechanisms of central tolerance for B cells. Nature Reviews Immunology 2017 17:5 *17*, 281–294. https://doi.org/10.1038/nri.2017.19.

Nemazee, D., and Buerki, K. (1989). Clonal deletion of autoreactive B lymphocytes in bone marrow chimeras. Proc Natl Acad Sci U S A *86*, 8039–8043. https://doi.org/10.1073/PNAS.86.20.8039.

Ng, K.W., Faulkner, N., Cornish, G.H., Rosa, A., Harvey, R., Hussain, S., Ulferts, R., Earl, C., Wrobel, A.G., Benton, D.J., et al. (2020). Preexisting and de novo humoral immunity to SARS-CoV-2 in humans. Science eabe1107. https://doi.org/10.1126/science.abe1107.

Ng, K.W., Faulkner, N., Finsterbusch, K., Wu, M., Harvey, R., Hussain, S., Greco, M., Liu, Y., Kjaer, S., Swanton, C., et al. (2022). SARS-CoV-2 S2–targeted vaccination elicits broadly neutralizing antibodies. Sci Transl Med *14*. https://doi.org/10.1126/scitranslmed.abn3715.

Nielsen, S.C.A., Roskin, K.M., Jackson, K.J.L., Joshi, S.A., Nejad, P., Lee, J.Y., Wagar, L.E., Pham, T.D., Hoh, R.A., Nguyen, K.D., et al. (2019). Shaping of infant B cell receptor repertoires by environmental factors and infectious disease. Sci Transl Med *11*. https://doi.org/10.1126/scitranslmed.aat2004.

Nielsen, S.C.A., Yang, F., Jackson, K.J.L., Hoh, R.A., Röltgen, K., Jean, G.H., Stevens, B.A., Lee, J.Y., Rustagi, A., Rogers, A.J., et al. (2020). Human B Cell Clonal Expansion and Convergent Antibody Responses to SARS-CoV-2. Cell Host Microbe *28*, 516. https://doi.org/10.1016/J.CHOM.2020.09.002.

Nkosi, T., Chasara, C., Papadopoulos, A.O., Nguni, T.L., Karim, F., Moosa, M.Y.S., Gazy, I., Jambo, K., Hanekom, W., Sigal, A., et al. (2022). Unsuppressed HIV infection impairs T cell responses to SARS-CoV-2 infection and abrogates T cell cross-recognition. Elife *11*, 78374. https://doi.org/10.7554/ELIFE.78374.

Noe, S., Ochana, N., Wiese, C., Schabaz, F., Von Krosigk, A., Heldwein, S., Rasshofer, R., Wolf, E., and Jonsson-Oldenbuettel, C. (2021). Humoral response to SARS-CoV-2 vaccines in people living with HIV. Infection *1*, 1. https://doi.org/10.1007/S15010-021-01721-7.

Nomah, D.K., Reyes-Urueña, J., Díaz, Y., Moreno, S., Aceiton, J., Bruguera, A., Vivanco-Hidalgo, R.M., Llibre, J.M., Domingo, P., Falcó, V., et al. (2021). Sociodemographic, clinical, and immunological factors associated with SARS-CoV-2 diagnosis and severe COVID-19 outcomes in people living with HIV: a retrospective

cohort study. Lancet HIV *8*, e701–e710. https://doi.org/10.1016/S2352-3018(21)00240-X.

Oberhardt, V., Luxenburger, H., Kemming, J., Schulien, I., Ciminski, K., Giese, S., Csernalabics, B., Lang-Meli, J., Janowska, I., Staniek, J., et al. (2021). Rapid and stable mobilization of CD8 + T cells by SARS-CoV-2 mRNA vaccine Vaccine-elicited CD8 + T cells. Nature *597*. https://doi.org/10.1038/s41586-021-03841-4.

Oettinger, M.A., Schatz, D.G., Gorka, C., and Baltimore, D. (1990). RAG-1 and RAG-2, adjacent genes that synergistically activate V(D)J recombination. Science *248*, 1517–1523. https://doi.org/10.1126/SCIENCE.2360047.

Ogbe, A., Pace, M., Bittaye, M., Tipoe, T., Adele, S., Alagaratnam, J., Aley, P.K., Ansari, M.A., Bara, A., Broadhead, S., et al. (2022). Durability of ChAdOx1 nCoV-19 vaccination in people living with HIV. JCI Insight *7*. https://doi.org/10.1172/JCI.INSIGHT.157031.

Ogega, C.O., Skinner, N.E., Blair, P.W., Park, H.S., Littlefield, K., Ganesan, A., Dhakal, S., Ladiwala, P., Antar, A.A.R., Ray, S.C., et al. (2021). Durable SARS-CoV-2 B cell immunity after mild or severe disease. J Clin Invest *131*. https://doi.org/10.1172/JCI145516.

Okba, N.M.A., Müller, M.A., Li, W., Wang, C., Geurtsvankessel, C.H., Corman, V.M., Lamers, M.M., Sikkema, R.S., De Bruin, E., Chandler, F.D., et al. (2020). SARS-CoV-2 specific antibody responses in COVID-19 patients. Emerg Infect Dis *26*. https://doi.org/10.1101/2020.03.18.20038059.

Oliviero, B., Mantovani, S., Ludovisi, S., Varchetta, S., Mele, D., Paolucci, S., Baldanti, F., and Mondelli, M.U. (2015). Skewed B cells in chronic hepatitis C virus infection maintain their ability to respond to virus-induced activation. J Viral Hepat *22*, 391–398. https://doi.org/10.1111/JVH.12336.

Oliviero, B., Varchetta, S., Mele, D., Mantovani, S., Cerino, A., Perotti, C.G., Ludovisi, S., and Mondelli, M.U. (2020). Expansion of atypical memory B cells is a prominent feature of COVID-19. Cell Mol Immunol *17*, 1101–1103. https://doi.org/10.1038/s41423-020-00542-2.

O'Nions, J., Muir, L., Zheng, J., Rees-Spear, C., Rosa, A., Roustan, C., Earl, C., Cherepanov, P., Gupta, R., Khwaja, A., et al. (2021). SARS-CoV-2 antibody responses in patients with acute leukaemia. Leukemia *35*, 289–292. https://doi.org/10.1038/s41375-020-01103-2.

Palanichamy, A., Barnard, J., Zheng, B., Owen, T., Quach, T., Wei, C., Looney, R.J., Sanz, I., and Anolik, J.H. (2009). Novel Human Transitional B Cell Populations Revealed by B Cell Depletion Therapy. The Journal of Immunology *182*, 5982–5993. https://doi.org/10.4049/jimmunol.0801859.

Pallikkuth, S., De Armas, L.R., Pahwa, R., Rinaldi, S., George, V.K., Sanchez, C.M., Pan, L., Dickinson, G., Rodriguez, A., Fischl, M., et al. (2018). Impact of aging and HIV infection on serologic response to seasonal influenza vaccination. AIDS *32*, 1085–1094. https://doi.org/10.1097/QAD.0000000000001774.

Pan, P., Shen, M., Yu, Z., Ge, W., Chen, K., Tian, M., Xiao, F., Wang, Z., Wang, J., Jia, Y., et al. (2021). SARS-CoV-2 N protein promotes NLRP3 inflammasome activation to induce hyperinflammation. Nat Commun *12*. https://doi.org/10.1038/S41467-021-25015-6.

Pape, K.A., Taylor, J.J., Maul, R.W., Gearhart, P.J., and Jenkins, M.K. (2011). Different B cell populations mediate early and late memory during an endogenous immune response. Science *331*, 1203–1207. https://doi.org/10.1126/science.1201730.

Pape, K.A., Dileepan, T., Kabage, A.J., Kozysa, D., Batres, R., Evert, C., Matson, M., Lopez, S., Krueger, P.D., Graiziger, C., et al. (2021). High-affinity memory B cells induced by SARS-CoV-2 infection produce more plasmablasts and atypical memory B cells than those primed by mRNA vaccines. Cell Rep *37*, 109823. https://doi.org/10.1016/J.CELREP.2021.109823.

Park, L.S., McGinnis, K.A., Gordon, K.S., Justice, A.C., Leyden, W., Silverberg, M.J., Skarbinski, J., Jefferson, C., Horberg, M., Certa, J., et al. (2022). SARS-CoV-2 testing and positivity among persons with and without HIV in 6 United States cohorts. J Acquir Immune Defic Syndr *90*, 249. https://doi.org/10.1097/QAI.0000000000002943.

Paschold, L., Klee, B., Gottschick, C., Willscher, E., Diexer, S., Schultheiß, C., Simnica, D., Sedding, D., Girndt, M., Gekle, M., et al. (2022). Rapid Hypermutation B

Cell Trajectory Recruits Previously Primed B Cells Upon Third SARS-Cov-2 mRNA Vaccination. Front Immunol *13*, 876306. https://doi.org/10.3389/FIMMU.2022.876306/BIBTEX.

Patterson, E.I., Prince, T., Anderson, E.R., Casas-Sanchez, A., Smith, S.L., Cansado-Utrilla, C., Solomon, T., Griffiths, M.J., Acosta-Serrano, Á., Turtle, L., et al. (2020). Methods of Inactivation of SARS-CoV-2 for Downstream Biological Assays. J Infect Dis *222*, 1462–1467. https://doi.org/10.1093/INFDIS/JIAA507.

Payne, R.P., Longet, S., Austin, J.A., Skelly, D.T., Dejnirattisai, W., Adele, S., Meardon, N., Faustini, S., Al-Taei, S., Moore, S.C., et al. (2021). Immunogenicity of standard and extended dosing intervals of BNT162b2 mRNA vaccine. Cell *184*, 5699-5714.e11. https://doi.org/10.1016/j.cell.2021.10.011.

Pensieroso, S., Cagigi, A., Palma, P., Nilsson, A., Capponi, C., Freda, E., Bernardi, S., Thorstensson, R., Chiodi, F., and Rossi, P. (2009). Timing of HAART defines the integrity of memory B cells and the longevity of humoral responses in HIV-1 vertically-infected children. Proc Natl Acad Sci U S A *106*, 7939–7944. https://doi.org/10.1073/pnas.0901702106.

Pensieroso, S., Galli, L., Nozza, S., Ruffin, N., Castagna, A., Tambussi, G., Hejdeman, B., Misciagna, D., Riva, A., Malnati, M., et al. (2013). B-cell subset alterations and correlated factors in HIV-1 infection. AIDS *27*, 1209–1217. https://doi.org/10.1097/QAD.0b013e32835edc47.

Phad, G.E., Pinto, D., Foglierini, M., Akhmedov, M., Rossi, R.L., Malvicini, E., Cassotta, A., Fregni, C.S., Bruno, L., Sallusto, F., et al. (2022). Clonal structure, stability and dynamics of human memory B cells and circulating plasmablasts. Nat Immunol *23*, 1–10. https://doi.org/10.1038/s41590-022-01230-1.

Piccoli, L., Park, Y.J., Tortorici, M.A., Czudnochowski, N., Walls, A.C., Beltramello, M., Silacci-Fregni, C., Pinto, D., Rosen, L.E., Bowen, J.E., et al. (2020). Mapping Neutralizing and Immunodominant Sites on the SARS-CoV-2 Spike Receptor-Binding Domain by Structure-Guided High-Resolution Serology. Cell *183*, 1024-1042.e21. https://doi.org/10.1016/j.cell.2020.09.037.

Pickering, S., Betancor, G., Galão, R.P., Merrick, B., Signell, A.W., Wilson, H.D., Kia Ik, M.T., Seow, J., Graham, C., Acors, S., et al. (2020). Comparative assessment of

multiple COVID-19 serological technologies supports continued evaluation of point-of-care lateral flow assays in hospital and community healthcare settings. PLoS Pathog *16*, e1008817. https://doi.org/10.1371/journal.ppat.1008817.

Pinder, C.L., Jankovic, D., Fox, T.A., Kirkwood, A., Enfield, L., Alrubayyi, A., Touizer, E., Ford, R., Pocock, R., Shin, J.S., et al. (2023). Humoral and cellular responses to SARS-CoV-2 in patients with B-cell haematological malignancies improve with successive vaccination. Br J Haematol https://doi.org/10.1111/BJH.18962.

Pinto, D., Park, Y.J., Beltramello, M., Walls, A.C., Tortorici, M.A., Bianchi, S., Jaconi, S., Culap, K., Zatta, F., De Marco, A., et al. (2020). Cross-neutralization of SARS-CoV-2 by a human monoclonal SARS-CoV antibody. Nature *583*, 290–295. https://doi.org/10.1038/s41586-020-2349-y.

Planas, D., Saunders, N., Maes, P., Guivel-Benhassine, F., Planchais, C., Buchrieser, J., Bolland, W.H., Porrot, F., Staropoli, I., Lemoine, F., et al. (2021). Considerable escape of SARS-CoV-2 Omicron to antibody neutralization. Nature *602*, 671–675. https://doi.org/10.1038/s41586-021-04389-z.

Planchais, C., Molinos-Albert, L.M., Rosenbaum, P., Hieu, T., Kanyavuz, A., Clermont, D., Prazuck, T., Lefrou, L., Dimitrov, J.D., Hüe, S., et al. (2023). HIV-1 treatment timing shapes the human intestinal memory B-cell repertoire to commensal bacteria. Nat Commun *14*, 1–17. https://doi.org/10.1038/s41467-023-42027-6.

Polack, F.P., Thomas, S.J., Kitchin, N., Absalon, J., Gurtman, A., Lockhart, S., Perez, J.L., Pérez Marc, G., Moreira, E.D., Zerbini, C., et al. (2020). Safety and Efficacy of the BNT162b2 mRNA Covid-19 Vaccine. New England Journal of Medicine *383*, 2603–2615. https://doi.org/10.1056/NEJMOA2034577/SUPPL_FILE/NEJMOA2034577_PROTOCOL.PDF.

Polvere, J., Fabbiani, M., Pastore, G., Rancan, I., Rossetti, B., Durante, M., Zirpoli, S., Morelli, E., Pettini, E., Lucchesi, S., et al. (2023). B cell response after SARS-CoV-2 mRNA vaccination in people living with HIV. Communications Medicine *3*, 1–10. https://doi.org/10.1038/s43856-023-00245-5.

Poon, M.M.L., Rybkina, K., Kato, Y., Kubota, M., Matsumoto, R., Bloom, N.I., Zhang, Z., Hastie, K.M., Grifoni, A., Weiskopf, D., et al. (2021). SARS-CoV-2 infection

generates tissue-localized immunological memory in humans. Sci Immunol *6*. https://doi.org/10.1126/sciimmunol.abl9105.

Popovic, M., Sarngadharan, M.G., Read, E., and Gallo, R.C. (1984). Detection, Isolation, and Continuous Production of Cytopathic Retroviruses (HTLV-III) from Patients with AIDS and Pre-AIDS. Science *224*, 497–500. https://doi.org/10.1126/SCIENCE.6200935.

Pormohammad, A., Ghorbani, S., Khatami, A., Farzi, R., Baradaran, B., Turner, D.L., Turner, R.J., Bahr, N.C., and Idrovo, J.P. (2020). Comparison of confirmed COVID-19 with SARS and MERS cases - Clinical characteristics, laboratory findings, radiographic signs and outcomes: A systematic review and meta-analysis. Rev Med Virol *30*, e2112. https://doi.org/10.1002/RMV.2112.

Portugal, S., Tipton, C.M., Sohn, H., Kone, Y., Wang, J., Li, S., Skinner, J., Virtaneva, K., Sturdevant, D.E., Porcella, S.F., et al. (2015). Malaria-associated atypical memory B cells exhibit markedly reduced B cell receptor signaling and effector function. Elife *4*, 1–21. https://doi.org/10.7554/eLife.07218.

Pozzetto, B., Legros, V., Djebali, S., Barateau, V., Guibert, N., Villard, M., Peyrot, L., Allatif, O., Fassier, J.B., Massardier-Pilonchéry, A., et al. (2021). Immunogenicity and efficacy of heterologous ChAdOx1–BNT162b2 vaccination. Nature *600*, 701–706. https://doi.org/10.1038/s41586-021-04120-y.

Prendecki, M., Clarke, C., Edwards, H., McIntyre, S., Mortimer, P., Gleeson, S., Martin, P., Thomson, T., Randell, P., Shah, A., et al. (2021). Humoral and T-cell responses to SARS-CoV-2 vaccination in patients receiving immunosuppression. Ann Rheum Dis *80*, 1322–1329. https://doi.org/10.1136/ANNRHEUMDIS-2021-220626.

Psevdos, G., Kim, J.H., Groce, V., and Sharp, V. (2010). Efficacy of double-dose hepatitis B rescue vaccination in HIV-infected patients. AIDS Patient Care STDS *24*, 403–407.
https://doi.org/10.1089/APC.2009.0340/ASSET/IMAGES/LARGE/FIGURE2.JPEG.

Pušnik, J., König, J., Mai, K., Richter, E., Zorn, J., Proksch, H., Schulte, B., Alter, G., and Streeck, H. (2022). Persistent Maintenance of Atypical Memory B Cells Following SARS-CoV-2 Infection and Vaccination Recall Response. J Virol *96*. https://doi.org/10.2139/ssrn.4072040.

Rambaut, A., Loman, N., Pybus, O., Barclay, W., Barrett, J., Carabelli, A., Connor, T., Peacock, T., Robertson, D., and Volz, E. (2020). Preliminary genomic characterisation of an emergent SARS-CoV-2 lineage in the UK defined by a novel set of spike mutations - SARS-CoV-2 coronavirus / nCoV-2019 Genomic Epidemiology - Virological.

Raybould, M.I.J., Kovaltsuk, A., Marks, C., and Deane, C.M. (2021). CoV-AbDab: The coronavirus antibody database. Bioinformatics *37*, 734–735. https://doi.org/10.1093/bioinformatics/btaa739.

Rees-Spear, C., Muir, L., Griffith, S.A., Heaney, J., Aldon, Y., Snitselaar, J.L., Thomas, P., Graham, C., Seow, J., Lee, N., et al. (2021). The effect of spike mutations on SARS-CoV-2 neutralization. Cell Rep *34*. https://doi.org/10.1016/J.CELREP.2021.108890.

Regev-Yochay, G., Gonen, T., Gilboa, M., Mandelboim, M., Indenbaum, V., Amit, S., Meltzer, L., Asraf, K., Cohen, C., Fluss, R., et al. (2022). Efficacy of a Fourth Dose of Covid-19 mRNA Vaccine against Omicron. New England Journal of Medicine *386*, 1377–1380. https://doi.org/10.1056/NEJMC2202542/SUPPL_FILE/NEJMC2202542_DISCLOSURES.PDF.

Reincke, M.E., Payne, K.J., Harder, I., Strohmeier, V., Voll, R.E., Warnatz, K., and Keller, B. (2020). The Antigen Presenting Potential of CD21 low B Cells. Front Immunol *11*. https://doi.org/10.3389/fimmu.2020.535784.

Reth, M., Petrac, E., Wiese, P., Lobel', L., and Alt', F.W. (1987). Activation of Vx gene rearrangement in pre-B cells follows the expression of membrane-bound immunoglobulin heavy chains. EMBO J *6*, 3299–3305. .

Reyes, R.A., Batugedara, G., Dutta, P., Reers, A.B., Garza, R., Ssewanyana, I., Jagannathan, P., Feeney, M.E., Greenhouse, B., Bol, S., et al. (2023). Atypical B cells consist of subsets with distinct functional profiles. IScience *26*, 108496. https://doi.org/10.1016/j.isci.2023.108496.

Reynolds, C.J., Pade, C., Gibbons, J.M., Butler, D.K., Otter, A.D., Menacho, K., Fontana, M., Smit, A., Sackville-West, J.E., Cutino-Moguel, T., et al. (2021). Prior

SARS-CoV-2 infection rescues B and T cell responses to variants after first vaccine dose. Science *372*, 1418–1423. https://doi.org/10.1126/science.abh1282.

Reynolds, C.J., Gibbons, J.M., Pade, C., Lin, K.M., Sandoval, D.M., Pieper, F., Butler, D.K., Liu, S., Otter, A.D., Joy, G., et al. (2022a). Heterologous infection and vaccination shapes immunity against SARS-CoV-2 variants. Science *375*, 183–192. https://doi.org/10.1126/SCIENCE.ABM0811/SUPPL_FILE/SCIENCE.ABM0811_MDAR_REPRODUCIBILITY_CHECKLIST.PDF.

Reynolds, C.J., Pade, C., Gibbons, J.M., Otter, A.D., Lin, K.M., Sandoval, D.M., Pieper, F.P., Butler, D.K., Liu, S., Joy, G., et al. (2022b). Immune boosting by B.1.1.529 (Omicron) depends on previous SARS-CoV-2 exposure. Science *377*. https://doi.org/10.1126/science.abq1841.

Richman, D.D., Wrin, T., Little, S.J., and Petropoulos, C.J. (2003). Rapid evolution of the neutralizing antibody response to HIV type 1 infection. Proc Natl Acad Sci U S A *100*, 4144. https://doi.org/10.1073/PNAS.0630530100.

Riddell, A.C., Kele, B., Harris, K., Bible, J., Murphy, M., Dakshina, S., Storey, N., Owoyemi, D., Pade, C., Gibbons, J.M., et al. (2022). Generation of Novel Severe Acute Respiratory Syndrome Coronavirus 2 (SARS-CoV-2) Variants on the B.1.1.7 Lineage in 3 Patients With Advanced Human Immunodeficiency Virus (HIV)-1 Disease. Clin Infect Dis *75*, 2016–2018. https://doi.org/10.1093/CID/CIAC409.

Robbiani, D.F., Gaebler, C., Muecksch, F., Lorenzi, J.C.C., Wang, Z., Cho, A., Agudelo, M., Barnes, C.O., Gazumyan, A., Finkin, S., et al. (2020). Convergent antibody responses to SARS-CoV-2 in convalescent individuals. Nature *584*, 437–442. https://doi.org/10.1038/s41586-020-2456-9.

Roco, J.A., Mesin, L., Binder, S.C., Nefzger, C., Gonzalez-Figueroa, P., Canete, P.F., Ellyard, J., Shen, Q., Robert, P.A., Cappello, J., et al. (2019). Class-Switch Recombination Occurs Infrequently in Germinal Centers. Immunity *51*, 337-350.e7. https://doi.org/10.1016/j.immuni.2019.07.001.

Rodger, A.J., Cambiano, V., Phillips, A.N., Bruun, T., Raben, D., Lundgren, J., Vernazza, P., Collins, S., Degen, O., Corbelli, G.M., et al. (2019). Risk of HIV transmission through condomless sex in serodifferent gay couples with the HIV-positive partner taking suppressive antiretroviral therapy (PARTNER): final results of

a multicentre, prospective, observational study. The Lancet *393*, 2428–2438. https://doi.org/10.1016/S0140-6736(19)30418-0.

Rogers, T.F., Zhao, F., Huang, D., Beutler, N., Burns, A., He, W.T., Limbo, O., Smith, C., Song, G., Woehl, J., et al. (2020). Isolation of potent SARS-CoV-2 neutralizing antibodies and protection from disease in a small animal model. Science *369*, 956–963. https://doi.org/10.1126/science.abc7520.

Roitt, I.M., Greaves, M.F., Torrigiani, G., Brostoff, J., and Playfair, J.H. (1969). The cellular basis of immunological responses. A synthesis of some current views. Lancet *2*, 367–371. https://doi.org/10.1016/s0140-6736(69)92712-3.

Rolink, A.G., Andersson, J., and Melchers, F. (1998). Characterization of immature B cells by a novel monoclonal antibody, by turnover and by mitogen reactivity. Eur J Immunol *28*, 3738–3748. https://doi.org/10.1002/(SICI)1521-4141(199811)28:11<3738::AID-IMMU3738>3.0.CO;2-Q.

Röltgen, K., Powell, A.E., Wirz, O.F., Stevens, B.A., Hogan, C.A., Najeeb, J., Hunter, M., Wang, H., Sahoo, M.K., Huang, C.H., et al. (2020). Defining the features and duration of antibody responses to SARS-CoV-2 infection associated with disease severity and outcome. Sci Immunol *5*. https://doi.org/10.1126/SCIIMMUNOL.ABE0240.

Röltgen, K., Nielsen, S.C.A., Silva, O., Younes, S.F., Zaslavsky, M., Costales, C., Yang, F., Wirz, O.F., Solis, D., Hoh, R.A., et al. (2022). Immune imprinting, breadth of variant recognition, and germinal center response in human SARS-CoV-2 infection and vaccination. Cell *185*, 1025-1040.e14. https://doi.org/10.1016/J.CELL.2022.01.018.

Roskin, K.M., Jackson, K.J.L., Lee, J.Y., Hoh, R.A., Joshi, S.A., Hwang, K.K., Bonsignori, M., Pedroza-Pacheco, I., Liao, H.X., Moody, M.A., et al. (2020). Aberrant B cell repertoire selection associated with HIV neutralizing antibody breadth. Nat Immunol *21*, 199–209. https://doi.org/10.1038/s41590-019-0581-0.

Rota, P.A., Oberste, M.S., Monroe, S.S., Nix, W.A., Campagnoli, R., Icenogle, J.P., Peñaranda, S., Bankamp, B., Maher, K., Chen, M., et al. (2003). Characterization of a Novel Coronavirus Associated with Severe Acute Respiratory Syndrome. Science *300*, 1394–1399. https://doi.org/10.1126/science.1085952.

Rutherford, G.W., Lifson, A.R., Hessol, N.A., Darrow, W.W., O'Malley, P.M., Buchbinder, S.P., Barnhart, J.L., Bodecker, T.W., Cannon, L., Doll, L.S., et al. (1990). Course of HIV-I infection in a cohort of homosexual and bisexual men: An 11 year follow up study. Br Med J *301*, 1183–1188. https://doi.org/10.1136/bmj.301.6762.1183.

Rutishauser, R.L., and Trautmann, L. (2022). CD8+ T-cell responses in HIV controllers: potential implications for novel HIV remission strategies. Curr Opin HIV AIDS *17*, 315. https://doi.org/10.1097/COH.0000000000000748.

Rydyznski Moderbacher, C., Ramirez, S.I., Dan, J.M., Grifoni, A., Hastie, K.M., Weiskopf, D., Belanger, S., Abbott, R.K., Kim, C., Choi, J., et al. (2020). Antigen-Specific Adaptive Immunity to SARS-CoV-2 in Acute COVID-19 and Associations with Age and Disease Severity. Cell *183*, 996-1012.e19. https://doi.org/10.1016/J.CELL.2020.09.038.

Sabouri, Z., Schofield, P., Horikawa, K., Spierings, E., Kipling, D., Randall, K.L., Langley, D., Roome, B., Vazquez-Lombardi, R., Rouet, R., et al. (2014). Redemption of autoantibodies on anergic B cells by variable-region glycosylation and mutation away from self-reactivity. Proc Natl Acad Sci U S A *111*, E2567. https://doi.org/10.1073/PNAS.1406974111.

Sadoff, J., Gray, G., Vandebosch, A., Cárdenas, V., Shukarev, G., Grinsztejn, B., Goepfert, P.A., Truyers, C., Fennema, H., Spiessens, B., et al. (2021). Safety and Efficacy of Single-Dose Ad26.COV2.S Vaccine against Covid-19. New England Journal of Medicine *384*, 2187–2201. https://doi.org/10.1056/NEJMOA2101544/SUPPL_FILE/NEJMOA2101544_DATA-SHARING.PDF.

Sahin, U., Muik, A., Vogler, I., Derhovanessian, E., Kranz, L.M., Vormehr, M., Quandt, J., Bidmon, N., Ulges, A., Baum, A., et al. (2021). BNT162b2 vaccine induces neutralizing antibodies and poly-specific T cells in humans. Nature *595*, 572–577. https://doi.org/10.1038/s41586-021-03653-6.

Sanchez, J.L., Hunt, P.W., Reilly, C.S., Hatano, H., Beilman, G.J., Khoruts, A., Jasurda, J.S., Somsouk, M., Thorkelson, A., Russ, S., et al. (2015). Lymphoid Fibrosis Occurs in Long-Term Nonprogressors and Persists With Antiretroviral Therapy but

May Be Reversible With Curative Interventions. J Infect Dis *211*, 1068. https://doi.org/10.1093/INFDIS/JIU586.

Sansonetti, P., Sali, M., Fabbiani, M., Morandi, M., Martucci, R., Danesh, A., Delogu, G., Bermejo-Martin, J.F., Sanguinetti, M., Kelvin, D., et al. (2014). Immune response to influenza A(H1N1)v in HIV-infected patients. J Infect Dev Ctries *8*, 101–109. https://doi.org/10.3855/jidc.3147.

Sanz, I., Wei, C., Jenks, S.A., Cashman, K.S., Tipton, C., Woodruff, M.C., Hom, J., and Lee, F.E.H. (2019). Challenges and opportunities for consistent classification of human b cell and plasma cell populations. Front Immunol *10*, 1–17. https://doi.org/10.3389/fimmu.2019.02458.

Sarzotti-Kelsoe, M., Bailer, R.T., Turk, E., Lin, C. li, Bilska, M., Greene, K.M., Gao, H., Todd, C.A., Ozaki, D.A., Seaman, M.S., et al. (2014). Optimization and validation of the TZM-bl assay for standardized assessments of neutralizing antibodies against HIV-1. J Immunol Methods *409*, 131–146. https://doi.org/10.1016/j.jim.2013.11.022.

Schacker, T.W., Nguyen, P.L., Beilman, G.J., Wolinsky, S., Larson, M., Reilly, C., and Haase, A.T. (2002). Collagen deposition in HIV-1 infected lymphatic tissues and T cell homeostasis. J Clin Invest *110*, 1133. https://doi.org/10.1172/JCI16413.

Schacker, T.W., Reilly, C., Beilman, G.J., Taylor, J., Skarda, D., Krason, D., Larson, M., and Haase, A.T. (2005). Amount of lymphatic tissue fibrosis in HIV infection predicts magnitude of HAART-associated change in peripheral CD4 cell count. AIDS *19*, 2169–2171. https://doi.org/10.1097/01.AIDS.0000194801.51422.03.

Schatz, D.G., and Ji, Y. (2011). Recombination centres and the orchestration of V(D)J recombination. Nat Rev Immunol *11*, 251–263. https://doi.org/10.1038/nri2941.

Schatz, D.G., Oettinger, M.A., and Baltimore, D. (1989). The V(D)J Recombination Activating Gene, RAG-1. Cell *59*, 1035–1048. .

Scherer, K.M., Mascheroni, L., Carnell, G.W., Wunderlich, L.C.S., Makarchuk, S., Brockhoff, M., Mela, I., Fernandez-Villegas, A., Barysevich, M., Stewart, H., et al. (2022). SARS-CoV-2 nucleocapsid protein adheres to replication organelles before viral assembly at the Golgi/ERGIC and lysosome-mediated egress. Sci Adv *8*, 4895. https://doi.org/10.1126/SCIADV.ABL4895/SUPPL_FILE/SCIADV.ABL4895_.

Schickel, J.N., Glauzy, S., Ng, Y.S., Chamberlain, N., Massad, C., Isnardi, I., Katz, N., Uzel, G., Holland, S.M., Picard, C., et al. (2017). Self-reactive VH4-34–expressing IgG B cells recognize commensal bacteria. J Exp Med *214*, 1991. https://doi.org/10.1084/JEM.20160201.

Schiepers, A., van't Wout, M.F.L., Greaney, A.J., Zang, T.M., Muramatsu, H., Lin, P.J.C., Tam, Y.K., Mesin, L., Starr, T.N., Bieniasz, P.D., et al. (2023a). Molecular fate-mapping of serum antibody responses to repeat immunization. Nature https://doi.org/10.1038/s41586-023-05715-3.

Schiepers, A., Van 't Wout, M.F.L., Hobbs, A., Mesin, L., and Victora, G.D. (2023b). Opposing effects of pre-existing antibody and memory T cell help on the dynamics of recall germinal centers. BioRxiv 2023.12.15.571936. https://doi.org/10.1101/2023.12.15.571936.

Schnittman, S.M., Lane, H.C., Higgins, S.E., Folks, T., and Fauci, A.S. (1986). Direct polyclonal activation of human B lymphocytes by the acquired immune deficiency syndrome virus. Science *233*, 1084–1086. https://doi.org/10.1126/science.3016902.

Schramm, C.A., and Douek, D.C. (2018). Beyond Hot Spots: Biases in Antibody Somatic Hypermutation and Implications for Vaccine Design. Front Immunol *9*, 1. https://doi.org/10.3389/FIMMU.2018.01876.

Schultheiß, C., Paschold, L., Simnica, D., Mohme, M., Willscher, E., von Wenserski, L., Scholz, R., Wieters, I., Dahlke, C., Tolosa, E., et al. (2020). Next-Generation Sequencing of T and B Cell Receptor Repertoires from COVID-19 Patients Showed Signatures Associated with Severity of Disease. Immunity *53*, 442. https://doi.org/10.1016/J.IMMUNI.2020.06.024.

Schuster, D.J., Karuna, S., Brackett, C., Wesley, M., Li, S.S., Eisel, N., Tenney, D.A., Hilliard, T., Yates, N.L., Heptinstall, J.R., et al. (2022). Lower SARS-CoV-2–specific humoral immunity in people living with HIV-1 recovered from nonhospitalized COVID-19. JCI Insight *7*. https://doi.org/10.1172/JCI.INSIGHT.158402.

Schwickert, T.A., Victora, G.D., Fooksman, D.R., Kamphorst, A.O., Mugnier, M.R., Gitlin, A.D., and Nussenzweig, M.L.D. (2011). A dynamic T cell–limited checkpoint regulates affinity-dependent B cell entry into the germinal center. J Exp Med *208*, 1243. https://doi.org/10.1084/JEM.20102477.

Seow, J., Graham, C., Merrick, B., Acors, S., Pickering, S., Steel, K.J.A., Hemmings, O., O'Byrne, A., Kouphou, N., Galao, R.P., et al. (2020). Longitudinal observation and decline of neutralizing antibody responses in the three months following SARS-CoV-2 infection in humans. Nat Microbiol *5*. https://doi.org/10.1038/s41564-020-00813-8.

Setliff, I., McDonnell, W.J., Raju, N., Bombardi, R.G., Murji, A.A., Scheepers, C., Ziki, R., Mynhardt, C., Shepherd, B.E., Mamchak, A.A., et al. (2018). Multi-Donor Longitudinal Antibody Repertoire Sequencing Reveals the Existence of Public Antibody Clonotypes in HIV-1 Infection. Cell Host Microbe *23*, 845. https://doi.org/10.1016/J.CHOM.2018.05.001.

Shang, J., Ye, G., Shi, K., Wan, Y., Luo, C., Aihara, H., Geng, Q., Auerbach, A., and Li, F. (2020). Structural basis of receptor recognition by SARS-CoV-2. Nature *581*, 221–224. https://doi.org/10.1038/s41586-020-2179-y.

Shannon, C.E., and Weaver, W. (1949). THE MATHEMATICAL THEORY OF COMMUNICATION. University of Illinois Press.

Sharp, P.M., and Hahn, B.H. (2011). Origins of HIV and the AIDS pandemic. Cold Spring Harb Perspect Med *1*, a006841. https://doi.org/10.1101/cshperspect.a006841.

Sheikh-Mohamed, S., Isho, B., Chao, G.Y.C., Zuo, M., Cohen, C., Lustig, Y., Nahass, G.R., Salomon-Shulman, R.E., Blacker, G., Fazel-Zarandi, M., et al. (2022). Systemic and mucosal IgA responses are variably induced in response to SARS-CoV-2 mRNA vaccination and are associated with protection against subsequent infection. Mucosal Immunology 2022 15:5 *15*, 799–808. https://doi.org/10.1038/s41385-022-00511-0.

Shi, R., Shan, C., Duan, X., Chen, Z., Liu, P., Song, J., Song, T., Bi, X., Han, C., Wu, L., et al. (2020). A human neutralizing antibody targets the receptor-binding site of SARS-CoV-2. Nature *584*, 120–124. https://doi.org/10.1038/s41586-020-2381-y.

Shih, T.A.Y., Meffre, E., Roederer, M., and Nussenzweig, M.C. (2002). Role of BCR affinity in T cell-dependent antibody responses in vivo. Nat Immunol *3*, 570–575. https://doi.org/10.1038/ni803.

Shrock, E., Fujimura, E., Kula, T., Timms, R.T., Lee, I.H., Leng, Y., Robinson, M.L., Sie, B.M., Li, M.Z., Chen, Y., et al. (2020). Viral epitope profiling of COVID-19 patients

reveals cross-reactivity and correlates of severity. Science *370*. https://doi.org/10.1126/SCIENCE.ABD4250.

Shrock, E.L., Timms, R.T., Kula, T., Mena, E.L., West, A.P., Guo, R., Lee, I.H., Cohen, A.A., McKay, L.G.A., Bi, C., et al. (2023). Germline-encoded amino acid–binding motifs drive immunodominant public antibody responses. Science *380*. https://doi.org/10.1126/science.adc9498.

Siegal, F.P., Lopez, C., Hammer, G.S., Brown, A.E., Kornfeld, S.J., Gold, J., Hassett, J., Hirschman, S.Z., Cunningham-Rundles, C., Adelsberg, B.R., et al. (1981). Severe Acquired Immunodeficiency in Male Homosexuals, Manifested by Chronic Perianal Ulcerative Herpes Simplex Lesions. New England Journal of Medicine *305*, 1439–1444. https://doi.org/10.1056/NEJM198112103052403.

Sievers, B.L., Cheng, M.T.K., Csiba, K., Meng, B., and Gupta, R.K. (2023). SARS-CoV-2 and innate immunity: the good, the bad, and the “goldilocks.” Cellular & Molecular Immunology 2023 1–13. https://doi.org/10.1038/s41423-023-01104-y.

Simpson, E.H. (1949). Measurement of diversity. Nature *163*, 688. https://doi.org/10.1038/163688a0.

Smith, N., Goncalves, P., Charbit, B., Grzelak, L., Beretta, M., Planchais, C., Bruel, T., Rouilly, V., Bondet, V., Hadjadj, J., et al. (2021). Distinct systemic and mucosal immune responses during acute SARS-CoV-2 infection. Nat Immunol *22*, 1428–1439. https://doi.org/10.1038/s41590-021-01028-7.

Snyman, J., Hwa, S.H., Krause, R., Muema, D., Reddy, T., Ganga, Y., Karim, F., Leslie, A., Sigal, A., Ndung’U, T., et al. (2022). Similar Antibody Responses Against Severe Acute Respiratory Syndrome Coronavirus 2 in Individuals Living Without and With Human Immunodeficiency Virus on Antiretroviral Therapy During the First South African Infection Wave. Clin Infect Dis *75*, e249. https://doi.org/10.1093/CID/CIAB758.

Sokal, A., Chappert, P., Barba-Spaeth, G., Roeser, A., Fourati, S., Azzaoui, I., Vandenberghe, A., Fernandez, I., Meola, A., Bouvier-Alias, M., et al. (2021). Maturation and persistence of the anti-SARS-CoV-2 memory B cell response. Cell *184*, 1201-1213.e14. https://doi.org/10.1016/J.CELL.2021.01.050.

Sokal, A., Broketa, M., Barba-Spaeth, G., Meola, A., Fernández, I., Fourati, S., Azzaoui, I., de La Selle, A., Vandenberghe, A., Roeser, A., et al. (2022). Analysis of mRNA vaccination-elicited RBD-specific memory B cells reveals strong but incomplete immune escape of the SARS-CoV-2 Omicron variant. Immunity *55*, 1096-1104.e4. https://doi.org/10.1016/j.immuni.2022.04.002.

Sokal, A., Barba-Spaeth, G., Hunault, L., Fernández, I., Broketa, M., Meola, A., Fourati, S., Azzaoui, I., Vandenberghe, A., Lagouge-Roussey, P., et al. (2023). SARS-CoV-2 Omicron BA.1 breakthrough infection drives late remodeling of the memory B cell repertoire in vaccinated individuals. Immunity *56*, 2137-2151.e7. https://doi.org/10.1016/J.IMMUNI.2023.07.007.

Solera, J.T., Ierullo, M., Arbol, B.G., Mavandadnejad, F., Kurtesi, A., Qi, F., Hu, Q., Gingras, A.C., Ferreira, V.H., Humar, A., et al. (2023). Bivalent COVID-19 mRNA vaccine against omicron subvariants in immunocompromised patients. Lancet Infect Dis *23*, e266–e267. https://doi.org/10.1016/S1473-3099(23)00357-2.

Søndergaard, M.H., Thavarajah, J.J., Churchill Henson, H., and Wejse, C.M. (2023). SARS-CoV-2 vaccine immunogenicity for people living with HIV: A systematic review and meta-analysis. HIV Med 1–22. https://doi.org/10.1111/hiv.13537.

Song, G., He, W. ting, Callaghan, S., Anzanello, F., Huang, D., Ricketts, J., Torres, J.L., Beutler, N., Peng, L., Vargas, S., et al. (2021). Cross-reactive serum and memory B-cell responses to spike protein in SARS-CoV-2 and endemic coronavirus infection. Nat Commun *12*. https://doi.org/10.1038/s41467-021-23074-3.

Song, W., Antao, O.Q., Condiff, E., Sanchez, G.M., Chernova, I., Zembrzuski, K., Steach, H., Rubtsova, K., Angeletti, D., Lemenze, A., et al. (2022). Development of Tbet- and CD11c-expressing B cells in a viral infection requires T follicular helper cells outside of germinal centers. Immunity *55*, 290-307.e5. https://doi.org/10.1016/j.immuni.2022.01.002.

Sonoda, E., Pewzner-Jung, Y., Schwers, S., Taki, S., Jung, S., Eilat, D., and Rajewsky, K. (1997). B Cell Development under the Condition of Allelic Inclusion. Immunity *6*, 225–233. https://doi.org/10.1016/S1074-7613(00)80325-8.

Spinelli, M.A., Lynch, K.L., Yun, C., Glidden, D. V, Peluso, M.J., Henrich, T.J., Gandhi, M., and Brown, L.B. (2021a). SARS-CoV-2 seroprevalence, and IgG concentration

and pseudovirus neutralising antibody titres after infection, compared by HIV status: a matched case-control observational study. Lancet HIV *8*, e334–e341. https://doi.org/10.1016/S2352-3018(21)00072-2.

Spinelli, M.A., Peluso, M.J., Lynch, K.L., Yun, C., Glidden, D. V, Henrich, T.J., Deeks, S.G., and Gandhi, M. (2021b). Differences in Post-mRNA Vaccination Severe Acute Respiratory Syndrome Coronavirus 2 (SARS-CoV-2) Immunoglobulin G (IgG) Concentrations and Surrogate Virus Neutralization Test Response by Human Immunodeficiency Virus (HIV) Status and Type of Vaccine: A Ma. Clinical Infectious Diseases https://doi.org/10.1093/CID/CIAB1009.

Srivastava, K., Carreño, J.M., Gleason, C., Monahan, B., Singh, G., Abbad, A., Tcheou, J., Raskin, A., Kleiner, G., Bakel, H. van, et al. (2024). SARS-CoV-2-infection- and vaccine-induced antibody responses are long lasting with an initial waning phase followed by a stabilization phase. Immunity *0*, 1–13. https://doi.org/10.1016/J.IMMUNI.2024.01.017.

Stacey, A.R., Norris, P.J., Qin, L., Haygreen, E.A., Taylor, E., Heitman, J., Lebedeva, M., Decamp, A., Li, D., Grove, D., et al. (2009). Induction of a Striking Systemic Cytokine Cascade prior to Peak Viremia in Acute Human Immunodeficiency Virus Type 1 Infection, in Contrast to More Modest and Delayed Responses in Acute Hepatitis B and C Virus Infections. J Virol *83*, 3719–3733. https://doi.org/10.1128/JVI.01844-08.

Stahl, R.E., Friedman-Kien, A., Dubin, R., Marmor, M., and Zolla-Pazner, S. (1982). Immunologic abnormalities in homosexual men. Relationship to Kaposi's sarcoma. Am J Med *73*, 171–178. https://doi.org/10.1016/0002-9343(82)90174-7.

Stamatatos, L., Czartoski, J., Wan, Y.H., Homad, L.J., Rubin, V., Glantz, H., Neradilek, M., Seydoux, E., Jennewein, M.F., MacCamy, A.J., et al. (2021). mRNA vaccination boosts cross-variant neutralizing antibodies elicited by SARS-CoV-2 infection. Science *372*, 1413–1418. https://doi.org/10.1126/SCIENCE.ABG9175/SUPPL_FILE/ABG9175_STAMATATOS_SM.PDF.

Starr, T.N., Greaney, A.J., Addetia, A., Hannon, W.W., Choudhary, M.C., Dingens, A.S., Li, J.Z., and Bloom, J.D. (2021). Prospective mapping of viral mutations that

escape antibodies used to treat COVID-19. Science *371*, 850–854. https://doi.org/10.1126/science.abf9302.

Sterlin, D., Mathian, A., Miyara, M., Mohr, A., Anna, F., Claër, L., Quentric, P., Fadlallah, J., Devilliers, H., Ghillani, P., et al. (2021). IgA dominates the early neutralizing antibody response to SARS-CoV-2. Sci Transl Med *13*, 2223. .

Stern, J.N.H., Yaari, G., Vander Heiden, J.A., Church, G., Donahue, W.F., Hintzen, R.Q., Huttner, A.J., Laman, J.D., Nagra, R.M., Nylander, A., et al. (2014). B cells populating the multiple sclerosis brain mature in the draining cervical lymph nodes. Sci Transl Med *6*, 248ra107. https://doi.org/10.1126/SCITRANSLMED.3008879.

Sungnak, W., Huang, N., Bécavin, C., Berg, M., Queen, R., Litvinukova, M., Talavera-López, C., Maatz, H., Reichart, D., Sampaziotis, F., et al. (2020). SARS-CoV-2 entry factors are highly expressed in nasal epithelial cells together with innate immune genes. Nat Med *26*, 681–687. https://doi.org/10.1038/s41591-020-0868-6.

Sutton, H.J., Aye, R., Idris, A.H., Vistein, R., Nduati, E., Kai, O., Mwacharo, J., Li, X., Gao, X., Andrews, T.D., et al. (2021). Atypical B cells are part of an alternative lineage of B cells that participates in responses to vaccination and infection in humans. Cell Rep *34*. https://doi.org/10.1016/j.celrep.2020.108684.

Suzuki, K., Grigorova, I., Phan, T.G., Kelly, L.M., and Cyster, J.G. (2009). Visualizing B cell capture of cognate antigen from follicular dendritic cells. J Exp Med *206*, 1485. https://doi.org/10.1084/JEM.20090209.

Swadling, L., Diniz, M.O., Schmidt, N.M., Amin, O.E., Chandran, A., Shaw, E., Pade, C., Gibbons, J.M., Le Bert, N., Tan, A.T., et al. (2022). Pre-existing polymerase-specific T cells expand in abortive seronegative SARS-CoV-2. Nature *601*, 110. https://doi.org/10.1038/S41586-021-04186-8.

Tan, A.T., Linster, M., Tan, C.W., Le Bert, N., Chia, W.N., Kunasegaran, K., Zhuang, Y., Tham, C.Y.L., Chia, A., Smith, G.J.D., et al. (2021). Early induction of functional SARS-CoV-2-specific T cells associates with rapid viral clearance and mild disease in COVID-19 patients. Cell Rep *34*, 108728. https://doi.org/10.1016/J.CELREP.2021.108728.

Tan, L., Wang, Q., Zhang, D., Ding, J., Huang, Q., Tang, Y.Q., Wang, Q., and Miao, H. (2020). Lymphopenia predicts disease severity of COVID-19: a descriptive and predictive study. Signal Transduct Target Ther *5*, 1–3. https://doi.org/10.1038/s41392-020-0148-4.

Tang, J., Zeng, C., Cox, T.M., Li, C., Son, Y.M., Cheon, I.S., Wu, Y., Behl, S., Taylor, J.J., Chakaraborty, R., et al. (2022). Respiratory mucosal immunity against SARS-CoV-2 after mRNA vaccination. Sci Immunol *7*, 1–11. https://doi.org/10.1126/sciimmunol.add4853.

Tangye, S.G., Liu, Y.J., Aversa, G., Phillips, J.H., and De Vries, J.E. (1998). Identification of Functional Human Splenic Memory B Cells by Expression of CD148 and CD27. J Exp Med *188*, 1691. https://doi.org/10.1084/JEM.188.9.1691.

Tanriover, M.D., Doğanay, H.L., Akova, M., Güner, H.R., Azap, A., Akhan, S., Köse, Ş., Erdinç, F.Ş., Akalın, E.H., Tabak, Ö.F., et al. (2021). Efficacy and safety of an inactivated whole-virion SARS-CoV-2 vaccine (CoronaVac): interim results of a double-blind, randomised, placebo-controlled, phase 3 trial in Turkey. The Lancet *398*, 213–222. https://doi.org/10.1016/S0140-6736(21)01429-X.

Tarke, A., Coelho, C.H., Zhang, Z., Dan, J.M., Yu, E.D., Methot, N., Bloom, N.I., Goodwin, B., Phillips, E., Mallal, S., et al. (2022). SARS-CoV-2 vaccination induces immunological T cell memory able to cross-recognize variants from Alpha to Omicron. Cell *185*, 847-859.e11. https://doi.org/10.1016/J.CELL.2022.01.015.

Tauzin, A., Beaudoin-Bussières, G., Gong, S.Y., Chatterjee, D., Gendron-Lepage, G., Bourassa, C., Goyette, G., Racine, N., Khrifi, Z., Turgeon, J., et al. (2022). Humoral immune responses against SARS-CoV-2 Spike variants after mRNA vaccination in solid organ transplant recipients. IScience *25*. https://doi.org/10.1016/j.isci.2022.104990.

Tegally, H., Wilkinson, E., Giovanetti, M., Iranzadeh, A., Fonseca, V., Giandhari, J., Doolabh, D., Pillay, S., San, E.J., Msomi, N., et al. (2021). Detection of a SARS-CoV-2 variant of concern in South Africa. Nature *592*, 438–443. https://doi.org/10.1038/s41586-021-03402-9.

Terpstra, F.G., J. M. Al, B., Roos, M.T.H.L., Wolf, F. De, Goudsmit, J., Schellekens, P.T.H.A., and Miedema, F. (1989). Longitudinal study of leukocyte functions in

homosexual men seroconverted for HIV: rapid and persistent loss of B cell function after HIV infection. Eur J Immunol *19*, 667–673. https://doi.org/10.1002/eji.1830190415.

Terreri, S., Piano Mortari, E., Vinci, M.R., Russo, C., Alteri, C., Albano, C., Colavita, F., Gramigna, G., Agrati, C., Linardos, G., et al. (2022). Persistent B cell memory after SARS-CoV-2 vaccination is functional during breakthrough infections. Cell Host Microbe *30*, 400-408.e4. https://doi.org/10.1016/J.CHOM.2022.01.003.

Tesoriero, J.M., Swain, C.A.E., Pierce, J.L., Zamboni, L., Wu, M., Holtgrave, D.R., Gonzalez, C.J., Udo, T., Morne, J.E., Hart-Malloy, R., et al. (2021). COVID-19 Outcomes among Persons Living with or without Diagnosed HIV Infection in New York State. JAMA Netw Open *4*. https://doi.org/10.1001/jamanetworkopen.2020.37069.

The Antiretroviral Therapy (ART) Cohort Collaboration (2003). Prognostic importance of initial response in HIV-1 infected patients starting potent antiretroviral therapy: Analysis of prospective studies. Lancet *362*, 679–686. https://doi.org/10.1016/S0140-6736(03)14229-8.

The INSIGHT START Study Group (2015). Initiation of Antiretroviral Therapy in Early Asymptomatic HIV Infection. N Engl J Med *373*, 795. https://doi.org/10.1056/NEJMOA1506816.

The TEMPRANO ANRS 12136 Study Group (2015). A Trial of Early Antiretrovirals and Isoniazid Preventive Therapy in Africa. New England Journal of Medicine *373*, 808–822. https://doi.org/10.1056/NEJMOA1507198/SUPPL_FILE/NEJMOA1507198_DISCLOSURES.PDF.

Tiegs, S.L., Russell, D.M., and Nemazee, D. (1993). Receptor editing in self-reactive bone marrow B cells. Journal of Experimental Medicine *177*, 1009–1020. https://doi.org/10.1084/jem.177.4.1009.

Tiller, T., Meffre, E., Yurasov, S., Tsuiji, M., Nussenzweig, M.C., and Wardemann, H. (2008). Efficient generation of monoclonal antibodies from single human B cells by single cell RT-PCR and expression vector cloning. J Immunol Methods *329*, 112. https://doi.org/10.1016/J.JIM.2007.09.017.

Tipton, C.M., Fucile, C.F., Darce, J., Chida, A., Ichikawa, T., Gregoretti, I., Schieferl, S., Hom, J., Jenks, S., Feldman, R.J., et al. (2015). Diversity, cellular origin and autoreactivity of antibody-secreting cell population expansions in acute systemic lupus erythematosus. Nat Immunol *16*, 755–765. https://doi.org/10.1038/NI.3175.

Titanji, K., De Milito, A., Cagigi, A., Thorstensson, R., Grützmeier, S., Atlas, A., Hejdeman, B., Kroon, F.P., Lopalco, L., Nilsson, A., et al. (2006). Loss of memory B cells impairs maintenance of long-term serologic memory during HIV-1 infection. Blood *108*, 1580–1587. https://doi.org/10.1182/blood-2005-11-013383.

To, K.K.W., Tsang, O.T.Y., Leung, W.S., Tam, A.R., Wu, T.C., Lung, D.C., Yip, C.C.Y., Cai, J.P., Chan, J.M.C., Chik, T.S.H., et al. (2020). Temporal profiles of viral load in posterior oropharyngeal saliva samples and serum antibody responses during infection by SARS-CoV-2: an observational cohort study. Lancet Infect Dis *20*, 565–574. https://doi.org/10.1016/S1473-3099(20)30196-1.

Tomaras, G.D., Yates, N.L., Liu, P., Qin, L., Fouda, G.G., Chavez, L.L., Decamp, A.C., Parks, R.J., Ashley, V.C., Lucas, J.T., et al. (2008). Initial B-Cell Responses to Transmitted Human Immunodeficiency Virus Type 1: Virion-Binding Immunoglobulin M (IgM) and IgG Antibodies Followed by Plasma Anti-gp41 Antibodies with Ineffective Control of Initial Viremia. J Virol *82*, 12449–12463. https://doi.org/10.1128/jvi.01708-08.

Tonegawa, S. (1983). Somatic generation of antibody diversity. Nature *302*, 575–581. https://doi.org/10.1038/302575a0.

Touizer, E., Alrubayyi, A., Rees-Spear, C., Fisher-Pearson, N., Griffith, S.A., Muir, L., Pellegrino, P., Waters, L., Burns, F., Kinloch, S., et al. (2021). Failure to seroconvert after two doses of BNT162b2 SARS-CoV-2 vaccine in a patient with uncontrolled HIV. Lancet HIV *8*, e317–e318. https://doi.org/10.1016/S2352-3018(21)00099-0.

Touizer, E., Alrubayyi, A., Ford, R., Hussain, N., Gerber, P.P., Shum, H.-L., Rees-Spear, C., Muir, L., Gea-Mallorquí, E., Kopycinski, J., et al. (2023). Attenuated humoral responses in HIV infection after SARS-CoV-2 vaccination linked to global B cell defects and altered immune profiles. IScience *26*, 105862,. https://doi.org/10.1101/2022.11.11.516111.

Trampert, D.C., Hubers, L.M., van de Graaf, S.F.J., and Beuers, U. (2018). On the role of IgG4 in inflammatory conditions: lessons for IgG4-related disease. Biochimica et Biophysica Acta (BBA) - Molecular Basis of Disease *1864*, 1401–1409. https://doi.org/10.1016/J.BBADIS.2017.07.038.

Turner, J.S., Zhou, J.Q., Han, J., Schmitz, A.J., Rizk, A.A., Alsoussi, W.B., Lei, T., Amor, M., McIntire, K.M., Meade, P., et al. (2020). Human germinal centres engage memory and naive B cells after influenza vaccination. Nature *586*, 127–132. https://doi.org/10.1038/s41586-020-2711-0.

Turner, J.S., Kim, W., Kalaidina, E., Goss, C.W., Rauseo, A.M., Schmitz, A.J., Hansen, L., Haile, A., Klebert, M.K., Pusic, I., et al. (2021). SARS-CoV-2 infection induces long-lived bone marrow plasma cells in humans. Nature *595*, 421–425. https://doi.org/10.1038/s41586-021-03647-4.

Tuttle, D.J., Castanha, P.M.S., Nasser, A., Wilkins, M.S., Galarza, T.G., Alaoui-El-Azher, M., Cuff, D.E., Chhibbar, P., Das, J., Li, Y., et al. (2023). SARS-CoV-2 mRNA Vaccines Induce Greater Complement Activation and Decreased Viremia and Nef Antibodies in Men With HIV-1. J Infect Dis jiad544. https://doi.org/10.1093/infdis/jiad544.

UK Government (2022). Prime Minister sets out plan for living with COVID - GOV.UK.

UKHSA (2023a). COVID-19 Dashboard in the UK.

UKHSA (2023b). SARS-CoV-2 variant surveillance and assessment: technical briefing 55.

unaids.org (2019). Global HIV & AIDS statistics — 2019 fact sheet | UNAIDS. Http://Www.Unaids.Org/En/Resources/Fact-Sheet *1*, 1–6. .

Veit, O., Niedrig, M., Chapuis-Taillard, C., Cavassini, M., Mossdorf, E., Schmid, P., Bae, H.G., Litzba, N., Staub, T., Hatz, C., et al. (2009). Immunogenicity and safety of yellow fever vaccination for 102 HIV-infected patients. Clinical Infectious Diseases *48*, 659–666. https://doi.org/10.1086/597006/2/48-5-659-TBL002.GIF.

Veit, O., Domingo, C., Niedrig, M., Staehelin, C., Sonderegger, B., Héquet, D., Stoeckle, M., Calmy, A., Schiffer, V., Bernasconi, E., et al. (2018). Long-term Immune Response to Yellow Fever Vaccination in Human Immunodeficiency Virus (HIV)–

Infected Individuals Depends on HIV RNA Suppression Status: Implications for Vaccination Schedule. Clinical Infectious Diseases *66*, 1099–1108. https://doi.org/10.1093/CID/CIX960.

Verburgh, M.L., van Pul, L., Grobben, M., Boyd, A., Wit, F.W.N.M., van Nuenen, A.C., van Dort, K.A., Tejjani, K., van Rijswijk, J., Bakker, M., et al. (2023). Robust Vaccine-Induced as Well as Hybrid B- and T-Cell Immunity across SARS-CoV-2 Vaccine Platforms in People with HIV. Microbiol Spectr *11*. https://doi.org/10.1128/spectrum.01155-23.

Vergori, A., Cozzi Lepri, A., Cicalini, S., Matusali, G., Bordoni, V., Lanini, S., Meschi, S., Iannazzo, R., Mazzotta, V., Colavita, F., et al. (2022). Immunogenicity to COVID-19 mRNA vaccine third dose in people living with HIV. Nat Commun *13*, 1–13. https://doi.org/10.1038/s41467-022-32263-7.

Viana, R., Moyo, S., Amoako, D.G., Tegally, H., Scheepers, C., Althaus, C.L., Anyaneji, U.J., Bester, P.A., Boni, M.F., Chand, M., et al. (2022). Rapid epidemic expansion of the SARS-CoV-2 Omicron variant in southern Africa. Nature *603*, 679–686. https://doi.org/10.1038/s41586-022-04411-y.

Victora, G.D., Schwickert, T.A., Fooksman, D.R., Kamphorst, A.O., Meyer-Hermann, M., Dustin, M.L., and Nussenzweig, M.C. (2010). Germinal Center Dynamics Revealed by Multiphoton Microscopy Using a Photoactivatable Fluorescent Reporter. Cell *143*, 592. https://doi.org/10.1016/J.CELL.2010.10.032.

De Vito, D., Di Ciaula, A., Palmieri, V.O., Trerotoli, P., Larocca, A.M.V., Montagna, M.T., and Portincasa, P. (2022). Reduced COVID-19 mortality linked with early antibodies against SARS-CoV-2, irrespective of age. Eur J Intern Med *98*, 77. https://doi.org/10.1016/J.EJIM.2022.02.010.

Volpe, J.M., and Kepler, T.B. (2008). Large-scale analysis of human heavy chain V(D)J recombination patterns. Immunome Res *4*. https://doi.org/10.1186/1745-7580-4-3.

Volz, E., Hill, V., McCrone, J.T., Price, A., Jorgensen, D., O'Toole, Á., Southgate, J., Johnson, R., Jackson, B., Nascimento, F.F., et al. (2021). Evaluating the Effects of SARS-CoV-2 Spike Mutation D614G on Transmissibility and Pathogenicity. Cell *184*, 64. https://doi.org/10.1016/J.CELL.2020.11.020.

Voss, W.N., Hou, Y.J., Johnson, N. V., Delidakis, G., Kim, J.E., Javanmardi, K., Horton, A.P., Bartzoka, F., Paresi, C.J., Tanno, Y., et al. (2021). Prevalent, protective, and convergent IgG recognition of SARS-CoV-2 non-RBD spike epitopes. Science eabg5268. https://doi.org/10.1126/science.abg5268.

Voysey, M., Clemens, S.A.C., Madhi, S.A., Weckx, L.Y., Folegatti, P.M., Aley, P.K., Angus, B., Baillie, V.L., Barnabas, S.L., Bhorat, Q.E., et al. (2021). Safety and efficacy of the ChAdOx1 nCoV-19 vaccine (AZD1222) against SARS-CoV-2: an interim analysis of four randomised controlled trials in Brazil, South Africa, and the UK. The Lancet *397*, 99–111. https://doi.org/10.1016/S0140-6736(20)32661-1.

Walker, B.D., Chakrabarti, S., Moss, B., Paradis, T.J., Flynn, T., Durno, A.G., Blumberg, R.S., Kaplan, J.C., Hirsch, M.S., and Schooley, R.T. (1988). HIV-specific cytotoxic T lymphocytes in seropositive individuals. Nature *328*, 345–348. https://doi.org/10.1038/328345a0.

Walker, C.M., Moody, D.J., Stites, D.P., and Levy, J.A. (1986). CD8+ lymphocytes can control HIV infection in vitro by suppressing virus replication. Science *234*, 1563–1566. https://doi.org/10.1126/science.2431484.

Wallace, M.R., Hooper, D.G., Graves, S.J., and Malone, J.L. (1994). Measles seroprevalence and vaccine response in HIV-infected adults. Vaccine *12*, 1222–1224. https://doi.org/10.1016/0264-410X(94)90247-X.

Walls, A.C., Park, Y.-J., Tortorici, M.A., Wall, A., Mcguire, A.T., and Correspondence, D.V. (2020). Structure, Function, and Antigenicity of the SARS-CoV-2 Spike Glycoprotein. Cell *181*, 281-292.e6. https://doi.org/10.1016/j.cell.2020.02.058.

Walsh, E.E., Shin, J.H., and Falsey, A.R. (2013). Clinical impact of human coronaviruses 229E and OC43 infection in diverse adult populations. Journal of Infectious Diseases *208*, 1634–1642. https://doi.org/10.1093/infdis/jit393.

Walsh, E.E., Robert W. Frenck, Jr., Falsey, A.R., Kitchin, N., Absalon, J., Gurtman, A., Lockhart, S., Neuzil, K., Mulligan, M.J., Bailey, R., et al. (2020). Safety and Immunogenicity of Two RNA-Based Covid-19 Vaccine Candidates. N Engl J Med *383*, 2439–2450. https://doi.org/10.1056/NEJMOA2027906.

Wang, C., Liu, Y., Cavanagh, M.M., Le Saux, S., Qi, Q., Roskin, K.M., Looney, T.J., Lee, J.Y., Dixit, V., Dekker, C.L., et al. (2015). B-cell repertoire responses to varicella-zoster vaccination in human identical twins. Proc Natl Acad Sci U S A *112*, 500–505. https://doi.org/10.1073/PNAS.1415875112/-/DCSUPPLEMENTAL/PNAS.1415875112.SAPP.PDF.

Wang, P., Nair, M.S., Liu, L., Iketani, S., Luo, Y., Guo, Y., Wang, M., Yu, J., Zhang, B., Kwong, P.D., et al. (2021a). Antibody resistance of SARS-CoV-2 variants B.1.351 and B.1.1.7. Nature *593*, 130–135. https://doi.org/10.1038/s41586-021-03398-2.

Wang, R., Han, Y., Zhang, R., Zhu, J., Nan, X., Liu, Y., Yang, Z., Zhou, B., Yu, J., Lin, Z., et al. (2023). Dissecting the intricacies of human antibody responses to SARS-CoV-1 and SARS-CoV-2 infection. Immunity *56*, 2635-2649.e6. https://doi.org/10.1016/J.IMMUNI.2023.10.007.

Wang, Y., Zhang, L., Sang, L., Ye, F., Ruan, S., Zhong, B., Song, T., Alshukairi, A.N., Chen, R., Zhang, Z., et al. (2020). Kinetics of viral load and antibody response in relation to COVID-19 severity. Journal of Clinical Investigation *130*, 5235–5244. https://doi.org/10.1172/JCI138759.

Wang, Z., Muecksch, F., Schaefer-Babajew, D., Finkin, S., Viant, C., Gaebler, C., Hoffmann, H.H., Barnes, C.O., Cipolla, M., Ramos, V., et al. (2021b). Naturally enhanced neutralizing breadth against SARS-CoV-2 one year after infection. Nature 2021 595:7867 *595*, 426–431. https://doi.org/10.1038/s41586-021-03696-9.

Wang, Z., Lorenzi, J.C.C., Muecksch, F., Finkin, S., Viant, C., Gaebler, C., Cipolla, M., Hoffmann, H.H., Oliveira, T.Y., Oren, D.A., et al. (2021c). Enhanced SARS-CoV-2 neutralization by dimeric IgA. Sci Transl Med *13*, 1555. https://doi.org/10.1126/SCITRANSLMED.ABF1555.

Wang, Z.Q., Horowitz, H.W., Orlikowsky, T., Hahn, B.I., Trejo, V., Bapat, A.S., Mittler, R.S., Rayanade, R.J., Young Yang, S., and Hoffmann, M.K. (1999). Polyspecific Self-Reactive Antibodies in Individuals Infected with Human Immunodeficiency Virus Facilitate T Cell Deletion and Inhibit Costimulatory Accessory Cell Function. J Infect Dis *180*, 1072–1079. https://doi.org/10.1086/314974.

Wardemann, H., Yurasov, S., Schaefer, A., Young, J.W., Meffre, E., and Nussenzweig, M.C. (2003). Predominant autoantibody production by early human B cell precursors. Science *301*, 1374–1377. https://doi.org/10.1126/science.1086907.

Waters, L., Winston, A., Reeves, I., Boffito, M., Churchill, D., Cromarty, B., Dunn, D., Fink, D., Fidler, S., Foster, C., et al. (2022). BHIVA guidelines on antiretroviral treatment for adults living with HIV-1 2022. HIV Med *23*, 3–115. https://doi.org/10.1111/HIV.13446.

Weber, T., Dähling, S., Rose, S., Affeldt, P., Vanshylla, K., Ullrich, L., Gieselmann, L., Teipel, F., Gruell, H., Di Cristanziano, V., et al. (2023). Enhanced SARS-CoV-2 humoral immunity following breakthrough infection builds upon the preexisting memory B cell pool. Sci Immunol *8*. https://doi.org/10.1126/SCIIMMUNOL.ADK5845.

Wec, A.Z., Wrapp, D., Herbert, A.S., Maurer, D.P., Haslwanter, D., Sakharkar, M., Jangra, R.K., Dieterle, M.E., Lilov, A., Huang, D., et al. (2020). Broad neutralization of SARS-related viruses by human monoclonal antibodies. Science eabc7424. https://doi.org/10.1126/science.abc7424.

Wei, C., Anolik, J., Cappione, A., Zheng, B., Pugh-Bernard, A., Brooks, J., Lee, E.-H., Milner, E.C.B., and Sanz, I. (2007). A New Population of Cells Lacking Expression of CD27 Represents a Notable Component of the B Cell Memory Compartment in Systemic Lupus Erythematosus. The Journal of Immunology *178*, 6624–6633. https://doi.org/10.4049/jimmunol.178.10.6624.

Wei, X., Decker, J.M., Wang, S., Hui, H., Kappes, J.C., Wu, X., Salazar-Gonzalez, J.F., Salazar, M.G., Kilby, J.M., Saag, M.S., et al. (2003). Antibody neutralization and escape by HIV-1. Nature *422*, 307–312. https://doi.org/10.1038/nature01470.

Weisel, F., and Shlomchik, M. (2017). Memory B cells of mice and humans. Annu Rev Immunol *35*, 255–284. https://doi.org/10.1146/annurev-immunol-041015-055531.

Weisel, F.J., Zuccarino-Catania, G. V., Chikina, M., and Shlomchik, M.J. (2016). A Temporal Switch in the Germinal Center Determines Differential Output of Memory B and Plasma Cells. Immunity *44*, 116. https://doi.org/10.1016/J.IMMUNI.2015.12.004.

Weissman, D., Alameh, M.-G., De Silva, T., Haynes, B.F., Korber, B., Correspondence, D.C.M., Collini, P., Hornsby, H., Brown, R., Labranche, C.C., et al.

(2021). D614G Spike Mutation Increases SARS CoV-2 Susceptibility to Neutralization ll D614G Spike Mutation Increases SARS CoV-2 Susceptibility to Neutralization. Cell Host Microbe *29*, 23–31. https://doi.org/10.1016/j.chom.2020.11.012.

Wheatley, A.K., Kristensen, A.B., Lay, W.N., and Kent, S.J. (2016). HIV-dependent depletion of influenza-specific memory B cells impacts B cell responsiveness to seasonal influenza immunisation. Sci Rep *6*. https://doi.org/10.1038/srep26478.

Wheatley, A.K., Juno, J.A., Wang, J.J., Selva, K.J., Reynaldi, A., Tan, H.X., Lee, W.S., Wragg, K.M., Kelly, H.G., Esterbauer, R., et al. (2021). Evolution of immune responses to SARS-CoV-2 in mild-moderate COVID-19. Nat Commun *12*, 1–11. https://doi.org/10.1038/s41467-021-21444-5.

Whitt, M.A. (2010). Generation of VSV pseudotypes using recombinant ΔG-VSV for studies on virus entry, identification of entry inhibitors, and immune responses to vaccines. J Virol Methods *169*, 365–374. https://doi.org/10.1016/j.jviromet.2010.08.006.

WHO (2020a). Naming the coronavirus disease (COVID-19) and the virus that causes it.

WHO (2020b). WHO Director-General's opening remarks at the media briefing on COVID-19 - 11 March 2020.

WHO (2024). WHO COVID-19 dashboard.

Wilhelm, A., Widera, M., Grikscheit, K., Toptan, T., Schenk, B., Pallas, C., Metzler, M., Kohmer, N., Hoehl, S., Marschalek, R., et al. (2022). Limited neutralisation of the SARS-CoV-2 Omicron subvariants BA.1 and BA.2 by convalescent and vaccine serum and monoclonal antibodies. EBioMedicine *82*, 104158. https://doi.org/10.1016/j.ebiom.2022.104158.

Willett, B.J., Grove, J., MacLean, O.A., Wilkie, C., De Lorenzo, G., Furnon, W., Cantoni, D., Scott, S., Logan, N., Ashraf, S., et al. (2022). SARS-CoV-2 Omicron is an immune escape variant with an altered cell entry pathway. Nat Microbiol *7*, 1161–1179. https://doi.org/10.1038/s41564-022-01143-7.

Winslow, G.M., Papillion, A.M., Kenderes, K.J., and Levack, R.C. (2017). CD11c+ T-bet+ memory B cells: Immune maintenance during chronic infection and inflammation? Cell Immunol *321*, 8–17. https://doi.org/10.1016/j.cellimm.2017.07.006.

Wit, F.W.N.M., Reiss, P., Rijnders, B., Rokx, C., Roukens, A., Brinkman, K., and Van Der Valk, M. (2023). COVID-19 in people with HIV in the Netherlands. AIDS *37*, 1671. https://doi.org/10.1097/QAD.0000000000003597.

Woldemeskel, B.A., Karaba, A.H., Garliss, C.C., Beck, E.J., Wang, K.H., Laeyendecker, O., Cox, A.L., and Blankson, J.N. (2022). The BNT162b2 mRNA Vaccine Elicits Robust Humoral and Cellular Immune Responses in People Living With Human Immunodeficiency Virus (HIV). Clinical Infectious Diseases ® *74*, 1268–1270. https://doi.org/10.1093/cid/ciab648.

Woodruff, M.C., Ramonell, R.P., Nguyen, D.C., Cashman, K.S., Saini, A.S., Haddad, N.S., Ley, A.M., Kyu, S., Howell, J.C., Ozturk, T., et al. (2020). Extrafollicular B cell responses correlate with neutralizing antibodies and morbidity in COVID-19. Nat Immunol *21*, 1506–1516. https://doi.org/10.1038/s41590-020-00814-z.

Woodruff, M.C., Ramonell, R.P., Haddad, N.S., Anam, F.A., Rudolph, M.E., Walker, T.A., Truong, A.D., Dixit, A.N., Han, J.E., Cabrera-Mora, M., et al. (2022). Dysregulated naive B cells and de novo autoreactivity in severe COVID-19. Nature *611*, 139–147. https://doi.org/10.1038/s41586-022-05273-0.

Woof, J.M., and Mestecky, J. (2005). Mucosal immunoglobulins. Immunol Rev *206*, 64–82. https://doi.org/10.1111/J.0105-2896.2005.00290.X.

Wrapp, D., Wang, N., Corbett, K.S., Goldsmith, J.A., Hsieh, C.L., Abiona, O., Graham, B.S., and McLellan, J.S. (2020). Cryo-EM structure of the 2019-nCoV spike in the prefusion conformation. Science *367*, 1260–1263. https://doi.org/10.1126/science.aax0902.

Wright, E., Temperton, N.J., Marston, D.A., McElhinney, L.M., Fooks, A.R., and Weiss, R.A. (2008). Investigating antibody neutralization of lyssaviruses using lentiviral pseudotypes: a cross-species comparison. J Gen Virol *89*, 2204. https://doi.org/10.1099/VIR.0.2008/000349-0.

Wu, F., Zhao, S., Yu, B., Chen, Y.M., Wang, W., Song, Z.G., Hu, Y., Tao, Z.W., Tian, J.H., Pei, Y.Y., et al. (2020). A new coronavirus associated with human respiratory disease in China. Nature *579*, 265–269. https://doi.org/10.1038/s41586-020-2008-3.

Wu, W., Cheng, Y., Zhou, H., Sun, C., and Zhang, S. (2023). The SARS-CoV-2 nucleocapsid protein: its role in the viral life cycle, structure and functions, and use as a potential target in the development of vaccines and diagnostics. Virology Journal 2023 20:1 *20*, 1–16. https://doi.org/10.1186/S12985-023-01968-6.

Wu, Y.C.B., Kipling, D., and Dunn-Walters, D.K. (2011). The Relationship between CD27 Negative and Positive B Cell Populations in Human Peripheral Blood. Front Immunol *2*. https://doi.org/10.3389/FIMMU.2011.00081.

Xia, S., Zhang, Y., Wang, Y., Wang, H., Yang, Y., Gao, G.F., Tan, W., Wu, G., Xu, M., Lou, Z., et al. (2021). Safety and immunogenicity of an inactivated SARS-CoV-2 vaccine, BBIBP-CorV: a randomised, double-blind, placebo-controlled, phase 1/2 trial. Lancet Infect Dis *21*, 39. https://doi.org/10.1016/S1473-3099(20)30831-8.

Yang, F., Nielsen, S.C.A., Hoh, R.A., Röltgen, K., Wirz, O.F., Haraguchi, E., Jean, G.H., Lee, J.Y., Pham, T.D., Jackson, K.J.L., et al. (2021a). Shared B cell memory to coronaviruses and other pathogens varies in human age groups and tissues. Science *372*, 738–741. https://doi.org/10.1126/science.abf6648.

Yang, J., Zheng, Y., Gou, X., Pu, K., Chen, Z., Guo, Q., Ji, R., Wang, H., Wang, Y., and Zhou, Y. (2020). Prevalence of comorbidities and its effects in coronavirus disease 2019 patients: A systematic review and meta-analysis. International Journal of Infectious Diseases *94*, 91–95. https://doi.org/10.1016/j.ijid.2020.03.017.

Yang, R., Avery, D.T., Jackson, K.J.L., Ogishi, M., Benhsaien, I., Du, L., Ye, X., Han, J., Rosain, J., Peel, J.N., et al. (2022). Human T-bet governs the generation of a distinct subset of CD11chighCD21low B cells. Sci Immunol *7*, eabq3277. https://doi.org/10.1126/SCIIMMUNOL.ABQ3277/SUPPL_FILE/SCIIMMUNOL.ABQ3277_SM.PDF.

Yang, X., Sun, J., Patel, R.C., Zhang, J., Guo, S., Zheng, Q., Olex, A.L., Olatosi, B., Weissman, S.B., Islam, J.Y., et al. (2021b). Associations between HIV infection and clinical spectrum of COVID-19: a population level analysis based on US National

COVID Cohort Collaborative (N3C) data. Lancet HIV *8*, e690–e700. https://doi.org/10.1016/S2352-3018(21)00239-3.

Yang, X., Zhang, J., Liu, Z., Chen, S., Olatosi, B., Poland, G.A., Weissman, S., and Li, X. (2024). COVID-19 breakthrough infections among people living with and without HIV: A statewide cohort analysis. International Journal of Infectious Diseases *139*, 21–27. https://doi.org/10.1016/j.ijid.2023.11.029.

Yates, J.L., Ehrbar, D.J., Hunt, D.T., Girardin, R.C., Dupuis, A.P., Payne, A.F., Sowizral, M., Varney, S., Kulas, K.E., Demarest, V.L., et al. (2021). Serological analysis reveals an imbalanced IgG subclass composition associated with COVID-19 disease severity. Cell Rep Med *2*. https://doi.org/10.1016/J.XCRM.2021.100329.

Yates, N.L., Lucas, J.T., Nolen, T.L., Vandergrift, N.A., Soderberg, K.A., Seaton, K.E., Denny, T.N., Haynes, B.F., Cohen, M.S., and Tomaras, G.D. (2011). Multiple HIV-1-specific IgG3 responses decline during acute HIV-1: Implications for detection of incident HIV infection. AIDS *25*, 2089–2097. https://doi.org/10.1097/QAD.0b013e32834b348e.

Yendewa, G.A., Perez, J.A., Schlick, K., Tribout, H., and McComsey, G.A. (2021). Clinical Features and Outcomes of Coronavirus Disease 2019 among People with Human Immunodeficiency Virus in the United States: A Multicenter Study from a Large Global Health Research Network (TriNetX). Open Forum Infect Dis *8*. https://doi.org/10.1093/ofid/ofab272.

Yisimayi, A., Song, W., Wang, J., Jian, F., Yu, Y., Chen, X., Xu, Y., Yang, S., Niu, X., Xiao, T., et al. (2023). Repeated Omicron exposures override ancestral SARS-CoV-2 immune imprinting. Nature *625*, 2023.05.01.538516. https://doi.org/10.1038/s41586-023-06753-7.

Yu, X., Tsibane, T., McGraw, P.A., House, F.S., Keefer, C.J., Hicar, M.D., Tumpey, T.M., Pappas, C., Perrone, L.A., Martinez, O., et al. (2008). Neutralizing antibodies derived from the B cells of 1918 influenza pandemic survivors. Nature *455*, 532–536. https://doi.org/10.1038/nature07231.

Yuan, M., Liu, H., Wu, N.C., Lee, C.C.D., Zhu, X., Zhao, F., Huang, D., Yu, W., Hua, Y., Tien, H., et al. (2020). Structural basis of a shared antibody response to SARS-CoV-2. Science *369*, 1119–1123. https://doi.org/10.1126/science.abd2321.

Zaki, A.M., van Boheemen, S., Bestebroer, T.M., Osterhaus, A.D.M.E., and Fouchier, R.A.M. (2012). Isolation of a Novel Coronavirus from a Man with Pneumonia in Saudi Arabia. New England Journal of Medicine *367*, 1814–1820. https://doi.org/10.1056/NEJMOA1211721/SUPPL_FILE/NEJMOA1211721_DISCLOSURES.PDF.

Zhang, H., Li, H.B., Lyu, J.R., Lei, X.M., Li, W., Wu, G., Lyu, J., and Dai, Z.M. (2020). Specific ACE2 expression in small intestinal enterocytes may cause gastrointestinal symptoms and injury after 2019-nCoV infection. International Journal of Infectious Diseases *96*, 19–24. https://doi.org/10.1016/J.IJID.2020.04.027.

Zhang, J., Wu, Q., Liu, Z., Wang, Q., Wu, J., Hu, Y., Bai, T., Xie, T., Huang, M., Wu, T., et al. (2021). Spike-specific circulating T follicular helper cell and cross-neutralizing antibody responses in COVID-19-convalescent individuals. Nat Microbiol *6*, 51–58. https://doi.org/10.1038/s41564-020-00824-5.

Zhang, Z., Nomura, N., Muramoto, Y., Ekimoto, T., Uemura, T., Liu, K., Yui, M., Kono, N., Aoki, J., Ikeguchi, M., et al. (2022a). Structure of SARS-CoV-2 membrane protein essential for virus assembly. Nat Commun *13*, 1–12. https://doi.org/10.1038/s41467-022-32019-3.

Zhang, Z., Mateus, J., Coelho, C.H., Dan, J.M., Moderbacher, C.R., Gálvez, R.I., Cortes, F.H., Grifoni, A., Tarke, A., Chang, J., et al. (2022b). Humoral and cellular immune memory to four COVID-19 vaccines. Cell *185*, 2434-2451.e17. https://doi.org/10.1016/J.CELL.2022.05.022.

Zhou, J.Q., and Kleinstein, S.H. (2019). Cutting Edge: Ig H Chains Are Sufficient to Determine Most B Cell Clonal Relationships. The Journal of Immunology *203*, 1687–1692. https://doi.org/10.4049/jimmunol.1900666.

Zhou, Q., Liu, Y., Zeng, F., Meng, Y., Liu, H., and Deng, G. (2023). Correlation between CD4 T-Cell Counts and Seroconversion among COVID-19 Vaccinated Patients with HIV: A Meta-Analysis. Vaccines (Basel) *11*. https://doi.org/10.3390/vaccines11040789.

Zila, V., Margiotta, E., Turoňová, B., Müller, T.G., Zimmerli, C.E., Mattei, S., Allegretti, M., Börner, K., Rada, J., Müller, B., et al. (2021). Cone-shaped HIV-1 capsids are

transported through intact nuclear pores. Cell *184*, 1032. https://doi.org/10.1016/J.CELL.2021.01.025.

Zonozi, R., Walters, L.C., Shulkin, A., Naranbhai, V., Nithagon, P., Sauvage, G., Kaeske, C., Cosgrove, K., Nathan, A., Tano-Menka, R., et al. (2023). T cell responses to SARS-CoV-2 infection and vaccination are elevated in B cell deficiency and reduce risk of severe COVID-19. Sci Transl Med *15*, eadh4529. https://doi.org/10.1126/scitranslmed.adh4529.

Zost, S.J., Gilchuk, P., Case, J.B., Binshtein, E., Chen, R.E., Nkolola, J.P., Schäfer, A., Reidy, J.X., Trivette, A., Nargi, R.S., et al. (2020). Potently neutralizing and protective human antibodies against SARS-CoV-2. Nature *584*, 443–449. https://doi.org/10.1038/s41586-020-2548-6.

Zufferey, R., Nagy, D., Mandel, R.J., Naldini, L., and Trono, D. (1997). Multiply attenuated lentiviral vector achieves efficient gene delivery in vivo. Nat Biotechnol *15*, 871–875. https://doi.org/10.1038/nbt0997-871.

Zufferey, R., Dull, T., Mandel, R.J., Bukovsky, A., Quiroz, D., Naldini, L., and Trono, D. (1998). Self-Inactivating Lentivirus Vector for Safe and Efficient In Vivo Gene Delivery. J Virol *72*, 9873–9880. .

Zuo, F., Abolhassani, H., Du, L., Piralla, A., Bertoglio, F., de Campos-Mata, L., Wan, H., Schubert, M., Cassaniti, I., Wang, Y., et al. (2022). Heterologous immunization with inactivated vaccine followed by mRNA-booster elicits strong immunity against SARS-CoV-2 Omicron variant. Nat Commun *13*, 1–8. https://doi.org/10.1038/s41467-022-30340-5.

Zurbuchen, Y., Michler, J., Taeschler, P., Adamo, S., Cervia, C., Raeber, M.E., Acar, I.E., Nilsson, J., Warnatz, K., Soyka, M.B., et al. (2023). Human memory B cells show plasticity and adopt multiple fates upon recall response to SARS-CoV-2. Nat Immunol *24*. https://doi.org/10.1038/s41590-023-01497-y.